

**DESIGN AND DEVELOPMENT OF A
NOVEL AUTONOMOUS MOORED UNDERWATER PROFILER**

by © Joseph Singleton

A Thesis submitted
to the School of Graduate Studies in partial fulfillment of the
requirements for the degree of

Master of Ocean and Naval Architectural Engineering

Faculty of Engineering and Applied Science

Memorial University of Newfoundland

October 2019

St. John's, Newfoundland and Labrador

Abstract

The ocean is a dynamic and complex system. Understanding it through observation is critical to predicting and adapting to it. This thesis details a new approach to making vertical profiles at a fixed geographic location. It describes the design of a novel autonomous moored underwater profiler to characterize the water column of the continental shelf. The theory supporting the design is detailed, and the results of laboratory and field tests are presented. The rationale for the system, sub-system, and component design and selection is supported through calculations, and/or validated through bench testing. The resulting prototype is a hybrid of a wire follower type profiler. The profiler is attached to a subsea mooring and it is capable of profiling the entire water column. Using a buoyancy engine and compound pulley system, the unique propulsion system only requires power for the ascent. Performance analysis of the prototype during open water field trials indicated a high potential for the profiler to operate as intended.

Acknowledgements

The Marine Environmental Observation Prediction and Response Network (MEOPAR)
for providing the funding for this thesis.

The Marine Institute of Memorial University of Newfoundland
for providing the time for me to pursue this thesis.

Dr. Brad de Young and Dr. Ralf Bachmayer for their guidance and supervision. Glenn Cutler for the support he provided with the control system, and deployments during field trials. Mark Downey for the support he provided with the subsea mooring development, and deployments during field trials. The staff at the Autonomous Oceans Systems Laboratory for providing their expertise when requested.

Table of Contents

| | |
|---|------|
| Abstract | ii |
| Acknowledgements | iii |
| List of Tables | viii |
| List of Figures | ix |
| 1 Introduction | 1 |
| 2 Overview of Autonomous Profilers | 5 |
| 2.1 Lagrangian Profilers | 5 |
| 2.1.1 Argo Floats | 5 |
| 2.1.2 Gliders | 7 |
| 2.2 Eulerian Measurements: Moored Profilers | 8 |
| 2.2.1 Winched Systems | 9 |
| 2.2.2 Wire Followers | 11 |
| 3 Goals and Objectives of the Development | 13 |
| 3.1 Operational Requirements | 13 |
| 3.2 Water Column Characteristics | 14 |
| 4 Profiler Design Concept | 15 |
| 4.1 Mode of Ascent and Descent | 18 |
| 4.1.1 Position A - Hibernation | 19 |
| 4.1.2 Position B – Primary Ascent | 20 |
| 4.1.3 Position C- Contact with the Upper Stop | 20 |
| 4.1.4 Position D – Secondary Ascent | 22 |
| 4.1.5 Position E – Surface Breach | 24 |

| | | |
|-----------|---|----|
| 5 | Profiler Design | 25 |
| 5.1 | Sensor Float Design | 26 |
| 5.1.1 | The Effect of Current on the Position of the Sensor Float..... | 30 |
| 5.1.2 | Sensor Float Shape and Size | 34 |
| 5.1.2.1 | Sensor Float Enclosure Design..... | 39 |
| 5.1.2.2 | Streamlined Shape of Sensor Float..... | 44 |
| 5.1.2.3 | Size of the Sensor Float | 45 |
| 5.1.2.4 | Sensor Float Structure..... | 47 |
| 5.1.3 | Upright Orientation and Stability of the Sensor Float | 48 |
| 5.1.4 | Buoyancy Verification and Trimming of the Sensor Float..... | 50 |
| 5.2 | Electromechanical Cable Assembly Design | 51 |
| 5.3 | Passive Float Design | 58 |
| 5.3.1 | Sheave Design..... | 60 |
| 5.3.2 | Passive Float Shape and Size | 61 |
| 5.3.3 | Buoyancy and Balancing of the Passive Float | 62 |
| 5.3.4 | Buoyancy and Stable Equilibrium Verification of the Passive Float | 67 |
| 5.4 | Main Body Design | 71 |
| 5.4.1 | Buoyancy Engine Module..... | 72 |
| 5.4.1.1 | Operation of the Hydraulic Circuit | 74 |
| 5.4.1.2 | Buoyancy Engine..... | 80 |
| 5.4.1.3 | Hydraulic Components | 81 |
| 5.4.1.3.1 | Hydraulic Pump and Motor | 81 |
| 5.4.1.3.2 | Hydraulic Oil Selection | 87 |
| 5.4.1.3.3 | Hydraulic Valves Selection | 88 |

| | | |
|-------------|--|-----|
| 5.4.1.3.4 | Accumulator Selection | 91 |
| 5.4.1.3.5 | Pilot Operated Check Valve and Accumulator Design | 93 |
| 5.4.1.3.6 | Oil Reservoir Design | 95 |
| 5.4.1.3.6.1 | Filter Unit Selection | 96 |
| 5.4.1.3.6.2 | Custom Breather Vent Design..... | 98 |
| 5.4.1.3.6.3 | Oil Level Sensor Selection | 100 |
| 5.4.1.3.7 | Hydraulic System Frame Design..... | 102 |
| 5.4.1.4 | Bladder Design | 103 |
| 5.4.1.4.1 | Bladder Cage Design..... | 104 |
| 5.4.1.5 | Subsea Enclosure Design..... | 105 |
| 5.4.1.6 | Hydraulic Tubing, Hoses, and Fittings | 108 |
| 5.4.1.7 | Buoyancy Engine Bench Testing..... | 109 |
| 5.4.1.7.1 | Automatic Drain Functionality and Reliability Test | 110 |
| 5.4.1.7.2 | Temperature Effects on Power Consumption and Flow Rate | 112 |
| 5.4.1.7.3 | Pump Validation Tests | 115 |
| 5.4.2 | Profiler Power Source | 116 |
| 5.4.3 | Frame | 117 |
| 5.4.3.1 | Pump Emergency Kill Switch | 121 |
| 5.4.4 | Buoyancy of the Main Body | 124 |
| 5.4.5 | Verification and Trimming of Profiler's Buoyancy..... | 127 |
| 6 | Subsea Mooring Design | 128 |
| 7 | Control System, Electrical and Electronics..... | 129 |
| 8 | Field Deployment..... | 132 |
| 8.1 | Transportation Skid..... | 132 |

| | |
|--|-----|
| 8.2 Deployment Procedure..... | 133 |
| 9 Field Deployment Test Results | 136 |
| 9.1 First Field Deployment | 136 |
| 9.2 Second Field Deployment..... | 145 |
| 9.3 Third Field Deployment..... | 148 |
| 9.4 Fourth Field Deployment | 154 |
| 10 Conclusion and Future Work | 159 |
| Bibliography | 164 |
| Appendix A Product Specification Sheets | 172 |
| Appendix B SolidWorks CAD Fabrication Drawings | 270 |
| Appendix C Custom Accumulator Design Calculations Worksheet | 402 |
| Appendix D ATL Bladder Design Work Sheet | 406 |
| Appendix E Buoyancy Engine Subsea Enclosure Tender Specifications..... | 411 |

List of Tables

| | |
|--|-----|
| Table 1 Sensor float suit of sensors | 29 |
| Table 2 Sensor float data logging and controller components..... | 29 |
| Table 3 Sensor float telemetry components..... | 30 |
| Table 4 Sensor float variables and results..... | 37 |
| Table 5 Variables and factors for sensor float enclosure | 41 |
| Table 6 2-437 O-ring design dimensions for a radial industrial static male gland seal | 43 |
| Table 7 Power spring design parameters and values | 57 |
| Table 8 Passive float free body diagram variables and solution..... | 67 |
| Table 9 THF-40 pump input torque and power requirements | 83 |
| Table 10 Accumulator rated volume variables and results | 92 |
| Table 11 Enclosure volume calculation variables..... | 107 |
| Table 12 Pump flow rate validation results | 116 |
| Table 13 Profiler energy consumption estimate for 50 m field trials and 200 m full deployment..... | 117 |
| Table 14 Magnetic field strength calculation variables | 123 |
| Table 15 Freshwater and sea water buoyant forces of the profiler components and the profiler's net buoyancy (empty bladder)..... | 124 |
| Table 16 Main body free-body-diagram variable | 126 |

List of Figures

| | |
|---|----|
| Figure 1 Argo float (Argo, 2018)..... | 6 |
| Figure 2 Argo float profile cycle (Argo, 2018)..... | 6 |
| Figure 3 Argo float global distribution for May 2018 (Argo, 2018) | 7 |
| Figure 4 Slocum G2 Glider (Teledyne Webb Research, 2018) | 8 |
| Figure 5 Glider sawtooth profile (Glanders, 2018) | 8 |
| Figure 6 Vertical Profiling System (InterOcean, 2013)..... | 10 |
| Figure 7 SeaCycler overall design and deployed configuration (Send, et al., 2013)..... | 10 |
| Figure 8 McLane Moored Profiler (McLane Moored Profiler, 2018) | 12 |
| Figure 9 Seahorse profiler mooring and component details (Fowler, Hamilton, Beanlands, & Furlong, 1997) | 12 |
| Figure 10 Profiler prototype CAD model | 16 |
| Figure 11 Significant points during the profiler ascent and descent..... | 19 |
| Figure 12 Profiler 3:1 compound pulley system and its free-body diagrams | 21 |
| Figure 13. Electromechanical cable pay out during the secondary ascent..... | 23 |
| Figure 14. Final sensor float design: full and sectioned view..... | 27 |
| Figure 15 Sensor float - Orthographic projections with dimensions | 28 |
| Figure 16 Simple subsea mooring with an anchor point..... | 32 |
| Figure 17 Spherical sensor float trajectory | 38 |
| Figure 18. Streamline sensor float trajectory | 38 |
| Figure 19 Sensor float subsea enclosure with blind body sectioned and the enclosure components segregated | 40 |
| Figure 20 Geometric Chart for Components Under External or Compressive Loading (ASME, 2015)..... | 42 |

| | |
|--|----|
| Figure 21 Chart for Determining Shell Thickness of Components Under External Pressure Developed for Welded Aluminum Alloy 6061-T6 (ASME, 2015) | 42 |
| Figure 22. Parker design guide for industrial static seal glands (Parker Hannifin Corporation, 2007) | 43 |
| Figure 23 Streamline profile shape of the sensor float | 45 |
| Figure 24 Sensor float mechanical structure with the HDPE base and shell sectioned..... | 48 |
| Figure 25 Sensor float stable equilibrium position with cable tension | 49 |
| Figure 26 Sensor float stable equilibrium position with no cable tension | 49 |
| Figure 27 Buoyancy verification tank set up | 50 |
| Figure 28 Electromechanical cable assembly | 51 |
| Figure 29 Sinusoidal progressive waveform (Randall, 2010) | 54 |
| Figure 30 Electromechanical cable assembly attached to the sensor float aluminum base | 58 |
| Figure 31 Passive float with only the shell and HCP50 foam sectioned | 59 |
| Figure 32 Passive float - Orthographic projections with dimensions | 60 |
| Figure 33 Sheave design | 61 |
| Figure 34 Passive float and sensor float free-body diagrams | 63 |
| Figure 35 Passive float free-body diagram | 66 |
| Figure 36 Passive float trim ring with sectioned view indicating the sloped surface | 68 |
| Figure 37 Passive float stable equilibrium verification set up | 68 |
| Figure 38 Initial equilibrium position of the passive float, 28° tilt..... | 69 |
| Figure 39 Corrected equilibrium position of the passive float | 69 |
| Figure 40 Passive float moment diagram to calculate weight position | 70 |
| Figure 41 Profiler main body design | 71 |
| Figure 42 Profiler main body - Orthographic projections with dimensions | 72 |

| | |
|--|-----|
| Figure 43 Buoyancy engine hydraulic circuit | 73 |
| Figure 44 Hydraulic circuit during the primary ascent with the high pressure lines and components highlighted red | 75 |
| Figure 45 Hydraulic circuit after completion of the primary and secondary ascent with the intermediate (orange) and high pressure (red) lines and components highlighted | 76 |
| Figure 46 Hydraulic circuit when draining the bladder with the intermediate (orange) and high pressure (red) lines and components highlighted..... | 77 |
| Figure 47 Hydraulic circuit to relieve pressure from the pilot operated check valve | 78 |
| Figure 48 Hydraulic circuit to pump oil from the bladder to the reservoir..... | 79 |
| Figure 49 Buoyancy engine with enclosure sectioned and hydraulic system separate..... | 80 |
| Figure 50 BLWS234D-36V-4000 torque vs. speed plot with 25.5 oz·in, 2000 RPM, and 18VDC lines (solid red) added (Anaheim Automation, 2016) | 85 |
| Figure 51 Pump and motor assembly..... | 86 |
| Figure 52 Bio-MIL-PRF-32073 temperature vs. viscosity plot..... | 88 |
| Figure 53 RH-2 pilot pressure vs. line pressure with the 2 bar line pressure overlay (Hawe Hydraulik, 2017) | 90 |
| Figure 54 Custom accumulator assembly with sleeve sectioned..... | 95 |
| Figure 55 Hydraulic reservoir with the sidewall sectioned..... | 96 |
| Figure 56. Filter application guideline chart (Donaldson Company, Inc., 2017). | 98 |
| Figure 57 Gore Polyvent XL PMF200542 sectioned view (GORE, 2016) | 100 |
| Figure 58 Sensor voltage and level vs. volume plot | 102 |
| Figure 59 Hydraulic system support frame..... | 103 |
| Figure 60 Bladder cage design..... | 105 |
| Figure 61 Assembly model of the hydraulic system..... | 108 |
| Figure 62 Buoyancy engine bench test set up with hydraulic cylinder simulating the bladder..... | 110 |

| | |
|--|-----|
| Figure 63 Ambient temperature vs. power consumption..... | 114 |
| Figure 64 Ambient temperature vs. drainage flow rate | 114 |
| Figure 65 Main body frame design | 119 |
| Figure 66 Main body - Orthographic projections with dimensions | 120 |
| Figure 67 Pump emergency kill switch design | 123 |
| Figure 68 Main body free-body diagram | 125 |
| Figure 69 Main body trim foam shape..... | 127 |
| Figure 70 Profiler hardware/software architecture (Cutler, 2018)..... | 131 |
| Figure 71 Transportation skid design | 133 |
| Figure 72 Skid on the Inquisitor deck..... | 133 |
| Figure 73 Schematic of Field Trial Profiler Mooring Deployment | 135 |
| Figure 74 First field deployment - Sensor float depth vs. time plot for the ascent..... | 138 |
| Figure 75 First field deployment - Sensor float breaching the surface during ascent | 138 |
| Figure 76 First field deployment - Profiler battery voltage vs. time and battery current vs. time plots..... | 140 |
| Figure 77 CTD and ECO FLS sensor water column measurements | 142 |
| Figure 78 Velocimeter measurements..... | 143 |
| Figure 79 Unfiltered Altimeter measurements | 143 |
| Figure 80 Filtered Altimeter measurements | 144 |
| Figure 81 Vector ARHS measurements..... | 144 |
| Figure 82 Second field deployment sensor float depth vs. time plot for the descent | 146 |
| Figure 83 Second Field Trial - Profiler at the bottom of the mooring | 147 |
| Figure 84 Second Field Trial- Profiler descent from the top of the mooring | 148 |
| Figure 85 Empty bladder state (0 l) | 148 |

| | |
|--|-----|
| Figure 86 Full Bladder state (6.5 l) | 148 |
| Figure 87 Third Field Trial - Profiler at the bottom of the mooring | 149 |
| Figure 88 Third Field Trial- Profiler at the top of the mooring. | 150 |
| Figure 89 Third field deployment sensor float depth vs. time plot for the ascent with the 1.2 kg of mass added to the sensor float | 151 |
| Figure 90 Third field deployment - Sensor float depth vs. time plot for the ascent with the 0.84 kg of mass added to the float | 152 |
| Figure 91. Third field deployment - Sensor float electromechanical cable payout during the ascent (0.84 kg of mass added) | 153 |
| Figure 92 Third field deployment - Sensor float breaching the surface (0.84 kg of mass added)..... | 153 |
| Figure 93 Fourth field deployment - Sensor float depth vs. time plot | 155 |
| Figure 94 Fourth field deployment – ROV screenshot of the maximum sensor float payout..... | 156 |
| Figure 95 Fourth field deployment – GoPro picture of the maximum sensor float payout | 156 |
| Figure 96 Fourth field deployment - Bladder not filled with 7.5 litres of oil | 156 |
| Figure 97 Fourth field deployment – Battery voltage and current vs. time | 157 |

1 Introduction

The ocean is a dynamic and complex system, physically, chemically, and biologically. Each of these characteristics are interconnected and influence one another. Ocean observation is critical to understanding these characteristics and interactions. To ensure safe and effective maritime operations, nations provide marine service weather forecasts and warnings which rely on vital data from ocean observations. The data from observations is also crucial for addressing scientific ocean and climate research. The data is used to validate, calibrate, and refine models which then may be used to make informed decisions and policies (National Academies of Sciences, Engineering, and Medicine, 2017). The ability to collect the required accurate and precise data with sufficient temporal and spatial resolution depends on the availability of appropriate technologies to make observations (Siedler, Griffies, Gould, & Church, 2013). Expanding the suite of instruments to measure more properties over a larger scale range, and deploying more instruments in networks to cover larger areas over longer times are also needed to improve observations (Davis, et al., 2019).

In the case of heat and carbon dioxide (CO₂) transportation, understanding the vertical stratification of the water column is critical. Heat and CO₂ are absorbed at the surface where it is then transported throughout the ocean depths along complex pathways (National Academies of Sciences, Engineering, and Medicine, 2017). The vertical structure of the upper ocean is primarily defined by the temperature and salinity which control the water column's density structure (Sprintall & Cronin, 2008). At the surface

exchange can occur rapidly in hours or days. However, as the water column stratifies with depth and time such as the seasonal and permanent pycnocline, significant water exchange and transportation of heat and CO₂ occurs over months, years and decades (National Academies of Sciences, Engineering, and Medicine, 2017).

Ocean change can influence species distribution in the ocean, human settlements, human activity such as fisheries, and have a profound economic influence on people around the world. Concerning North Atlantic cod, water temperature influences growth rates, reproduction, abundance, distribution, and migration (Drinkwater, 2005). The cod fishery is an important component of the Newfoundland and Labrador economy. As another example, oscillations in the equatorial Pacific referred to as the El Niño Southern Oscillation can influence weather patterns around the world. This affects ecosystems, agriculture, freshwater supplies, hurricanes and other severe weather events worldwide (Collins, et al., 2010).

The ocean is vast and remote; its environment is harsh. Equipment is exposed to a corrosive liquid environment, extreme pressures, and the hostility of mother nature. Observation of the ocean progressed as a result of advancements in technical capability and prioritization of understanding the ocean (National Academies of Sciences, Engineering, and Medicine, 2017). Technical development accelerated in the 1960s and early 1970s lead to observational methods that are now regard as routine and greatly enhanced by improvements in navigation. Some of the major drivers of these advancements in equipment and sensor technologies are solid state electronics,

minimizing computer power, battery chemistry, material science, and satellite communication (Siedler, Griffies, Gould, & Church, 2013). Current profiling is one of many great example of ocean observation progression. Subsurface current measurements evolved from single point mechanical based instruments such as the Aanderaa RCM 5 which employed a Savonius rotor-and-vane; to the much more capable and sophisticated Acoustic Current Doppler Profilers (ACDP) which transmit and receives acoustic signals to measure the current at different depths simultaneously (Joseph, 2013). Early work done on single point mooring designs by Berteaux which tend to experienced fatigue failure in rough sea conditions have been further developed by engineers such as Mark Grosenbaugh. Dynamic analysis of single point moorings has shown that the large oscillatory tensions cause fatigue which is primarily due to the mass and dampening of the components attached to the mooring. An increase in fatigue resistance which would allow for longer deployments can be achieved through the development and use of smaller and lighter sensors and components (Grosenbaugh, 1995).

People have been observing the ocean for centuries. It is a challenging, dangerous, and expensive endeavor. Often information is required at many different depths, thus we need to profile it in time and space (longitude, latitude, and depth) to develop a thorough understanding. A sustained in situ global ocean observing system is required. The dominant in situ elements of ocean observing systems include profiling floats, ocean gliders, global drifters, and moorings (National Academies of Sciences, Engineering, and Medicine, 2017). These systems have continued to evolve and grow

to augment the more traditional ship-based observations. A continual effort must be made to find new solutions, and to further enhance current solutions. In particular, the challenge of developing a profiling instrument on a mooring at a fixed location is one such effort to contribute to a global ocean observing network.

2 Overview of Autonomous Profilers

Satellite remote sensing yields high resolution spatial coverage of ocean surface features such as wave height and surface temperature. However, it lacks the ability to observe the subsurface environment. Autonomous profiling platforms have been developed to provide high temporal and vertical resolution data of the water column for the open ocean and continental shelf. These platforms vary in functionality and ability. They can be deployed as either Lagrangian (drifting) or Eulerian (fixed) profilers.

2.1 Lagrangian Profilers

Lagrangian profilers are not bound to a specific geographic location. These profilers move about passively, driven by the ocean currents. As a result, they do not provide data at a fixed location. This provides good spatial resolution but limits the temporal resolution for a location. Two common types of Lagrangian profilers are Argo floats and surface drifters (Thorpe, 2009). Active profilers such as ocean gliders move about under their own power.

2.1.1 Argo Floats

The Argo float shown Figure 1 is a true Lagrangian profiler, its ever-changing location is determined by the ocean current. The typical ten day profile cycle is shown in Figure 2. The float begins its profile at a depth of 2,000 m and during the six hour ascent to the surface it measures and records the water salinity, temperature and depth. Once at the surface it transmits its position and the recorded data via a satellite connection. When the

transmission is complete the float descends to a depth of 1,000 m to avoid strong surface currents and wave action. It holds its depth at 1,000 m for approximately nine days before descending to 2,000 m and starting another cycle (Argo, 2018). To control the profiles, oil is transferred between an internal reservoir and an external bladder to regulate the buoyancy. Moving oil into the bladder causes it to rise, and subsequently moving it back into the reservoir causes it to sink. These battery powered floats can operate in the ocean for up to five years. The Argo network achieves high spatial resolution through the sheer number of deployments. Figure 3 shows that as of May 21, 2018, there were 3833 of these floats distributed across the oceans (Argo, 2018).

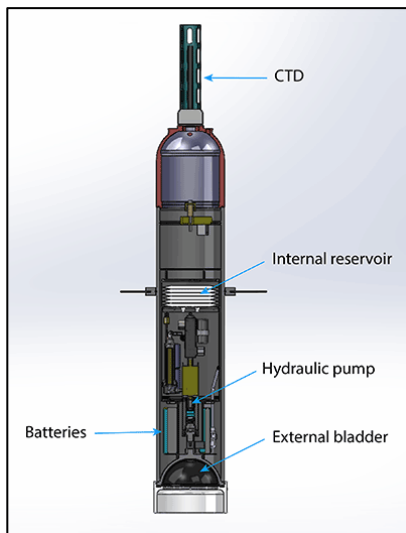


Figure 1 Argo float (Argo, 2018)

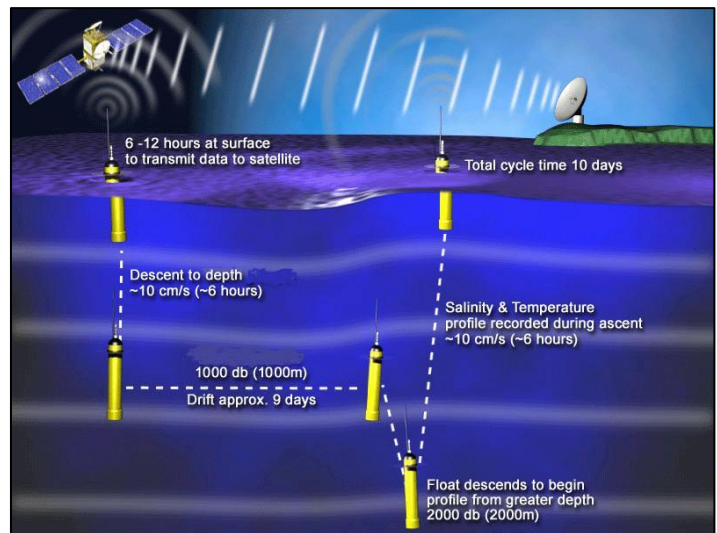


Figure 2 Argo float profile cycle (Argo, 2018)

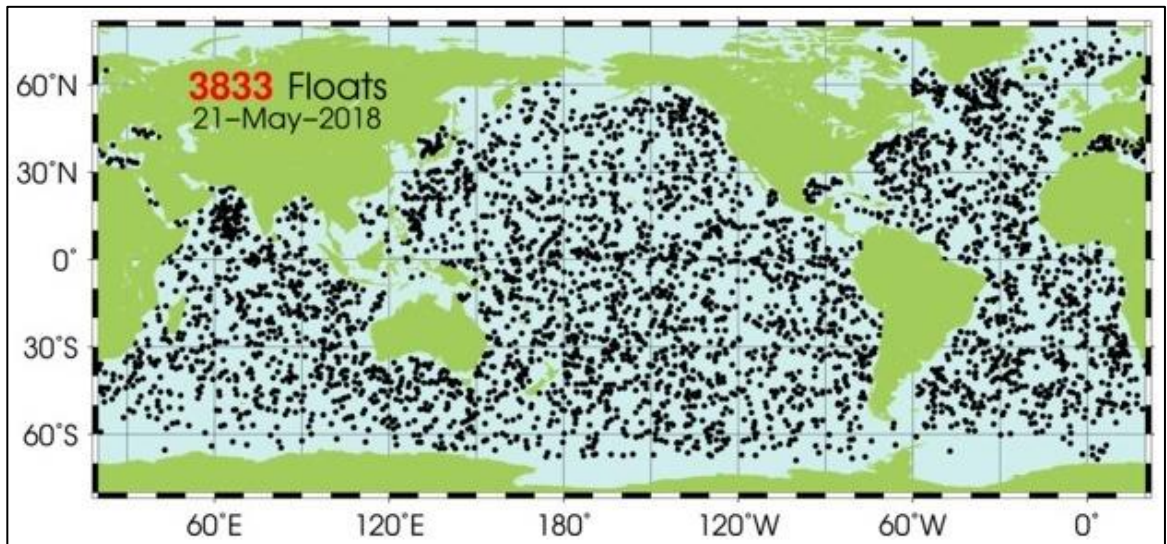


Figure 3 Argo float global distribution for May 2018 (Argo, 2018)

2.1.2 Gliders

Gliders like the Slocum G2 shown in Figure 4 control their profiling locations based on a predetermined mission plan (Gliders, 2018). Like the Argo floats they collect conductivity, temperature, and depth data. Gliders can also be used to collect other physical, chemical, and biological data by equipping them with the appropriate sensors. Gliders control their profile by transferring fluid into and out of an external bladder to regulate their buoyancy. Actively adjusting the glider's center of gravity causes it to tilt up or down. Fixed wings generate forward motion when the nose is tilted down during the descent, and tilted up during the ascent. The result is a sawtooth motion as indicated in Figure 5 (Gliders, 2018). Periodically the glider will surface at which time it uses Global Positioning System (GPS) and an Attitude and Heading Reference System (AHRS) to determine its location and adjust its trajectory if necessary. The trajectory is controlled by

adjusting a rudder. These battery powered vehicles have mission durations of a few weeks, to many months, or up to a year depending upon the types of power supply used.

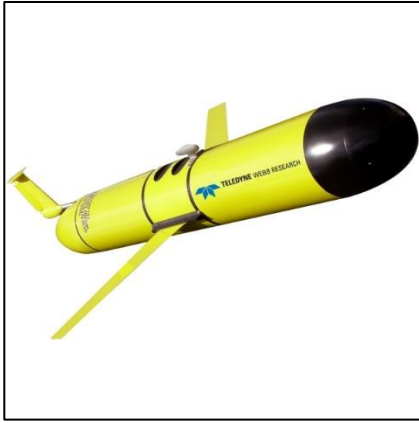


Figure 4 Slocum G2 Glider (Teledyne Webb Research, 2018)

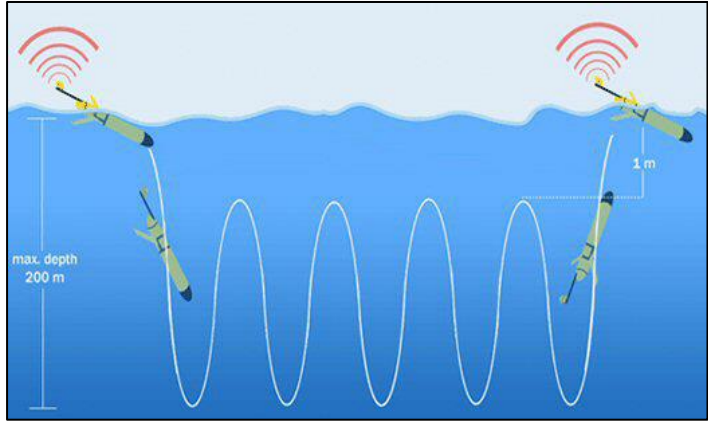


Figure 5 Glider sawtooth profile (Gliders, 2018)

2.2 Eulerian Measurements: Moored Profilers

A moored profiler is bound to a specific geographic location. They provide high temporal and vertical resolution for a specific location. Profiling the water column at a fixed geographic location over time can capture high frequency, seasonal, or episodic ocean processes (Carlson, Ostrovskii, Kebkal, & Gildor, 2013).

The static approach to sampling in the vertical consists of a series of sensors set at fixed intervals on a mooring line. To obtain good vertical resolution, the sensors must be placed close together. Adequately equipping a mooring over hundreds of meters quickly becomes cost prohibitive. Autonomous mobile moored profilers have emerged to provide high resolution temporal and vertical data by repeatedly moving through the water

column at a fixed location. The key advantage of the autonomous profiler is that only one sensor needs to be used to measure a variable. The two most common systems are those with a sensor package that either follows a fixed cable or is attached to a moving cable; wire followers and winched systems.

2.2.1 Winched Systems

Winched systems such as the Miniature Autonomous Moored Profiler (Benard, 2006) and the Vertical Profiling System (InterOcean, 2013) shown in Figure 6, profile the water column by using an electric motor to reel a cable on and off a drum. One of the advantages of the winched profilers is the ability to reach the surface. This provides a complete profile of the water column and enables the capability to transmit data. To reach the surface these systems require a large positive buoyancy to overcome near-surface currents. As a result, they require substantial power when working against the buoyancy (Carlson, Ostrovskii, Kebkal, & Gildor, 2013). These systems have also been challenged by snarling of the cable drum which must be repeatedly spooled and unspooled neatly to operate efficiently.

The Sea Cycler shown in Figure 7 is a unique winched type profiler that utilizes an energy conservation mechanism to resolve the high energy consumption exhibited by other winched profilers (Send, et al., 2013). The profiler consists of a communication float, sensor float, and mechanism float. Drums on the mechanism float share a common shaft and spool both the anchored mooring cable and the sensor float cable. The diameter of the drum for the sensor float cable is larger than that of the mooring cable. The cables

are also spooled onto their respective drums in opposite directions. The opposite spooling of the cables in conjunction with careful design consideration of the drum diameter ratios and the net buoyancy of the floats results in a static balance of the system which requires minimal torque to rotate the drums. When the drum shaft is rotated such that the mooring cable spools onto the drum, the mechanism float will move deeper. At the same time the sensor float cable will unspool and allow the sensor float to rise towards the surface. Likewise, the opposite rotation will unspool the mooring cable and spool the sensor float cable which moves the mechanism float upwards and the sensor float downwards. During these profiling motions, sensors measure and record data that is transmitted via satellites when the communications float reaches the surface.



Figure 6 Vertical Profiling System (InterOcean, 2013)

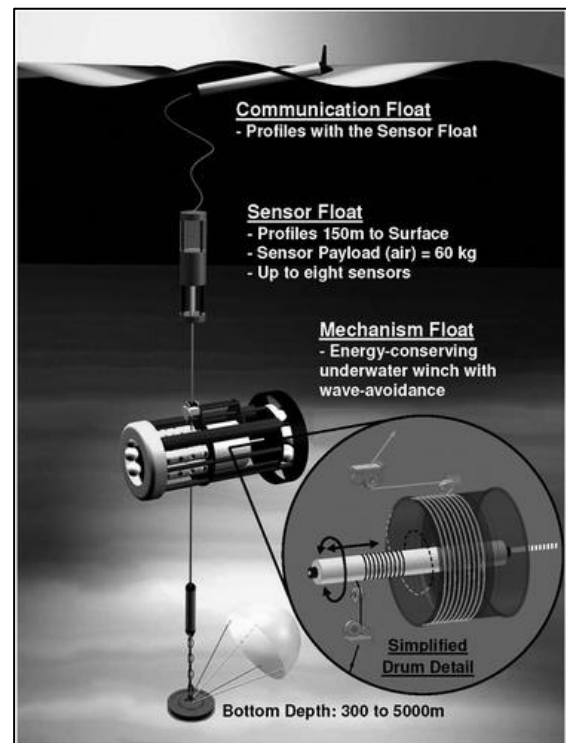


Figure 7 SeaCycler overall design and deployed configuration (Send, et al., 2013)

2.2.2 Wire Followers

Profilers that follow a fixed mooring line require the line to be vertical and taught. The most prominent is the McLane profiler shown in Figure 8 (Morrison III, Billings, & Doherty, 2000). It uses a motorized traction wheel to move up and down the mooring line. It is designed to have neutral buoyancy at a specific depth, which significantly minimizes the power required to drive it. The taught mooring line requirement means that the buoy at the top of the mooring line must sit below the surface to minimize the harmful effects of waves. This limits the profiling range to exclude the very significant region of the water column near the surface. It also restricts the opportunity for telemetry.

In benign conditions, where the mooring buoy can be positioned on the surface, profilers like the Seahorse (Figure 9) can be used. It uses a wave powered ratcheting system requiring minimal power for locomotion (Fowler, Hamilton, Beanlands, & Furlong, 1997). The jacketed wire of the mooring line passes through a one-way clamp in the body of the Seahorse. When engaged, the mechanics of the clamp only allow the wire to pass through it in the upward vertical direction. Thus, when the surface buoy is lifted up by a wave it pulls the cable through the clamp which positions the instrumented body of the Seahorse at a lower point on the mooring cable. Continuous wave action causes the body of the profiler to eventually move to the bottom of the mooring line. At this point the clamp is disengaged and the profiler rises to the surface due to its net positive buoyancy. It is during the smooth ascent that the oceanographic measurements are taken.

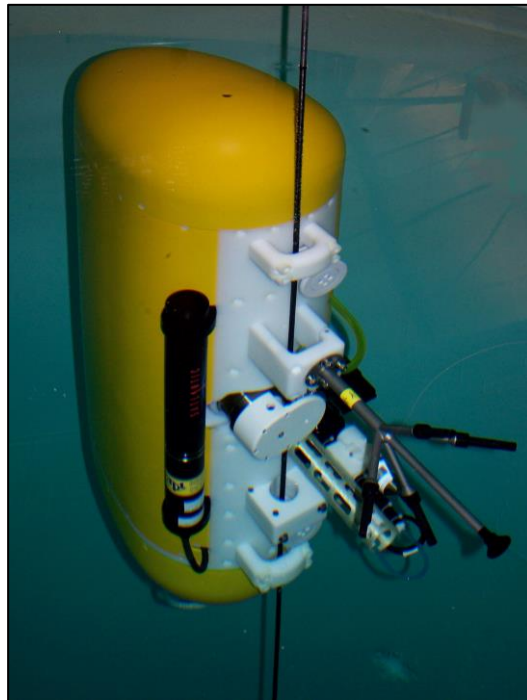


Figure 8 McLane Moored Profiler
(McLane Moored Profiler, 2018)

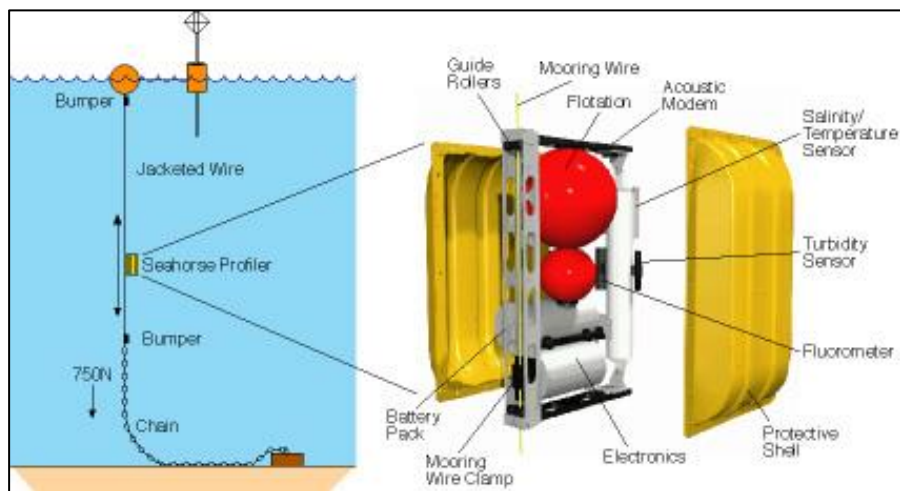


Figure 9 Seahorse profiler mooring and component details (Fowler, Hamilton, Beanlands, & Furlong, 1997)

3 Goals and Objectives of the Development

This thesis focuses on the development of a viable autonomous moored profiler to characterize the oceans water column as an alternative to existing profiling systems. The design, fabrication, and testing of the prototype is detailed in this document.

3.1 Operational Requirements

The profiler should provide long term high resolution oceanographic data of the water column in near real-time, under the typical environmental conditions expected in areas such as the Scotian Shelf. In order to do this, the profiler is designed to meet the following nine operational requirements.

1. Operate to depths of 200 m
2. Operate in horizontal currents up to 1 m/s
3. Operate in waves heights up to 5 meters
4. Operate in temperatures ranging from -5°C to 30°C
5. Profile from the bottom of the water column to the surface
6. Profiles 5 times every 24 hours
7. Profile at a speed of $0.3 \text{ m/s} \pm 0.1 \text{ m/s}$
8. Communicate data while at the surface
9. Operate continuously for 365 days

3.2 Water Column Characteristics

The profiler is designed to measure the following six water column properties. However, the system is capable of adding or exchanging other sensors depending on the end users need, deployment time, and available power supply.

1. Salinity
2. Temperature
3. Depth
4. Dissolved Oxygen
5. Current Velocity
6. Chlorophyll

4 Profiler Design Concept

After a thorough literature review of the various ocean observation systems as described in the previous section, the concept development process began. The aim was to design a moored profiler that could breach the surface of the ocean while utilizing the protection of a subsea mooring. Several design ideas were proposed and assessed before a final concept, which is detailed in this document, was chosen to be developed and prototyped. The moored profiler design is considered a hybrid between a wire follower and a “drumless” winched system. A Computer Aided Design (CAD) model of the prototype is detailed in Figure 10.

This design allows the sensor float to measure and record oceanographic data via a suite of integrated sensors as the profiler moves upward through the water column from the ocean floor to the surface. A buoyancy engine located in the main body is the means of propulsion. The buoyancy engine changes the buoyancy of the main body of the profiler by inflating and deflating an external bladder with an incompressible fluid from an internal reservoir. Based on Archimedes principle, inflating the external bladder increases the volume of water displaced by the system while maintain the same mass; this results in the system becoming more positively buoyant (Munson, Young, & Okiishi, 1994). The net buoyancy of the system is trimmed such that it is negatively buoyant (sinks) when the bladder is deflated and positively buoyant (floats) when the bladder is inflated. While at the surface the profiler can transmit and receives data to and from a remote site. Once the communication is completed the profiler returns to the bottom of the mooring to

hibernate. During the hibernation state energy is conserved where possible until the next scheduled profile. While at the bottom the system is protected from human interference, and the harsher environmental conditions at the surface such as waves. The environmental conditions that promote biofouling also decrease with depth. (Durr & Thomason, 2010).

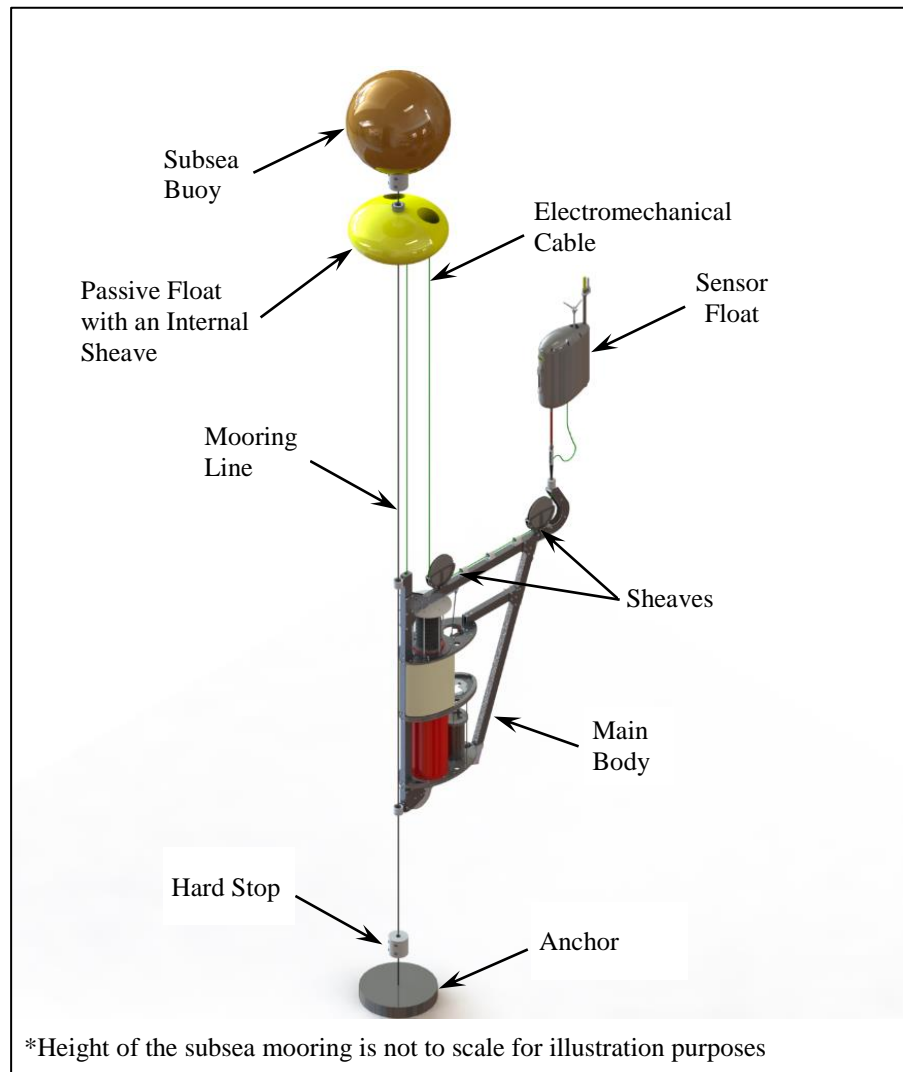


Figure 10 Profiler prototype CAD model

The complete system is made up of five major components.

1. Sensor Float
2. Passive Float
3. Main Body
4. Electromechanical Cable
5. Subsea Mooring (subsea buoy, mooring line, and anchor)

The sensor float has a fixed positive buoyancy and houses the necessary sensors that are required to measure the water column characteristics. It also contains a control system that records and stores the data until it can be transmitted to shore via the attached antennas and a satellite constellation.

The passive float also has a fixed positive buoyancy. Its main purpose is to keep the sensor float retracted until the profiler is near the surface. Details of how this simple component influences the movement of the sensor float is described later in greater detail

The main body has a variable negative buoyancy. It secures the power supply and the buoyancy engine for the profiler. The variable buoyancy of the main body produced by the buoyancy engine causes the complete profiler system to either ascend or descend in the water column.

The electromechanical cable links the sensor float, passive float, and main body together. One end of the electromechanical cable terminates at a connection on the sensor float while the other end terminates at a connection on the main body. Following the

electromechanical cable from the bottom of the sensor float, it first passes through two sheaves on the main body, then through a sheave within the passive float before ending at bottom of the main body.

The subsea mooring cable constrains the passive float and main body to the geographic location of the mooring. The cable passes through a guide tube located at the center of the passive float and then through two eyelets at the end of the frame of main body. The anchor connected at the bottom of the cable coupled with the subsea buoy connected at the top produce a taught mooring line.

4.1 Mode of Ascent and Descent

Five significant points along the profiler's ascent and descent through the water column are illustrated in Figure 11. The system has two modes of dynamic behaviour during its operation which are dependent on its position along the subsea mooring line, and the buoyancy of the main body, passive float, and sensor float.

- The positive buoyancy of the passive float must be more than twice the positive buoyancy of the sensor float.
- The maximum negative buoyancy of the main body must be greater than the sum of the positive buoyancy of the passive and sensor floats.
- The minimum negative buoyancy of the main body must be less than three times the positive buoyancy of the sensor float.

The first dynamic mode of behaviour occurs during the majority of the profile when the passive float is not in contact with the subsea buoy (Position A and B in Figure 11). The second dynamic mode occurs when the passive float is in contact with the subsea buoy (Positions C to E in Figure 11).

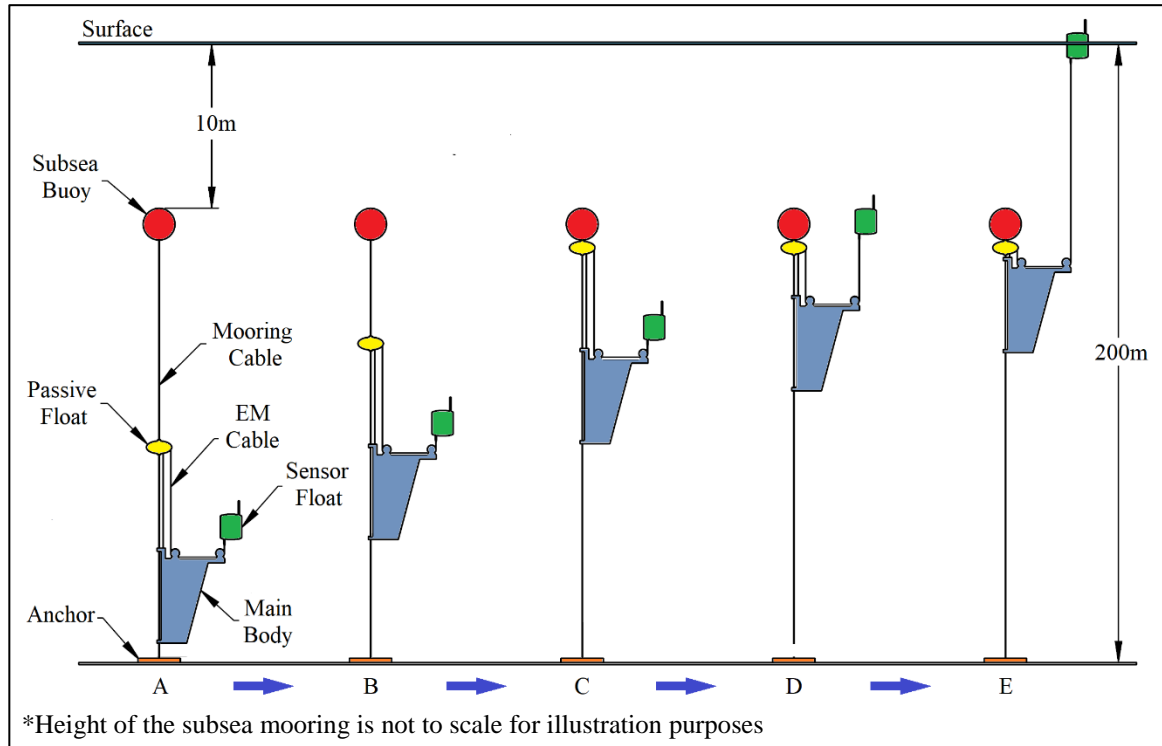


Figure 11 Significant points during the profiler ascent and descent

4.1.1 Position A - Hibernation

In its hibernation position the profiler is located at the bottom of the subsea mooring. To achieve this position, the buoyancy of the main body is adjusted to its maximum negative buoyancy which is greater than the combined positive buoyancy of the passive and sensor floats. Since the passive float has more than twice the buoyancy of the sensor float, it

generates more tension on the electromechanical cable than the sensor float can exert.

Therefore, the sensor float will be retracted against the main body, and the passive float is positioned at its maximum distance from the main body. The full retraction of the sensor float is critical to ensure that it will not become entangled around the mooring cable.

4.1.2 Position B – Primary Ascent

To initiate an ascent, the negative buoyancy of the main body is adjusted to its minimum negative buoyancy. This is less than the combined positive buoyancy of the passive float and the sensor float, and less than three times the positive buoyancy of the sensor float; thus the profiler rises. Again, since the passive float has more than twice the buoyancy of the sensor float it generates more tension on the electromechanical cable than the sensor float can exert. Therefore, the sensor float remains retracted against the main body, and the passive float maintains its position at a maximum distance from the main body during the primary ascent.

4.1.3 Position C- Contact with the Upper Stop

A hard stop located on the mooring line immediately below the subsea buoy prevents the passive float from moving further up the mooring line. The mode in which the sensor float continues to ascend towards the surface is initiated at this point. The passive float is now static and acts as an anchored component of the system.

The arrangement of the sheaves on the main body of the profiler and the passive float provides a 3:1 mechanical advantage. A simplified schematic of this compound pulley

arrangement and its corresponding free body diagrams for static conditions are shown in Figure 12. The upper pulley represents the sheave connected to the passive float, and the lower pulley represents the sheaves attached to the main body. The arrow end of the cable in the leftmost schematic is the point where the sensor float would be attached. To maintain static equilibrium, the tension in the cable (T_E) must be one third of the negative buoyancy of the main body (B_{MB}). The positive buoyancy of the sensor float is greater than one third of the negative buoyancy of the main body. Therefore, it can lift the main body. The anchoring force (F_A) for the system requires twice the static equilibrium cable tension. Again, since the buoyancy of the passive float is more than twice that of the sensor float it is able to maintain its anchor function.

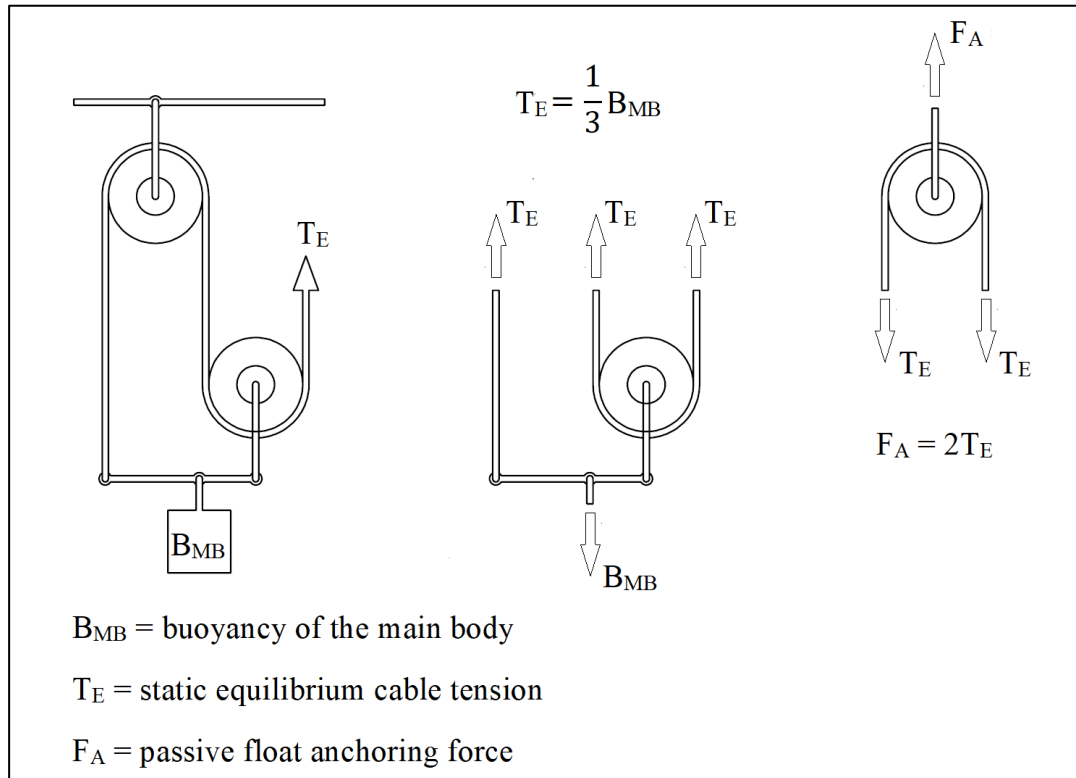


Figure 12 Profiler 3:1 compound pulley system and its free-body diagrams

4.1.4 Position D – Secondary Ascent

During the secondary ascent, the sensor float is released from the main body. It moves upwards towards the surface and away from the main body. The cable to be payed out is stored between the pulleys on the passive float and the main body. While ascending the sensor float lifts the main body towards the anchored passive float. The vertical displacement of the sensor float is three time the vertical displacement of the main body due to the 3:1 mechanical advantage of the compound pulley system. Referring to Figure 13, if the length of the electromechanical cable payout required for the sensor float to reach the surface is Y , then the secondary ascent would begin when the sensor float is $1.5Y$ below the surface. To reach the surface during the secondary ascent the sensor float moves $1.5Y$, and simultaneously the main body moves $0.5Y$. The basic behaviour of the secondary ascent satisfies that the work done by the sensor float is equal to or greater than the work done on the main body. Work is the product of the force on a body and its displacement in the direction of the force (Hibbeler, 2007).

Releasing the sensor float from the main body while only at the top of the subsea mooring reduces the possibility of entanglement in the mooring line. Ocean currents can create drag on the sensor float and cause a horizontal displacement. In the unlikely event the displacement is directed towards the mooring line, there could be an entanglement if they cross over. The amount of displacement increases with the length of electromechanical cable that must be payed out. Therefore, the sensor float should not be released from the main body until it is near the subsea buoy. The critical point during the release of the

sensor float is when it is at the same depth as the subsea buoy as shown in Figure 13.

Above this point, the sensor float is in the space above the mooring, and the cables cannot cross over. To mitigate this issue, the release point of the sensor float on the main body must be far enough from the mooring line to ensure that the horizontal displacement developed by a 1 m/s current is not sufficient to allow contact between the sensor float and the mooring.

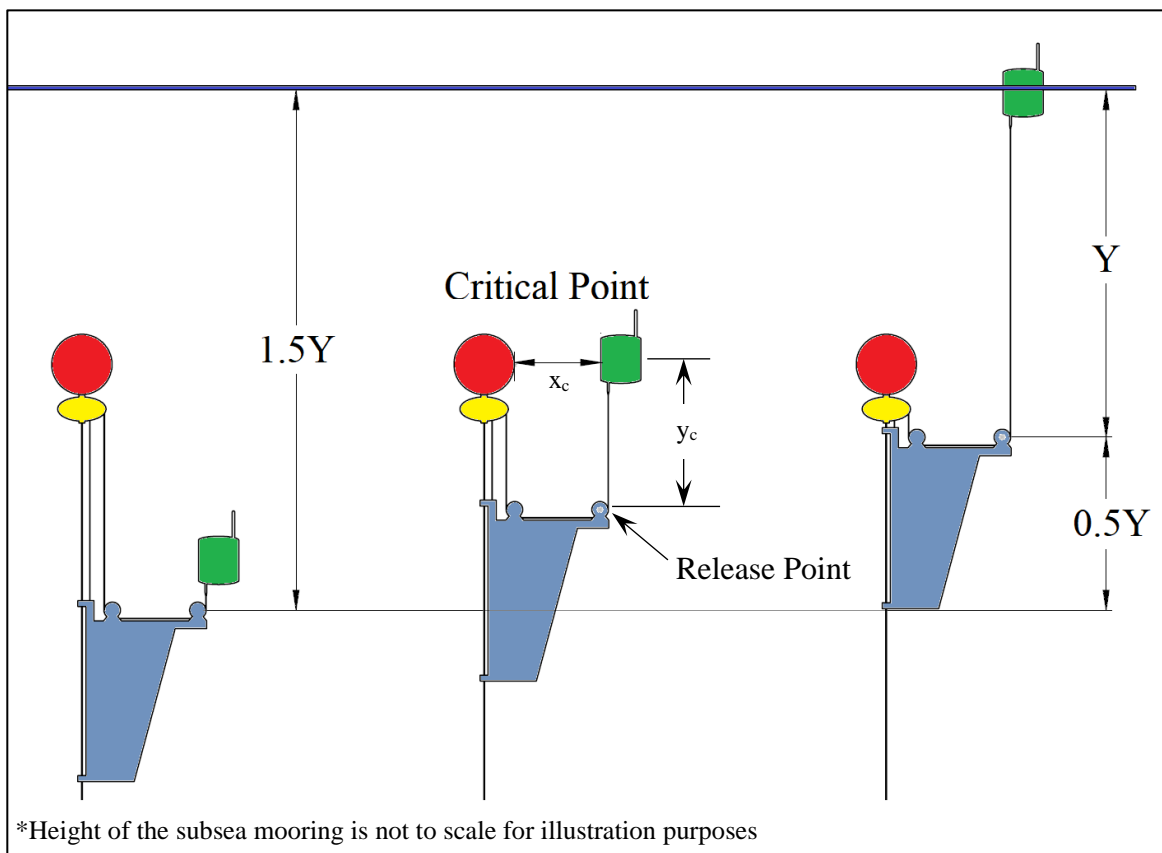


Figure 13. Electromechanical cable payout during the secondary ascent

4.1.5 Position E – Surface Breach

A surface breach occurs when the sensor float reaches the surface and exposes the antennae to the atmosphere. At this point, the profiler will be able to communicate with a remote site. The amount that the antennae breaches the surface depends on the excess buoyancy of the sensor float. Once the profiler has completed sending and receiving data, the buoyancy of the main body is adjusted to its maximum negative buoyancy. Since this is greater than the sum of the positive buoyancy of the passive float and sensor float, the profiler will descend to the bottom of the mooring in essentially a rewind of the ascent order, back to position A where it hibernates waiting to complete the next profile.

5 Profiler Design

This chapter details the design of the system and components that make up the profiler. Due to the dependent relationship between the components, especially their buoyancy, they were designed in series. The starting point was the sensor float, followed by the electromechanical cable, then the passive float, and finally the main body. As part of the design cycle each component went through several iterations before arriving at the final designs detailed in the following sections.

Throughout the design, careful consideration was given to the material selection for components given the harsh operating environment of seawater. While plastics such as Ultra High Molecular Weight Polyethylene (UHMW) are useful and have good compatibility in seawater, they lack the strength required for the structural members or pressure vessels. As detailed further in the designs, aluminum was the material of choice for most of the strength components, and 316 stainless steel for the fasteners. The combination of stainless steel and aluminum is not ideal due to the potential for galvanic corrosion between the dissimilar metals. However, the alternative of using all stainless, titanium, and/or nickel alloys was cost prohibitive, especially for a prototype. To mitigate the potential for failure of the components or system due to galvanic corrosion, several solutions were implemented in the design. The first was to anodize all of the aluminum components. The second was to include attachment points on the aluminum components for sacrificial zinc anodes; especially near areas where stainless steel fasteners are in contact with the aluminum. The third was to separate physical contact between the

stainless steel fasteners and the aluminum component with non-metallic washers and bushings.

5.1 Sensor Float Design

The final sensor float design is shown in Figures 14 and 15. It was designed to house the sensors, a controller and data logger, and the telemetry system. To perform properly under the operating conditions specified, it was designed to provide low drag and positive buoyancy to ensure it can reach the surface while mitigating the risk of entanglement in the mooring line. It provides an upright orientation of the antenna for telemetry while at the surface. A strong structure with a mechanical connection point on the bottom allows the addition of a strain relief to dampen the impact energy from wave action when the profiler is near the surface.

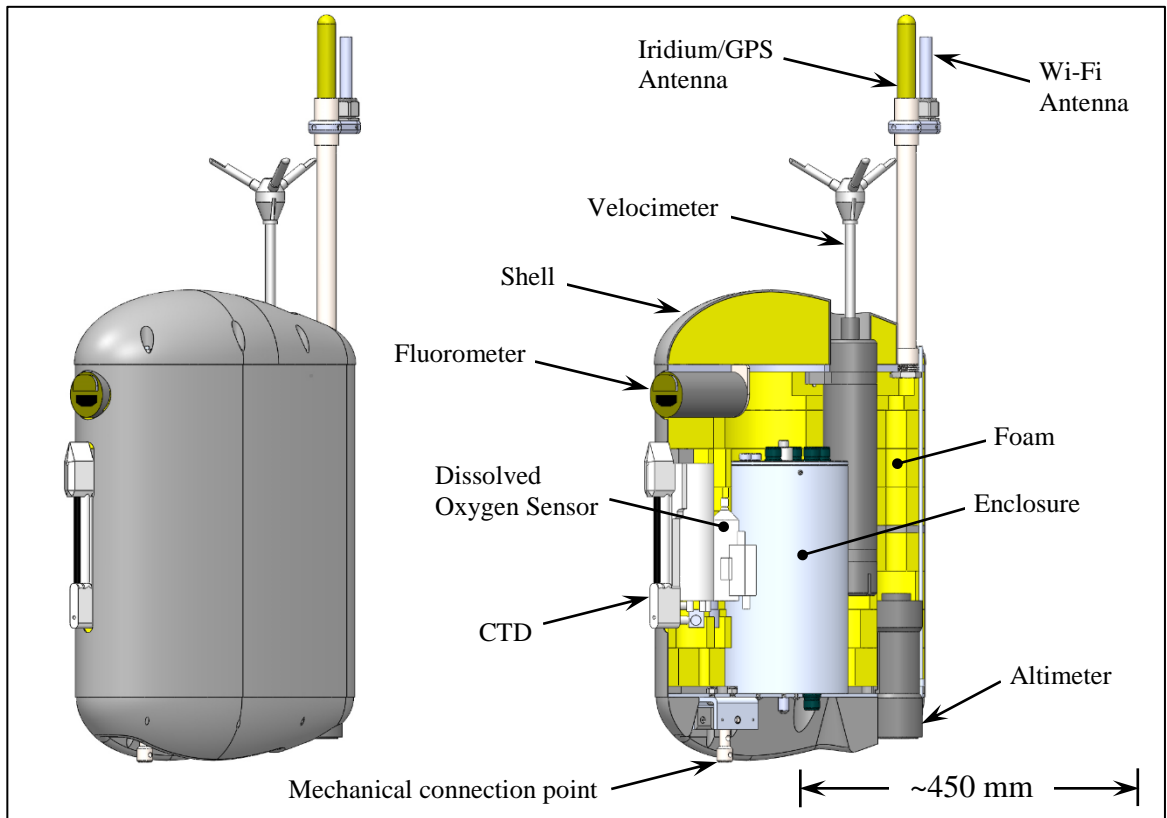


Figure 14. Final sensor float design: full and sectioned view

The suite of sensors that was chosen for the sensor float are listed in Table 1. The sensors were selected based on performance specifications such as power consumption, accuracy, range, resolution, and size. All of the sensors are rated for a depth of 200 m or greater.

The exception to the depth rating are the Altitude Heading Reference System (AHRS) and Global Positioning System (GPS) receiver which are housed within the enclosure and not exposed to the ambient water pressure.

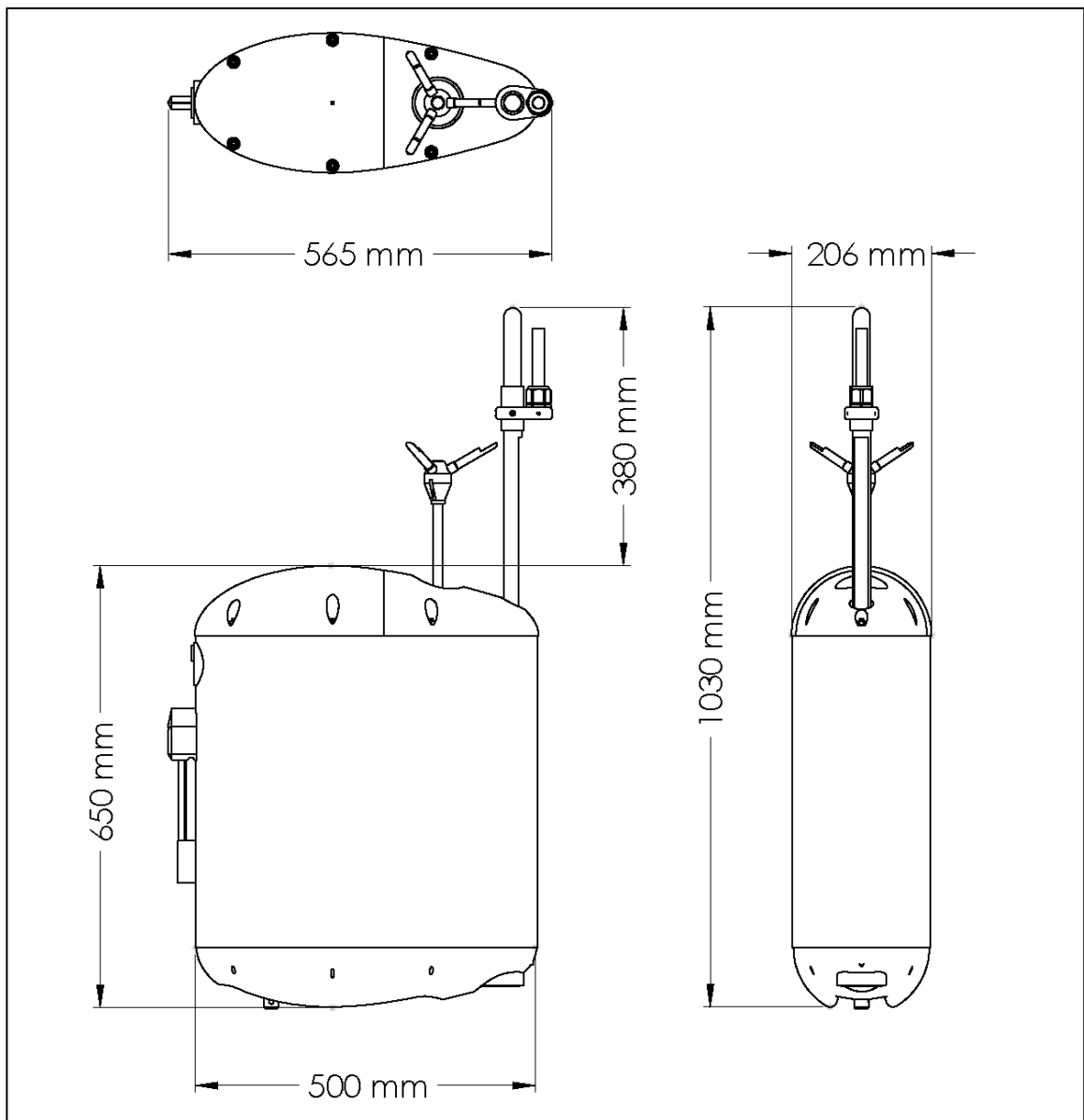


Figure 15 Sensor float - Orthographic projections with dimensions

Table 1 Sensor float suit of sensors

| Manufacture | Model # | Parameter(s) | Range | Accuracy | Power |
|------------------|------------|---------------------------|-----------------------|-------------------------------|--------|
| Seabird | GPCTD | Conductivity | 0-9 S/m | ± 0.0003 S/m | 190 mW |
| | | Temperature | -5-42 °C | ± 0.0002 °C | |
| | | Depth | 0-300 m | $\pm 0.1\%$ FSR | |
| Seabird | 43F | Dissolved Oxygen | 120% of saturation | $\pm 2\%$ of saturation | 45 mW |
| Seabird | ECO FLS | Chlorophyll-a Florescence | 0-125 $\mu\text{g/L}$ | 0.02 $\mu\text{g/L}$ | 0.6 mW |
| Nortek | Vector | Velocity | ± 0.1 -7 m/s | $\pm 0.5\%$ of measured value | 1.2 W |
| LORD MicroStrain | 3DM-GX4-24 | Attitude and Heading | 360° about all axes | $\pm 2.0^\circ$ | 800 mW |
| Tritech | LRPA200 | Altitude | 2-200 m | $\pm 0.025\%$ FSR | 2.2 W |
| Sparkfun | GPS-10920 | Latitude & Longitude | N/A | 2.5 m | 67 mW |

The components listed in Table 2 make up the sensor float data logger and controller which are housed in the subsea enclosure.

Table 2 Sensor float data logging and controller components

| Manufacturer | Model # | Description | Power |
|--------------|-----------------|-----------------------|---------------|
| BeagleBone | Black | Single Board Computer | < 1 W |
| PJRC | Teensy 3.2 | Microcontroller | <150 mW |
| CUI | PBY30-Q48-S12-U | 24V DC-DC Converter | 88% efficient |

The telemetry systems components are listed in Table 3. The Iridium/GPS and Wi-Fi antenna are affixed to the top of the sensor float while their respective electronic modules reside in the subsea enclosure.

Table 3 Sensor float telemetry components

| Manufacturer | Model # | Description | Power |
|--------------|----------------------------|--------------------------------------|--------------|
| Trident | Dual Element GPS & Iridium | Active GPS & Passive Iridium Antenna | < 50 mW |
| Iridium | A3LA-RS | Satellite Modem | 1.75 W (max) |
| Digi | XTP9B-PKI-R | RF Modem | < 3W |
| Ubiquiti | BM5HP | Wi-Fi Transceiver | 6 W (max) |
| Teledyne | CCR-33S | Coaxial Switch | 1.7 W |
| AOSL | N/A | Wi-Fi Antenna | N/A |

The manufacturer specification data sheets for all the components listed in the three tables above are included in Appendix A, pages 173-203.

5.1.1 The Effect of Current on the Position of the Sensor Float

Under ideal environmental conditions with no current acting on the system, the sensor float would rise to the surface following a straight vertical trajectory during the secondary ascent (Figure 11). However, when a horizontal current is imposed on the sensor float and the electromechanical cable, the effect is a horizontal displacement of the sensor float.

The profiler is designed to turn into the current such that the sensor float moves away from the mooring line when displaced by a current. However, if opposing currents acted

on the main body of the profiler and the sensor float, the consequence is a risk of the sensor float becoming entangled with the mooring line. This could impede its operation. To prevent entanglement, the horizontal displacement of the sensor float needs to be minimized. The release point of the sensor float must be positioned such that the horizontal displacement does not subject it to the entanglement conditions described in section 4.1.4.

At any instant in time during the secondary ascent, the sensor float behaves as its own simple subsea mooring with the anchor point being the release point on the main body. Assuming the electromechanical cable is short and lightweight, Equations 5.1, 5.2, and 5.3 can be used to determine the length of the cable (s), the horizontal (x), and vertical (y) distance from the release point, respectively when exposed to a current (Figure 16) (Berteaux, 1976).

$$s = \frac{T_0}{R} (\cot \theta_1 - \cot \theta_2) \quad (5.1)$$

$$x = \frac{T_0}{R} (\csc \theta_2 - \csc \theta_1) \quad (5.2)$$

$$y = \frac{T_0}{R} \left\{ \log_e \left(\tan \frac{\theta_2}{2} \right) - \log_e \left(\tan \frac{\theta_1}{2} \right) \right\} \quad (5.3)$$

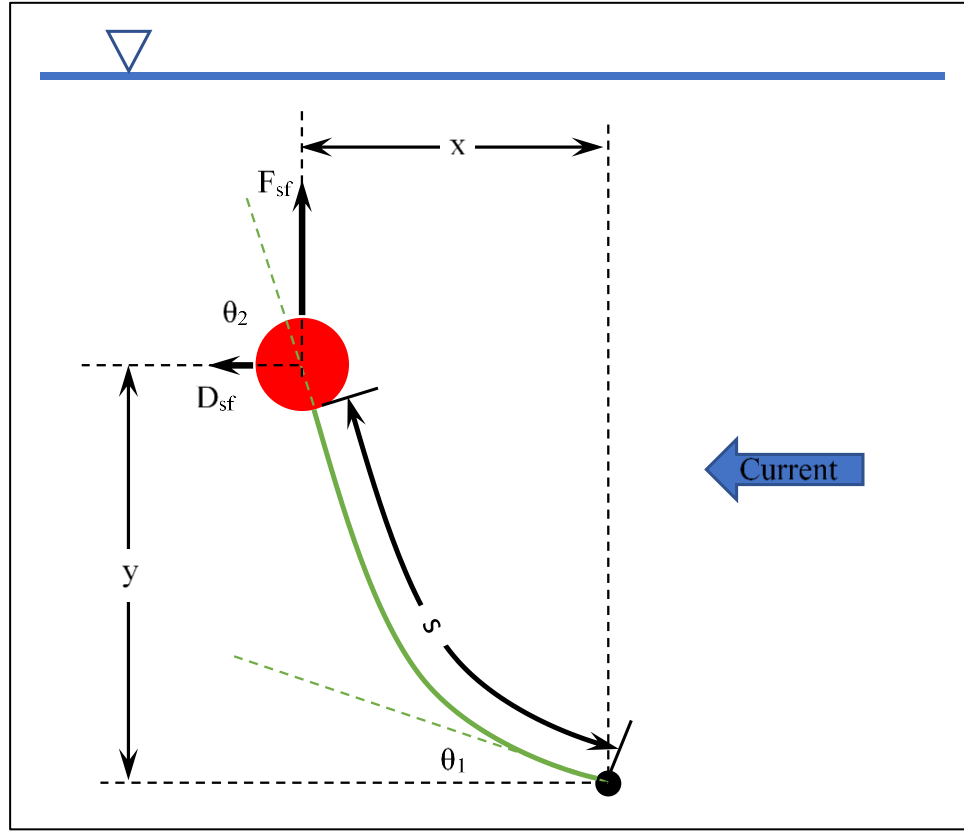


Figure 16 Simple subsea mooring with an anchor point

The tension (T_0) is the resultant force of the vertical buoyant force (F_{sf}), and the horizontal drag force (D_{sf}) on the sensor float. The vertical buoyant force is determined from Equation 5.4 which is the difference between the buoyant force of the sensor float (B_{sf}) and the weight of the sensor float (W_{sf}).

$$F_{sf} = B_{sf} - W_{sf} \quad (5.4)$$

The buoyant force of any submerged body is equivalent to the weight of the water it displaces (Munson, Young, & Okiishi, 1994). Equation 5.5 determines the buoyant force

of the sensor float (B_{sf}) from the density of the water (ρ_w) and the volume of water it displaces (V_{sf}).

$$B_{sf} = \rho_w V_{sf} \quad (5.5)$$

The drag force on the sensor float (D_{sf}) is dependent on the drag coefficient of the sensor float (C_{Dsf}), the density of the water, the velocity of the water (v), and the projected areas of the sensor float perpendicular to the water velocity (A_{sf}) (Munson, Young, & Okiishi, 1994). Equation 5.6 gives the drag force on the sensor float.

$$D_{sf} = \frac{1}{2} C_{Dsf} \rho_w v^2 A_{sf} \quad (5.6)$$

The drag force per unit length of the electromechanical cable (R) is calculated from Equation 5.7. It is dependent on the drag coefficient of the electromechanical cable (C_{Dec}), the density of the water, the velocity of the water, and the diameter of the electromechanical cable (θ_{ec}).

$$R = \frac{1}{2} C_{Dec} \rho_w v^2 \theta_{ec} \quad (5.7)$$

The drag coefficient (C_D) of an object is dependent on the Reynolds Number (Re). The Reynolds Number is dependent the density of water, the velocity of the water, the dynamic viscosity of the water (μ), and the characteristic linear dimension of the object (D). The characteristic linear dimension of a sphere and cylinder (cable) are its diameters, θ_{sf} and θ_{ec} . Equation 5.8 is used to calculate the Reynolds number (Munson, Young, & Okiishi, 1994).

$$Re = \frac{\rho_w v D}{\mu} \quad (5.8)$$

θ_1 is the angle between the horizontal and the electromechanical cable at the release point of the main body, which is determined by rearranging Equation 5.3 to give Equation 5.9.

$$\theta_1 = 2 \tan^{-1} \frac{\tan \frac{\theta_2}{2}}{e^{\frac{yR}{T_0}}} \quad (5.9)$$

The angle between the horizontal and the electromechanical cable at the buoy is θ_2 , determined from the basic trigonometry of the vertical buoyant force and the horizontal drag force acting on the sensor float, Equation 5.10.

$$\theta_2 = \tan^{-1} \frac{F_{sf}}{D_{sf}} \quad (5.10)$$

Based on the equations presented, the horizontal displacement of the sensor float and subsequently the length of electromechanical cable required to reach the surface can be minimized by increasing the positive buoyancy of the sensor float and reducing the drag on the sensor float. Reducing the drag on the electromechanical cable also helps but at a lesser magnitude.

5.1.2 Sensor Float Shape and Size

A systematic and iterative approach was used to determine the appropriate size and shape of the sensor float. The first step determined a rough estimate of the buoyancy and drag required by the sensor float. This estimate is based on restricting the location of the sensor

float release point on the main body to a maximum of 1.5 meters from the mooring line. This is to keep the size of the main body within reasonable limits. This means that the horizontal displacement of the sensor float at the critical point (the same height as the subsea buoy) cannot exceed 1.5 m. The horizontal displacement from the release point at the critical point (x_c) is solved using Equation 5.2. It is dependent on the vertical displacement from the release point to the critical point (y_c) (Figure 13). Equation 5.11 is used to approximate y_c . It depends on the length of cable required to reach the surface (s_s) which is calculated from Equation 5.1. If the amount of cable required for the sensor float to reach the surface is s_s ; then the sensor float is half the length of s_s below the subsea buoy when the profiler is about to start the secondary ascent. This is because the amount of electromechanical cable required to reach the surface is stored equally between the pulleys in the passive float and on the main body. Due to the 3:1 ratio of the pulleys, the y_c value indicated in Figure 13 can be approximated as two thirds the distance from the passive float to the subsea buoy at the start of the secondary ascent.

$$y_c \cong \frac{2}{3} \left(\frac{1}{2} s_s \right) \quad (5.11)$$

The initial estimate of the buoyancy and drag of the sensor float assumed the following:

- The sensor float is spherical and its weight in sea water (W_{sf}), including the instrumentation and enclosure is 200 N;
- The electromechanical cable diameter (θ_{ec}) is 0.01 m and is cylindrical;

- The vertical distance of the sensor float to the release point when at the surface (y_s) is 10 m.

This information and the other variables (such as the 1 m/s current) required to solve for the horizontal displacement from the release point at the critical point (x_c) are listed in

Table 4. An Excel spreadsheet was used to solve for x_c while incrementally increasing the diameter of the sensor float by 0.005 m. When the sensor float reached a diameter of 0.385 m it produced a calculated x_c value of 1.5 m. The corresponding buoyancy and drag on the sensor float were 101 N and 29.9 N respectively. This was considered a reasonable size for the sensor float. Thus it was used as a baseline for the size and shape. The spherical sensor float trajectory plot in Figure 17 indicates the trajectory of the 0.385 m diameter sensor float (green line) from the release point (black line) to when it reaches the surface (blue line). The trajectory does not intersect the mooring cable (red line) therefore reducing the risk of entanglement. Reducing the drag on the sensor float can further reduce the risk of entanglement by decreasing the horizontal displacement. Adopting a streamline body for the sensor float can reduce the drag coefficient to 0.1 or less. A streamline sensor float with a conservative drag coefficient estimate of 0.1 and the same characteristics and operating conditions as the spherical sensor float has an 80% reduction of the drag of force. The 6 N drag force of the streamline float results in a 0.53 m horizontal displacement at the critical point. The equivalent streamlined sensor float trajectory shown in Figure 18 provides excellent risk mitigation of entanglement. Limiting the critical distance x_c to 1.5 m under these parameters will permit the subsea

buoy to be submerged to a depth up to 17 m without risking entanglement. This means the profiler can accommodate a discrepancy of 7 meters in depth beyond the expected subsea buoy depth of 10 m. This depth discrepancy is expected due to waves, tides, tolerances in assembling of the subsea mooring, and bathymetry uncertainty at deployment sites.

Table 4 Sensor float variables and results

| | |
|---|------------------------|
| Depth of the subsea buoy, y_s | 10 m |
| Sensor float diameter, θ_{sf} | 0.385 m |
| Sensor Float weight, W_{sf} | 200 N |
| Sensor float drag coefficient, C_{Dsf} | 0.5 |
| Electromechanical cable diameter, θ_{ec} | 0.01 m |
| Electromechanical cable drag coefficient, C_{Dec} | 1 |
| Density of water, ρ_w | 1047 kg/m ³ |
| Dynamic viscosity of water, μ | 0.00141 Pa·s |
| Water velocity, v | 1 m/s |
| Gravity, g | 9.81 m/s ² |
| Re for the sensor float | 2.6×10^5 |
| Re for the electromechanical cable | 7.3×10^3 |
| Buoyant force of the sensor float, B_{sf} | 301.0 N |
| Vertical force on the sensor float, F_{sf} | 101.0 N |
| Drag force on the sensor float, D_{sf} | 29.3 |
| Tension in the electromechanical cable, T_0 | 105.2 N |
| Drag force per unit length of electromechanical cable, R | 5.1 N/m |
| Angle between the horizontal and cable at the subsea buoy, θ_2 | 73.8° |
| Angle between the horizontal and cable at the anchor point, θ_1 | 49.5° |
| Amount of electromechanical cable required to reach the surface, s_s | 11.6 m |
| Vertical displacement from the release point to the critical point, y_c | 3.9 m |
| Critical horizontal displacement (x_c) | 1.5 m |

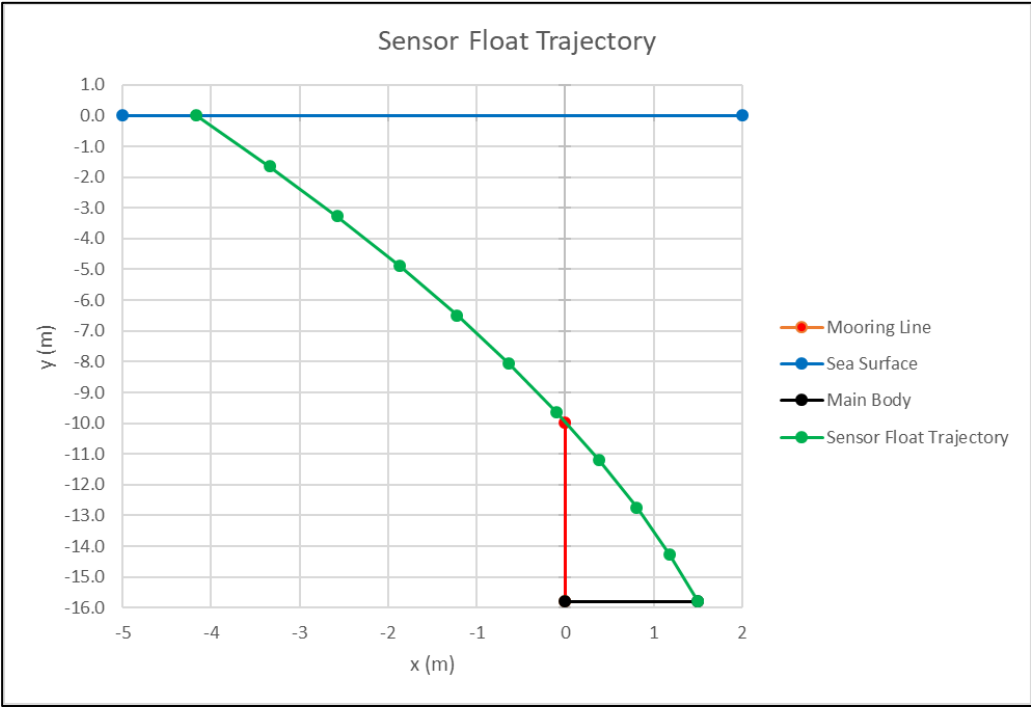


Figure 17 Spherical sensor float trajectory

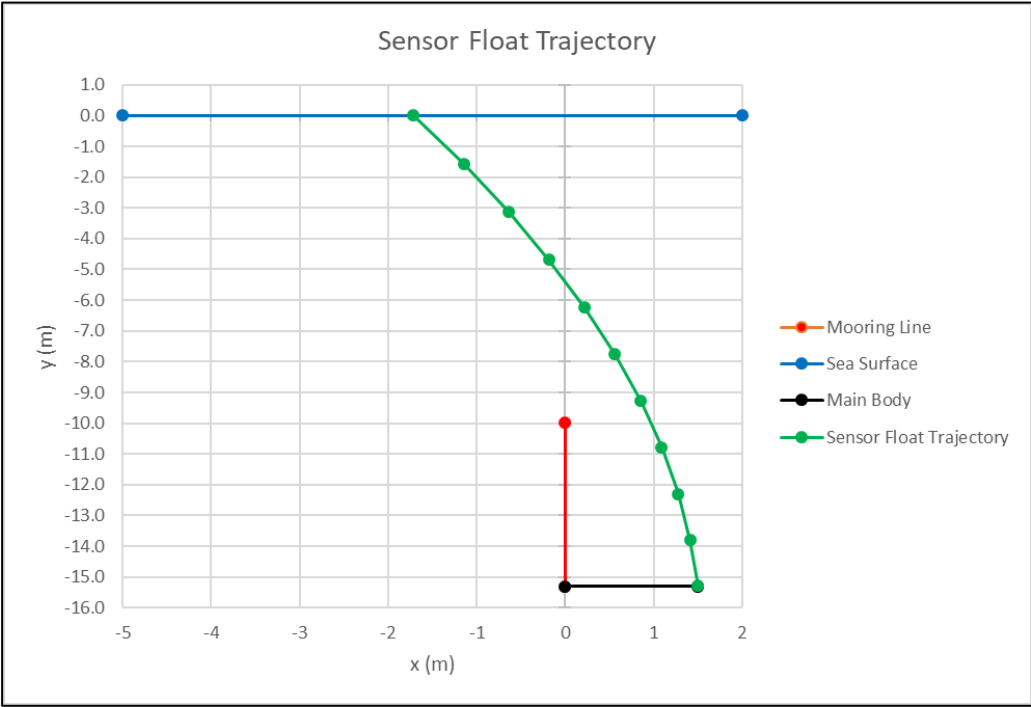


Figure 18. Streamline sensor float trajectory

Based on these calculations, the design goal for the sensor float was to ensure it provided a minimum of 100 N of buoyancy and a drag of less than 30 N to ensure it could reach the surface without interfering with the mooring line. To minimize the drag, a sensor float with a streamline body was designed and the volume of the float was optimized to reduce its projected area. To optimize the volume of the sensor float, the iterative design process entailed modeling the sensors and enclosure, then arranging them closely together in a free space such that a streamlined shape could enclose the components. Once the shape was defined, it was determined how much foam would be required to provide a net buoyancy of 100N. Detailed CAD drawing of the parts required to fabricate the sensor float are provided in Appendix B, pages 271-305.

5.1.2.1 Sensor Float Enclosure Design

To minimize its size, a custom cylindrical subsea enclosure was designed and fabricated for the sensor float (Figure 19). The detailed CAD drawings are available in Appendix B, pages 302-305. The enclosure has a blind body with a removable end cap held in place by three radial set screws.

The enclosure requires an inside diameter of 162 mm and an internal length of 277 mm (with the endcap on) to house the components as arranged in Figure 19. The subsea enclosure is fabricated from 6061-T6 Aluminum and is designed to withstand a minimum allowable external pressure of 30 bar (~300 m depth).

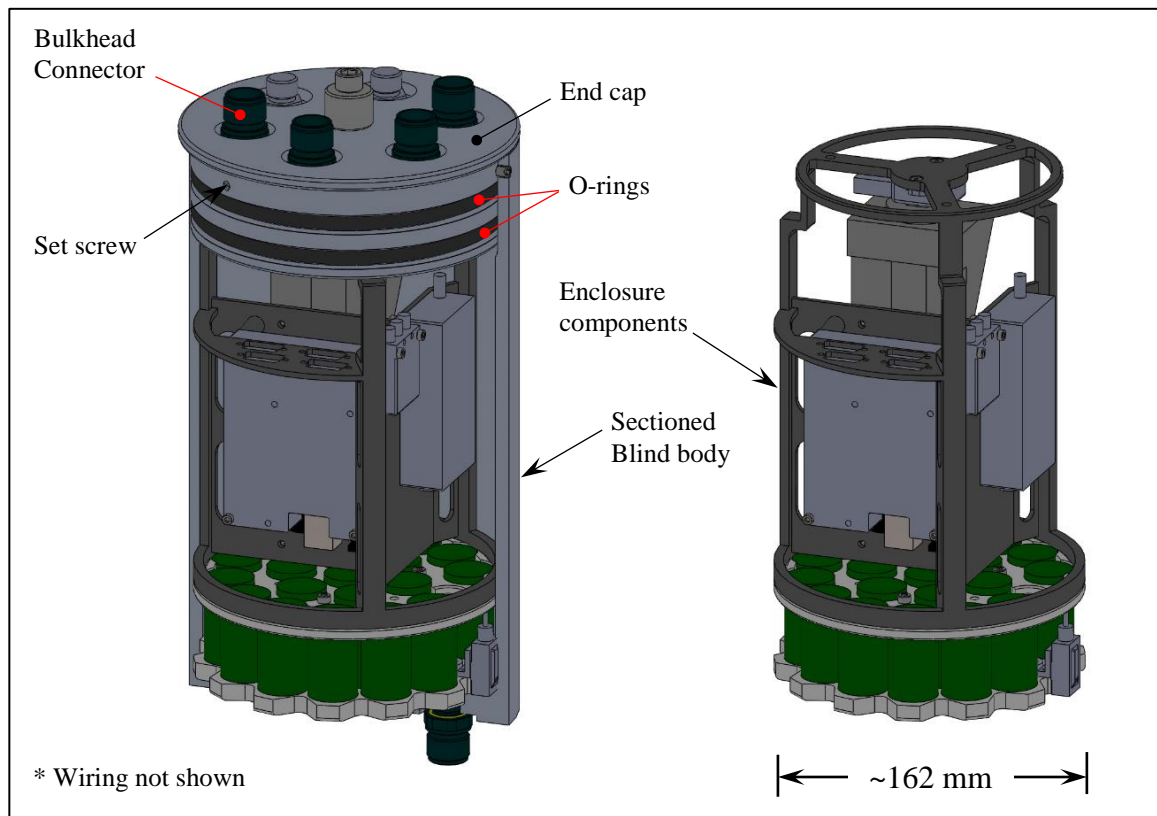


Figure 19 Sensor float subsea enclosure with blind body sectioned and the enclosure components segregated

The external design pressure (P_a) of the enclosure was verified using Equation 5.12 and the procedures from the American Society for Mechanical Engineers (ASME) Boiler and Pressure Vessel Code; specifically Section 8 Division 1, Unfired General 28 (VIII-1 UG28) THICKNESS OF SHELLS AND TUBES UNDER EXTERNAL PRESSURE (ASME International, 2015). The external design pressure is dependant on the outside diameter of the enclosure (D_o), the side wall thickness (t), and a factor based on the material properties, and the dimensions of the enclosure (B). Given the variables in Table 5, the 7.62 mm sidewall thickness of sensor float enclosure allows for an external design pressure of 38.9 bar (~389 m depth).

The first step of the procedure was to verify that that D_o/t was greater than 10 in order to validate the procedure used. Next, “Factor A” was determined from the intersection of the L/D_o and D_o/t lines on the Geometric Chart for Components Under External or Compressive Loading (Figure 20). Finally, the “Factor B” was determined from the intersection of the Factor A and the “up to 200 °F” lines on the Chart for Determining Shell Thickness of Components Under External Pressure Developed for Welded Aluminum Alloy 6061-T6 (Figure 21).

$$P_a = \frac{4B}{3 \left(\frac{D_o}{t} \right)} \quad (5.12)$$

Table 5 Variables and factors for sensor float enclosure

| | |
|---|-----------------------|
| Inside diameter of enclosure, D_i | 162.6 mm |
| Outside diameter of enclosure, D_o | 177.8 mm |
| Sidewall thickness, t | 7.6 mm |
| Unsupported length of enclosure, L | 295.3 mm |
| Factor A ($L/D_o = 1.66$ and $D_o/t = 23.4$) | 0.007 |
| Factor B (Aluminum 6061-T6) | 9,900 psi (682.6 bar) |
| Allowable external design pressure, P_a | 38.9 bar |

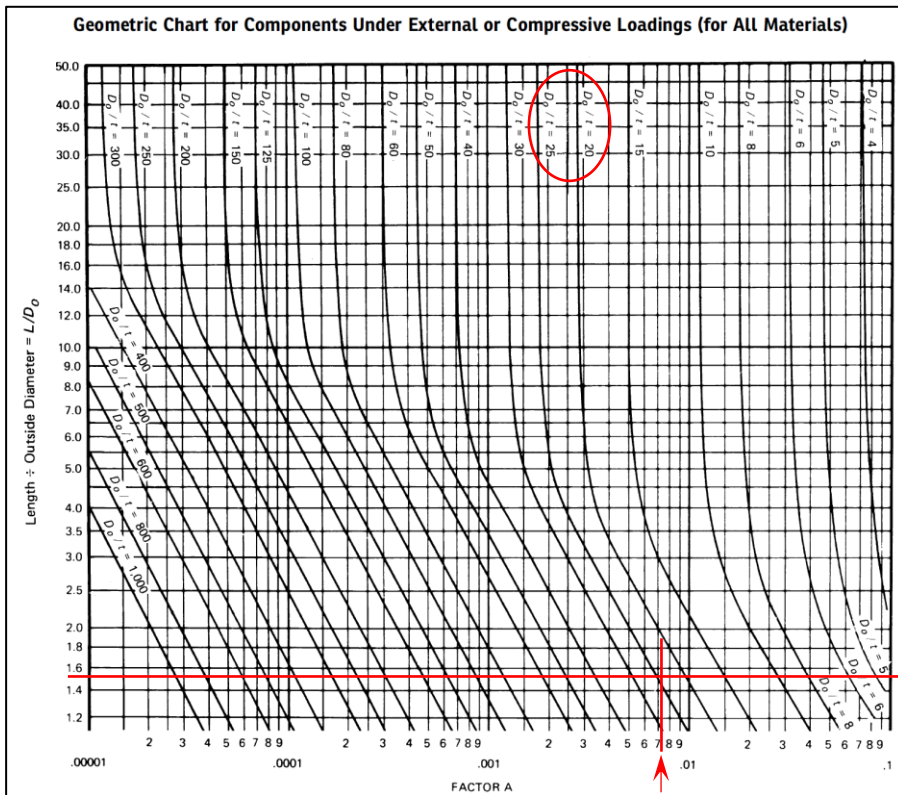


Figure 20 Geometric Chart for Components Under External or Compressive Loading (ASME, 2015)

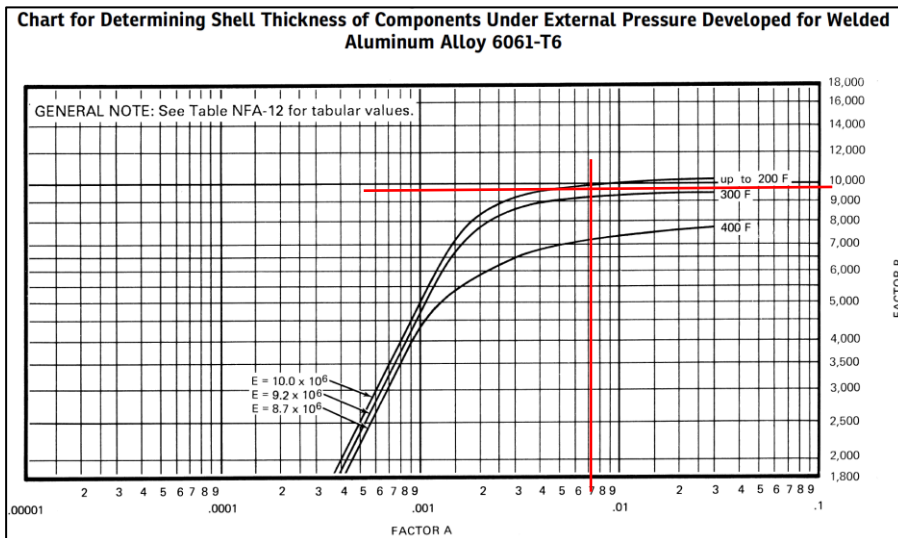


Figure 21 Chart for Determining Shell Thickness of Components Under External Pressure Developed for Welded Aluminum Alloy 6061-T6 (ASME, 2015)

The removable end cap of the enclosure is sealed with two radial male glands. The two 2-437 O-rings are seated in grooves on the end cap (with no backing). This industrial O-ring static seal is designed for a pressure of 103.5 bar as per the guidelines and specifications provided in the Parker O-Ring Handbook ORD700 (Parker Hannifin Corporation, 2007).

Table 6 summarizes the O-ring and enclosure design dimensions as referenced to the Parker design guide schematic in Figure 22.

Table 6 2-437 O-ring design dimensions for a radial industrial static male gland seal

| | |
|------------------------------|----------------------|
| O-ring inside diameter, I.D. | 151.77 ± 0.94 mm |
| O-ring diameter, W | 6.99 ± 0.15 mm |
| Groove width, G | 9.53 – 9.65 mm |
| Bore diameter, A | 165.10 – 165.15 mm |
| Groove diameter, B-1 | 153.52 – 153.62 mm |
| Plug diameter, C | 164.97 – 165.00 |
| Diametral clearance, E | 0.10 – 0.18 mm |
| Groove radius, R | 0.51 – 0.89 mm |

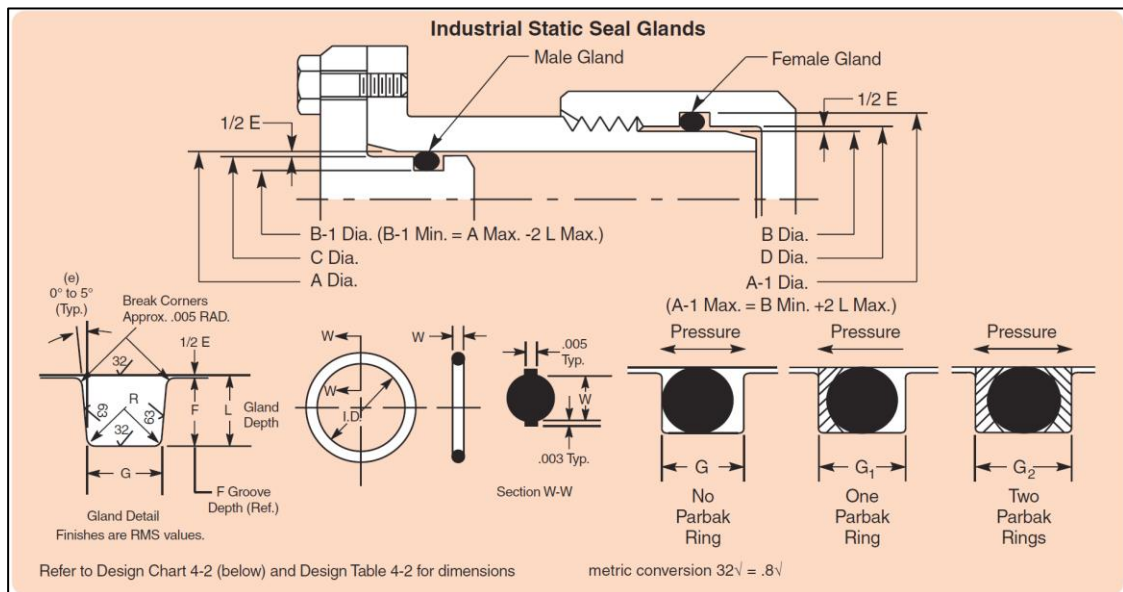


Figure 22. Parker design guide for industrial static seal glands (Parker Hannifin Corporation, 2007)

The enclosure is fitted with seven subsea bulkhead connectors. The four Teledyne Impulse Miniature High Density (MHDG) series subsea connectors on the top are for the GPCTD, Velocimeter, Altimeter, and ECO FLS sensors. The other two top connectors are Teledyne DGO 110 series coaxial connectors. They are for the Iridium/GPS and Wi-Fi antennas. The single MHDG connector on the bottom is for the electromechanical cable connection. The specifications for the bulkhead connectors are available in Appendix A, pages 204-208. With a pressure rating of 5000 psi (345 bar) and greater, the connectors exceed the 30 bar design pressure.

5.1.2.2 Streamlined Shape of Sensor Float

A method frequently used to develop a streamline shape is to use a combination of simple geometric shape such as ellipses. Figure 23 shows the profile shape of the sensor float that is able to enclose the sensors and enclosure as arranged in Figure 14. The profile was developed after the shape suggested by the National Physics Laboratory where the major axis of the ellipse that makes up the back is $\sqrt{2}$ time greater than the major axis of the front ellipse (Kale, Joshi, & Pant, 2005). The sensor float profile can be considered streamlined since the major axis of the back ellipse is $1.5 (> \sqrt{2})$ times greater than the front ellipse. The major axis of the front and back ellipse is 400 mm and 600 mm, respectively. The total length or chord of the profile is 500 mm and the thickness is 200 mm. A streamlined strut with a thickness to chord ratio of 0.4 (same as the sensor float profile) has a drag coefficient ≤ 0.1 at Reynolds Number (Re) $\geq 10^4$ (Cimbala & Cengel, 2006). The sensor float improves streamlining of the strut shape by rounding and tapering

the top and bottom. The rounding and tapering shape is produced from a 180° revolution of half of the streamline profile (Figure 23), about the long axis of symmetry.

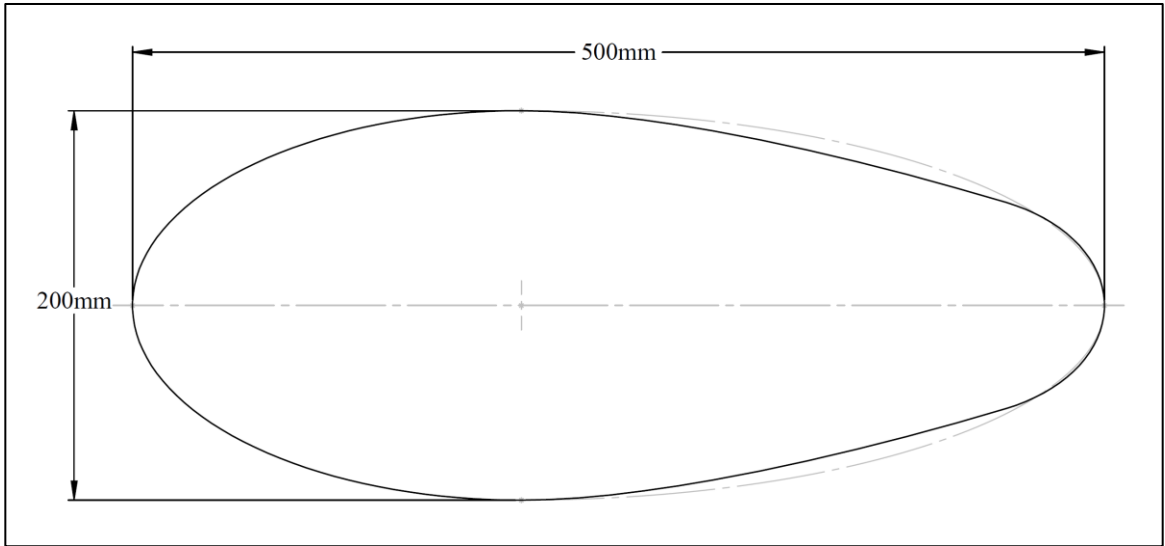


Figure 23 Streamline profile shape of the sensor float

5.1.2.3 Size of the Sensor Float

The sensors, enclosure, and structural components of the sensor float all have a negative buoyancy. To achieve the positive 100 N buoyancy goal, foam was added to the sensor float. The foam used was Divinycell HCP50, the full specifications are available from the technical data sheets in Appendix A, pages 209-210. HCP50 is a high performance, low density closed cell foam designed for subsea applications. Its salt water operational depths specification of 300 m is suitable for this profiler's 200 m application.

To estimate the volume of the foam required, the buoyancy of everything that makes up the sensor float excluding the foam (sensors, enclosure, and structural components) had to

be determined. If the buoyancy of a sensor was not known from the product data sheet, it was determined by using a load cell to measure the buoyancy in a tank of water. The buoyancy of the enclosure was determined using a load cell and tank of water as well. The buoyancy of the sensor float components to be fabricated was determined from the analytical tool in SolidWorks. First the density of each component was set to the density of the material of construction minus the density of sea water. Then the buoyancy of the part was determined by multiplying gravity (9.81 m/s^2) by the mass value from the mass property analytical tool. The total of wet weight (buoyancy) of the sensor float components excluding the foam was negative 48 N. Therefore, to provide 100 N of positive buoyancy there must be a sufficient volume of foam to generate 148 N of positive buoyancy (B_+). Given the specification that the HCP50 foam provides 775 kg/m^3 of positive buoyant density (ρ_{bm}), Equation 5.13 was used to determine that $1.95 \times 10^{-2} \text{ m}^3$ of Divinycell HCP50 foam was required.

$$V_{foam} = \frac{B_+}{\rho_{bm}g} \quad (5.13)$$

To optimize the volume of the sensor float and reduce the projected area of the float, the 53 mm thick sheets HCP50 foam were machined to match the streamline profile. Pockets were machined within the shape to allow routing of cables and tubing, and to fit tightly around the tie rods, sensors, and the enclosure. Due to the complex shapes and geometries the SolidWorks mass property analytical tool was used to determine the volume of foam used. Engineering drawings for the ten pieces of HCP50 foam that make up a volume of

$1.95 \times 10^{-2} \text{ m}^3$ (eight layers in the body and two pieces in the top cap) are available in Appendix B, pages 280-288 and 295-296.

The resulting height of the sensor float (excluding the antenna and Velocimeter) is 0.650 m. For drag calculation purposes the projected area of the sensor float is 0.125 m^2 . Using Equation 5.8 with the environmental variable from the spherical sensor float analysis and the physical variables from the streamlined sensor float, the Reynolds Number is 1.5×10^5 . This is greater than 1×10^4 , therefore the drag coefficient can be conservatively estimated as 0.1. This will generate a drag force of 6.4 N. Including the 6.6 N of calculated drag from the antenna and Velocimeter, the resultant 0.81 m horizontal displacement of the sensor float at the critical point is within the 1.5 m tolerance placed on the critical horizontal displacement.

5.1.2.4 Sensor Float Structure

The main mechanical structure of the sensor float is shown in Figure 24. It relies on a 5 mm thick aluminum base plate and seven 6 mm diameter aluminum tie rods equally spaced around the perimeter. The tie rods are threaded into the base and a flanged nut at the top to compress and hold the foam and intermediate layers of High Density Polyethylene (HDPE) in place. A HDPE shell attached to the HDPE layers helps to protect and confine the foam. The subsea enclosure and a strain relief attachment point are rigidly attached to the aluminum base plate with fasteners. The strain relief attachment point is mounted near the front of the sensor float to help ensure that the GPCTD sensor located in the nose will orientate into the current. This is the optimal position for the

sensors since they will be exposed to an undisturbed parcel of water during the upward profile.

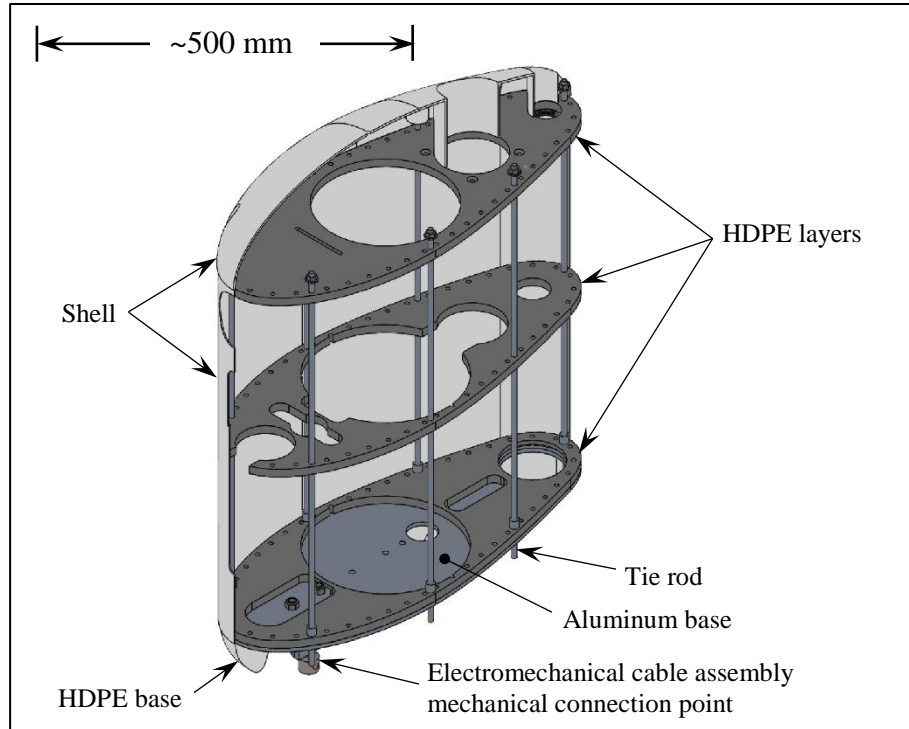


Figure 24 Sensor float mechanical structure with the HDPE base and shell sectioned

5.1.3 Upright Orientation and Stability of the Sensor Float

A fully or partially submerged object is considered to be in stable equilibrium if it returns to its equilibrium position after it has been displaced (Munson, Young, & Okiishi, 1994). To ensure a clear telemetry link, the top mounted antennas on the sensor float must be out of the water when in the equilibrium position at the surface. Due to the buoyant force of the sensor float and the tension in the cable, the equilibrium position provides the antennas with an upright and out of the water orientation as shown in Figure 25.

However, the tension in the electromechanical cable can be permanently or temporarily removed from the float during events such as a detachment from the electromechanical cable or exposure to wave action. In either situation the equilibrium position of the sensor float should ensure the antennas remain out of the water to transmit data. To guarantee an upright stable equilibrium position of the antennas when there is no tension on the cable the center of buoyancy must be above the center of gravity (Munson, Young, & Okiishi, 1994). To promote this, more of the positive buoyant foam was positioned at the top of the float and the negative buoyant components were located as close as possible to the bottom of the float. Figure 26 shows that the stable equilibrium position of the sensor float with no tension in the cable keeps the antennae out of the water; however not as prominently as when there is cable tension.



Figure 25 Sensor float stable equilibrium position with cable tension



Figure 26 Sensor float stable equilibrium position with no cable tension

5.1.4 Buoyancy Verification and Trimming of the Sensor Float

Verification and trimming of the buoyancy of the sensor float was completed in the Faculty of Engineering deep tank. The buoyancy of the sensor float was verified using the two set up arrangements illustrated in Figure 27. The first arrangement had a load cell connected at the top of the sensor float and the sinker weight attached to the bottom to submerge it. The second arrangement only has the submerged sinker weight attached to the load cell. The difference between the load cell values gives the buoyancy measurement of the sensor float. The initial measurement of the sensor floats buoyancy was 82.3 N. To trim the buoyancy of the sensor float to 97.5 N, $2.1 \times 10^{-2} \text{ m}^3$ (15.2 N) of HCP50 foam was added within the void above the enclosure. Since sea water is approximately 2.5% more dense than freshwater the sensor float should have a buoyancy of 100 N in sea water.

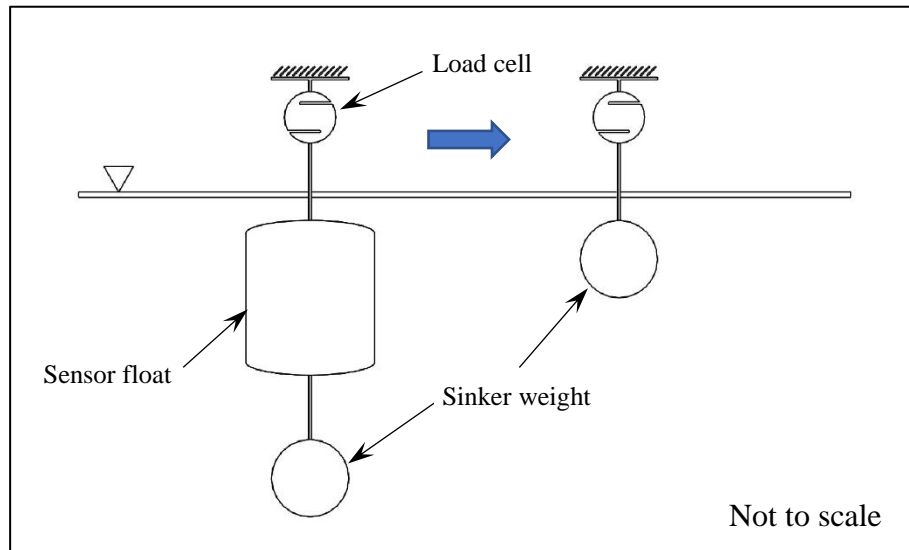


Figure 27 Buoyancy verification tank set up

5.2 Electromechanical Cable Assembly Design

The electromechanical cable assembly was designed as illustrated in Figure 28. It is made up of four main components; an electromechanical cable, connectors, a strain relief, and a shock absorber. The assembly provides five functions; (i) power for the sensor float; (ii) data transfer to and from the sensor float; (iii) a mechanical connection between the sensor float, passive float, and main body; (iv) strain relief to the connectors and cable; and (v) shock load absorption.

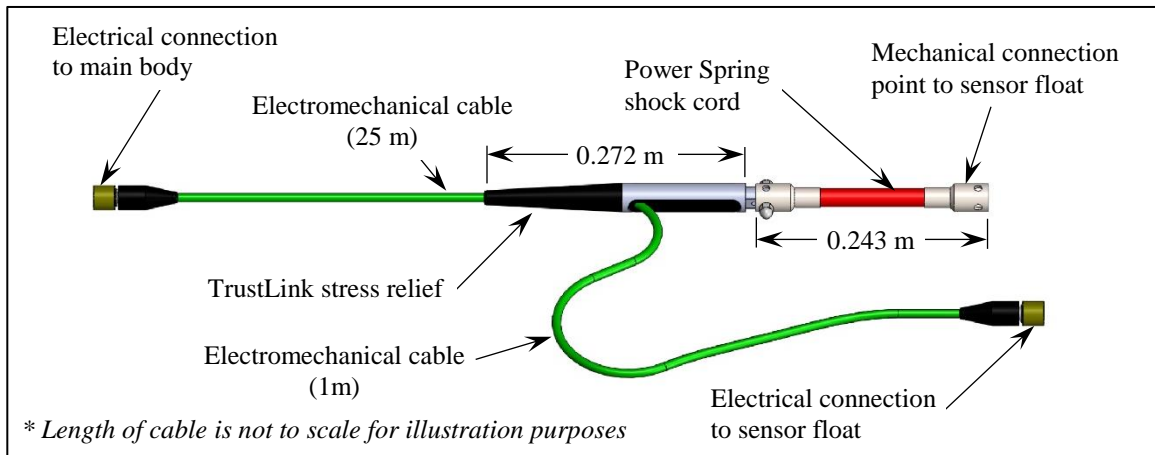


Figure 28 Electromechanical cable assembly

To reduce cost and lead time, a suitable off-the-shelf cable was selected rather than designing and specifying a unique cable solution to satisfy the profiler requirements. The electromechanical cable selected was a Falmat FM022208-04 12K Xtreme-Net ruggedized deep water ethernet cable. The cable has two 18 AWG conductors for power, and a pair of 24 AWG conductors for data transmission. In addition, there is an aramid

fiber layer which provides 1,200 lb. (5,338 N) of breaking strength. The specification sheet for the cable is in Appendix A, page 211.

The 8.8 mm diameter cable is less than the 10 mm diameter previously assumed.

Therefore, there will be less drag on the cable, a decrease in the expected amount of horizontal displacement, and a reduction in the length of electromechanical cable required to reach the surface. Replacing the 10 mm cable diameter value with 8.8 mm reduces the drag per unit length of cable from 5.14 N/m to 4.52 N/m. Applying this value to the critical horizontal displacement in section 5.1.2.3 results in a reduction from 0.81 m to 0.76m.

The electromechanical cable is the lifeline for the system, and it must be protected from failure. As per the manufacture's recommendation, the maximum safe working load for the cable is 20% of the breaking strength. Setting the safe working load of the electromechanical cable at 1,000 N satisfies the recommended maximum limit for the safe working load. Under static operating conditions, the ~100 N load that the cable would experience is much less than the safe working load. However, while at the surface the sensor float is exposed to cyclical and potentially shock loading due to wave action.

Aramid fiber properties are characterized by a high modulus of elasticity due to their high strength and low elongation, and excellent tension fatigue (Horn, Riewald, & Zweben, 1977). The high strength and excellent tension fatigue help permit the electromechanical cable to withstand the potentially high tension and cyclical loads caused by waves. However, the low elongation limits its ability to absorb energy during shock loading.

Shock loading will occur when the sensor float is at the surface and it reaches the extension limit of the electromechanical cable while moving up a wave. This will cause the float to stop immediately. This is analogous to dropping the sensor float from a height while attached to a fixed length of cable. The kinetic energy developed by the moving mass of the sensor float must be absorbed by the electromechanical cable assemblies shock cord.

The kinetic energy (KE) possessed by the sensor float as it moves up and down with the wave motion is determined by Equation 5.14 (Hibbeler, 2007). It is dependent on the mass of the sensor float (m_{sf}) and the velocity of the sensor float (v_{sf}). Since the mass of the sensor float is constant, the maximum kinetic energy will occur when the velocity of the sensor float is at its maximum. The mass of the sensor float excludes any ‘added mass’ effect of the surrounding sea water due to acceleration imposed on the seawater by the sensor float.

$$KE = \frac{1}{2} m_{sf} v_{sf}^2 \quad (5.14)$$

A simplified model of deep water surface gravity waves can be characterized by a sinusoidal wave as illustrated in Figure 29 (Randall, 2010). A water particle at the surface traveling along the wave will have a horizontal and vertical velocity component. The magnitude and direction are dependent on the position along the wave. Equation 5.15 is used to determine the vertical velocity (w) of the particle (Randall, 2010). It depends on the wave height (H), period (T), wave number (k), vertical distance of the particle at the

surface of the wave from the Still Water Line (SWL) (z), and the phase angle (θ). The phase angle is 0° at the crest of the wave. The maximum upward vertical velocity occurs when the particle is at the SWL and on the upward slope of the wave. At this point the phase angle is 270° and the distance from the SWL is 0. Substituting these values into Equation 5.15 simplifies it to $w_{\max} = \pi H/T$.

$$w = \frac{\pi H}{T} e^{kz} \sin \theta \quad (5.15)$$

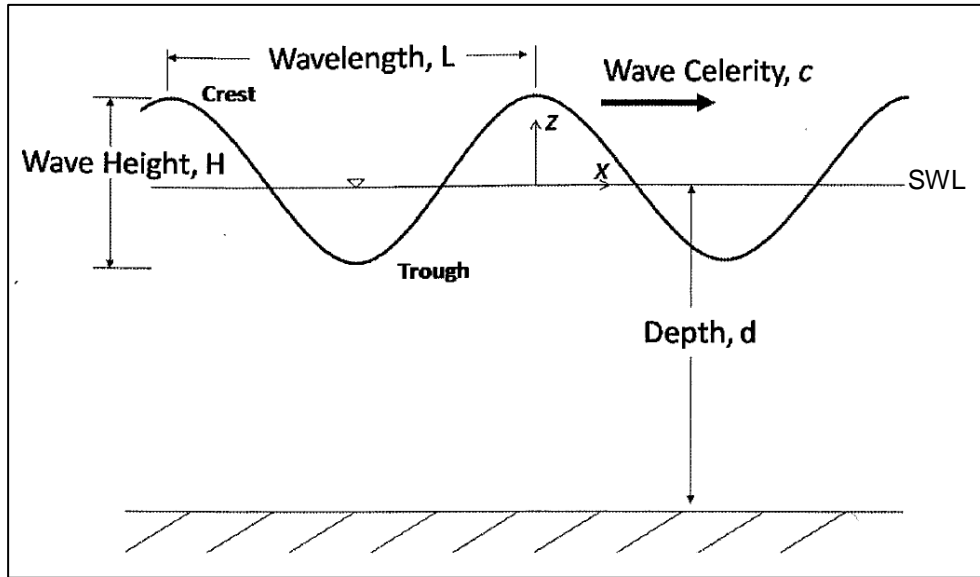


Figure 29 Sinusoidal progressive waveform (Randall, 2010)

A wave height of 5 m and a period of 6 seconds was used in Equation 5.15 to determine that 2.62 m/s is the maximum upward velocity the sensor float may experience at the surface. The 5 m wave height was set as one of the operational limits of the profiler. A period of 6 seconds was chosen based on 59 years of Meteorological Service of Canada (MSC) 50 North Atlantic Wave Hindcast at Grid Point 2124 (42.2°N , 62.9°W) of the

Scotian Shelf. Hourly wave data from 1954-2012 indicated that the lowest wave period recorded for a 5 m wave was 6 seconds (Stantec, 2014).

With a sensor float mass of 29.9 kg, and a maximum velocity of 2.62 m/s, Equation 5.14 results in a maximum kinetic energy of 103 J. This is the energy that must be absorbed by the shock absorber of the electromechanical cable assembly without exceeding the safe working load of 1,000 N.

A shock cord (or bungee cord) was chosen over a more traditional constant force extension spring as the energy absorbing component. An extension springs relatively short life of the tens of thousand of cycles was a severe limitation for an application which would expose it to regular cyclical loading from wave action (Shigley & Mischke, 1996). The shock cord is able to endure 5×10^6 cycles before failure; an order of magnitude greater than the extension spring. The shock cord is also more compatible with sea water than a stainless-steel spring. Natural rubber is able to endure long term submerged exposure in a salt water environment (Mott & Roland, 2001).

A 19 mm diameter Ibex Marina Power Spring was selected as the shock absorber for the electromechanical cable assembly. The full specifications for the Power Spring is available in Appendix A, page 212. Its maximum load rating of 1,125 N is able to withstand the safe working load of the electromechanical cable and the 'E' type end fittings provide a secure means of attachment. The length of the Power Spring was sized to ensure that under a 1,000 N load it would deflect a sufficient amount to absorb 103 J of energy; the maximum kinetic energy developed by the sensor float. The energy absorbed

by a spring (U_s) with an initial tension (T_i) is determined by Equation 5.16 (Hibbeler, 2007). It is dependent on the initial tension (T_i), the spring constant (k), and the amount of deflection (x). The (kx) term is the load on the spring and the initial tension is the load required to initiate the deflection.

$$U_s = \frac{1}{2} (kx) x + T_i x \quad (5.16)$$

Unlike an extension spring, the spring constant for a shock cord depends on its original length. The manufacturer's specifications for the Power Spring provides Equation 5.17 to determine the load (Ibex Marina, 2015). It is dependent on the spring rate specification (S), the percentage of extension (E) of its original length, and the initial tension specification (F_0). The load and initial tension in Equation 5.17 is the same as the kx and T_i terms in Equation 5.16, respectively.

$$Load = S \times E + F_0 \quad (5.17)$$

The minimum required original length (x_0) of the Power Spring can be determined using Equation 5.18. It is dependent on the amount of deflection (x) and the percentage of extension (E)

$$x_0 = \frac{x}{E} \quad (5.18)$$

Given the parameters provided in Table 7 and using Equations 5.16, 5.17, and 5.18 the original length of Power Spring required for the electromechanical cable assembly that limits the load to 1,000 N while absorbing 103 J of energy was determined to be 0.184 m.

Table 7 Power spring design parameters and values

| | |
|---|----------------|
| Spring energy, U_s | 103 J |
| Spring load, $Load$ and (kx) | 1,000 N |
| Initial spring tension, F_0 and T_i | 248 N |
| Spring deflection, x | 0.138m |
| Percentage of deflection, E | 74.9% |
| Original spring length, x_0 | 0.184 m |

To connect the electromechanical cable assembly to the sensor float the Power Spring is coupled to a Type II-F McCartney Trustlink Stress Termination (Figure 28). One end of the Power Spring connects to the sensor float via the electromechanical cable assembly mechanical attachment point. This connection can pivot to avoid putting a bending stress on the Power Spring. The other end of the Power Spring connects to the Trustlink, and the electromechanical cable is secured and molded into the Trustlink. The specification for the Trustlink is given in Appendix A, pages 213-214. The watertight Trustlink is designed as a rugged, safe, and reliable solution for connecting cables to towed and profiling subsea systems (McCartney, 2015). Its purpose is to eliminate the stress on the connectors of the electromechanical cable as illustrated by the slack cable shown in Figure 30. The slack section of the cable is longer than the Power Spring at full extension. Therefore, when the Power Spring is loaded to 1,000 N or less, the slack section of the electromechanical cable will remain slack and not experience any stress. The Trustlink selected has a maximum safe working load of 600 kg (5886 N). This is much greater than the electromechanical cables 1,000 N limit, but it was the smallest one suitable for the 8.8 mm diameter electromechanical cable. It would be cost and time prohibitive to design and fabricate a specific Trustlink with a lower safe working load.

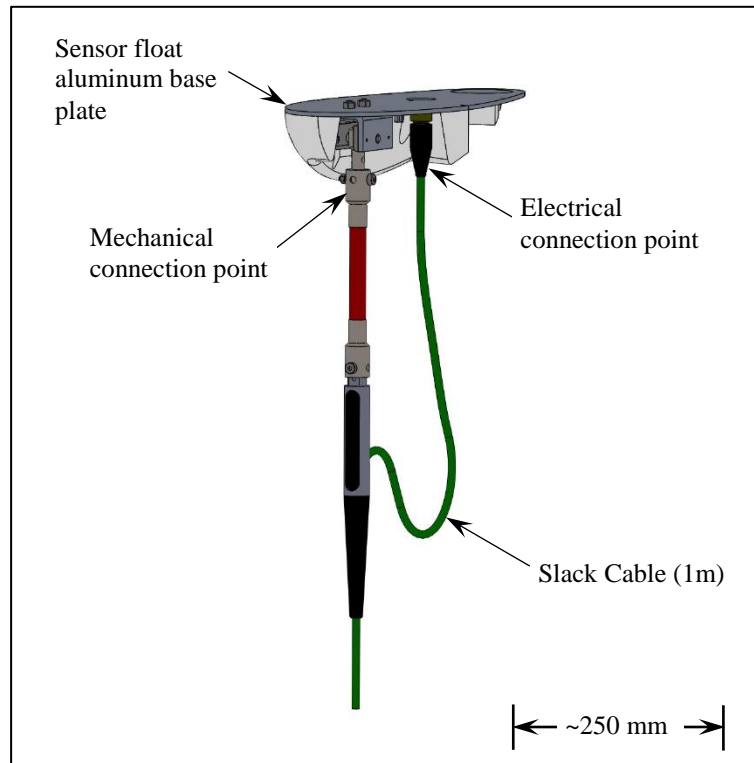


Figure 30 Electromechanical cable assembly attached to the sensor float aluminum base

5.3 Passive Float Design

The main function of the passive float is to keep the sensor float retracted during the primary ascent and the descent. The final design of the passive float is shown in Figures 31 and 32. Detailed CAD drawings for the passive float components are given in Appendix B, pages 306-323. The passive float is constrained to the sensor float and main body by the electromechanical cable via an internal sheave, and to the mooring line via the guide tube. The sheave is mounted to a bracket on the guide tube to provide mechanical strength and structure. Collars mounted at each end of the guide tube hold the buoyant section of the passive float in place. The ellipsoidal shaped section is formed by a

3mm thick fiberglass shell. One half of the shell protects an HCP50 foam core and the other half is hollow and vented. The foam half of the passive float forms a pocket to fit the sheave and guide tube structure. Through-holes in the design allow for the addition of trim weight and/or foam plugs to fine tune the buoyancy. The float was fabricated as four separate quarters; the top foam quarter, the bottom foam quarter, the top shell quarter, and the bottom shell quarter. All four pieces were then joined together with a final common fiberglass shell.

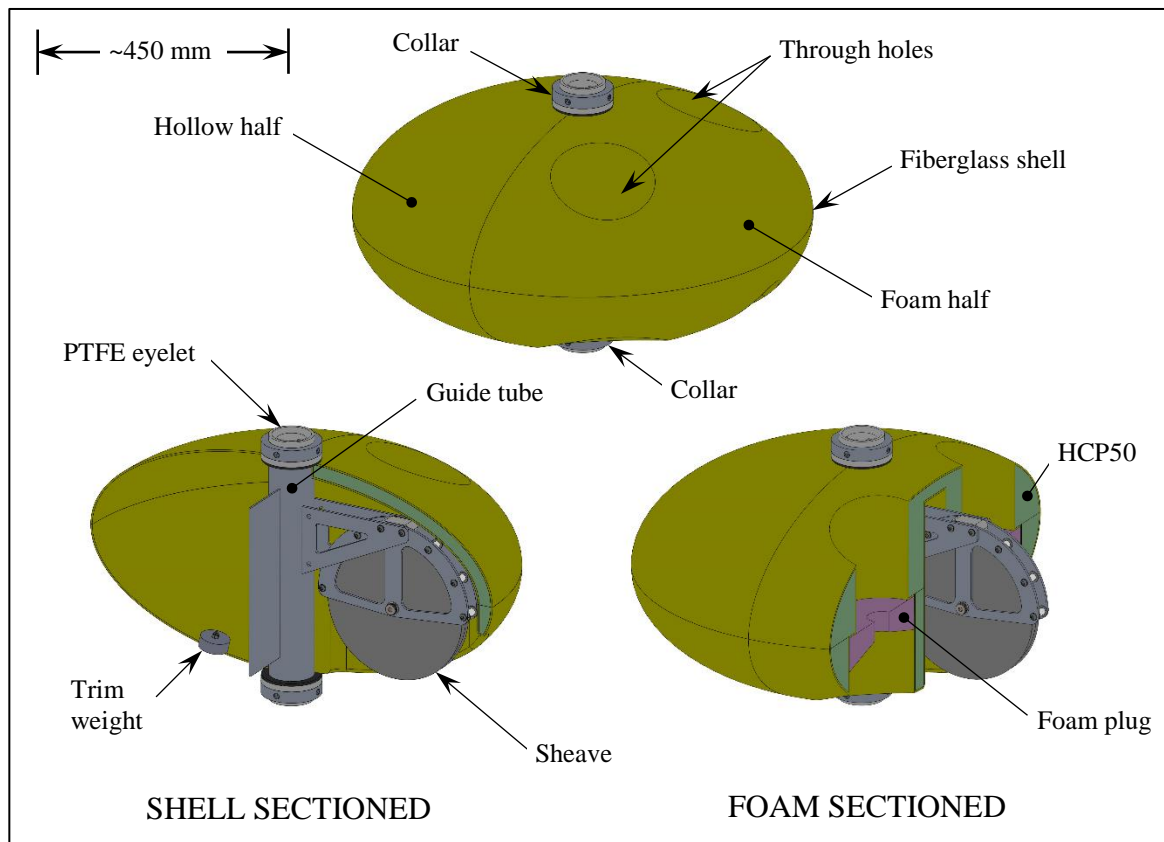


Figure 31 Passive float with only the shell and HCP50 foam sectioned

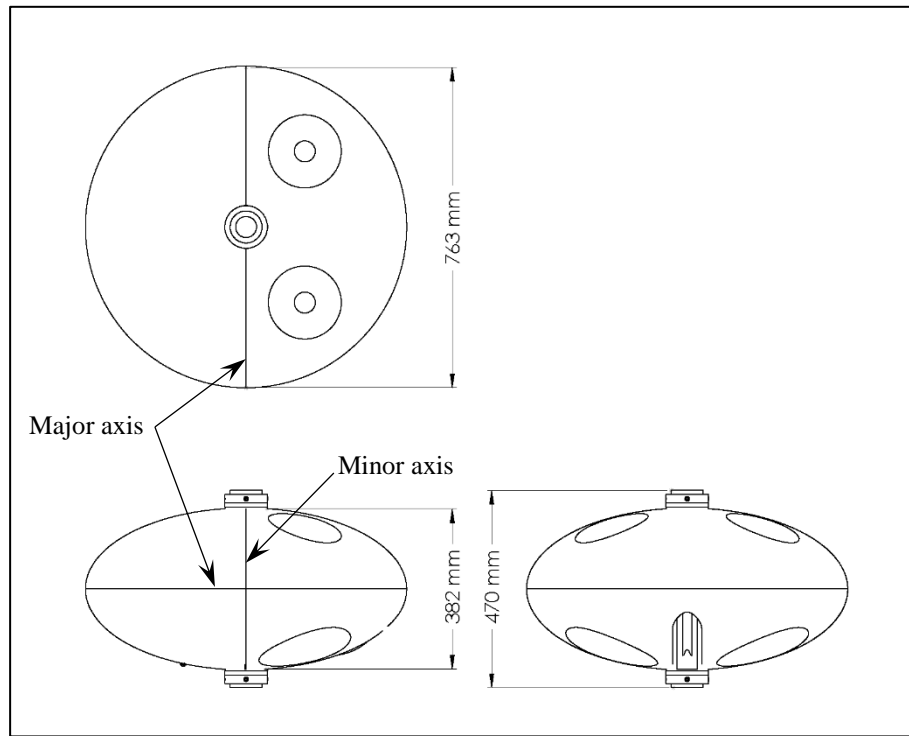


Figure 32 Passive float - Orthographic projections with dimensions

5.3.1 Sheave Design

The size of the sheave is constrained by good design practice. To ensure that the integrity of the electromechanical cable is preserved the supplier's minimum bending radius of 10 times the cable radius is maintained. The sheave's pulley design limits the bending radius to 120 mm which is 27 times the 4.4 mm radius of the electromechanical cable. To ensure the cable remains seated in the pulley, the groove depth is 1.5 times the diameter of the cable and the throat angle is 40° . The groove radius is dimensioned as 0.530 – 0.535 times the cable diameter. If the groove diameter is too small the cable can be crushed and if too large the cable could flatten (All Rigging Co., 2016). A detailed drawing indicating the pulley dimensions is provided in Appendix B, page 314.

The sheave uses a Rulon plain bearing. Rulon is a low friction polytetrafluoroethylene (PTFE) based material that is intended for wet applications. PTFE thrust washers are also used to minimize the friction between the side walls of the sheave and the side plates. PTFE spacers located around the perimeter of the side plates constrain the electromechanical cable in the groove. This requires the sheave to be assembled around the cable, but it ensures the cable will remain in the sheave (Figure 33). Detailed CAD drawings of the sheave components are provided in Appendix B, pages 311-315.

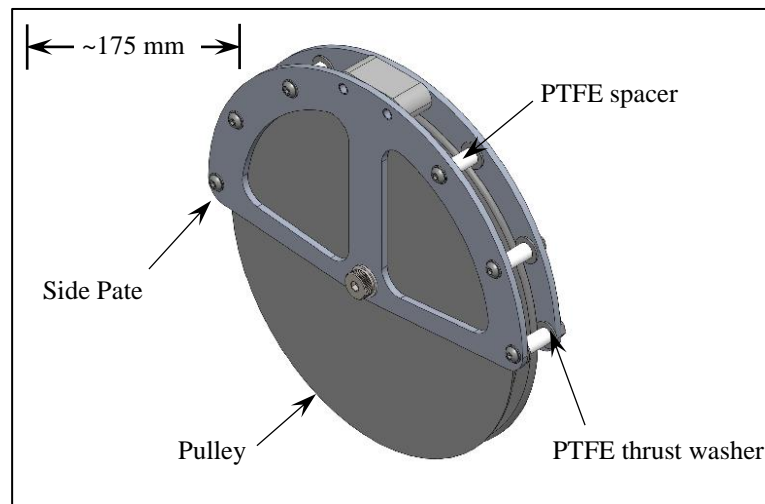


Figure 33 Sheave design

5.3.2 Passive Float Shape and Size

The chosen shape for the passive float is an ellipsoid (oblate spheroid) shape with a 2:1 major to minor axis ratio. An oblate spheroid is generated by rotating an ellipse about its minor axis. The major axis of the final design is 760 mm and the minor axis is 380 mm.

The size of the passive float was determined based on the size of the sheave that had to be enveloped, and to contain a sufficient amount of foam to generate the required buoyancy.

An ellipsoid shape was chosen over a more traditional spherical shape because spherical subsea buoys are known to experience undesirable oscillations under certain flow conditions (Govardhan & Williamson, 1997). Oscillations of the float can increase the drag force on the float and impart additional stress and strain on the electromechanical cable. Streamlining the shape of a subsea buoy to reduce its drag has proven to reduce these oscillations (Hurley, de Young, & Williams, 2008). Under the same conditions, the drag coefficient of an ellipsoid is less than that of a sphere with an equivalent projected area. Therefore, it would reduce the occurrence of unwanted oscillations (Cimbala & Cengel, 2006).

Due to the symmetry of its ellipsoid shape the orientation of the passive float is not strongly affected by the current. The placement of the sheave within the body of the float also eliminates it from acting like a fin and driving the orientation with the direction of the current. Maintaining an orientation independent of the current helps eliminate twisting of the electromechanical cable about the mooring line under conditions which could expose the main body and passive float to currents in different directions. The orientation of the passive float should only be influenced by the main body since they are coupled together by the electromechanical cable.

5.3.3 Buoyancy and Balancing of the Passive Float

The positive buoyancy of the passive float must be more than twice that of the sensor float to keep it retracted during the primary ascent and the descent. Because of the sheave in the passive float, the greatest tension it can develop in the electromechanical cable is

half of its own buoyancy as indicated in by the free body diagram given in Figure 34. The passive float was designed to have a positive buoyancy of 220 N (F_{PF}) in sea water. This can produce a cable tension of 110 N (T_{EC}) which is 10 N greater than the 100 N buoyancy of the sensor float (F_{SF}). Although small, a magnitude the 10 N is sufficient to keep the sensor float retracted. Increasing the magnitude of the passive float to produce more buoyancy to retract the sensor float will require a larger buoyancy engine. The buoyancy engine is required to vary the weight of the main body from greater than the sum of the sensor float and passive float buoyancy, to less than three times the sensor float buoyancy. Increasing the buoyancy of the passive float increases the magnitude of this variation. Therefore, employing a larger buoyancy engine capacity which necessitates more power.

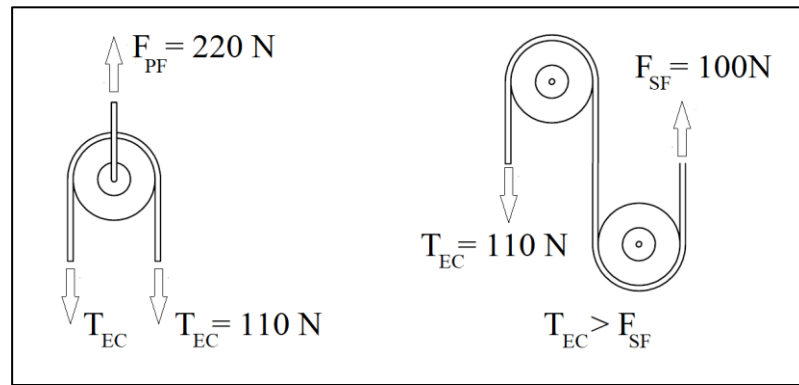


Figure 34 Passive float and sensor float free-body diagrams

To achieve a passive float design with 220 N of positive buoyancy, a systematic and iterative process was used. First, based on a 760 mm \times 380 mm ellipsoid, the buoyancy of the HCP50 foam, fiberglass shell, and the sheave and guide tube structure were determined using the SolidWorks analytical tools. The net value of the first iteration

exceeded the desired 220 N. Due to the requirement to enclose the sheave within the passive float, altering the dimensions of the ellipsoid shape was not an option. Two equal and symmetric through-hole features were incorporated into the design to reduce the volume of foam in the passive float. The through-holes were iteratively dimensioned until the volume of foam material remaining resulted in the final buoyancy of the passive float equalling 220 N. Again, due to the complex geometries involved in cutting through a curved surface, the mass and volume information from SolidWorks analytical tools were used to determine the net buoyancy values for varying through-hole sizes. The center of the through-holes are positioned 140 mm from centerline of the guide tube and 180 mm from the plane of symmetry. This position aligns the through-holes near the center of buoyancy of the floats foam core.

The reasoning for two symmetric through holes was to keep all the float components symmetric to avoid unwanted tilting. The location of the sheave prevents a single through-hole in the center. The ideal natural position of the float is to have its major axis aligned horizontally. This position will position the guide tube parallel to the mooring line. Excessive tilting of the passive float combined with currents could cause undesirable forces on the float such as lift and thrust. Excessive tilting alone could cause additional friction between the guide tube and the mooring due to contact forces that would develop between the tube and cable to counteract the tilting. This friction will reduce the buoyant force of the passive float.

The rationale for the through-holes rather than pockets is it to eliminate the opportunity for air to become entrapped within the pockets that would alter the buoyancy. There is also an expected buoyancy discrepancy between the design and fabrication of the passive float. The through holes provide a convenient means to secure additional ring-shaped material to increase or decrease the passive floats buoyancy. The through-hole in the top half of the passive float is designed with a smaller diameter than the matching through-hole in the lower half. Decreasing the diameter of the upper through-hole provides a shoulder to securely constrain a foam insert. For tank testing this is sufficient security and allows different sized foam rings to be quickly and easily interchanged without additional securing methods such as fasteners or adhesives.

Additional foam and weight were required to trim the passive float such that its major axis is horizontal when it is in its stable equilibrium position. The passive float is designed with the sheave offset from the minor axis to match up with the sheave on the main body so that the electromechanical cable transitions from one sheave to the other in a vertical line. This arrangement generates a moment on the passive float that acts to displace it from the required stable equilibrium position. Half of the passive float is hollow so it does not generate any upward buoyant force on the opposite side of the sheave which would magnify the offsetting moment. The buoyant force generated by the foam on the same side of the passive float as the sheave counteracts the moment caused by the cable tension. Unfortunately, due to the location of the tension force in the cable and the buoyant force in the float, the stable equilibrium position can not be obtained without adding weight to the hollow side of the passive float. Any negatively buoyant

force (weight) added to the passive float must be counteracted by an equivalent positive buoyant force to ensure the 220 N of positive buoyancy is maintained.

An assessment of the passive floats free-body diagram illustrated in Figure 35 provided an initial estimate of the additional trim weight and foam required to ensure the major axis of the passive float is horizontal when it is in the stable equilibrium position. The SolidWorks analytical tools were used to determine the positive and negative buoyant forces acting on the float and the location of the forces. A value of 20 N was assumed for the trim weight (F_{TW}) and trim foam (F_{TF}). Equation 5.19 represents the sum of the moments about the centerline of the guide tube for the stable equilibrium position. Using the variables from the free body diagram listed in Table 8, the location of the trim weight (L_1) that produce a 0 N·m moment was determined to be 283 mm from the centerline of the guide tube on the empty shell side of the passive float.

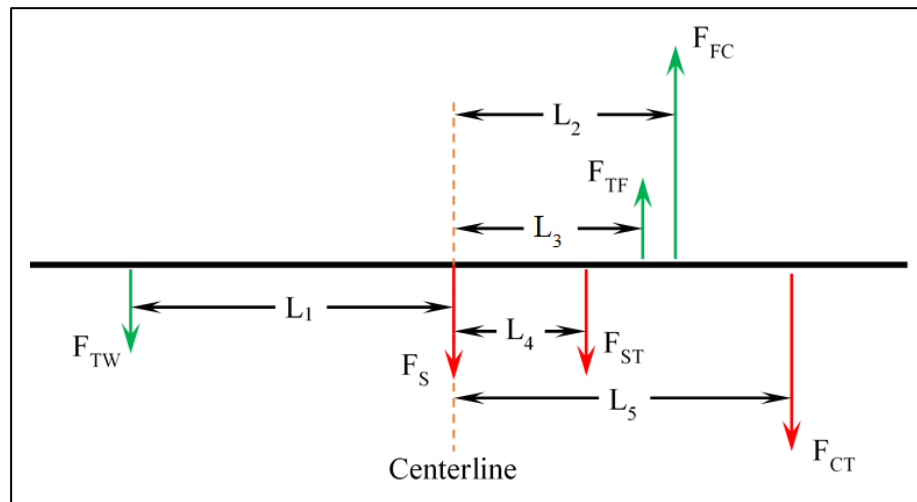


Figure 35 Passive float free-body diagram

$$F_{TW}L_1 + F_{FC}L_2 + F_{TF}L_3 + F_{ST}L_4 + F_{CT}L_5 = 0 \quad (5.19)$$

Table 8 Passive float free body diagram variables and solution

| | |
|--|---------------|
| Force due to trim weight, F_{TW} | -20 N |
| Force due to trim foam, F_{TF} | 20 N |
| Force due to foam core, F_{FC} | 261.2 N |
| Force due to sheave and tube structure, F_{ST} | -15.3 N |
| Force due to sheave and cable tension, F_{CT} | -220 N |
| Force due to shell, F_s | -25.9 N |
| Distance from centerline to F_{TF} , L_2 | 140 mm |
| Distance from centerline to F_{FC} , L_3 | 144 mm |
| Distance from centerline to F_{ST} , L_4 | 90 mm |
| Distance from centerline to F_{CT} , L_4 | 203 mm |
| Distance from centerline to F_{TW}, L_1 | 289 mm |

5.3.4 Buoyancy and Stable Equilibrium Verification of the Passive Float

The buoyancy of the passive float was determined using the same method as for the sensor float as described in section 5.1.4. The initial verification indicated that the passive float produced 198 N of positive buoyancy. To trim the passive floats buoyancy to 214.5 N (220 N in sea water) $2.2 \times 10^{-2} \text{ m}^3$ (16.5 N) of HCP50 foam was added. They were added in the form of two $1.1 \times 10^{-2} \text{ m}^3$ rings as shown in Figure 36. The rings are designed to fit tightly within the lower through-hole on the passive float and they have a sloped surface to encourage air escapement.

To verify the stable equilibrium position of the passive float a simple jig was designed and fabricated to allow the float to be submerged in the deep tank by cable tension acting on the sheave to simulate the submerged conditions when incorporated into the profiler system. Figure 37 illustrates the deep tank set up using the jig. The jig is position at the

bottom of the tank with one end of a cable anchored to it. The cable first passes through the sheave on the passive float and then through a sheave on the jig. The jig cable anchor point and the jig sheave are positioned such that the cable engages the sheave on the passive float vertically. The cable is then anchored to a point above the surface such that the passive float is completely submerged. The tension in the cable is generated by the buoyancy of the passive float.

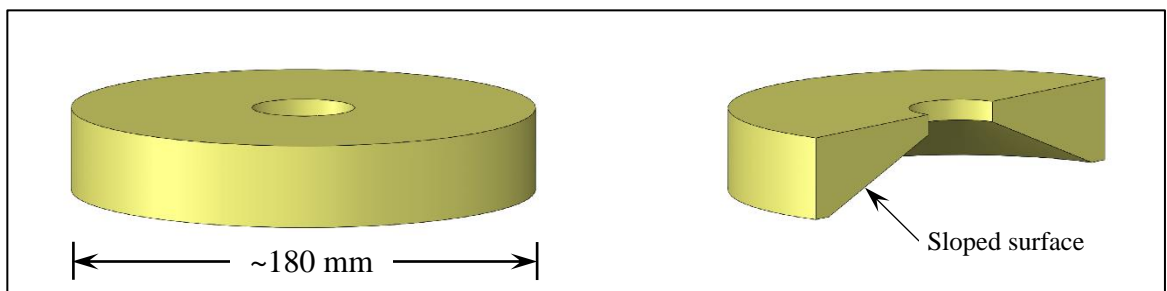


Figure 36 Passive float trim ring with sectioned view indicating the sloped surface

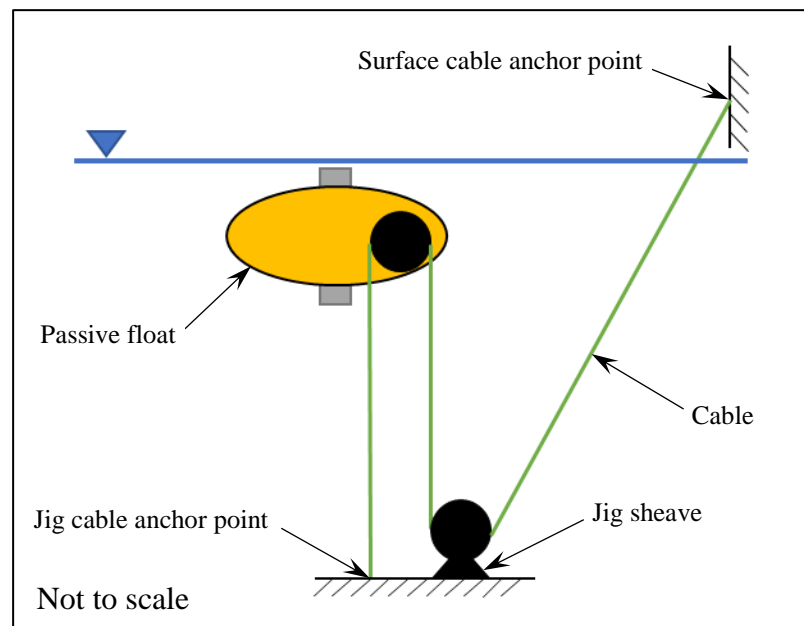


Figure 37 Passive float stable equilibrium verification set up

The verification of the initial equilibrium position of the passive float demonstrated that it was tilted approximately 28° as shown in Figure 38. Another jig was designed and fabricated to attach to the guide tube at the top of the passive float to measure the tilt and to help fine tune the equilibrium position. A single axis tilt indicator attached to the jig measures the inclination and a symmetrically mounted t-slot bar allows for the variable positioning of a mass to alter the equilibrium position. Symmetric construction and mounting of the jig are critical in order to not introduce other tilt inducing moments onto the passive float.

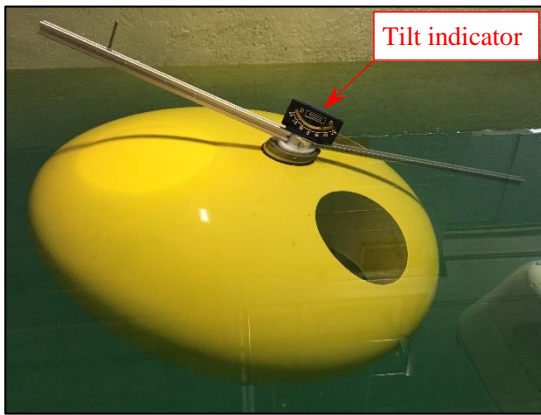


Figure 38 Initial equilibrium position of the passive float, 28° tilt

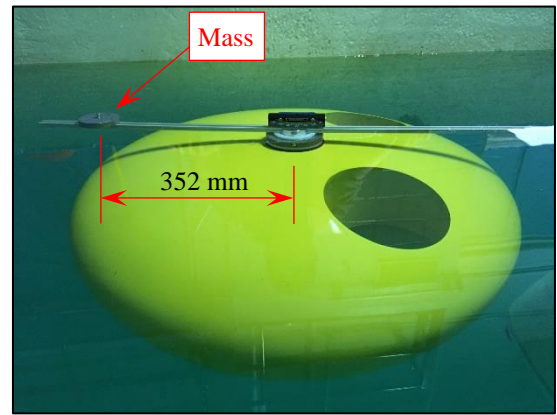


Figure 39 Corrected equilibrium position of the passive float

The moment required for the passive float to achieve the required stable equilibrium position can be determined from knowing the magnitude and relative position of the weight that produces a 0° tilt. Figure 39 shows the passive float in the required stable equilibrium position (0° tilt). This position was attained by placing a 10.4 N weight, 352 mm from the centerline of the guide tube. This equates to a 3.66 N·m moment about the centerline of the guide tube (minor axis of the float).

To correct the stable equilibrium position of the passive float, a $3.66 \text{ N}\cdot\text{m}$ moment was generated by adding a weight to the hollow section and additional foam to the sheave section. As indicated in Section 5.3, when adding weight to correct the stable equilibrium position, foam with a buoyant force of equivalent magnitude must also be added to ensure the required buoyancy of the passive float is not altered. The design of the passive float restricts the position of additional foam to the through-holes. Therefore, the location of the weight had to be determined. Based on the moment diagram in Figure 40, Equation 5.20 was used to determine that a 10.4 N weight must be symmetrically located 212 mm (L_0) from the centerline of the guide tube along with two 5.2 N ($6.8 \times 10^{-3} \text{ m}^3$) foam rings positioned in the through-holes.

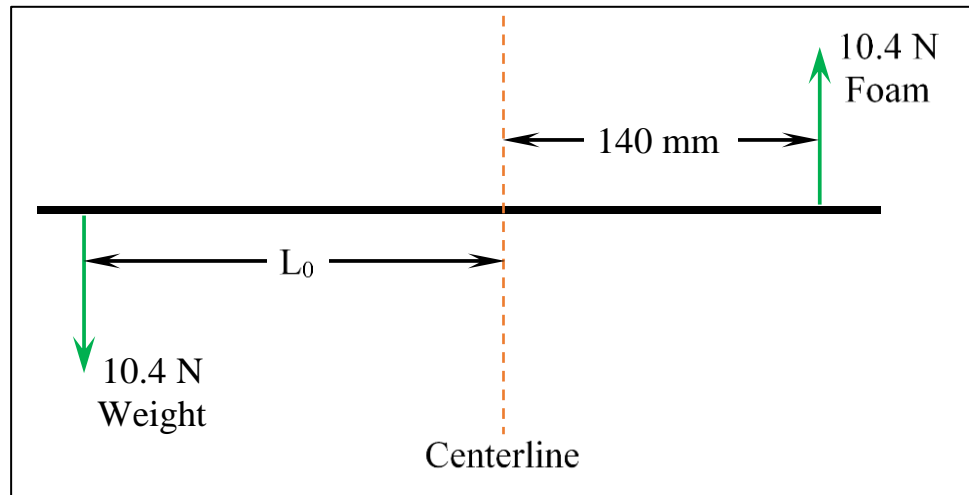


Figure 40 Passive float moment diagram to calculate weight position

$$10.4 \text{ N} \times 0.14 \text{ m} + 10.4 \text{ N} \times L_0 = 3.66 \text{ N} \cdot \text{m} \quad (5.20)$$

A 10.4 N lead weight was secured to the inside wall of the passive float at a distance of 212 mm from the centerline of the guide tube, and two $6.8 \times 10^{-3} \text{ m}^3$ (10.4 N total) foam rings were positioned in the through-holes. The result was a passive float with 214.5 N (220 N salt water) of buoyant force, and the major axis horizontal (0°) in the stable equilibrium position.

5.4 Main Body Design

The main body of the profiler illustrated in Figures 41 and 42 consists of the buoyancy engine, the power supply, the frame, and the trim foam. Details of each of these components is provided in the subsequent sections.

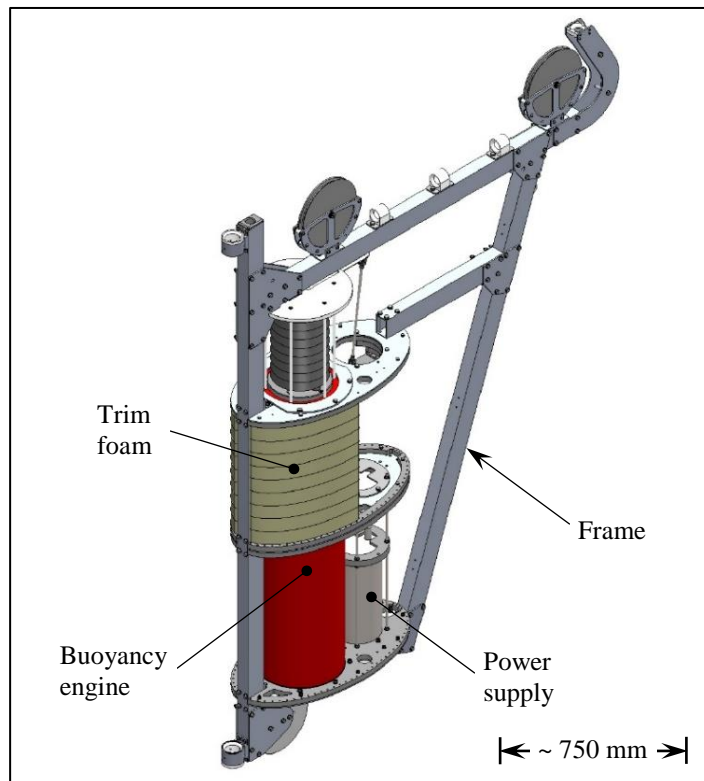


Figure 41 Profiler main body design

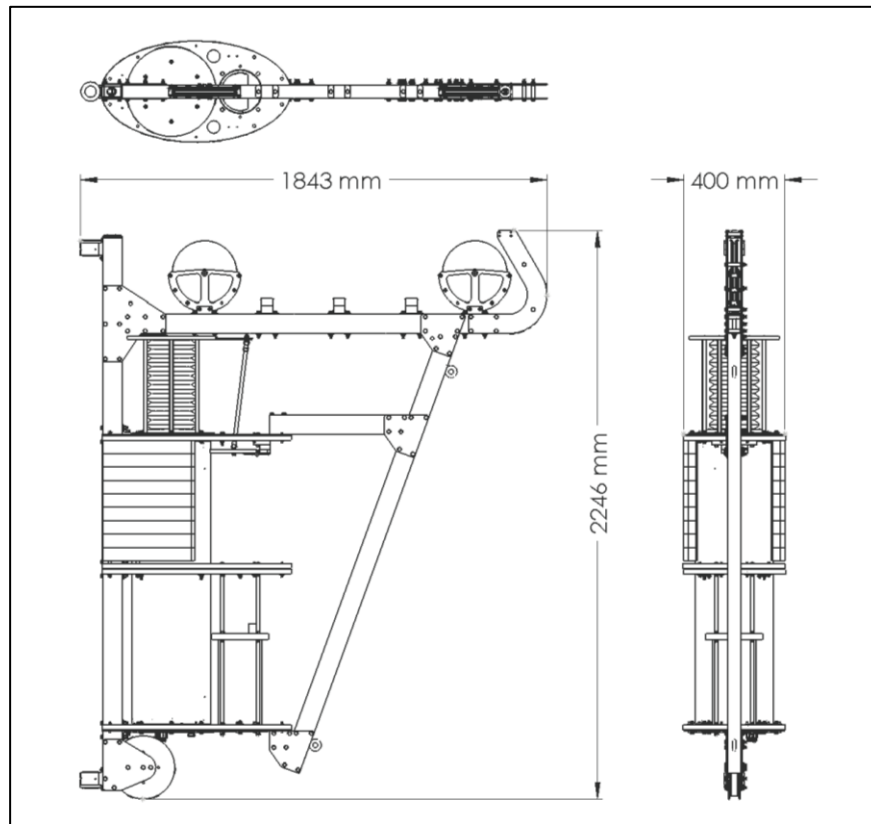


Figure 42 Profiler main body - Orthographic projections with dimensions

5.4.1 Buoyancy Engine Module

The purpose of the buoyancy engine is to adjust the buoyancy of the main body. This is accomplished by pumping an incompressible fluid from a reservoir within the enclosure to a bladder outside of the enclosure. A buoyancy engine was chosen as the method of propulsion based on its successful use in other profiling systems such as Argo floats and gliders (Davis, Eriksen, & Jones, 2003). The hydraulic components required to build the system are used reliably in various industrial applications and are readily available. The hydraulic diagram representing the buoyancy engine designed for the profiler is illustrated in Figure 43. It consists of the following components.

1. An internal reservoir to store hydraulic fluid
2. A motor and pump to push hydraulic fluid through the system
3. Check valves to restrict flow to a single direction
4. Solenoid valves to control flow through the system
5. An accumulator to store hydraulic energy
6. A pressure relief valve to protect the system
7. An expandable/collapsible external bladder to store hydraulic fluid
8. Tubing to connect components and direct hydraulic fluid through the system

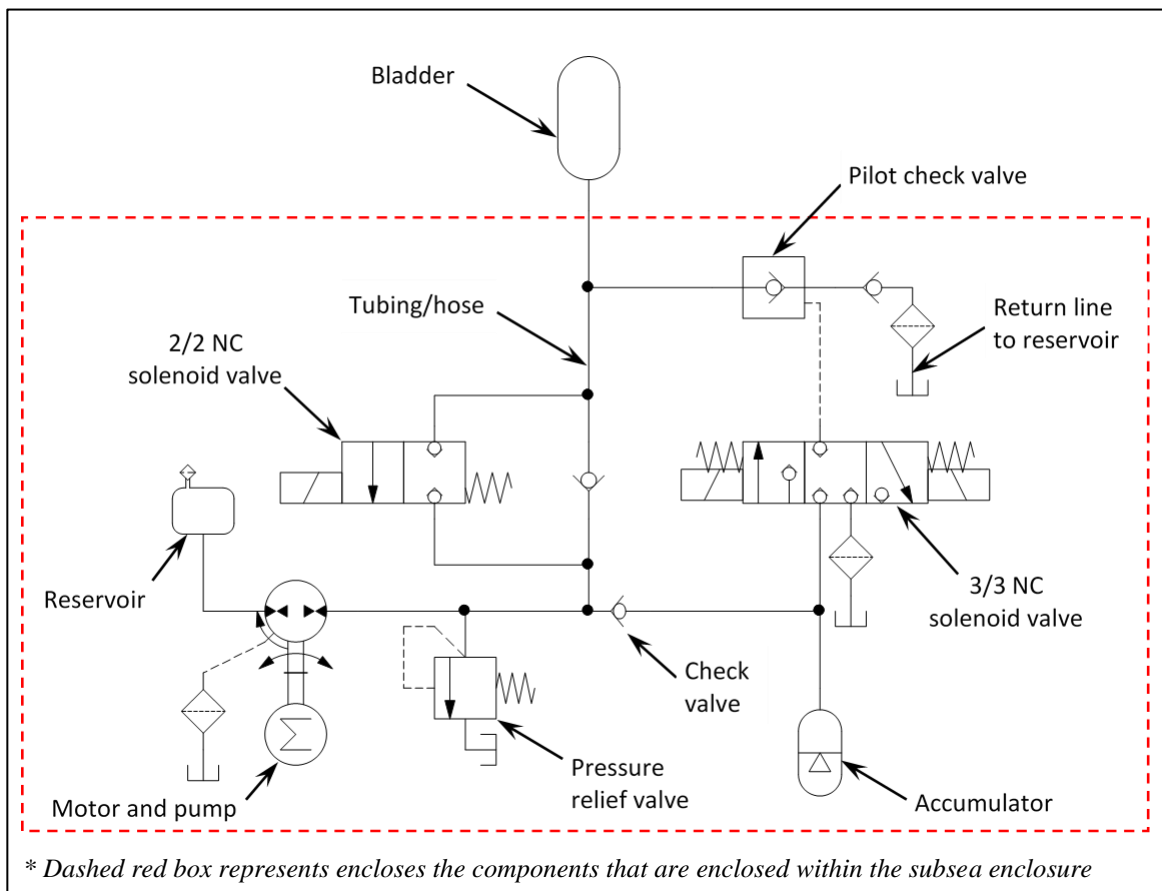


Figure 43 Buoyancy engine hydraulic circuit

This particular arrangement of hydraulic components allows the profiler to operate through the ascent and descent cycle while only requiring hydraulic fluid to be pumped into the external flexible bladder to ascend. At the top of the ascent, the bladder will be located approximately 10 m below the surface. At this depth, there is approximately 1 bar of gauge pressure acting on the exterior of the bladder. The internal reservoir will be at approximately 0 bar (gauge). This pressure differential will cause the oil to flow from the bladder to the reservoir when a pathway is opened. Eliminating the requirement to pump the oil back into the reservoir reduces the energy requirement of the profiler.

5.4.1.1 Operation of the Hydraulic Circuit

To initiate the profiler's primary ascent from its hibernation position at the bottom of the mooring line the pump begins to pressurize and fill the bladder. The pressure required is equivalent to the pressure generated at the submerged depth of the bladder; approximately one bar for every ten meters. No power is supplied to the solenoid valves during the initial ascent therefore they maintain their normally closed (NC) state. The check valves and solenoid valves direct the high pressure oil into the bladder and accumulator. The high pressure lines and components of the hydraulic system are highlighted red in Figure 44.

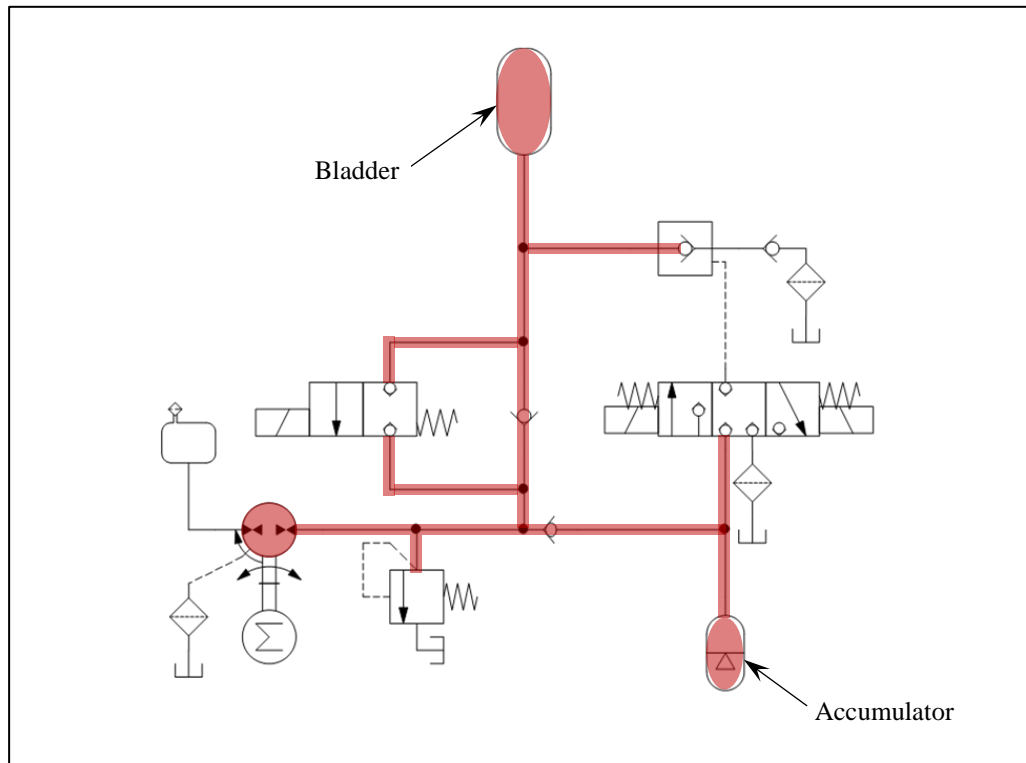


Figure 44 Hydraulic circuit during the primary ascent with the high pressure lines and components highlighted red

Once the required quantity of oil has been pumped into the bladder, the profiler will continue through the primary ascent and then through the secondary ascent to allow the sensor float to breach the surface. At this point the pressure in the bladder and connected tubing has decreased to an intermediate value since it depends on the external water pressure which is now approximately 1 bar (gauge). The oil is trapped in the bladder by a check valve, the pilot operated check valve, and the de-energized 2/2 NC solenoid valve. A check valve and the de-energized 3/3 NC solenoid valve trap high pressure oil in the accumulator. The oil pressure in the accumulator maintains a high pressure because the valves isolates it from the bladder pressure. The intermediate and high pressure lines and

components in the hydraulic circuit are highlighted orange and red, respectively in Figure 45.

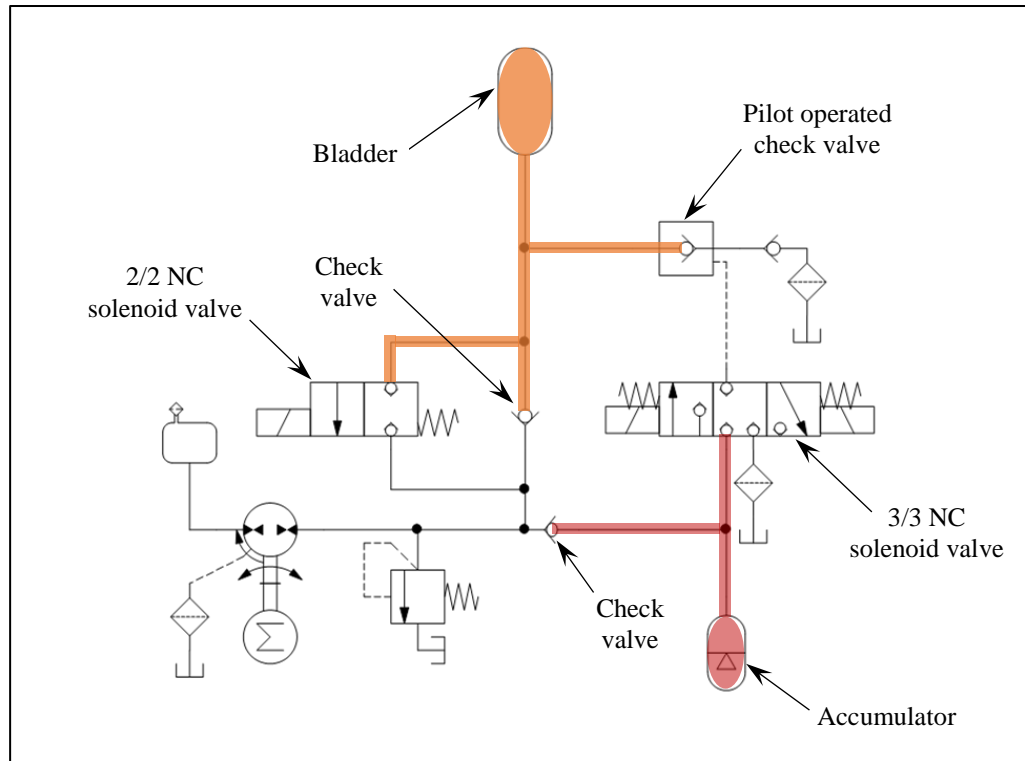


Figure 45 Hydraulic circuit after completion of the primary and secondary ascent with the intermediate (orange) and high pressure (red) lines and components highlighted

To allow the profiler to descend back to its hibernation position at the bottom of the mooring line, the oil in the bladder is drained back into the internal reservoir. This is accomplished by using the hydraulic energy stored in the accumulator to open the pilot operated check valve via the 3/3 NC solenoid valve. Energizing the left side of the solenoid valve allows the high pressure fluid in the accumulator to flow through to the pilot operated check valve. The high pressure in the pilot opens the check valve which

opens a pathway to allow the intermediate pressure fluid in the bladder to flow back to the internal reservoir. It is not necessary to keep the solenoid valve energized until the bladder is completely drained. This is another energy economizing feature of the hydraulic circuit. Deenergized, the solenoid returns it to the closed position trapping the high pressure fluid in the pilot. This keeps the pilot operated check valve open to allow the bladder to continue draining. Therefore, the solenoid only needs to be temporarily energized. The intermediate pressure and the high pressure lines and components in the hydraulic circuit are highlighted orange and red, respectively in Figure 46.

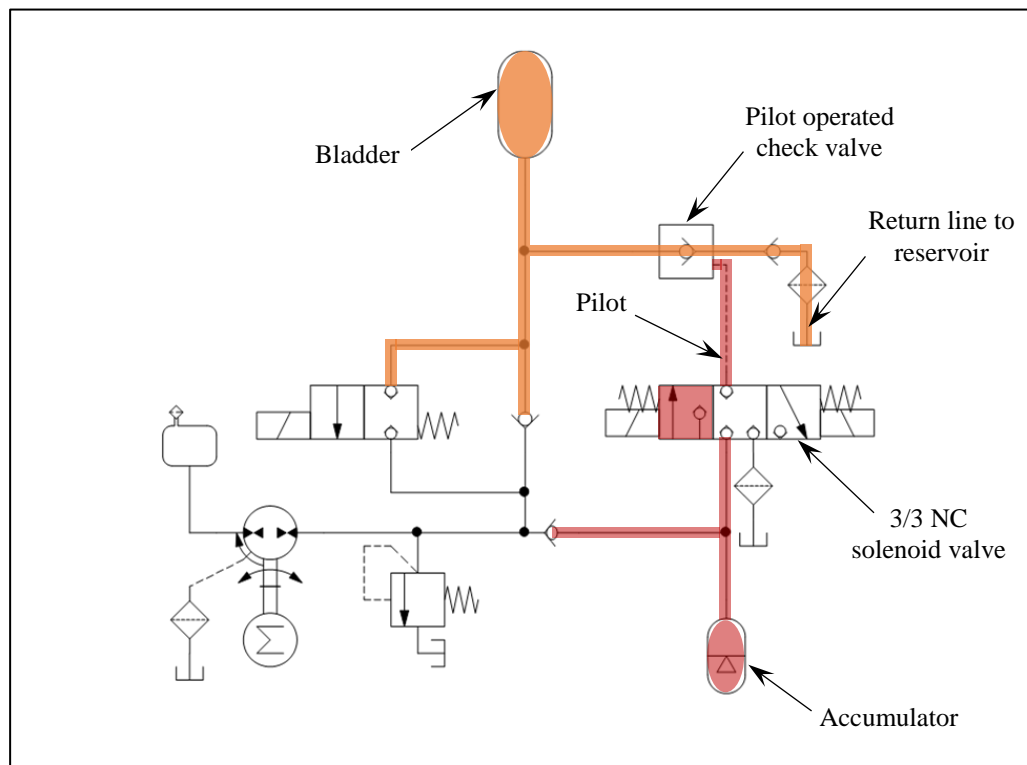


Figure 46 Hydraulic circuit when draining the bladder with the intermediate (orange) and high pressure (red) lines and components highlighted

When the profiler has descended back to the bottom of the mooring the pilot operated check valve is still being held in the open position due to the high pressure oil trapped in the pilot line. Oil will be pumped back into the reservoir rather than the bladder on the next ascent cycle if the pilot operated check valve is not closed. The pilot operated check valve is closed by relieving the pressure in the pilot line. Temporarily energizing the right side of the 3/3 NC solenoid valve opens a pathway for the high pressure oil to flow back to the internal reservoir. This reduces the pressure in the pilot and results in the pilot operated check valve closing. The low pressure pilot line and components are highlighted in green in Figure 47.

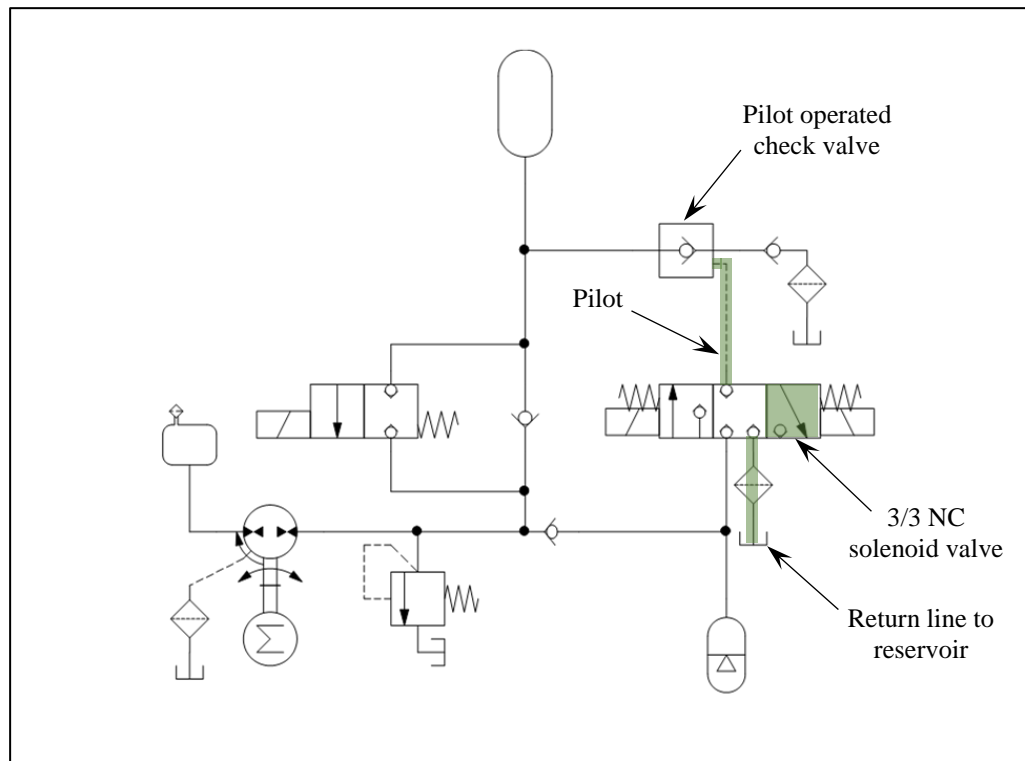


Figure 47 Hydraulic circuit to relieve pressure from the pilot operated check valve

The hydraulic circuit also allows for a redundant emptying process which is achieved by pumping the oil out of the bladder and back into the internal reservoir. Reversing the rotation of the bi-directional pump reverses the direction of flow. To drain the oil from the bladder via the pump, it needs to be rotated in the opposite direction and the 2/2 NC solenoid valve must be energized to allow the flow to bypass the check valve. This method requires the solenoid valve and pump to be powered until the bladder is completely empty. Since this is a much more energy intensive process, it is only intended to be used for emergency and testing purposes. The intermediate pressure lines and components of the hydraulic circuit are highlighted orange in Figure 48.

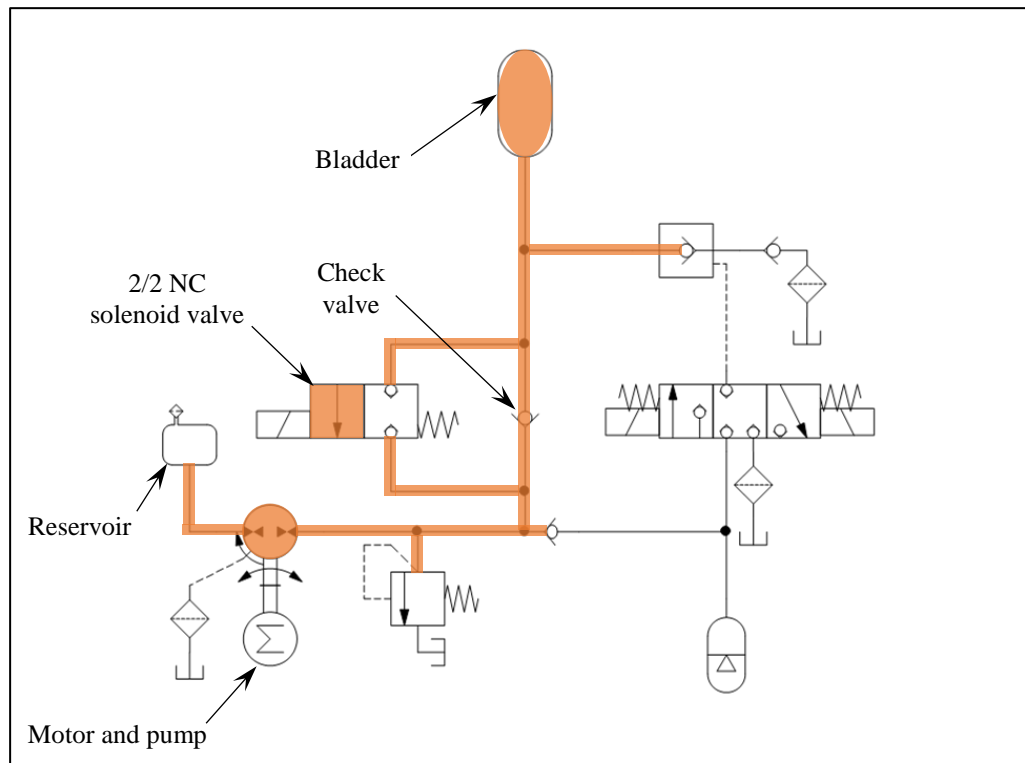


Figure 48 Hydraulic circuit to pump oil from the bladder to the reservoir

5.4.1.2 Buoyancy Engine

The final design of the buoyancy engine is shown in Figure 49. Detailed fabrication drawings are available in Appendix B, pages 324-350 and 392-393, and Appendix E, pages 417-426. Aside from the external bladder, the hydraulic and electronic/electrical components of the buoyancy engine are contained and protected inside the subsea enclosure. Two bulkhead connectors on the bottom of the enclosure allow for a connection to the electromechanical cable and the power source. A bellow type bladder is connected at the top of enclosure where it is constrained and protected by a cage.

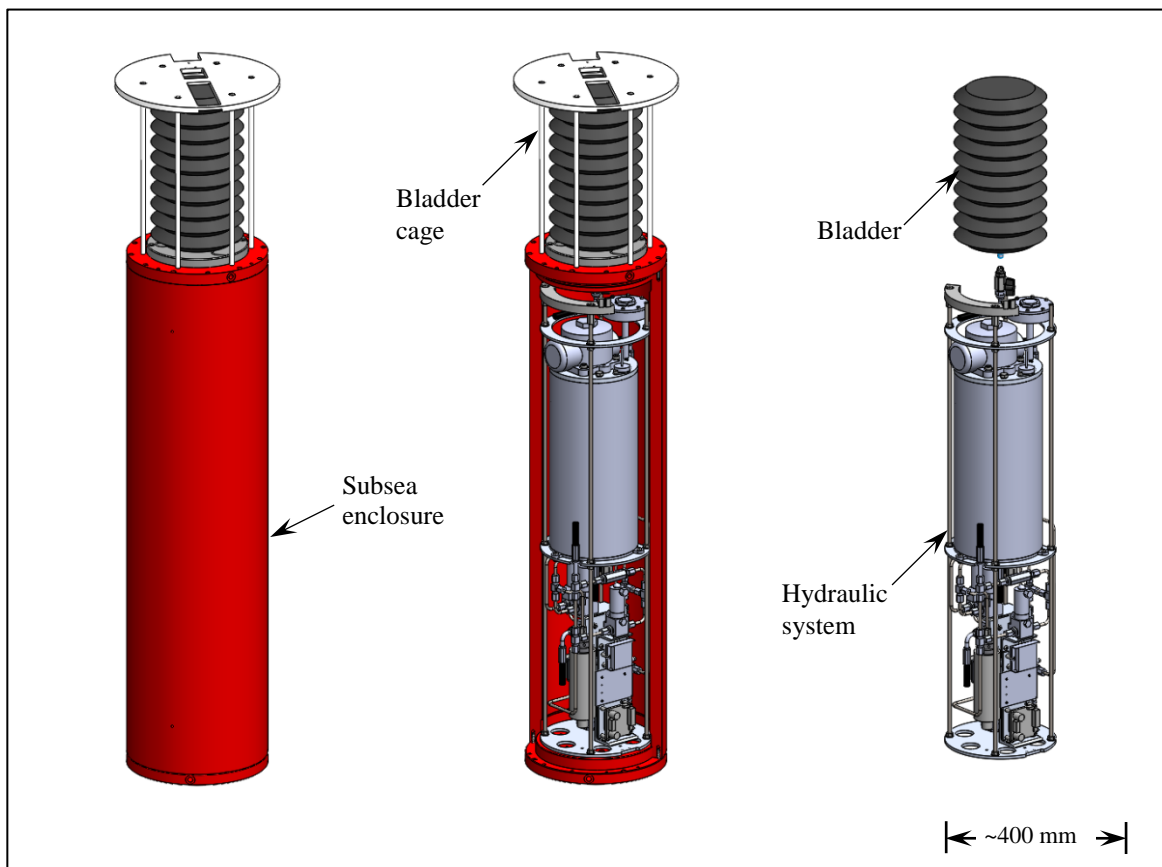


Figure 49 Buoyancy engine with enclosure sectioned and hydraulic system separate

The buoyancy engine was designed through a systematic process similar to the other subsystems of the profiler. First, the components identified in the hydraulic diagram were sourced and purchased from vendors, or designed and fabricated. Next the off-the-shelf components were modeled in SolidWorks and arranged together with the designed components in free space to form the final assembly. Then the hydraulic system was assembled and tested to verify its operation. Finally, the subsea enclosure was sized such that the hydraulic system could be adequately contained within it.

5.4.1.3 Hydraulic Components

5.4.1.3.1 Hydraulic Pump and Motor

The pump chosen for the hydraulic system was a Takako TFH-40 bi-directional, inline axial piston pump. The specifications and performance curve for the TFH-40 pump can be found in Appendix A, pages 215-217. An axial piston pump was chosen in order to economize energy consumption. Axial piston pumps are capable of operating at a high pressure with a high overall operational efficiency (Eaton Fluid Power Training, 2010). As indicated by the performance curve, the TFH-40 has a maximum overall efficiency of 85% when operating at 100 bar. When operating at the expected 20 bar (~200 m) the overall efficiency is 67%.

The TFH-40 pump was also selected based on its small size. The linear dimensions of the pump are 77 mm × 30 mm × 30 mm. Compare to axial piston pumps typically used in other industrial application, the TFH-40 is diminutive. The small physical size of the

pump minimizes the space required for the hydraulic system and subsequently the subsea enclosure.

The small physical size of the pump also translates into a small volumetric displacement. The TFH-40 pump has a volumetric displacement of 0.4 cm³ per revolution. The volumetric displacement along with the mechanical efficiency and maximum operating pressure results in a maximum input torque specification of 0.9 N·m. This torque can be produced by a small direct drive DC motor. A pump requiring a higher torque would need to use a motor with a gear reduction. The gear reduction would decrease the systems efficiency and therefore require more power.

The motor that drives the pump must be able to deliver the torque and power required by the pump. The input torque (M) required by the pump is determine from Equation 5.21 (Hatami , 2013). It is dependent on the pumps volumetric displacement (V), the operating pressure (p), and the mechanical efficiency (η_m).

$$M = \frac{1.59 \cdot V \cdot p}{100 \cdot \eta_m} \quad (5.21)$$

The input power (P) required by the pump is determined from Equation 5.22 (Hatami , 2013). It is dependent on the pumps flow rate (Q), the operating pressure (p), and the overall efficiency (η_o).

$$P = \frac{Q \cdot p}{600 \cdot \eta_o} \quad (5.22)$$

The pump flow rate (Q) is determined from Equation 5.23 (Hatami , 2013). It is dependent on the volumetric displacement (V), the operating speed (N), and the volumetric efficiency (η_v).

$$Q = \frac{V \cdot N \cdot \eta_v}{1,000} \quad (5.23)$$

Based on an operating pressure of 20 bar (~200 m), and applying the THF-40 pump specification, the torque and power required by the pump are 0.18 N·m and 39.8 W, respectively. Table 9 summarizes the variables for, and the results from Equations 5.21, 5.22, and 5.23.

Table 9 THF-40 pump input torque and power requirements

| | |
|---------------------------------------|---------------------|
| Operating pressure, p | 200 bar |
| Volumetric displacement, V | 0.4 cm ³ |
| Pump speed, N | 2,000 RPM |
| Mechanical efficiency, η_m | 67 % |
| Volumetric efficiency, η_v | 100% |
| Overall efficiency, η_o | 67% |
| Pump flow rate, Q | 0.8 l/min |
| Input Torque, M | 0.18 N·m |
| Input Power, P | 0.398 kW |

Through consultation with technical personnel at Anaheim Automation the BLWS234D-36V-4000 brushless DC motor was selected to power the hydraulic pump. The specification sheets for the motor is available in Appendix A, pages 218-219. The rated voltage, speed, power, and torque of the motor are 36 V, 4,000 RPM, 134 W, and 45.32 oz·in (0.32 N·m), respectively. The application for the hydraulic system requires the

pump to run at a maximum voltage of 24 VDC and at a maximum speed of 2000 RPM.

The Torque vs. Speed plots displayed in Figure 50 indicates that at 24 VDC the motor can deliver the required 0.18 N·m (25.5 oz·in) of torque at a speed of 2800 RPM. The speed of a DC motor decreases with an increase in torque (Guru & Hiziroglu, 1995). Therefore, the selected motor will have additional torque capacity when operating at 24VDC and 2000 RPM. Extrapolation of the 24 VDC Torque-Speed line to the 2000 RPM point gives a torque of 1.17 N·m (165 oz·in). This is more than sufficient to deliver the 0.26 N·m (36.8 oz·in) of torque required by the pump if operating at 30 bar (~300m) of pressure. As well, the torque required from the motor is less than the rated torque of 0.32 N·m (45.32 oz·in). Therefore, the motor can run continuously without overheating.

Through interpolation between the 24 VDC and 12 VDC Torque-Speed lines, it was determined that the voltage at the 2000 RPM and 0.18 N·m (25.5 oz·in) point is 18 VDC. Given the torque constant for the motor is 8.5 oz·in/A the motor is expected to draw 3 A to deliver a torque of 0.18 N·m (25.5 oz·in). The resulting power required by the motor will be 54 W. As indicated earlier, the power required by the pump is 39.8 W therefore the motor is operating at 73.7% efficiency. Ideally a brushless DC motor with a better efficiency would be used. Brushless DC motors are capable of efficiency in the range of 85%-90% (Telco Intercontinental Corp., 2016). A more exhaustive search or purpose-built motor could improve the efficiency. A 90% efficient DC motor would only require 44.2 W to power the pump when delivering 20 bar of pressure.

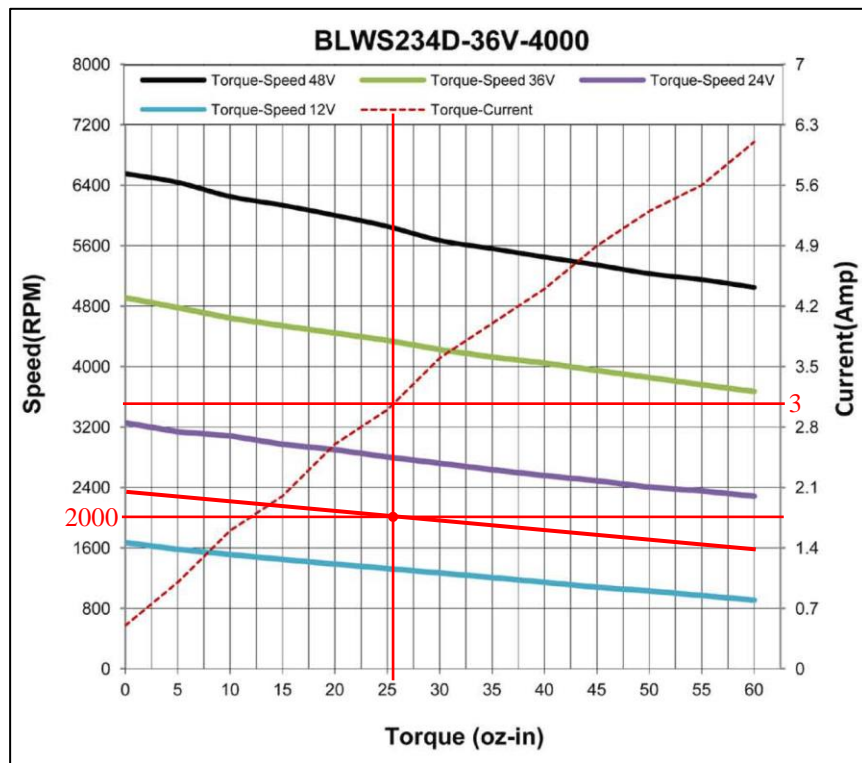


Figure 50 BLWS234D-36V-4000 torque vs. speed plot with 25.5 oz-in, 2000 RPM, and 18VDC lines (solid red) added (Anaheim Automation, 2016)

Figure 51 illustrates the motor and pump assembly for the hydraulic system. Three key components aside from the pump and motor are the manifold, the shaft coupling, and the encoder. The THF-40 pump is not supplied with a manifold for directing the flow out of or into the pump. The manifold shown was designed and fabricated to accept hydraulic fittings to connect the inlet, outlet, and drain line of the pump to the hydraulic system. The flexible helical shaft coupling joins the motor to the pump. The Ruland PCR12-1/4"-6MM-H shaft coupling accommodates parallel (0.20 mm), angular (3°), and axial (0.13 mm) misalignment between the shafts. The 0.79 N·m torque and 6000 RPM speed rating meet the demand from the application. The coupling also produces no backlash therefore

it can be used for encoder applications. The detailed product specification sheet for the shaft coupling is available in Appendix A, page 220. The CUI Inc. AMT110 Modular Incremented Encoder is mounted to the shaft at the bottom of the motor. The encoder monitors the speed, position, and number of revolutions of the shaft. This data is used by the RoboteQ SBL1330 motor controller to control the speed of the motor. The product data sheets for the encoder and controller are available in Appendix A, pages 221-228. Controlling the motor speed and duration determines the volume of oil pumped. The flow of a positive displacement pumps is dependent on the volumetric displacement and is independent of pressure (Eaton Fluid Power Training, 2010). This characteristic allows control of the total pumped volume by dividing the required volume by the volumetric displacement to determine the number of revolutions required from the motor/pump. Once the count equals the number of revolutions, the motor is stopped.

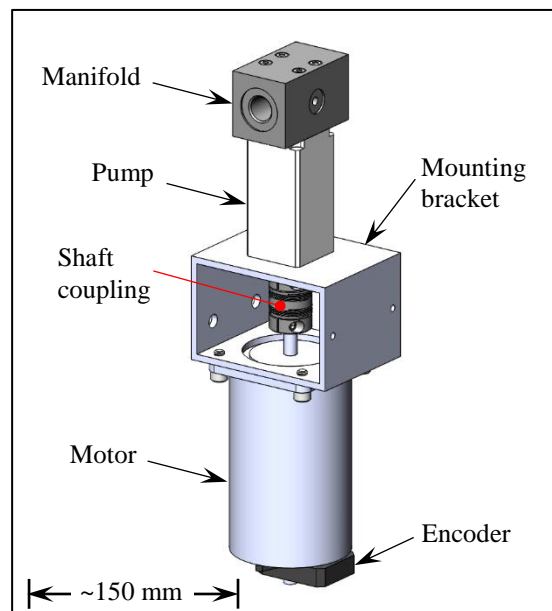


Figure 51 Pump and motor assembly

5.4.1.3.2 Hydraulic Oil Selection

The TFH-40 pump specifications indicate that the acceptable viscosity range of the fluid is 15 to 370 cSt while the suitable viscosity range is 20 to 160 cSt. This information was used to select the hydraulic oil for the profiler. The oil selected is ISO 15 Bio-MIL-PRF-32073 from Renewable Lubricants. The product data sheet is available in Appendix A, pages 231-232. The viscosity specifications for the oil are 170 cSt at -15°C, 14.18 cSt at 40°C, and 3.81 cSt at 100°C. The specified operating temperature range for the profiler is -5°C to 30°C. To verify the viscosity at these temperatures the specification points for the oil were plotted with a vertical viscosity axis in the logarithmic scale (Figure 52). The logarithmic scale causes the characteristic curve for most hydraulic fluids to become linear (Hunt & Vaughan, 1998). The plot indicated that the oil viscosities for -5°C and 30°C are 108 and 22 cSt, respectively. These values are within the suitable viscosity range for the TFH-40 pump. Aside from meeting the viscosity specifications, the selected oil is a biodegradable biosynthetic fluid intended for use in environmentally sensitive areas. Given the fact that the profiler will be operating in a marine environment, practicing sound environmental stewardship is a responsibility.

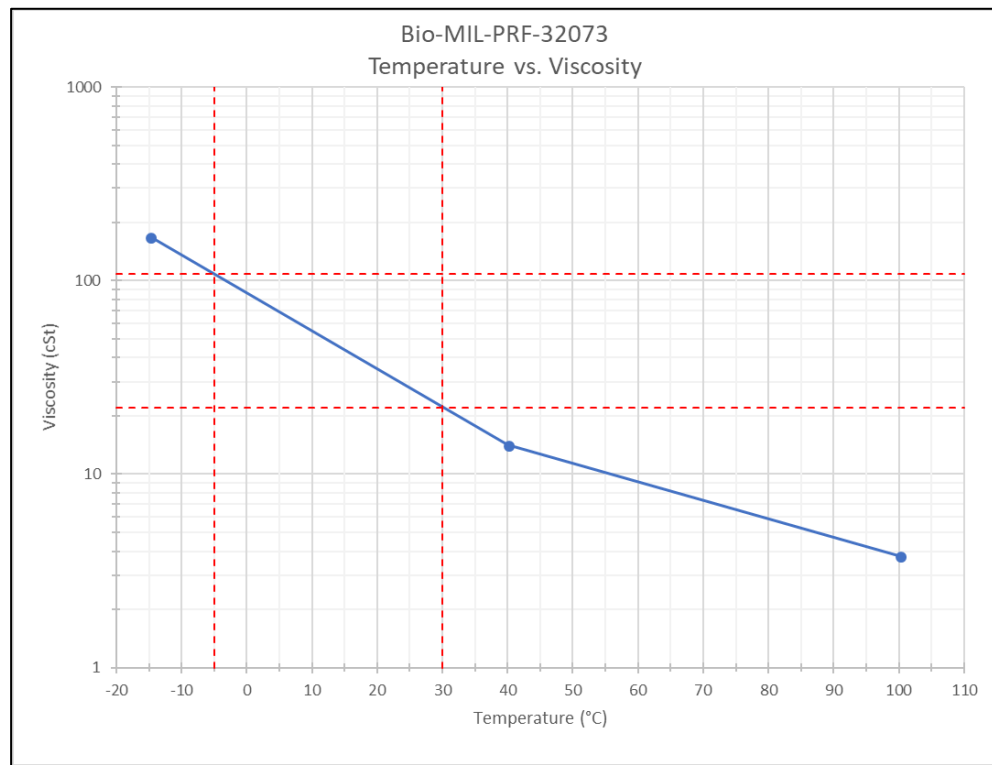


Figure 52 Bio-MIL-PRF-32073 temperature vs. viscosity plot

5.4.1.3.3 Hydraulic Valves Selection

The valves in the hydraulic system were selected based on their compatibility with the viscosity range of the oil (108 cSt to 22 cSt) and their ability to function at the operating pressure (20 bar) and flow rate (0.8 l/min) of the of the pump. The solenoid valves were also selected against the additional criteria of the operating voltage (24 VDC maximum). All the valves were selected from the Hawe Hydraulik product line. Poppet style valves were chosen over spool valves to guarantee against internal leaks within the valve (Parambath, 2016). An internal leak could result in the accumulator depressurizing and thus become unable to activate the pilot operated check valve to drain the bladder.

The specification sheets for the valves used in the hydraulic system are available in Appendix A, pages 233-243. The valves used in the hydraulic system are as follows.

- One MV41 F R-250 pressure relief valve. The valve can operate at 700 bar with a flow through of 20 l/min. The pressure relief is set at 25 bars and can be manually adjusted from 0-80 bar. The optimal viscosity range of the oil is 10 cSt to 500 cSt.
- Three B2-1 check valves. The valves can operate at 500 bar and a flow through of 15 l/min. The optimal viscosity range of the oil is 10 to 500 cSt. The valve opening pressure is 0.4 - 0.5 bar therefore it will function under the minimum expected system pressure of 1 bar (~10 m) which is during the draining process.
- One G 21-0-1/4-G24 directional control 3/3 normally closed solenoid valve. The valve can operate at 500 bar and a flow through of 6 l/min. The optimal viscosity range of the oil is 10 to 200 cSt. The solenoid operates on 24 VDC and has a 16 W maximum power consumption.
- One G R2-0-1/4-G24 directional control 2/2 normally closed solenoid valve. The valve can operate at 500 bar and a flow through of 6 l/min. The optimal viscosity range of the oil is 10 to 200 cSt. The solenoid operates on 24 VDC and has a 16 W maximum power consumption.
- One RH-2 pilot operated check valve. The valve can operate at 700 bar and a flow through of 35 l/min. The optimal viscosity range of the oil is 10 to 500 cSt. The volume of oil required to fully open the valve is 0.25 cm³. Since the valve is opened to drain the bladder when the profiler is at the top of the mooring line the

conservatively estimated pressure in the line connected to the valve is 2 bar. A worse case scenario could put the line pressure at 5 bar (p_A). This will require a pilot pressure of 13 bar to initially open the pilot operated check valve (Figure 53). The 13 bar (opening pressure is less than the 20 bar that can be generated and stored in the accumulator when at 200 m depth. Therefore, the valve is adequate for the hydraulic system. To keep the valve fully open a pilot pressure (p_{st}) of 10.6 bar is required as determined by Equation 5.24 (Hawe Hydraulik, 2017). It is dependent on the outlet pressure (p_B), the pressure drop across the valve (Δp), and the pressure constant of the valve (k). The valve specifications for the pressure drop and pressure constant are 0.5 bar and 10 bar, respectively. An outlet pressures of 0.1 bar is based on a maximum expected hydrostatic head of 1m.

$$p_{st} = p_B + \Delta p + k \quad (5.24)$$

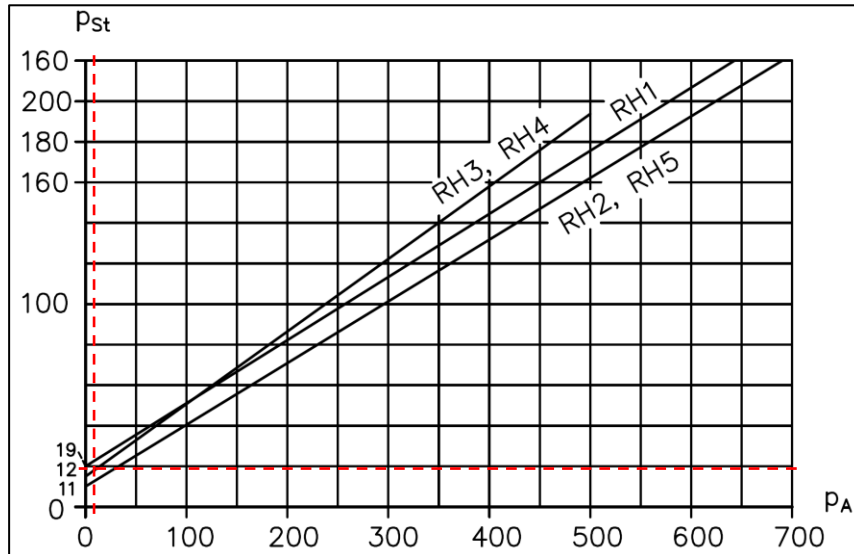


Figure 53 RH-2 pilot pressure vs. line pressure with the 2 bar line pressure overlay (Hawe Hydraulik, 2017)

5.4.1.3.4 Accumulator Selection

The accumulator for the hydraulic systems was selected based on its ability to deliver 0.25 cm³ of oil at a pressure of 13 bar to the RH-2 pilot operated check valve. The compatibility with the viscosity range of the oil (22 to 108 cSt) and the ability to function at the operating pressure (20 bar) were also considered. A Hawe Hydraulik AC13-10 miniature accumulator was selected. The AC-13-10 is a diaphragm style accumulator with a rated volume of 13 cm³ and a nitrogen pre-charge pressure of 10 bar. The specification sheets for the accumulator are in Appendix A, pages 244-245.

To verify that the AC-13-10 miniature accumulator is capable of operating the RH-2 check valve its 13 cm³ rated volume specification was compared against the required rated volume (V_0) determined from Equation 5.25 (Sizing Accumulators, 2013).

$$V_0 = C_a \frac{\Delta V}{\left(\frac{p_0}{p_1}\right)^{1/n} - \left(\frac{p_0}{p_1}\right)^{1/n}} \quad (5.25)$$

The rated volume depends on several factors. The amount of oil required from the accumulator (ΔV) is the 0.25 cm³ of oil demanded by the pilot operated check valve. The minimum working pressure (p_1) of the accumulator is the 13 bar of pressure required to open the pilot operated check valve. The maximum working pressure (p_2) of the accumulator is the 20 bar of pressure developed by the pump when the profiler is at its nominal operational depth (200 m). A pre-charge pressure (p_0) of 10 bar was selected based on the suggested criteria of being less than 90% of the minimum working pressure.

The gas expansion process (n) is 1.4 based on an expected adiabatic process due to the fast change in volume when opening the pilot operated check valve.

Based on the variables listed and summarized in Table 10, 1.42 cm^3 is the required rated volume of the accumulator. This is less than the 13 cm^3 available, therefore the AC 13-10 is adequate for the system. Using the same assessment formula, it was determined that 13.6 bar (136 m) is the minimum operating pressure that the accumulator can operate the pilot operated check valve. The specifications for the AC 13-10 product line also indicates that for an adiabatic process the maximum working pressure should not exceed three times the minimum working pressure. Given the minimum working pressure is 13 bar the maximum working pressure should not exceed 39 bar. The maximum operating pressure of the profiler is 30 bar ($\sim 300\text{m}$). Therefore, the maximum working pressure will not exceed its limit.

Table 10 Accumulator rated volume variables and results

| | |
|---|---------------------------------------|
| Oil required from the accumulator, ΔV | 0.25 cm^3 |
| Accumulator pre-charge pressure, p_0 | 10 bar |
| Minimum working pressure, p_1 | 13 bar |
| Maximum working pressure, p_2 | 20 bar |
| Gas expansion process, n | 1 (adiabatic) |
| Pressure ratio, p_2/p_1 | 1.54 |
| Correction factor, C_a | 1.25 |
| Rated Volume, V_0 | 1.42 cm^3 |

5.4.1.3.5 Pilot Operated Check Valve and Accumulator Design

The RH-1 pilot operated check valve identified in Sections 5.4.1.3.3 is not suitable for low pressure bench testing and shallow water field trials planned for water depths of 25 to 50 m. The 11 bar minimum cracking pressure of the check valve is greater than the 5 bar of pressure that will be produced by the pump when the profiler is at a depth of 50 m. Due to the typical high pressure application of hydraulics, there were limited options for a replacement pilot operated check valve with a suitable cracking pressure.

The pilot operated check valve was replaced with a Versa two way, normally closed, BSP-208 pilot operated check valve for bench testing and field trials. The specification sheets for this valve is available in Appendix A, page 246. The valve is suitable for hydraulic applications where the pressure does not exceed 34.5 bar (500 psi). A pilot pressure of 2.5 bar (36 psi) can open the valve with a line pressure up to 13.8 bar (200 psi), therefore the valve is suitable for a 25 m deep (or greater) field test.

The Versa valve requires 18.4 cm^3 (1.12 in^3) of oil to fully open which is a greater quantity than the 13 cm^3 capacity of the AC-13 accumulator. Therefore, another accumulator was required to meet the demand of the Versa valve. Again, due to the typical high pressure application of hydraulics there were no options identified for an off-the-shelf replacement accumulator. The lowest minimum pre-charge pressure of an off-the-shelf accumulators was 5 bar. This value is greater than the 2.5 bar (~25 m) operational pressure therefore the accumulator would not be able to store any hydraulic

energy. A custom spring loaded accumulator was designed and fabricated for bench testing and shallow water field trials.

The custom accumulator design is illustrated in Figure 54. The design required selecting a piston with the appropriate bore, stroke, and return spring rate to supply the required amount of oil at an adequate pressure to the pilot. It consists of a single acting hydraulic cylinder which was custom ordered without the internal return spring. An external sleeve was designed to thread onto the body of the cylinder to preload a compression spring and engage it with the cylinder's piston. As oil is pumped into the cylinder the spring compresses and hydraulic energy is stored for use with the pilot operated check valve. This design is capable of delivering 18.4 cm^3 (1.12 in^3) of oil at a pressure of 1.4 bar (20 psi) or greater when the profiler operates at a depth of 25 m. Therefore, it is suitable for low pressure bench testing and a minimum shallow water field trial of 25 meters. Details of the design calculations are available from the Custom Accumulator Worksheet in Appendix C, pages 403-405. Specifications for the Vektex cylinder and McMaster-Carr spring are available in Appendix A, pages 247-249. Fabrication drawings for the parts are available in Appendix B, pages 347-348.

It should be noted that the custom accumulator and Versa pilot operated check valve are not adequate substitutions for the originally selected accumulator and pilot check valve during regular operations. The 18.4 cm^3 of oil required by the Versa pilot operated check valves is 73.6 times greater than the Hawe (0.25 cm^3). Therefore, it would require ~75 times more hydraulic power to operate.

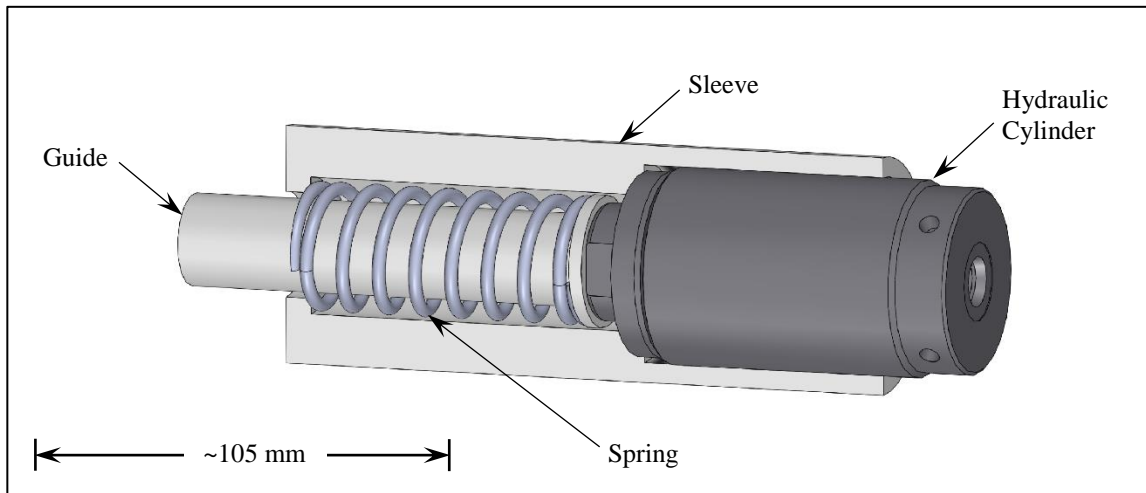


Figure 54 Custom accumulator assembly with sleeve sectioned

5.4.1.3.6 Oil Reservoir Design

The oil reservoir shown in Figure 55 was designed to hold 7.5 litres of pumpable oil. Pumpable oil refers to the quantity of oil above the protruding reservoir outlet to the pump. This protrusion into the reservoir helps to mitigate the risk of contaminants entering the system since they will tend to settle on the bottom below the level of the outlet. Three ancillary components of the reservoir are the filter unit, oil level sensor, and the breather vent. Detailed fabrication drawings for the hydraulic reservoir and breather vent are available in Appendix B pages 336-342.

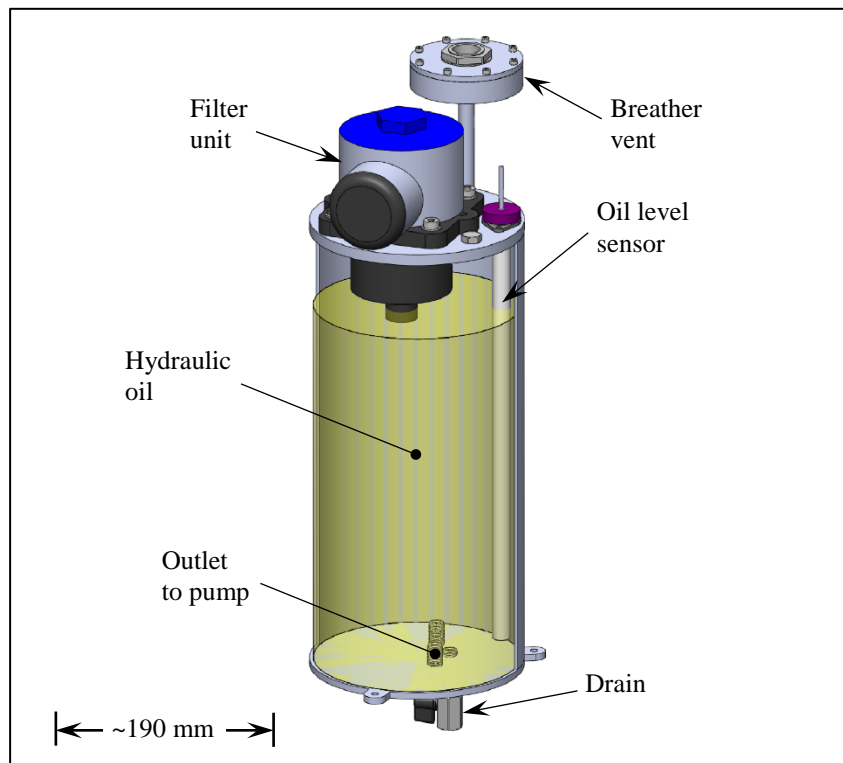


Figure 55 Hydraulic reservoir with the sidewall sectioned

5.4.1.3.6.1 Filter Unit Selection

An oil filter is required to protect the hydraulic system. The filter unit is located in the return line at the top of the hydraulic reservoir. All of the hydraulic oil passes through the filter before returning to the reservoir. If contaminants are not removed from the oil it can cause wear and damage of components and block flow creating a loss of lubrication. The results cause a degradation of system and component performance or outright system failure (Eaton Fluid Power Training, 2010).

The filter unit selected was a Donaldson K040811. It was chosen based on its ability to fit the reservoir and to house the required filter element. The filter element was selected

based on the requirement of the axial piston pump. The pump is the system component most sensitive to contamination. The recommended ISO 4406 contamination code for an axial piston pump is 18/16/14 (Donaldson Company, Inc., 2017). ISO 4406 expresses the degree of oil contamination, and the 18/16/14 designation indicates the quantity of particles greater than 4 μm , 6 μm , and 14 μm in one millilitres of oil. The filter element selected to satisfy the filtration requirement was a Donaldson Synteq Synthetic P171525. The filter has a beta performance rating of $\beta_{11(c)} = 1000$ as per ISO 16889 test standards (99.9% of particles $\geq 11 \mu\text{m}$ removed). It is suitable for the application because it exceeds the $\beta_{12(c)} = 1000$ synthetic filter performance. This is indicated by the red overlaid 18/16/14 line in the application guideline chart being above the $\beta_{12(c)}$ line, as illustrated in Figure 56. The filter element also has $\beta_{<4(c)} = 200$ and $\beta_{10(c)} = 200$ performance ratings which satisfies the $\beta_{7(c)} = 200$ and $\beta_{10(c)} = 200$ recommended performance ratings for axial piston pumps (Donaldson Company, Inc., 2017). The specification sheets for the filter unit and element are available in Appendix A, pages 250-256.

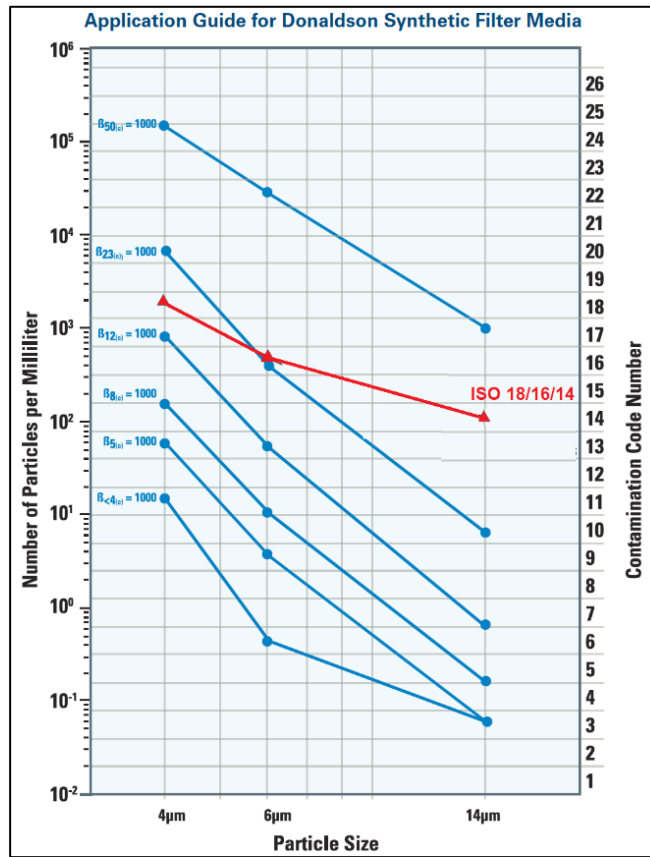


Figure 56. Filter application guideline chart (Donaldson Company, Inc., 2017).

5.4.1.3.6.2 Custom Breather Vent Design

The profiler's hydraulics system uses an open reservoir design. The open design means that it must be able to exchange the air in the reservoir with air outside the reservoir for the oil to flow properly. As oil is pumped out of the reservoir air needs to be let in, and as oil is drained back into the reservoir air needs to be let out. Otherwise, an excessive vacuum pressure that exceeds the suction pressure of the pump can form while pumping oil out. Excessive positive pressure that equals the flow generating bladder pressure can develop when draining oil back in the reservoir causing the flow to stop.

The filter unit selected for the profiler has a filtered breather vent that is incorporated into the design. Unfortunately, this breather vent does not keep oil from leaking out of the reservoir if the breather vent is located below the oil level of the reservoir. Typical hydraulic applications would not subject the breather vent to such a condition. However, it is reasonable to assume the breather vent for the profiler application could be subject to this condition. The profiler is expected to be transported and stored in a horizontal position. During deployment it could experience excessive tilting and motion that sloshes the oil in the reservoir.

The breather vent built into the filter unit was capped and a custom breather vent was designed using a Gore Polyvent XL PMF200542. The specifications are available in Appendix A, pages 257-258. The intended industrial application is for equalizing the pressure in outdoor electronic enclosures while keeping out exterior contaminants such as oil. The vent consists of an oleophobic expanded polytetrafluoroethylene membrane housed and protected in a sealable cap (Figure 57). The membrane repels and prevents the penetration of oil while allowing air to pass through it. The model selected allows a maximum of 16 l/min to pass through it at a pressure differential of 0.012 bar. Based on the pumps specified flow rate of 0.8 l/min and a minimum suction pressure of -0.1 bar (gauge), the vent is suitable for the application.

The vent must be installed such that proper side of the membrane is exposed to the oil. For the reservoir the vent must be installed such that the face with the O-ring is against an

interior surface of the reservoir. To keep the vent out of the splash zone it was mounted to the reservoir in a snorkel to position it above the top of the reservoir (Figure 55).

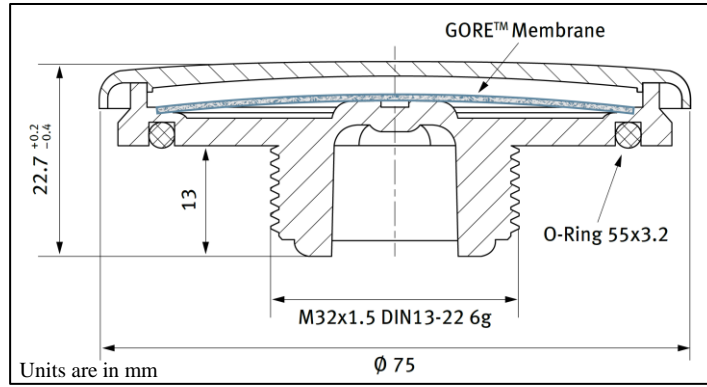


Figure 57 Gore Polyvent XL PMF200542 sectioned view (GORE, 2016)

To verify the performance of the custom breather vent the reservoir was filled with 8 l of oil and held in a horizontal position. The reservoir was also orientated such that the breather vent was at the lowest point and completely submerge below the oil. After a 64 hours there was no leakage visually detected.

5.4.1.3.6.3 Oil Level Sensor Selection

The oil level in the reservoir is a critical parameter to monitor. The oil level is directly related to the quantity of oil in the reservoir. If the amount of the oil in the reservoir is known, then the quantity of oil in the external bladder can be determined. It can also be used to detect system leaks if there is a change in level over time. The oil level sensor chosen is a Gill 4233-2TN-390-B capacitance liquid level sensor. It was selected based on its compatibility with the hydraulic oil being used, the operational voltage, a low power

consumption, and its dimensions are configurability to fit the reservoir. The specifications for the sensor are available in Appendix A, pages 259-261. As noted in the specifications, the lower 8mm of the probe does not have a linear relationship. Therefore, the length of the probe was configured such that when it is installed in the reservoir the non-linear section of the probe is positioned below the outlet to the pump. The oil can not be pumped below this level; therefore, all the sensor readings will be in the linear range.

To use the liquid level sensor to determine the volume of oil in the reservoir its voltage output was calibrated against the volume of oil in the reservoir. This was done empirically by varying the quantity of oil in the reservoir and plotting the volume of oil versus the output reading of the sensor. The volume was determined from the oil's specific gravity and the mass of oil in the reservoir. The volume is equal to the mass divided by the density. Based on the 0.88 specific gravity specification, the density of the oil is 880 kg/m^3 . The mass of the oil was determined from a bench scale.

To collect the data required for the calibration plot, the empty reservoir was placed on a scale and zeroed. Then the reservoir was filled with oil until the sensor reading was close to 100% full reading. The mass, voltage, and sensor level were recorded at this point. Increments of approximately 250 ml of oil were drained from the reservoir into a graduated beaker. After each increment, the mass, voltage, and sensor level were recorded. The mass values were converted to volume, and the sensor voltage and level readings were plotted against the reservoir volume (Figure 58). The plot indicates the relationship between the volume of oil in the reservoir and the voltage output from the

sensor. The equation of the linear line of best fit for the voltage versus the volume plot is, $y = 1.713x + 0.172$; where the reservoir volume is y and the sensor voltage is x.

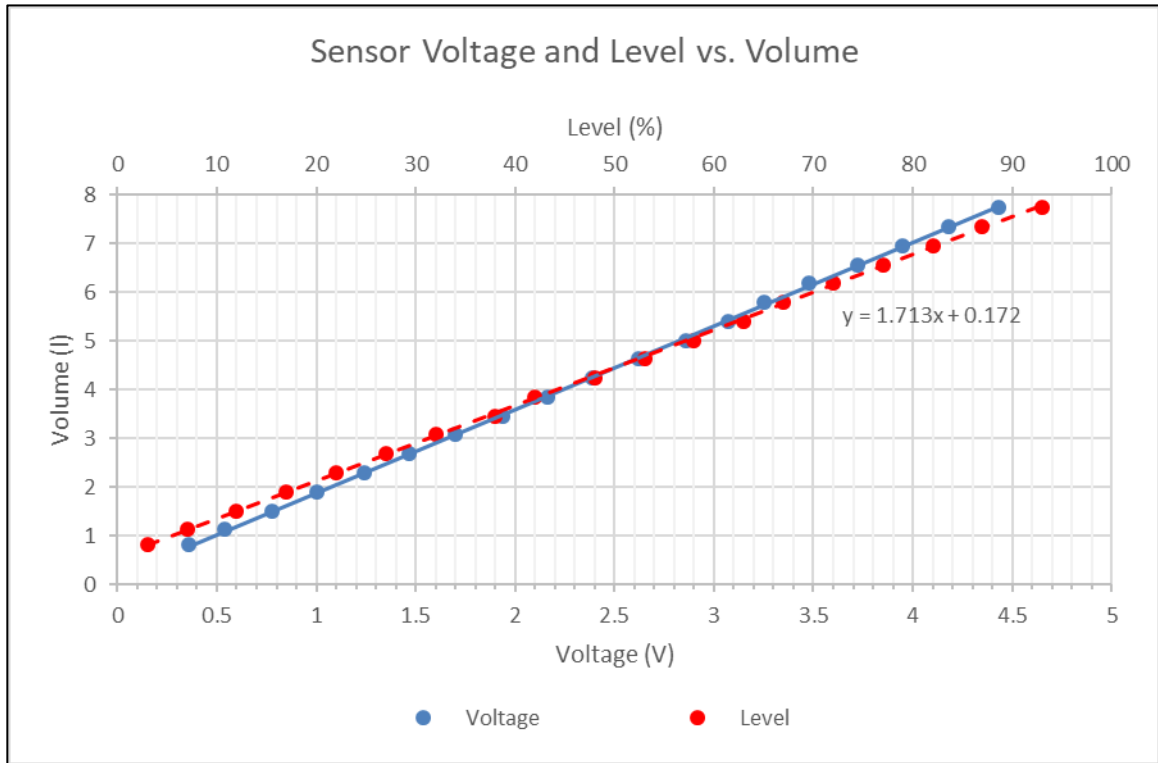


Figure 58 Sensor voltage and level vs. volume plot

5.4.1.3.7 Hydraulic System Frame Design

To provide structure, rigidity, and support to the hydraulic system a simple frame was designed (Figure 59). Detailed fabrication drawings are available in Appendix B, pages 324-335. The aluminum baseplate of the frame has through holes that allow it to be securely connected to the bottom end cap of the enclosure and for wiring to pass through it. A series of brackets attached to the baseplate provides a rigid mounting surfaces for the hydraulic, electrical, and electronic components. The four threaded rods attached to the

baseplate are also attached to an intermediate ring plate and an end ring plate to support and secure the reservoir, and to provide rigidity. Rubber inserts on the periphery of the plates fill the gap between the outside diameter of the frame and the inside diameter of the enclosure. This constrains the lateral movement of the frame within the enclosure and eliminates metal on metal contact between the frame and the enclosure.

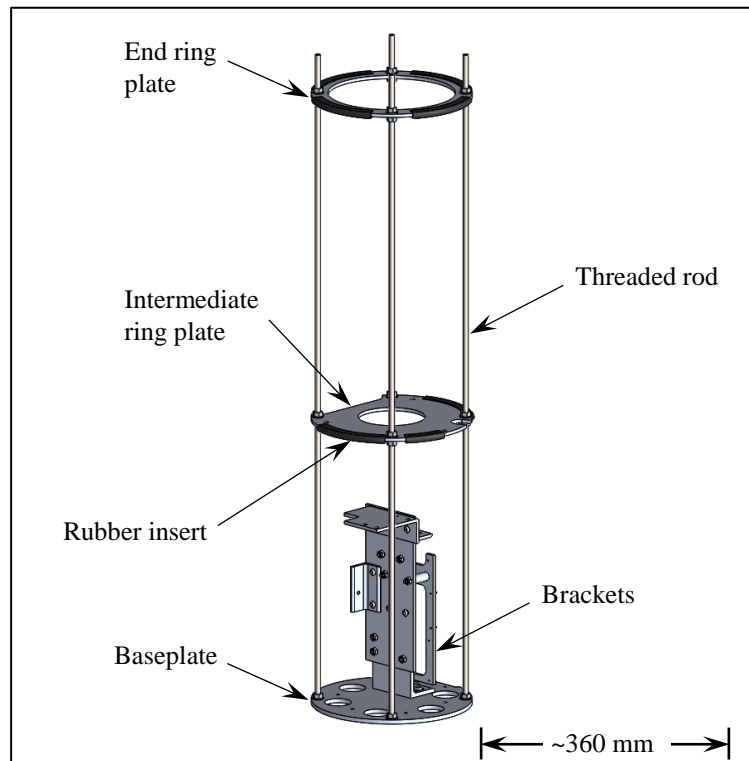


Figure 59 Hydraulic system support frame

5.4.1.4 Bladder Design

The external bladder was custom fabricated by Aero Tech Laboratories (ATL). The company specializes in the design and manufacture of bladder containment systems. They have experience making bladders for subsea operations, gliders, and Argo floats. Their

clients include Wood Hole Oceanographic Institute (WHOI) and Scrips Institute of Oceanography (SIO). The design worksheets for the bladder fabricated by ATL is included in Appendix D, pages 407-410. The final product was a bellows style bladder with a capacity to hold 8 litres of hydraulic oil. The bladder is also furnished with an SAE-4 ORB flange fitting for connecting it to end cap of the enclosure.

5.4.1.4.1 Bladder Cage Design

The bladder cage illustrated in Figure 60 is designed to contain and protect the bladder; especially when it is in the inflated state. Detailed fabrication drawing for the components are available in Appendix B, pages 389-392. The top plate constrains it from extending past its inflation limit, and the rods keep it from excessively deviating off center which could apply unwanted stress to the bottom flange and connection to the enclosure.

Threaded rods provide mechanical structure for the cage. The rods thread into the top endcap of the enclosure and bolts onto the end plate of the cage. A PTFE sleeve covers the exposed threads of the rods between the cap and end plate. All other surfaces that the bladder could potentially contact are rounded, smooth, and fabricated from PTFE or Ultra High Molecular Weight Polyethylene (UHMW). This minimizes wear and abrasion on the bladder if it rubs against these surfaces during inflation and deflation or from oscillations caused by moving water.

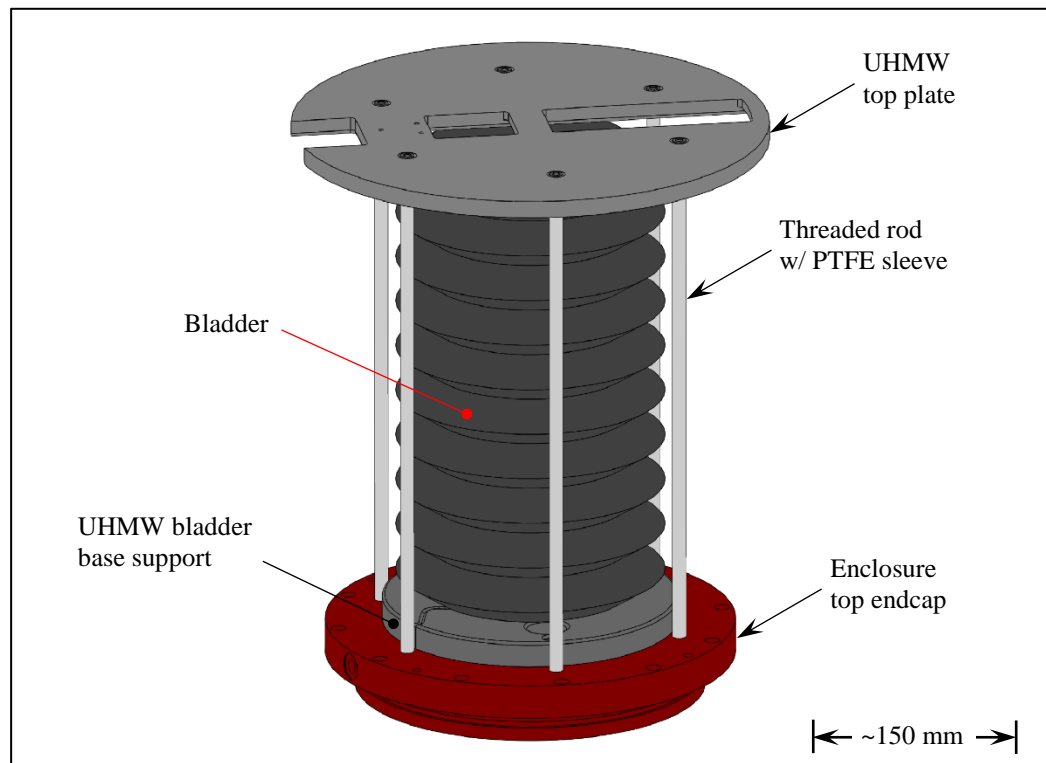


Figure 60 Bladder cage design

5.4.1.5 Subsea Enclosure Design

The subsea enclosure is designed to contain and protect the hydraulic, electronic, and electrical components. It was designed and fabricated by NV Mechanical Design based on the tender specifications available in Appendix E, pages 412-416. The detailed fabrication drawings for the subsea enclosure are also available in Appendix E, pages 417-426. The tender addresses the enclosures working environment, the seals, and the securement of the end caps. It also provides details for threaded features required to attach the bladder and bladder cage, the hydraulic system, and bulkhead connectors for the electromechanical cable and power cable.

One of the key specifications of the tender are the interior dimensions of the enclosure. The interior dimensions define the volume of the enclosure. The enclosure must have a sufficient volume to permit the pump to operate within its pressure limits, specifically the suction pressure at the inlet. The inlet suction pressure specification for pump is -0.1 to 0.3 bar (gauge).

As oil is pumped out of the reservoir and into the bladder, the air pressure decreases in the enclosure. This phenomenon is described by the ideal gas law (Equations 5.26). The law is dependent on the pressure (p), volume (V), Temperature (T), number of moles (n), and the ideal gas constant (R). Absolute pressure and temperature in degrees Kelvin must be used with the ideal gas law. Since the enclosure is a sealed system, the quantity of air does not change; i.e. n is constant. Therefore, the ideal gas law can be used to equate two states (Equation 5.27).

$$pV = nRT \quad (5.26)$$

$$\frac{p_1 V_1}{T_1} = \frac{p_2 V_2}{T_2} \quad (5.27)$$

In state 1 is the volume of air in the enclosure is at its minimum (no oil pumped into the bladder). In state 2 the volume of air in the enclosure is at it maximum (7.5 litres of oil pumped into the bladder). The enclosure must have a sufficient volume of air in state 1 such that the pressure does not drop below -0.1 bar (0.9 bar absolute) after the volume has increased by 7.5 litres. It should also be assumed the enclosure would be sealed in an environment at atmospheric pressure (1 bar absolute) and room temperature (293 °K).

When the oil is pumped out, it could be in an environment where the temperature is as low as 268 °K (-5 °C). Under these conditions, Equation 5.27 was used to determine that 450 litres of air space is required in the enclosure at state 1. The variables used are summarized in Table 11.

Table 11 Enclosure volume calculation variables

| | |
|--------------------------------------|-----------------------|
| Initial enclosure pressure, p_1 | 1 bar (absolute) |
| Final enclosure pressure, p_2 | 0.9 bar (absolute) |
| Initial enclosure temperature, T_1 | 293 °K |
| Final enclosure temperature, T_2 | 268 °K |
| Initial enclosure volume, V_1 | V_1 |
| Initial enclosure volume, V_2 | $V_1 + 7.5 \text{ l}$ |

It is not feasible or functional to use an enclosure that has an interior air volume of 450 litres. Therefore, it was decided to pressurize the enclosure in state 1 to reduce the volume of air space required. Pressurizing the enclosure to 0.2 bar (1.2 bar absolute) results in a more reasonable state 1 volume requirement of 34.1 litres.

The hydraulic system components that are housed in the enclosure require a minimum space that is 240 mm in diameter and 994 mm high. Based on the SolidWorks analytical tools, within this space the components occupy a volume of 12.7 litres. Therefore, the minimum enclosure volume required is 46.8 l. The minimum dimension specification in the tender for the enclosure were set to a 254 mm inside diameter and 1,000 mm inside length. These dimensions produce an enclosure with a satisfactory internal volume of 47.1 litres.

5.4.1.6 Hydraulic Tubing, Hoses, and Fittings

The majority of the high pressure plumbing used to connect the hydraulic components is custom bent steel tubing to allow for a compact assembly. A high pressure hose was used where flexibility was a requirement for ease of assembly; from the reservoir outlet to the pump inlet; from the main return line to the filter inlet; and from the outlet to the bladder. Flexible tubing was used to avoid fabricating complex rigid routes required for the pumps low pressure drain line, and the low pressure pilot drain line. British Standard Parallel Pipe (BSPP) and compression fittings were used to plumb the components together. A model of the hydraulic system highlighting the components, and the type of plumbing and fittings used is shown in Figure 61.

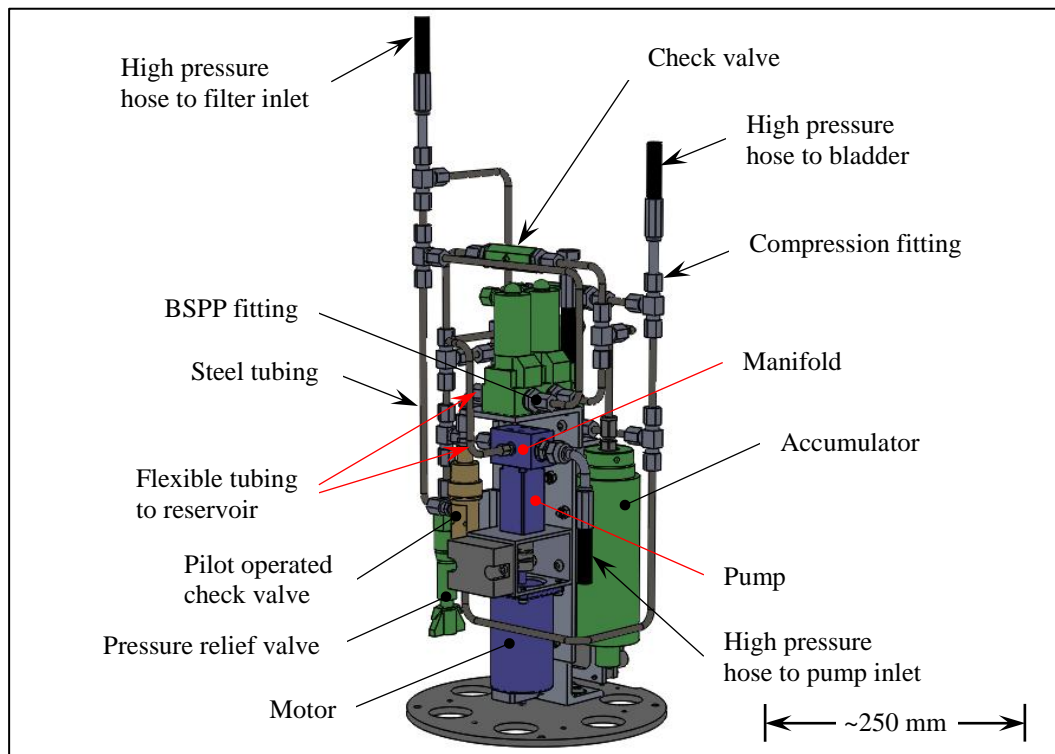


Figure 61 Assembly model of the hydraulic system

5.4.1.7 Buoyancy Engine Bench Testing

A series of validation tests were conducted on the buoyancy engine prior to installing it within the enclosure. The first test was to verify the function and reliability of the automatic drain feature using the accumulator to open the pilot operated check valve. The second test was to observe the effects of temperature change on the flow rates, and the power consumption of the pump. The third test was conducted to determine the pumps output volumes for each rotational direction.

The bench testing used a double acting hydraulic cylinder to simulate the submerged bladder (Figure 62). The cylinder was mounted vertically such that the rod end actuated upwards when oil was pumped into the lower port, and the upper port was vented to atmosphere. To simulate bladder pressure, lead weight was added to a plate attached to the rod end. The weight required to develop a desired pressure is determined by multiplying the pressure by the area of the cylinder bore. The mass is determined from dividing the weight by the acceleration due to gravity. The bore diameter of the cylinder is 50.8 mm (2 in.) and the stroke length is 152.4 mm (6 in.).

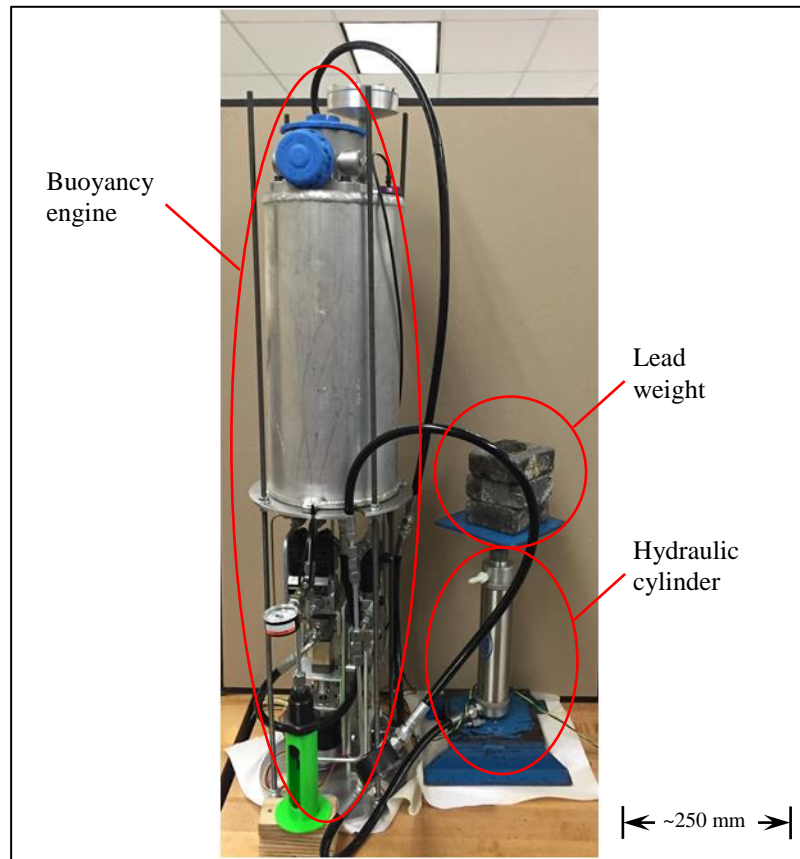


Figure 62 Buoyancy engine bench test set up with hydraulic cylinder simulating the bladder

5.4.1.7.1 Automatic Drain Functionality and Reliability Test

The test procedure listed below was followed to assess the functionality and the reliability of the automatic drain feature. The procedure simulates a profile cycle from a depth of 25 meters (2.5 bar) to a depth of 10 meters (1 bar).

1. Place 50.6 kg of lead on the cylinder plate to simulate a pressure of 2.5 bar (~25 m depth).

2. Send a command to the pump to fill the cylinder with 0.3 litres of oil to raise the lead weight by filling and pressurizing the accumulator.
3. Wait a minimum of 30 seconds.
4. Replace the 50.6 kg of lead on the cylinder plate with 30.3 kg to simulate a pressure of 1 bar (~10 m depth).
5. Send a command to open solenoid one for one second to pressurize the pilot line of the pilot operated check valve to cause it to open.
6. Wait until the cylinder completely drains to lower the lead weight.
7. Send a command to open solenoid two for one second to relieve the pressure on the pilot line of the pilot operated solenoid valve to cause it to close.
8. Repeat steps 1-8.

The initial tests failed due to a failure to depressurize the pilot line which resulted in the pilot operated check valve not closing. When the cycle was repeated, the oil would flow directly into the reservoir rather than filling the cylinder. This issue was resolved by plumbing the pilot drain line separately to the reservoir rather than through the same drain line as the bladder.

With the new plumbing route for the pilot drain line implemented, the procedure was successfully repeated two hundred times without any observed problems. The results validated the functionality of the feature and provided confidence in the reliability. The system was also able to drain automatically when a 50.6 kg mass was left on the cylinder for the full cycle. This indicates that the automatic drain feature can function when the

line pressure is 2.5 bar. 2 bar is the maximum line pressure expected due to variations in the depth of the subsea buoy beyond 10 m.

5.4.1.7.2 Temperature Effects on Power Consumption and Flow Rate

The typical operating environment expected for the profiler during field tests is about 5°C. A decrease in temperature increases the viscosity of the oil, as demonstrated by the plot in Figure 52. The viscosity of the oil affects the resistance to flow. The flow resistance increases with an increase in viscosity due to higher frictional effects due to the fluids resistance to shearing (Munson, Young, & Okiishi, 1994). This can result in sluggish operation of the valves and an increase in energy consumption (Eaton Fluid Power Training, 2010).

To observe the temperature effects on the hydraulic system, profiles were simulated using the bench test setup in environments with four different temperatures, and four different operating pressures. The ambient temperatures were 4.5°C, 10.5°C, 13.0°C, and 23.5°C. The pressures were 0.98 bar (20.3 kg), 2.01 bar (41.5 kg), 2.88 bar (59.6 kg), and 3.73 bar (77.0 kg). The pressure was limited to 3.73 bar due to the instability of the stacked weights creating a safety concern.

During the pumping process, to raise the applied load, the current drawn by the motor was recorded. The total drain time was also recorded. The drain time was measured from the time the pilot line to the pilot operated check valve was pressurized to the time the cylinder rod bottomed out. The tests were repeated three times and averaged. The current

drawn was converted to power consumption by multiplying it by the 24 VDC supplied to the motor. The drain time was converted to flow rate by dividing the volume of the cylinder by the time required for the cylinder empty.

The graph in Figure 63 characterizes the effect of temperature on the pump's power consumption. All four pressures scenarios experience an increase in power demand as the temperature decreased from 23.5 °C to 4.5 °C. The drainage flow rate decreases as the temperature decreased from 23.5 °C to 4.5 °C (Figure 64). The power data can be used to estimate the pump's power consumption during field trials where the expected depth and temperature are 50 m (5 bar) and 5°C, respectively. Extrapolating the 4.5 °C data to a pressure of 5 bar (50 m) gives a power requirement of approximately 30 W per profile. The flow rate data can be used to estimate the bladder drainage time during field trials. Assuming the bladder is filled to 6.5 l, the time required to drain the bladder will be approximately 10 minutes when the line pressure is 1 bar, and the ambient temperature is 5°C. It is important not to begin filling the bladder again until it is fully drained or else the bladder could rupture, or the profiler may not operate as intended. The fill and drain control will initially be based on a time schedule but eventually needs to improve to one based on feedback from the tank level sensor.

During the cold (4.5 °C) oil temperature testing, the pilot operated check valve consistently failed to open resulting in the failure of the cylinder to drain. Increasing the energization time from one to two seconds resolved the issue. The slower flow rate due to the higher viscosity at low temperatures was the issue.

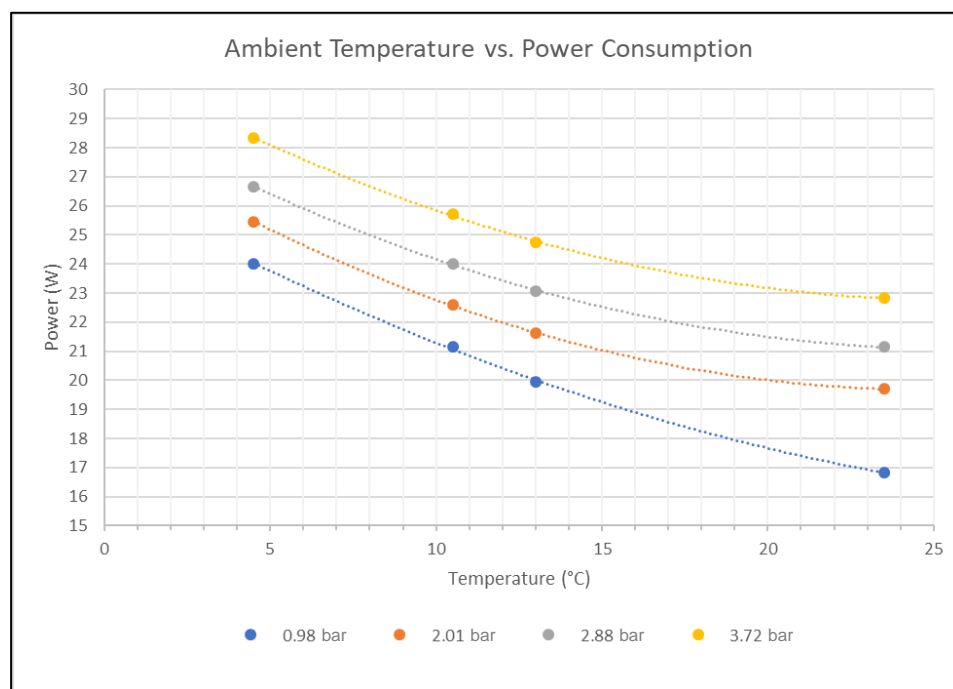


Figure 63 Ambient temperature vs. power consumption

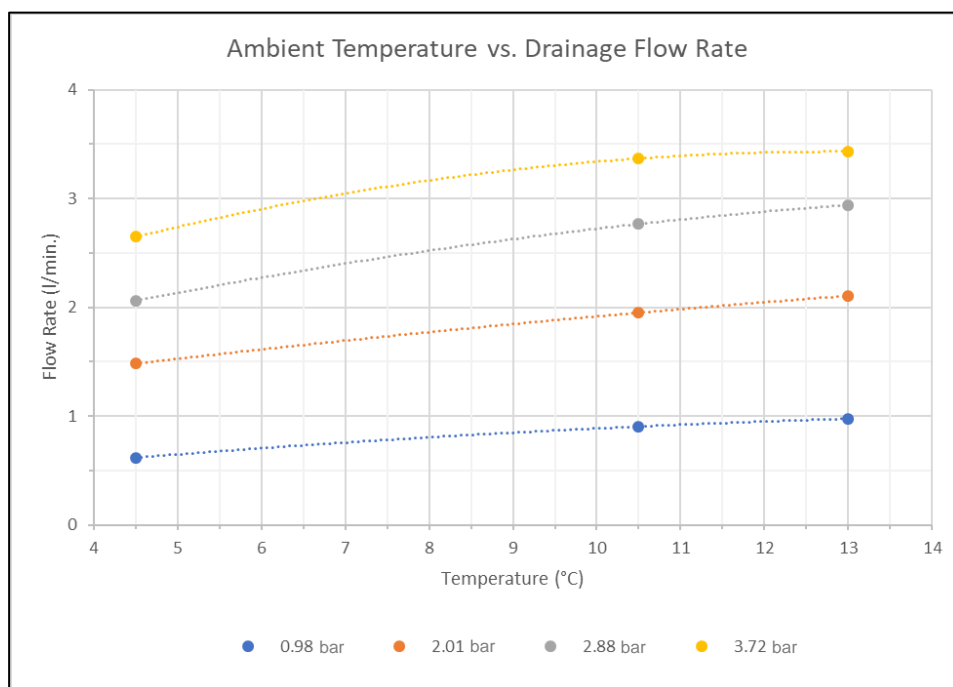


Figure 64 Ambient temperature vs. drainage flow rate

5.4.1.7.3 Pump Validation Tests

During bench testing operations it was observed that the pump delivers a different flow rate depending on the rotational direction of the pump. Validating the flow rates in both directions is critical to ensuring the intended quantity of oil is pumped into or out of the bladder. The initial validation was quantified with a graduated cylinder. The hydraulic cylinder was removed from the bench test setup and replaced with a 1,000 ml graduated cylinder. A hydraulic fitting was installed on the bottom of the graduated cylinder and connect to the buoyancy engine. 2000 counter clockwise revolutions of the pump delivered 815 ml of oil to the graduated cylinder while 2000 clockwise revolutions only removed 660 ml from the graduated cylinder. The 0.408 cm^3 per revolution flow rate while pumping into the cylinder matches the pump specification of 0.4 cm^3 per revolution. However, the 0.33 cm^3 per revolution flow rate while pumping out of the cylinder is 18% less than the specification.

The flow rate bench test was extended to filling and emptying the larger volume of the bladder. The bench test for this set up consisted of replacing the graduated cylinder with the bladder. The bladder was positioned on a scale and zeroed. Using the 0.88 kg/m^3 density specification for the oil, the mass for various volumes from 4 to 6.5 litres was determined. The pump output revolutions were then adjusted until the mass indicated on the scales matched the mass for the desired volume. Similarly, once the volume matching mass was achieved the number of pump revolutions to empty the bladder were adjusted until the scale mass returned to zero. Table 12 summarizes the masses, volumes, and

corresponding pump revolutions flow rates to fill and empty the bladder. The larger volume reveals an average fill flow rate of 0.396 cm³ per revolution and an average empty flow rate of 0.327 cm³ per revolution. This information is required for programming the volume of oil being pumped.

Table 12 Pump flow rate validation results

| Volume (l) | Mass (kg) | Fill Revolutions | Fill flow rate (cm ³ /revolution) | Empty Revolutions | Empty flow rate (cm ³ /revolution) |
|------------|-----------|------------------|--|-------------------|---|
| 4 | 3.52 | 10,089 | 0.396 | 12,229 | 0.325 |
| 5 | 4.40 | 12,598 | 0.397 | 15,277 | 0.327 |
| 6 | 5.28 | 15,137 | 0.396 | 18,347 | 0.327 |
| 6.5 | 5.72 | 16,402 | 0.396 | 19,882 | 0.327 |

5.4.2 Profiler Power Source

The power source selected for the profiler was a rechargeable lithium-ion battery. The specific battery selected was a Standard “Big Jim” “A” type high capacity battery from SubCtech. The battery has a nominal voltage of 25.2 VDC, a 90Ah capacity, and 2279 Wh of energy. The maximum continuous discharge current of the battery is 7A and it is submersible in sea water up to 300 m. The specification sheets for the battery are available in Appendix A, pages 267-269. This battery was selected because it is capable of supplying 24 VDC and the estimated 4.5 A maximum current demand required by the profiler. It also satisfies the 200 m operating depth and -5 to 30°C temperature conditions.

The high energy density available from lithium ion batteries results in more energy in a smaller volume.

Table 13 below summarizes the expected energy demand per profile based on the information available from the component specification sheets. The duration of the power consumption was based on an estimated profiling rate of 0.25 m/s, and an assumed 6.5 litre bladder volume with a 0.8 l/min flow rate. Field deployments of 50 m are estimated to consume 4.75 Wh per profile and full deployments of 200 m are estimated to consume 14.53 Wh. The selected battery will provide a maximum endurance of 480 profiles for a 50 m deployment and 157 profiles for a 200 m deployment.

Table 13 Profiler energy consumption estimate for 50 m field trials and 200 m full deployment

| System | Power (W) | | Duration (h) | | Energy (Wh) | |
|-------------------------------|--------------|------|-----------------|-------|----------------|--------------|
| | 50m | 200m | 50m | 200m | 50m | 200m |
| Hydraulic | 30 | 90 | 0.135 | 0.135 | 4.06 | 12.18 |
| Sensors and controller system | 10 | 10 | 0.056 | 0.222 | 0.56 | 2.22 |
| Telemetry | 4 | 4 | 0.033 | 0.033 | 0.13 | 0.13 |
| Total | | | | | 4.75 | 14.53 |

5.4.3 Frame

The frame for the main body which is illustrated in Figures 65 and 66 is a basic but important component of the system. Detailed fabrication drawing for the frame are available in Appendix B, pages 351-388. The main purpose of the frame is to house the

buoyancy engine and battery, as well as to mount two of the pulleys that make up the compound pulley system. The structural members of the frame are fabricated from rectangular aluminum tubing connected together with aluminum gussets plates and brackets using stainless steel fasteners. This method of construction was chosen over weldments for the ease of making modifications. The mooring cable passes through the eyelets of the frame to secure the profiler to the subsea mooring. The UHMW lined eyelets have the same opening diameter as the guide tube on the passive float to allow for the mooring cable assembly to pass through it.

Since the electromechanical cable routes through and attaches to components on the frame, potential contact points are designed with smooth and rounded surfaces, and use low friction materials (PTFE/UHMW) to minimize wear and abrasion. A series of cable guides aid in the routing of the electromechanical cable through the frame. A drum on the bottom of the frame can store excess electromechanical cable to allow control over the amount of cable available to be payed out during the secondary ascent. The drum also acts as a locked capstan to reduce the stress on electromechanical cable connection point at the buoyancy engine enclosure.

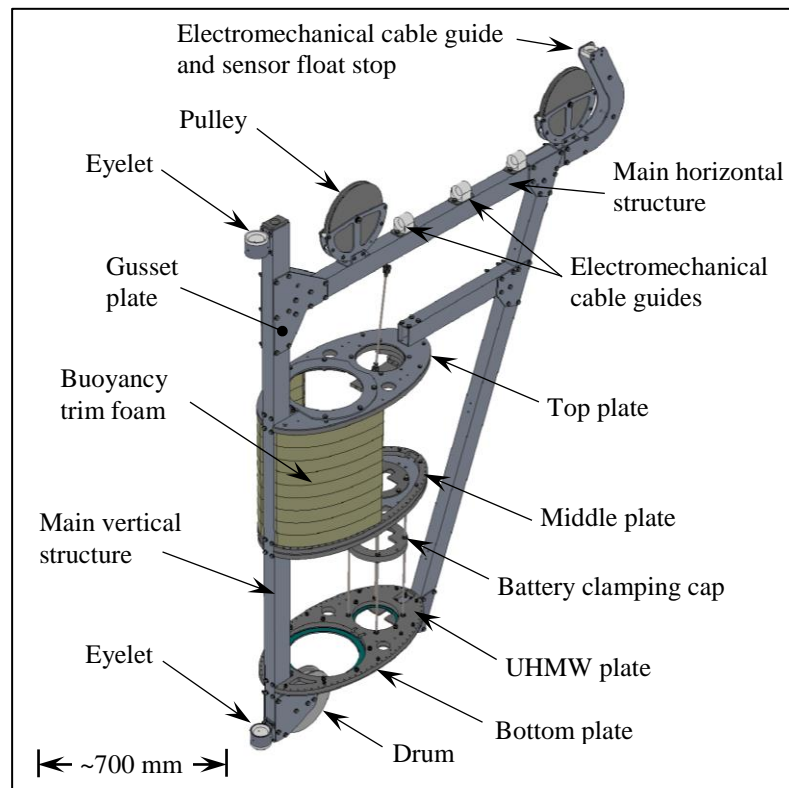


Figure 65 Main body frame design

The buoyancy engine is positioned adjacent to the main vertical structural member. It is constrained in the vertical direction by the top and bottom plates. In the lateral direction, it is constrained by all three plates and the attached UHMW plate. The UHMW plate and rubber gasket material between the end plates eliminate metal on metal contact between the frame and the buoyancy engine enclosure. A radially protruding pin located on the circumference the bottom end cap of the enclosure mates with a groove in the bottom UHMW plate to constrain the buoyancy engine from rotating. The locating pin also ensures the enclosure is positioned correctly within the frame for connecting the battery and electromechanical cables to the bulkhead connectors. Its also ensures it is positioned correctly for operation of the pump emergency kill switch.

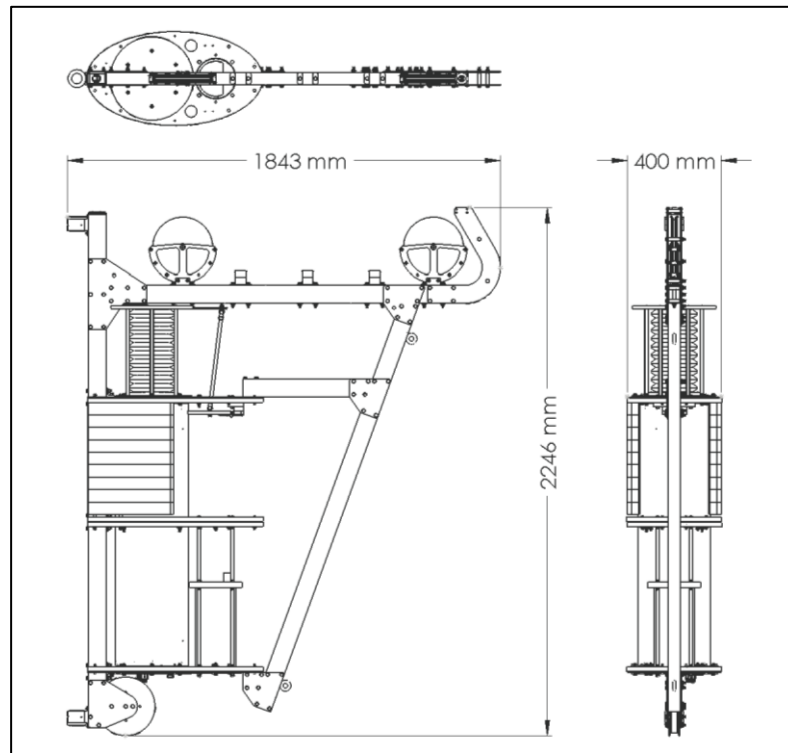


Figure 66 Main body - Orthographic projections with dimensions

The battery is positioned adjacent to the buoyancy engine and is constrained vertically and laterally within the frame in a similar manner as the buoyancy engine. An adjustable battery clamping cap allows for the length variations between the standard and XL SubCtech batteries. A notch in the clamping cap engages the batteries bulkhead connector to prevent the battery from rotating.

The pulleys located on the top horizontal structural member are constructed in the same manner as the pulley on the passive float apart from the mounting bracket. The pulleys are located such that the sensor payload float is positioned 1.5 m from the mooring cable and to ensure the electromechanical cable transitions from the frame pulley to the passive float pulley in a vertical line.

The electromechanical cable guide located at the end of the top horizontal structural member serves two purposes. It is aligned above the pulley to transition the electromechanical cable vertically into the pulley groove. It also prevents the tapered end of the Trustlink from retracting into the pulley groove which could jam it due to a wedge effect.

5.4.3.1 Pump Emergency Kill Switch

Ensuring that the bladder does not rupture due to over inflation is a critical requirement of the profiler. Proper monitoring of the pump output and/or the oil level in the reservoir will prevent the bladder from overfilling and rupturing. However, an emergency kill switch was designed as a fail safe. The kill switch design uses a magnet and Hall-effect switch to signal the pump to turn off when the bladder expands to the end limit of the bladder cage.

A Hall-effect sensor is a transducer that varies its output voltage depending on the influence from a magnetic field. The switch design takes advantage of the low magnetic permeability property of the aluminum buoyancy engine enclosure. Aluminum has the same magnetic permeability property as air and water, thus it has negligible influence on the magnetic field. This allows for the Hall-effect sensor to be housed inside the enclosure while the magnet is located outside. The magnetic field, if strong enough, can penetrate the water gap, aluminum side wall, and interior air gap to influence the sensor. The main benefit of this switch design is that it does not require an external sensor with

wires that would need to connect through an additional bulkhead connector. Every bulkhead connector used is a source for leaks to occur and should be minimized.

A D68-N52 neodymium magnet was selected based on its ability to produce a magnetic field strong enough to activate the AH9246 Hall-effect switch. The specification sheets for the magnet and Hall-effect switch are available in Appendix A, pages 262-266. The specifications for the Hall-effect switch indicate that a minimum magnetic field strength of 9 Gauss is required for operation. Equation 5.28 was used to determine the flux density of the magnetic field (B_z) for a cylindrical magnet (Camacho & Sosa, 2013). It is dependent on the strength of the magnet (B_r), the relative permeability of the media surrounding the magnet (μ_r), the length of the magnet (L), the radius of the magnet (R), and the axial distance from the end of the magnet (z).

$$B_z = \frac{\mu_r B_r}{2} \left(\frac{z}{\sqrt{z^2 + R^2}} - \frac{z - L}{\sqrt{(z - L)^2 + R^2}} \right) \quad (5.28)$$

When the bladder reaches the end plate of the bladder cage the axial distance from the south pole face of the magnet to the marked face of the AH9246 Hall-effect switch is 32 mm. The resulting magnetic field produced at the location of the Hall-effect sensor is 36 Gauss. The equation variables are summarized in Table 14. Since the 9 Gauss requirement for operation is exceeded, the magnet is sufficient for the application. The magnet can produce a magnetic field ≥ 9 Gauss at an axial distance up to 55 mm from the switch.

Table 14 Magnetic field strength calculation variables

| | |
|---|--------------|
| Strength of the magnet, B_z | 14,800 Gauss |
| Relative permeability (water, air, aluminum), μ_r | 1 |
| Length of the magnet, L | 12.7 mm |
| Radius of the magnet, R | 4.76 mm |
| Axial distance from the end of the magnet, z | 32 mm |

The profiler frame has a mounted pivot arm with the neodymium magnet potted at the end (Figure 67). A linkage connects it to another pivot arm mounted on the bladder cage. As the bladder is filled it raised the arm mounted on the bladder cage which through the linkage, simultaneously raises the arm with the embedded magnet. When the bladder reaches the end limit of the bladder cage the south pole face of the magnet will be positioned 32 mm from the marked face of the Hall-effect switch that is mounted inside the buoyancy engine enclosure. CAD drawings of the components are available in Appendix B, pages 384-389.

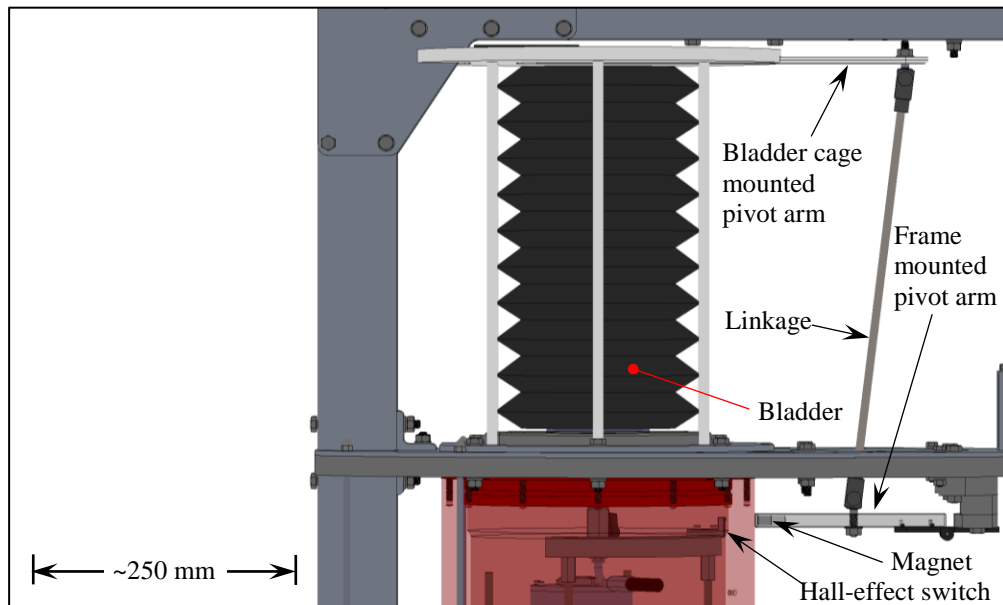


Figure 67 Pump emergency kill switch design

5.4.4 Buoyancy of the Main Body

The total buoyancy of the main body (buoyancy engine, battery, and frame) with the bladder empty is negative 484.7 N. The buoyancy of the individual components was determined by submerging them in the deep tank and measuring the weight with a load cell. The buoyancy engine is -224.6 N with the bladder empty, the battery is -61.7 N, and the frame is -198.4 N. With the bladder empty the net buoyancy of the profiler should be negative 20 N in sea water (negative 42.9 N in freshwater) for the profiler to sink. Therefore, the buoyancy of the main body must be trimmed with foam to add 130.3 N of freshwater buoyant force to achieve the desired net buoyancy. Table 15 below summarizes the freshwater and sea water buoyant forces of the profiler components and the net buoyancy of the system with an empty bladder.

Table 15 Freshwater and sea water buoyant forces of the profiler components and the profiler's net buoyancy (empty bladder)

| Component | Freshwater Buoyancy (N) | Sea water Buoyancy (N) |
|------------------------------|-------------------------|------------------------|
| Sensor Float | +97 | +99.4 |
| Passive Float | +214.5 | +219.9 |
| Buoyancy Engine | -224.6 | -219.1 |
| Battery | -61.7 | -60.2 |
| Frame | -198.4 | -193.6 |
| Main Body Trim Foam | +130.3 | +133.6 |
| Net buoyancy of the profiler | -42.9 | -20.0 |

The trim foam must be positioned on the frame of the main body such that the stable equilibrium position has the vertical strength member orientated vertically. To determine the required location point of the trim foam the sum of the moments for the free-body-diagram of the main body in the desired equilibrium position was solved using sea water buoyancy values. Based on the diagram in Figure 68, Equation 5.29 was used with the variables summarized in

Table 16 to determine that centre of buoyancy of the trim foam must be located 148 mm from the centerline of the eyelets. As the quantity of oil changes in the bladder so to does the stable equilibrium position of the main body. Therefore, for the calculation it was chosen to use the buoyant force for the buoyancy engine with 3.5 litres of oil in the bladder (about half full) rather than the empty or full state.

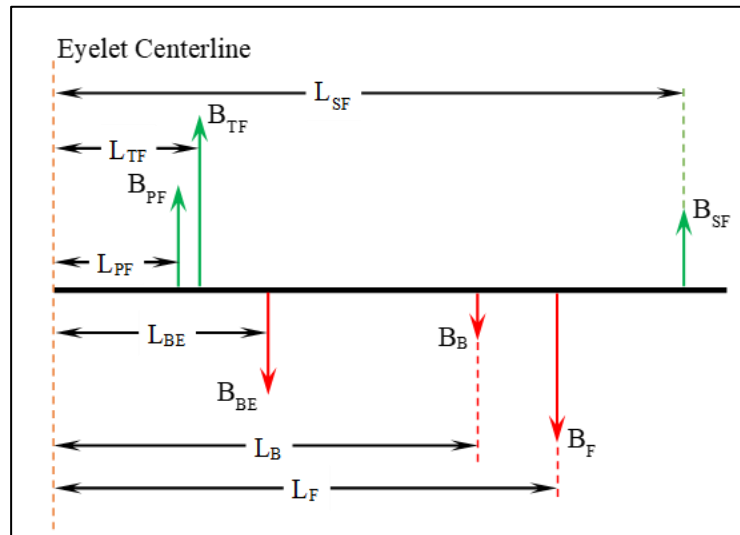


Figure 68 Main body free-body diagram

$$B_{PF}L_{PF} + B_{TF}L_{TF} + B_{SF}L_{SF} - B_{BE}L_{BE} - B_B L_B - B_F L_F = 0 \quad (5.29)$$

Table 16 Main body free-body-diagram variable

| | |
|--|---------------|
| Passive float buoyancy, B_{PF} | 219.9 N |
| Trim foam buoyancy, B_{TF} | 133.6 N |
| Sensor float buoyancy, B_{SF} | 99.4 N |
| Buoyancy engine buoyancy, B_{BE} | 185.1 N |
| Battery buoyancy, B_B | 60.2 N |
| Frame buoyancy, B_F | 193.6 N |
| Distance from eyelet centerline to B_{PF} , L_{PF} | 203 mm |
| Distance from eyelet centerline to B_{SF} , L_{SF} | 1639 mm |
| Distance from eyelet centerline to B_{BE} , L_{BE} | 319 mm |
| Distance from eyelet centerline to B_B , L_B | 591 mm |
| Distance from eyelet centerline to B_F , L_F | 686 mm |
| Distance from eyelet centerline to B_{TF}, L_{TF} | 148 mm |

Through an iterative process, the shape of the trim foam block was developed until its center of buoyancy, when installed on the frame, matched the required position. The buoyant force and center of buoyancy for the foam was determined using the SolidWorks analytical tool. The shape of the foam is illustrated in Figure 69. It follows the contour of the frame plates which have a 2:1 elliptical shape to provide a streamlining effect.

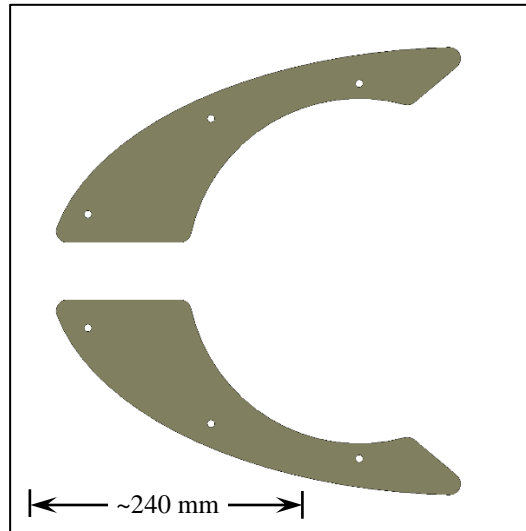


Figure 69 Main body trim foam shape

5.4.5 Verification and Trimming of Profiler's Buoyancy

The complete profiler was assembled and placed in the deep tank for final buoyancy trimming and verification. To completely submerge the system in the deep tank, the sensor float and passive float had to be retracted and attached as close to the main body as possible. A load cell was then used to measure the weight of the system. As indicated in section 5.4.4 the freshwater buoyancy of the profiler should be -42.9 N to have a sea water buoyancy of -20 N. The initial test indicated the value was -29.9 N. An additional 13 N of weight was added to the bottom of the profiler to achieve the required -42.9 N buoyancy.

6 Subsea Mooring Design

The subsea mooring (excluding the hard stops) used for the field trial was designed and fabricated by Mark Downey an Oceanographic Assistant with the Physical Oceanography research group at Memorial University. The subsea mooring consists of a pair of 16 inch spherical subsea buoys and a 200 kg anchor to provide 72 kg of buoyant force to keep the mooring line taught. The mooring line is a 0.25 inch diameter vinyl coated steel cable terminated at each end with thimbles. The thimbles allow the mooring cable to be easily connected with shackles to the buoys and the anchor. They also allow the cable to be thread through the passive float guide tube and the frame eyelets. This feature allows the profiler to be easily and quickly secured to the subsea mooring at the deployment site. An additional feature added to the subsea mooring design were upper and lower limit hard stops. The two-piece hard stops clamp onto the cable at the top and bottom of the mooring. The purpose of the hard stop is to safely limit the travel of the profiler. Without the stops, the shackles at the ends of the mooring cable can wedge in the opening of the guide tube or eyelets and impede the operation of the profiler. Detailed fabrication drawing of the hard stop is available in Appendix B, page 397.

7 Control System, Electrical and Electronics

The architecture for the profilers control system was developed by Glenn Cutler at the Autonomous Oceans Systems Laboratory of Memorial University. This included sourcing the majority of required electrical and electronic components for the control system; interfacing the components; and writing the software to operate the system.

Within the sensor float and the buoyancy engine module, the profiler incorporates the many sensors, actuators, instruments, controllers, and devices outline in this document. The software/hardware architecture for the profiler is illustrated in Figure 70. The system is controlled with three programmable microcontrollers, a BeagleBone Black and two Teensy 3.2. It also uses several data transmission methods between the various components; ethernet, RS232, and CAN (Controller Area Network) Bus.

The BeagleBone Black (BBB) single board computer is located in the sensor float and is used as the primary controller. The custom Linux software running on the BeagleBone Black is the most complex of the three controllers. All commands, responses, and data sent to and from various parts of the system go through the BeagleBone (Cutler, 2018). The two other controllers (main body controller and secondary controller) are connected to the primary controller via a CAN Bus, the AHRS and Vector instruments are connected to the BBB via RS232, and the Iridium and Wi-Fi antenna are connected via ethernet.

The Teensy 3.2 secondary controller which is also located in the sensor float serves as an expansion for the primary controller. The Altimeter, GPCTD (with 43F pump), and GPS are connected to it via RS232. This controller operates based on commands from the primary controller via the CAN bus.

The Teensy 3.2 main body controller is located in the buoyancy engine subsea enclosure. This controller operates the buoyancy engine. It controls the valves, power to the motor controller, and the speed and number of revolutions of the hydraulic pump motor. It receives data from the hydraulic tank level sensor, the motor controller, Hall-effect switch, and the main battery through RS232 serial ports. It communicates with the primary controller via CAN Bus.

Aside from controlling the motion and data collection and transmission of the profiler, the custom software developed and embedded into the controllers also ensures optimal power management. To maximize the deployment duration components are only powered when necessary. The motor controller, tank level sensor, and Hall-effect switch are only powered while the pump is on. The oceanographic sensors are only powered during the ascent to the surface. The telemetry components are only powered while at the surface. Since the profiler spends the majority of the time at the sea bottom waiting to profile, the software puts the system in hibernation. While in hibernation, 0.3 Watts of power is consumed. This is just enough power to maintain an internal alarm clock to awaken the profiler at the next set time interval.

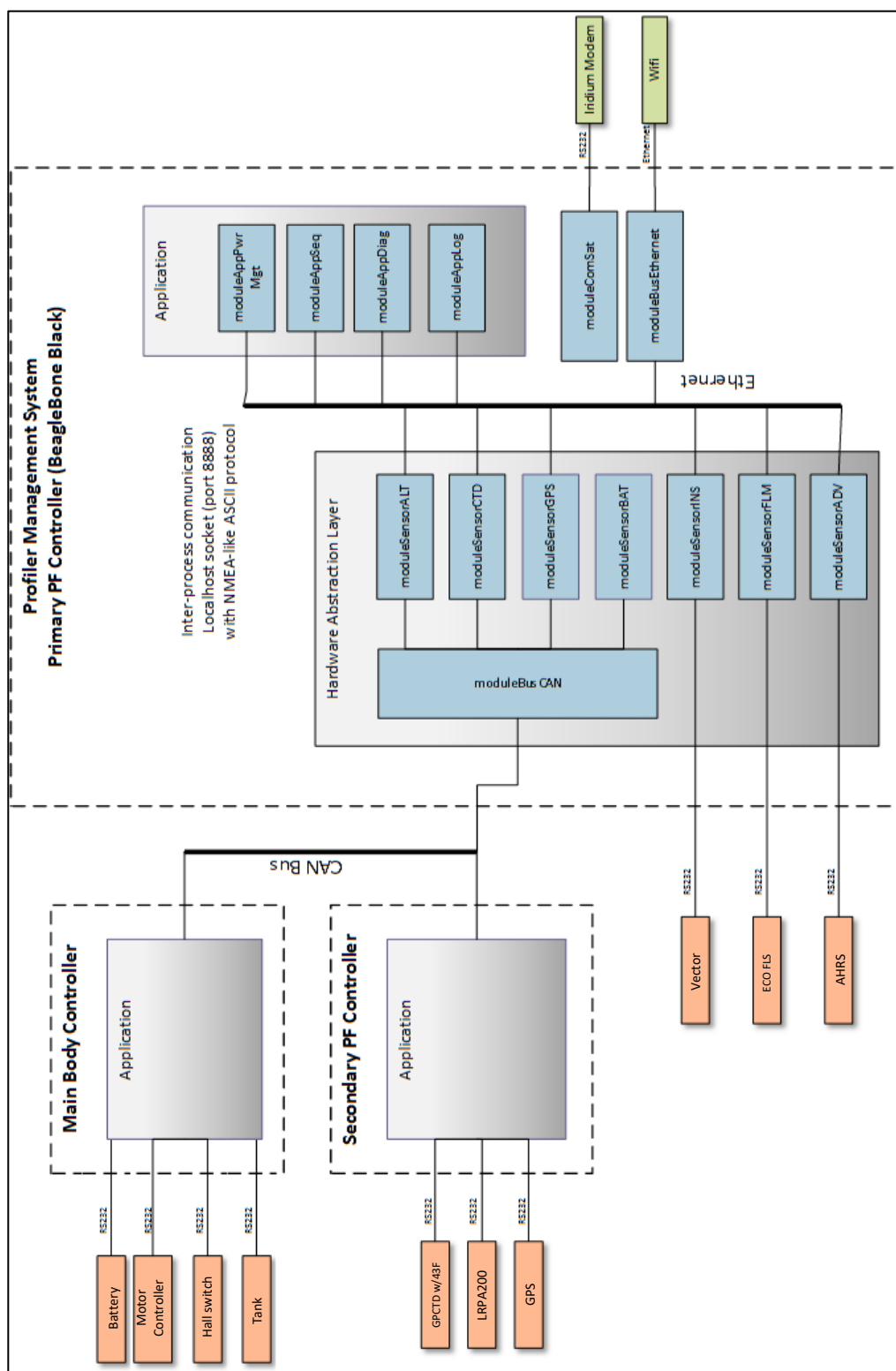


Figure 70 Profiler hardware/software architecture (Cutler, 2018)

8 Field Deployment

South Arm of Holyrood Bay was selected as the test site for the field deployment tests.

The water depths in this area range up to 52 meters within 2 km from the vessel support site, Holyrood Marine Base. The profiler deployment requires support from two vessels.

One vessel must be equipped with a crane for hoisting the profiler into and out of the water and a winch for lowering and raising the mooring anchor. The second vessel provides support on the water to release the profiler from the crane and to ensure there are no entanglements. The two vessels used for the field trial deployments were the Marine Institute's M.V. Inquisitor (117 t, 24.9 m) for the main deployment and the Narwhal (2.56 t, 11 m) for support.

8.1 Transportation Skid

A skid was designed and fabricated to safely secure the profiler during vehicle and vessel transportation. Figure 71 illustrates the skid design and Figure 72 shows the skid in use on the deck of the Inquisitor. The skid was designed with a footprint that allows it to fit in the back of a pickup truck for conveniences of transportation. Detailed CAD drawings of the skid components and assembly are available in Appendix B, pages 398-401.

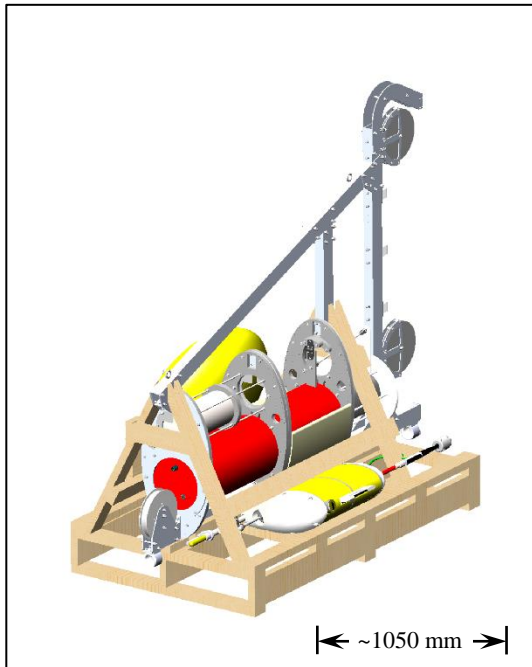


Figure 71 Transportation skid design



Figure 72 Skid on the Inquisitor deck

8.2 Deployment Procedure

The basic procedure listed below was followed to deploy the profiler.

1. Anchor main support vessel at deployment site.
2. Thread the mooring cable through the guide tube on the passive float and the eyelets on the frame.
3. Attach the hard stops at the top and bottom of the mooring cable.
4. Attach the anchor chain to the bottom of the mooring line and the subsea floats to the top.
5. Attach the anchor to the winch.
6. Deploy the subsea mooring buoy(s) off the aft end of the vessel.

7. Deploy the sensor float and passive float off the aft end of the vessel.
8. Use the crane to position the main body in the water at the aft end of the vessel.
9. Use the small support vessel (Narwhal) to ensure there are no entanglements.
10. Release the main body from the crane.
11. Use the winch to lower the chain anchor to the sea floor.

Steps 9 and 10 of the deployment procedure proved to be the most complicated and riskiest part of the deployment. In step 9 all of the components are in the water but not yet set in their final position. They are highly susceptible to entanglement at this point since there are two independent cable systems (mooring and electromechanical) with limited constraints, and four separate bodies at the surface (subsea buoy, main body, passive float and the sensor float). Once the main body is released from the crane it quickly sinks below the surface, pulling on the cables, floats and the buoy. It took two alert people aboard the support vessel to manage the position and orientation of the system and components to ensure a proper deployment as shown in Figure 73. It should be noted that a typical deployment would not have a surface marker buoy attached to the profile. As well, the winch cable would be removed and an acoustic release would be used to recover the profiler.

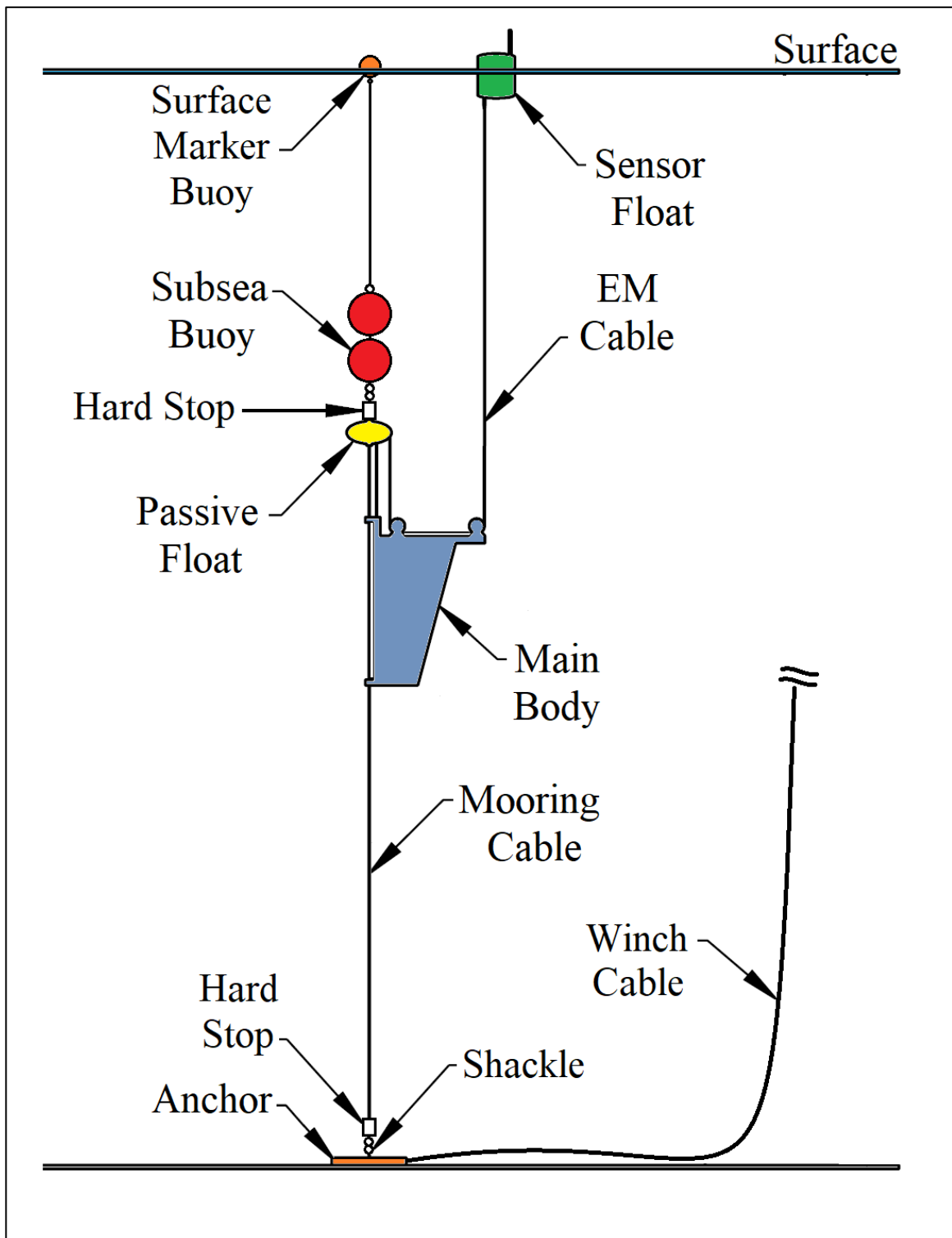


Figure 73 Schematic of Field Trial Profiler Mooring Deployment

9 Field Deployment Test Results

Field testing was done over four separate deployments in South Arm to assess the operation of the profiler. The main features to assess were; the ability of the buoyancy engine to cycle through the primary and secondary ascent and descent; the ability of the sensors to measure and collect data, the power consumed by the system; and the overall performance of the profiler. All four deployments used a subsea mooring with the subsea buoy positioned approximately 10 meters below the surface. The quantity of electromechanical cable made available for payout was 19 meters.

9.1 First Field Deployment

The goal of the first deployment was to become familiar with deploying and operating the profiler, and to assess its performance. The deployment was performed in a water depth of 32 meters. The buoyancy engine was set to pump 6.5 litres of oil into and out of the bladder for the ascent and descent. The automatic drain feature using the pilot operated check valve was omitted from the first field test to limit the functions to assess.

The depth versus time plot for the ascent of one of the profile cycles is shown in Figure 74. There are several points of interest as follows.

- The solid blue line indicates the sensor float begins the ascent at a depth of 23.5 m and the rate of ascent increases with time. The sensor float reaches the surface which was also confirmed from visual observation (Figure 75).

- The vertical purple dashed line indicates the time that the sensor float reached the surface, 240 s.
- The vertical red dashed line indicates the time that the pump stopped, 417 s.
- The sloped green dashed line indicates the maximum rate of ascent, 0.25 m/s

The 0.25 m/s maximum rate of ascent is within the 0.3 ± 0.1 m/s specification goal identified in section 3.1. A profile depth greater than 23.5 m should experience a higher maximum rate of ascent. The sensor float reached the surface 170 seconds before the pump stopped, therefore, there will be more buoyant force available for propulsion on deeper profiles. The profiler does not reach the 0.2 m/s lower limit of the ascent rate until 190 seconds have elapsed. At this point, the profiler had ascended 11.5 m. Over a 23.5 m profile, approximately 50% of the water column is profiled at a rate less than the specified range. However, this percentage will decrease as the depth of the profile increases. Over a 200 m profile only the lower 6% would be sampled below the specified ascent rate.

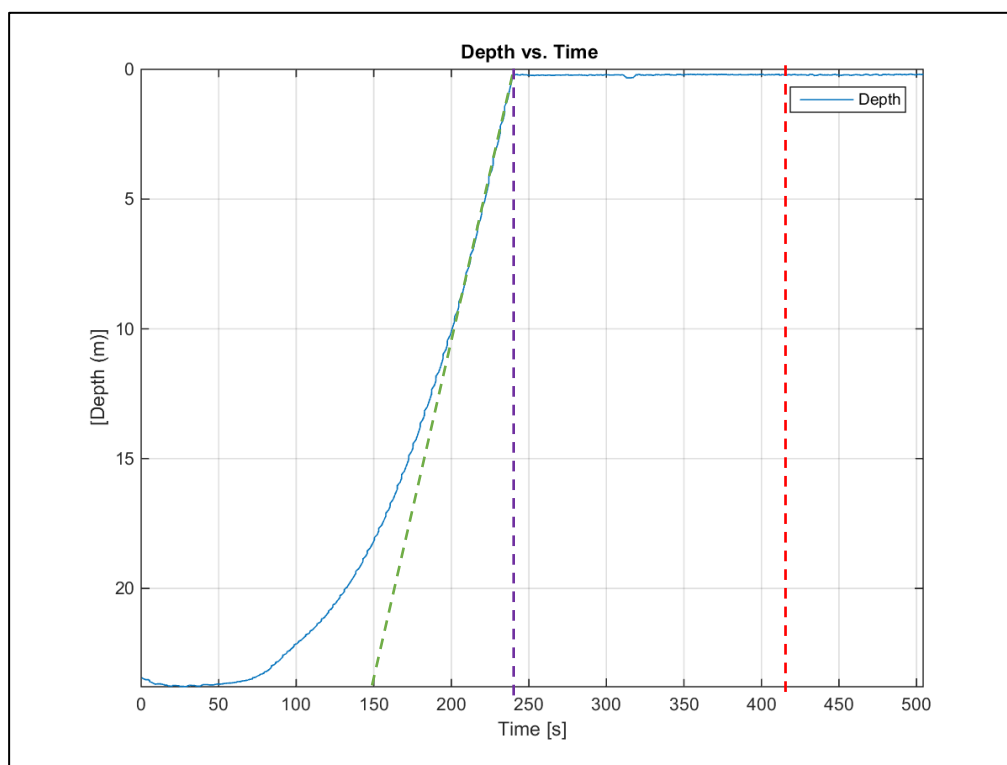


Figure 74 First field deployment - Sensor float depth vs. time plot for the ascent

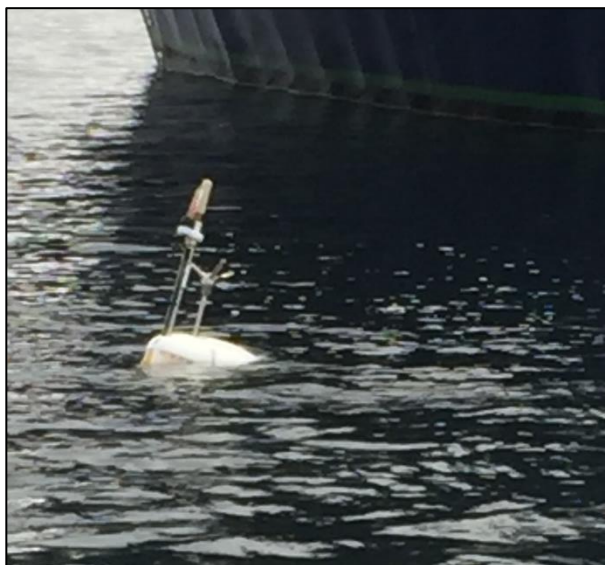


Figure 75 First field deployment - Sensor float breaching the surface during ascent

Due to calm and clear conditions, the profiler's descent could be observed only partially from the deck of the vessel. It appeared that the passive float was unable to retract the sensor float to the frame during the descent. This observation explains the start of the sensor float ascent at a depth of 23.5 m. Based on the 32.5 m depth of the water at the deployment site and the dimensions of the profiler, the sensor float should start the profile at approximately 28 meters if it was fully retracted to the frame. This information implies the sensor float had 4.5 m (28 m – 23.5 m) of electromechanical cable released. This observation was further verified by the Remotely Operated Vehicle video taken during the second deployment, which is detailed in the next section.

The profiler's battery voltage and battery current versus time plots are shown in Figure 76. Points of interest on the plot are as follows.

- The red circle indicates the point when that the sensor float reached the surface.
- The green circle indicates the point when the pump stops.

When the pump stops, the hydraulic system is no longer demanding power from the battery. The horizontal line of the plot after the green circle indicates that the power required by the sensors and control system is constant. At this point the supply current is 0.506 A and the battery voltage is 26.15 V. Therefore, the power required by the sensors and control system is 13.2W.

When the profile begins, the battery supplies 26.15 V and 1.442 A to the pump, sensors, and control system. This maximum power demand from the system is 37.7 W. As the

sensor float first reaches the surface it reduces to 33.2 W (1.268 A and 26.15 V).

Therefore, the maximum and minimum power required from the hydraulic system are 24.5 W and 20 W, respectively. The decrease in the hydraulic power demand is expected because the power is dependent on the pressure it is working against. The pressure acting on the bladder decreases as the depth decreases. The 24.5 W power requirement from the hydraulics is comparable to the pump power versus temperature plots in Figure 63. At a temperature of 10°C and a simulated depth of 29 m (2.9 bar), the power demand was approximately 24.2 W.

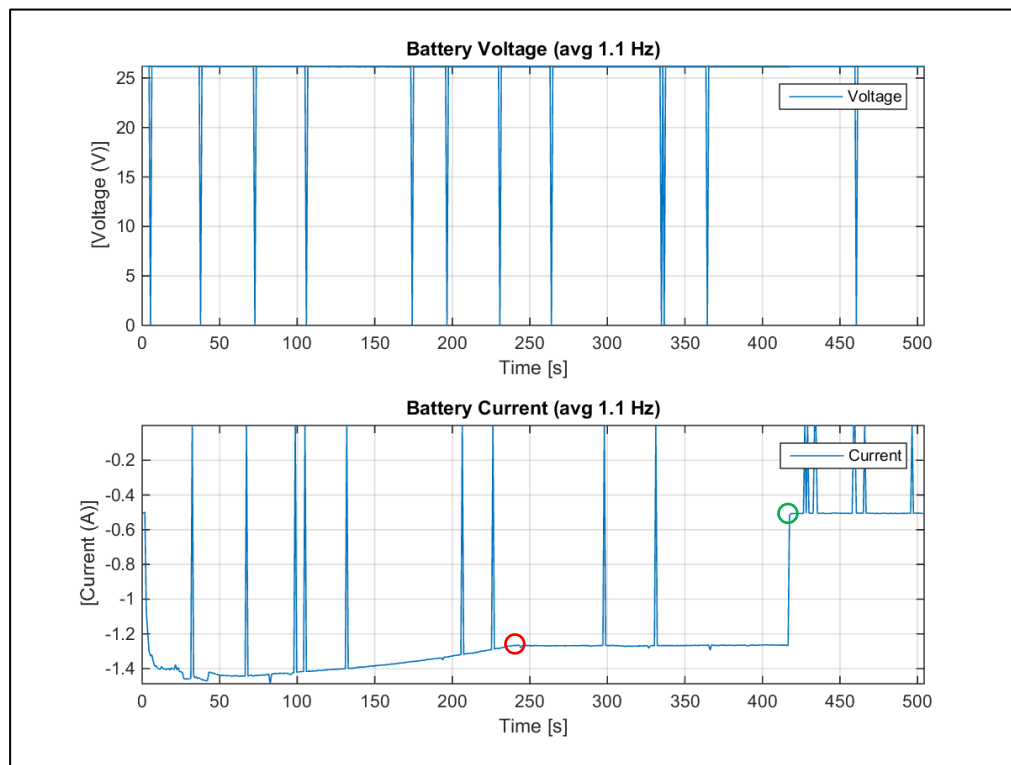


Figure 76 First field deployment - Profiler battery voltage vs. time and battery current vs. time plots

The profiler was successful collecting oceanographic and performance data from its suite of sensors during the ascents. Figure 77 displays the data from the CTD (Salinity, Temperature, Depth, and Dissolved Oxygen) and the ECO FLS (Chlorophyll) sensors. The sea water of the upper two meters of the water column has less salinity than the water below it. The temperature decreases from 10.4 °C at the surface to 9.5 °C at the bottom of the profile. The dissolved oxygen also decreases with depth, from 7.5 ml/l to 7.25 ml/l. The chlorophyll value spikes to 1.45 µg/l at a depth of 10 m but drops back to 0.7 µg/l near the surface and at the bottom of the profile.

Figure 78 displays the Velocimeter sensor measurements. This raw data has not been post-processed to correct for the motion of the sensor float. The profiler reaches the surface at the 240 s mark and at this point the Velocimeter protrudes from the water into the air. This corresponds with the spike in the beam 1 velocity measurement, and it is also the point at which all the measurements become more erratic due to wave motion.

The unfiltered Altimeter measurements are displayed in Figure 79. There appears to be a significant amount of corrupt measurements present in the plot. These measurements are represented by the 200 m points which is the maximum range of the altimeter. The cause may be attributed to the orientation of the sensor float which positions the altimeter with an ~10 to 15° pitch from vertical. The ideal orientation of the altimeter is vertical, and error in the head alignment can give rise to unreliable results. Filtering the 200 m points from the data results in a plot that clarifies the sensor floats altitude from the sea floor (Figure 80).

The measurement from the Vector's AHRS (Roll, Pitch, and Yaw rates of the sensor float) are displayed in Figure 81. The sensor float exhibits good stability with respect to pitch and roll. This is attributed to the ability of the buoyant force of the sensor float to develop a moment that resists those motions. The lever arm of the buoyant force is greater for the pitch than it is for the roll which is evident by the pitch and roll rates experienced. The buoyant force of the sensor float is perpendicular to the yaw motion and therefore cannot develop a moment to resist it. As a result, the sensor float experiences its greatest rate of motion in this direction. All three motions are very erratic when the sensor float reaches the surface (240 s mark) where it is subjected to wave action.

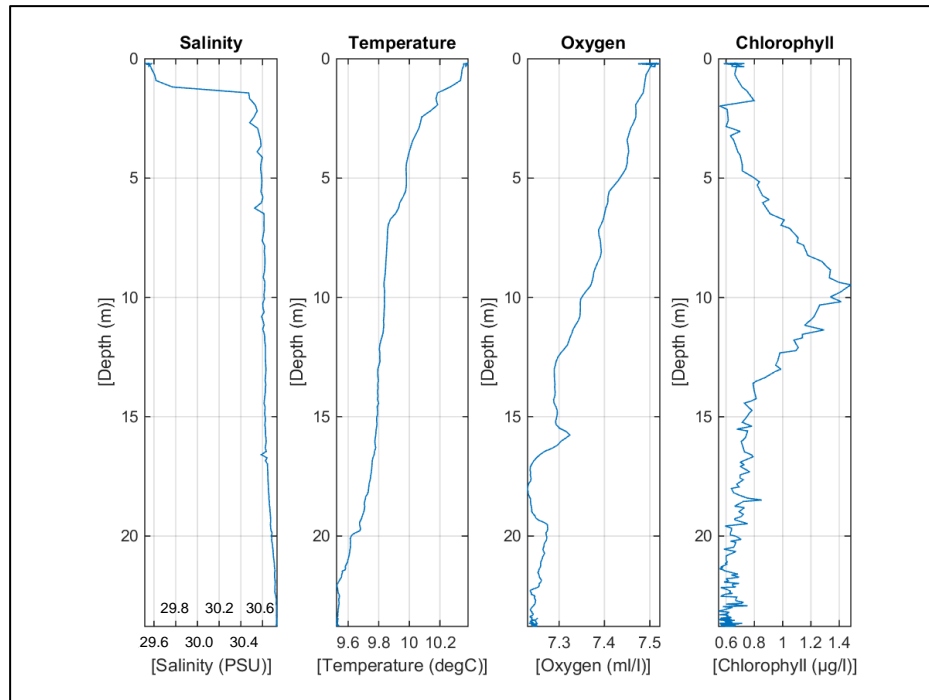


Figure 77 CTD and ECO FLS sensor water column measurements

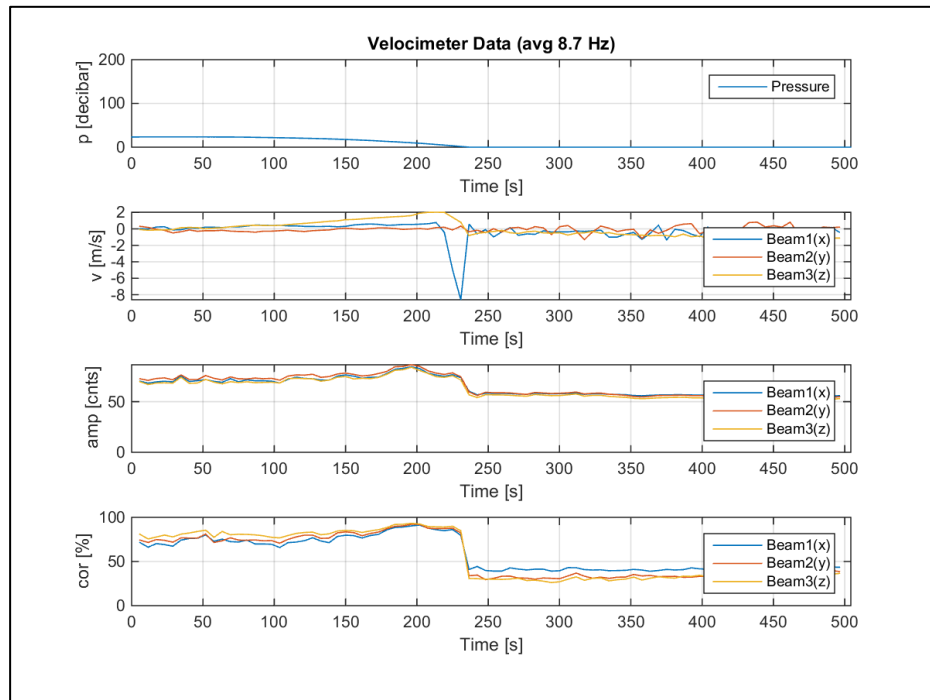


Figure 78 Velocimeter measurements

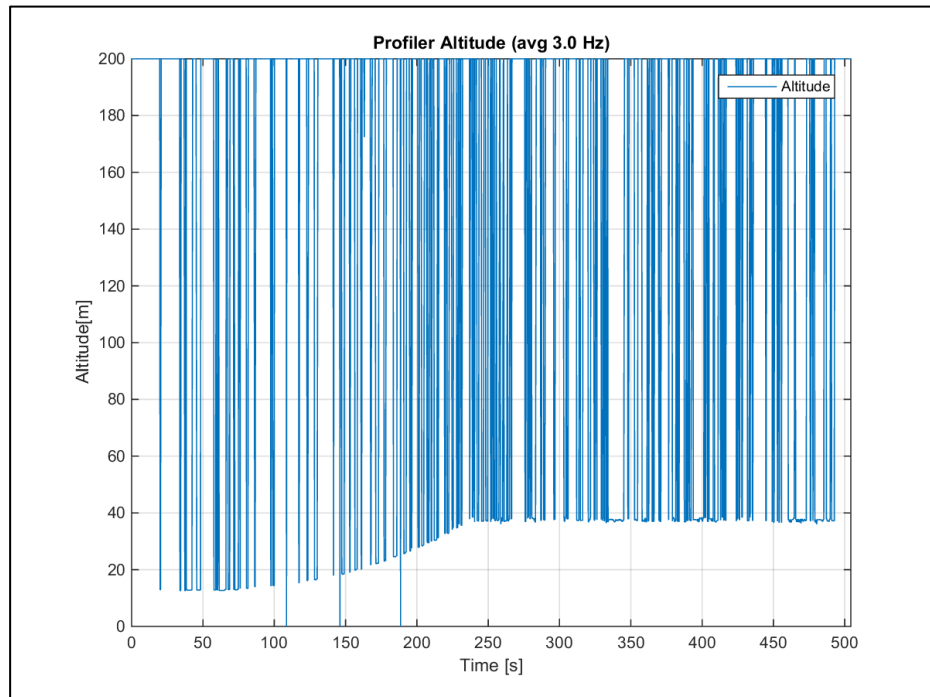


Figure 79 Unfiltered Altimeter measurements

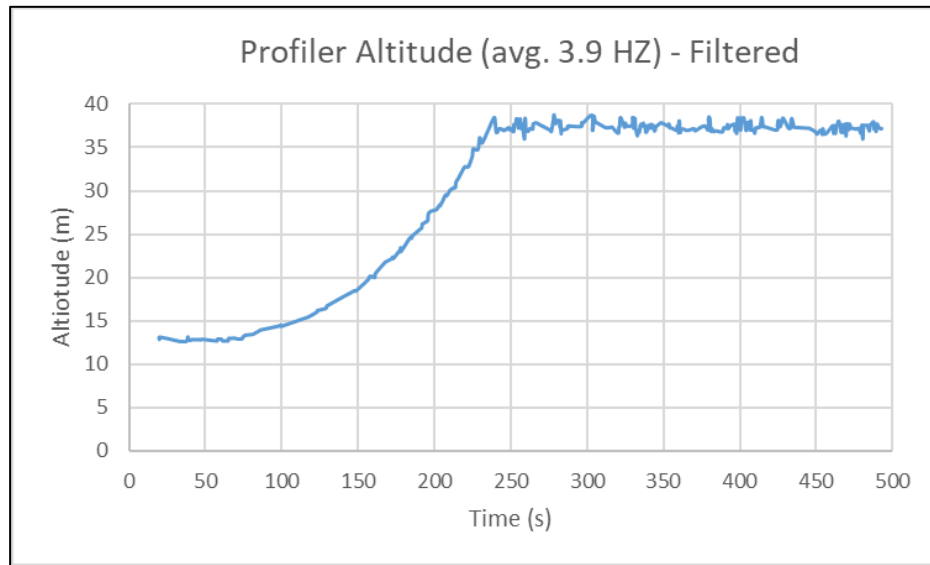


Figure 80 Filtered Altimeter measurements

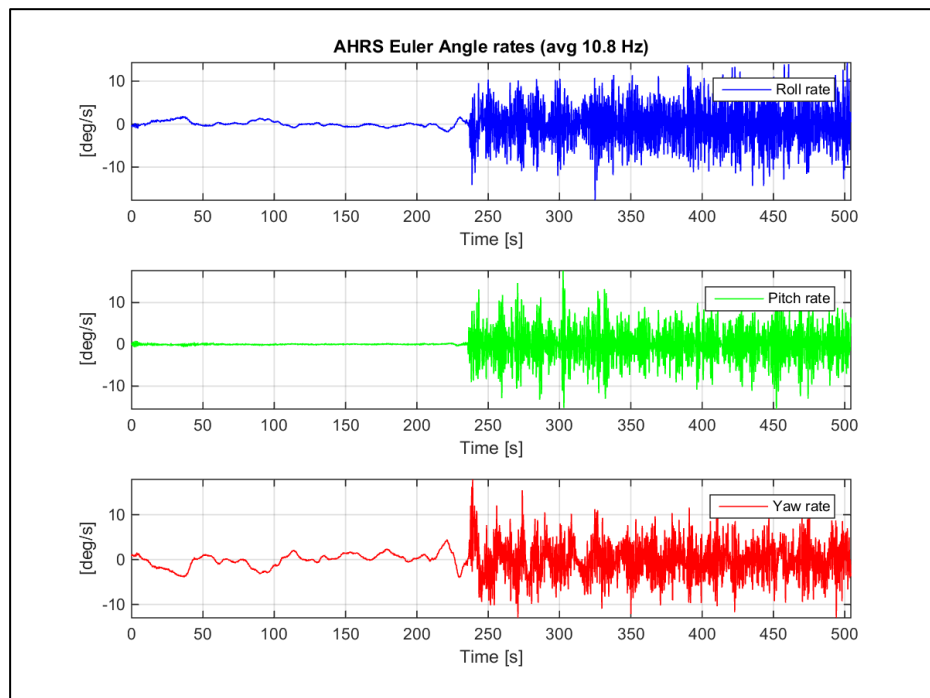


Figure 81 Vector ARHS measurements

9.2 Second Field Deployment

The goal of the second field deployment was to test the automatic drain function of the profiler and to visually observe the operation using a small eyeball class Remote Operated Vehicle (ROV) and submersible cameras mounted to the profiler's frame. The deployment was conducted at a location with a water depth of 40 meters. The buoyancy engine was set to pump 6.5 litres of oil into the bladder and the automatic drain feature using the pilot operated check valve and accumulator was used to drain the oil from the bladder back into the reservoir.

The depth versus time plot for the descent of the profiler is shown in Figure 82. Points of interest on the plot are as follows.

- The vertical red dashed line indicates the time that the pilot operated check valve is opened, 1,021 s.
- The vertical green dashed line indicates the time when the oil in the reservoir has returned to its original level (80.1%), 1,443 s.
- The sloped purple dashed line indicates the maximum rate of descent, 0.11 m/s

The accumulator and pilot operated check valve combination was successful in draining the bladder. At a flow rate of 0.92 l/min it took 422 s to drain the 6.5 litres of oil from the bladder into the reservoir. This is comparable to the ambient temperature versus drainage flow rate data in Figure 64 of section 5.4.1.7.2. At a temperature of 5°C and a simulated depth of 15 m (1.5 bar) the drainage flow rate was approximately 1.1 l/min.

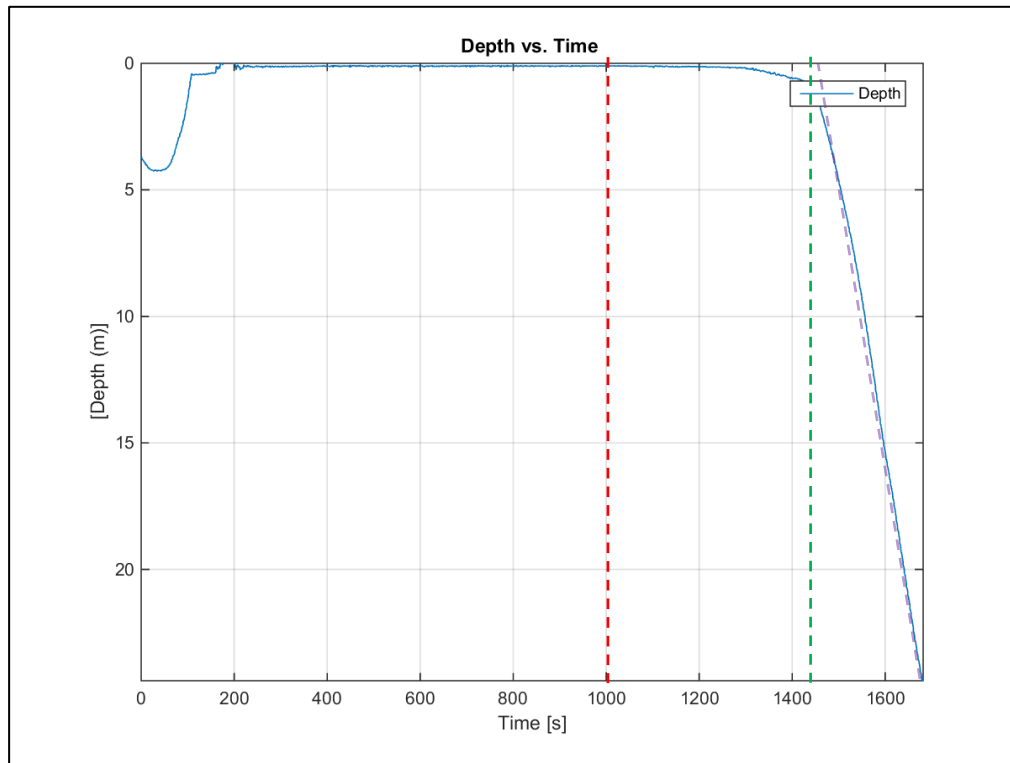


Figure 82 Second field deployment sensor float depth vs. time plot for the descent

Two points of interest observed with the ROV during the second field trial was the arrangement of the profiler at the bottom and the top of the mooring line, as well as, its arrangement as it ascended and descended.

Figure 83 is a screenshot from the ROV video while observing the profiler at the bottom of the mooring line. As expected from the first field trial the profiler is not behaving as expected. At the bottom of the profile the sensor float should be retracted back to the frame. As highlighted in the screenshot, the sensor float is not retracted back to the frame and is approximately 12-15 m of electromechanical cable is still payed out. The red oval indicates where the sensor float should be positioned at this time. The same situation

occurs during the descent from the top of the mooring line (Figure 84). The vertical separation between the passive float and the upper stop indicates that the profiler is descending at this point. The red oval is where the sensor float should be positioned but it is out of the shot due to the payout of electromechanical cable. This is due to the passive float not having the buoyant capacity to retract the sensor float. Visual observation from the ROV confirmed that the profiler maintains this arrangement during the ascent and descent cycles.

Screenshots of the bladder in its empty state (0 l) and full state (6.5 l) are shown in Figures 85 and 86, respectively. They appear relatively similar to the tank test and bench test observations.

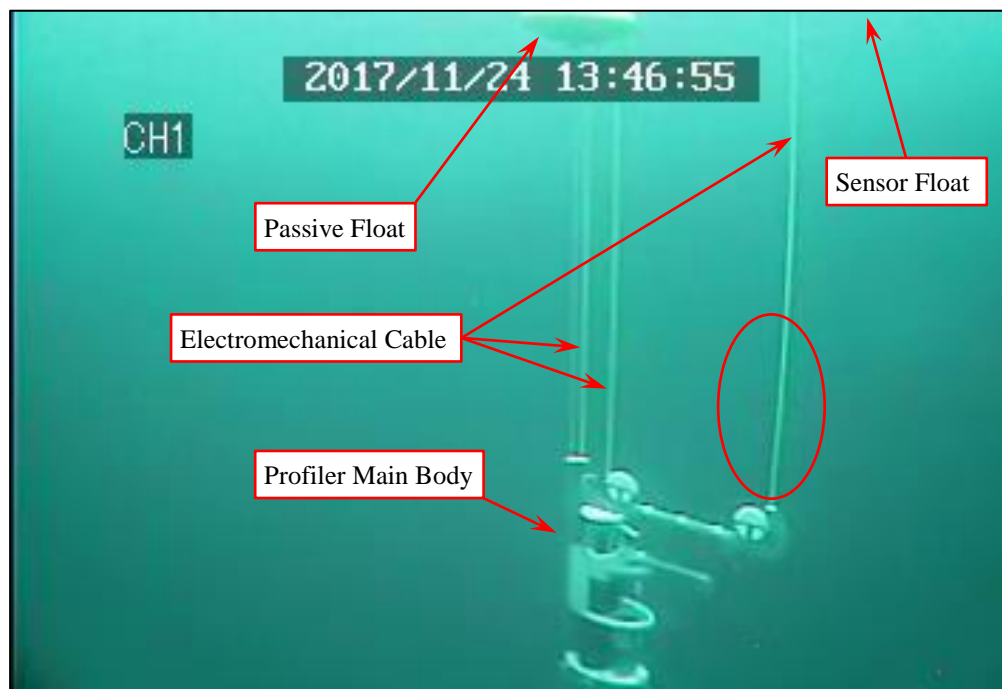


Figure 83 Second Field Trial - Profiler at the bottom of the mooring

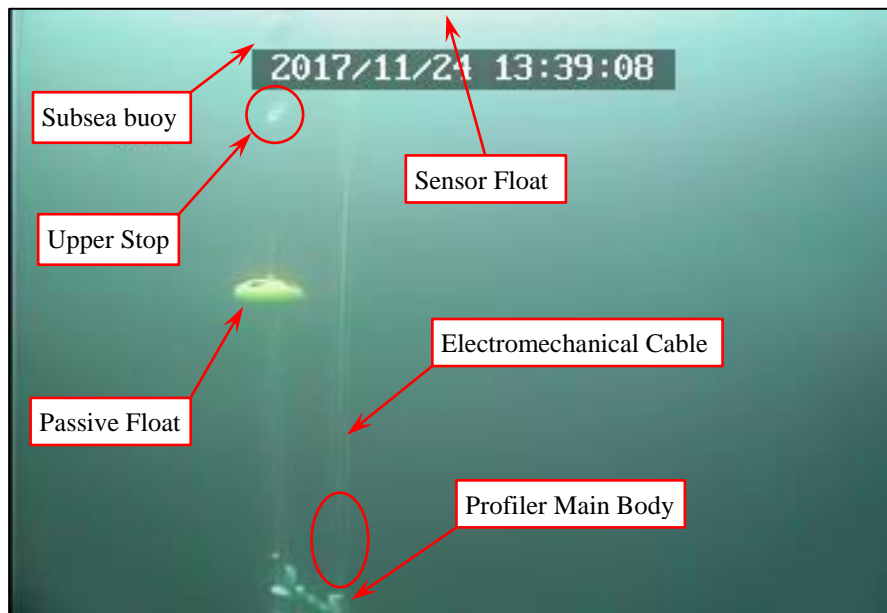


Figure 84 Second Field Trial- Profiler descent from the top of the mooring

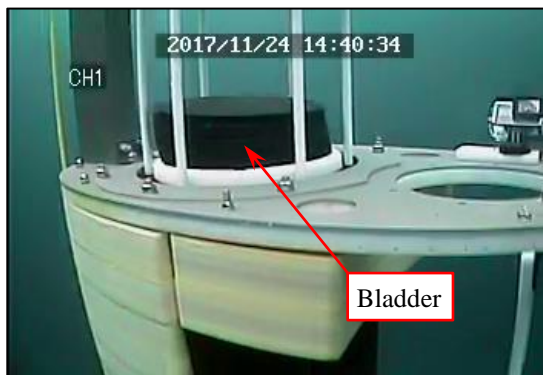


Figure 85 Empty bladder state (0 l)



Figure 86 Full Bladder state (6.5 l)

9.3 Third Field Deployment

The goal of the third deployment was to trim the buoyancy of the sensor float such that the passive float would be able to retract it. This was accomplished through an iterative process of adding 0.28 kg shackles to the antenna mast of the sensor float when it breached the surface during the ascent cycle. The option of adding foam to the passive

float was not viable since it is submerged, and the profiler would need to be retrieved for each iteration of foam addition. The third deployment was located at N 47°24' W 53°08' in a water depth of 52 m. The buoyancy engine was set to pump 6.5 litres of oil into and out of the bladder for the ascent and descent.

The mass required to be added to the sensor float to ensure it retracted was 1.12 kg (4 shackles). Figures 87 and 88 show the ROV screenshots of the profiler at the bottom and the top of the mooring, respectively. It is evident from the screenshots that the sensor float is retracted back to the frame at these points.

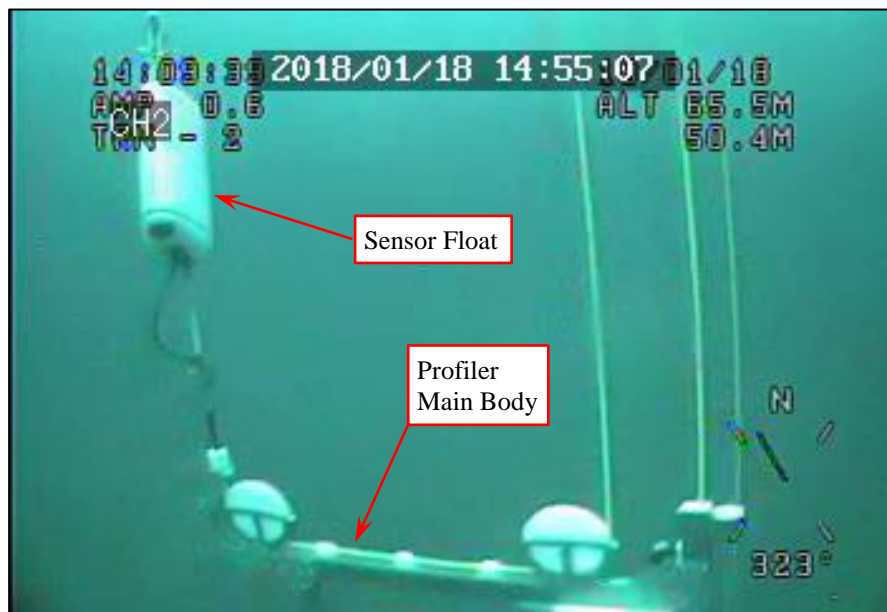


Figure 87 Third Field Trial - Profiler at the bottom of the mooring

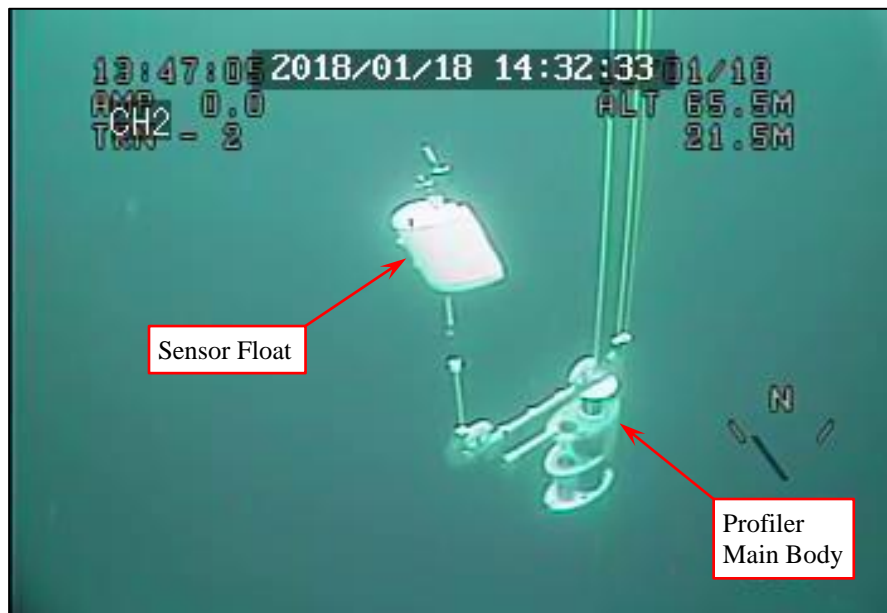


Figure 88 Third Field Trial- Profiler at the top of the mooring.

Through observations with the ROV, the profiler maintains the sensor float in the retracted position during the primary and secondary ascent. The added mass was successful in reducing the buoyancy of the sensor float such that the passive float could retract it. Unfortunately, the magnitude of the sensor float's reduced buoyancy did not have the capacity to lift the weight of the main body to progress through the secondary ascent. This is illustrated from the depth versus time plot for the profile in Figure 89. The sensor float maintains a depth of 20 m after the pump stops at the 417 s mark as indicated by the vertical red dashed line. Additional buoyancy needs to be added to the main body by pumping more oil into the bladder to decrease its weight. Unfortunately, at this point communication could not be made with the profiler since it was submerged. There was also insufficient time remaining in the day to retrieve the profiler to make a communication link and continue with testing.

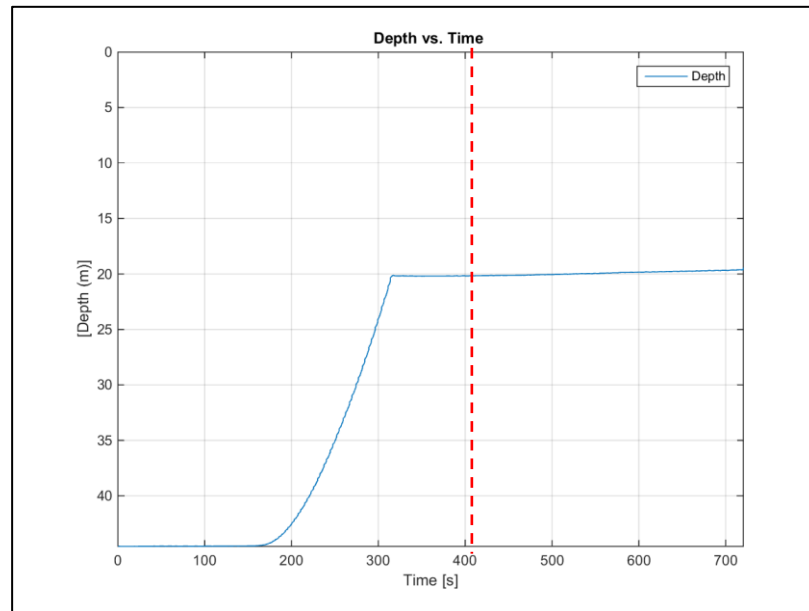


Figure 89 Third field deployment sensor float depth vs. time plot for the ascent with the 1.2 kg of mass added to the sensor float

An interesting observation was made from the sensor float depth versus time plot when only 0.84 kg of mass was added (3 shackles), Figure 90. The sensor float begins the ascent profile at 41.2 meters compared to 44.5 meters for the fully retracted profile with 1.2 kg of mass added to the sensor float. Therefore, the sensor float is not fully retracted during the ascent but only 3.3 meters of cable are payed out. This is evident from the screen shot from the ROV video, Figure 91. The payout is much less then the 12-15 m from previous field tests with no mass added to the sensor float. At the 284 s mark the passive float reaches the upper mooring stop and the sensor float hold at a depth of 15 m until approximately the 376 s mark. This is indicated by the purple and blue dashed lines. During this time the weight of the main body exceeds the 3:1 capacity of the sensor float. Oil is still pumping into the bladder at this point and continues to until the 418 s mark; the

red dashed line. At the 376 s mark the wet weight of the main body is reduced sufficiently to allow the sensor float to lift it and start the secondary ascent. The average rate of ascent during the secondary ascent is 0.06 m/s. At the 642 s mark the sensor float breaches the surface, Figure 92. This data and the observations made with the ROV indicate the profiler has the ability to operate as intended. The buoyancy of the sensor float, passive float, and/or main body need to be optimized.

When the sensor float mass was increased by 0.28 kg from 0.84 kg to 1.12 kg it lost the ability to cycle through the secondary ascent. Since the sensor float has a 3:1 mechanical advantage the mass of the main body needs to reduce by 0.84 kg ($3 \times 0.28 \text{ kg}$) to allow the profiler to cycle through the primary and secondary ascent. This is equivalent to 8.24 N, or increasing the output of the buoyancy engine by ~ 0.824 litres.

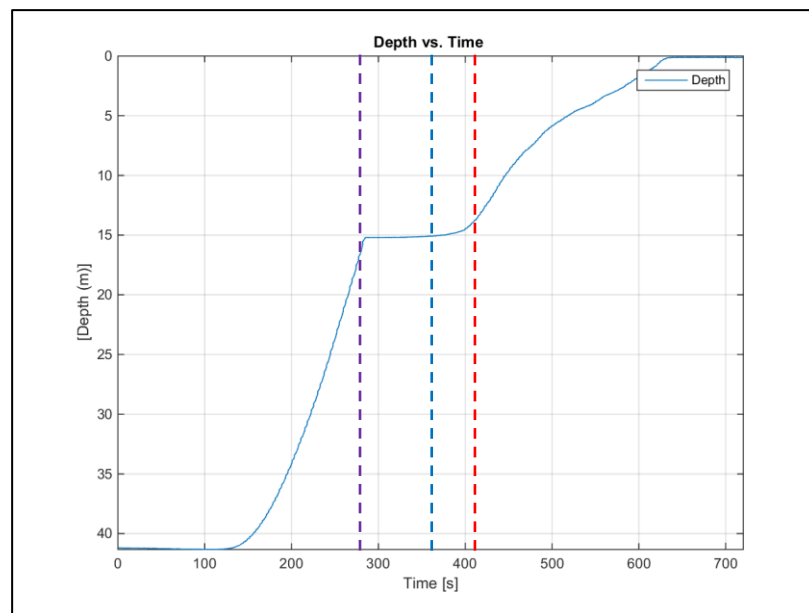


Figure 90 Third field deployment - Sensor float depth vs. time plot for the ascent with the 0.84 kg of mass added to the float

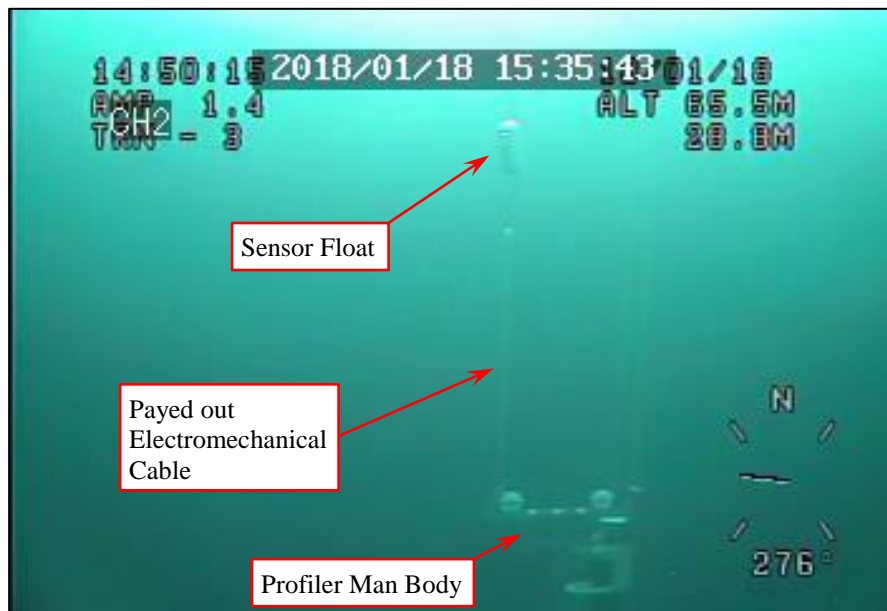


Figure 91. Third field deployment - Sensor float electromechanical cable payout during the ascent (0.84 kg of mass added)

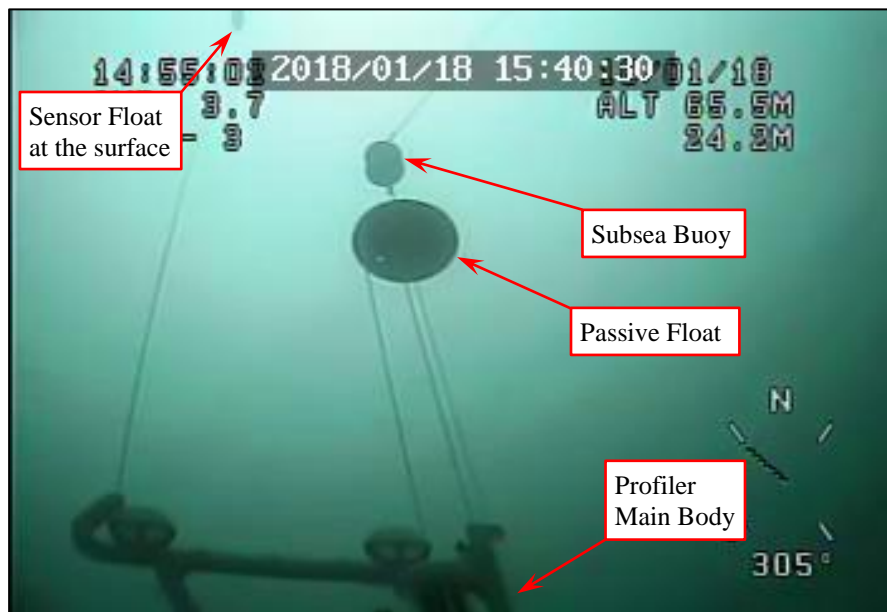


Figure 92 Third field deployment - Sensor float breaching the surface (0.84 kg of mass added)

9.4 Fourth Field Deployment

The goal of the fourth deployment was to test the profiler with an increase in the buoyancy of the main body to adjust for the 1.12 kg of mass added to the sensor float.

The option of adding foam to the passive float was considered but excluded due to the uncertainty of introducing a different variable. The fourth deployment was located at the same location as the third deployment; N 47°24' W 53°08' in a water depth of 52.

The buoyancy engine was set to pump 7.5 litres (an additional litre from the 3rd field trial) of oil into and out of the bladder for the ascent and descent. The result of the depth vs time plot is shown in Figure 93. The profiler only makes a partial secondary ascent and does not breach the surface. The plot and raw data indicate that 2.3 meters of electromechanical cable was payed out during the secondary ascent. However, observations from the ROV (Figure 94), and the GoPro (Figure 95), show that the sensor float payed out an estimated 6 meters of cable. The system stopped measuring data before this point.

Post-deployment review of the ROV videos and the raw data indicated that 7.5 litres of oil was not pumped into the bladder. Figure 96 shows a screenshot of the bladder filled to its maximum point for the profile. Observations from prior bench testing and a manual fill and empty cycle prior to the fourth deployment indicated the bladder should contact the top of the bladder cage when it is filled with 7.5 litres of oil. This did not occur as indicated in the screenshot. The level is comparable to the bladder fill level seen in the 6.5 litre profiles (Figure 86). Review of the battery voltage and current plot in Figure 97 show

that power was cut off from the pump at the 417 s mark. This is the same amount of time as the previous three field trials when pumping 6.5 litres of oil into the bladder. A positive displacement pump needs more time to pump more volume. Without the additional 1 litre of oil pumped into the bladder, the profiler was not capable of performing the secondary ascent to breach the surface.

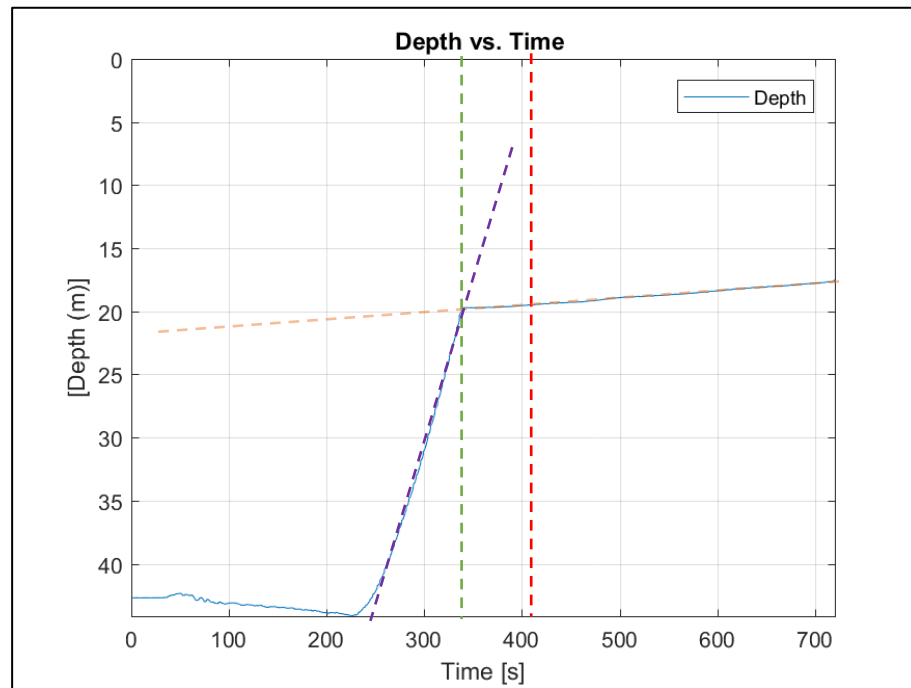


Figure 93 Fourth field deployment - Sensor float depth vs. time plot

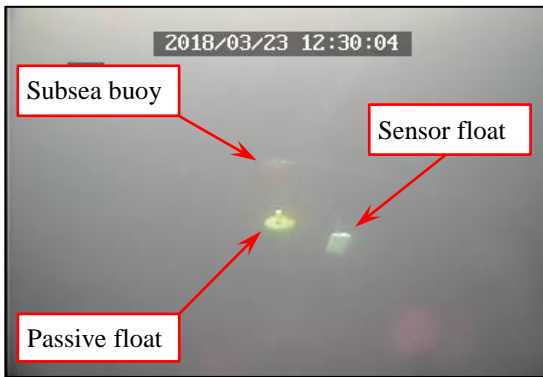


Figure 94 Fourth field deployment – ROV screenshot of the maximum sensor float payout

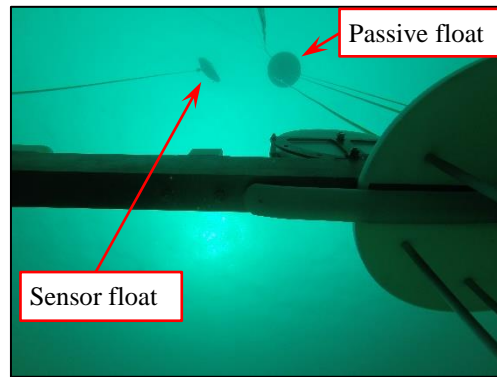


Figure 95 Fourth field deployment – GoPro picture of the maximum sensor float payout

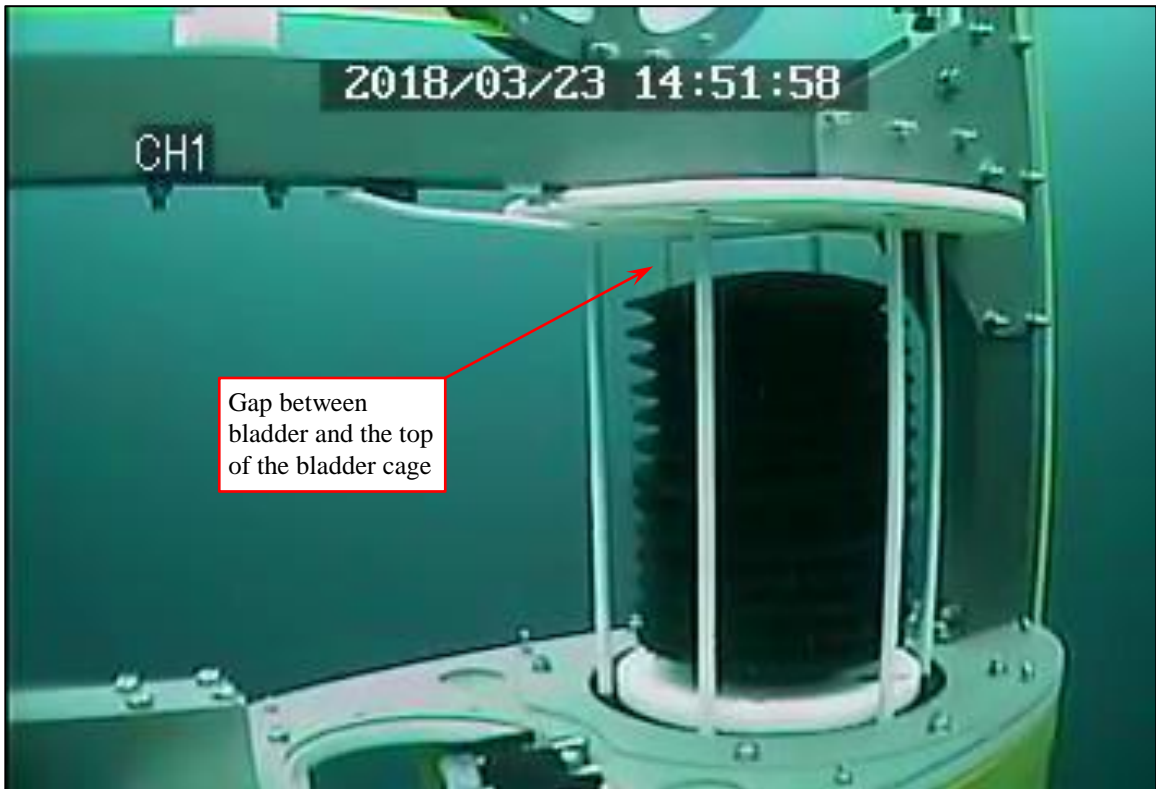


Figure 96 Fourth field deployment - Bladder not filled with 7.5 litres of oil

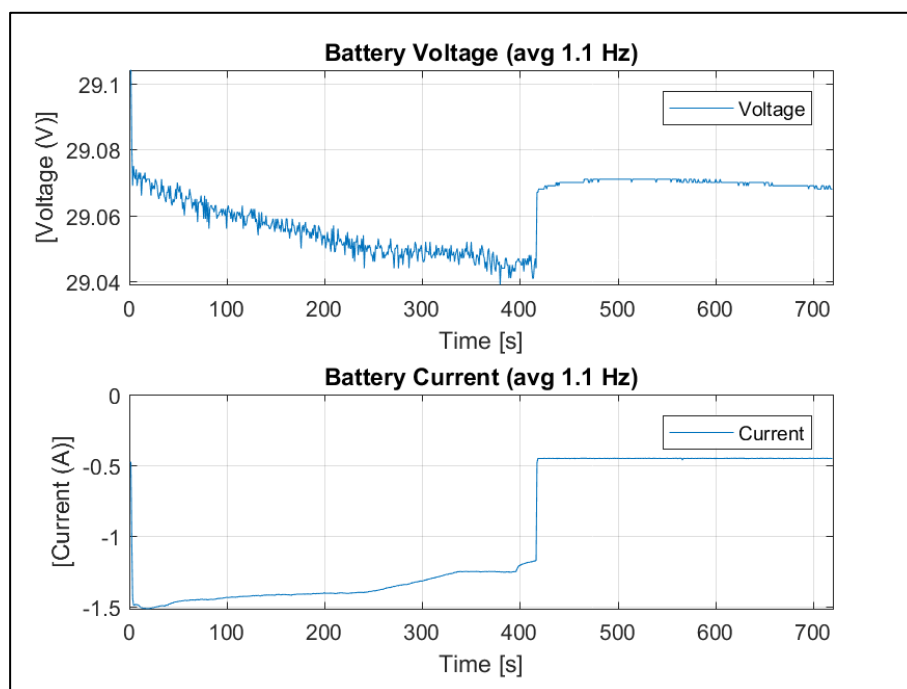


Figure 97 Fourth field deployment – Battery voltage and current vs. time

Additional analysis of the raw data available from the depth versus time plot and the battery voltage and current versus time plots revealed the following information about the profile.

- The average rate of the primary ascent was 0.27 m/s. Compared to the other field trials with less weight on the sensor float, the start of the ascent takes longer due to the need to overcome the additional weight.
- The average rate of the secondary ascent was 0.006 m/s. It starts at the 338 s mark which is similar to the 376 s experienced in the third field trials. There is little to no holding period between the primary and secondary ascent for the fourth field trial. This is due to the slower time it takes for the passive float to reach the upper

stop. There is enough oil pumped into the bladder when the passive float reaches the subsea buoy to start the secondary ascent.

- The maximum system power demand is 43.6 W (29.05 V and 1.5 A) at the start of the profile where the bladder is at a depth of 47 m. Once the pump cuts off and only the sensors and control system are operating, the power demand is 13 W (29.07 V and 0.45 A). This is the same power demand as the other field trials. The resulting maximum power demand from the hydraulic system is 30.6 W.

Two key observations were made during the fourth field trial to provide assurance of the system operation. The first observation was that the sensor float could be raised to the surface through the secondary ascent cycle by pushing upwards on the bottom of the profiler's frame with the ROV. This is essentially simulating additional buoyant force.

The pushing force from the ROV was removed when the sensor float breached the surface and the sensor float was able to maintain its position at the surface rather than retracting.

This implies that the system is very close to achieving the buoyancy required. The second observation was that the descending profile after the sensor float was at the surface behaved as expected. The sensor float first retracted back to the frame before the complete system descended to the bottom of the mooring line.

Due to time and budget constraints the fourth field trial was the last test conducted with the profiler.

10 Conclusion and Future Work

The principal aim of this work was to pursue a novel approach to a viable alternative autonomous moored profiler to characterize the water column of the continental shelf. A concept was theorized then designed and developed into a functional prototype capable of operating in an open ocean environment for field testing.

The profiler design can be considered a hybrid of a wire follower type profiler. A unique characteristic of the system is that it is constrained by a subsea mooring to protect it from the harsh environment of the surface. However, it can also sample the water column above the mooring and make a telemetry link at the surface. The profiler relies on a hydraulic buoyancy engine for the primary means of propulsion and a compound pulley arrangement as the secondary means. Another unique characteristic of the systems is that the hydraulic buoyancy engine only requires power for propulsion during the ascent.

Field testing was conducted over four separate deployments at Holyrood Bay in water depths up to 50 meters. The system closely exhibited the behaviours expected but ultimately did not perform exactly as intended. However, the data collected from the profiler's instruments and sensors, in conjunction with the visual observation made with an ROV indicate a high potential for the profiler to operate successfully. The inability to perform as designed was attributed to a lack of buoyancy output from the buoyancy engine. An increase in the output volume of the buoyancy engine provides more lifting capacity to sensor float which allows it to deploy to the surface during the secondary ascent. This is an issue that can be easily remedied by increasing the capacity from the

intended 6.5 l to 7.5 l, or greater. Unfortunately, the increase in buoyancy capacity from the buoyancy engine requires more energy. In an attempt to minimize the energy consumption, the system was designed with low limits on the balance of the system/component buoyancy values. Based on the buoyancy values provided previously in Table 15, the passive float only has 10.6 N of extra lifting capacity to retract the sensor float, and the sensor float only has 13.7 N of extra capacity to deploy from the main body. The low limits on the buoyancy capacities does not provide a lot of tolerance for parasitic loads on the system such as friction in the pulleys, and contact between the electromechanical cable and the guides, or the mooring cable and the guides. As well, drag on the components caused by currents could impose a resistive lifting or depressing force. The impact of these forces coupled with the low buoyancy limits may have been the cause failure of the system to behave as intended under the initial deployment setup (before adjusting the system/component buoyancy values).

The profiler was successful in sequentially completing the primary and secondary ascent to breach the surface with the sensor float before completing the secondary and primary descent. The only issue was that the sensor float was not fully retracted during the primary ascent and descent which increases the risk of entanglement. During the profiles the sensors were able to successfully measure and record the characteristics of the water column. The only exception was the altimeter which exhibited unreliable data.

Minimizing energy consumption was a key objective during the design process. Field testing revealed the instrumentation, sensors, and control system profiler consumed more

power than expected. It required approximately 13 W compared to the estimated 10 W expected. The maximum demand from the buoyancy engine was 30.6 W at ~50 meters. This was very close to the 30 W expected, based on the bench temperature test results. The power demand needs to be further minimized to make it a viable solution for long term profiling up to five times a day. There are several approaches that can be considered which are indicated at the end of this section

Due to the mobility between the cables, sensor float, passive float, and main body, the deployment of the profiler was a tedious ordeal. It required favourable sea conditions, support from secondary vessel, and multiple able bodied personnel. Temporarily constraining the components of the profiler together as one cohesive unit would significantly improve the ease of deployment, reduce the number of personnel required, and possibly eliminate the need for a secondary vessel requirement.

There is a significant amount of potential work that should be completed in order to further validate the design, and to improve power consumption and ease of deployment. The following work is listed in order of priority.

- Develop and implement a method to communicate with the profiler when it is submerged. This would only be required during field testing where it would be advantageous to have the capability to take over control of the buoyancy engine.
- Complete a fifth field deployment under the same conditions as the fourth field deployment to verify that the profiler performs exactly as intended when 7.5 litres of oil is pumped into the bladder.

- Complete further field deployments of longer durations, greater depths, and more adverse conditions to assess the performance.
- Focus on the development of a more efficient buoyancy engine. Optimize the brushless DC motor paired with the pump. Investigate using a de-intensifier in the hydraulic system. A de-intensifier is a hydraulic intensifier operated in reverse. A de-intensifier requires oil at high pressure and low volume from the pump to output low pressure and high volume to the bladder. The axial piston pump used in this application has a maximum efficiency of 85%, but only at a pressure of 100 bar. When operating at 20 bar (~200 m) the efficiency is only 67%. A 5:1 de-intensifier would cause the pump to work at 100 bar and 85% efficiency to deliver 20 bar to the bladder. The volume pumped into the de-intensifier is only 20 percent of what is injected into the bladder. The hydraulic system can be customized for the depth of the deployment to always ensure the system is operating at its peak efficiency. Intensifiers operate at 95% efficiency, when used with an 85% efficient pump the maximum system efficiency is improved to 81%.
- A two-stage buoyancy engine should also be investigated to reduce the energy consumption. The primary ascent should be completed with an axial piston pump due to the high pressure requirement. The additional buoyancy required for the secondary ascent may be achieved from a pump that operates more efficiently at the lower pressure of 2 bar (~20 m). Splitting the profile into two stages also provides an excellent opportunity to assess the sea state before proceeding through the secondary ascent.

- Investigate the possibility of using a latching solenoid valve to control the flow of oil in the hydraulic circuit. A latching solenoid valve only requires a momentary energization to switch from open to close (or close to open). If applicable, two latching solenoid valve could replace all the hydraulic components between the pump and bladder. Such a system would be much less complex to plumb, and possibly require less power.
- Continue to work on a deployment solution. Promising preliminary investigative, and assessment work was complete on using polyvinyl alcohol (PVA) release tabs. PVA is a water-soluble plastic. It was envisioned to use these tabs with rope to help constrain the passive and sensor float to the frame, and manage the electromechanical cable. Controlled and timely release of these constrained components would significantly improve the ease of deployment. The tabs that were 3D printed and tested exhibited good initial strength, and the ability to maintain adequate strength for up to 30 minutes when submersed in water. A decrease in water temperature also decreased the solubility rate which provides more working time.
- Modify the sensor payload float to ensure the altimeter is mounted vertically. This is required to collect reliable altimeter data.

Bibliography

All Rigging Co. (2016, January 1). *Technical Information Related With Wire Ropes*.

Retrieved from All Rigging Co.: <http://allrigging.com/drum-data/>

Anaheim Automation. (2016, 05 14). *Anaheim Automation*. Retrieved from BLWS23

Series - Brushless DC Motors:

<http://www.anaheimautomation.com/manuals/brushless/L010229%20-%20BLWS23%20Series%20Product%20Sheet.pdf>

Argo. (2018, June 3). Retrieved from Argo:

http://www.argo.ucsd.edu/How_Argo_floats.html

ASME. (2015). *An International Code 2015 ASME Boiler & Pressure Vessel Code, Section II, Part D (Properties (Customary))*. New York: ASME.

ASME International. (2015). *Guide for ASME Section VIII Division 1 Stamp Holders PTB-10 - 2015*. New York , NY, USA: ASME International.

Benard, A. (2006). The Minature Autonomous Moored Profiler (Mini AMP). Retrieved

from

[http://www.researchgate.net/publication/228957963_The_Miniaturized_Autonomous_Moored_Profiler_\(Mini_AMP\)](http://www.researchgate.net/publication/228957963_The_Miniaturized_Autonomous_Moored_Profiler_(Mini_AMP))

Berteaux, H. (1976). Buoy Engineering. In H. Berteaux, *Buoy Engineering* (pp. 107-108). New York: Wiley.

- Camacho, J. M., & Sosa, V. (2013). Alternative method to calculate the magnetic field of permanent magnets with azimuthal symmetry. *Revista mexicana de física E*, 59, 8-17.
- Carlson, D. F., Ostrovskii, A. G., Kebkal, K., & Gildor, H. (2013). Moored automatic mobile profilers and their application. In O. Gal, *Advanced in Marine Robotics*, 169-206.
- Cimbala, J. M., & Cengel, Y. A. (2006). *Fluid Mechanics Fundamentals and Applications* (1st Edition ed.). New York, NY, USA: McGraw-Hill Education.
- Collins, M., An, S.-I., Cai, W., Ganachaud, A., Guilyardi, E., Jin, F.-F., . . . Wittenberg, A. (2010). The impact of global warming on the tropical Pacific Ocean and El Niño. *Nature Geoscience*, 3, 391. doi:10.1038/ngeo868
- Cutler, G. (2018). *MAVP Software Documentation*. Unpublished manuscript, AOSL.
- Davis, R. E., Eriksen, C. C., & Jones, C. P. (2003). Autonomous Buoyancy-Driven Underwater Gliders. In G. (. Griffiths, *Technology and Applications of Autonomous Underwater Vehicles* (pp. 37-58). London: CRC Press.
- Davis, R. E., Talley, L. D., Roemmich, D., Owens, W. B., Rudnick, D. L., Toole, J., . . . Barth, J. A. (2019). 100 Years of Progress in Ocean Observing Systems. *Meteorological Monographs*.

Donaldson Company, Inc. (2017). Hydraulic Filtration Product Guide. *Catalog No. F112100 ENG (1/17)*. Minneapolis, MN, USA: Donaldson Company, Inc.

Retrieved from <https://www.donaldson.com/content/dam/donaldson/engine-hydraulics-bulk/catalogs/Hydraulic/North-America/F112100-ENG/Hydraulic-Filtration-Product-Guide.pdf>:

<https://www.donaldson.com/content/dam/donaldson/engine-hydraulics-bulk/catalogs/Hydraulic/North-America/F112100-ENG/Hydraulic-Filtration-Product-Guide.pdf>

Drinkwater, K. F. (2005). The response of Atlantic cod (*Gadus morhua*) to future climate change. *ICES Journal of Marine Science*, 62(7), 1327-1333. Retrieved from <https://doi.org/10.1016/j.icesjms.2005.05.015>

Durr, S., & Thomason, J. (2010). *Biofouling*. Oxford, UK: Wiley-Blackwell.

Eaton Fluid Power Training. (2010). *Industrial Hydraulics Manual*. Maumee, OH, USA: Eaton Corporation.

Fowler, G. A., Hamilton, J. M., Beanlands, B. D., & Furlong, A. R. (1997). A Wave-Powered Profiler for Long-Term Monitoring. *Oceans '97 MTS/IEEE*, (pp. 225-228).

Gliders. (2018, June 03). Retrieved from National Oceanography Centre: <http://noc.ac.uk/facilities/marine-autonomous-robotic-systems/gliders>

GORE. (2016, May 01). *Protective Vents*. Retrieved from GORE Crative Technologies

Worlwide: <https://www.gore.com/sites/g/files/ypyipe116/files/2016-07/PTV-Datasheet-Screw-In-Series-US.pdf>

Gould, J. (2004, May 11). Argo profiling floats bring new era of in situ ocean observations. *EOS*(19), pp. 179,190-191. doi:10.1029/2004EO190002

Govardhan, R., & Williamson, C. (1997). Vortex-induced motions of a tethered sphere. *Journal of Wind Engineering and Industrial Aerodynamics*, 69–71, 375-385. doi:10.1016/S0167-6105(97)00170-0

Grosenbaugh, ,. M. (1995). Designing Oceanographic Surface Moorings to Withstand Fatigue. *Journal of Atmospheric and Oceanic Technology*, 1101-1110.

Guru, B. S., & Hiziroglu, H. R. (1995). *Elictrical Machinery and Transformers* (2nd ed.). Orlando, Florida, USA: Harcourt Brace College Publishers.

Hatami , H. (2013, October 01). *Hydraulic Formulary*. Retrieved from Rexroth Bosch

Group:

https://www.boschrexroth.com/business_units/bri/de/downloads/hyd_formelsammlung_en.pdf

Hawe Hydraulik. (2017, March 01). *Releasable check valves*. Retrieved from Hawe

Hydraulik: <http://downloads.hawe.com/6/1/D6105-en.pdf>

- Hibbeler, R. C. (2007). *Engineering Mechanics Statics and Dynamics* (11th ed.). Upper Saddle River, New Jersey, USA: Pearson Prentice Hall.
- Horn, M., Riewald, P., & Zweben, C. (1977). Strength and durability characteristics of ropes and cables from Kevlar aramid fibers. *CEANS '77 Conference Record* (pp. 313-324). Los Angeles: IEEE-MTS. doi:10.1109/OCEANS.1977.1154444
- Hunt, T. M., & Vaughan, N. (1998). *The Hydraulic Handbook*. Kidlington, Oxford, UK: Elsevier Advanced Technology.
- Hurley, J., de Young, B., & Williams, C. D. (2008). Reducing Drag and Oscillation of Spheres Used for Buoyancy in Oceanographic Moorings. *Journal of Atmospheric and Oceanic Technology*, 1823–1833. Retrieved from <https://doi.org/10.1175/2006JTECHO472.1>
- Ibex Marina. (2015, March 06). *Power Spring*. Retrieved from Ibex MARina: <https://online.flowpaper.com/754b071d/PowerSpringsBrochures5/>
- InterOcean. (2013, September 16). *InterOceans Systems VPS - Vertical Profilling System*. Retrieved from <http://www.interoceansystems.com/vps.htm>: <http://www.interoceansystems.com/vps.htm>
- Joseph, A. (2013). *Measuring Ocean Currents: Tools, Technologies, and Data*. San Diego: Elsevier.

- Kale, S., Joshi, P., & Pant, R. (2005). A generic methodology for determination of drag coefficient of an aerostat envelope using CFD. *AIAA 5th ATIO and 16th Lighter-Than-Air Sys Tech. and Balloon Systems Conferences*. Arlington.
doi:<https://doi.org/10.2514/6.2005-7442>
- McArtney. (2015, May 10). *TrustLink Stress Termination*. Retrieved from McArtney Underwater Solutions: <https://www.macartney.com/media/5321/trustlink-stress-terminations.pdf>
- McLane Moored Profiler*. (2018, June 03). Retrieved from McLane Labs:
<http://mclanelabs.com/mclane-moored-profiler/>
- Morrison III, A. T., Billings, J. D., & Doherty, K. W. (2000). The McLane moored profiler: an autonomous platform for oceanographic measurements. *Oceans 2000 MTS/IEEE Conference and Exhibition, 1*. doi:0.1109/OCEANS.2000.881284
- Mott, P. H., & Roland, C. H. (2001). Aging of Natural Rubber in Air and Seawater. *Chemistry and Technology*, 74(1), 97-88.
- Munson, B. R., Young, D. F., & Okiishi, T. H. (1994). *Fundamentals of Fluid Mechanics* (2nd ed.). New York: John Wiley & Sons Inc.
- National Academies of Sciences, Engineering, and Medicine. (2017). *Sustaining Ocean Observations to Understand Future Changes in Earth's Climate*. Washington, DC: The National Academies Press. doi:10.17226/24919

Parambath, J. (2016). *Industrial Hydraulic Systems - Theory and Practice*. Boca Raton, FL, USA: Universal-Publishers.

Parker Hannifin Corporation. (2007). *Parker O-Ring Handbook ORD 5700*. Cleveland, Ohio, USA: Parker Hannifin Corporation.

Randall, R. E. (2010). *Elements of Ocean Engineering*. Jersey City, NJ Society of Naval Architects & Marine Engineers, USA: Society of Naval Architects & Marine Engineers.

Send, U., Fowler, G., Siddall, G., Beanlands, B., Pittman, M., Waldmann, C., . . .

Lampitt, R. (2013). SeaCycler: A Moored Open-Ocean Profiling System for the Upper Ocean in Extended Self-Contained Deployments. *The Journal of Atmospheric and Oceanic Technology*, 30(7), 1555-1565. Retrieved from <https://doi.org/10.1175/JTECH-D-11-00168.1>

Shigley, J. E., & Mischke, C. R. (1996). *Standard Book of Machine Design*. New York, USA: McGraw-Hill.

Siedler, G., Griffies, S. M., Gould, J., & Church, J. A. (2013). *Ocean Circulation and Climate: A 21st Century Perspective*. Oxford: Academic Press.

Sizing Accumulators. (2013, March 01). Retrieved from Hydac: <http://www.hydac-na.com/sites/hydac-na/SiteCollectionDocuments/AOSS-%20accumulators.pdf>

Sprintall, J., & Cronin, M. F. (2008). Upper Ocean Vertical Structure. (J. H. Steele, Ed.)

Encyclopedia of Ocean Sciences, Second Edition, pp. 217-224.

Stantec. (2014). *Shelburn Basin Exploration Drilling Project Environmental Impact*

Statement. Edmonton: Stantec. Retrieved from

<https://www.ceaa.gc.ca/050/documents/p80058/99342E.pdf>

Telco Intercontinental Corp. (2016, June 02). *DC Brushless Motor*. Retrieved from Telco:

<http://www.telcointercon.com/article/dc-brushless-motor>

Teledyne Webb Research. (2018, June 03). Retrieved from Naval Technology:

<https://www.naval-technology.com/contractors/sonar/teledyne-webb-research/attachment/teledyne-webb-research1/>

Thorpe, S. A. (Ed.). (2009). *Measurement Techniques, platforms & sensors: A derivative of the encyclopedia of ocean sciences*. San Diego: Academic Press.

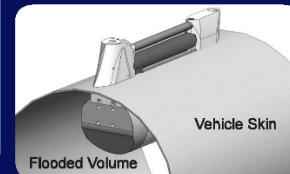
Appendix A

Product Specification Sheets

Glider Payload CTD (optional DO) GPCTD

The GPCTD is a modular, low-power profiling instrument for autonomous gliders with the high accuracy necessary for research, inter-comparison with moored observatory sensors, updating circulation models, and leveraging data collection opportunities from operational vehicle missions. The externally powered, continuously pumped CTD consumes only 175 mW recording at 1 Hz (190 mW for real-time data). One Alkaline D cell could operate the CTD continuously for 114 hours (9.5 days at 50% duty cycle, profiling continuously at 1 Hz on every glider upcast); one Lithium DD cell could provide 48 days continuous profiling on every upcast. Data are output in engineering units.

The GPCTD can optionally be equipped with an SBE 43F Dissolved Oxygen sensor, but does not support other auxiliary sensors.



Features

- Conductivity, Temperature, Pressure, and (optional) Dissolved Oxygen (modular SBE 43F DO sensor).
- Pressure-proof module allows for exchange of CTD (and DO sensor) without opening glider pressure hull.
 - Assembly visible on glider exterior consists of intake sail (with integral T-C duct and anti-foulant device), internal field conductivity cell, and exhaust sail with pump connections. Intake sail allows measurements to be made outside vehicle's boundary flow (where old water is thermally contaminated by vehicle). Pump pulls water into intake sail, past temperature sensor, through anti-foulant device and conductivity cell, and out exhaust sail (preventing exhaust re-circulation and Bernoulli pressure differences from changing flow rate). Outside of conductivity cell is free-flushed, minimizing salinity errors. Connecting neck, electronics, pump, and DO sensor are in a flooded space inside hull, placed so that tubing lengths are minimized (between conductivity cell and pump intake, and from pump outlet to sail exhaust fitting), sharp bends are avoided, and pump and tubing are oriented to avoid trapping air that will interfere with pump priming.
- RS-232 interface, memory, real-time output, no batteries (for use on vehicles that can supply power).
- Four sampling modes: Continuous (1 Hz), Fast Interval (5-14 sec intervals), Slow Interval (15-3600 sec intervals; CTD only), and Polled.
 - Continuous sampling time series suitable for corrections (e.g. response filtering, alignment, thermal mass correction) for dynamic errors in data.
 - File headers (maximum 1000) contain beginning and ending sample numbers, sampling mode and interval, and starting date/time.
- Unique flow path, pumping regimen, and expendable anti-foulant device, for maximum bio-fouling protection.
- Pump-controlled, T-C ducted flow to minimize salinity spiking.
- Depths to 350 or 1500 m.
- Field-proven design based on Argo float CTD, with more than 10,000 Argo float CTDs deployed.
- Seasoft® V2 Windows software package (setup, data upload, data processing).
- Five-year limited warranty.

Components

- Unique internal-field conductivity cell permits use of expendable anti-foulant device, for long-term bio-fouling protection.
- Aged and pressure-protected thermistor has a long history of exceptional accuracy and stability.
- Pressure sensor with temperature compensation is available in four strain-gauge ranges (to 2000 m).
- (optional) Oxygen sensor is field-proven, individually calibrated SBE 43F Dissolved Oxygen sensor.
- For Continuous and Fast Interval sampling, pump runs continuously, providing bio-fouling protection and correlation of CTD (and optional DO) measurements.

Options

- Strain-gauge pressure sensor in one of 4 ranges (to 2000 m).
- SBE 43F interface in GPCTD, and modular SBE 43F Dissolved Oxygen Sensor in 600 or 7000 m housing.
- Plastic (350 m) or titanium (1500 m) housing.

Measurement Range

| | |
|--------------|---|
| Conductivity | 0 to 9 S/m (calibrated 0 to 6 S/m) |
| Temperature | -5 to +42 °C (calibrated +1 to +32 °C) |
| Pressure | 0 to 100 / 350 / 1000 / 2000 m (calibrated to full scale) |

Initial Accuracy

| | |
|--------------|--|
| Conductivity | In calibration range: ± 0.0003 S/m; Outside calibration range: ± 0.0010 S/m ¹ |
| Temperature | In calibration range: ± 0.002 °C; Outside calibration range: ± 0.004 °C ¹ |
| Pressure | In calibration range: $\pm 0.1\%$ of full scale range |

Typical Stability

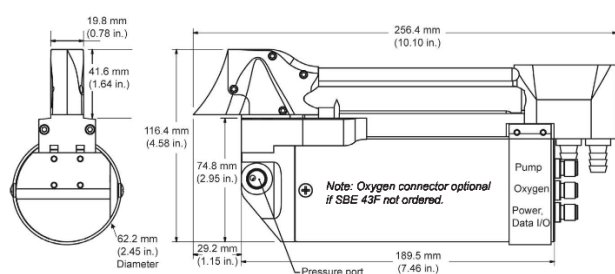
¹ Due to fit extrapolation errors.

| | |
|--------------|---|
| Conductivity | 0.0003 S/m per month |
| Temperature | 0.0002 °C per month |
| Pressure | $\pm 0.05\%$ of full scale range per year |

Resolution

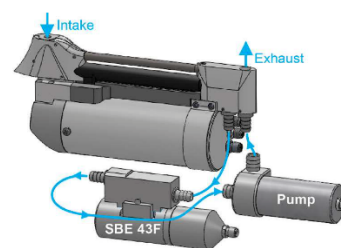
| | |
|--------------|----------------------------|
| Conductivity | 0.00001 S/m |
| Temperature | 0.001 °C |
| Pressure | 0.002% of full scale range |

| | |
|---------------------------------|--|
| Sampling Speed | 1 Hz (1 sample/sec) maximum |
| External Power Requirements | 8 to 20 VDC nominal. CTD only: 175 mW recording at 1 Hz; 190 mW transmitting real-time data. CTD & DO: 265 mW recording at 1 Hz; 280 mW transmitting real-time data. |
| Memory | 8 Mbytes; 699,000 samples CTD (194 hours at 1 Hz) or 559,000 samples of CTD & DO (155 hours at 1 Hz) |
| Data Format | Real-time and uploaded data in decimal or Hex: S/m, °C, decibars, DO frequency. |
| Housing, Depth Rating, & Weight | CTD & pump: Plastic, 350 m, in air 1.0 kg, in water 0.2 kg; Titanium, 1500 m, in air 1.2 kg, in water 0.4 kg. SBE 43F DO sensor: Plastic, 600 m, in air 0.3 kg, in water 0.1 kg; Titanium, 7000 m, in air 0.4 kg, in water 0.2 kg. |



Forward End View

Side View

With SBE 43F Oxygen Sensor
(plumbing approximate)

Specifications subject to change without notice. ©2014 Sea-Bird Scientific. All rights reserved. Rev. August 2015

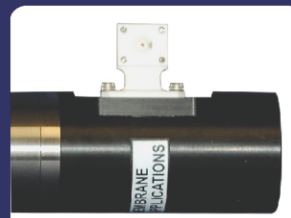


Sea-Bird Electronics
+1 425-643-9866
sales@seabird.com
www.seabird.com

SBE 43 Dissolved Oxygen Sensor

The SBE 43 is an individually calibrated, high-accuracy oxygen sensor to assist in critical hypoxia and ocean stoichiometric oxygen chemistry research on a variety of profiling and moored platforms. Careful choices of materials, geometry, and sensor chemistry are combined with superior electronics and calibration methodology to yield significant gains in performance.

The SBE 43 is designed for use in a CTD's pumped flow path, providing optimal correlation with CTD measurements. Elapsed time between the CTD and associated oxygen measurement is easily quantified, and corrected for, in post-processing. The black plenum and plumbing's black tubing blocks light, reducing in-situ algal growth. Plumbing isolates the SBE 43 from continuous exposure to the external environment, allowing trapped water to go anoxic and minimizing electrolyte consumption between samples for moored deployments.



Features

- Voltage or frequency output.
- Fully and individually calibrated; calibration drift rates of less than 0.5% over 1000 hours of operation (*on time*).
- For use in CTD pumped flow path, optimizing correlation with CTD measurements.
- Oxygen measurement dramatically improved because of improved temperature response.
- Signal resolution increased by on-board temperature compensation.
- Continuous polarization eliminates stabilization wait-time after power-up.
- Hysteresis largely eliminated in upper ocean (1000 m) due to improved temperature response. Hysteresis at greater depths predictable and correctable in post-processing.
- No degradation of signal or calibration when used for profiling in hydrogen sulfide environments.
- 600 or 7000 m housing.
- Five-year limited warranty (during warranty period, one sensor re-charge [electrolyte refill, membrane replacement, recalibration] performed free of charge).

Configuration Options

- SBE 43 voltage output sensor can be integrated with any Sea-Bird CTD that accepts 0-5 volt auxiliary sensor input. It is available with 600 m plastic or 7000 m titanium housing; XSG or wet-pluggable MCBH connector; 0.5-mil membrane (fast response, typically for profiling applications) or 1-mil membrane (slower response but more rugged for enhanced long-term stability, typically for moored applications).
- SBE 43F frequency output sensor can be integrated with SBE 52-MP or Glider Payload CTD, or used for OEM applications (requires OEM circuit board); it is available with 600 m plastic or 7000 m titanium housing. Another 43F version is used as an integral part in SBE 37-SIP-IDO MicroCATs.

Performance

| | |
|--------------------|--|
| Measurement Range | 120% of surface saturation in all natural waters (fresh and salt) |
| Initial Accuracy | ± 2% of saturation |
| Typical Stability | 0.5% per 1000 hours of deployed time (clean membrane) |
| Response Time Tau* | 2 to 5 sec for 0.5-mil membrane, 8 to 20 sec for 1.0-mil membrane *Time to reach 63% of final value for a step change in oxygen; dependent on ambient water temperature and flow rate (see Application Note 64 for discussion) |

Electrical

| | |
|---------------|---|
| Input Power | 6.5 - 24 VDC; 60 milliwatts (SBE 43) or 45 milliwatts (SBE 43F) |
| Output Signal | 0 - 5 VDC (SBE 43), frequency (SBE 43F) |

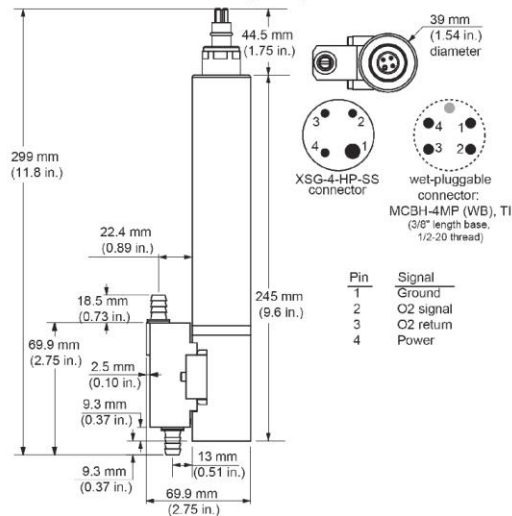
Mechanical

| | |
|----------------------------|--|
| SBE 43 (voltage output) | 600 m Plastic housing - 0.5 kg in air, 0.1 kg in water 7000 m Titanium housing - 0.7 kg in air, 0.4 kg in water |
| SBE 43F (frequency output) | 600 m Plastic housing - 0.3 kg in air, 0.1 kg in water 7000 m Titanium housing - 0.4 kg in air, 0.2 kg in water |



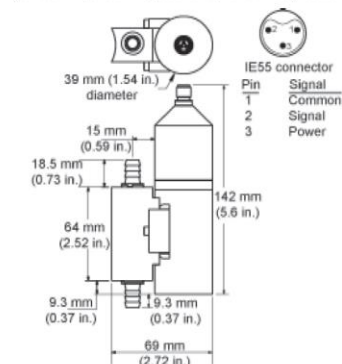
SBE 43 voltage output
sensor integrated with
SBE 19plus V2 CTD

SBE 43 Voltage Output Sensor



SBE 43F Frequency Output Sensor

(for 52-MP, Glider Payload CTD, & OEM applications)



Specifications subject to change without notice. ©2016 Sea-Bird Scientific. All rights reserved. Rev. June 2016



Sea-Bird Electronics
+1 425-643-9866
sales@seabird.com
www.seabird.com

ECO FL Fluorescence

The Environmental Characterization Optics (ECO) series of single channel fluorometers delivers both high resolution and wide ranges across our entire line of parameters using 14 bit digital processing. The ECO series excels in biological monitoring and dye trace studies. The potted optics block results in long term stability of the instrument and the optional anti-biofouling technology delivers truly long term field measurements.

ECO FL fluorometers measure fluorescence from chlorophyll-a, CDOM, uranine, rhodamine, and phycocyanin and phycoerythrin.

Chlorophyll-a fluorescence is an indicator of active phytoplankton biomass and chlorophyll concentrations. This measurement is used for tracking biological variability and abundance in the water column.

Colored Dissolved Organic Matter (CDOM) ECO allows you to obtain CDOM fluorescence across a wide range of environments, from mangrove swamps to oligotrophic blue water.

Uranine (fluorescein) & Rhodamine: The ideal combination of linearity, sensitivity and range for dye studies. Detection limits in parts per trillion allows for precise patch determination and first arrival timing as well as reducing the necessary initial dye concentration.

ECO phycobilin fluorometers have the high resolution necessary for early detection of either blue-green (**phycocyanin**) or brown (**phycoerythrin**)



Features

- Ships with ECOView Host software
- Analog and Digital Output
- Analog scaling to maximize analog resolution
- Optional integrated Bio-wiper™ and/or copper faceplate for antifouling
- Optional internal batteries and memory; 100K + samples
- Full ocean depth model available

Optical

| | |
|---|--|
| Chlorophyll-a ex/em: Sensitivity Range | 470/695 nm 0.02 µg/L 0–125 µg/L |
| CDOM: Sensitivity Range | ex/em: 370/460 nm 0.09 ppb 0–500 ppb |
| Uranine: Sensitivity Range | ex/em: 470/530 nm 0.05 ppb 0–400 ppb |
| Rhodamine: | ex/em: 540/570 nm |
| Phycocerythrin: | ex/em: 540/570 nm |
| Phycocyanin: Sensitivity Range | ex/em: 630/680 0.03 ppb 0–230 ppb |
| Linearity (all) | 99% R ² |

Environmental

| | |
|-------------------|------------------------------|
| Temperature Range | 0 - 30 °C |
| Depth Rating* | 600 m (std) 6000 m (deep) |

Mechanical

| | |
|-----------------|------------------|
| Diameter | 6.3 cm |
| Length | 12.7 cm |
| Weight in air | 0.4 kg |
| Weight in water | 0.02 kg |
| Materials | Acetal copolymer |

Options*

- **FL(RT)** Provides analog or RS-232 serial output with 16,300-count (approximate) range. "Real Time" instruments provide continuous operation when powered.
- **FL(RT)D** Provides the capabilities of the FL(RT) with 6,000-meter depth rating.
- **FLS** Provides the capabilities of the FL with an integrated anti-fouling Bio-wiper™.
- **FLB** Provides the capabilities of the FL with internal memory and batteries for autonomous operation.
- **FLSB** Provides the capabilities of the FLS with internal memory and batteries for autonomous operation.

Electrical

| | |
|---------------------------|-------------------------|
| Digital output resolution | 14 bit |
| Internal data logging | Optional |
| Internal batteries | Optional |
| Connector | MCBHEMP |
| Input | 7–15 VDC |
| Current, typical | 50 mA |
| Current, sleep | 140 µA |
| Data memory | 108,000 samples |
| Sample rate | User selectable to 8 Hz |
| RS-232 output | 19200 baud |
| Analog output signal | 0–5 v |
| Anti-fouling Bio-wiper™ | Optional* |

*The limit depth for ECO with Anti-fouling Bio-wiper™ and Internal Batteries (models B, S and SB) rated to 300 m.



Specifications subject to change without notice. ©2016 Sea-Bird Scientific. All rights reserved. Rev. September 2017

seabird@seabird.com
seabird.com

VELOCIMETER

Vector - 300 m



Sample 3D velocity at up to 64 Hz for small-scale research in coastal areas

The Vector is a high-accuracy single-point current meter that is capable of acquiring 3D velocity in a very small volume at rates up to 64 Hz. It is widely used for sediment transport applications, small-scale turbulence measurements and coastal engineering studies. It has an excellent track record of delivering outstanding data quality in a variety of applications. This version is suitable for use down to a depth of 300 m. The Vector's titanium version is suitable for investigating deep- water currents.

VELOCIMETER

Vector - 300 m



Highlights

- ✓ Small-scale turbulence
- ✓ Sampling up to 64 Hz
- ✓ Small sampling volume for measurements close to boundaries

Applications

- ✓ Wave orbital studies
- ✓ Studies of bottom boundary layers
- ✓ Ocean engineering projects
- ✓ Coastal studies
- ✓ River turbulence
- ✓ Low flow measurements
- ✓ Flux measurements

Vector - 300 m

Technical specifications

→ Water velocity measurements

| | |
|--|---|
| Maximum profiling range | N/A |
| Distance from probe | 0.15 m |
| Sampling volume diameter | 15 mm |
| Sampling volume height (user-selectable) | 5-20 mm |
| Cell size | N/A |
| Velocity range | ±0.01, 0.1, 0.3, 1, 2, 4, 7 m/s (software-selectable) |
| Adaptive ping interval | N/A |
| Accuracy | ±0.5% of measured value ±1 mm/s |
| Velocity precision | typ. 1% of velocity range (at 16 Hz) |
| Sampling rate (output) | 1-64 Hz |
| Internal sampling rate | 100-250 Hz |

→ Distance measurements

| | |
|---------------|-----|
| Minimum range | N/A |
| Maximum range | N/A |
| Cell size | N/A |
| Accuracy | N/A |
| Sampling rate | N/A |

→ Echo intensity

| | |
|--------------------|---------|
| Acoustic frequency | 6 MHz |
| Resolution | 0.45 dB |
| Dynamic range | 90 dB |

→ Sensors

| | |
|--------------|---------------------------------|
| Temperature: | Thermistor embedded in end bell |
| Temp. range | -4 to +40 °C |

Vector - 300 m

→ Sensors

| | |
|---------------------------|--|
| Temp. accuracy/resolution | 0.1 °C/0.01 °C |
| Temp. time response | 10 min |
| Compass: | Magnetometer |
| Accuracy/resolution | 2°/0.1° for tilt < 20° |
| Tilt: | Liquid level |
| Accuracy/resolution | 0.2°/0.1° |
| Maximum tilt | 30° |
| Up or Down | Automatic detect |
| Pressure: | Piezoresistive |
| Standard range | 0-20 m (inquire for options) |
| Accuracy/precision | 0.5% FS / Better than 0.005% of full scale |

→ Analog inputs

| | |
|---|--|
| No. of channels | 2 |
| Supply voltage to analog output devices | Three options selectable through firmware commands: 1) Battery voltage/500 mA, 2) +5 V/250 mA, 3) +12 V/100 mA |

→ Data recording

| | |
|------------------------|---|
| Capacity (standard): | 9 MB, can add 4/16 GB |
| Data record (Standard) | 24 bytes at sampling rate + 28 bytes/second |
| Data record (IMU) | 72 bytes at sampling rate |

→ Real-time clock

| | |
|----------------------------|-------------|
| Accuracy | ±1 min/year |
| Backup in absence of power | 4 weeks |

→ Data communications

| | |
|-----------------------------|---|
| I/O | RS-232 or RS-422 |
| Communication baud rate | 300-115 200 Bd |
| Recorder download baud rate | 600/1200 kBd for both RS-232 and RS-422 |

Vector - 300 m

→ Data communications

| | |
|-----------------|--|
| User control | Handled via "Vector" software, ActiveX® function calls, or direct commands. |
| Analog outputs | 3 channels standard, one for each velocity component or two velocities and pressure. |
| Output range | 0–5 V, scaling is user-selectable. |
| Synchronization | TTL (5V tolerant) sync in/sync out, start on sync, sample on sync |

→ Connectors

| | |
|--------------------|---------------------------------------|
| Bulkhead (Impulse) | MCBH-8-FS |
| Cable | PMCIL-8-MP on 10 m polyurethane cable |

→ Software

| | |
|-----------|--|
| Functions | Deployment planning, instrument configuration, data retrieval and conversion (for Windows®). |
|-----------|--|

→ Multi unit operation

| | |
|----------|-----|
| Software | N/A |
| I/O | N/A |

→ Power

| | |
|---------------------------|---------------------|
| DC input | 9–15V DC |
| Maximum peak current | 3 A |
| Max. consumption | 1.5 W at 64 Hz |
| Typical consumption, 4 Hz | 0.6 - 1 W |
| Sleep consumption | < 100 µA |
| Transmit power | 2 adjustable levels |

→ Batteries

| | |
|--------------------------|--|
| Battery capacity | 50 Wh (alkaline or Li-ion), 165 Wh (lithium), single or dual |
| New battery voltage | 13.5 V DC (alkaline) |
| Data collection capacity | Refer to planning section in software |

VELOCIMETER

Vector - 300 m



→ Environmental

Operating temperature

-4 to +40 °C

VELOCIMETER



Vector - 300 m

→ Environmental

Storage temperature -20 to +60 °C

Shock and vibration IEC 721-3-2

Depth rating 300m

→ Materials

Standard model POM housing, titanium probe and fasteners

→ Dimensions

Maximum diameter 75 mm

Maximum length 468 mm (housing only), 246 mm (fixed stem) add 110 mm for double battery

→ Weight

No batteries Weight in air: 2.32 kg, in water: buoyant

2 batteries Weight in air: 3.20 kg, in water: 0.54 kg

→ Options

Probe mounted on fixed stem or on 2 m cable

Vertical or horizontal probes

Alkaline, lithium or Li-ion external batteries

IMU - Inertial Measurement Unit

LORD DATASHEET

3DM-GX4-45™

GPS-Aided Inertial Navigation System (GPS/INS)

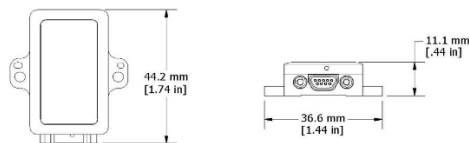


3DM-GX4-45™ - miniature industrial-grade all-in-one navigation solution with integrated GPS and magnetometers, high noise immunity, and exceptional performance

The LORD MicroStrain® family of **industrial** and **tactical grade inertial sensors** provides a wide range of triaxial inertial measurements and computed attitude and navigation solutions.

In all models, the Inertial Measurement Unit (IMU) includes direct measurement of acceleration, angular rate, and atmospheric pressure. Sensor measurements are processed through an on-board processor running a sophisticated estimation filter or fusion algorithm to produce high accuracy computed outputs with compensation options for magnetic and linear acceleration anomalies, sensor biases, auto-zero update, and noise offsets. The computed outputs vary between models and can include pitch, roll, yaw, a complete attitude, heading, and reference solution (AHRS) or a complete position, velocity and attitude solution (PVA), as well as integrated GNSS outputs. All sensors are fully temperature compensated and calibrated over the operating temperature. The use of Micro-Electro-Mechanical System (MEMS) technology allows for highly accurate, small, lightweight devices.

The LORD MicroStrain® **MIP™ Monitor** software can be used for device configuration, live data monitoring, and recording. Alternatively, the **MIP™ Data Communications Protocol** is available for development of custom interfaces and easy OEM integration.



Best in Class Inertial Measurement

Product Highlights

- High performance integrated GPS receiver and MEMS sensor technology provide direct satellite and inertial measurements, and computed position, velocity, and attitude outputs in a small package
- Triaxial accelerometer, gyroscope, magnetometer, temperature sensors, and a pressure altimeter achieve the best combination of measurement qualities
- Dual on-board processors run a sophisticated Extended Kalman Filter (EKF) for excellent PVA estimates

Features and Benefits

Best in Class Performance

- Fully calibrated, temperature-compensated, and mathematically-aligned to an orthogonal coordinate system for highly accurate outputs
- Bias tracking, error estimation, threshold flags, and adaptive noise, magnetic, and gravitational field modeling allow for fine tuning to conditions in each application
- High-performance, low-drift gyros with noise density of 0.005°/sec/√Hz and VRE of 0.001°/s/g²RMS
- Smallest and lightest industrial GPS/INS available

Ease of Use

- User-defined sensor-to-vehicle frame transformation
- Easy integration via comprehensive and fully backwards-compatible communication protocol
- Common protocol between 3DM-GX3, GX4, RQ1, GQ4, and GX5 inertial sensor families for easy migration

Cost Effective

- Out-of-the box solution reduces development time
- Volume discounts

Applications

- GPS-aided navigation system
- Unmanned vehicle navigation
- Platform stabilization, artificial horizon


LORD SENSING
MicroStrain

3DM-GX4-45™ GPS-Aided Inertial Navigation System (GPS/INS)

Specifications

| General | | | |
|--------------------------------------|---|----------------------------------|--|
| Integrated sensors | Triaxial accelerometer, triaxial gyroscope, triaxial magnetometer, temperature sensors, pressure altimeter, and GPS receiver | | |
| Data outputs | Inertial Measurement Unit (IMU) outputs: acceleration, angular rate, magnetic field, ambient pressure, deltaTheta, deltaVelocity Computed outputs: Extended Kalman Filter (EKF): filter status, GPS timestamp, LLH position, NED velocity, attitude estimates (in Euler angles, quaternion, orientation matrix), linear and compensated acceleration, bias compensated angular rate, pressure altitude, gyroscope and accelerometer bias, scale factors and uncertainties, gravity and magnetic models, and more. Complementary Filter (CF): attitude estimates (in Euler angles, quaternion, orientation matrix), stabilized north and gravity vectors, GPS correlation timestamp Global Positioning System outputs (GPS): LLH position, ECEF position and velocity, NED velocity, UTC time, GPS time, SV, GPS protocol access mode available. | | |
| | Inertial Measurement Unit (IMU) Sensor Outputs | | |
| | Accelerometer | Gyroscope | Magnetometer |
| | Measurement range | ±5 g (standard) ±16g (option) | 300°/sec (standard) ±75, ±150, ±900 °/sec (options) |
| Non-linearity | ±0.03 % fs | ±0.03 % fs | ±0.4% fs |
| Resolution | <0.1 mg | <0.008°/sec | -- |
| Bias instability | ±0.04 mg | 10°/hr | -- |
| Initial bias error | ±0.002 g | ±0.05°/sec | ±0.003 Gauss |
| Scale factor stability | ±0.05 % | ±0.05 % | ±0.1 % |
| Noise density | 100 µg/√Hz | 0.005°/sec/√Hz | 100 µGauss/√Hz |
| Alignment error | ±0.05° | ±0.05° | ±0.05° |
| Adjustable bandwidth | 225 Hz (max) | 250 Hz (max) | - |
| Offset error over temperature | 0.06% (typ) | 0.05 % (typ) | -- |
| Gain error over temperature | 0.05% (typ) | 0.05% (typ) | -- |
| Scale factor non-linearity (@ 25° C) | 0.02% (typ) 0.06% (max) | 0.02% (typ) 0.06% (max) | ±0.0015 Gauss |
| Vibration induced noise | -- | 0.072°/s RMS/g RMS | -- |
| Vibration rectification error (VRE) | -- | 0.001°/s/g ² RMS | -- |
| IMU filtering | 4 stage filtering: analog bandwidth filter to digital sigma-delta wide band anti-aliasing filter to (user adjustable) digital averaging filter sampled at 4 kHz and scaled into physical units: coning and sculling integrals computed at 1 kHz | | |
| Sampling rate | 4 kHz | 4 kHz | 50 Hz |
| IMU data output rate | 1 Hz to 500 Hz | | |
| Pressure Altimeter | | | |
| Range | -1800 m to 10,000 m | | |
| Resolution | <0.1 m | | |
| Noise density | 0.01 hPa RMS | | |
| Sampling rate | 25 Hz | | |

| Computed Outputs | |
|---|--|
| Position accuracy | ±2.5 m RMS horizontal, ±5 m RMS vertical (typ) |
| Velocity accuracy | ±0.1 m/s RMS (typ) |
| Attitude accuracy | EKF outputs: ±0.25° RMS roll & pitch, ±0.8° RMS heading (typ) CF outputs: ±0.5° roll, pitch, and heading (static, typ), ±2.0° roll, pitch, and heading (dynamic, typ) |
| Attitude heading range | 360° about all axes |
| Attitude resolution | <0.01° |
| Attitude repeatability | 0.3° (typ) |
| Calculation update rate | 500 Hz |
| Computed data output rate | EKF outputs: 1 Hz to 500 Hz CF outputs: 1 Hz to 1000 Hz |
| Global Positioning System (GPS) Outputs | |
| Receiver type | 50-channel u-Blox 6 engine GPS, L1 frequency, C/A code SBAS: WAAS, EGNOS, MSAS |
| GPS data output rate | 1 Hz to 4 Hz |
| Time-to-first-fix | Cold start: 27 second, aided start: 4 second, hot start: 1 second |
| Sensitivity | Tracking: -159 dBm, cold start: -147 dBm, hot start: -156 dBm |
| Velocity accuracy | 0.1 m/sec |
| Heading accuracy | 0.5° |
| Horizontal position accuracy | GPS: 2.5 m CEP SBAS: 2.0 m CEP |
| Time pulse signal accuracy | 30 nsec RMS <60 nsec 99% |
| Acceleration limit | ≤ 4 g |
| Altitude limit | No limit |
| Velocity limit | 500 m/sec (972 knots) |
| Operating Parameters | |
| Communication | USB 2.0 (full speed) RS232 (9,600 bps to 921,600 bps, default 115,200) |
| Power source | +3.2 to +36 V dc |
| Power consumption | 170 mA (typ), 200 mA (max) @ Vpri = 3.2 - 5.5 Vdc 750 mW (typ), 900 mW (max) @ Vaux = 5.2 - 36 Vdc |
| Operating temperature | -40 °C to +85 °C |
| Mechanical shock limit | 500 g (calibration unaffected) 1000 g (bias may change), 5000 g (survivability) |
| MTBF | 180,000 hours (Telcordia method I, GL/35C) 67,000 hours (Telcordia method I, GM/35C) |
| Physical Specifications | |
| Dimensions | 44.2 mm x 24.0 mm x 36.6 mm |
| Weight | 20 grams |
| Enclosure material | Aluminum |
| Regulatory compliance | ROHS, CE |
| Integration | |
| Connectors | Data/power output: micro-DB9 GPS antenna: MMCX type |
| Software | MIP™ Monitor, MIP™ Hard and Soft Iron Calibration, Windows XP/Vista/7/8 compatible |
| Compatibility | Protocol compatibility across 3DM-GX3, GX4, RQ1, GQ1, and GX5 product families |
| Software development kit (SDK) | MIP™ data communications protocol with sample code available (OS and platform independent) |



LORD SENSING
MicroStrain

LORD Corporation
MicroStrain® Sensing Systems

LORD SENSING
MicroStrain

LORD Corporation
MicroStrain® Sensing Systems
450 Hurricane Lane, Suite 102
Williston, VT 05495 USA

ph: 802-862-6620
sensing_sales@LORD.com
sensing_support@LORD.com

Copyright © 2016 LORD Corporation
Document 8400-0059 Revision B. Subject to change without notice.

www.microstrain.com

LRPA200

Long Range Precision Altimeter



The Long-range Precision Altimeter LRPA200 is both a stand-alone and network device and offers the same reliable features and flexibility of Tritech's standard altimeter series (PA200).

The LRPA200 may be supplied with simultaneous analogue and digital outputs allowing it to be interfaced to a wide range of PC devices, data loggers, ROV telemetry systems and multiplexers.

Control of the altimeters may be performed directly from a PC, from a suitable control system or as part of a multidrop network.

For long range and high accuracy echosounding applications

Full digital synthesis of transmit and receive frequencies, together with a wide dynamic input range offer, unsurpassed levels of performance from a compact unit. The altimeter is also highly configurable and can provide interrogated or free-running modes and a variety of analogue outputs.

Benefits

- Millimetre resolution capability
- Use for distance measurement
- 4000m or 6800m depth rating
- Various connector options
- Highly configurable design

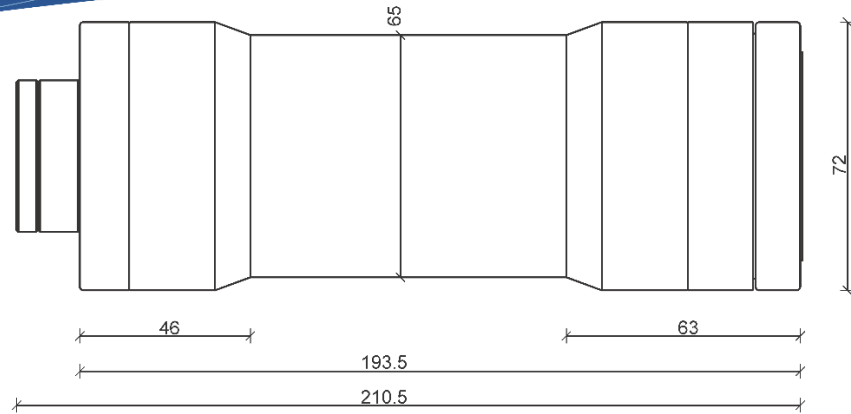
Features

- Analogue output
- Digital output
- Simultaneous analogue and digital output
- Free-running output
- Interrogated output

Applications

- ROV and AUV altitude
- Under-ice measurement
- Integration with oceanographic sensors
- Low-cost hydrographic surveys
- Integration with bathymetric systems
- Touchdown monitoring of subsea structures
- Wave height measurement
- Monitoring of scouring on bridge supports

Specification



All dimensions are in mm. Not to scale.

Diagram shows standard 4000m rated version

| Acoustic | |
|---------------------------|-----------------|
| Operating frequency | 200kHz |
| Beamwidth | 10° conical |
| Range | 2 to 200m |
| Digital timing resolution | 1mm |
| Analogue resolution | 0.025% of range |

| Electrical and Communication | |
|------------------------------|--|
| Power supply | 24V DC at 90mA (12V DC optional) |
| Analogue output | 0 to 10V DC (with 24V power supply) 0 to 5V DC 4 to 20mA |
| Communication protocols | RS232 or RS485 |
| Output modes | Free running, interrogated or part of multidrop network |

| Physical | Standard model | Deep rated model |
|-----------------------|--|------------------|
| Weight in air | 1.3kg | 4.33kg |
| Weight in water | 0.95kg | 2.93kg |
| Depth rating | 4000m | 6000m |
| Materials | Aluminium alloy (stainless steel optional) | |
| Operating temperature | -10 to 35°C | |
| Storage temperature | -20 to 50°C | |



Note

The deep rated unit is larger than the standard unit with a diameter of 76mm and a length of 222mm (with Burton connector). The Burton 5506 series connector is standard, but other connectors are available on request.

Specifications subject to change according to a policy of continual development.

Document: 0266-SOM-00003, Issue: 04

Marketed by:

Tritech International Ltd
Peregrine Road, Westhill Business Park
Westhill, Aberdeenshire, AB32 6JL
United Kingdom
sales@tritech.co.uk
+44(0)1224 744 111



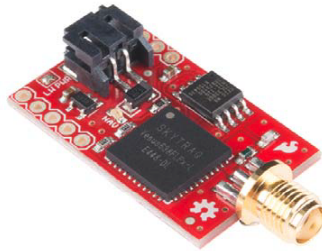
sparkfun

Export Restrictions

This product has some level of export control/restriction, so may be delayed by 2-3 business days when shipping outside the United States. [Contact us](#) with questions, or we will contact you after you place your order.

SparkFun Venus GPS Logger - SMA Connector

GPS-10920 ROHS ✓ ⚡



Images are CC BY-NC-SA 3.0

Description: The smallest, most powerful, and most versatile GPS receiver we carry just got more powerful. The Venus638FLPx is the successor to the Venus634LPx and has improved sensitivity and a faster update rate. The new module can be configured to an amazingly powerful 20Hz update rate. With 29mA operating current and high sensitivity, this receiver seriously opens new doors for tracking. Module outputs the standard NMEA-0183 or SkyTraQ Binary sentences at a default rate of 9600bps (adjustable to 115200bps).

The Venus638FLPx has improved sensitivity, an integrated LNA (with multipath detection and suppression), built-in RTC, and integrated single power supply making it very simple to use.

Not sure which GPS module is right for you? Check out our [GPS Buying Guide](#)!

Features:

- 20Hz Update rate
- -148dBm cold start sensitivity
- -165dBm tracking sensitivity
- 29 second cold start TTFF

- 3.5 second TTFF with AGPS
- 1 second hot start
- 2.5m accuracy
- Multipath detection and suppression
- Jamming detection and mitigation
- SBAS (WAAS / EGNOS) support
- 67mW full power navigation
- Works directly with active or passive antenna
- Supports external SPI flash memory data logging
- IC 32M Serial Flash Memory
- Complete receiver in 10mm x 10mm x 1.3mm size
- Contains LNA, SAW Filter, TCXO, RTC Xtal, LDO
- Can be powered by a 3.7V LiPo battery (or any 3.5 - 12V supply) through the JST connector or 3.3V regulated supply.

Dimensions: 1.25 x 0.75 inches

4.0 BeagleBone Black Features and Specification

This section covers the specifications and features of the BeagleBone Black and provides a high level description of the major components and interfaces that make up the board.

Table 2 provides a list of the BeagleBone Black features.

Table 2. BeagleBone Black Features

| | Feature | |
|------------------------|--|------------------------------------|
| Processor | AM3358/9 600MHZ-USB Powered (TBD) 800MHZ-DC Powered | |
| SDRAM Memory | 512MB DDR3L 606MHZ | |
| Flash eMMC | 2GB, 8bit | |
| PMIC TPS65217C | PMIC regulator and one additional LDO. | |
| Debug Support | Optional Onboard 20-pin CTI JTAG | |
| Power | miniUSB USB or DC Jack | 5VDC External Via Expansion Header |
| PCB | 3.4" x 2.1" | 6 layers |
| Indicators | 1-Power, 2-Ethernet, 4-User Controllable LEDs | |
| HS USB 2.0 Client Port | Access to the USB1 Client mode via miniUSB | |
| HS USB 2.0 Host Port | USB Type A Socket, 500mA LS/FS/HS | |
| Serial Port | UART0 access via 6 pin Header. Header is populated | |
| Ethernet | 10/100, RJ45 | |
| SD/MMC Connector | microSD , 3.3V | |
| User Input | 1-Reset Button, 1-User Boot Button | |
| Video Out | 16b HDMI , w/ CEC | |
| Audio | Via HDMI Interface | |
| Expansion Connectors | Power 5V, 3.3V , VDD_ADC(1.8V) 3.3V I/O on all signals McASP0, SPI1, I2C, GPIO(65), LCD, GPMC, MMC1, MMC2, 7 AIN(1.8V MAX), 4 Timers, 3 Serial Ports, CAN0, EHRPWM(0,2),XDMA Interrupt, Power button, Expansion Board ID (Up to 4 can be stacked) | |
| Weight | 1.4 oz (39.68 grams) | |

NOTE: THE INITIAL A4 VERSIONS WERE BUILT USING THE AM3352 PROCESSOR. THIS WAS A RESULT OF RECEIVING MISMARKED PARTS FROM THE SUPPLIER. DUE TO THE TIGHT SCHEDULE, THE DECISION WAS MADE TO BUILD WITH THE AM3352 VERSION AS REV A4. PRODUCTION VERSION IS REV A5 AND WILL HAVE THE CORRECT PROCESSOR. REV A4 DOES NOT HAVE SUPPORT FOR THE PRU OR SGX

4.1 Board Component Locations

Figure 4 below shows the locations of the key components on the PCB layout of the BeagleBone Black.

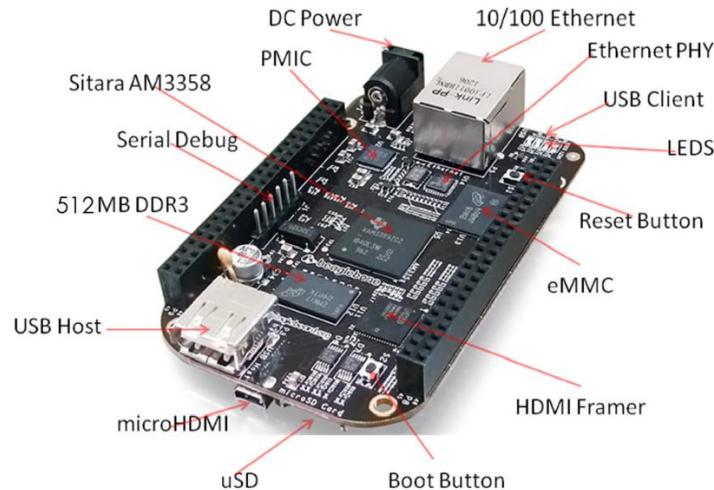


Figure 4. Key Components

The **Sitara AM3358** is the processor.

512MB DDR3 is the processor dynamic RAM memory.

Serial Debug is the serial debug port.

PMIC provides the power rails to the various components on the board.

DC Power is the main DC input that accepts 5V power.

10/100 Ethernet is the connection to the LAN.

Ethernet PHY is the physical interface to the network.

USB Client is a miniUSB connection to a PC that can also power the board.

There are four blue **LEDs** that can be used by the user.

Reset Button allows the user to reset the processor.

eMMC is an onboard MMC chip that hold sup to 2GB of data.

HDMI Framer provides control for an HDMI or DVI-D display.

BOOT Button can be used to force a boot from the SD card or from the USB port.

uSD slot is where a uSD card can be installed.

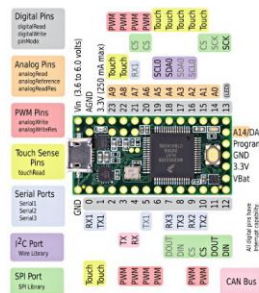
The **microHDMI** connector is where the display is connected.

USB Host can be connected different USB interfaces such as Wifi, BT, Keyboard, etc,

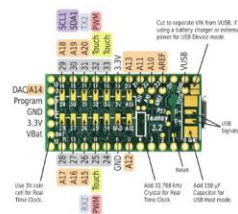
Teensy Technical Specifications

| Feature | Teensy 2.0 | Teensy++ 2.0 | Teensy LC | Teensy 3.2 | Teensy 3.5 | Teensy 3.6 | Units |
|----------------------|-------------------------|-------------------------|-------------------------|-------------------------|-------------------------|-------------------------|------------|
| Price | \$16.00 | \$24.00 | \$11.65 | \$19.80 | \$24.25 | \$29.25 | US Dollars |
| Processor | ATMEGA32U4 | AT90USB1286 | MKL26Z64VFT4 | MK20DX256VLH7 | MK64FX512VMD12 | MK66FX1M0VMD18 | |
| Core | AVR | AVR | Cortex-M0+ | Cortex-M4 | Cortex-M4F | Cortex-M4F | |
| Rated Speed | 16 | 16 | 48 | 72 | 120 | 180 | MHz |
| Overclockable | - | - | - | 96 | - | 240 | MHz |
| Flash Memory | 31.5 | 127 | 62 | 256 | 512 | 1024 | kbytes |
| Bandwidth | 32 | 32 | 96 | 192 | 192 | 411 | Mbytes/sec |
| Cache | - | - | 64 | 256 | 256 | 8192 | Bytes |
| RAM | 2.5 | 8 | 8 | 64 | 256 | 256 | kbytes |
| EEPROM | 1024 | 4096 | 128 (emu) | 2048 | 4096 | 4096 | bytes |
| Direct Memory Access | - | - | 4 | 16 | 16 | 32 | Channels |
| Digital I/O | 25 | 46 | 27 | 34 | 58 | 58 | Pins |
| Breadboard I/O | 22 | 36 | 24 | 24 | 40+2 | 40+2 | Pins |
| Voltage Output | 5V | 5V | 3.3V / 5V | 3.3V | 3.3V | 3.3V | Volts |
| Current Output | 20mA | 20mA | 5mA / 20mA | 10mA | 10mA | 10mA | milliAmps |
| Voltage Input | 5V | 5V | 3.3V Only | 5V Tolerant | 5V Tolerant | 3.3V Only | Volts |
| Interrupts | 4 | 8 | 18 | 34 | 58 | 58 | Pins |
| Analog Input | 12 | 8 | 13 | 21 | 27 | 25 | Pins |
| Converters | 1 | 1 | 1 | 2 | 2 | 2 | |
| Usable Resolution | 10 | 10 | 12 | 13 | 13 | 13 | Bits |
| Prog Gain Amp | 1 | 1 | - | 2 | - | - | |
| Touch Sensing | - | - | 11 | 12 | - | 11 | Pins |
| Comparators | 1 | 1 | 1 | 3 | 3 | 4 | |
| Analog Output | - | - | 1 | 1 | 2 | 2 | Pins |
| DAC Resolution | - | - | 12 | 12 | 12 | 12 | Bits |
| Timers | 4 Total | 4 Total | 7 Total | 12 Total | 17 Total | 19 Total | |
| PWM, 16 bit | 2 | 2 | 3 | 3 | 4 | 6 | |
| PWM, 8-10 bit | 2 | 2 | - | - | - | - | |
| Total PWM Outputs | 7 | 9 | 10 | 12 | 20 | 22 | Pins |
| PDB Type | - | - | - | 1 | 1 | 1 | |
| CMT Type | - | - | - | 1 | 1 | 1 | |
| LPTMR Type | - | - | 1 | 1 | 1 | 1 | |
| PIT/Interval | - | - | 2 | 4 | 4 | 4 | |
| IEEE1588 | - | - | - | - | 4 | 4 | |
| Systick | - | - | 1 | 1 | 1 | 1 | |
| RTC | - | - | 0 ** | 1 ** | 1 | 1 | |
| Communication | | | | | | | |
| USB | 1 | 1 | 1 | 1 | 1 | 2 | |
| Serial | 1 | 1 | 3 | 3 | 6 | 6 | |
| With FIFOs | - | - | - | 2 | 2 | 2 | |
| High Res Baud | - | - | - | 3 | 6 | 5 | |
| SPI | 1 | 1 | 2 | 1 | 3 | 3 | |
| With FIFOs | - | - | 1 | 1 | 1 | 1 | |
| I2C | 1 | 1 | 2 | 2 | 3 | 4 | |
| CAN Bus | - | - | - | 1 | 1 | 2 | |
| Digital Audio | - | - | 1 | 2 | 2 | 2 | |
| SD Card | - | - | - | - | 1 | 1 | |
| Ethernet | - | - | - | - | 1 | 1 | |

Teensy 3.2



Teensy 3.2





SERIES: PYB30-U | DESCRIPTION: DC-DC CONVERTER

FEATURES

- up to 30 W isolated output
- industry standard pinout
- 4:1 input range (9~36 Vdc, 18~75 Vdc)
- smaller package
- single/dual/triple regulated outputs
- 1,500 Vdc isolation
- continuous short circuit, over current protection, over voltage protection
- temperature range (-40~85°C)
- six-sided metal shielding
- efficiency up to 90%

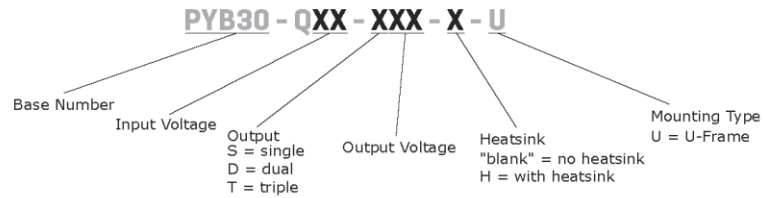


MODEL

| | input voltage | | output voltage | output current | | output power | ripple and noise ¹ | efficiency |
|------------------|---------------|-------------|----------------|----------------|--------------|--------------|-------------------------------|------------|
| | typ (Vdc) | range (Vdc) | | min (mA) | max (mA) | | | |
| PYB30-Q24-S5-U | 24 | 9~36 | 5 | 300 | 6000 | 30 | 100 | 88 |
| PYB30-Q24-S12-U | 24 | 9~36 | 12 | 125 | 2500 | 30 | 100 | 88 |
| PYB30-Q24-S15-U | 24 | 9~36 | 15 | 100 | 2000 | 30 | 100 | 90 |
| PYB30-Q24-D5-U | 24 | 9~36 | ±5 | ±150 | ±3000 | 30 | 100 | 86 |
| PYB30-Q24-D12-U | 24 | 9~36 | ±12 | ±63 | ±1250 | 30 | 100 | 89 |
| PYB30-Q24-D15-U | 24 | 9~36 | ±15 | ±50 | ±1000 | 30 | 100 | 90 |
| PYB30-Q24-T312-U | 24 | 9~36 | 3.3 ±12 | 175 ±31 | 3500 ±625 | 26.5 | 100 | 85 |
| PYB30-Q24-T315-U | 24 | 9~36 | 3.3 ±15 | 175 ±25 | 3500 ±500 | 26.5 | 100 | 86 |
| PYB30-Q24-T512-U | 24 | 9~36 | 5 ±12 | 150 ±31 | 3000 ±625 | 30 | 100 | 88 |
| PYB30-Q24-T515-U | 24 | 9~36 | 5 ±15 | 150 ±25 | 3000 ±500 | 30 | 100 | 88 |
| PYB30-Q48-S5-U | 48 | 18~75 | 5 | 300 | 6000 | 30 | 100 | 88 |
| PYB30-Q48-S12-U | 48 | 18~75 | 12 | 125 | 2500 | 30 | 100 | 88 |
| PYB30-Q48-S15-U | 48 | 18~75 | 15 | 100 | 2000 | 30 | 100 | 89 |
| PYB30-Q48-D5-U | 48 | 18~75 | ±5 | ±150 | ±3000 | 30 | 100 | 86 |
| PYB30-Q48-D12-U | 48 | 18~75 | ±12 | ±63 | ±1250 | 30 | 100 | 87 |
| PYB30-Q48-D15-U | 48 | 18~75 | ±15 | ±50 | ±1000 | 30 | 100 | 87 |
| PYB30-Q48-T312-U | 48 | 18~75 | 3.3 ±12 | 175 ±31 | 3500 ±625 | 26.5 | 100 | 85 |
| PYB30-Q48-T315-U | 48 | 18~75 | 3.3 ±15 | 175 ±25 | 3500 ±500 | 26.5 | 100 | 85 |
| PYB30-Q48-T512-U | 48 | 18~75 | 5 ±12 | 150 ±31 | 3000 ±625 | 30 | 100 | 88 |
| PYB30-Q48-T515-U | 48 | 18~75 | 5 ±15 | 150 ±25 | 3000 ±500 | 30 | 100 | 87 |

Notes: 1. Ripple and noise are measured at 20 MHz BW by "parallel cable" method with 1 µF ceramic and 10 µF electrolytic capacitors on the output.

PART NUMBER KEY



INPUT

| parameter | conditions/description | min | typ | max | units |
|-------------------------------------|---|------|-----|------|-------|
| operating input voltage | 24 Vdc input models | 9 | 24 | 36 | Vdc |
| | 48 V input models | 18 | 48 | 75 | Vdc |
| start-up voltage | 24 Vdc input models | | | 9 | Vdc |
| | 48 Vdc input models (single/dual output models) | | | 18 | Vdc |
| | 48 Vdc input models (triple output models) | | | 17.8 | Vdc |
| under voltage shutdown ¹ | 24 Vdc input models | 7.8 | | | Vdc |
| | 48 Vdc input models | 16 | | | Vdc |
| surge voltage | for maximum of 1 second | | | | |
| | 24 Vdc input models | -0.7 | | 50 | Vdc |
| | 48 Vdc input models | -0.7 | | 100 | Vdc |
| start-up time | | | 10 | | ms |
| filter | pi filter | | | | |
| CTRL ² | models ON (CTRL open or connect high level, 2.5~12 Vdc) | | | | |
| | models OFF (CTRL connect GND or low level, 0~1.2 Vdc) | | | | |
| | input current (models OFF) | | 1 | | mA |

Notes: 1. Contact CUI if you are planning to use this feature in your application.
2. CTRL pin voltage is referenced to GND.

OUTPUT

| parameter | conditions/description | min | typ | max | units |
|------------------------------|---|-----|------|-------|-------|
| line regulation | full load, input voltage from low to high | | ±0.2 | ±0.5 | % |
| | single and dual output models | | | ±1 | % |
| | triple output models (main output) | | | ±5 | % |
| | triple output models (auxiliary outputs) | | | | % |
| load regulation ³ | 5% to 100% load, nominal input | | ±0.5 | ±1 | % |
| | single and dual output models | | | ±2 | % |
| | triple output models (main output) | | | ±5 | % |
| | triple output models (auxiliary outputs) | | | | % |
| cross regulation | dual output models: main output 50% load, secondary output from 10% to 100% load | | | ±5 | % |
| voltage accuracy | single and dual output models | | ±1 | ±3 | % |
| | triple output models (main output) | | ±1 | ±3 | % |
| | triple output models (auxiliary outputs) | | ±3 | ±5 | % |
| adjustability ⁴ | | | ±10 | | % |
| switching frequency | PWM mode | | 400 | | kHz |
| transient recovery time | 25% load step change | | 300 | 500 | µs |
| transient response deviation | 25% load step change | | ±3 | ±5 | % |
| temperature coefficient | 100% load, single and dual output models | | | ±0.02 | %/°C |
| | 100% load, triple output models | | | ±0.03 | %/°C |

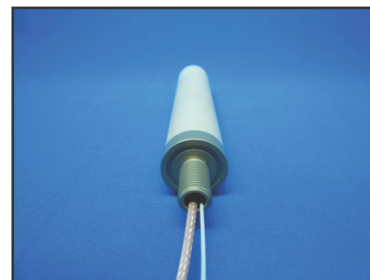
Notes: 3. For dual output models, unbalanced load can not exceed ±5%. If ±5% is exceeded, it may not meet all specifications.
4. Output trimming available on single and dual output models only.

Trident Sensors' Dual Element Active GPS & Passive Iridium Antenna



Features

- Pressure rated to 6,000 m
- Active GPS & Passive Iridium antenna elements
- Dual cables & connectors for GPS & Iridium
- Rapid position acquisition at the sea-surface
- Small, light-weight, low drag
- Iridium element allows two-way data communications
- Various cable lengths available with a choice of GPS & Iridium connectors



150 mm Dual Element Active GPS & Passive Iridium Antenna with Separate Cables & Connectors for GPS & Iridium

Feed-through Connection

- For antenna mounting directly onto pressure housing
- 7/16" UNF thread

Applications

- AUVs
- ROVs
- Drifters
- Profiling floats
- Manned submersibles
- Location & recovery
- Mission data transmission
- Command & control

| | Active GPS | Passive Iridium |
|--------------|---------------------|---------------------|
| Type | Quadrifilar Helix | Octafilar Helix |
| Frequency | 1573.42-1577.42 MHz | 1616-1626 MHz |
| Polarization | Right-hand circular | Right-hand circular |
| Voltage | 2.8 to 3.6 V | |
| Current | 13 mA | |
| Gain | +24 dBic | +2.0 dBic @zenith |
| Beamwidth | 135 Degrees | >120 Degrees |
| Bandwidth | 20 MHz | {1 dB} 15 MHz |
| Axial Ratio | <2.0 @Zenith | <1.5 @Zenith |
| VSWR | <2.0:1 | <2.0:1 |
| Impedance | 50 | 50 |
| Temperature | -40 to +85 °C | -40 to +85 °C |



Dual Element Active GPS & Passive Iridium Mounted Directly onto Pressure Housing

| | Active GPS & Passive Iridium |
|------------------------|------------------------------------|
| Length (excl. thread) | 150 mm |
| Diameter (housing) | 25 mm |
| Thread Length | 19 mm |
| Thread | 7/16" - 20 UNF |
| Weight* | ~130 g |
| Face-seal O-ring | BS017 (17.17 id x 1.78 mm section) |
| Cable* | Hirose U.FL Coax / RG-316 |
| GPS/Iridium Connector* | MCX, SMA, U.FL Plug |

* Approximate values as customers' requirements vary. Please specify desired cable length & connectors. Other connectors may be available.



SATELLITE MODEM: A3LA-RS

Key Features

- Low cost
- Small form factor
- Data-only modem capable of SBD, SMS, data switch and RUDICS.
- Does not support voice
- RS-232 interface
- Functionally is the same as the 9522B
- ~70% smaller in volume than the 9522B
- ~70% lighter than the 9522B

Description

The A3LA-RS is a satellite modem comprised of an Iridium 9523 transceiver. It allows SBD, SMS, data switch and RUDICS connectivity to the Iridium satellite network. It does not support voice.



A3LA-RS Specifications

Mechanical

| | |
|-----------------------|---|
| Dimensions: | 3.63" x 1.88" x 0.92" (92 mm x 48 mm x 23 mm) |
| Weight: | ~4.3 ounces (122 g) |
| Data/Power Interface: | 15-Pin D-Sub |
| Antenna Interface: | SMA female connector |
| Enclosure: | Hard-anodized aluminum (EMI/EMC shielded) |

Electrical

| | |
|----------------------|--------------|
| Input Voltage Range: | 3.5V to 5.4V |
| Nominal Input: | 5VDC |
| Idle Power: | 60mA @ 5V |
| Transmitted Power: | 350mA @ 5V |

RF Boards

| | |
|----------------------|--------------|
| Iridium Transceiver: | Iridium 9523 |
|----------------------|--------------|

Environmental

| | |
|------------------------|----------------------------------|
| Operating Temperature: | -22°F to +158°F (-30°C to +70°C) |
| Operating Humidity: | < 75% RH |



POWERED by the **IRIDIUM NETWORK**



9300 W. Courthouse Rd, Manassas, VA 20110
www.nalresearch.com

XTend®-PKG RF Modems

1 Watt/900 MHz Stand-Alone Radio Modems

900 MHz radio modems offer long-range performance, advanced networking and simple out-of-the-box operation with multiple data interface options.



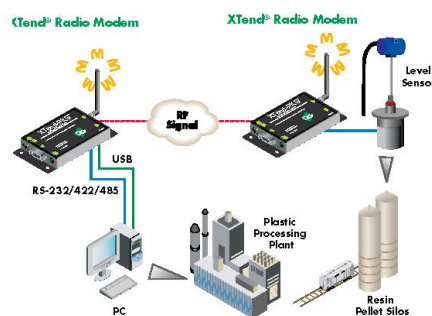
Overview

Digi's XTend-PKG RF modems provide everything you need for out-of-the-box serial cable replacement, enabling quick wireless connectivity of electronic devices across a broad range of applications. Simply feed data into one modem and the data is transported to the other end of a long range wireless link. Data security is provided by 256-bit AES encryption (128-bit AES is available outside of North America). If more advanced functionality is needed, the modems support an extensive set of AT and binary commands.

With superior receiver sensitivity, XTend modems hear what others can't, yielding two- to eight- times the range of competing RF modems. This allows OEMs and integrators to cover more ground with fewer transceivers, reducing the cost of deployment. And with no configuration required, complexity is minimized.

Available in multiple interface options, including RS-232/422/485 and USB, and with an optional NEMA 4-rated enclosure, XTend modems are ideally suited for remote monitoring, building automation/security, industrial automation/SCADA, fleet management/asset tracking and sensor data capture in embedded systems. For hazardous locations, a Class 1, Division 2 rated model is also available.

Application Highlight



Features/Benefits

- Indoor/urban range up to 3000 feet
- Outdoor line-of-sight range up to 40 miles (with high gain antenna)
- Outstanding receiver sensitivity (-110 dBm @ 9600 bps)
- Adjustable power output from 1 mW to 1 W; up to 4 W EIRP (with 6 dB antenna)
- Low power consumption for power-sensitive applications
 - Pin, serial port and cyclic sleep modes available
- Streaming, acknowledged and multi-transmit modes supported
- Easy out-of-the box operation — no configuration necessary
- Durable industrial grade enclosure



www.digi.com

Features/Specifications

PERFORMANCE

- Indoor/Urban range (w/ 2.1 dB dipole antenna): Up to 3000 feet (900 m)
- Outdoor RF line-of-sight range (w/ high gain antenna): Up to 40 miles (64 km)
- Outdoor RF line-of-sight range (w/ 2.1 dB dipole antenna): Up to 14 miles (22 km)
- Transmit power output (software selectable): 1mW - 1W (0 - 30 dBm)
- Interface data rate: 10 - 230,400 bps (including non-standard baud rates)
- Receiver sensitivity: -110 dBm (@9,600 bps throughput data rate), -100 dBm (@115,200 bps)
- Throughput data rate (software selectable): 9,600 or 115,200 bps
- RF data rate:
 - 10,000 bps (@9,600 bps throughput data rate)
 - 125,000 bps (@115,200 bps)

CONNECTION OPTIONS

- RS-232/422/485, DB-9 (XTend-PKG-R)
- USB (XTend-PKG-U)
- RS-232/422/485, DB-9/screw terminal (XTend-PKG-NEMA)

DIMENSIONS

- XTend-PKG-R, XTend-PKG-U,
- Length: 2.75 in (6.99 cm)
 - Width: 5.50 in (13.97 cm)
 - Depth: 1.13 in (2.86 cm)
 - Weight: 7.10 oz (200 g)
- XTend-NEMA
- Length: 5.13 in (13.02 cm)
 - Width: 7.13 in (18.10 cm)
 - Depth: 1.50 in (3.81 cm)
 - Weight: 12.30 oz (348.70 g)

ENVIRONMENTAL

- XTend-PKG-R, XTend-PKG-NEMA
- 40° C to 85° C (industrial)
- XTend-PKG-U
- 0° C to 70° C (commercial)

POWER REQUIREMENTS

- All models**
- Power supply voltage: 7 - 28V
- XTend-PKG-R**
- Receive current: 110 mA
 - Pin sleep power-down: 17 mA
 - Serial port sleep power-down: 45 mA
 - Idle current (various cyclic sleep intervals): 19 - 39 mA
 - Transmit current (1 mW - 1W TX power output): 110 - 900 mA
- XTend-PKG-U**
- Receive current: 100 mA (Self Power)
 - Pin sleep power-down: 17 mA
 - Serial port sleep power-down: 45 mA
 - Idle current (various cyclic sleep intervals): 21 - 35 mA (Self Power)
 - Transmit current (1 mW - 1W TX power output): 88 - 480 mA
- XTend-NEMA**
- Receive current: 100 mA
 - Pin sleep power-down: 17 mA
 - Serial port sleep power-down: 45 mA
 - Idle current (various cyclic sleep intervals): 19 - 39 mA
 - Transmit current (1 mW - 1W TX power output): 110 - 900 mA

ANTENNA

- XTend-PKG-R, XTend-PKG-U**
- Connector: RPSMA (Reverse Polarity SMA)
 - Impedance: 50 ohms unbalanced
- XTend-NEMA (Weatherproof)**
- External antenna version
 - Connector: RPTNC
 - Impedance: 50 ohms unbalanced
 - Internal antenna version
 - Connector: MMCX
 - Impedance: 50 ohms unbalanced

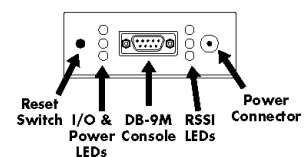
CERTIFICATIONS

- All models**
- FCC Part 15.247: OUR-9XTEND
 - Industry Canada (IC): 4214A-9XTEND
- NEMA enclosure**
- IP 66/67, IP 66
 - IK 08
 - NEMA 1, 4, 4X, 6 (12 and 13)
 - UL 94-V0, UL 508

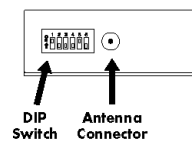
NETWORKING AND SECURITY

- Frequency: ISM 902 - 928 MHz
- Spread Spectrum: FHSS (Frequency Hopping Spread Spectrum)
- Modulation: FSK (Frequency Shift Keying)
- Supported Network Topologies: Peer-to-peer (no master/slave dependencies), point-to-point, point-to-multipoint and multidrop
- Channel Capacity: 10 hop sequences share 50 frequencies
- Encryption: 256-bit AES Encryption
 - AES algorithm meets Federal Information Processing Standard-197 (FIPS-197)

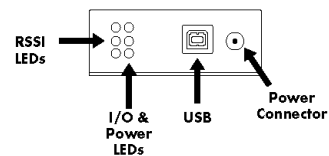
XTend-PKG-R - Front



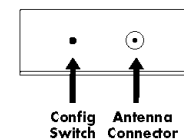
XTend-PKG-R - Back



XTend-PKG-U - Front



XTend-PKG-U - Back



You can purchase with confidence knowing that Digi is always available to serve you with expert technical support and our industry leading warranty. For detailed information visit www.digi.com/support

91001399
82/911

Digi International
Worldwide HQ
877-912-3444
952-912-3444
www.digi.com

Digi International
France
+33-1-55-61-98-98
www.digi.fr

Digi International
Japan
+81-3-5428-0261
www.digi-intl.co.jp

Digi International
Singapore
+65-6213-5380

Digi International
China
+86-21-50492199
www.digi.com.cn



© 1996-2015 Digi International Inc. All rights reserved. All other trademarks are the property of their respective owners.



BULLET M

Zero-Variable Wireless Infrastructure Deployment

Models: BM2HP, BM5HP

Completely integrated Radio

Directly plugs into any Antenna
that has a Type N female connector

Robust Weatherproof Design

UBIQUITI
NETWORKS

BULLET M | Datasheet

Specifications

05

| System Information | |
|----------------------|---|
| Processor Specs | Atheros MIPS 24KC, 400MHz |
| Memory Information | 32MB SDRAM, 8MB Flash |
| Networking Interface | 1 X 10/100 BASE-TX (Cat. 5, RJ-45) Ethernet |

| Regulatory / Compliance Information | |
|-------------------------------------|-------------------------------|
| Wireless Approvals | FCC Part 15.247, IC RS210, CE |
| RoHS Compliance | YES |

| Physical / Electrical / Environmental | | |
|---------------------------------------|--|---------|
| RF Connector | Integrated N-type Male Jack (connects directly to antenna) | |
| Enclosure Size | 15.2 x 3.7 x 3.1 cm (length, width, height) | |
| Weight | 0.18kg | |
| Enclosure Characteristics | Outdoor UV Stabilized Plastic | |
| Power Rating | Up to 24V | |
| Power Method | Passive Power over Ethernet (pairs 4, 5+; 7, 8 return)* | |
| Operating Temperature | -40C to 80C | |
| Operating Humidity | 5 to 95% Condensing | |
| Shock and Vibration | ETSI300-019-1.4 | |
| | M2 | M5 |
| Max Power Consumption | 7 Watts | 6 Watts |

| Range Performance | |
|-----------------------------|-----------|
| Outdoor (Antenna Dependent) | Over 50km |

* POE Adapter is sold separately

Ubiquiti Networks, Inc. Copyright © 2011, All Rights Reserved

 www.ubnt.com

| PART NUMBER | DESCRIPTION |
|-------------|------------------------------------|
| CCR-33S | Commercial Latching SPDT, DC-18GHz |
| CR-33S | Elite Latching SPDT, DC-22GHz |

The CCR-33S/CR-33S is a broadband, SPDT, electromechanical, coaxial switch designed to switch a microwave signal from a common input to either of two outputs. The characteristic impedance is 50 Ohms. The small switches incorporate SMA connectors. The CCR-33S/CR-33S series switch is offered with a latching actuator. This design is compatible with the two most common mounting hole patterns. The CCR-33S/CR-33S series switch is interchangeable with a variety of switches.



ENVIRONMENTAL AND PHYSICAL CHARACTERISTICS

| | |
|--|--------------------------|
| Operating Temperature | |
| Commercial Model, CCR-33S | –40°C to 65°C |
| Elite Model, CR-33S | –55°C to 85°C |
| Vibration (MIL-STD-202 Method 214, Condition D, non-operating) | 10 g's RMS |
| Shock (MIL-STD-202 Method 213, Condition D, non-operating) | 500 g's |
| Standard Actuator Life | 5,000,000 cycles |
| Actuator Life w/ Additional Features | 1,000,000 cycles |
| Connector Type | SMA |
| Humidity (Moisture Seal) | Available |
| Weight | 1.65 oz. (46.78g) (max.) |

ELECTRICAL CHARACTERISTICS

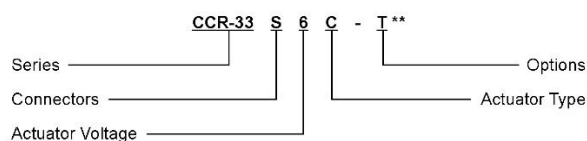
| | |
|-----------------------------------|-------------------------|
| Form Factor | SPDT, break before make |
| Frequency Range | |
| CCR-33S | DC–18 GHz |
| CR-33S | DC–22 GHz |
| Characteristic Impedance | 50 Ohms |
| Operate Time | 10 ms (max.) |
| Actuation Voltage Available | 12 15 24 28 V |
| Actuation Current, max. @ ambient | 140 170 90 65 mA |

TYPICAL PERFORMANCE CHARACTERISTICS

| Frequency | DC–4 GHz | 4–8 GHz | 8–12 GHz | 12–16 GHz | 16–20 GHz | 20–22 GHz |
|------------------------------|----------|---------|----------|-----------|-----------|-----------|
| Insertion Loss, dB, typical. | 0.1 | 0.2 | 0.2 | 0.3 | 0.4 | 0.4 |
| Isolation, dB, typical. | 90 | 90 | 80 | 70 | 65 | 65 |
| VSWR, typical. | 1.1:1 | 1.1:1 | 1.1:1 | 1.2:1 | 1.2:1 | 1.2:1 |

For maximum limits, please see charts on page 3-5

PART NUMBERING SYSTEM



Connector
S: SMA Female

Actuator Voltage
6: 28 Vdc Latching
7: 15 Vdc Latching
8: 12 Vdc Latching
9: 24 Vdc Latching

Actuator Type
0: Standard Contacts
C: Indicator Contacts
D: Self Cutoff Only
E: Indicators and Self Cutoff

**SEE PARTS LIST ON PAGES 3-9

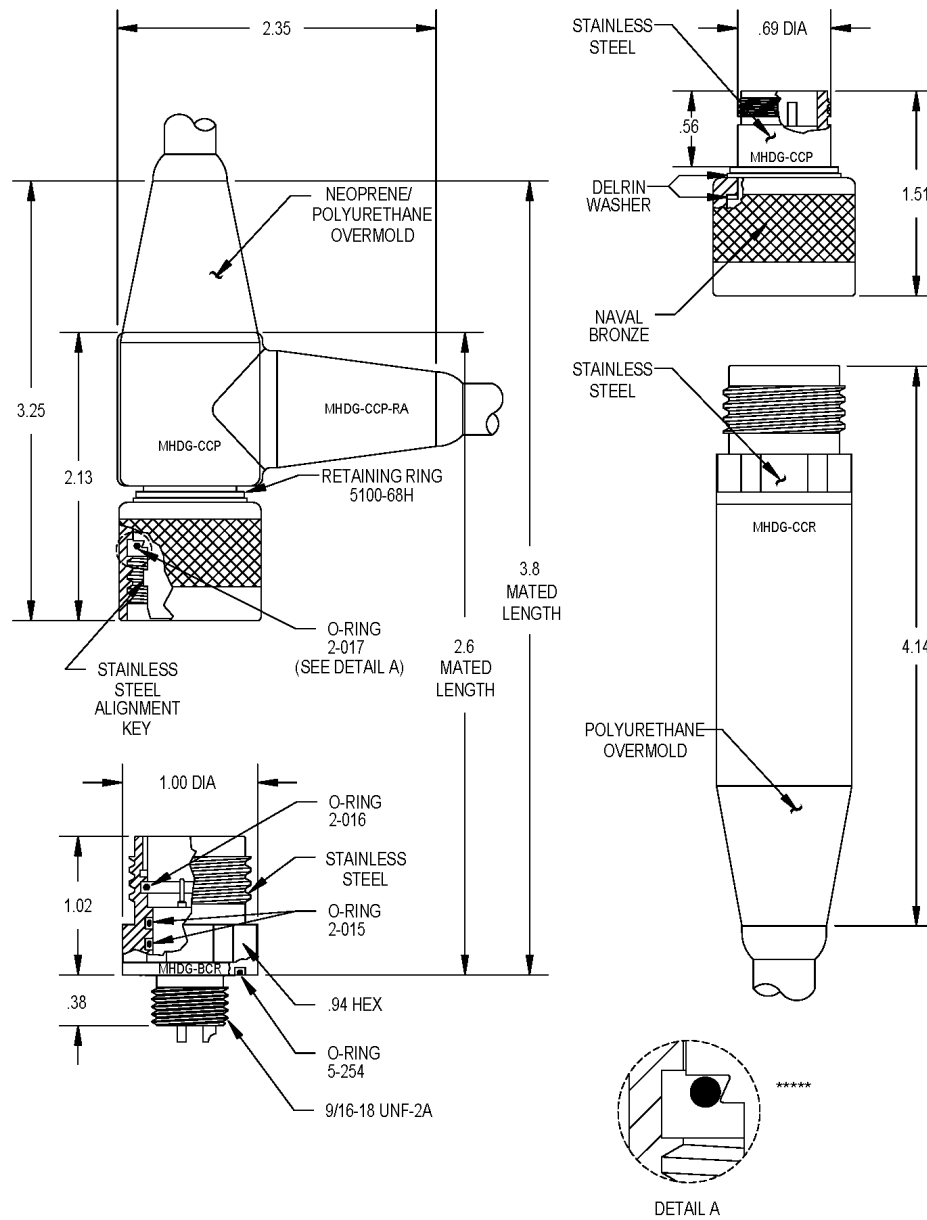
Options
T: TTL Drivers with Diodes
D: Transient Suppression Diodes
R: Positive + Common
N: Narrow Body
M: Moisture Seal
S: 9 Pin D-Sub Connector

For other options, contact factory.

| | |
|--------------------------|---|
| DESCRIPTION AND MATERIAL | <ul style="list-style-type: none">• 316 stainless steel passivated per QQ-P-35 Type VI with naval bronze engaging nut.• Special alloys are available upon request (contact factory).• Contains a removable glass reinforced epoxy insert. (Except for MHDG series and CCP's)• Up to 96 contacts.• Up to 600 VDC.• 10,000 PSI in mated condition (higher pressure rating available using special alloy metal shell; please contact factory).• Bulkhead connector design open face pressure rated to 5,000 psi.• MHD-CCR/CCP connectors can be overmolded with polyurethane.• Contacts are gold plated per MIL-G-45204. |
| CABLE | <ul style="list-style-type: none">• Connector's amperage and voltage may be limited by the amperage and voltage ratings of the cable to which the connector is molded.• This series is not molded to cable unless specified at the time of order. |
| USES | <ul style="list-style-type: none">• Signal telemetry.• Hazardous environment.• FCR is mounted by use of four equally spaced bolts around the flange surface.• FCR is used in place of the BCR when the use of a bulkhead nut and washer is impractical.• For all open face pressures above 5,000 PSI the BCR, FCR must be back potted (please contact the factory).• The CCR is used in a variety of environments where cable to cable termination is necessary. |
| GUIDELINES | <ul style="list-style-type: none">• Mounting torque should not exceed 150 in lbs. for this series.• All mounting surfaces require a 32 finish.• Align indexes.• Keep o-ring grooves clean.• Avoid o-ring cuts and nicks.• Lubricate o-rings with Dow Corning #111 Valve Lubricant or equivalent.• Replace o-rings when re-using connectors.• Avoid contact with noxious solvents.• Elastomers can be seriously degraded if exposed to direct sunlight or high ozone levels for extended periods of time. |

MHDG

MINIATURE HIGH DENSITY SERIES

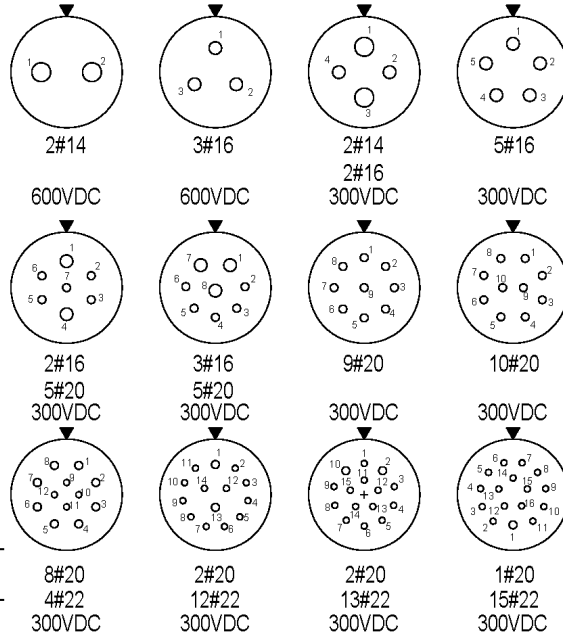
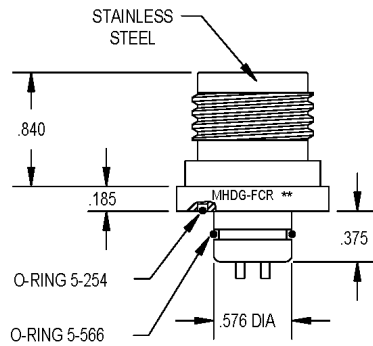
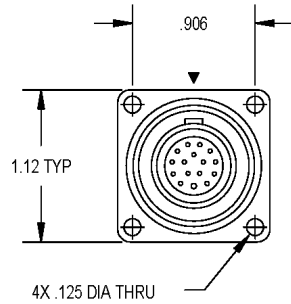


MHDG

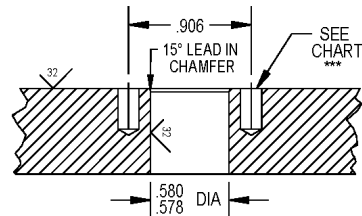
MINIATURE HIGH DENSITY SERIES



CONTACT CONFIGURATION (BCR FACE VIEW)



MOUNTING INSTRUCTIONS



| | | | |
|---------------------------------|--------------------------|-----------------------------|----------|
| MOUNTING TORQUE FOR MHDG-BCR | not to exceed 150 in lbs | MATED PRESSURE RATING (psi) | 10,000 |
| DUMMY PLUG FOR MHDG-BCR/FCR/CCR | MHDG-SCP | DUMMY PLUG FOR MHDG-CCP | MHDG-SCR |

NOTE: CCP is not terminated to cable unless specified.

* Please specify number of contacts.

** Internal assembly same as MHDG-BCR (facing page).

*** Blind tapped hole not to penetrate bulkhead, minimum full thread depth 2 times bolt diameter.

**** Oil filled version available. See section 86.

***** O-Ring installation tool available - Contact factory for further details.



110 SERIES | RECEPTACLE OPTIONS

PAGE 23

FEATURES

- 50 Ohm Coax
- Glass-to-metal seal pressure barrier in the receptacle for maximum protection of equipment
- Dual O-ring seals – primary face seal with secondary piston seal
- Simple, durable construction; excellent for cameras or instruments used in or around water or other harsh environments

MATERIALS (STANDARD)

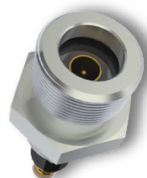
Body: 316/316L Stainless Steel
Coupling Rings: 316
Insulators, Plugs: Nylon
Insulators, Receptacles: Glass
O-rings: Buna-N
Note: Alternate material options are available, e.g. Titanium, Monel and Inconel, consult factory for details

PERFORMANCE

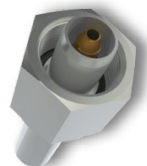
Impedance: 50 Ohms
Frequency Range: 0-1.5 GHz
Insulation Resistance: 5 Gohms at 500 VDC
Max Operating Voltage: 1000 VRMS
Max Operating Current: 3 amps
Temp Range, Operating: -40°F to 165°F
Temp Range, Storage: -65°F to 175°F
Max Operational Pressure: 2,000 psi for molded cable assemblies (-4500 ft/1372 m)
10,000 psi open face receptacle

RECOMMENDED CABLES

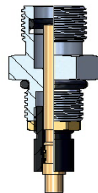
For General Use: MIL-2-17/28 RG-58 (including shallow water, non-critical applications)
For Deep Submergence / Critical Applications: TRC CN-4 (50 Ohm)
Note: Alternate cables can be accommodated; consult factory for details



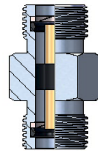
RECEPTACLE



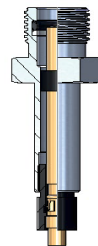
PLUG ASSEMBLY



BULKHEAD



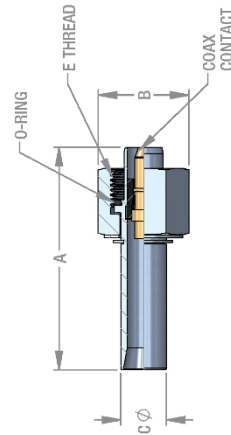
SPLICE



INLINE



PLUG KITS | STRAIGHT PLUGS

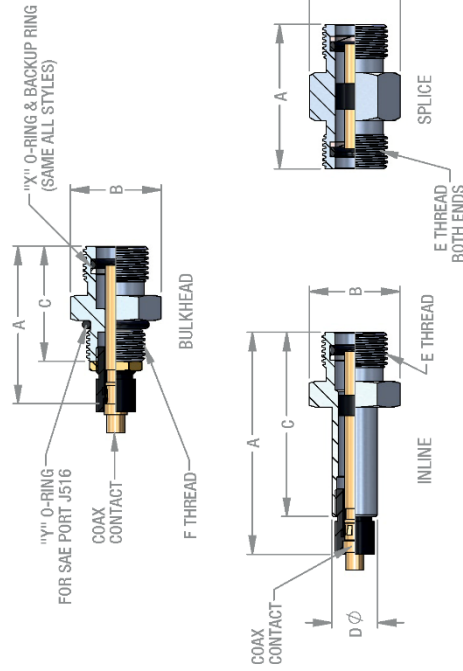


| Plug Kit Number | 1101001-101 |
|--------------------------|---------------|
| A | 2.13 |
| B (across hex nut flats) | 0.75 |
| C | .436 Diameter |
| E | 5/8-18UNF |
| O-ring | MS28775-013 |
| Coax Contact | 1131016-101 |
| Cable Accommodated | RG-58, CN-4 |

(Dimensions in inches)

22

RECEPTACLE KITS | STANDARD



| Receptacle Part No. | Bulkhead | Inline | Splice |
|--------------------------|--------------|---------------|-------------|
| 1100001-101 | 1.5 | 2.07 | 1.38 |
| A | 0.75 | 0.75 | 0.75 |
| B (across hex nut flats) | 1.1 | 1.76 | n/a |
| C | n/a | .436 Diameter | n/a |
| D | 5/8-18UNF | 5/8-18UNF | 5/8-18UNF |
| E | 9/16-18UNF | n/a | n/a |
| F | MS28775-012 | MS28775-012 | MS28775-012 |
| O-ring "X" | 1102109-501 | 1102109-501 | 1102109-501 |
| Back-up Ring | MS3461/2-906 | n/a | n/a |
| O-ring "Y" | 1131016-101 | 1131016-101 | n/a |
| Coax Contact | RG-58, CN-4 | RG-58, CN-4 | n/a |
| Cable Accommodated | n/a | n/a | n/a |

(Dimensions in inches)

23

www.djco.com

The high performance sandwich core

Divinycell HCP grade meets the demand for a high performance, low density buoyancy material with excellent characteristics. It is widely used in subsea buoyancy units, ROVs, diving bells and impact protection structures. As a result of its excellent hydraulic compressive properties and closed cell structure, it has very low buoyancy loss and water absorption under long-term loading conditions. The insulation properties of HCP are also good. HCP stands for Hydraulic Crush Point and is defined as the point of pressure in Bar, where the

material when subjected to an increasing pressure of 1-2 Bar/sec has lost 5% of its initial volume. The design of subsea buoyancy applications is complex and consideration has to be given to the required buoyancy loss and updrift over the expected lifetime and service conditions, with respect to long and short term hydraulic compressive creep, water absorption and hydraulic fatigue. Please contact Diab Technical Services for design proposal.

Mechanical properties Divinycell® HCP

| Property | Test Procedure | Unit | HCP 30 | HCP50 | HCP70 | HCP90 | HCP100 |
|-----------------------------|----------------|-------------------|-------------------------------|-------------------|-------------|--------------|-------------------|
| Hydraulic Crush Point | | Bar | | | | | |
| Compressive Strength | ASTM D 1621 | MPa | Nominal Minimum | 5.4 7.2 | 8.1 10.2 | 10.2 11.6 | 11.6 10.0 |
| E-modulus (extension meter) | ASTM D1621 | MPa | Nominal Minimum | 310 265 | 400 350 | 500 480 | 590 540 |
| Tensile Strength | ASTM D 1623 | MPa | Nominal Minimum | 7.1 6.3 | 9.2 8.0 | 11.0 10.0 | 12.8 11.5 |
| Shear Strength | ASTM C 273 | MPa | Nominal Minimum | 3.5 3.2 | 4.5 3.9 | 5.2 4.2 | 6.5 6.0 |
| Shear Modulus | ASTM C 273 | MPa | Nominal Minimum | 73 65 | 97 81 | 115 90 | 147 126 |
| Shear Strain | ASTM C 273 | % | Nominal Minimum | 45 200 | 45 250 | 35 310 | 35 380 |
| Density | ISO 845 | kg/m ³ | Nominal Maximum Minimum | 230 290 180 | 290 240 | 340 295 | 415 355 390 |

All values measured at +23°C

1. Properties measured perpendicular to the plane

Nominal value is an average value of a mechanical property at a nominal density

Minimum value is a minimum guaranteed mechanical property a material has independently of density

Technical Data

Product Characteristics

- Excellent buoyancy performance
- High impact resistance
- Low water absorption
- Thermoflexible
- Superior damage tolerance
- Fast and easy to machine
- Good chemical resistance
- High temperature resistance

Technical Characteristics

| Type | Buoyancy (kg/m ³) | Operational depth ¹ (m) | Crush depth (m) |
|--------|-------------------------------|------------------------------------|-----------------|
| HCP30 | 825 | 190 | 300 |
| HCP50 | 775 | 300 | 500 |
| HCP70 | 715 | 450 | 700 |
| HCP90 | 645 | 550 | 900 |
| HCP100 | 615 | 650 | 1000 |

- Operational depth above is calculated with a max 5% buoyancy loss over 10 years operational time. Depth shown are for guidance only and can be optimized for individual conditions. Always contact Diab for advice before selecting material. Buoyancy calculated from salt water (density 1025 kg/m³).

Technical Characteristics Divinycell® HCP

| Characteristics ¹ | Unit | HCP30 | HCP50 | HCP70 | HCP90 | HCP100 | Test method |
|-----------------------------------|-----------------------|-------------|-------------|-------------|-------------|-------------|-------------|
| Closed cells | % | >99 | >99 | >99 | >99 | >99 | - |
| Thermal conductivity ² | W/(m·K) | 0.049 | 0.051 | 0.057 | 0.058 | 0.060 | EN 12667 |
| Coeff. linear heat expansion | ×10 ⁻⁶ /°C | 37 | 37 | 37 | 37 | 37 | ASTM D 696 |
| Continuous temp range | °C | -200 to +80 | -200 to +80 | -200 to +80 | -200 to +80 | -200 to +80 | - |
| Max process temp | °C | +90 | +90 | +90 | +90 | +90 | - |
| Dissipation factor | - | 0.0015 | 0.0020 | 0.0024 | 0.0030 | 0.0034 | ASTM D 2520 |
| Dielectric constant | - | 1.25 | 1.32 | 1.39 | 1.47 | 1.53 | ASTM D 2520 |

- Typical values
 - Thermal conductivity at +10°C
- Operating temperature is typically -200°C to +80°C. Normally Divinycell HCP can be processed up to +90°C without dimensional changes.
- Maximum processing temperature is dependent on time, pressure and process conditions. Therefore users are advised to contact Diab Technical Services to confirm that Divinycell HCP is compatible with their particular processing parameters.

Physical characteristics

| Format | Unit | HCP30 | HCP50 | HCP70 | HCP90 | HCP100 |
|-----------|------|-------|-------|-------|-------|--------|
| Length | mm | 1730 | 1640 | 1410 | 1340 | 1310 |
| Width | mm | 850 | 800 | 700 | 660 | 640 |
| Thickness | mm | 56 | 53 | 30 | 27 | 23 |

Can be bonded to larger dimensions upon request.

Disclaimer:
This data sheet may be subject to revision and changes due to development and changes of the material. The data is derived from tests and experience. If not stated as minimum values, the data is average data and should be treated as such. Calculations should be verified by actual tests. The data is furnished without liability for the company and does not constitute a warranty or representation in respect of the material or its use. The company reserves the right to release new data sheets in replacement.

All content in this publication is protected by international copyright laws. Copyright © Diab Feb 2018

Issued: Feb 2018 Doc No: HCP Feb 2018 rev16 SI

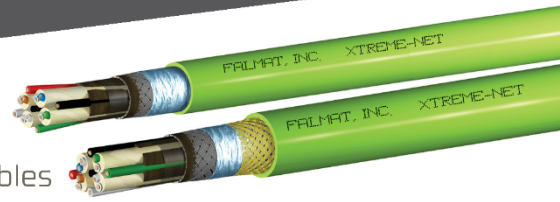
Diab Group
Box 201
312 22 Laholm, Sweden
Phone: +46 (0)430 163 00
E-mail: info@se.diabgroup.com



The Original and Still
The Best!

Xtreme-Net

Ruggedized Deepwater Ethernet Cables



Application

XtremeNet® Cables are designed for use in deep-water, subsea applications or where high-speed Ethernet data transmission is required.

Design

- These uniquely designed cables are able to maintain high-speed Ethernet data transmission while under extreme water pressure, even exceeding 10,000 PSI.
- Optional constructions with additional power conductors, shielding, synthetic strength layers or steel armor can be ordered.
- Jacket made of Falmat's specially formulated, high-temp "Xtreme" grade polyurethane with excellent abrasion and cut resistance, low coefficient of friction and good flexibility with overmold compatibility. Hot rubber mold compatible to 120C up to 90 minutes.
- Extensively tested and validated to meet industry Ethernet standard TIA/EIA-568B, with less than 2% change in values when tested to 6,000 PSI.
- Data rates of 100Mbps Fast Ethernet, 270Mbps Digital Video and up to 1Gigabit Ethernet can be achieved, as well as RS-485 and DSL rates.
- Rating: -25C to 90C, 600V. Some power wires to 1kv. (Ratings not UL listed)

Ordering Options

- Optional Aramid fiber layer of 1,200 lb. break strength will not increase diameter listed. Please use suffix K12 after each part number when inquiring about cables with optional aramid fiber rated for 1,200 lb.
- Higher strength ratings can be ordered up to 50K lbs.
- Armored versions using braided stainless steel or double served steel can be special ordered.

| PART NUMBER | DATA RATE | DESCRIPTION | SHIELD | DIA. (in.) | DIA. (mm) |
|-------------|---------------|----------------------------------|------------|------------|-----------|
| FM022208-01 | 100mb Cat5E | 2pr-24AWG Data, 2C-14AWG Power | Alum/Braid | 0.422 | 10.7 |
| FM022208-02 | 100mb Cat5E | 2pr-24AWG Data, 2C-14AWG Power | | 0.397 | 10.1 |
| FM022208-03 | 100mb Cat5E | 2pr-24AWG Data, 2C-18AWG Power | Alum/Braid | 0.371 | 9.4 |
| FM022208-04 | 100mb Cat5E | 2pr-24AWG Data, 2C-18AWG Power | | 0.364 | 8.8 |
| FM022208-05 | 1Gig Cat5E-6* | 4pr-24AWG Data | | 0.440 | 11.2 |
| FM022208-06 | 1Gig Cat5E-6* | 4pr-24AWG Data | Alum/Braid | 0.462 | 17.7 |
| FM022208-07 | 1Gig Cat6^ | 4pr-23AWG Data | | 0.472 | 12.0 |
| FM022208-08 | 1Gig Cat6^ | 4pr-23AWG Data | Alum/Braid | 0.495 | 12.6 |
| FM022208-09 | 1Gig Cat6^ | 4pr-23AWG Data 4C-22AWG Control | | 0.472 | 12.0 |
| FM022208-10 | 1Gig Cat6^ | 4pr-23AWG Data 4C-20AWG Control | | 0.472 | 12.0 |
| FM022208-11 | 1Gig Cat6^ | 4pr-23AWG Data 10C-20AWG Control | | 0.616 | 15.6 |
| FM022208-12 | 1Gig Cat6^ | 4pr-23AWG Data 10C-20AWG Control | Alum/Braid | 0.640 | 16.3 |
| FM022208-14 | 1Gig Cat6^ | 4pr-23AWG Data 4C-18AWG Control | Alum/Braid | 0.500 | 12.7 |

*100 Mb rates up to 100 mtr., 1Gig rates over shorter distances up to 50 mtr.

^ 1Gig rates up to 70 mtr. and potentially 90 mtr. lengths.

Rev. 2.2.17



Falmat, Inc.
1873 Diamond Street
San Marcos, CA 92078 USA

760.471.5400 Tel/
760.471.4970 Fax
www.falmat.com

©2016 Falmat, Inc. All rights reserved. Made in the USA.

Power Springs



POWERSPRINGS ARE AVAILABLE IN SIX DIAMETERS.

At each of these diameters length is available from 100mm to 100m with a length tolerance of $\pm 1\%$ or 5mm. PowerSprings can be specified in a similar way to a steel extension spring. A typical specification chart is shown in the table.

The load at any extension can be calculated using the formula:

$$\text{Load} = S \times E + F0$$

(where S = spring rate, E = % extension and F0 = initial tension)

Designed to harness the power of the elemental materials, Power Springs are high-strength elastic tension/extension springs manufactured from a natural rubber core encased in braided fibre inner and outer covers.

PowerSprings deliver a unique combination of power and load characteristics that offer a high performance alternative to coiled steel springs.

- Exceptional load - weight ratio
- Virtually no restriction on length
- Outstanding flexibility
- Tested beyond 5,000,000 cycles
- Non magnetic
- Chemical resistance
- Wide temperature service range
- Available in endless ring applications

Essential to the versatility of *PowerSprings* is its patented termination options.

In external tests carried out by the Institute of Spring Technology, in excess of 5,000,000 load cycles had been achieved.

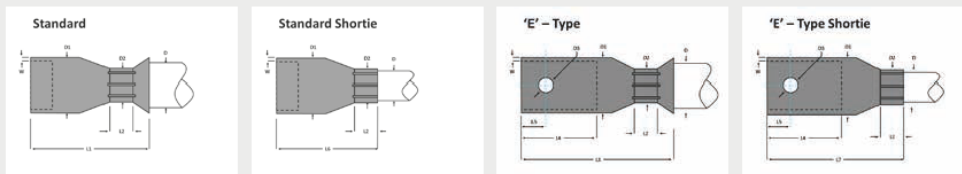
A range of stainless steel and aluminium end fittings are used as standard, but customised end options can be fitted to meet application demands. Additionally for special requirements, to meet British Standard 3F70:1991 for example, or when high performance is required, different fibre sheathing cover materials can be used.

| Cord diameter mm (in) | Maximum load N (lb) | Initial Tension N (lb) | Preload N (lb) | Nominal free length | Spring rate N (lb) | Maximum extension % |
|-----------------------|---------------------|------------------------|----------------|---------------------|--------------------|---------------------|
| 12.5 (0.49) | 487 (109) | 135 (30) | 174 (39) | Any | 3.91 (0.88) | 90 |
| 16.0 (0.63) | 826 (186) | 190 (43) | 261 (59) | Any | 7.07 (1.59) | 90 |
| 19.0 (0.75) | 1152 (259) | 248 (56) | 348 (78) | Any | 10.04 (2.26) | 90 |
| 22.0 (0.87) | 1565 (352) | 367 (82) | 500 (112) | Any | 13.31 (2.99) | 90 |
| 26.0 (1.02) | 1957 (440) | 538 (121) | 696 (156) | Any | 15.77 (3.54) | 90 |
| 32.0 (1.26) | 3326 (747) | 782 (176) | 1065 (239) | Any | 28.27 (6.35) | 90 |

Pre-load = load at 10% extension.

Initial tension = calculated value that assumes the modulus is constant to zero extension.

POWERSPRINGS STANDARD TERMINATIONS



| Cord Diameter (mm) | Aluminium | | | | | | | | | | | Steel | | | | | | | | | | |
|--------------------|-----------|----|----|----|----|-----|----|----|----|----|-----|-------|----|----|----|----|-----|----|----|----|----|-----|
| | D1 | D2 | D3 | L1 | L2 | L3 | L4 | L5 | L6 | L7 | W | D1 | D2 | D3 | L1 | L2 | L3 | L4 | L5 | L6 | L7 | W |
| 12.5 | 19 | 16 | 7 | 46 | 26 | 64 | 18 | 11 | 38 | 56 | 2.6 | 19 | 15 | 7 | 46 | 26 | 64 | 18 | 11 | 38 | 56 | 2.6 |
| 16 | 25.4 | 21 | 7 | 51 | 26 | 75 | 21 | 11 | 41 | 66 | 3.3 | 25.4 | 21 | 7 | 51 | 26 | 75 | 21 | 11 | 41 | 66 | 3.3 |
| 19 | 28.6 | 19 | 7 | 55 | 26 | 79 | 21 | 11 | 44 | 67 | 3.3 | 28.6 | 19 | 7 | 55 | 26 | 79 | 21 | 11 | 44 | 67 | 3.3 |
| 22 | 31.8 | 23 | 10 | 59 | 27 | 83 | 22 | 15 | 46 | 70 | 3.3 | 31.8 | 23 | 10 | 59 | 27 | 83 | 22 | 15 | 46 | 70 | 3.3 |
| 26 | 38.1 | 26 | 10 | 65 | 27 | 96 | 36 | 15 | 50 | 80 | 3.3 | 38.1 | 26 | 10 | 65 | 27 | 96 | 36 | 15 | 50 | 80 | 4 |
| 32 | 44.5 | 30 | 10 | 75 | 29 | 111 | 38 | 15 | 57 | 93 | 3.3 | 44.5 | 30 | 10 | 75 | 29 | 111 | 38 | 15 | 57 | 93 | 3.3 |

This information may be subject to change.

TrustLink Stress Terminations

Rugged connectivity solutions for heavy loads



TrustLink stress terminations represent a range of rugged, safe and reliable solutions for connecting a cable to a towed or profiling system or for handling a heavy piece of cabled underwater equipment or a subsea installation. Terminating and moulding the cable to a connector ensures a watertight connection from the cable to the subsea equipment.

MacArtney holds TrustLink stress terminations in stock for steel or kevlar armoured cables with a broad variety of industry standard diameters.

TrustLink stress terminations are available in either a 'shackle' or 'fork' termination design. While standard TrustLink stress terminations are available with safe working loads (SWL) ranging from 400 to 14,500 kg, MacArtney also holds extensive experience in designing custom stress termination solutions for loads of up to 100 tons.

Specifications

- Standard SWL range 400-14,500 kg
- Body material: stainless steel AISI 316

Features and benefits

- Simple, rugged, dependable and flexible connectivity solutions for multiple applications
- 'Shackle' and 'fork' termination designs available
- Extremely high durability
- Easy to re-terminate
- Watertight connection from cable to system
- Wide range of loads handled

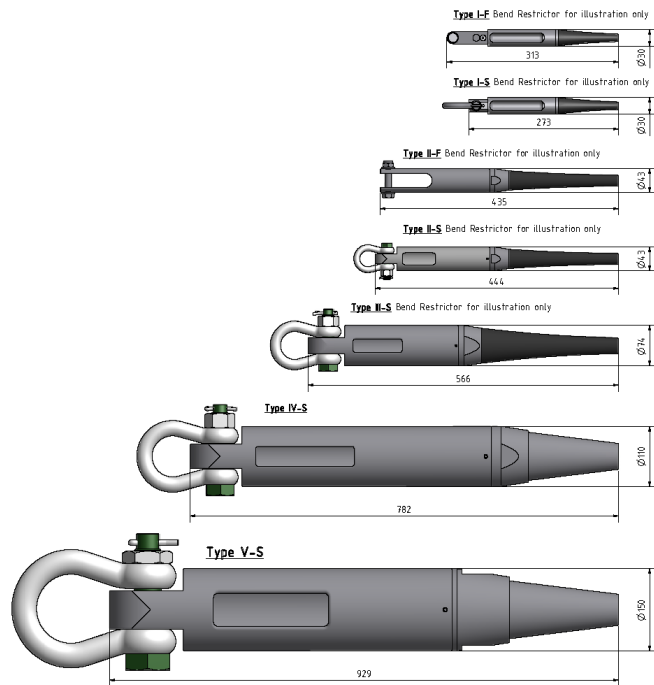
Applications

- Subsea drilling, coring and CPT systems
- Drop-camera systems
- Remotely operated towed vehicles (ROTV)
- Custom towed sensor platforms and towfish applications
- Side scan sonars
- CTD systems and sampling rosettes
- Sound velocity sensors
- Dive support equipment
- Dredging support systems
- Installing and recovering cabled subsea installations
- General lifting and handling of towed systems
- General lifting and handling of profiling systems and equipment

Options

- Customisable from 1 to 100,000 kg SWL
- Termination and moulding to connectors and cables
- Moulded bend stiffeners





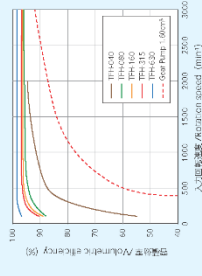
Specifications

| | Cable range | Max SWL | Overall OD | Calculated weight of termination |
|------------|-------------|---------|------------|----------------------------------|
| Type | mm | kg | mm | kg |
| Type I-F | ø3 to ø8 | 400 | ø30 | 0.4 |
| Type I-S | ø3 to ø8 | 660 | ø30 | 0.4 |
| Type II-F | ø8 to ø14 | 800 | ø43 | 1.6 |
| Type II-S | ø8 to ø14 | 1,500 | ø43 | 2 |
| Type III-S | ø14 to ø25 | 4,250 | ø74 | 8 |
| Type IV-S | ø25 to ø35 | 8,000 | ø110 | 32.8 |
| Type V-S | ø35 to ø45 | 14,500 | ø150 | 77.7 |

マイクロポンプ Small Axial Piston Pump

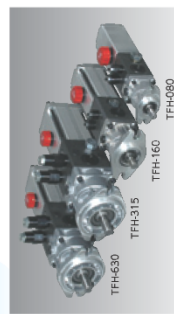


| 型式 Model | 最大瞬間 出力 Maximum output (kW) | 最大回転 速度 Max. rotation speed (rpm) | 全長 Overall length (mm) | 質量 Weight (kg) | 寸法 Size (mm) |
|-------------|---|--|------------------------------|----------------------|--------------------|
| TFH-040 | 0.40 | 14 | 2000 | 0.40 | 30×77 |
| TFH-080 | 0.80 | 21 | 3000 | 0.80 | 40×97 |
| TFH-160 | 1.61 | 21 | 3000 | 4.83 | 60×112 |
| TFH-315 | 3.13 | 21 | 3000 | 9.39 | 80×137 |
| TFH-630 | 6.25 | 21 | 3000 | 18.87 | 80×140 |



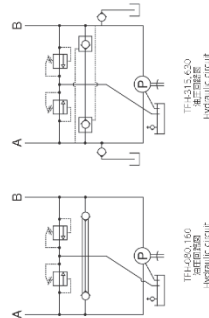
- フラココ膜設計により、使用性、耐久性に優れている。
- 入力軸を回転方向に自動で調整できる。
- 低コストな減速回路で、使用でも、効率が高い。
- 閉回路でも使用できる。
- Superior characteristic of maintaining pressure and boosting property thanks to the spherical valve plate.
- Input shaft is bi-rotational.
- High efficiency, capable from low speed to high speed.
- The pump could be used also in closed loop circuit.

マイクローポンプユニット

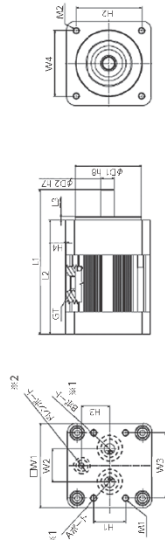


| 型式 Model | 機體重量 Weight kg | 全高 Overall height mm | 全幅 Overall width mm | 全長 Overall length mm | 最大速度 Max speed km/h | 最大出力 Max power HP | 機體構造 機體構造 機體構造 |
|---------------|----------------------|----------------------------|---------------------------|----------------------------|---------------------------|-------------------------|----------------------|
| TFH-080-U-V | 2.40 | 1,545 | 249 | 3,000 | 21 | 0.80 | 機體構造 機體構造 機體構造 |
| TFH-160-U-V | 2.5 | 1,600 | 271 | 3,000 | 21 | 1.61 | 機體構造 機體構造 機體構造 |
| TFH-315-U-PCV | 6.3 | 1,800 | 349 | 3,000 | 21 | 3.13 | 機體構造 機體構造 機體構造 |
| TFH-630-U-PCV | 6.5 | 1,800 | 349 | 3,000 | 21 | 6.29 | 機體構造 機體構造 機體構造 |

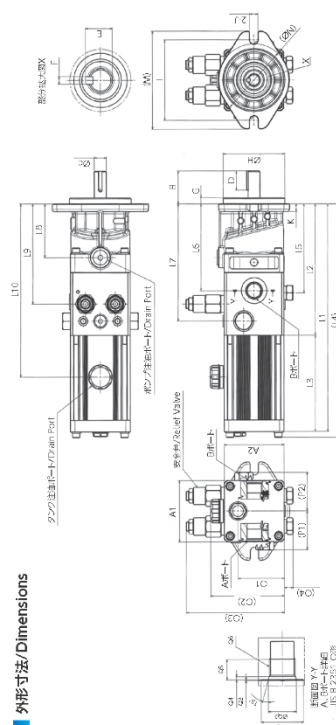
- 従来型、付力付きできつてしまっているスペースへの取付け方が可能である場所、必要な時だけ油圧圧入、省エネルギーである。
- 最新型はクレーンやクレーンに電動で、容易に搬入される。
- 電動機は三相電圧400Vの組合せで、燃焼油システム、EHA、Electric Hydraulic Actuator) として、簡単に使用できる。
- possible to mount on small space where it was not possible in the past.
- Energy saving as you can use hydraulic only at necessary place and time.
- input shaft could be driven in bi-rotational wise with high responsiveness.
- Wide application is possible as EHA; Electric Hydraulic Actuator, combined with motor and activator



Small Axial Piston Pump / Small Axial Piston Pump Unit

[illegible]

外形寸法/Dimensions

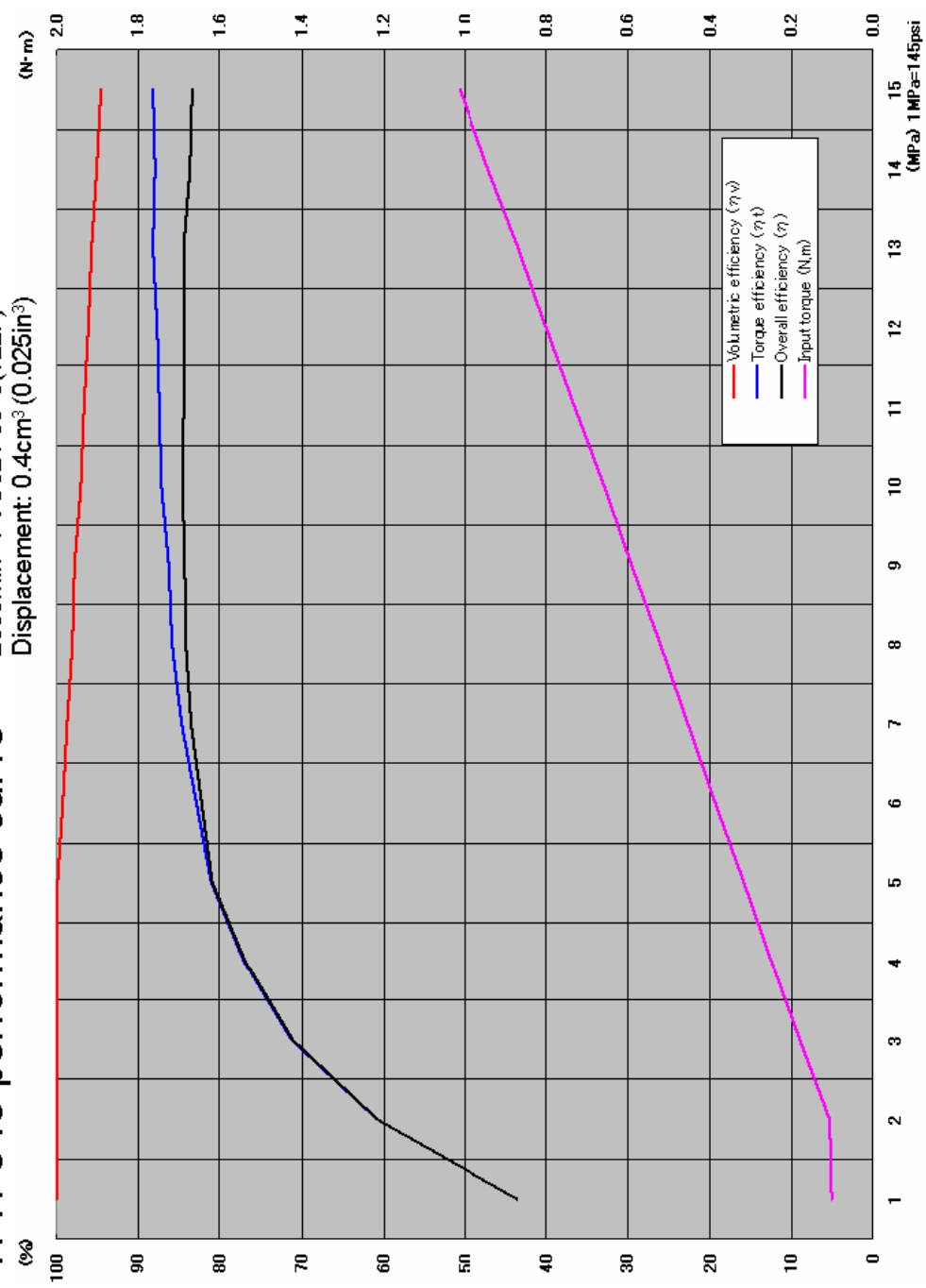


| 形式 Series | A | B | C | D | E | F | G | H | I | J | K | L | M | N | O | P | Q | R | S | T | U | V | W | X | Y | Z | 合計 | | |
|--------------|----|----|----|----|------|---|---|----|----|---|------|------|----|-----|-----|------|----|-----|----|----|----|-----|----|---|----|----|----|----|----|
| TPH-100 | 48 | 48 | 28 | 19 | 11.5 | 4 | 5 | 30 | 38 | 6 | 1542 | 1011 | 36 | 202 | 362 | 1562 | 63 | 180 | 72 | 60 | 27 | 165 | 76 | 1 | 33 | 34 | 1 | 38 | 15 |
| TPH-150 | 48 | 48 | 28 | 19 | 11.5 | 4 | 5 | 30 | 38 | 6 | 1542 | 1011 | 36 | 202 | 362 | 1562 | 63 | 180 | 72 | 60 | 27 | 165 | 76 | 1 | 33 | 34 | 1 | 38 | 15 |
| TPH-200 | 48 | 48 | 27 | 19 | 11.5 | 4 | 6 | 30 | 38 | 6 | 1536 | 1013 | 36 | 202 | 360 | 1560 | 63 | 180 | 72 | 60 | 27 | 165 | 76 | 1 | 33 | 34 | 1 | 38 | 15 |
| TPH-250 | 48 | 48 | 27 | 19 | 11.5 | 4 | 6 | 30 | 38 | 6 | 1536 | 1013 | 36 | 202 | 360 | 1560 | 63 | 180 | 72 | 60 | 27 | 165 | 76 | 1 | 33 | 34 | 1 | 38 | 15 |
| TPH-300 | 48 | 48 | 27 | 19 | 11.5 | 4 | 6 | 30 | 38 | 6 | 1536 | 1013 | 36 | 202 | 360 | 1560 | 63 | 180 | 72 | 60 | 27 | 165 | 76 | 1 | 33 | 34 | 1 | 38 | 15 |
| TPH-350 | 48 | 48 | 27 | 19 | 11.5 | 4 | 6 | 30 | 38 | 6 | 1536 | 1013 | 36 | 202 | 360 | 1560 | 63 | 180 | 72 | 60 | 27 | 165 | 76 | 1 | 33 | 34 | 1 | 38 | 15 |
| TPH-400 | 48 | 48 | 27 | 19 | 11.5 | 4 | 6 | 30 | 38 | 6 | 1536 | 1013 | 36 | 202 | 360 | 1560 | 63 | 180 | 72 | 60 | 27 | 165 | 76 | 1 | 33 | 34 | 1 | 38 | 15 |
| TPH-450 | 48 | 48 | 27 | 19 | 11.5 | 4 | 6 | 30 | 38 | 6 | 1536 | 1013 | 36 | 202 | 360 | 1560 | 63 | 180 | 72 | 60 | 27 | 165 | 76 | 1 | 33 | 34 | 1 | 38 | 15 |
| TPH-500 | 48 | 48 | 27 | 19 | 11.5 | 4 | 6 | 30 | 38 | 6 | 1536 | 1013 | 36 | 202 | 360 | 1560 | 63 | 180 | 72 | 60 | 27 | 165 | 76 | 1 | 33 | 34 | 1 | 38 | 15 |
| TPH-550 | 48 | 48 | 27 | 19 | 11.5 | 4 | 6 | 30 | 38 | 6 | 1536 | 1013 | 36 | 202 | 360 | 1560 | 63 | 180 | 72 | 60 | 27 | 165 | 76 | 1 | 33 | 34 | 1 | 38 | 15 |
| TPH-600 | 48 | 48 | 27 | 19 | 11.5 | 4 | 6 | 30 | 38 | 6 | 1536 | 1013 | 36 | 202 | 360 | 1560 | 63 | 180 | 72 | 60 | 27 | 165 | 76 | 1 | 33 | 34 | 1 | 38 | 15 |
| TPH-650 | 48 | 48 | 27 | 19 | 11.5 | 4 | 6 | 30 | 38 | 6 | 1536 | 1013 | 36 | 202 | 360 | 1560 | 63 | 180 | 72 | 60 | 27 | 165 | 76 | 1 | 33 | 34 | 1 | 38 | 15 |
| TPH-700 | 48 | 48 | 27 | 19 | 11.5 | 4 | 6 | 30 | 38 | 6 | 1536 | 1013 | 36 | 202 | 360 | 1560 | 63 | 180 | 72 | 60 | 27 | 165 | 76 | 1 | 33 | 34 | 1 | 38 | 15 |
| TPH-750 | 48 | 48 | 27 | 19 | 11.5 | 4 | 6 | 30 | 38 | 6 | 1536 | 1013 | 36 | 202 | 360 | 1560 | 63 | 180 | 72 | 60 | 27 | 165 | 76 | 1 | 33 | 34 | 1 | 38 | 15 |
| TPH-800 | 48 | 48 | 27 | 19 | 11.5 | 4 | 6 | 30 | 38 | 6 | 1536 | 1013 | 36 | 202 | 360 | 1560 | 63 | 180 | 72 | 60 | 27 | 165 | 76 | 1 | 33 | 34 | 1 | 38 | 15 |
| TPH-850 | 48 | 48 | 27 | 19 | 11.5 | 4 | 6 | 30 | 38 | 6 | 1536 | 1013 | 36 | 202 | 360 | 1560 | 63 | 180 | 72 | 60 | 27 | 165 | 76 | 1 | 33 | 34 | 1 | 38 | 15 |
| TPH-900 | 48 | 48 | 27 | 19 | 11.5 | 4 | 6 | 30 | 38 | 6 | 1536 | 1013 | 36 | 202 | 360 | 1560 | 63 | 180 | 72 | 60 | 27 | 165 | 76 | 1 | 33 | 34 | 1 | 38 | 15 |
| TPH-950 | 48 | 48 | 27 | 19 | 11.5 | 4 | 6 | 30 | 38 | 6 | 1536 | 1013 | 36 | 202 | 360 | 1560 | 63 | 180 | 72 | 60 | 27 | 165 | 76 | 1 | 33 | 34 | 1 | 38 | 15 |
| TPH-1000 | 48 | 48 | 27 | 19 | 11.5 | 4 | 6 | 30 | 38 | 6 | 1536 | 1013 | 36 | 202 | 360 | 1560 | 63 | 180 | 72 | 60 | 27 | 165 | 76 | 1 | 33 | 34 | 1 | 38 | 15 |



TFH-040 performance curve

2000min⁻¹ / VG32 / 50°C (122F)
Displacement: 0.4cm³ (0.025in³)

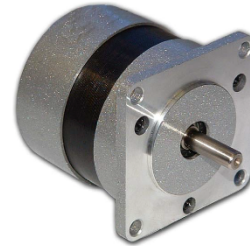


BLWS23 Series - Brushless DC Motors



FEATURES

- NEMA Size 23 BLDC Motors
- Compact Size and Power Density
- Cost-Effective Solution
- Long Life and Highly Reliable
- Can be Customized for
 - Maximum Speed
 - Winding Current
 - Shaft Options
 - Cables and Connectors
- CE Certified and RoHS Compliant



DESCRIPTION

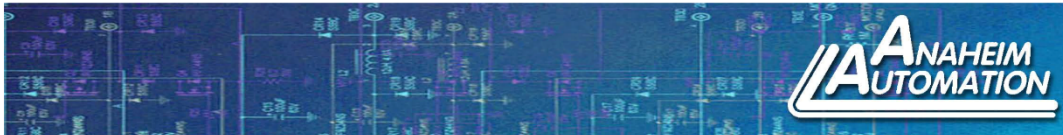
The BLWS23 Series Brushless DC Motors come in a compact package with high power density. These motors are cost-effective solutions to many velocity control applications. They come in five different stack lengths to provide you with just the right torque for your application. The motors come in a standard 8-lead configuration. We can also customize the windings to perfectly match your voltage, current, and maximum operating speed. Special shaft modifications, cables and connectors are also available upon request.

SPECIFICATIONS

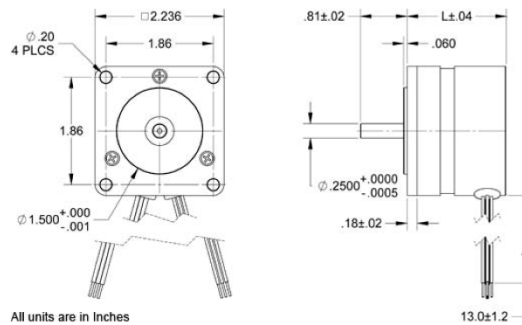
| Model # | Rated Voltage (V) | Rated Speed (RPM) | Rated Power (W) | Rated Torque (oz-in) | No Load Current (A) | Torque Constant (oz-in/A) | Back EMF Voltage (V/kRPM) | Line to Line Resistance (ohms) | Line to Line Inductance (mH) | Rotor Inertia (oz-in-sec ²) | Weight (lbs) | "L" Length (in) |
|--------------------|-------------------|-------------------|-----------------|----------------------|---------------------|---------------------------|---------------------------|--------------------------------|------------------------------|---|--------------|-----------------|
| BLWS231D-24V-2000 | 24 | 2000 | 11.5 | 7.79 | 0.40 | 7.50 | 5.50 | 6.00 | 12.70 | 0.00042 | 0.84 | 1.72 |
| BLWS231S-24V-2000 | 24 | 2000 | 11.5 | 7.79 | 0.40 | 7.50 | 5.50 | 6.00 | 12.70 | 0.00042 | 0.84 | 1.72 |
| BLWS231D-36V-4000 | 36 | 4000 | 23 | 7.79 | 0.20 | 7.50 | 5.50 | 4.20 | 9.70 | 0.00042 | 0.84 | 1.72 |
| BLWS231S-36V-4000 | 36 | 4000 | 23 | 7.79 | 0.20 | 7.50 | 5.50 | 4.20 | 9.70 | 0.00042 | 0.84 | 1.72 |
| BLWS232D-12V-500 | 12 | 255 | 1.3 | 7.08 | 0.18 | 27.33 | 16.10 | 22.00 | 56.00 | 0.00106 | 1.10 | 2.11 |
| BLWS232S-12V-500 | 12 | 255 | 1.3 | 7.08 | 0.18 | 27.33 | 16.10 | 22.00 | 56.00 | 0.00106 | 1.10 | 2.11 |
| BLWS232D-24V-1350 | 24 | 1350 | 16 | 15.58 | 0.30 | 16.43 | 9.50 | 6.88 | 18.00 | 0.00106 | 1.10 | 2.11 |
| BLWS232S-24V-1350 | 24 | 1350 | 16 | 15.58 | 0.30 | 16.43 | 9.50 | 6.88 | 18.00 | 0.00106 | 1.10 | 2.11 |
| BLWS232D-24V-4000 | 24 | 4000 | 46 | 15.58 | 0.50 | 5.48 | 4.00 | 0.82 | 2.30 | 0.00106 | 1.10 | 2.11 |
| BLWS232S-24V-4000 | 24 | 4000 | 46 | 15.58 | 0.50 | 5.48 | 4.00 | 0.82 | 2.30 | 0.00106 | 1.10 | 2.11 |
| BLWS232D-36V-4000 | 36 | 4000 | 4 | 14.16 | 0.40 | 8.50 | 4.50 | 2.40 | 4.39 | 0.00106 | 1.10 | 2.11 |
| BLWS232S-36V-4000 | 36 | 4000 | 4 | 14.16 | 0.40 | 8.50 | 4.50 | 2.40 | 4.39 | 0.00106 | 1.10 | 2.11 |
| BLWS233D-24V-4000 | 24 | 4000 | 92 | 31.15 | 0.50 | 6.09 | 3.50 | 0.35 | 1.00 | 0.00169 | 1.65 | 2.90 |
| BLWS233S-24V-4000 | 24 | 4000 | 92 | 31.15 | 0.50 | 6.09 | 3.50 | 0.35 | 1.00 | 0.00169 | 1.65 | 2.90 |
| BLWS233D-36V-4000 | 36 | 4000 | 92 | 31.15 | 0.50 | 8.92 | 4.80 | 0.58 | 2.10 | 0.00169 | 1.65 | 2.90 |
| BLWS233S-36V-4000 | 36 | 4000 | 92 | 31.15 | 0.50 | 8.92 | 4.80 | 0.58 | 2.10 | 0.00169 | 1.65 | 2.90 |
| BLWS234D-36V-4000 | 36 | 4000 | 134 | 45.32 | 0.50 | 8.50 | 4.80 | 0.45 | 1.50 | 0.00245 | 2.20 | 3.69 |
| BLWS234S-36V-4000 | 36 | 4000 | 134 | 45.32 | 0.50 | 8.50 | 4.80 | 0.45 | 1.50 | 0.00245 | 2.20 | 3.69 |
| BLWS234D-45V-1400 | 45 | 1400 | 44 | 42.48 | 0.50 | 28.32 | 16.00 | 4.20 | 15.00 | 0.00245 | 2.20 | 3.69 |
| BLWS234S-45V-1400 | 45 | 1400 | 44 | 42.48 | 0.50 | 28.32 | 16.00 | 4.20 | 15.00 | 0.00245 | 2.20 | 3.69 |
| BLWS235D-24V-500 | 24 | 240 | 5.7 | 31.86 | 0.15 | 59.48 | 34.10 | 18.00 | 55.00 | 0.00326 | 2.76 | 4.47 |
| BLWS235S-24V-500 | 24 | 240 | 5.7 | 31.86 | 0.15 | 59.48 | 34.10 | 18.00 | 55.00 | 0.00326 | 2.76 | 4.47 |
| BLWS235D-36V-4000 | 36 | 4000 | 184 | 62.31 | 0.40 | 8.92 | 4.60 | 0.38 | 1.00 | 0.00326 | 2.76 | 4.47 |
| BLWS235S-36V-4000 | 36 | 4000 | 184 | 62.31 | 0.40 | 8.92 | 4.60 | 0.38 | 1.00 | 0.00326 | 2.76 | 4.47 |
| BLWS235D-36V-10000 | 36 | 10000 | 183 | 24.78 | 1.50 | 4.53 | 2.30 | 0.09 | 0.25 | 0.00326 | 2.76 | 4.47 |
| BLWS235S-36V-10000 | 36 | 10000 | 183 | 24.78 | 1.50 | 4.53 | 2.30 | 0.09 | 0.25 | 0.00326 | 2.76 | 4.47 |
| BLWS235D-160V-3000 | 160 | 3000 | 157 | 70.80 | 0.20 | 46.73 | 26.00 | 11.00 | 33.50 | 0.00326 | 2.76 | 4.47 |
| BLWS235S-160V-3000 | 160 | 3000 | 157 | 70.80 | 0.20 | 46.73 | 26.00 | 11.00 | 33.50 | 0.00326 | 2.76 | 4.47 |

L010229 Note: The 8th character "S" denotes a single shaft, use "D" for double shaft. Custom leadwires, cables, connectors, and windings are available upon request.

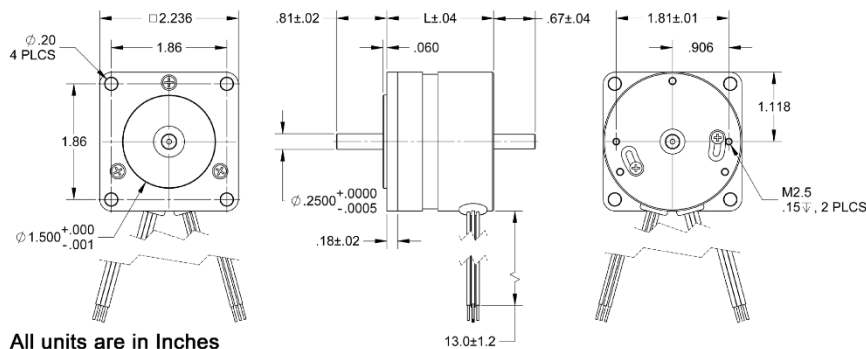
4985 E. Landon Drive Anaheim, CA 92807 Tel. (714) 992-6990 Fax: (714) 992-0471 www.anaheimautomation.com



SINGLE SHAFT DIMENSIONS

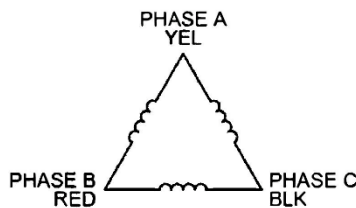


DUAL SHAFT DIMENSIONS



SPECIFICATIONS / WIRING

| Wire Color | Description |
|------------|-------------|
| Red | Hall Supply |
| Blue | Hall A |
| Green | Hall B |
| White | Hall C |
| Black | Hall Ground |
| Yellow | Phase A |
| Red | Phase B |
| Black | Phase C |



| Hall Sensor Specifications | |
|------------------------------|-------------------|
| Supply Voltage: | 4.5VDC to 28VDC |
| Current, I_{off} : | 10mA max |
| Current, I_{on} : | 11.3mA max |
| Rated Sinking Current: | 20mA |
| Saturation Voltage: | 0.4VDC max @ 25°C |
| Output Leakage Current: | 10µA |
| Output Switching Time @ 25°C | |
| Rise, 10% to 90% | 1.5µs |
| Fall, 90% to 10% | 1.5µs |
| Output Type: | Open Collector |

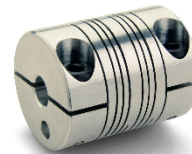
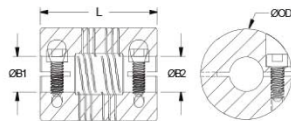
| | | | |
|--------------------|-----------------------------|------------------------|----------------------------|
| Winding Type: | Delta, 4 Poles | Max. Radial Force: | 75N @ 20mm from the Flange |
| Hall Effect Angle: | 120 Degree Electrical Angle | Max. Axial Force: | 10N |
| Shaft Run Out: | 0.025mm | Insulation Class: | Class B |
| Radial Play: | 0.02mm@450g | Dielectric Strength: | 500VDC for one Minute |
| End Play: | 0.08mm@450g | Insulation Resistance: | 100MOhm, 500VDC |

4985 E. Landon Drive Anaheim, CA 92807 Tel. (714) 992-6990 Fax. (714) 992-0471 www.anaheimautomation.com



PCR12-1/4"-6MM-A

Ruland PCR12-1/4"-6MM-A, 1/4" x 6mm Four Beam Coupling, Aluminum, Clamp Style, 0.750" (19.1mm) OD, 0.900" (22.9mm) Length



Description

Ruland PCR12-1/4"-6MM-A is a four beam coupling with 1/4" x 6mm bores, 0.750" (19.1mm) OD, and 0.900" (22.9mm) length. It is machined from a single piece of material and feature two sets of two spiral cuts. This gives it higher torque capacity, lower windup, and larger body sizes than single beam couplings. PCR12-1/4"-6MM-A is well suited for applications such as encoders that require high positioning accuracy. This four beam spiral coupling is zero-backlash and has a balanced design for reduced vibration at high speeds of up to 6,000 RPM. All hardware is metric and tests beyond DIN 912 12.9 standards for maximum torque capabilities. PCR12-1/4"-6MM-A is made from 7075 aluminum for lightweight and low inertia. It is machined from bar stock that is sourced exclusively from North American mills and is RoHS2 and REACH compliant. PCR12-1/4"-6MM-A is manufactured in our Marlborough, MA factory under strict controls using proprietary processes.

Product Specifications

| | | | |
|-------------------------------|--|-------------------------------------|---|
| Large Bore B1 | 0.250 in | Small Bore B2 | 6 mm |
| B1 Shaft Penetration | 0.422 in, 10.7 mm | B2 Shaft Penetration | 0.422 in, 10.7 mm |
| Outer Diameter OD | 0.750 in / 19.1 mm | Bore Tolerance | +0.001 in / -.000 in, +.025 mm / -.000 mm |
| Length L | 0.900 in / 22.9 mm | Cap Screw | M2.5 |
| Screw Material | Alloy Steel | Hex Wrench Size | 2.0 mm |
| Screw Finish | Black Oxide | Seating Torque | 1.21 Nm |
| Number of Screws | 2 ea | Static Torque | 14 lb-in, 1.58 Nm |
| Angular Misalignment | 3° | Dynamic Torque Non-Reversing | 7 lb-in, 0.79 Nm |
| Parallel Misalignment | 0.008 in, 0.20 mm | Dynamic Torque Reversing | 3.5 lb-in, 0.40 Nm |
| Axial Motion | 0.005 in, 0.13 mm | Torsional Stiffness | 0.330 Deg/lb-in, 2.92 Deg/Nm |
| Moment of Inertia | 0.0025 lb-in ² , 0.731 x10 ⁻⁶ kg-m ² | Maximum Speed | 6,000 RPM |
| Material Specification | 7075-T651 Extruded and Drawn Aluminum Bar | Temperature | -40°F to 225°F -40°C to 107°C |
| Finish Specification | Bright | Manufacturer | Ruland Manufacturing |
| Country of Origin | USA | Weight (lbs.) | 0.0590 |
| Note 1 | Torque ratings are at maximum misalignment. | | |
| Note 2 | Performance ratings are for guidance only. The user must determine suitability for a particular application. | | |
| Note 3 | Torque ratings for the couplings are based on the physical limitations/failure point of the machined beams. Under normal/typical conditions the hubs are capable of holding up to the rated torque of the machined beams. In some cases, especially when the smallest standard bores are used or where shafts are undersized, slippage on the shaft is possible below the rated torque of the machined beams. Keyways are available to provide additional torque capacity in the shaft/hub connection when required. Please consult technical support for more assistance. | | |
| Prop 65 | ⚠️ WARNING This product can expose you to the chemical Ethylene Thiourea, known to the State of California to cause cancer and birth defects or other reproductive harm. For more information go to www.P65Warnings.ca.gov . | | |

30A Forward/Reverse Brushless DC Motor Controller with Hall and Encoder Inputs, USB and CAN



Roboteq's SBL13xx is a high-current controller for hall-sensor equipped Brushless DC motors. The controller uses the position information from the sensors to sequence power on the motor's 3 windings in order to generate smooth continuous rotation. The controller also uses the Hall sensor or encoder input information to compute speed and measure travelled distance inside a 32-bit counter. The motor may be operated in open or closed loop speed mode. Using low-cost position sensors, they may also be set to operate as heavy-duty position servos.

The SBL13xx accepts commands received from an RC radio, Analog Joystick, wireless modem, or microcomputer. Using CAN bus, up to 127 controllers can be networked on a single twisted pair cable. Numerous safety features are incorporated into the controller to ensure reliable and safe operation.

The controller's operation can be extensively automated and customized using Basic Language scripts. The controller can be configured, monitored and tuned in realtime using a Roboteq's free PC utility. The controller can also be reprogrammed in the field with the latest features by downloading new operating software from Roboteq.

Applications

- Electric Bikes
- Machine Control
- Terrestrial and Underwater Robotic Vehicles
- Automatic Guided Vehicles
- Police and Military Robots
- Hazardous Material Handling Robots
- Telepresence Systems
- Animatronics
- Industrial Controls
- Hydraulic Pumps control

Key Features

- RS232, 0-5V Analog, or Pulse (RC radio) command modes
- Available in version with CAN bus up to 1 Mbit/s
- Auto switch between RS232, Analog, or Pulse based on user-defined priority
- Built-in 3-phase high-power drivers for one brushless DC motor at up to 30A
- Trapezoidal switching based on Hall Sensor position information
- Full forward & reverse motor control. Four quadrant operation. Supports regeneration
- Operates from a single power source
- Programmable current limit up to 30A for protecting controller, motor, wiring and battery.
- Connector for Hall Sensors
- Accurate speed and Odometry measurement using Hall Sensor or encoder data
- Quadrature encoder input with 32-bit counter
- Up to 4 Analog Inputs for use as command and/or feedback
- Up to 4 Pulse Length, Duty Cycle or Frequency Inputs for use as command and/or feedback
- Up to 6 Digital Inputs for use as Deadman Switch, Limit Switch, Emergency stop or user inputs
- Two general purpose 40V, 1.5A output for brake release or accessories
- Custom scripting in Basic language. Execution speed 50000 lines per second
- Selectable min, max, center and deadband in Pulse and Analog modes
- Selectable exponentiation factors for each command inputs

- Trigger action if Analog, Pulse, Encoder or Hall counter capture are outside user selectable range (soft limit switches)
- Open loop or closed loop speed control operation
- Closed loop position control with encoder, analog or pulse/frequency feedback
- PID control loop
- Configurable Data Logging of operating parameters on RS232 Output for telemetry or analysis
- Built-in Battery Voltage and Temperature sensors
- Optional 12V backup power input for powering safely the controller if the main motor batteries are discharged
- Power Control wire for turning On or Off the controller from external microcomputer or switch
- No consumption by output stage when motors stopped
- Regulated 5V output for powering RC radio, RF Modem or microcomputer
- Separate Programmable acceleration and deceleration for each motor
- Support for two simplified CAN protocols
- Efficient 10 mOhm ON resistance MOSFETs
- Auto stop if no motion is detected
- Stall detection and selectable triggered action if Amps is outside user-selected range
- Short circuit protection with selectable sensitivity levels
- Overvoltage and Undervoltage protection
- Watchdog for automatic motor shutdown in case of command loss
- Overtemperature protection
- Diagnostic LED
- Efficient heat sinking using conduction bottom plate. Operates without a fan in most applications
- Power wiring via screw terminals
- 70mm x 70mm x 27mm
- -40o to +85o C operating environment
- 2oz (60g)
- Easy configuration, tuning and monitory using provided PC utility
- Field upgradeable software for installing latest features via the internet

Orderable Product References

| Reference | Number of Channels | Amps/Channel | Volts | CAN | USB |
|-----------|--------------------|--------------|-------|-----|-----|
| SBL1330 | 1 | 30 | 30 | Yes | Yes |
| SBL1360 | 1 | 30 | 60 | Yes | Yes |

Note: Brushless DC motor controllers require Hall Sensors to drive motors.

Electrical Specifications

Absolute Maximum Values

The values in the table below should never be exceeded. Permanent damage to the controller may result.

TABLE 6.

| Parameter | Measure point | Model | Min | Typ | Max | Units |
|-----------------------------------|--|---------|-----|-----|---------|-------|
| Battery Leads Voltage | Ground to VMot | SBL1330 | | | 35 | Volts |
| | | SBL1360 | | | 60 | Volts |
| Reverse Voltage on Battery Leads | Ground to VMot | All | -1 | | | Volts |
| Power Control Voltage | Ground to Pwr Control wire | All | | | 65 | Volts |
| Motor Leads Voltage | Ground to U, V, W wires | SBL1330 | | | 30 (1) | Volts |
| | | SBL1360 | | | 60 (1) | Volts |
| Digital Output Voltage | Ground to Output pins | All | | | 40 | Volts |
| Analog and Digital Inputs Voltage | Ground to any signal pin on 15-pin & Hall inputs | All | | | 15 | Volts |
| RS232 I/O pins Voltage | External voltage applied to Rx/Tx pins | All | | | 15 | Volts |
| Case Temperature | Case | All | -40 | | 85 | °C |
| Humidity | Case | All | | | 100 (2) | % |

Note 1: Maximum regeneration voltage in normal operation. Never inject a DC voltage from a battery or other fixed source
 Note 2: Non-condensing

Power Stage Electrical Specifications (at 25°C ambient)

TABLE 7.

| Parameter | Measure point | Model | Min | Typ | Max | Units |
|---|--|---------|-------|-----------|--------|---------------|
| Battery Leads Voltage | Ground to VMot | SBL1330 | 0 (1) | | 30 | Volts |
| | | SBL1360 | 0 (1) | | 60 | Volts |
| Motor Leads Voltage | Ground to U, V, W wires | SBL1330 | 0 (1) | | 30 (2) | Volts |
| | | SBL1360 | 0 (1) | | 60 (2) | Volts |
| Power Control Voltage | Ground to Power Control wire | All | 0 (1) | | 65 | Volts |
| Minimum Operating Voltage | VMot or Pwr Ctrl wires | All | 9 (3) | | | Volts |
| Over Voltage protection range | Ground to VMot | SBL1330 | 5 | 55 (4) | 30 | Volts |
| | | SBL1360 | 5 | 55 (4) | 60 | Volts |
| Under Voltage protection range | Ground to VMot | SBL1330 | 0 | 5 (4) | 30 | Volts |
| | | SBL1360 | 0 | 5 (4) | 60 | Volts |
| Idle Current Consumption | VMot or Pwr Ctrl wires | All | 50 | 100 (5) | 150 | mA |
| ON Resistance (Excluding wire resistance) | VMot to U, V or W. Ground to U, V or W | All | | 10 | | mOhm |
| Max Current for 30s | Motor current | All | | | 30 | Amps |
| Continuous Max Current per channel | Motor current | All | | | 20 (7) | Amps |
| Current Limit range | Motor current | All | 5 | 20 (8) | 30 | Amps |
| Stall Detection Amps range | Motor current | All | 5 | 30 (8) | 30 | Amps |
| Stall Detection timeout range | Motor current | All | 1 | 65000 (9) | 65000 | milli-seconds |

TABLE 7

| Parameter | Measure point | Model | Min | Typ | Max | Units |
|--|---|-------|---|----------|----------|---------------|
| Short Circuit Detection threshold (10) | Between Motor wires or Between Motor wires and Ground | All | 100 (11) | | 200 (11) | Amps |
| Short Circuit Detection threshold | Between Motor wires and VMot | All | No Protection. Permanent damage will result | | | |
| Motor Acceleration/Deceleration range | Motor Output | All | 100 | 500 (12) | 65000 | milli-seconds |
| <p>Note 1: Negative voltage will cause a large surge current. Protection fuse needed if battery polarity inversion is possible</p> <p>Note 2: Maximum regeneration voltage in normal operation. Never inject a DC voltage from a battery or other fixed source</p> <p>Note 3: Minimum voltage must be present on VMot or Power Control wire</p> <p>Note 4: Factory default value. Adjustable in 0.1V increments</p> <p>Note 5: Current consumption is lower when higher voltage is applied to the controller's VMot or PwrCtrl wires</p> <p>Note 6: Max value is determined by current limit setting. Duration is estimated and is dependent on ambient temperature cooling condition</p> <p>Note 7: Estimate. Limited by heatsink temperature. Current may be higher with better cooling</p> <p>Note 8: Factory default value. Adjustable in 0.1A increments</p> <p>Note 9: Factory default value. Time in ms that Stall current must be exceeded for detection</p> <p>Note 10: Controller will stop until restarted in case of short circuit detection</p> <p>Note 11: Sensitivity selectable by software</p> <p>Note 12: Factory default value. Time in ms for power to go from 0 to 100%</p> | | | | | | |

Command, I/O and Sensor Signals Specifications

TABLE 8.

| Parameter | Measure point | Min | Typ | Max | Units |
|--------------------------------|----------------------------|--------|------|-------|------------------------|
| Main 5V Output Voltage | Ground to 5V pin on DSub15 | 4.7 | 4.9 | 5.1 | Volts |
| 5V Output Current | 5V pin on DSub15 | | | 100 | mA |
| Digital Output Voltage | Ground to Output pins | | | 40 | Volts |
| Digital Output Current | Output pins, sink current | | | 1 | Amps |
| Output On resistance | Output pin to ground | | 0.75 | 1.5 | Ohm |
| Output Short circuit threshold | Output pin | 1.05 | 1.4 | 1.75 | Amps |
| Input Impedances | AIN/DIN Input to Ground | | 53 | | kOhm |
| Digital Input 0 Level | Ground to Input pins | -1 | | 1 | Volts |
| Digital Input 1 Level | Ground to Input pins | 3 | | 15 | Volts |
| Analog Input Range | Ground to Input pins | 0 | | 5.1 | Volts |
| Analog Input Precision | Ground to Input pins | | 0.5 | | % |
| Analog Input Resolution | Ground to Input pins | | 1 | | mV |
| Pulse durations | Pulse inputs | 20000 | | 10 | us |
| Pulse repeat rate | Pulse inputs | 50 | | 250 | Hz |
| Pulse Capture Resolution | Pulse inputs | | 1 | | us |
| Frequency Capture | Pulse inputs | 100 | | 10000 | Hz |
| Encoder count | Internal | -2.147 | | 2.147 | 10 ⁹ Counts |

TABLE 8.

| Parameter | Measure point | Min | Typ | Max | Units |
|--|--------------------|-----|-----|-------|----------|
| Encoder frequency | Encoder input pins | | | 1M(1) | Counts/s |
| Note1: Encoder input requires RC inputs 1, 2 and 3 to be disabled. Encoders are disabled in factory default. | | | | | |

Operating & Timing Specifications

TABLE 9.

| Parameter | Measure Point | Min | Typ | Max | Units |
|---|--------------------------|-------|------------|-------|--------|
| Command Latency | Command to output change | 0 | 2.5 | 5 | ms |
| PWM Frequency | Motor outputs | 10 | 18 (1) | 20 | kHz |
| Closed Loop update rate | Internal | | 1000 | | Hz |
| RS232 baud rate | Rx & Tx pins | | 115200 (2) | | Bits/s |
| RS232 Watchdog timeout | Rx pin | 1 (3) | | 65000 | ms |
| Note 1: May be adjusted with configuration program | | | | | |
| Note 2: 115200, 8-bit, no parity, 1 stop bit, no flow control | | | | | |
| Note 3: May be disabled with value 0 | | | | | |

Scripting

TABLE 10.

| Parameter | Measure Point | Min | Typ | Max | Units |
|-----------------------------|---------------|--------|---------|------|-----------|
| Scripting Flash Memory | Internal | | 8192 | | Bytes |
| Max Basic Language programs | Internal | | 1000 | 1500 | Lines |
| Integer Variables | Internal | | | 1024 | Words (1) |
| Boolean Variables | Internal | | | 1024 | Symbols |
| Execution Speed | Internal | 50 000 | 100 000 | | Lines/s |
| Note 1: 32-bit words | | | | | |

Thermal Specifications

TABLE 11.

| Parameter | Measure Point | Min | Typ | Max | Units |
|--|-----------------------------|-----|-----|--------|-------|
| Board Temperature | PCB | -40 | | 85 (1) | oC |
| Thermal Protection range | PCB | 70 | | 80 (2) | oC |
| Thermal resistance | Power MOSFETs to heats sink | | | 2 | oC/W |
| Note 1: Thermal protection will protect the controller power | | | | | |
| Note 2: Max allowed power out starts lowering at minimum of range, down to 0 at max of range | | | | | |

The SBL13xx uses a conduction plate at the bottom of the board for heat extraction. For best results, attach firmly with thermal compound paste against a metallic chassis so that heat transfers to the conduction plate to the chassis. If no metallic surface is available, mount the controller on spacers so that forced or natural air flow can go over the plate surface to remove heat.



date 07/18/2014
page 1 of 8

SERIES: AMT10 | DESCRIPTION: MODULAR INCREMENTAL ENCODER

FEATURES

- patented capacitive ASIC technology
- low power consumption
- CMOS outputs
- 16 DIP switch selectable resolutions
- index pulse
- modular package design
- straight (radial) and right-angle (axial) versions
- 9 mounting hole options for radial version
- 8 mounting hole options for axial version
- -40~100°C operating temperature



ELECTRICAL

| parameter | conditions/description | min | typ | max | units |
|---------------------|------------------------------|---------|-----|-----|-------|
| power supply | VDD | 3.6 | 5 | 5.5 | V |
| current consumption | with unloaded output | | 6 | | mA |
| output high level | | VDD-0.8 | | | V |
| output low level | | | | 0.4 | V |
| output current | CMOS sink/source per channel | | | 2 | mA |
| rise/fall time | | | 30 | | ns |

INCREMENTAL CHARACTERISTICS

| parameter | conditions/description | min | typ | max | units |
|--|---|-----|------|-----|---------|
| channels | quadrature A, B, and X index | | | | |
| waveform | CMOS voltage square wave | | | | |
| phase difference | A leads B for CCW rotation (viewed from front) | | 90 | | degrees |
| quadrature resolutions ¹ | 48, 96, 100, 125, 192, 200, 250, 256, 385, 400, 500, 512, 800, 1000, 1024, 2048 | | | | PPR |
| index ² | one pulse per 360 degree rotation | | | | |
| accuracy | | | 0.25 | | degrees |
| quadrature duty cycle (at each resolution) | 256, 512, 1024, 2048 | 49 | 50 | 51 | % |
| | 48, 96, 100, 125, 192, 200, 250, 384, 400, 500 | 47 | 50 | 53 | % |
| | 800, 1000 | 43 | 50 | 56 | % |

Notes: 1. Resolution selected via adjustable DIP switch
2. Some stepper motors may leak a magnetic field causing the AMT index pulse to not function properly (non-magnetic version available with 8 pulses per revolution).

MECHANICAL

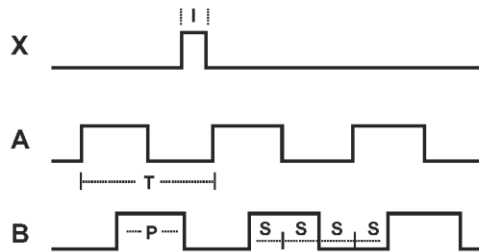
| parameter | conditions/description | min | typ | max | units |
|---------------------------------------|---|-----|------|-------|-------|
| motor shaft length | | 9 | | | mm |
| weight | AMT102 | | 20.5 | | g |
| | AMT103 | | 14.0 | | g |
| axial play | | | | ±0.3 | mm |
| rotational speed (at each resolution) | 192, 384, 400, 500, 800, 1000, 1024, 2048 | | | 7500 | RPM |
| | 48, 96, 100, 125, 200, 250, 256, 512 | | | 15000 | RPM |

ENVIRONMENTAL

| parameter | conditions/description | min | typ | max | units |
|-----------------------|-------------------------------|-----|-----|-----|-------|
| operating temperature | | -40 | | 100 | °C |
| humidity | non-condensing | | | 95 | % |
| vibration | 20~500 Hz, 1 hour on each XYZ | | | 10 | G |
| shock | 11 ms, ±XYZ direction | | | 50 | G |
| RoHS | 2011/65/EU | | | | |

WAVEFORMS**Figure 1**

Quadrature signals with index showing counter-clockwise rotation

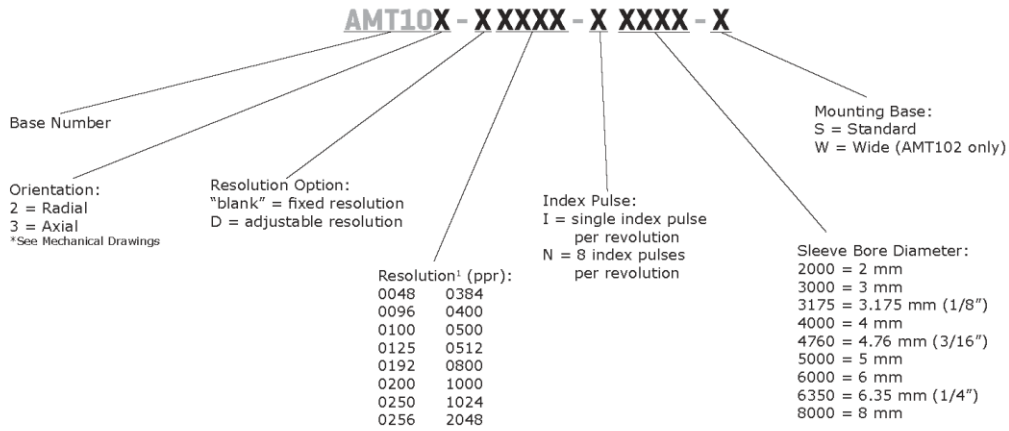


The following parameters are defined by the resolution selected for each encoder, where R = resolution.

| Parameter | Description | Expression | Units |
|-----------|-----------------|------------|--------------------|
| T | period | $360/R$ | mechanical degrees |
| P | pulse width | $T/2$ | mechanical degrees |
| I | index width | $P/2$ | mechanical degrees |
| S | A/B state width | $P/2$ | mechanical degrees |

PART NUMBER KEY

For customers that prefer a specific AMT10 configuration, please reference the custom configuration key below.



Note: 1. Fixed resolutions are permanently set at this value; adjustable resolutions are preset via DIP switch to this value upon shipment.










AMT10-V KITS









In order to provide maximum flexibility for our customers, the AMT10 series is provided in kit form standard. This allows the user to implement the encoder into a range of applications using one sku#, reducing engineering and inventory costs.

ORDERING GUIDE

AMT10X-V

Orientation:
2 = Radial
3 = Axial
*See Mechanical Drawings

| SLEEVES | | | | | | | | |
|---|---|---|---|---|---|---|---|---|
|  |  |  |  |  |  |  |  |  |
| 8mm | 1/4 inch (6.35mm) | 6mm | 5mm | 3/16 inch (4.76mm) | 4mm | 1/8 inch (3.175mm) | 3mm | 2mm |
| Blue | Snow | Red | Green | Yellow | Gray | Purple | Orange | Light Sky Blue |

| | | | |
|--|---|---|---|
| 102 BASE  | 102 WIDE BASE  | 102 TOP COVER  | SHAFT ADAPTER  |
| 103 BASE  | 103 TOP COVER  | TOOL A  | TOOL B  |



1-DC Series

- Ratings from 7 A to 40 A @ 200 VDC and from 7 A to 10 A @ 500VDC
- Mosfet Output
- UL Approved, CE Compliant to EN60950-1
- Improved SEMS screw and washer
- Redesigned housing with anti-rotation barriers

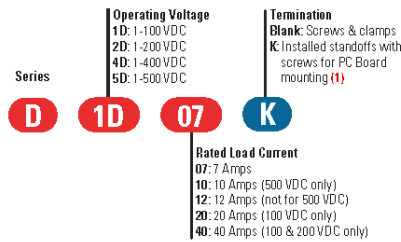
- DC control
- EMC Compliant to Level 3
- Epoxy Free Design

For **Generation 3** datasheet [click here](#)

PRODUCT SELECTION

| Load Voltage | 7 A | 10 A | 12 A | 20 A | 40 A |
|--------------|-------|-------|-------|-------|-------|
| 100 VDC | D1D07 | | D1D12 | D1D20 | D1D40 |
| 200 VDC | D2D07 | | D2D12 | | D2D40 |
| 400 VDC | D4D07 | | D4D12 | | |
| 500 VDC | D5D07 | D5D10 | | | |

AVAILABLE OPTIONS



- Required for valid part number
- For options only and not required for valid part number
- Not all part number combinations are available. Contact Crydom Technical Support for information on the availability of a specific part number.

OUTPUT SPECIFICATIONS ⁽²⁾

| Description | 7 A | 12 A | 20 A | 40 A | 7 A | 12 A | 40 A | 7 A | 12 A | 7 A | 10 A |
|--|------|-------|-------|-------|-------|-------|-------|-------|-------|-------|-------|
| Recommended Operating Voltage [Vdc] | 1-72 | 1-72 | 1-72 | 1-72 | 1-150 | 1-150 | 1-150 | 1-300 | 1-300 | 1-365 | 1-365 |
| Absolute Maximum Rating [Vdc] | 100 | 100 | 100 | 100 | 200 | 200 | 200 | 400 | 400 | 500 | 500 |
| Maximum Off-State Leakage Current @ Rated Voltage [mA] | 0.1 | 0.2 | 0.3 | 0.3 | 0.1 | 0.3 | 0.3 | 0.3 | 0.3 | 0.2 | 0.3 |
| Maximum Load Current [Adc] (3) | 7 | 12 | 20 | 40 | 7 | 12 | 40 | 7 | 12 | 7 | 10 |
| Minimum Load Current [mA] (4) | 1 | 1 | 1 | 1 | 1 | 1 | 1 | 1 | 1 | 1 | 1 |
| Maximum Surge Current (10msec) [Adc] | 23 | 28 | 42 | 106 | 22 | 31 | 106 | 18 | 36 | 19 | 29 |
| Maximum On-State Voltage Drop @ Rated Current [Vdc] | 0.5 | 0.9 | 0.8 | 1 | 1.5 | 0.7 | 0.8 | 2.3 | 2.6 | 3.5 | 3.3 |
| Maximum On-State Resistance [RDS-ON] [Ohms] | 0.07 | 0.072 | 0.039 | 0.025 | 0.21 | 0.062 | 0.021 | 0.33 | 0.22 | 0.5 | 0.33 |
| Thermal Resistance Junction to Case [Rjc] [°C/W] | 2 | 2 | 1.71 | 0.68 | 1.24 | 0.71 | 0.22 | 0.56 | 0.39 | 0.6 | 0.43 |
| Minimum Heat Sink for Rated Current @ 40°C [°C/W] | 5 | 3 | 2 | 1 | 3 | 3 | 0.7 | 2 | 1 | 1 | 0.7 |
| Maximum Pulse Width Modulation Frequency [Hz] (5) | 5000 | 4000 | 3500 | 2500 | 3500 | 2000 | 950 | 1200 | 900 | 1100 | 900 |

INPUT SPECIFICATIONS ⁽²⁾

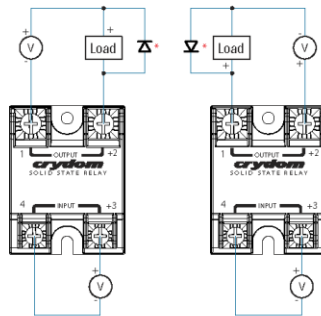
| Description | DC Control |
|--------------------------------------|-------------------|
| Control Voltage Range | 3.5-32 VDC |
| Maximum Reverse Voltage | -32 VDC |
| Minimum Turn-On Voltage (6) | 3.5 VDC |
| Must Turn-Off Voltage | 1 VDC |
| Minimum Input Current (for on-state) | 10 mA |
| Maximum Input Current | 15 mA |
| Nominal Input Impedance | Current Regulated |
| Maximum Turn-On Time [µsec] | 100 |
| Maximum Turn-Off Time [µsec] | 100 |

GENERAL SPECIFICATIONS ⁽²⁾

| Description | Parameters |
|--|--------------------------------|
| Dielectric Strength, Input/Output/Base (50/60Hz) | 3750 Vrms |
| Minimum Insulation Resistance (@ 500 VDC) | 10 ⁹ Ohms |
| Maximum Capacitance, Input/Output | 8 pF |
| Ambient Operating Temperature Range ⁽⁷⁾ | -40 to 100 °C |
| Ambient Storage Temperature Range | -40 to 125 °C |
| Weight (typical) | 2.66 oz (75.5 g) |
| Housing Material | UL94 V-0 |
| Baseplate Material | Aluminum |
| Input Terminal Screw Torque Range (in-lb/Nm) | 13-15 / 1.5-1.7 |
| Load Terminal Screw Torque Range (in-lb/Nm) | 18-20 / 2-2.2 |
| SSR Mounting Screw Torque Range (in-lb/Nm) | 18-20 / 2-2.2 |
| Input/Load Terminal Screw Torque Range (in-lb/Nm) ⁽¹⁾ | wt/"K" option 8-10 / 0.9-1.13 |
| Input/Output Terminal Screw Thread Size | #6-32 UNC / #8-32 UNC |
| Humidity per IEC60068-2-78 | 93% non-condensing |
| MTBF (Mean Time Between Failures) at 40°C ambient temperature ⁽⁸⁾ | 21,395,130 hours (2,441 years) |
| MTBF (Mean Time Between Failures) at 60°C ambient temperature ⁽⁸⁾ | 11,545,504 hours (1,317 years) |

WIRING DIAGRAM

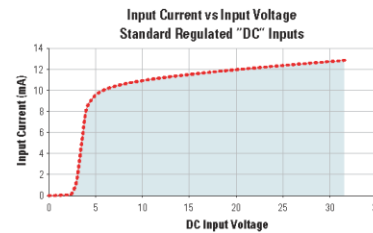
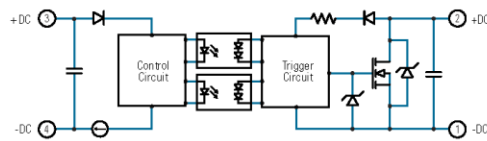
* Inductive loads must be diode suppressed.



Recommended Wire Sizes

| Terminals | Wire Size (Solid / Stranded) | Wire Pull-Out Strength (lbs [N]) |
|-----------|---|----------------------------------|
| Input | 24 AWG (0.2 mm ²) / 0.2 [minimum] | 10 [44.5] |
| | 2 x 12 AWG (3.3 mm ²) / 3.3 [maximum] | 90 [400] |
| Output | 20 AWG (0.5 mm ²) / 0.518 [minimum] | 30 [133] |
| | 2 x 10 AWG (5.3 mm ²) / 5.3 [maximum] | 110 [490] |
| | 2 x 8 AWG (8.4 mm ²) / 8.4 [maximum] | 90 [400] |

EQUIVALENT CIRCUIT BLOCK DIAGRAMS





Renewable Lubricants, Inc.

476 Griggy Rd., P.O. Box 474
Hartville, Ohio 44632-0474
Voice: 330.877.9982 Fax 330.877.2266
Web: www.renewablelube.com

Bio-MIL-PRF-32073 Hydraulic Fluid (ISO 15, 22, 32, 46, 68)



"Biobased Lubricants that Perform Like Synthetics"

Bio-MIL-PRF-32073 Hydraulic Fluids are ultimately biodegradable¹ biosynthetic (biobased) formulas that were designed to replace mineral oil based hydraulic fluids for environmentally sensitive areas. They have been specifically formulated to provide additional seal swell (10% to 30%) as required by MIL-PRF-32073 and ISO 15 or ISO 22 can replace obsolete specification MIL-PRF-5606 for ground support equipment. Bio-MIL-PRF-32073 Hydraulic Fluids are formulated to perform in hydraulic systems that require anti-wear, anti-foam, anti-rust, anti-oxidation, and demulsibility properties. They are highly inhibited against moisture and rusting in both fresh and sea water and pass both A and B Sequences of the ASTM D-665 Turbine Oil Rust Test. Incorporating the super high viscosity index of the Stabilized* High Oleic Base Stocks (HOBS) into the formula, gives multi-grade synthetic base oil performance by boosting the viscosity index to synthetic levels. This super high viscosity index of the HOBS naturally improves the thermal shear stability of the formula and increases load capacity. The HOBS's extremely low volatility increases the flash and fire safety features in the formula. An environmentally friendly, zinc-free additive system has also been developed that meets or exceeds high pressure pump requirements.

Bio-MIL-PRF-32073 Hydraulic Fluids have been used successfully in a wide variety of stationary and mobile hydraulic equipment. These patented super high VI fluids are designed for use in hydraulic vane, piston, and gear-type pumps. They also meet the requirements for ashless GL-1, GL-2, GL-3 and AGMA Non-EP gear oils in reduction units and gear sets where they meet the viscosity ranges. They have shown to have exceptional anti-wear performance in ASTM D-4172 Four Ball Wear Tests. **Very little wear was encountered in the field studies, and in accelerated pump tests using biobased formulations in Denison T-5D, Vickers 20VQ, 35VQ-25 (M-2950-S), and V-104C (ASTM D-2882), Vickers I-286-S pump stand tests.** Their anti-wear performance **exceeds the requirements** for US Steel 126, 136 and 127, load stage 10 in the FZG (DIN 51354).

Bio-MIL-PRF-32073 Hydraulic Fluids meet the Environmental Protection Agency (EPA) 2013 Vessel General Permit (VGP) guidelines for Environmentally Acceptable Lubricants (EALs), and should be used in hydraulic systems where **LOW TOXICITY, BIODEGRADABILITY** and **NON-BIOACCUMULATION** properties are required. They exceed the acute toxicity (LC-50 / EC-50 >1000 ppm) criteria adopted by the US Fish and Wildlife Service and the US EPA. Because they meet the environmental requirements they can also be used where ISO 15380 (HEES/HETG) Hydraulic Fluids are specified.

Bio-MIL-PRF-32073 Hydraulic Fluids are **ENVIRONMENTALLY ACCEPTED LUBRICANTS (EALs)** that are formulated from renewable biobased resources. We believe Earth's environmental future rests in the use of renewable materials.

¹Ultimate Biodegradation (Pw1) within 28 days in ASTM D-5864 Aerobic Aquatic Biodegradation of Lubricants

STABILIZED by Renewable Lubricants™ is RLI's trademark on their proprietary and patented anti-oxidant, anti-wear, and cold flow technology. High Oleic Base Stock (HOBS) are agricultural vegetable oils. This Stabilized technology allows the HOBS to perform as a high performance formula in high and low temperature applications, reducing oil thickening and deposits.

Patented Product: US Patent 6,383,992, US Patent 6,534,454 with additional Pending and Foreign Patents
™ Trademark of Renewable Lubricants™, Inc. Copyright 1999 Renewable Lubricants, Inc.

Availability **F.O.B.: Hartville, Ohio, USA** **1 Gallon** **5 Gallon Pail** **Drum** **Totes** **Bulk**

Bio-MIL-PRF-32073 Hydraulic Fluid

The test data below shows that the Bio-MIL-PRF-32073 Hydraulic Fluids provide high performance in a wide variety of stationary and transportation equipment that operate in broad ranges of environmental conditions. In equipment operating outside, wear from poor cold temperature pumpability, surge loads, moisture, and dusty environments are more prominent. Bio-MIL-PRF-32073 Hydraulic Fluids are formulated to improve performance in equipment that requires excellent anti-wear, rapid water separation and cold temperature pumpability as low as -40°C. In addition, the products may be used in machine tool hydraulic systems where higher seal swell fluids are required because of previously used MIL-Spec hydraulic Fluids.

| TYPICAL SPECIFICATIONS (MIL-PRF-32073A) | ISO Grade Military Grade | ISO 15 1 | ISO 22 2 | ISO 32 3 | ISO 46 4 | ISO 68 5 |
|---|--------------------------------------|------------------------------|------------------------------|------------------------------|------------------------------|------------------------------|
| Viscosity @ 40°C, cSt | ASTM D-445 | 14.18 | 21.1 | 30.87 | 43.8 | 64.1 |
| Viscosity @ 100°C, cSt | ASTM D-445 | 3.81 | 5.0 | 6.9 | 9.87 | 12.5 |
| Viscosity @ -15°C, cSt | ASTM D-445 | 170 | 330 | 479 | 595 | 1160 |
| Viscosity @ -25°C, Brookfield | ASTM D-2983 | 314 cP | 646 cP | 970 cP | 1260 cP | 2610 cP |
| Viscosity @ -30°C Brookfield | ASTM D-2983 | 480 cP | 1020 cP | 1530 cP | 2040 cP | 4800 cP |
| Viscosity @ -35°C Brookfield | ASTM D-2983 | 750 cP | 1680 cP | 2490 cP | | |
| Viscosity @ -40°C Brookfield | ASTM D-2983 | 1250 cP | 2800 cP | 4250 cP | | |
| Viscosity Index | ASTM D-2270 | 172 | 175 | 189 | 201 | 198 |
| Pour Point | ASTM D-97 | -60°C | -52°C | -48°C | -39°C | -36°C |
| Flash Point (COC) | ASTM D-92 | 180°C | 205°C | 243°C | 252°C | 263°C |
| Foam Sequence I, II, III (10 min) | ASTM D-892 | <30/0 Foam | <30/0 Foam | <30/0 Foam | <30/0 Foam | <30/0 Foam |
| Galvanic Corrosion | FTM 791-5322 | Pass | Pass | Pass | Pass | Pass |
| Rust Prevention Distilled Water Syn. Sea Water | ASTM D-665 | Pass Pass | Pass Pass | Pass Pass | Pass Pass | Pass Pass |
| Copper Corrosion Strip 3hr @ 100°C | ASTM D-130 | 1A | 1A | 1A | 1A | 1A |
| Rotary Bomb Oxidation, (minutes) | ASTM D-2272 | 400 | 400 | 400 | 400 | 400 |
| Dielectric Strength (KV) (Avg) | ASTM D-877 | 50 | 45 | 45 | 45 | 45 |
| Oxidation Stability, Pressure Differential Scanning Calorimeter PDSC (minutes) | ASTM D-6186 Modified | 95.0 (155°C) 25.0 (180°C) | 95.0 (155°C) 25.0 (180°C) | 90.0 (155°C) 25.0 (180°C) | 90.0 (155°C) 25.0 (180°C) | 90.0 (155°C) 25.0 (180°C) |
| Neutralization Number mg KOH/g | ASTM D-974 | <0.4 | <0.4 | <0.4 | <0.4 | <0.4 |
| Seal Swell NBR-L, % (Avg.) Volume Change (%) | FTM-791-3603 | 20 | 20 | 13 | 13 | 13 |
| Filterability A-No Water (s) (Avg) B-2% Water (s) (Avg) | Denison TP 02100 HF-0 Requirement | 113 187 | 268 271 | 335 449 | 355 470 | 355 470 |
| Demulsibility, ML Oil/Water/Emulsion | ASTM D-1401 | 40/ 40/ 0 (<10 minutes) | 40/ 40/ 0 (<10 minutes) | 40/ 40/ 0 (<10 minutes) | 40/ 40/ 0 (<10 minutes) | 40/ 40/ 0 (<10 minutes) |
| 4-Ball Wear, 1h, 167°F, 1200 RPM, 40 kg | ASTM D-4172 | .30-.40 | .30-.40 | .30-.40 | .03-.40 | .30-.40 |
| FZG Test | DIN 51354 | 11 | 11 | 12 | 12 | 12 |
| <u>Biodegradation Classification</u> | ASTM D-5864 | Ultimate PW1 | Ultimate PW1 | Ultimate PW1 | Ultimate PW1 | Ultimate PW1 |
| <u>Environmentally Friendly</u> | ISO 15380 | yes | yes | yes | yes | yes |
| <u>USDA Biobased Tested</u> | New Carbon | yes | yes | yes | yes | yes |
| <u>Environmental Management System</u> | ISO 14001 | yes | yes | yes | yes | yes |
| <u>Ecotoxicity LC-50 / EC-50</u> | EPA 560/6-82-002, 003 | meets/exceeds | meets/exceeds | meets/exceeds | meets/exceeds | meets/exceeds |
| Product Item # | | 81140 | 81150 | 81160 | 81170 | 81180 |

Pressure valves type MV.., DMV.. and SV..

Pressure limiting valves, differential pressure regulators

Pressure p_{max} = 700 bar
Flow Q_{max} = 160 lpm

Additional versions

- Versions as assembly kit see D 7000 E/1
- Versions with component approval (TÜV inspected) see D 7000 TÜV



Type MV and MVS
MVCS



Type MVE



Type MVP



Type DMV
DMVN



Type SV and SVC

1. General

Pressure valves primarily influence the pressure in hydraulic installations (DIN ISO 1219-1). The types listed here are to complete following tasks:

The pressure relief valves are not suited for safeguarding pressure devices acc. to Pressure Equipment Directive 97/23/EC. There are also versions available featuring unit approvals, see D 7000 TÜV, D 7710 TÜV, D 6905 TÜV.

• Pressure limiting valve

Protection against exceeding the maximum pressures approved for the system (relief valve) or limiting the working pressures. All valves listed in this leaflet can be used for this purpose.

• Differential pressure regulator

Generation of a constant pressure difference between the inlet and outlet of the flow. Valves with a housing in steel or spheroidal casting can be used for this purpose (see list of types on sect. 3.1).

• Pressure limiting valve without damping

For special operating conditions, e.g. to prevent creeping pressure rises in sealed cylinder chambers during temperature rise or compulsory creeping piston movement because of externally induced forces. Very low difference between opening and reseal pressure.

2. Typical construction

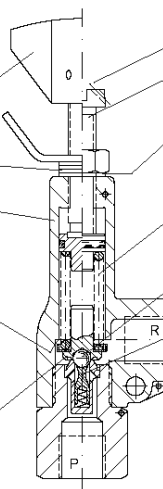
Means of adjustment with adjustable version
(Coding R = Wing screw
Coding V and H = Turn knob, see section 3.1)

Washer to limit the adjustment distance (see section 5)

Valve housing (spring dome) in zinc die casting, spheroidal casting or in steel for maximum adaption to local installation conditions (inline or manifold mounting, cartridge version)

Stroke limitation prevents the valve ball from being lifted out too far when the spring is completely relieved or when the flow through the valve is too high, also prevents the dampening plunger from blocking the flow passage.

Dynamically acting lift aid results in a pressure setting, which is rather flow independent (constant pressure characteristics)



Fixed design
Setting spindle
Setting limit to prevent spring blockage

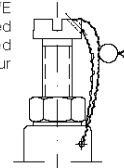
Valve spring depending on pressure range

Seated ball valve insensitive to contamination

Spring-loaded dampening plunger with a long guide ensures chatter free operation throughout a wide viscosity range
For undamped valves, see section 1.

The valve ball and dampening plunger are separate functional parts, which do not obstruct one another during dynamic stress (pressure peaks), thereby ensuring rapid response of the ball upon sudden pressure rise, the cushion plunger is missing in the undamped valve design

Lead seal provision (Lead sealing is available from HAWE when added in uncoded text to your order)



2.3

HAWE
HYDRAULIK

HAWE HYDRAULIK SE
STREITFELDSTR. 25 • 81673 MÜNCHEN

D 7000/1

© 1977 by HAWE Hydraulik

December 2013-00

3. Types available

3.1 Type code and main data

Order examples:

MVP 4 A - 650

MV 53 B R X

DMV 4 B/C

- 300/200
Desired pressure setting (bar) (without specification, see table 2)

X = Undamped version acc. to sect. 1

Table 1: Basic type and Size

| Brief description | Connection size and thread | | Spring dome material |
|--|----------------------------|-----------------|---|
| | Basic type Size | ISO 228/1 (BSP) | Port pressure rating |
| Pressure limiting valve | MV ⁵⁾ | 41 G 1/4 | Zinc die casting |
| | | 42 G 3/8 | |
| | | 52 G 3/8 | Perm. pressure P = 700 bar |
| | | 53 G 1/2 | R = 20 bar |
| | | 63 G 1/2 | see sect. 3.2 |
| | | 64 G 3/4 | |
| Pressure limiting valve and sequence valves | MVS ⁸⁾ | 41 G 1/4 | Spheroidal casting |
| | | 42 G 3/8 | |
| | | 52 G 3/8 | Perm. pressure P = 700 bar |
| | | 53 G 1/2 | R = 500 bar |
| | | 63 G 1/2 | see sect. 3.2 |
| | | 64 G 3/4 | |
| | MVE ¹⁰⁾ | 84 G 3/4 | Steel: Perm. pressure P and R = 400 bar |
| | | 85 G 1 | |
| | MVP ¹⁰⁾ | 4 | Stepped bore, see dimension. drawing |
| | | 5 | |
| | | 6 | |
| | | 8 | |
| Pressure limiting valve (as shock valve) | SV ¹⁾ | 42 G 3/8 | Steel: Perm. pressure P = 700 (400) bar |
| | | 53 G 1/2 | R = 500 (400) bar |
| | | 64 G 3/4 | |
| | | 85 G 1 | |
| | DMV ^{1) 3)} | 41 G 1/4 | |
| | | 42 G 3/8 | |
| | | 52 G 3/8 | Steel: Perm. pressure P and R = 350 bar |
| | | 53 G 1/2 | |
| | | 63 G 1/2 | |
| | DMVN ^{1) 3) 5)} | 64 G 3/4 | |
| | | 84 G 3/4 | |
| | | 85 G 1 | |
| | | 42 G 3/8 | Steel: Perm. pressure A, B = 350 bar |
| | | 53 G 1/2 | R = 20 bar |
| Pressure limiting valve with free return R → P via a by-pass check valve | MVT ^{1) 3) 5)} | 64 G 3/4 | Steel: Perm. pressure P and R = 315 bar |
| | | 63 G 1/2 | |
| | | 46 G 3/8 | |
| | | 56 G 1/2 | |
| | | 66 G 3/4 | |
| | MVCS ^{3) 5)} | 47 G 3/8 (A) | Spheroidal casting |
| | | 58 G 1/2 (A) | |
| | | 69 G 3/4 (A) | Perm. pressure P and R = 500 bar |
| | | 46 G 3/8 | |
| | | 56 G 1/2 | |
| Pressure limiting valve with free return R → P via a by-pass check valve | SVC ^{1) 3) 5)} | 66 G 3/4 | Steel: Perm. pressure P and R = 500 bar |
| | | 47 G 3/8 (A) | |
| | | 58 G 1/2 (A) | |
| | | 69 G 3/4 (A) | |
| | | 46 G 3/8 | |
| | MVCV ^{3) 5)} | 47 G 3/8 (A) | |
| | | 58 G 1/2 (A) | |
| | | 69 G 3/4 (A) | |
| | | 46 G 3/8 | |
| | | 56 G 1/2 | |

Table 3: Adjustment (during operation)

| Without coding | Standard, tool adjustable |
|---------------------|--|
| R | Manually adjustable (Wing screw+wing nut) |
| V ⁸⁾ 9) | Turn knob (self-locking) |
| H ⁹⁾ 10) | Turn knob lockable Keys conforming the regulations of the automotive industry; One key is scope of delivery (usually anyway in the possession of the authorized work staff) |

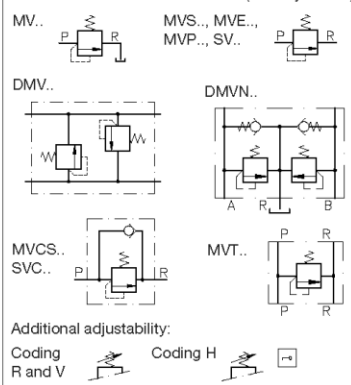
Table 2: Pressure range and flow

Attention: The pressure will be set acc. to the table below, if not ordered otherwise

| Pressure range | A ³⁾ | B | C | E | F |
|---|-----------------|--------|-----|-----|-----|
| (0) 4) ... | Size 700 | 500 | 315 | 160 | 80 |
| ... P _{max} (bar) | Size 4, 5, 6 | | | | |
| Size 8 | 700 | 400 9) | 315 | 160 | --- |
| Pressure setting from HAWC (bar) 2) | 450 | 400 | 315 | 160 | 80 |
| Corresponding flow Q _{max} (lpm) | Size 4 | 12 | | 20 | |
| | Size 5 | 20 | | 40 | |
| | Size 6 | 40 | | 75 | |
| | Size 8 | 100 | | 160 | |

Symbols

Illustration of the standard version (tool adjustable)



- 1) Tool adjustable version only
- 2) When not specified in the order
- 3) Pressure range coding A not avail. for type DMV, DMVN, MVT, MVCS, and SVC
- 4) A setting below 0.2 P_{max} is not effective. The min. pressure that can be achieved, when the spring is completely decompressed depends on the valve related back pressure and the flow (sect. 3.2)
- 5) Not available as size 8
- 6) Suction valves serve for the volume compensation, preventing the formation of a vacuum within hydraulic cylinders
- 7) Coding V not available for type MVS 4
- 8) Pressure range B not available for type SV 85
- 9) Coding H not available for type MVE 4 and MVP 4

Check valve type B

Pressure p_{max} = 500 bar
Flow Q_{max} = 160 lpm



1. General

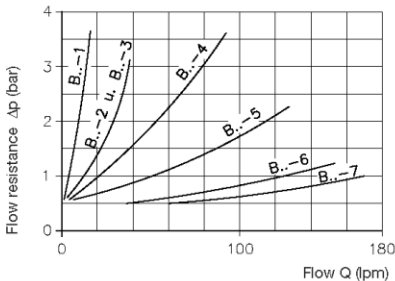
Check valves block the flow in one direction whilst permitting free flow in the opposite direction (DIN ISO 1219-1).

2. Available versions, main data

| | | | | Pressure p_{max} (bar) | Flow Q_{max} (lpm) |
|----------------------------|---------|---------|---------|--------------------------------|----------------------------|
| Coding and main data | B 1 - 1 | B 2 - 1 | B 3 - 1 | 500 | 15 |
| | B 1 - 2 | B 2 - 2 | B 3 - 2 | | 20 |
| | B 1 - 3 | B 2 - 3 | B 3 - 3 | | 30 |
| | B 1 - 4 | B 2 - 4 | B 3 - 4 | | 45 |
| | B 1 - 5 | B 2 - 5 | B 3 - 5 | | 75 |
| | B 1 - 6 | B 2 - 6 | B 3 - 6 | | 120 |
| | B 1 - 7 | B 2 - 7 | B 3 - 7 | | 160 |

| | |
|--------------------|--|
| Design | Spring-loaded, leakage free ball seated valve |
| Mounting | Type B 1 and B 3 with tapped journal, type B 2 is for in-line installation |
| Installed position | Arbitrarily |
| Mass (weight) | See unit dimensions in sect. 3 |
| Pressure fluid | Hydraulic oil conforming DIN 51 514 part 1 to 3: ISO VG 10 to 68 conforming DIN 51 519. Viscosity limits: min. approx. 4, max. approx. 1500 mm ² /s; optimal operation approx. 10 ... 500 mm ² /s. Also suitable are biologically degradable pressure fluids types HEPG (Polyalkylenglycol) and HEES (Synth. Ester) at service temperatures up to approx. +70 °C. |
| Temperature | Ambient: approx. -40 ... +80°C Fluid: -25 ... +80°C, note viscosity range Permissible temperature during start: -40°C (Note Start-viscosity!), as long as the service temperature is at least 20K higher for the following operation. Biological degradable pressure fluids: Note manufacturers information. Due the seals compatibility not above +70°C. |
| Opening pressure | approx. 0.4 to 0.5 bar B 2-2 and B 3-2 also available with an opening pressure of 3 bar (order coding e.g. B 2-2 - 3 bar) |

Δp -Q-Characteristic



Oil viscosity during measurement
approx. 30 mm²/s

2.5

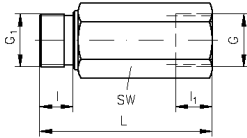
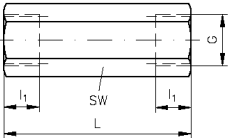
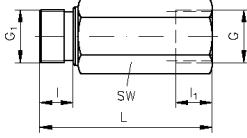


HAWES HYDRAULIK SE
STREITFELDSTR. 25 • 81673 MÜNCHEN

D 1191
Check valve type B

3. Unit dimensions

SW = a/f

| | | Ports DIN ISO 228/1 (BSPP) | | | | | | Mass (weight) approx. (kg) |
|---|-------|-------------------------------|----------------|-----|----|----------------|----|----------------------------------|
| Type | | G | G ₁ | L | l | l ₁ | SW | |
|  | B 1-1 | G 1/4 | G 1/4 A | 50 | 12 | 12 | 19 | 0.1 |
| | B 1-2 | G 3/8 | G 3/8 A | 58 | 12 | 13 | 24 | 0.2 |
| | B 1-3 | G 1/2 | G 1/2 A | 60 | 12 | 16 | 27 | 0.2 |
| | B 1-4 | G 3/4 | G 3/4 A | 70 | 16 | 16 | 36 | 0.4 |
| | B 1-5 | G 1 | G 1 A | 94 | 18 | 20 | 41 | 0.7 |
| | B 1-6 | G 1 1/4 | G 1 1/4 A | 110 | 20 | 23 | 55 | 1.3 |
| | B 1-7 | G 1 1/2 | G 1 1/2 A | 115 | 22 | 25 | 60 | 1.5 |
|  | B 2-1 | G 1/4 | -- | 55 | -- | 12 | 19 | 0.1 |
| | B 2-2 | G 3/8 | -- | 62 | -- | 12 | 24 | 0.2 |
| | B 2-3 | G 1/2 | -- | 70 | -- | 16 | 27 | 0.2 |
| | B 2-4 | G 3/4 | -- | 77 | -- | 16 | 36 | 0.4 |
| | B 2-5 | G 1 | -- | 102 | -- | 20 | 41 | 0.7 |
| | B 2-6 | G 1 1/4 | -- | 120 | -- | 23 | 55 | 1.5 |
| | B 2-7 | G 1 1/2 | -- | 122 | -- | 24 | 60 | 1.8 |
|  | B 3-1 | G 1/4 | G 1/4 A | 60 | 12 | 12 | 19 | 0.1 |
| | B 3-2 | G 3/8 | G 3/8 A | 67 | 12 | 13 | 24 | 0.2 |
| | B 3-3 | G 1/2 | G 1/2 A | 66 | 12 | 14 | 27 | 0.2 |
| | B 3-4 | G 3/4 | G 3/4 A | 58 | 16 | 16 | 36 | 0.3 |
| | B 3-5 | G 1 | G 1 A | 114 | 18 | 21 | 41 | 0.8 |
| | B 3-6 | G 1 1/4 | G 1 1/4 A | 130 | 20 | 23 | 55 | 1.7 |
| | B 3-7 | G 1 1/2 | G 1 1/2 A | 136 | 22 | 25 | 60 | 2.0 |

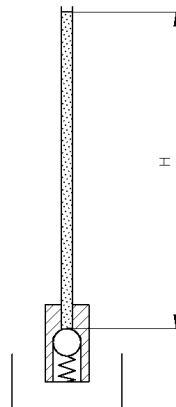
All dimensions in mm, subject to change without notice !

4. Note for installation

Check valves at return pipe ends

If the check valves are installed as final elements in return pipes, e.g. to prevent running empty of the pipes, they are capable of maintaining a head of oil $H \approx 4$ meter.

However, bearing in mind the tolerances on the spring preload, only about 75% of this load should be assumed in calculations.



Directional seated valves

Directly actuated, leakagefree for hydraulic systems

For the assembly on connection sub-plates

Valve for sub-plate mounting
Valve with individual connection sub-plate
Directional valve bank

Section 3
Section 5
D 7302

Pressure p_{\max} = 350...500 (700) bar
Flow Q_{\max} = 6...120 lpm

1. General information

Directional control valves are generally used for the direct, leakage free control of consumers and as pilot valves for hydraulically actuated valves (depending on the flow pattern). They are designed as spring returned ball seated valves. The valve elements are forced into their respective switching position against the spring force and fluid pressure by various actuation elements via an elbow lever acting on a pin. A strainer insert in the inlet port prevents the entry of coarse contamination.

The fluid ducts end as holes with O-ring seals at the ground, bottom surface of the valve body. Pipes may be connected either via customer furnished connection blocks or sub-plates (for individual valves with sub-plates see sect. 5 or for valve banks see D 7302).

These valves do not show any leakage in blocked switching position. Reliable shifting is ensured, as these valves are designed as ball seated valves where there is no seizing or sticking in working position under full pressure. The leverage between actuation and valve element ensures low actuation forces and smooth shifting. To avoid interaction, most of these directional control valves are available with check valve inserts and return pressure stops or orifice inserts to limit the inflow of oil.

Individual valves with sub-plate, enabling direct pipe connection, may be equipped with a by-pass check valve, a pressure limiting valve, or a rectifier circuit by means of check valves.

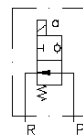
2. Overview

(For complete type overview, see sect. 8)

Individual valve for manifold mounting

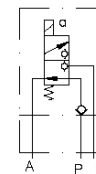
Individual valve with connection sub-plate for direct pipe connection

e.g. GS 2-1-G 24



Solenoid actuated
2/2-way directional
seated valve, size
1, free flow when
deenergized

e.g. GZ 3-2R-3/8-G 24



Solenoid actuated 3/2-way
directional seated valve, size
2 with check valve insert in
port P

Tapped ports in the
connection sub-plate, G 3/8
(BSPF)

Actuation modes

For detailed data, see section 4++.

(Max. pressure rating depending on flow pattern and size, see sect. 3.1 table 2)

| Code letter | Solenoid | | Pressure | | Mechanical | | Manual | |
|--------------------|----------|----|-----------|-----------|------------|-----|--------|-----------|
| | G | WG | hydraulic | pneumatic | roller | pin | feeler | turn-knob |
| Picture and symbol | | | | | | | | |

HAWE
HYDRAULIK

HAWE HYDRAULIK SE
STREITFELDSTR. 25 • 81673 MÜNCHEN

D 7300
Directional seated valves

© 1980 by HAWE Hydraulik

May 2007-06

3. Individual valves, manifold mounting

3.1 Valve

Order example:

G R2 - 3 R - G 24

Solenoid actuation (acc. to sect. 4.1)

G = DC

WG = AC

For actuation modes H, P, K, T, F, D, see sect. 2 and 4.2 ++

(For individual valves with connection sub-plate for pipe connection, see sect. 5)

solenoid voltage (standard)

G 24 = 24 V DC; WG 230 = 230 V AC

see sect. 4.1

Additional element (see table 3)

Size and main data (see table 2)

Table 1: Flow pattern

| Coding | 2/2-way valve | | 3/2-way valve | | 3/3-way valve | 4/3-way valve | 4/2-way valve | |
|--|------------------|------------------|-----------------|------------------|------------------|------------------|-----------------|------------------|
| | R2 ³⁾ | S2 ³⁾ | 3 ³⁾ | Z3 ³⁾ | 21 ³⁾ | 22 ¹⁾ | 4 ³⁾ | Z4 ³⁾ |
| Detailed symbols (must be completed by actuation symbol) | | | | | | | | |
| Simplified flow pattern symbol | | | | | | | | |

1) Not available for size 4! Note the arrangement of solenoids a and b in relation to the ports A and B, see dim. drawings sect. 3.3.3
 2) Only available for size 1
 3) Size 1 also available as explosion-proof version, see sect. 4.1.3

Table 2: Size, main data

| Coding | 0 | | 1 | | 2 | | 3 | | 4 | |
|---------------------------------|--------------------------------------|-----|-----|--------------------|-----|-------------------|-----|---------------|-----|---------------|
| Max. flow approx. lpm | 6 | | 12 | | 25 | | 65 | | 120 | |
| Directional valves (...-way) | 2/2; 3/2 | 3/3 | 4/3 | 2/2; 3/2; 3/3; 4/2 | 4/3 | 2/2; 3/2; 3/3 | 4/3 | 2/2; 3/2; 3/3 | 4/3 | 2/2; 3/2; 3/3 |
| Pressure p _{max} (bar) | Solenoid actuation Type G.. and WG.. | 500 | 350 | 500 ⁴⁾ | 350 | 500 ⁴⁾ | 350 | 400 | 350 | 350 |
| | Pressure actuation Type H.. | 500 | 500 | 700 | 500 | 500 | 500 | 400 | 400 | --- |
| | Pressure actuation Type P.. | --- | --- | 700 | 400 | 500 | 400 | 400 | 350 | --- |
| | Mechanical actuation Type K.. | --- | --- | 700 | 400 | 500 | 400 | 400 | 350 | --- |
| | Manual actuation Type F.. | --- | --- | 700 | 400 | 500 | 400 | 400 | 350 | --- |
| | Type D.. | 500 | --- | 700 | 400 | 500 | --- | --- | --- | --- |

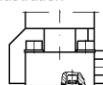
⁴⁾ For max. pressure during shifting, see sect. 4.1

Table 3: Additional elements to influence shifting operations, inserted in port P or R (can be retrofitted).

| Coding and symbol | Additional element | | Note |
|-------------------|--|---|--|
| | for size | Type | |
| | all | Insert check valves type ER acc. to D 7325 e.g. type ER 01 for valves size 0 | Not avail. for 3/3- and 4/3-way directional spool valves type ...21 and ...22 The check valve prevents an uncontrolled impact or reflow R→P or A→P, e.g. if the inlet pressure at P drops below the consumer pressure at A (during idle position or actuation of another consumer with a lower pressure requirement) when several valves are connected in parallel. A pressure reduction is prevented during such switching operations. |
| | all | size 0 = EB 0-0,6 1 = EB 1-0,8 2 = EB 2-1,2 3 = EB 3-2,5 4 = EB 4-4,0 Insert orifices type EB acc. to D 6465 | |
| | 0 | 7332 000 a | Only available for 3/2-way valves types ...3-.. or ...Z3-.. Check valves may be installed in the reflow ports R of 3/2-way valves size 0 and 1. With parallel shifting of several valves, they prevent pressure surges from migrating via the common reflow gallery into non-operated, easily moving and unloaded consumers if there is a connection A→R, thus preventing uncontrolled extension movements. Such pressure surges can be caused by shifting operations. These check valves are not intended for blocking off hydraulic oil, which depending on the combination of switching operations of other valves, can arise at port R. |
| | 1 | 7332 000 b | |
| | A combination with check valve or orifice in port P is possible e.g. G 3-1 BS-G 24, GZ 3-1 RS-G 24 | | |

Installation illustration

Check valve or orifice installed in port P



Return pressure stop installed in port R

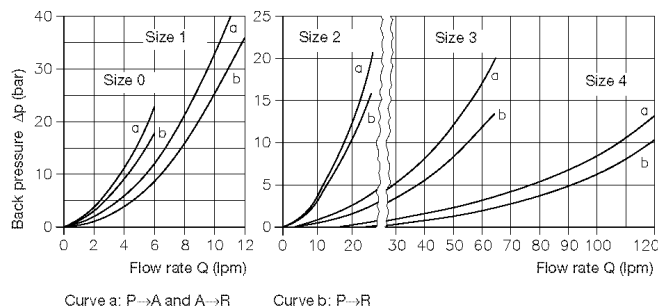


3.2 Further characteristic data

3.2.1 General and hydraulic parameters

| | | | | | | | |
|------------------------------------|---|-----------------------|---|---|----|----|----|
| Description | 2/2-, 3/2-, 3/3, 4/3- and 4/2-way valve | | | | | | |
| Design | Seated ball valve | | | | | | |
| Mounting type and leads connection | Manifold mounting | Size | 0 | 1 | 2 | 3 | 4 |
| | | corresp. to nom. size | 4 | 6 | 10 | 15 | 20 |
| Installation position | Any; Vertically with actuation up (best) | | | | | | |
| Direction of flow | Only in arrow direction acc. to flow pattern in sect. 3.1 The location of ports P (pump), R (return flow), A and B (consumers) are dictated by the internal design and can't be readily interchanged. | | | | | | |
| Overlap | Negative, i.e. the transition from shifting pos. 0 into a and vice versa is gradual, with 3/2-way valves all ports may be interconnected during this state. See also sect. 3.1 (table 3) „Additional orifice“ ! | | | | | | |
| Operation pressure | See sect. 3.1. All ports may be subject to the full oper. pressure, but a pressure drop must be maintained in flow direction acc. to the flow pattern in sect. 3.1, i.e. $P \geq A(B) \geq R$. With 4/3-way valves connection R must be employed as return flow only. For permissible pressure during switching operations, see sect. 4.1. | | | | | | |
| Static overload capacity | Approx. $2 \times p_{max}$, applies only to valves in idle position (p_{max} from table 2 sect. 3.1) | | | | | | |
| Flow rating | See sect. 3.1. Pay attention to the area ratio of double acting consumers (differential cylinders), i.e. the return might be higher than the inflow. | | | | | | |
| Pressure fluid | Hydraulic oil conforming DIN 51524 part 1 to 3; ISO VG 10 to 68 conforming DIN 51519 Viscosity limits: min. approx. 4, max. approx. 800 mm ² /s Optimal operation: Approx. 10 ... 200 mm ² /s Also suitable for biological degradable pressure fluids types HEPG (Polyalkylenglycol) and HEES (Synth. Ester) at service temperatures up to approx. +70 °C. For other fluids see sect. 6.2. | | | | | | |
| Temperature | Ambient: approx. -40...+80°C; Fluid: -25...+80°C, pay attention to the viscosity range! Start temperature down to -40°C are allowable (Pay attention to the viscosity range during start!), as long as the operation temperature during subsequent running is at least 20K higher. Biological degradable pressure fluids: Pay attention to manufacturer's information. With regard to the compatibility with sealing materials do not exceed +70°C. Restrictions for version with ex-proof solenoid! | | | | | | |

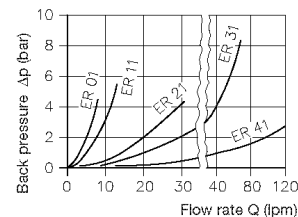
2/2- and 3/2-way valves



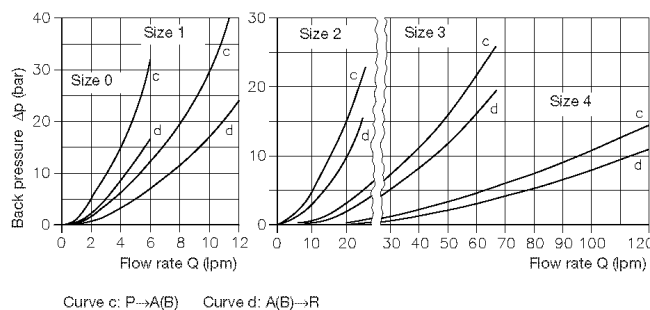
Additional elements

(the figures for Δp P→A(R) below are to be added !)

Check valve



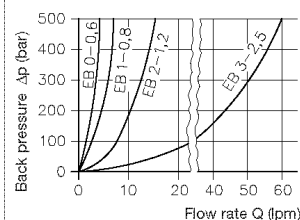
3/3-, 4/3- and 4/2-way valves



Δp-Q curves (guideline)

Oil viscosity during tests approx. 60 mm²/s

Orifice



1**Overview of releasable check valve type RH**

Check valves with hydraulic release are a type of check valve. They block one or both hydraulic consumer lines or are used as a hydraulically actuated drain or circulation valve.

In the closed state the check valve type RH has zero leakage. Available with hydraulic release. Hydraulic release suppresses relief surges that can occur at high pressure and with a large consumer volume.

Features and benefits:

- Pressures up to 700 bar
- with hydraulic release for smooth switching

Intended applications:

- Blocking of leak-free hydraulic cylinders



Releasable check valve type RH

2 Available versions, main data

Circuit symbol:



Order coding examples:

RH 3

Basic type and size Table 1 Basic type and size

Table 1 Basic type and size

| Basic type and size | | Pressure p_{max} (bar) | Flow rate Q_{max} (lpm) | Control volume (cm ³) | Ports ISO 228-1 (BSPP) | |
|---------------------------|------------------------|-----------------------------|------------------------------|--------------------------------------|------------------------|-------|
| Without hydraulic release | With hydraulic release | | | | A, B | Z |
| RH 1 | -- | 700 | 15 | 0.15 | G 1/4 | G 1/4 |
| RH 2 | -- | | 35 | 0.22 | G 3/8 | |
| RH 3 | RH 3 V | | 55 | 0.4 | G 1/2 | |
| RH 4 | RH 4 V | 500 | 100 | 1 | G 3/4 | |
| RH 5 | RH 5 V | | 160 | 1.8 | G 1 | |

3 Parameters

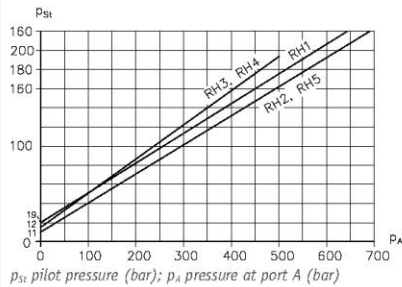
General information

| | |
|-----------------------|---|
| Designation | Releasable check valve |
| Design | Spring-loaded ball seated valve, zero-leakage |
| Model | Pipe connection |
| Material | Balls made of rolling bearing steel Steel; electro-galvanised valve housing; hardened and ground functional inner parts |
| Attachment | Freely suspended in the pipe |
| Installation position | As desired |
| Hydraulic fluid | Hydraulic oil: according to Part 1 to 3; ISO VG 10 to 68 according to DIN ISO 3448 Viscosity limits: min. approx. 4, max. approx. 1500 mm ² /s opt. operation approx. 10... 500 mm ² /s. Also suitable for biologically degradable hydraulic fluids type HEPG (polyalkylene glycol) and HEES (synthetic ester) at operating temperatures up to approx. +70°C. |
| Cleanliness level | ISO 4406 <hr/> 21/18/15...19/17/13 |
| Temperatures | Ambient: approx. -40 ... +80°C, Fluid: -25 ... +80°C, Note the viscosity range! Permissible temperature during start: -40°C (observe start-viscosity!), as long as the service temperature is at least 20K higher for the following operation. Biologically degradable pressure fluids: Observe manufacturer's specifications. By consideration of the compatibility with seal material not over +70°C. |

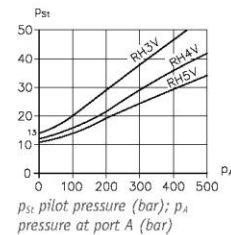
Characteristics

Oil viscosity approx. 60 mm²/s

To release ($p_B = 0$ bar)



To release the hydraulic release



To keep open:

$$p_{St} = p_B + \Delta p + k$$

p_B (bar) = pressure on B side

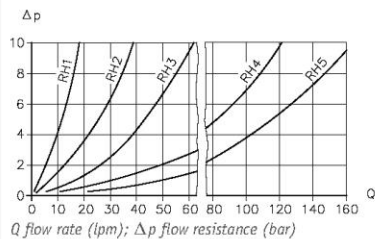
Δp (bar) = Flow resistance A → B according to Δp -Q characteristics

k = 10 bar for RH 1 and RH 2
7 bar for RH 3(V)
8 bar for RH 4(V) and RH 5(V)

Δp -Q characteristics

Valid for flow direction B → A and released direction A → B

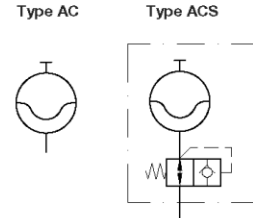
Opening pressure B → A 0.2 to 0.3 bar



At viscosities above approx. 500 mm²/s, a larger Δp - increase is to be expected with smaller types (RH 1 to RH 3).

Miniature hydraulic accumulators type AC for mounting in tapped ports

Operating pressure p_{max} = 500 bar
Rated volume V_0 = 13 or 40 cm³
Gas filling pressure $p_{0 max}$ = 250 bar



1. General information

The miniature accumulator described here are excepted from the pressure equipment regulation 97/23/EC section 3 (1) 1.1.a and 1.1.b. The pressure limiting valve used for the hydraulic system is sufficient for safe-guarding the permitted pressure level (i.e. the accumulator itself does not require a separate, specially homologated and approved safety valve). Whenever the accumulator is utilized in a section of the hydraulic system exposed to excessive pressure during operation (or in the event of a false setting), and such pressure peak possibly exceeding max pressure p_4 , a simple pressure limitation valve set to this or slightly below p_4 should be provided for this section only.

It is recommended to add a note to the operation manual for the system, which informs the operator to drain all pressure from the system prior to any service/repair on the hydraulic system (DIN 24 346, paragr. 7.4.7); see also sect. 6.

Application

- The miniature accumulators type AC may be used for compensation possible leakage loss in small systems operated in switch-off mode e.g. clamping circuits (prolongation of the off-periods when controlled by pressure switches), or as a source supplying compressed oil in an emergency when the oil supply pump fails to operate. Preference should be given to the AC 40 type in view of the reservoir volume available.
- AC miniature accumulator may also be used to support the switch-over process with fully hydraulic, pressure-controlled idle circulation valves (see D 7529, sect. 5.1).
- A further application of the miniature accumulators type AC is to compensate for changes in volume in specific oil cavities caused by fluctuations in ambient temperature (eg. long-term tests with small, static presses).
- A accumulator may serve furthermore to influence and increase the inherent of pressure scales or other components actuated by a difference in pressure. This makes it possible to avoid or quickly overcome excessive fluctuations in compensating for low-frequency vibration or yaw movements of hydromechanical components, such as crane booms, hydraulic motors on long pipelines, etc.

2. Available versions, type codings

Example:

AC 13 - 1/4 - 50 - ...

Optional extensions (also see section 4.1)
Order code: K 1/4 = Short version,
L 1/4 = Long version

| Basic type, rated volume and type of connection | Rated volume V ₀ (cm ³) | Gas filling pressure p _{0 max} (bar) | Perm. over-press. p _{4 max} (bar) | Highest perm. operating pressure ratio p _{2 max} : p _{1 max} isotherm adiabat | | Mass (weight) (kg) | Adjustm. range for closing valve from ... to (bar) |
|---|--|---|--|---|-----|-----------------------|--|
| AC 13 - 1/4 - ... | 13 | 250 | 500 | 4:1 | 3:1 | 0.3 | --- |
| ACS 13 - 1/4 - .../... ¹⁾ | 13 | 250 | 500 | 4:1 | 3:1 | 0.3 | 20 ... 100 or 80 ... 200 or 180 ... 300 |
| AC 40 - 1/4 - ... | 40 | 250 | 400 | 4:1 | 3:1 | 0.65 | --- |

¹⁾ The version with the closing valve is used when pressures of $p_{oil 2}$ which are greater than $4 p_0$ occur in the hydraulic circuit.
Example: One accumulator is intended to dampen in the low pressure range (low gas preloading) and another one is intended to dampen in the higher pressure range (high gas preloading). Type ACS 13 is selected for the accumulator operating in the lower pressure range and the closing valve is set to a closing pressure $\leq 4 p_0$, under adiabatic stress (constant load change) $\leq 3 p_0$.

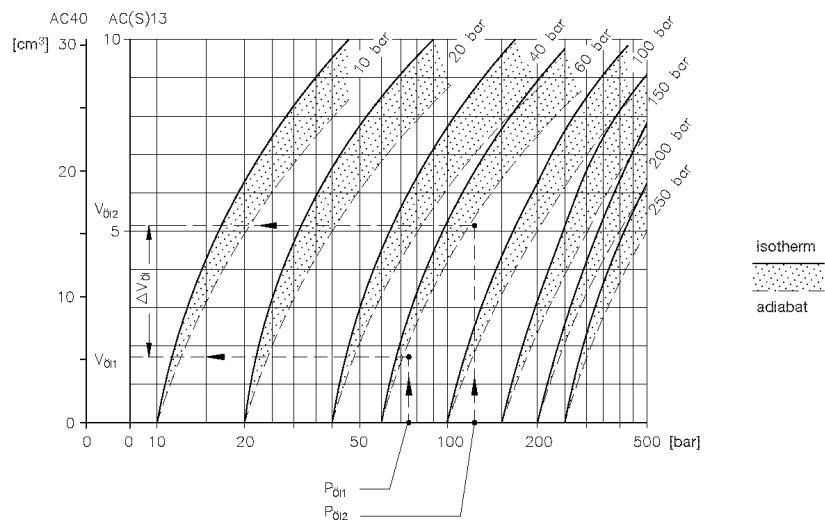


HAWE HYDRAULIK SE
STREITFELDSTR. 25 • 81673 MÜNCHEN

D 7571
Miniature hydraulic
accumulators AC

3. Additional characteristic data

| | |
|-----------------------|--|
| Nomenclature | Miniature diaphragm accumulator (ball accumulator) |
| Installation position | Any |
| Mounting | G 1/4 A ISO 228/1 (BSPP) tapped journal with sealing lip; max. torque approx. 39 Nm |
| Ambient temperature | -20 ... +60°C |
| Bursting pressure | approx. 4x max. permissible overpressure p_4 |
| Pressure fluid | Hydraulic oil conforming DIN 51524 part 1 to 3: ISO VG 10 to 68 conforming DIN 51519. Viscosity limits: min. approx. 4, max. approx. 1500 mm ² /sec; opt. operation approx. 10 ... 500 mm ² /sec |
| Operating pressure | Also see selection table, Page 1 p_0 (bar) gas filling pressure (desired), stamped on accumulator housing $p_{0 \max} = 250 \text{ bar}$; $p_{0 \min} = 5 \text{ bar}$ $p_{oil \ 1}$ (bar) lower operating pressure (oil side), $p_{oil \ 1 \ min} = 1.1 p_0$ $p_{oil \ 2}$ (bar) upper operating pressure (oil side), $p_{oil \ 2 \ max} = 4 p_0$ (isothermal), $= 3 p_0$ (adiabatic) |
| Filler gas | Nitrogen, class 4.0 |
| Refill possibility | Aparent, necessary filling fixture on request (section 5) |
| Δp -Q-curves | |

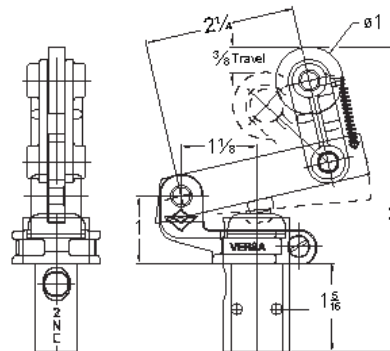


The characteristic represents theoretical recommended limit values only. The available removal volume calculated from the two operating points $p_{oil \ 2}$ and $p_{oil \ 1}$ at a given gas filling pressure p_0 is $\Delta V_{oil} = V_{oil \ 2} - V_{oil \ 1}$. Largely isothermal behavior can be expected when used for oil leakage compensation. More rapid load changes follow the adiabatic characteristic more closely.

TRIP-CAM LEVER



BCK-3208-35 Shown



Bracket and Trip-Cam Lever is sub-assembly BA-3200-40-35.

Actuated by cam travel in one direction only. Overriding device prevents actuation on return stroke. Cam follower is hardened.

| Trip-Cam Lever | Normally Closed | Normally Open |
|----------------|-----------------|---------------|
| TWO WAY | BCK-2208-35 | BCK-2206-35 |
| THREE WAY | BCK-3208-35 | BCK-3206-35 |

Suffix Options:

- 67 Stainless steel button
- 68 Mtg. holes clear #10 screw
- 155 Fluorocarbon seals
- 167 Body, brass internals, bracket and aluminum and aluminum button electroless nickel plated.
- S Strong spring for applications with marginal lubrication.

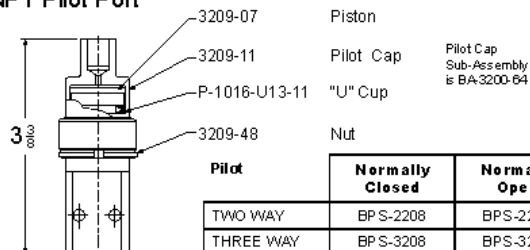
PILOT



BPS-2208 Shown



1/8 NPT Pilot Port



| Pilot | Normally Closed | Normally Open |
|-----------|-----------------|---------------|
| TWO WAY | BPS-2208 | BPS-2206 |
| THREE WAY | BPS-3208 | BPS-3206 |

| Minimum Pilot Pressure required for Actuation (PSI) | 18 | 20 | 22 | 24 | 26 | 28 | 30 | 32 | 34 | 36 |
|---|------|----|----|----|-----|-----|-----|-----|-----|-----|
| If Inlet Pressure (PSI) is: | 0-20 | 40 | 60 | 80 | 100 | 120 | 140 | 160 | 180 | 200 |

Suffix Options:

- 67 Brass and stainless steel internals
- 68 Mtg. holes clear #10 screw
- 155 Fluorocarbon seals
- 167 Body, brass internals, pilot cap are electroless nickel plated.
- S Strong spring for applications with marginal lubrication. Increases pilot pressure by 45%.





Cylinders

Threaded

Single and Double Acting

- Easy to use, basic hydraulic cylinders in SAE 4 ported designs.
- Designed for long life in high production applications.
- Reduce or eliminate part distortion by providing accurate, repeatable clamping force.
- Double Acting cylinders assure complete powered retraction for CNC controlled operations (where time is critical) or when using heavy end effectors. Single acting cylinders should be used with small end effectors only and where retraction speed is not critical.
- Coaxial spring design adds long life to Single Acting units.

Hardened chrome alloy steel pistons won't "mushroom" even when used without gripes.

Springs are designed to return the cylinder and contact points, not intended to pull mechanisms.



F-4

| Model No. | Cylinder Capacity (lb.)** | | Stroke (in.) | Body Thread | Minimum Length | Effective Piston Area (sq. in.) | | Oil Capacity (cu. in.) | |
|---------------------|---------------------------|---------|--|-------------|----------------|---------------------------------|---------|------------------------|---------|
| | Extend | Retract | | | | Extend | Retract | Extend | Retract |
| Single Acting (S/A) | | | Cylinders, actuated hydraulically 1 direction, spring returned | | | | | | |
| 20-0110-00 | | | 0.50 | | 2.68 | | | 0.393 | |
| 20-0110-01 | 3900 | N/A | 1.00 | 1 5/16-16 | 3.18 | 0.785 | N/A | 0.785 | N/A |
| 20-0110-04 | | | 1.50 | | 3.80 | | | 1.177 | |
| 20-0110-02 | | | 2.00 | | 4.30 | | | 1.570 | |
| 20-0115-00 | | | 0.50 | | 2.75 | | | 0.884 | |
| 20-0115-01 | 8800 | N/A | 1.00 | 1 7/8-16 | 3.25 | 1.767 | N/A | 1.767 | N/A |
| 20-0115-04 | | | 1.50 | | 3.75 | | | 2.650 | |
| 20-0115-02 | | | 2.00 | | 4.26 | | | 3.534 | |
| Double Acting (D/A) | | | Cylinders, actuated hydraulically both directions | | | | | | |
| 20-0210-00 | | | 0.50 | | 2.68 | | | 0.393 | 0.134 |
| 20-0210-01 | 3900 | 1300 | 1.00 | 1 7/8-16 | 3.18 | 0.785 | 0.267 | 0.785 | 0.267 |
| 20-0210-04 | | | 1.50 | | 3.80 | | | 1.177 | 0.400 |
| 20-0210-02 | | | 2.00 | | 4.30 | | | 1.570 | 0.534 |
| 20-0215-00 | | | 0.50 | | 2.75 | | | 0.884 | 0.386 |
| 20-0215-01 | 8800 | 3800 | 1.00 | 2 1/2-16 | 3.25 | 1.767 | 0.773 | 1.767 | 0.773 |
| 20-0215-04 | | | 1.50 | | 3.75 | | | 2.650 | 1.160 |
| 20-0215-02 | | | 2.00 | | 4.26 | | | 3.534 | 1.546 |

** Cylinder capacities are at 5,000 psi maximum operating pressure. The output force is adjustable by varying hydraulic system pressure. To determine the approximate output force for your application, multiply the piston area by your system operating pressure. (Actual force may vary slightly due to friction loss, seal and tapering, and/or air line springs.)

Dimensions at 3900 lb. Capacity, Extended

| Model No. | Extend Capacity (lb.) | A | B | C | D | E | F | G | H | J | K | L | M | N |
|---------------------|-----------------------|-----------|------|------|------|------|------|------|------|----------------|------|------|------|------|
| Single Acting (S/A) | | | | | | | | | | | | | | |
| 20-0110-00 | | | 2.68 | 0.50 | | 1.56 | | | | | | | | |
| 20-0110-01 | 3900 | 1 5/16-16 | 3.18 | 1.00 | | 2.06 | 0.32 | 0.81 | 0.68 | 5/16-18 X 0.44 | 0.28 | 1.22 | N/A | N/A |
| 20-0110-04 | | | 3.80 | 1.50 | 0.50 | 2.56 | | | | | | | | |
| 20-0110-02 | | | 4.30 | 2.00 | | 3.18 | | | | | | | | |
| Double Acting (D/A) | | | | | | | | | | | | | | |
| 20-0210-00 | | | 2.68 | 0.50 | | 1.56 | | | | | | | | |
| 20-0210-01 | 3900 | 1 7/8-16 | 3.18 | 1.00 | | 2.06 | 0.32 | 0.81 | 0.68 | 5/16-18 X 0.44 | 0.28 | 1.76 | 0.56 | 0.56 |
| 20-0210-04 | | | 3.80 | 1.50 | 0.50 | 2.56 | | | | | | | | |
| 20-0210-02 | | | 4.30 | 2.00 | | 3.18 | | | | | | | | |



© Vektex, September 2017

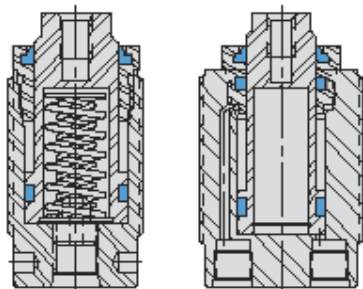
800-992-0236

www.vektek.com

Cylinders

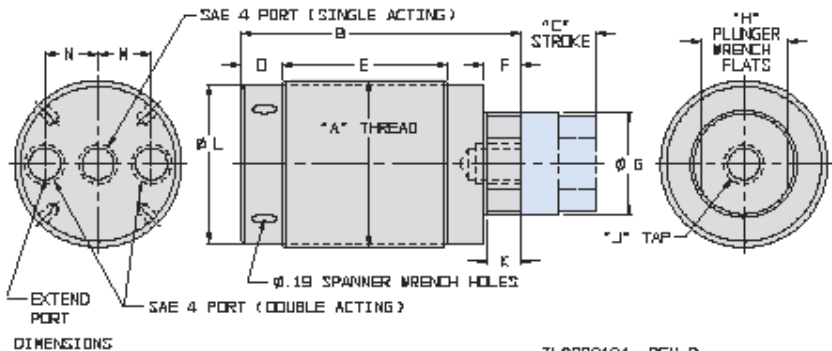


Threaded



ILS200103 REV B

F-5



ILS200104 REV D

Dimensions at 8800 lb. Capacity, Extended

| | Model No. | Extend Capacity (lb) | A | B | C | D | E | F | G | H | J | K | L | M | N |
|--|------------|----------------------|----------|------|------|------|---|------|------|------|---------------|------|------|------|------|
| | | | | | | | Cylinders, actuated hydraulically 1 direction, spring returned. | | | | | | | | |
| | 20-0115-00 | 8800 | 1 7/8-16 | 2.75 | 0.50 | 0.50 | 1.56 | 0.40 | 1.13 | 1.00 | 1/2-13 X 0.51 | 0.36 | 1.78 | N/A | N/A |
| | 20-0115-01 | | | 3.25 | 1.00 | | 2.06 | | | | | | | | |
| | 20-0115-04 | | | 3.75 | 1.50 | | 2.56 | | | | | | | | |
| | 20-0115-02 | | | 4.26 | 2.00 | | 3.06 | | | | | | | | |
| | | | | | | | Cylinders, actuated hydraulically both directions. | | | | | | | | |
| | 20-0215-00 | 8800 | 2 1/2-16 | 2.75 | 0.50 | 0.50 | 1.56 | 0.40 | 1.13 | 1.00 | 1/2-13 X 0.51 | 0.36 | 2.39 | 0.81 | 0.44 |
| | 20-0215-01 | | | 3.25 | 1.00 | | 2.06 | | | | | | | | |
| | 20-0215-04 | | | 3.75 | 1.50 | | 2.56 | | | | | | | | |
| | 20-0215-02 | | | 4.26 | 2.00 | | 3.06 | | | | | | | | |

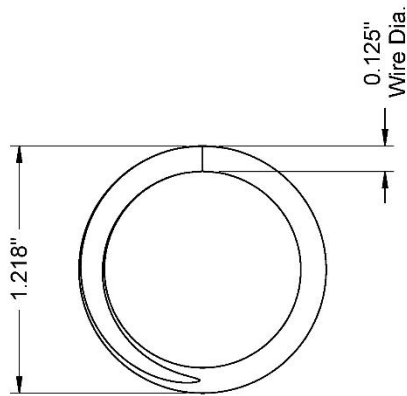
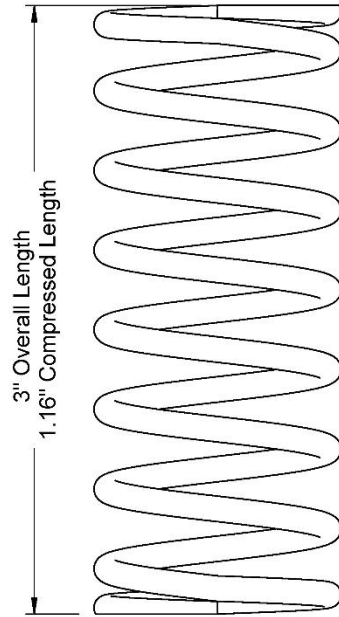
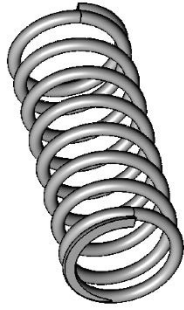
All dimensions are in inches. For mounting hardware details, see page L-1.



www.vektek.com

800-992-0236

© Vektex, September 2017



| | |
|--|--|
| McMASTER-CARR  | PART NUMBER 9657K445 |
| http://www.mcmaster.com © 2012 McMaster-Carr Supply Company <small>Information in this drawing is provided for reference only.</small> | Zinc-Plated Steel Music Wire Compression Spring |



FIK

Max Flow: 170 gpm (644 lpm)



FIK In-Tank Filters

Working Pressures to: 145 psi
1000 kPa
10 bar

Rated Static Burst to: 217 psi
1500 kPa
15 bar

Flow Range to: 170 gpm
644 lpm



Features

FIK in-tank filters are economical, space-saving units offering a variety of options including aluminum or plastic access covers, mounting options, and breathers. FIK filters, featuring a die-cast aluminum head and a steel or plastic canister are designed to handle heavy-duty applications. The head (and the inlet) sit above the tank, while the housing remains inside the tank, offering design-in flexibility. Optional air breather featuring T.R.A.P.[™] technology are available with style A and B, designed to allow the breather to be mounted directly in the FIK filter head, thus eliminating the cost associated with an additional penetration to the hydraulic tank for breather installation. FIK filters offer three service indicators to choose from: pressure gauge, visual indicator and electrical indicator. FIK filter assemblies are shipped from the factory with cellulose or Synteq[™] synthetic filter media, and replacement cartridges are offered in a range of media types and performance ratings.

Beta Rating

- Performance to $\beta_{(c)}=1000$

Porting Size Options

- 1/2", 3/4", 1" NPT
- SAE-8, SAE-12, SAE-16, SAE-20, SAE-24 O-ring
- 2" SAE 4-Bolt Flange Code 61

Standard Bypass Ratings

- 22 psi / 150 kPa / 1.5 bar

Operating Temperatures

- -4°F to 194°F / -20°C to 90°C

Collapse Ratings

- 145 psid / 1000 kPa / 10 bar

Redesigned with Features for Application Flexibility, Improved Servicing and Enhanced Filtration Performance

STYLE B Shown Below

Applications

- Cooling Circuits
- Fluid Conditioning Systems
- Lube Oil Systems
- Process Systems
- Return Lines
- Side Loop Systems

Multifunctional Ports (custom)

Contact your Donaldson sales representative for details

- Can be converted into auxiliary inlet ports
- The two secondary inlet ports can be used in conjunction with the main inlet port for higher flow rates

Flat Gasket Design

- For leak-tight operation

Service Indicator Ports

- Electrical, visual or pressure gauge options

T.R.A.P.™ Breather Technology

Breather ordered separately
Plug ships standard. Pressurized & atmospheric breathers available.

- Quick fit connection
- Anti-splash design allows smooth operation under tilt conditions
- Keeps reservoir free from condensation

Flexible Mounting Configurations

2 or 4 hole mounting option

- Better sealing and stability
- Enhanced stability on plastic tanks
- Reverse compatible – retrofit existing tanks with the new hole configuration

Built-In By-Pass Valve

- New by-pass valve installed with every filter replacement

Filter Media Technology

Wide range of Donaldson media offerings – to meet various performance targets and cleanliness standards


FIK

Max Flow: 170 gpm (644 lpm)



FIK Specification Illustrations

Low Flow Assemblies

< 32 gpm (120 lpm)

STYLE A
K030319

STYLE B
K040811
K040812
K040813
K041782


Improved Design Feature

- 2 or 4 hole mounting options
- Built-in by-pass valve in the cartridge
- Improved seal design
- Anti-splash air flow path
- Optional mini T.R.A.P. breather

Improved Design Feature

- 2 or 4 hole mounting options
- Built-in by-pass valve in the cartridge
- Improved seal design
- Anti-splash air flow path
- Optional mini T.R.A.P. breather
- Multifunctional ports for accessories

High Flow Assemblies

5 - 170 gpm (18 - 643 lpm)

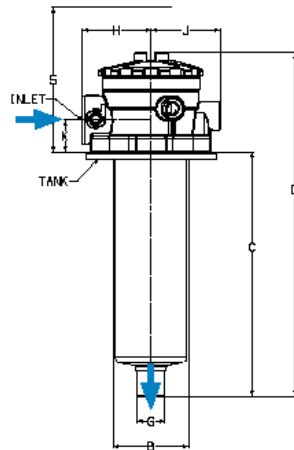
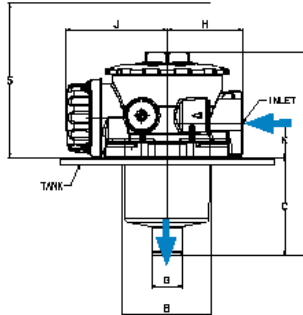
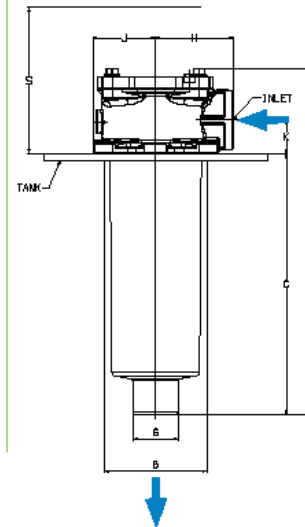
STYLE C, D, E

Assembly part numbers on following page

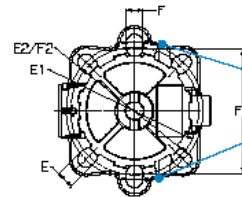
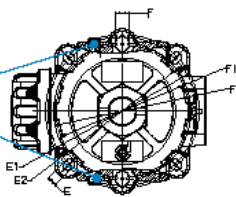
Improved Design Feature

- Improved seal design
- Built-in by-pass valve in the cartridge

Assembly - Side Views

STYLE A

STYLE B

STYLE C, D, E


Head - Top Views


Ports for
service
indicator


High Flow Assemblies

5 - 170 gpm (18 - 643 lpm)

STYLE C
K041770 K041774
K041771 K040799
K041772 K040798
K041773
K031027 (2 point mount only)

Improved Design Feature
• 2 or 4 hole mounting options



STYLE D
K070248 K070250
K071001 K071003
K070249 K071002

Design Feature
• 4 hole mounting



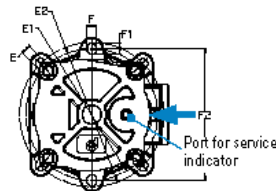
STYLE E
K051204
K052053

Design Feature
• 3 hole mounting

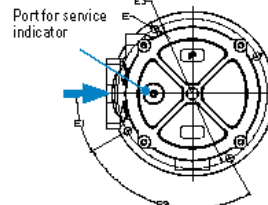


Head - Top Views

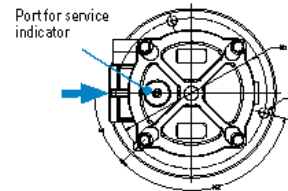
STYLE C



STYLE D



STYLE E



Dimensions

| ASSEMBLY DIMENSIONS | ASSEMBLY PART NUMBER | | | | | | | | | | | | | | | | | | | | | | | |
|---------------------|----------------------|---------|---------|---------|---------|---------|---------|---------|---------|---------|---------|---------|---------|---------|---------|---------|---------|---------|---------|---------|---------|-------|-------|-------|
| | STYLE A | | | | STYLE B | | | | STYLE C | | | | | | | | STYLE D | | | | STYLE E | | | |
| | K030819 | K040811 | K040812 | K040813 | K040813 | K041782 | K031027 | K041770 | K041771 | K041772 | K041773 | K041774 | K040799 | K070248 | K071001 | K070249 | K070250 | K071003 | K051204 | K052053 | | | | |
| C | 176.8 | 6.96 | 91.0 | 3.58 | 141.0 | 5.55 | 218.0 | 8.58 | 78.0 | 3.07 | 99.0 | 3.90 | 149.0 | 5.87 | 227.7 | 8.96 | 242.0 | 9.53 | 290.0 | 11.42 | 434.0 | 17.08 | 224.0 | 8.82 |
| D | 248.6 | 9.79 | 189.0 | 7.44 | 239.0 | 9.41 | 316.0 | 12.44 | 132.0 | 5.20 | 173.3 | 6.82 | 223.2 | 8.79 | 301.9 | 11.89 | 348.0 | 13.70 | 395.5 | 15.57 | 539.5 | 21.24 | 313.8 | 12.35 |
| S | 220.0 | 8.66 | 180.0 | 7.09 | 220.0 | 8.66 | 305.0 | 12.01 | 149.0 | 5.87 | 170.0 | 6.69 | 220.0 | 8.66 | 299.0 | 11.77 | 320.0 | 12.60 | 365.0 | 14.37 | 515.0 | 20.28 | 305.0 | 12.01 |
| G | 20.0 | 0.79 | 27.6 | 1.09 | 27.6 | 1.09 | 39.6 | 1.56 | 25.2 | 0.99 | 27.6 | 1.09 | 27.6 | 1.09 | 39.5 | 1.56 | 50.0 | 1.97 | 63.5 | 2.50 | 63.5 | 2.50 | 40.0 | 1.57 |
| B | 57.0 | 2.24 | 90.0 | 3.54 | 90.0 | 3.54 | 90.0 | 3.54 | 68.6 | 2.70 | 90.0 | 3.54 | 90.0 | 3.54 | 90.0 | 3.54 | 175.0 | 6.89 | 175.0 | 6.89 | 175.0 | 6.89 | 131.0 | 5.16 |
| H | 49.7 | 1.96 | 70.5 | 2.78 | 70.5 | 2.78 | 70.5 | 2.78 | 49.0 | 1.93 | 68.0 | 2.68 | 68.0 | 2.68 | 68.0 | 2.68 | 120.0 | 4.72 | 126.0 | 4.96 | 126.0 | 4.96 | 95.0 | 3.74 |
| J | 94.2 | 3.71 | 94.5 | 3.72 | 94.5 | 3.72 | 94.5 | 3.72 | 44.0 | 1.73 | 55.0 | 2.17 | 55.0 | 2.17 | 55.0 | 2.17 | 100.0 | 3.94 | 100.0 | 3.94 | 100.0 | 3.94 | 78.0 | 3.07 |
| K | 23.0 | 0.91 | 32.0 | 1.26 | 32.0 | 1.26 | 32.0 | 1.26 | 22.0 | 0.87 | 29.5 | 1.16 | 29.5 | 1.16 | 29.5 | 1.16 | 41.0 | 1.61 | 48.5 | 1.91 | 48.5 | 1.91 | 35.0 | 1.38 |
| F | 11.0 | 0.43 | 11.0 | 0.43 | 11.0 | 0.43 | 11.0 | 0.43 | 11.0 | 0.43 | 11.0 | 0.43 | 11.0 | 0.43 | 11.0 | 0.43 | 11.0 | 0.43 | 11.0 | 0.43 | 11.0 | 0.43 | 11.0 | 0.43 |
| F1 | Ø82 | Ø3.23 | Ø112 | Ø4.41 | Ø112 | Ø4.41 | Ø112 | Ø4.41 | Ø112 | Ø4.41 | Ø112 | Ø4.41 | Ø112 | Ø4.41 | Ø112 | Ø4.41 | Ø112 | Ø4.41 | Ø112 | Ø4.41 | Ø112 | Ø4.41 | Ø112 | Ø4.41 |
| F2 | Ø90 | Ø3.54 | Ø116 | Ø4.57 | Ø116 | Ø4.57 | Ø116 | Ø4.57 | Ø116 | Ø4.57 | Ø116 | Ø4.57 | Ø116 | Ø4.57 | Ø116 | Ø4.57 | Ø116 | Ø4.57 | Ø116 | Ø4.57 | Ø116 | Ø4.57 | Ø116 | Ø4.57 |
| N | N/A | N/A | N/A | N/A | N/A | N/A | N/A | N/A | N/A | N/A | N/A | N/A | N/A | N/A | N/A | N/A | N/A | N/A | N/A | N/A | N/A | N/A | N/A | N/A |
| N1 | N/A | N/A | N/A | N/A | N/A | N/A | N/A | N/A | N/A | N/A | N/A | N/A | N/A | N/A | N/A | N/A | N/A | N/A | N/A | N/A | N/A | N/A | N/A | N/A |
| N2 | N/A | N/A | N/A | N/A | N/A | N/A | N/A | N/A | N/A | N/A | N/A | N/A | N/A | N/A | N/A | N/A | N/A | N/A | N/A | N/A | N/A | N/A | N/A | N/A |
| N3 | N/A | N/A | N/A | N/A | N/A | N/A | N/A | N/A | N/A | N/A | N/A | N/A | N/A | N/A | N/A | N/A | N/A | N/A | N/A | N/A | N/A | N/A | N/A | N/A |
| E | 11.0 | 0.43 | 8.5 | 0.33 | 8.5 | 0.33 | 8.5 | 0.33 | 8.5 | 0.33 | 8.5 | 0.33 | 8.5 | 0.33 | 8.5 | 0.33 | 8.5 | 0.33 | 8.5 | 0.33 | 8.5 | 0.33 | 8.5 | 0.33 |
| E1 | Ø84 | Ø3.31 | Ø126 | Ø4.96 | Ø126 | Ø4.96 | Ø126 | Ø4.96 | Ø126 | Ø4.96 | Ø126 | Ø4.96 | Ø126 | Ø4.96 | Ø126 | Ø4.96 | Ø126 | Ø4.96 | Ø126 | Ø4.96 | Ø126 | Ø4.96 | Ø126 | Ø4.96 |
| E2 | Ø90 | Ø3.54 | Ø130 | Ø5.12 | Ø130 | Ø5.12 | Ø130 | Ø5.12 | Ø130 | Ø5.12 | Ø130 | Ø5.12 | Ø130 | Ø5.12 | Ø130 | Ø5.12 | Ø130 | Ø5.12 | Ø130 | Ø5.12 | Ø130 | Ø5.12 | Ø130 | Ø5.12 |
| E3 | N/A | N/A | N/A | N/A | N/A | N/A | N/A | N/A | N/A | N/A | N/A | N/A | N/A | N/A | N/A | N/A | N/A | N/A | N/A | N/A | N/A | N/A | N/A | N/A |
| WEIGHT | lbs | kg | lbs | kg | lbs | kg | lbs | kg | lbs | kg | lbs | kg | lbs | kg | lbs | kg | lbs | kg | lbs | kg | lbs | kg | lbs | kg |
| K | 1.8 | 0.8 | 2.1 | 0.95 | 3.2 | 1.45 | 4.1 | 1.86 | 1.1 | 0.5 | 1.8 | 0.8 | 2.1 | 0.95 | 2.43 | 1.1 | 10.0 | 4.5 | 13.1 | 5.9 | 18.6 | 8.4 | 7.0 | 3.2 |



FIK

Max Flow: 170 gpm (644 lpm)



FIK Components

Assembly Choices

| Port Size | Bypass Rating* | Assembly Part No. | R_{90} = 1000 | Filter Media† | Provided with Filter | Filter Diameter (in./mm) | Filter Length (in./mm) | Flow Range (@ ~5 psid / 34.5 kPa) |
|--|----------------|-------------------|--------------------|---------------|----------------------|--------------------------|------------------------|-----------------------------------|
| Additional filter choices on following pages to meet various performance requirements. | | | | | | | | |
| Low Flow Assemblies | | | | | | | | |
| STYLE A | | | | | | | | |
| SAE-8 O-Ring | 22 psi/1.5 bar | K030319 | 36 µm | Cellulose | P171839 | 1.69 / 43 | 6.38 / 162 | 10 gpm / 38 lpm |
| STYLE B | | | | | | | | |
| SAE-12 O-Ring | 22 psi/1.5 bar | K040811 | 36 µm | Cellulose | P171527 | 2.76 / 70 | 3.23 / 82 | 14 gpm / 53 lpm |
| SAE-16 O-Ring | 22 psi/1.5 bar | K040812 | 36 µm | Cellulose | P171533 | 2.76 / 70 | 5.04 / 128 | 23 gpm / 86 lpm |
| SAE-20 O-Ring | 22 psi/1.5 bar | K040813 | 36 µm | Cellulose | P171840 | 2.76 / 70 | 8.27 / 210 | 32 gpm / 120 lpm |
| SAE-20 O-Ring | 22 psi/1.5 bar | K041782 | 11 µm | Synthetic | P171846 | 2.76 / 70 | 8.27 / 210 | 28 gpm / 106 lpm |
| High Flow Assemblies | | | | | | | | |
| STYLE C | | | | | | | | |
| 1/2" NPT | 22 psi/1.5 bar | K031027 | 36 µm | Cellulose | P171503 | 2.05 / 52 | 2.64 / 67 | 5 gpm / 18 lpm |
| 1" NPT | 22 psi/1.5 bar | K041770 | 36 µm | Cellulose | P171527 | 2.76 / 70 | 3.23 / 82 | 15 gpm / 56 lpm |
| 3/4" NPT | 22 psi/1.5 bar | K041771 | 36 µm | Cellulose | P171533 | 2.76 / 70 | 5.04 / 128 | 18 gpm / 68 lpm |
| 1" NPT | 22 psi/1.5 bar | K041772 | 36 µm | Cellulose | P171533 | 2.76 / 70 | 5.04 / 128 | 21 gpm / 79 lpm |
| SAE-12 O-Ring | 22 psi/1.5 bar | K041773 | 36 µm | Cellulose | P171533 | 2.76 / 70 | 5.04 / 128 | 18 gpm / 68 lpm |
| SAE-12 O-Ring | 22 psi/1.5 bar | K041774 | 11 µm | Synteq | P171531 | 2.76 / 70 | 5.04 / 128 | 13 gpm / 49 lpm |
| SAE-16 O-Ring | 22 psi/1.5 bar | K040799 | 36 µm | Cellulose | P171533 | 2.76 / 70 | 5.04 / 128 | 21 gpm / 79 lpm |
| SAE-16 O-Ring | 22 psi/1.5 bar | K040798 | 36 µm | Cellulose | P171840 | 2.76 / 70 | 8.22 / 209 | 32 gpm / 120 lpm |
| STYLE D | | | | | | | | |
| SAE-24 O-Ring | 22 psi/1.5 bar | K070248 | 36 µm | Cellulose | P171557 | 5.51 / 140 | 7.49 / 203 | 66 gpm / 248 lpm |
| SAE-24 O-Ring | 22 psi/1.5 bar | K071001 | 11 µm | Synteq | P171555 | 5.51 / 140 | 7.49 / 203 | 44 gpm / 165 lpm |
| 2" SAE 4-Bolt | 22 psi/1.5 bar | K070249 | 36 µm | Cellulose | P171575 | 5.51 / 140 | 9.84 / 250 | 106 gpm / 399 lpm |
| 2" SAE 4-Bolt | 22 psi/1.5 bar | K071002 | 11 µm | Synteq | P171573 | 5.51 / 140 | 9.84 / 250 | 74 gpm / 278 lpm |
| 2" SAE 4-Bolt | 22 psi/1.5 bar | K070250 | 36 µm | Cellulose | P171581 | 5.51 / 140 | 15.75 / 400 | 170 gpm / 643 lpm |
| 2" SAE 4-Bolt | 22 psi/1.5 bar | K071003 | 11 µm | Synteq | P171579 | 5.51 / 140 | 15.75 / 400 | 120 gpm / 451 lpm |
| STYLE E | | | | | | | | |
| SAE-20 O-Ring | 22 psi/1.5 bar | K051204 | 36 µm | Cellulose | P171539 | 3.74 / 95 | 7.49 / 203 | 47 gpm / 177 lpm |
| SAE-20 O-Ring | 22 psi/1.5 bar | K052053 | 11 µm | Synteq | P171537 | 3.74 / 95 | 7.49 / 203 | 32 gpm / 120 lpm |

Note

*Bypass valve is an integral part of the replacement filter.
Service indicator port available for all assemblies.

Filter Notes





FIK filters utilize either glass fiber, cellulose, or wire mesh media.
All FIK filters are potted with polyurethane adhesives.
Synteq media designs are double wire-backed using epoxy-coated steel mesh for maximum pleat support and dirt capacity.
Buna-N® seals are standard on all FIK filters. Buna-N® is a registered trademark of E. I. DuPont de Nemours and Company.

T.R.A.P.™ Breather Choices



For Redesigned Style A and B Assemblies with 4 Hole Mounting Configurations Only

Note: T.R.A.P. breathers are not compatible on older style assemblies with 2 hole mounting configuration

| Part No. | Description | Efficiency | Fits Assembly Models: |
|---|--|-------------|------------------------------------|
| STYLE A | | | |
|  P967392 | Mini T.R.A.P. | 3 µm @ 97% | K030319 |
| STYLE B | | | |
|  P766528 | Black Standard plug (no air exchange) | N/A | K040811, K040812, K040813, K041782 |
|  P766530 | Blue Atmospheric pressure | 10 µm @ 98% | K040811, K040812, K040813, K041782 |
|  P766538 | Red 7.3 psi (½ bar) pressurized | 10 µm @ 98% | K040811, K040812, K040813, K041782 |



Standard Breather Choices

Replacement Breathers for Older Style A and B Assemblies with 2 Hole Mounting Configuration Only

| Part No. | Efficiency | Fits Assembly Models: |
|----------------|------------|---------------------------|
| STYLE A | | |
| P173330 | 10 µm | K030319 |
| STYLE B | | |
| P172434 | 10 µm | K040811, K040812, K040813 |



Service Indicators

Pressure Gauges
P171956
G 1/8"
(center back)



P171953
G 1/8"
(bottom mount)

-14.5 to 72 psi
-1 to +5 bar

DC Electrical Indicator
P171966
17 psi / 1.2 bar
(48V AC/DC)



G 1/8" →

Visual Indicator
P171958
17 psi / 1.2 bar



G 1/8" →



FIK

Max Flow: 170 gpm (644 lpm)



FIK Components

Filter Choices - Low Flow Assemblies

| Media | $\beta_{\text{req}} = 2$ | $\beta_{\text{req}} = 1000$ | Length | | Donaldson |
|------------------|---------------------------|-----------------------------|--------|---------|-----------|
| Type | Rating based on ISO 16889 | | in | mm | Part No. |
| STYLE A | | | | | |
| K030319 | | | | | |
| Synteq Synthetic | 6 μm | 6.38 | 162 | P569273 | |
| | 11 μm | 6.38 | 162 | P171845 | |
| | 23 μm | 6.38 | 162 | P171842 | |
| Cellulose | 7 μm | 6.38 | 162 | P171839 | |
| | 27 μm | 6.38 | 162 | P171836 | |
| Wire Mesh | 60 μm | 6.38 | 162 | P171833 | |
| | 90 μm | 6.38 | 162 | P171830 | |

Filter Choices - Low Flow Assemblies

| Media | $\beta_{\text{req}} = 2$ | $\beta_{\text{req}} = 1000$ | Length | | Donaldson |
|------------------|---------------------------|-----------------------------|--------|----|-----------|
| Type | Rating based on ISO 16889 | | in | mm | Part No. |
| STYLE B | | | | | |
| K040811 | | | | | |
| Synteq Synthetic | 11 μm | 3.23 | 82 | | P171525 |
| | 23 μm | 3.23 | 82 | | P171526 |
| Cellulose | 7 μm | 3.23 | 82 | | P171527 |
| | 27 μm | 3.23 | 82 | | P171528 |
| Wire Mesh | 60 μm | 3.23 | 82 | | P171529 |
| | 90 μm | 3.23 | 82 | | P171524 |
| K040812 | | | | | |
| Synteq Synthetic | 6 μm | 5.04 | 128 | | P569275 |
| | 11 μm | 5.04 | 128 | | P171531 |
| | 23 μm | 5.04 | 128 | | P171532 |
| Cellulose | 7 μm | 5.04 | 128 | | P171533 |
| | 27 μm | 5.04 | 128 | | P171534 |
| Wire Mesh | 60 μm | 5.04 | 128 | | P171535 |
| | 90 μm | 5.04 | 128 | | P171530 |
| K040813 | | | | | |
| Synteq Synthetic | 6 μm | 8.27 | 210 | | P569276 |
| | 11 μm | 8.27 | 210 | | P171846 |
| | 23 μm | 8.27 | 210 | | P171843 |
| Cellulose | 7 μm | 8.27 | 210 | | P171840 |
| | 27 μm | 8.27 | 210 | | P171837 |
| Wire Mesh | 60 μm | 8.27 | 210 | | P171834 |
| K041782 | | | | | |
| Synteq Synthetic | 6 μm | 8.27 | 210 | | P569276 |
| | 11 μm | 8.27 | 210 | | P171846 |
| | 23 μm | 8.27 | 210 | | P171843 |
| Cellulose | 7 μm | 8.27 | 210 | | P171840 |
| | 27 μm | 8.27 | 210 | | P171837 |
| Wire Mesh | 60 μm | 8.27 | 210 | | P171834 |



Protective Vents

SCREW-IN SERIES

Increase outdoor enclosure durability in harsh environments

VENTING FOR PROTECTION

Harsh or changing environmental conditions cause pressure changes that can stress outdoor enclosure seals to failure, allowing contaminants to enter and damage sensitive electronics.

GORE® Protective Vents effectively equalize pressure and reduce condensation in sealed enclosures, while keeping out solid and liquid contaminants. They can improve the safety, reliability and service life of outdoor electronic devices.

A VENTING PORTFOLIO FOR ANY APPLICATION




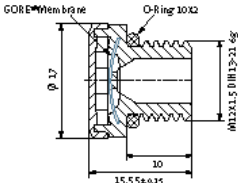
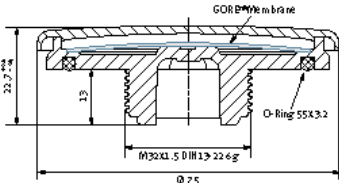
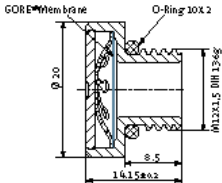
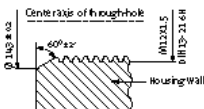

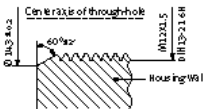





GORE® Vents Screw-In Series is engineered to provide oleophobic protection and withstand the mechanical stresses of rugged environments. Choose from a full range of sizes and performance options to meet all your application needs.

- GORE® PolyVent XS has a compact, low-profile design that meets some of the industry's toughest standards, making it ideal for today's smaller (up to 2 l) housings.
- GORE® PolyVent Standard offers reliable venting for volumes up to 5 l, and comes in two colors and two thread sizes for different wall thicknesses, with or without a counter nut.
- GORE® PolyVent High Airflow has the protection level of "Standard" – with nearly 10 times the airflow. For housings up to 50 l, it easily manages the strong pressure differentials caused by extreme weather.
- GORE® PolyVent XL maintains exceptionally high airflow in extra-large enclosures (volumes up to 200 l) and meets the most rigorous standards, such as solar resistance (IEC 62108).
- **NEW** GORE® PolyVent Stainless Steel offers premium-level durability, corrosion- and chemical resistance, to reliably protect enclosures up to 20 l in the most extreme conditions.



REALIZE THE BENEFITS OF GORE® VENTS SCREW-IN SERIES:

- **Easy to install:** ensures fast, foolproof integration for durable performance in any application.
- **Increased safety:** the rugged screw-in construction and improved O-ring keep the vent reliably secured in the housing.
- **Reliable protection:** even after immersion, the GORE™ Membrane blocks contaminant ingress.
- **Rugged durability:** engineered for chemical, UV and temperature resistance, and hydrolytic stability.
- **Product quality:** 100% quality control, plus full traceability for all vents with thread size M6 and M12.
- **Flammability resistance:** All PolyVent caps, bodies and O-rings are rated UL 94 V-0. PolyVent XS and Stainless Steel also incorporate a UL 94 VTM-0 rated membrane!

| | | | | |
|---|--|--|--|--|
|  |  |  | | |
| PolyVent High Airflow | PolyVent XL | PolyVent Stainless Steel | | |
| M12x1.5 | M32x1.5 | M12x1.5 | | |
| PMF100585 (black) / PMF100586 (grey) | PMF200542 | PMF200444 | | |
| 4000 ml/min (dp = 70 mbar) | 16 l/min (dp = 12 mbar) | 1600 ml/min (dp = 70 mbar) | | |
| ePTFE/Polyester (PET) | ePTFE/Polyester (PET) | ePTFE/- | | |
| Oleophobic | Oleophobic | Oleophobic | | |
| Polyamide (PA6) | Polycarbonate (PC) | Stainless steel (1.4404 / 316L) | | |
| Black: RAL 9011 / Grey: RAL 7035 | Grey: RAL 7035 | Metallic | | |
| 16 mm | 70 mm | 18 mm | | |
| Silicone 60 Shore A | Silicone 60 Shore A | Silicone 60 Shore A | | |
| Plastic/Grey / M10510-009 | Plastic/Grey / M10510-010 | Nickel-plated brass / M10510-008 | | |
| Yes: Individually laser-marked | No | Yes: Individually laser-marked | | |
|  |  |  | | |
|  |  |  | | |
| 0.7 ± 0.1 Nm | 5 Nm | 0.9 ± 0.3 Nm | | |
| 12.2 ± 0.1 mm | 33 ± 0.5 mm | 12.2 ± 0.1 mm | | |
|  Salt Fog Testing Vent resistance to salty environments METHODS: • IEC 60068-2-11 (salt fog) • IEC 60068-2-52 (cyclic salt fog) |  Corrosive Gas Testing Vent durability in corrosive gas environment (e.g., NO _x , SO _x , H ₂ S, Cl ₂) METHOD: • GR-3108-CORE |  Vibration Testing (Not applicable to PolyVent XL) Vent resistance against vibration METHOD: • ETSI EN 300 019-2-2 • IEC 60068-2-64 |  Flammability and UV Resistance Testing (Not applicable to stainless steel materials) Resistance to open flame, radiant heat and ultraviolet light METHOD: • UL 94V-0 and UL 746C F1 All non-metal PolyVent caps/bodies • UL 94V-0 All PolyVent O-ring materials • UL 94VTM-0 GORE™ Membranes in PolyVentXS and Stainless Steel |  Solar Industry Testing (PolyVent XL only) Durability in solar applications METHODS: • IEC 62108 10.8 (humidity freeze – high temperature / humidity followed by freezing temperature) • IEC 62108 10.9 (ball impact) |

GS level - 4223

Lightweight Liquid Level Sensor

GILL

Key Features

- Compatible use with fuels, oils and coolants
- Multiple and custom mounting arrangements
- Side or top exit cable options
- Lightweight Aluminium design
- Operating temperature range: -40°C to +125°C
- Custom lengths available: 100 – 750mm
- Temperature output option (coming soon)

The GSLevel 4223 is a lightweight capacitive liquid level sensor designed to provide accurate and reliable liquid level measurement to variety of applications.

The sensor is a form fit and function replacement for the R-Series sensors as well as bringing the flexibility to be adapted to an almost limitless range of mechanical mounting configurations. Standard stock adaptors are available for 1, 2, 3 & 5 bolt mounting as well as metric male thread designs.

For real product flexibility, you have the ability to design your own custom configurations to suit any flat gasket seal configuration, limitless thread adaptations to both Male and Female threads.



OUTPUT SPECIFICATION

| | |
|--|--|
| Primary output standard range | 0.25 – 4.75V Range is Datum A to Datum B (see drawing on page 2) |
| Primary output maximum range | 0.25 – 10V (configurable through user software. See page 4) |
| Primary output accuracy | ±1% @ 50% FSD (full scale deflection) 20°C. |
| Primary volumetric output | Configurable through user software. See page 4 Tank profiling Wizard or CSV file upload |
| Secondary output (option N) | Open collector output 50V / 1A max switch to ground (V-) |
| Secondary output hysteresis (option N) | Configurable through user software. See page 4 |

ELECTRICAL

| | |
|----------------|---|
| Supply voltage | 5-32VDC |
| Supply current | <20mA |
| Interface | Compatible with RS232 |
| Resolution | 10 bit (1024 points over measurement range) |
| Sample rate | 100Hz |

MECHANICAL

| | |
|--------------------|---|
| Lengths available | 100-750mm |
| Mounting options | 1 hole, 2 hole, 3 hole, 5 hole and M22x1.5 Threaded |
| Sealing options | Panel gasket or o-ring |
| Cable exit options | Top or Side |
| Weight (100mm) | 36.5g (100mm probe with 1000mm cable) +0.34g per mm (probe) thereafter |

ENVIRONMENTAL TESTING AND CERTIFICATION

| | |
|---------------------|--|
| Ingress Protection | IP68 |
| Shock tested to | BS EN 60068-2-27 (half-sine pulse 25g, 6ms 1000 shocks (positive and negative) in each 3 axis) |
| Vibration tested to | Resonant frequency search 5 to 2500Hz @ 0.5g peak |
| Pressure | 10 bar (absolute and differential) |
| Drop | 1m (in packaging) on all 3 sides |
| Thermal shock | to BS EN 60068-2-14, test Na |
| Dry heat | to BS EN 60068-2-2, test Bb |
| Cold | to BS EN 60068-2-1, test Ab |
| Damp Heat | to BS EN 60068-2-30, test Db |
| EMC Immunity level | BS EN 60945, BS EN 61326 and BS EN 61000-6-1/2/3/4 |

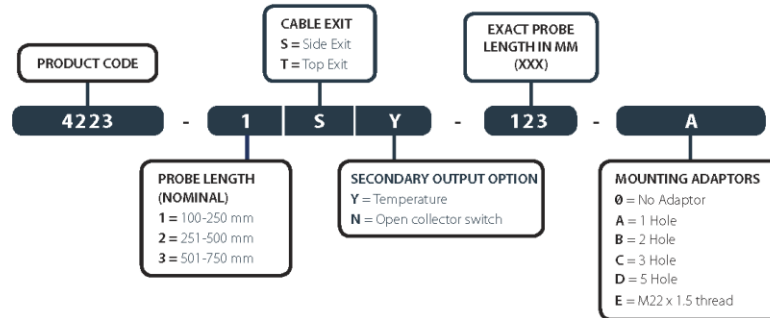
WIRING

| | |
|-----------------|---------------------|
| Cable | Flying lead, 1000mm |
| Number of cores | 6 with drain wire |
| Wire size | 26AWG 7/0.15 |
| Sleeving | XLPE |

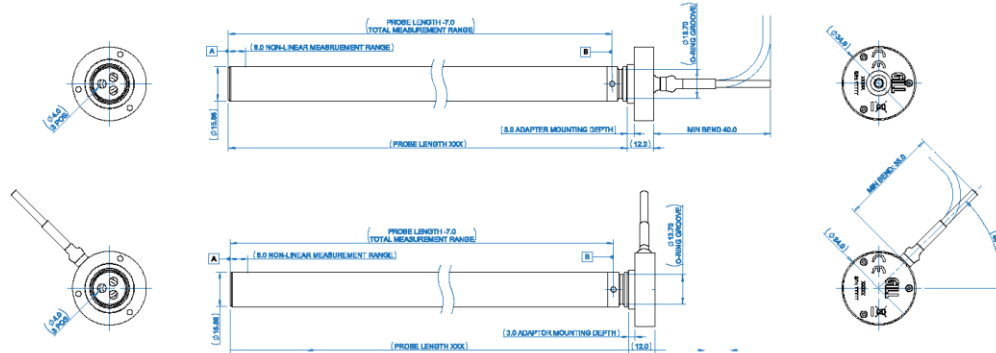
COMPATIBLE MEDIUM

| | |
|----------|---|
| Fuels | Diesel, Gasoline, Biofuels |
| Oils | Hydraulic, Gear, Motor, Vegetable, Synthetic ester, Polyalphaolefin, Polyglycol |
| Coolants | Ethylene Glycol, water |
| Other | Salt water |

PART NUMBER CONFIGURATOR



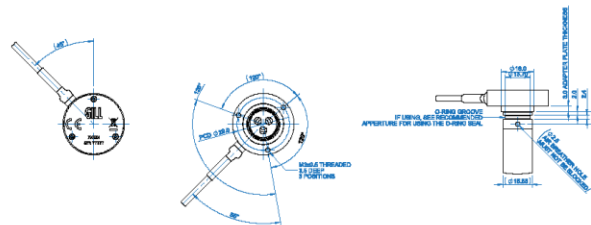
CABLE EXIT OPTIONS



CUSTOM ADAPTOR DESIGN INFO

TOLERANCES

| | |
|---------|--|
| LINEAR | 1 Decimal place $\pm 0.1\text{mm}$ 2 Decimal places $\pm 0.05\text{mm}$ |
| ANGULAR | $\pm 1^\circ$ |



CABLE LOOM

| WIRE COLOUR | DESIGNATION |
|-------------|------------------|
| RED | +V |
| BLACK | -V (GROUND) |
| ORANGE | PRIMARY OUTPUT |
| BLUE | SECONDARY OUTPUT |
| GREEN | Rx |
| WHITE | Tx |

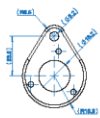
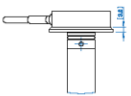
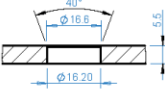
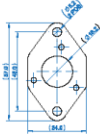
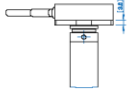
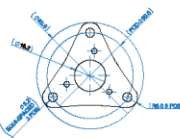
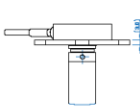

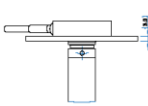
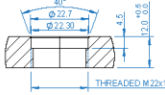
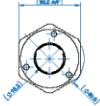
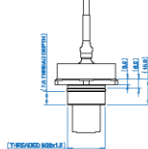
MOUNTING ADAPTORS

Design Notes – Adaptors & Fitting

Each adaptor is supplied in a kit which includes 3 x M3 CSK screws, with pre-applied adhesive, Fluorosilicone O-rings and a Fluorosilicone Gasket (options A through D only).

Notes – Adaptors can be fitted in 3 orientations (+/- 120° from top dead centre of TOP VIEW below)

Top Exit cable can be selected for use with options A through D
(Side exit cable shown for illustration only purposes)

| ADAPTOR | TOP VIEW | SIDE VIEW | |
|------------------------|---|--|--|
| A (1 HOLE) |  |  |  |
| B (2 HOLE) |  |  | RECOMMENDED MOUNTING APERTURE FOR USING THE O-RING SEAL. USE WITH 1 HOLE FLANGE ADAPTOR. CAN BE USED WITH 2/3/5 HOLE ADAPTORS. |
| C (3 HOLE) |  |  | RECOMMENDED MOUNTING APERTURE FOR THE PANEL GASKET SEAL. CAN BE USED WITH 2/3/5 HOLE FLANGE ADAPTORS. |
| D (5 HOLE) |  |  |  |
| E (THREADED) |  |  | RECOMMENDED MOUNTING APERTURE FOR FOR USE WITH M22x1.5 THREADED FLANGE ADAPTOR |

Description

The AH9246 is an ultra high sensitivity Hall-effect switch with internal pull-up resistor on the output, designed for battery operated handheld equipments to industrial applications.

A chopper stabilized architecture improves stability of magnetic switch points over the whole operating range. A sleep-awake logic controls the sleep and awake time to reduce the average operating current of the device. During the awake time, the output is changed with the magnetic flux density. During the sleep time, the output is latched in its previous state and the current consumption reduces to 4μA typical at 3V. The average current consumption is 8μA at 3V.

The output can be switched on with either north or south pole of sufficient strength. If the magnetic flux density perpendicular to the part marking surface is larger than operating point (B_{OP}), the output will be turned on; if it is less than releasing point (B_{RP}), the output will be turned off.

The AH9246 is available in industry standard TO92S and SC59 packages.

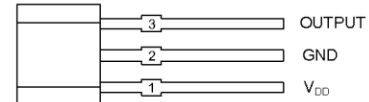
Features

- Omnipolar Operation (Switching with North or South Poles)
- Micropower Operation
- Built in Pull-up Resistor on the Output
- 2.5V to 5.5V Power Supply
- Stabilized Chopper
- Superior Temperature Stability
- Digital Output Signal
- -40°C to +85°C Operating Temperature
- ESD (HBM): 5000V
- Small Low Profile Industry Standard SC59 and TO92S Packages
- **Totally Lead-Free & Fully RoHS Compliant (Notes 1 & 2)**
- **Halogen and Antimony Free. "Green" Device (Note 3)**

Notes: 1. No purposely added lead. Fully EU Directive 2002/95/EC (RoHS) & 2011/65/EU (RoHS 2) compliant.
2. See http://www.diodes.com/quality/lead_free.html for more information about Diodes Incorporated's definitions of Halogen- and Antimony-free, "Green" and Lead-free.
3. Halogen- and Antimony-free "Green" products are defined as those which contain <900ppm bromine, <900ppm chlorine (<1500ppm total Br + Cl) and <1000ppm antimony compounds.

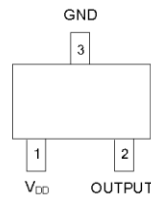
Pin Assignments

(Front View)



TO92S

(Top View)

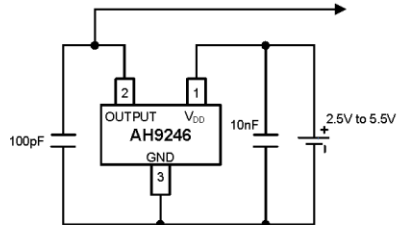


SC59

Applications

- Cover Switch in Notebook PC/PDA
- Handheld Wireless Application Awake Switch
- Magnet Switch in Low Duty Cycle Applications

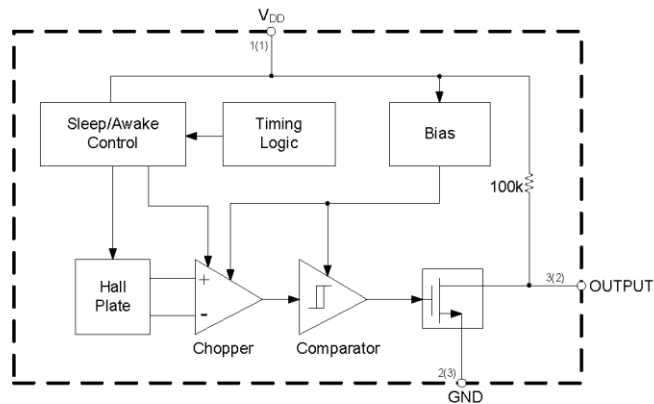
Typical Applications Circuit



Pin Descriptions

| Pin Number | | Pin Name | Function |
|------------|------|-----------------|------------------|
| TO92S | SC59 | | |
| 1 | 1 | V _{DD} | Power supply pin |
| 2 | 3 | GND | Ground pin |
| 3 | 2 | OUTPUT | Output pin |

Functional Block Diagram



A (B)
A for TO92S
B for SC59

Absolute Maximum Ratings (Note 4) (@T_A = +25°C, unless otherwise specified.)

| Symbol | Parameter | Rating | Unit |
|------------------|---------------------------------|-------------|-------|
| V _{DD} | Supply Voltage (Note 5) | 7 | V |
| I _{DD} | Supply Current (Fault) | 6 | mA |
| V _{OUT} | Output Voltage | 7 | V |
| I _{OUT} | Output Current | 2 | mA |
| B | Magnetic Flux Density | Unlimited | Gauss |
| P _D | Power Dissipation | TO92S | 230 |
| | | SC59 | 230 |
| T _{STG} | Storage Temperature | -55 to +150 | °C |
| T _J | Junction Temperature | +150 | °C |
| — | ESD (Human Body Model) (Note 6) | 5000 | V |
| — | ESD (Machine Model) (Note 6) | 400 | V |

- Notes:
- Stresses greater than the 'Absolute Maximum Ratings' specified above may cause permanent damage to the device. These are stress ratings only; functional operation of the device at these or any other conditions exceeding those indicated in this specification is not implied. Device reliability may be affected by exposure to absolute maximum rating conditions for extended periods of time.
 - The absolute maximum V_{DD} of 7V is a transient stress rating and is not meant as a functional operating condition. It is not recommended to operate the device at the absolute maximum rated conditions for any period of time.
 - Electronic semiconductor products are sensitive to Electro Static Discharge (ESD). Always observe Electro Static Discharge control procedures whenever handling semiconductor products.

Recommended Operating Conditions

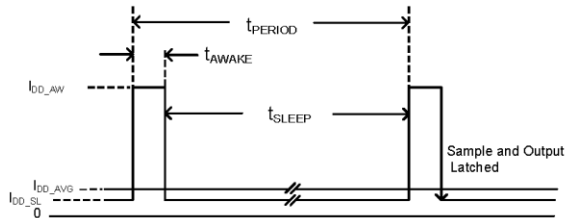
| Symbol | Characteristic | Conditions | Min | Max | Unit |
|-----------------|-----------------------------|------------|-----|-----|------|
| V _{DD} | Supply Voltage | Operating | 2.5 | 5.5 | V |
| T _A | Operating Temperature Range | Operating | -40 | +85 | °C |

Electrical Characteristics (Note 7) (@T_A = +25°C, V_{DD} = 3V, unless otherwise specified.)

| Symbol | Characteristic | Conditions | Min | Typ | Max | Unit |
|---------------------|--------------------------------------|---|----------------------|----------------------|-----|------|
| V _{DD} | Supply Voltage | Operating | 2.5 | 3 | 5.5 | V |
| I _{DD_AW} | Supply Current During "Awake" Period | T _A = -40 to +85°C, V _{DD} = 2.5V to 5.5V | — | 1.8 | 3 | mA |
| I _{DD_SL} | Supply Current During "Sleep" Period | T _A = -40 to +85°C, V _{DD} = 2.5V to 5.5V | — | 4 | 10 | μA |
| I _{DD_AVG} | Average Supply Current | T _A = -40 to +85°C, V _{DD} = 2.5V to 5.5V | — | 8 | 15 | μA |
| I _{OUT} | Output Current | — | — | — | 1.0 | mA |
| I _{OFF} | Output Leakage Current | V _{OUT} = 5.5V, Output off | — | <0.1 | 1 | μA |
| V _{OL} | Output Low Voltage (On) | I _{OUT} = 1.0mA | — | — | 0.4 | V |
| V _{OH} | Output High Voltage (Off) | I _{OUT} = -1.0mA | V _{DD} -0.2 | V _{DD} -0.1 | — | V |
| t _{AW} | Awake Mode Time | Operating | — | 150 | — | μs |
| t _{SL} | Sleep Mode Time | Operating | — | 100 | — | ms |
| D | Duty Cycle | — | — | 0.15 | — | % |
| f _C | Chopper Frequency | — | — | 15 | — | kHz |

- Note:
- Parameters values over operating temperature range are not tested in production, they are guaranteed by design, process control and characterization. The magnetic characteristics may vary with supply voltage, operating temperature and after soldering.

Electrical Characteristics (Cont.) (@T_A = +25°C, V_{DD} = 3V, unless otherwise specified.)

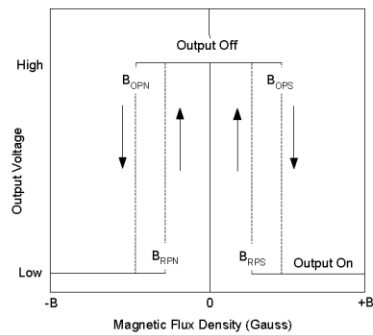


Magnetic Characteristics (Notes 8 & 9) (@T_A = -40°C to +85°C, V_{DD} = 3V, unless otherwise specified.)

| (1mT=10 Gauss) | | | | | | |
|--|-----------------|--|-----|-----|-----|-------|
| Symbol | Parameter | Conditions | Min | Typ | Max | Unit |
| B _{OPS} (South Pole to Part Marking Side) | Operating Point | B > B _{OPS} , V _{OUT} =Low (output on) | 9 | 18 | 27 | Gauss |
| B _{OPN} (North Pole to Part Marking Side) | | B > B _{OPN} , V _{OUT} =Low (output on) | -27 | -18 | -9 | Gauss |
| B _{RPS} (South Pole to Part Marking Side) | Releasing Point | B < B _{RPS} , V _{OUT} =High (output off) | 4 | 12 | 22 | Gauss |
| B _{RPN} (North Pole to Part Marking Side) | | B < B _{RPN} , V _{OUT} =High (output off) | -22 | -12 | -4 | Gauss |
| B _{HYS} (B _{OPX} - B _{RFX}) | Hysteresis | (Note 9) | — | 6 | — | Gauss |

Notes: 8. Parameters values over operating temperature range are not tested in production, they are guaranteed by design, process control and characterization. The magnetic characteristics may vary with supply voltage, operating temperature and after soldering.
9. Maximum and minimum hysteresis is guaranteed by design and characterization.
B_{OPX}=operating point (output turns on); B_{RFX}=releasing point (output turns off)

Operating Characteristics



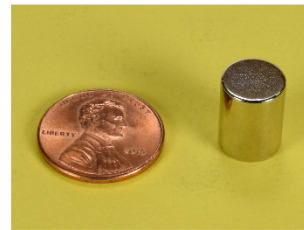
Output Voltage vs. Magnetic Flux Density



D68-N52 Specification Sheet

Product Specifications

Type: DISC
Dimensions: 0.375 dia x 0.5 thk (in)
Tolerance: All dimensions ± 0.004 in
Material: NdFeB, Grade N52
Plating: NiCuNi
Max Op Temp: 176°F (80°C)
Br max: 14,800 Gauss
BH max: 52 MGOe




Performance Specifications

Pull Force, Case 1,
Magnet to a Steel Plate: 10.52 lb

Surface Field values are derived from calculation and verification with experimental testing. These values are the field values at the surface of the magnet, centered on the axis of magnetization. Measurement of the B field with a magnetometer may yield varying results, depending on the geometry of your sensor. Pull Force values are based on extensive product testing in our laboratory. Different configurations of magnets and surrounding ferromagnetic materials may substantially alter your results.

| Specification | "Long-John" 90 mm battery | | | |
|-----------------|--|--------------|---|--------------|
| |  | | | |
| | 14.4V | 25.2V | 46.8V | 50.4V |
| Capacity | 47Ah | 26Ah | 16Ah | 16Ah |
| Energy | 674Wh | 655Wh | 730Wh | 768Wh |
| 2000m | Ø 90 mm x 512mm length. 8.5kg in air, 5.1kg in sea water | | Ø 90 mm x 560mm length. 8.9kg in air, 5.2kg in sea water | |
| 4000m | Ø 90 mm x 512mm length. 9.3kg in air, 5.8kg in sea water | | Ø 90 mm x 560mm length. 9.6kg in air, 6kg in sea water | |
| 6000m | Ø 90 mm x 512mm length. 8.5kg in air, 5.1kg in sea water | | Ø 90 mm x 560mm length. 8.9kg in air, 5.2kg in sea water | |

Notes: no high current output for Long-John batteries. High peaks on demand, please specify.
Optional: BMS with data interface, remote on/off input, DC/DC regulated outputs (the length is increased up to 150mm)

| Specification | "Big Jim" 168/180 mm battery | | | | | | | |
|-----------------|--|--------|--|--------|--------------|--------|--------------|--------|
| |  | | | | | | | |
| | 14.4V | | 25.2V | | 46.8V | | 50.4V | |
| Type | Standard | XL | Standard | XL | Standard | XL | Standard | XL |
| Capacity | 140Ah | 280Ah | 70Ah | 140Ah | 34Ah | 70Ah | 34Ah | 70Ah |
| Energy | 2020Wh | 4040Wh | 1769Wh | 3538Wh | 1582Wh | 3285Wh | 1704Wh | 3538Wh |
| 300m | Std.: Ø 168 mm x 372mm length. XL: Ø 168 mm x 638mm length. | | Weight: 17kg in air, 9kg in sea water Weight: 29kg in air, 5kg in sea water | | | | | |
| 2000m | Std.: Ø 180 mm x 390mm length. XL: Ø 180 mm x 630mm length. | | Weight: 24kg in air, 14kg in sea water Weight: 38kg in air, 22kg in sea water | | | | | |
| 4000m | Std.: Ø 180 mm x 390mm length. XL: Ø 180 mm x 630mm length. | | Weight: 25kg in air, 15kg in sea water Weight: 41kg in air, 25kg in sea water | | | | | |
| 6000m | Std.: Ø 180 mm x 390mm length. XL: Ø 180 mm x 630mm length. | | Weight: 25kg in air, 15kg in sea water Weight: 41kg in air, 25kg in sea water | | | | | |

Notes: continuously high current output is limited. Please call.
Optional: BMS with data interface, remote on/off input, DC/DC regulated outputs (the length is increased up to 150mm)

UN T38.8 certified batteries: see next page

SubCtech GmbH • Wellseedamm 3 • D-24145 Kiel • Germany
T +49 431-22039-880 • F +49 431-22039-881 • www.subctech.com • info@subctech.com

© SubCtech GmbH. All rights reserved. In view of our continual improvement policy, the design and specifications of our products may vary from those illustrated in this brochure. All pictures and trademarks mentioned in this user manual are property of their respective owners. MicroDL, NetDL, SmartDL, m8Bubler, PowerPack, SmartCharger, SmartBMS, OceanLine, OceanPack, OceanView, Gosubsea and SubCtech are registered or applied trademarks of SubCtech GmbH, Germany. 02.04.2017



Our new "A" type batteries incorporate our well known AUV (Autonomous Underwater Vehicle) battery cell for highest capacity. After usage only for high-sophisticated AUV battery systems up to 100 kWh and 400 V we provide this special Li-Ion technology now for our standard product portfolio.

The special features from the MNP technology are:

- ✦ Internal Temperature Coefficient Device (PTC) to protect over-heating on cell level
- ✦ Current Interrupt Device (CID) to protect over current on cell level
- ✦ Heat Resistance Layer (HRL) to protect over-heating and internal short-circuit

| Specification | NEW "Long-John" "A" type high capacity battery | | | |
|---------------|--|-------|-------|--------|
| | 14.4V | 25.2V | 46.8V | 50.4V |
| Capacity | 60Ah | 33Ah | 20Ah | 20Ah |
| Energy | 868Wh | 844Wh | 941Wh | 1013Wh |

All other specifications as above.

| Specification | NEW "Big-Jim" "A" type high capacity battery | | | | | | | |
|---------------|--|--------|----------|--------|----------|--------|----------|--------|
| | 14.4V | | 25.2V | | 46.8V | | 50.4V | |
| Type | Standard | XL | Standard | XL | Standard | XL | Standard | XL |
| Capacity | 180Ah | 362Ah | 90Ah | 181Ah | 43Ah | 90Ah | 43Ah | 90Ah |
| Energy | 2605Wh | 5210Wh | 2279Wh | 4559Wh | 2038Wh | 4233Wh | 2195Wh | 4559Wh |

Notes all other specifications as above.

| Specification | NEW "Big-Jim" "M" type high capacity battery | | | | | | | |
|---------------|--|--------|----------|--------|----------|--------|----------|--------|
| | 14.7V | | 25.7V | | 47.7V | | 51.4V | |
| Type | Standard | XL | Standard | XL | Standard | XL | Standard | XL |
| Capacity | 172Ah | 345Ah | 86Ah | 172Ah | 41Ah | 86Ah | 41Ah | 86Ah |
| Energy | 2536Wh | 5073Wh | 2220Wh | 4439Wh | 1984Wh | 4122Wh | 1984Wh | 4439Wh |

Notes all other specifications as above.
The yellow marked batteries are UN T38.3 tested to simplify shipping (still dangerous goods!)

| Specification | Certifications & approvals (all types) |
|-----------------------|--|
| Certifications | The cells are fully certified for UN/DOT 38.3 and listed at UL. |
| Production | Production following IPC-A-600 and IPS-A-610 class 2; or class 3 on request. |
| Environmental | Product testing for temperature, shock and vibration following e.g. MIL-STD 810G on request. |
| EMC | Our products comply with the IEC EMC directives, single tests on request. |
| Offshore | Our production and quality management is approved to ISO 13628-6 and API17f |
| Air cargo | Our standard products are approved by the "Bundesluftfahrtamt" no. LBA B32F/439.50/15 |
| Vendor | We are proved battery manufacturer of the German UBA (Umweltbundesamt) no. 21002655 |

SubCtech GmbH • Wellseedamm 3 • D-24145 Kiel • Germany
T +49 431-22039-880 • F +49 431-22039-881 • www.subctech.com • info@subctech.com

© SubCtech GmbH. All rights reserved. In view of our continual improvement policy, the design and specifications of our products may vary from those illustrated in this brochure. All pictures and trademarks mentioned in this user manual are property of their respective owners. MicroDL, NetDL, SmartDL, m8ubbler, PowerPack, SmartCharger, SmartBMS, OceanLine, OceanPack, OceanView, Gosubsea and SubCtech are registered or applied trademarks of SubCtech GmbH, Germany. 02.04.2017



| Specification | Voltage ranges (all types) | | | |
|-----------------------|----------------------------|------------|------------|------------|
| Battery type | 14V | 25V | 46V | 50V |
| Charging volt. | 16.8V | 29.4V | 54.6V | 58.8V |
| Minimal volt. | 12V | 21V | 39V | 42V |
| Cut-off | 10V | 17.5V | 32.5V | 35V |

Notes: the charge voltage is the max. voltage measured at the battery output. The min. voltage guarantees full performance and lifetime. The battery capacity is measured down to this level. More discharge will not provide more capacity. Cut-off protects electronically against under discharge. In case of cut-off our SmartCharger™ will revive the battery.

| Specification | Current options and connectors (High-currents for Big-Jim only) | | | | |
|----------------------------------|---|--|---|--|--|
| Current | 7A (standard) | 20A | 30A | 40A | 50A |
| Connector power only | BH-4F "Standard" | BH-4F | BH-10F | BH-12F | BH-16F |
| Connector with power+data | BH-8F | BH-8F | BH-10F | BH-12F | BH-16F |
| | 1, 4: V- 2, 3: V+ (SeaBattery™ compatible) | 1-2: V- 2-3: V+ 4-7: Data 8: On/Off | 1-3: V- 4-6: V+ 7-9: Data 10: On/Off | 1-4: V- 5-8: V+ 9-11: Data 12: On/Off | 1-6: V- 7-12: V+ 13-15: Data 16: On/Off |

Notes: all connectors are SubConn®. The connector BH-4F (e.g. standard 7A, 20A) is SeaBattery™ compatible. Other connectors on request. **For all current outputs larger than 7A the high-power option is required** (Big-Jim only; special electronic components and wiring).

| Specification | General (all types) |
|----------------------------------|---|
| Temperature | -20 ... +60 °C (operating), >0 ... +40 °C (charging), -20 ... +50 °C (storage) |
| Self discharge | <10 % per year at +25°C, < 5% per year at 0°C |
| Charge cycles | Standard >500 cycles; optional >3000 cycles using special electronic and less capacity |
| Protection | Over-charge, under voltage discharge, current limiting after 1s, over-temperature |
| Data interface (optional) | BMS (Battery Management System) with RS-232 (RS-485) data interface ASCII NMEA-0183 or binary MODBUS RTU data protocol. Optical isolated. |
| Remote On/Off (optional) | Remote on/off input pin. Connected to 0V (battery -) to switch the battery on. An open input or any voltage >1.2V up to Vbatt will switch off. The pin is internally connected to Vbatt with 1MΩ. |
| Charger | Our SmartCharger™ can be connected all time. Do not open the housing for charging. |
| Switches (optional) | Remote switches e.g. for ROV (ISO 13628-6 light torque tool) or simple linear magnetic switches e.g. for diver or ROV usage |
| DC Options (optional) | Customised DC/DC outputs e.g. 5V, 12V, 24V. High efficiency and low noise. LED control light, customized e.g. green/red highly visibility and low-power |
| Transportation | The battery must be transported as dangerous goods class 9. SubCtech is registered as a vendor of batteries. Transported by sea, air or road. We are pleased to advise you. |
| Storage | Storage at +5 to +20°C, approx. 50%-80% charged. Recharge after 3-6 months. We provide storage/transport boxes with low-power cooling devices and charging. |



Never use other chargers, modify cables or operate outside the specifications, risk of fire or explosion.

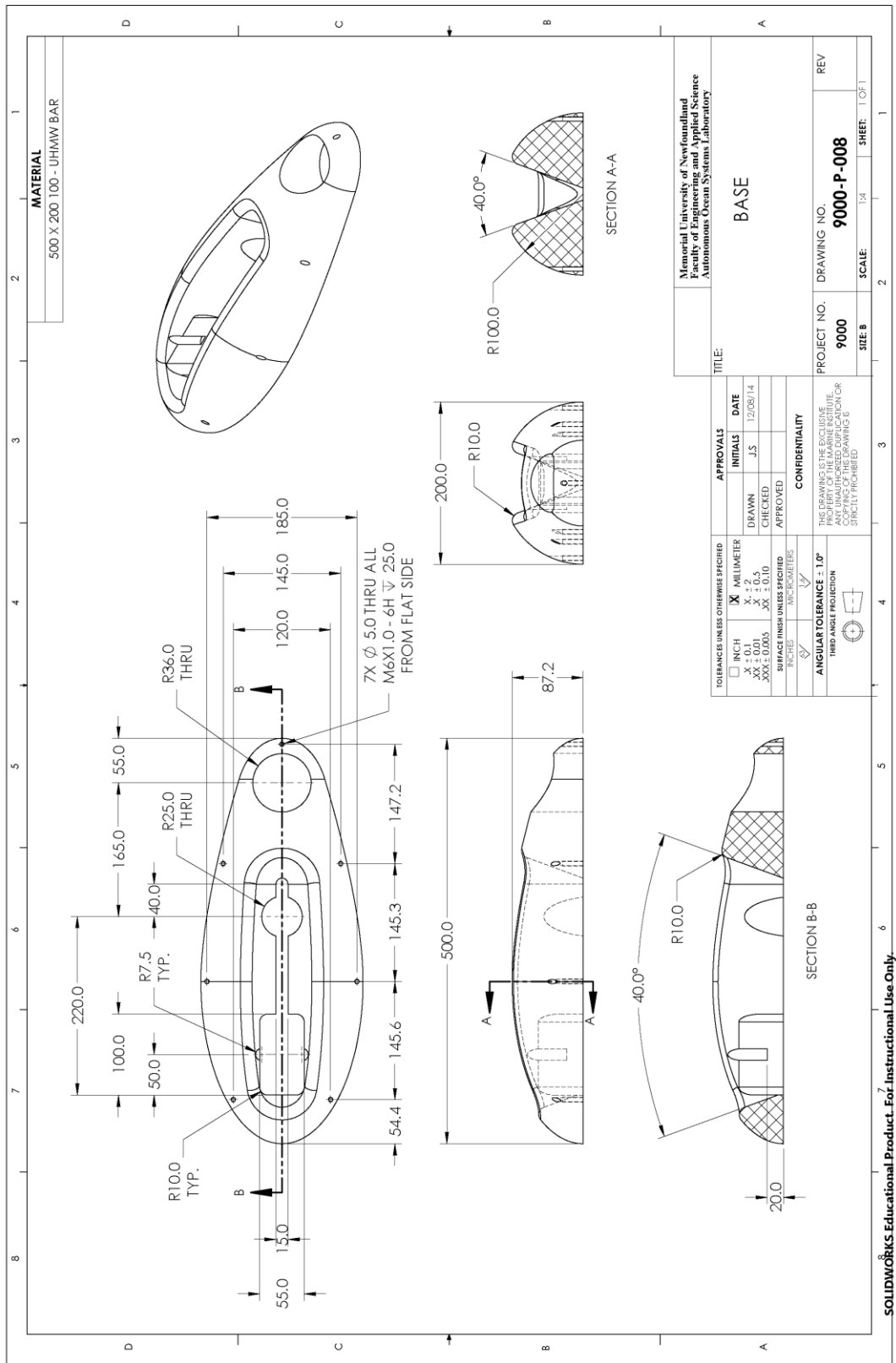
SubCtech GmbH • Wellseedamm 3 • D-24145 Kiel • Germany
T +49 431-22039-880 • F +49 431-22039-881 • www.subctech.com • info@subctech.com

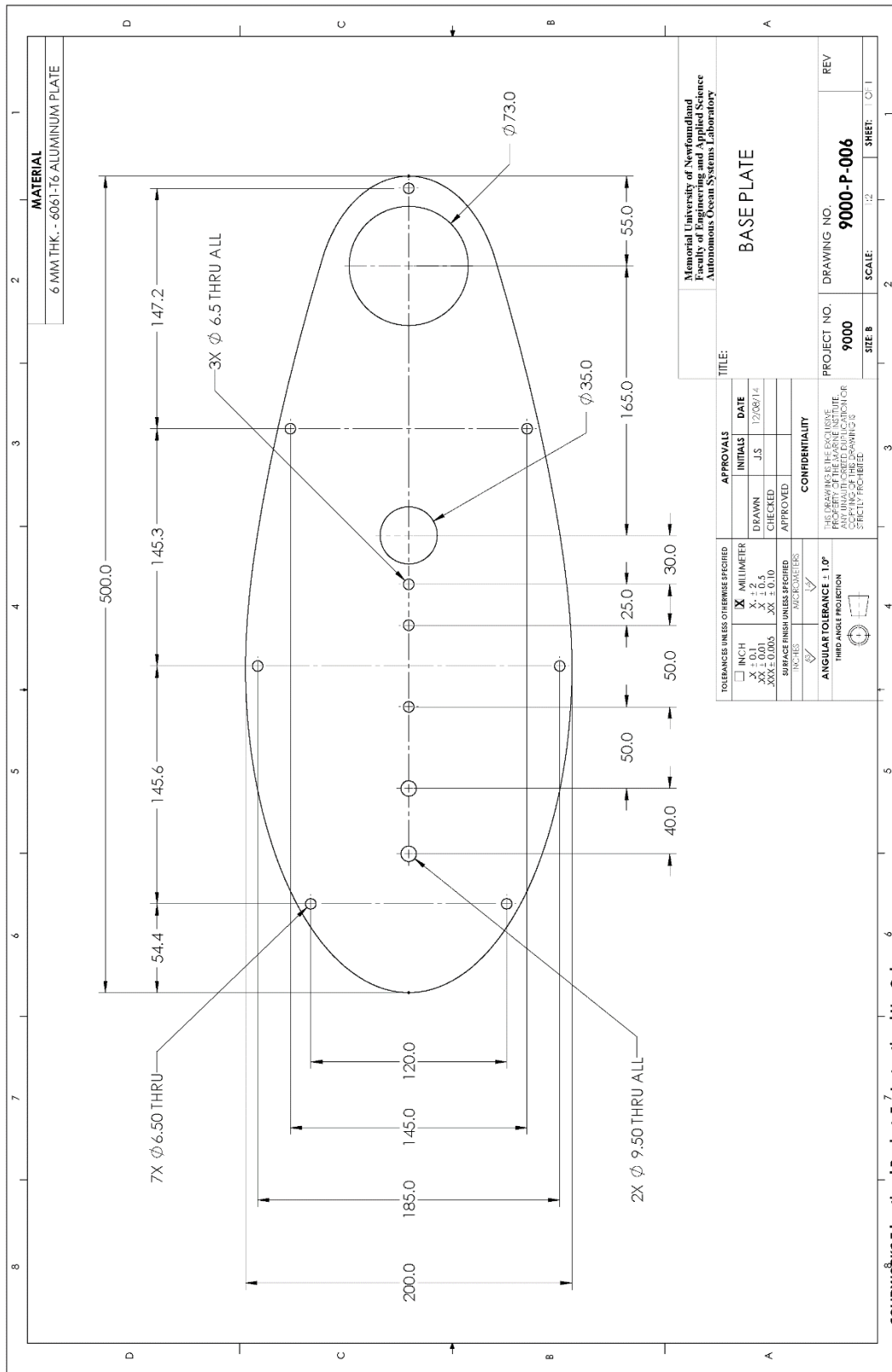
© SubCtech GmbH. All rights reserved. In view of our continual improvement policy, the design and specifications of our products may vary from those illustrated in this brochure. All pictures and trademarks mentioned in this user manual are property of their respective owners. MicroDL, NetDL, SmartDL, m8Bubler, PowerPack, SmartCharger, SmartBMS, OceanLine, OceanPack, OceanView, Gosubsea and SubCtech are registered or applied trademarks of SubCtech GmbH, Germany. 02.04.2017

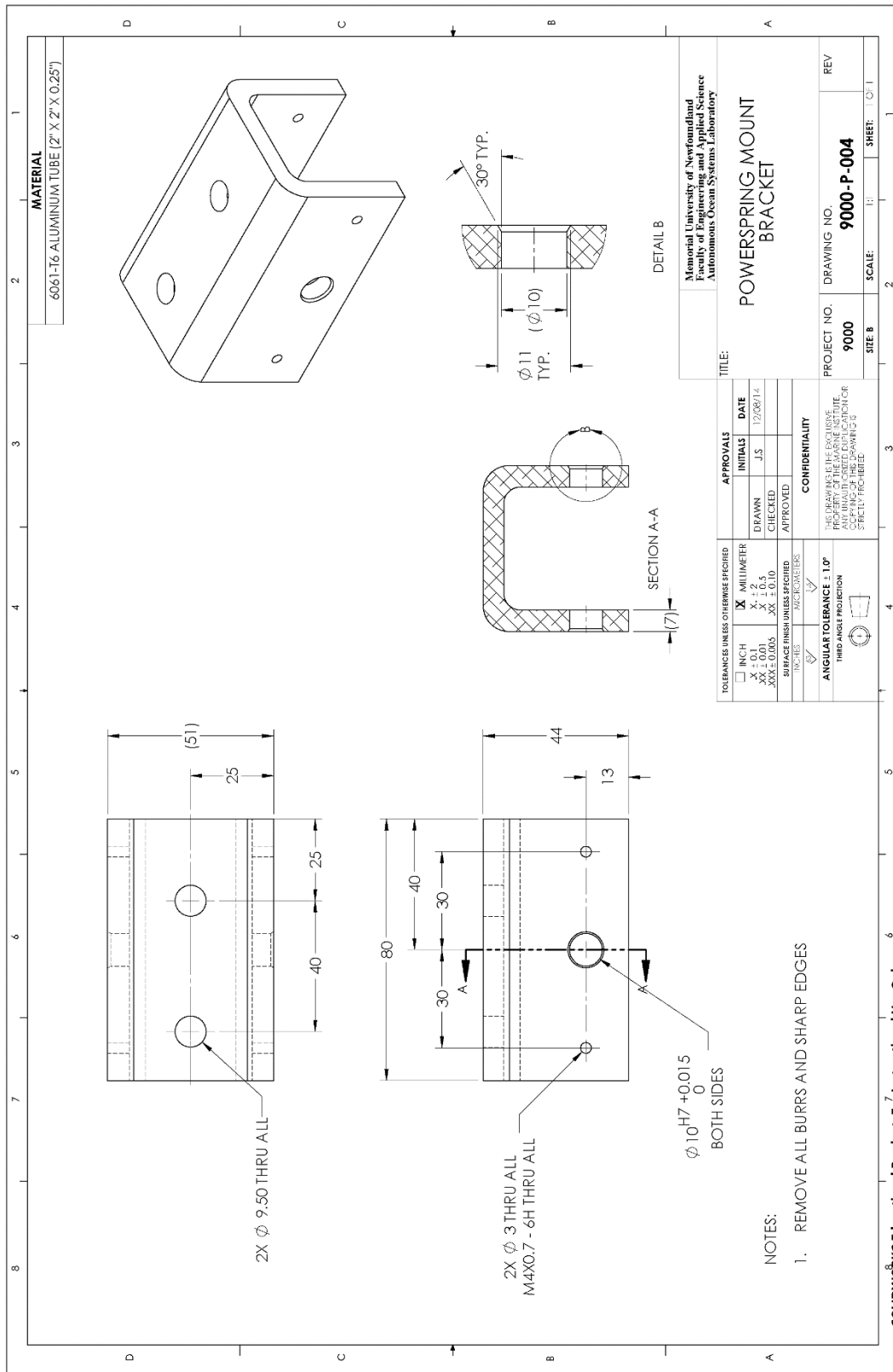


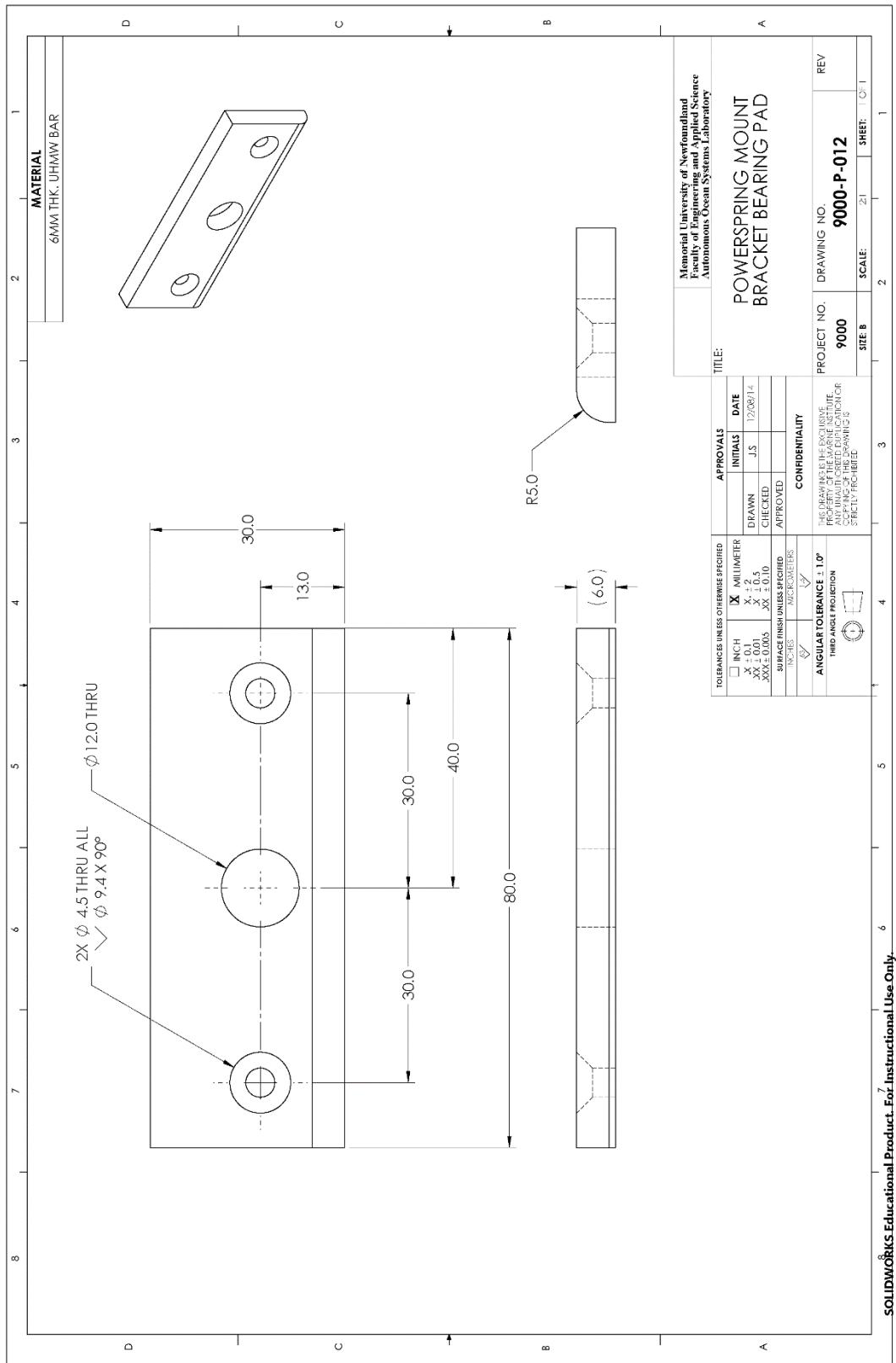
Appendix B

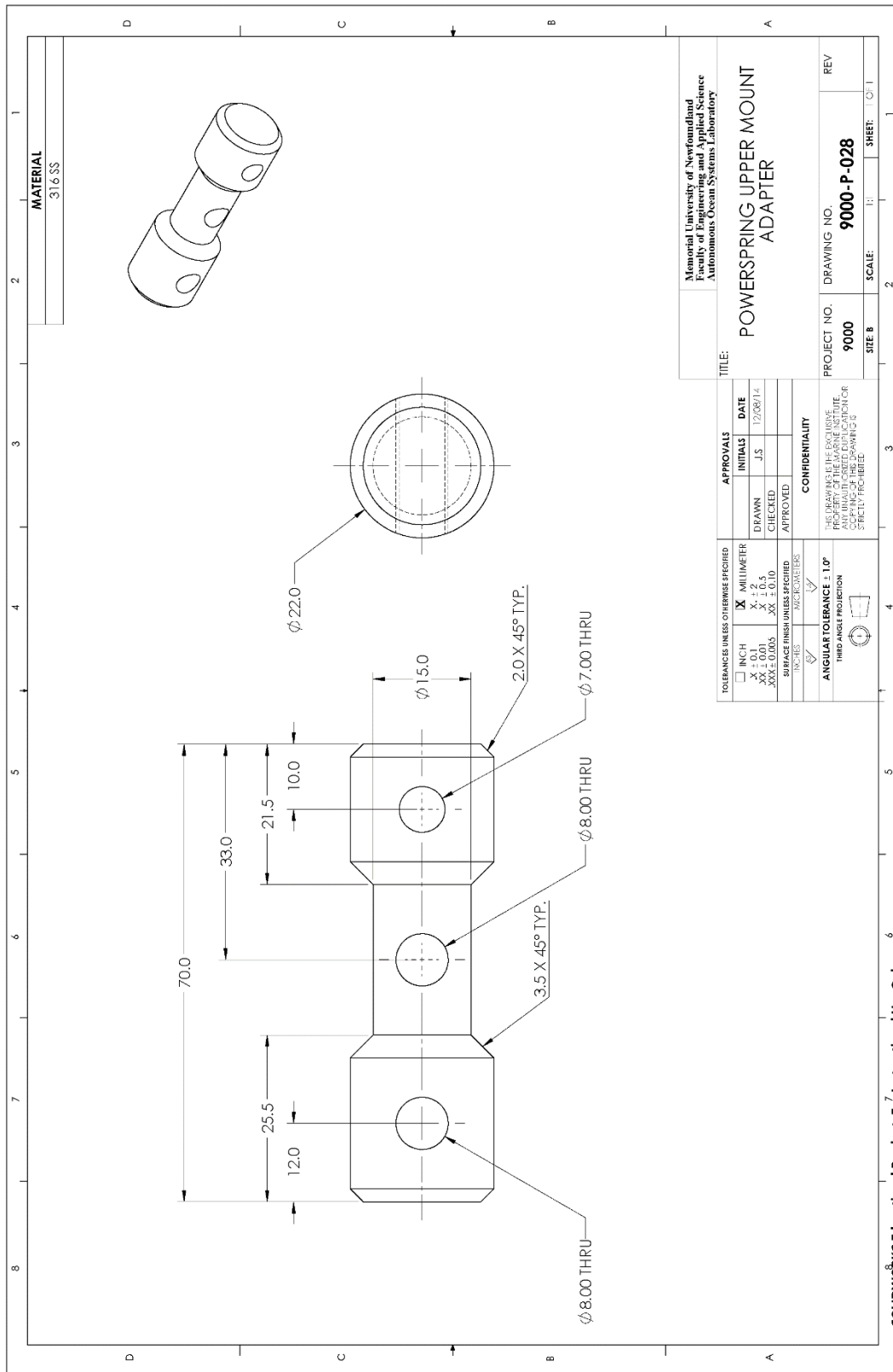
SolidWorks CAD Fabrication Drawings

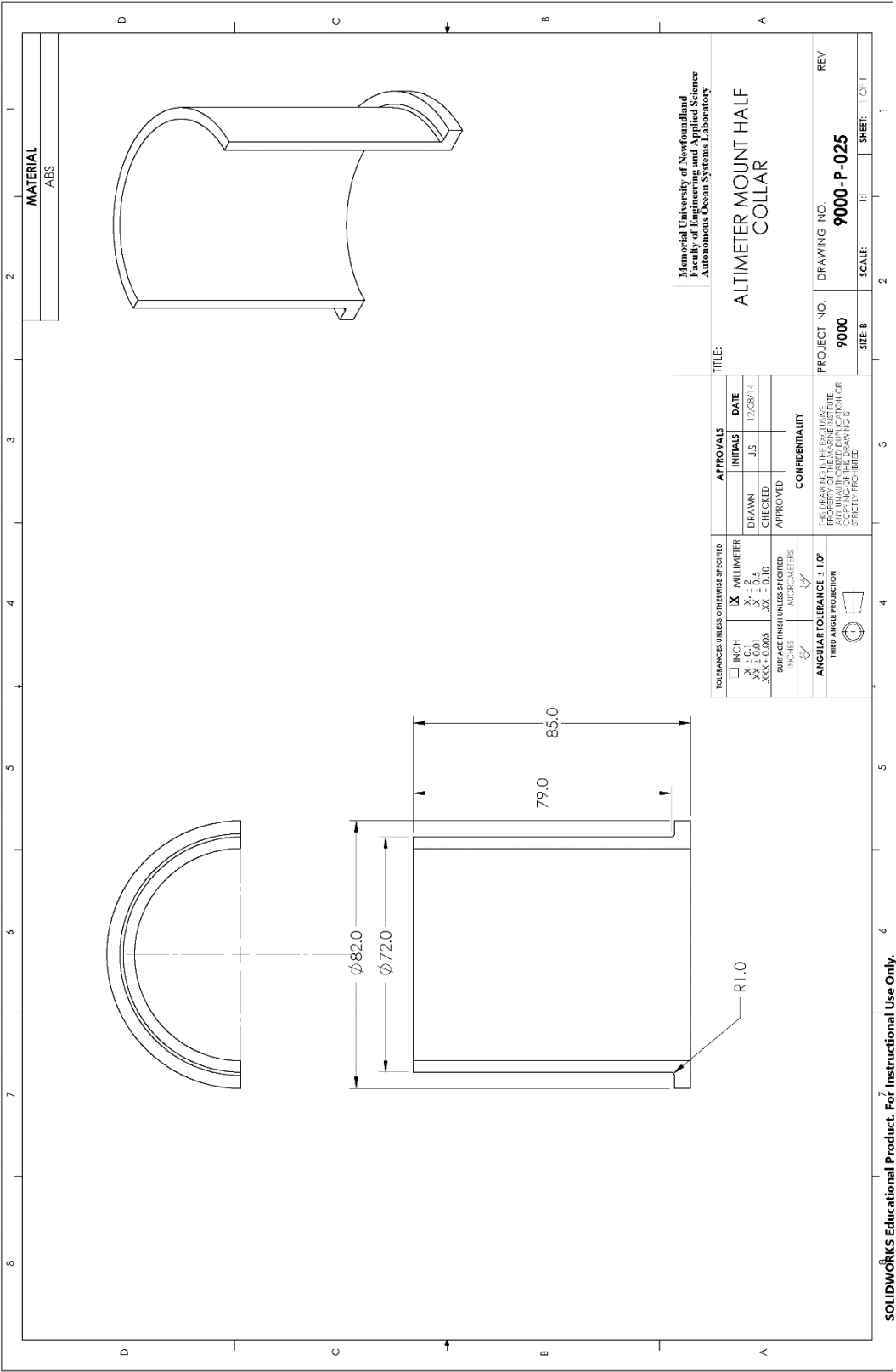


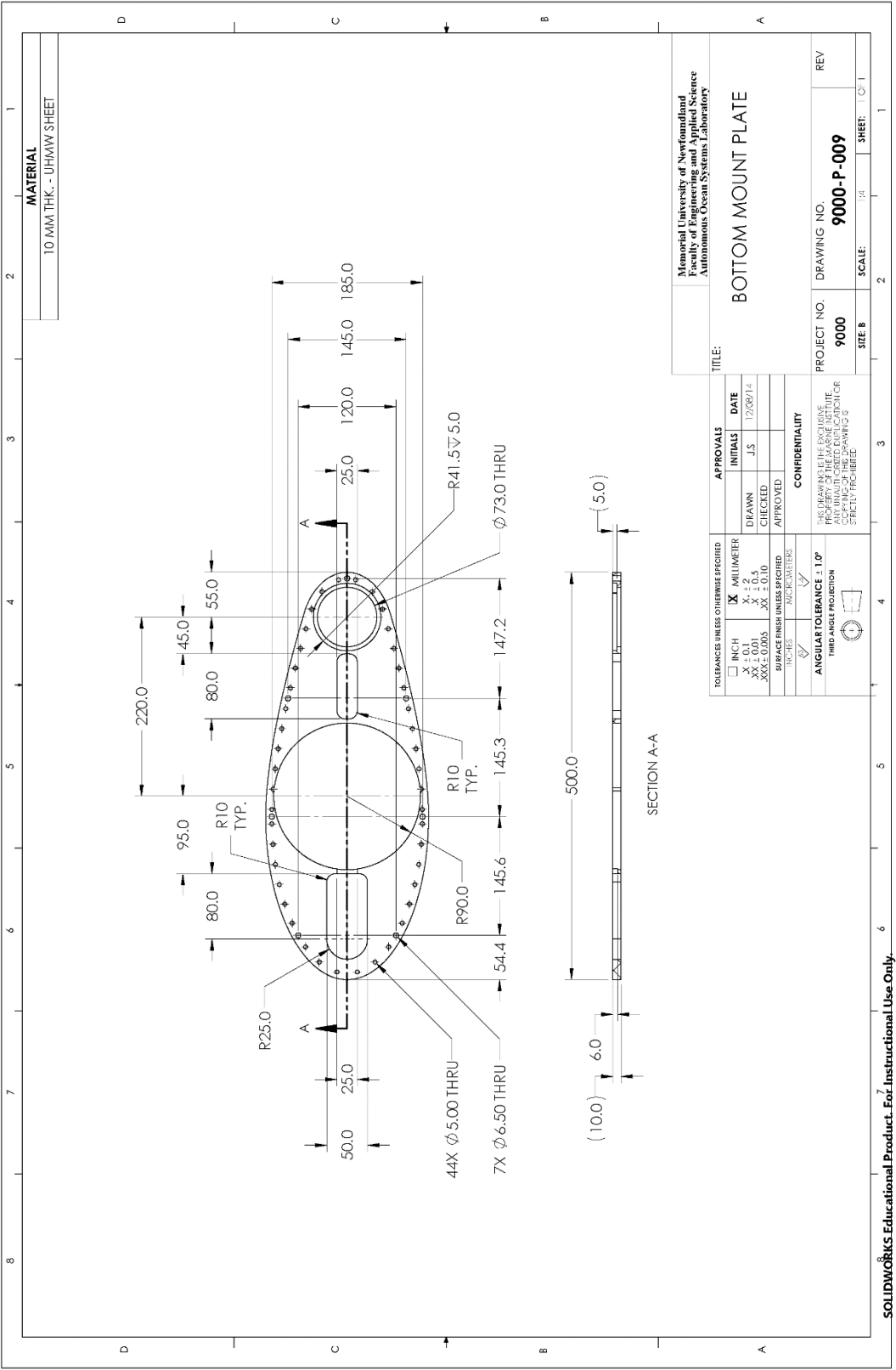





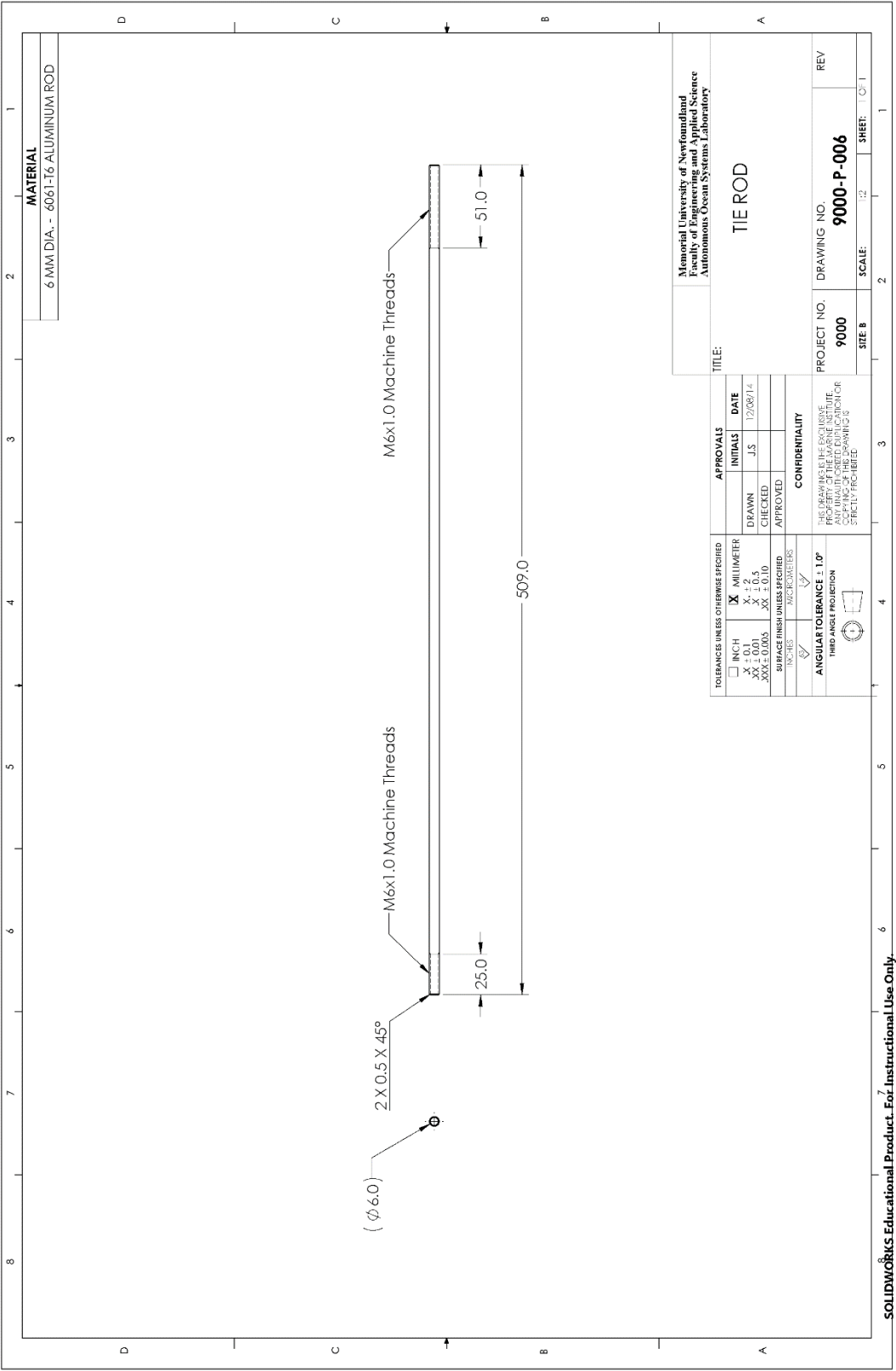


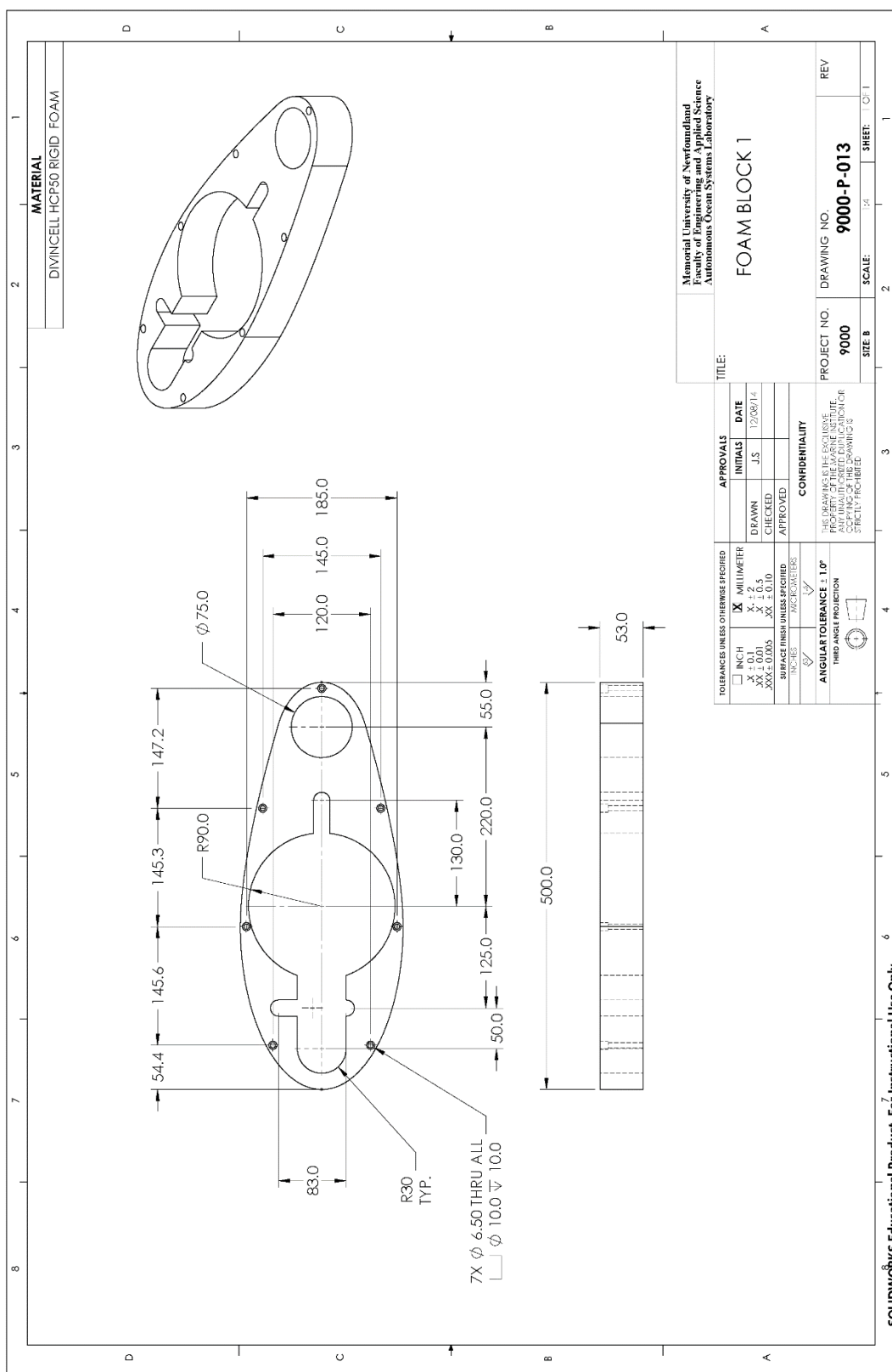


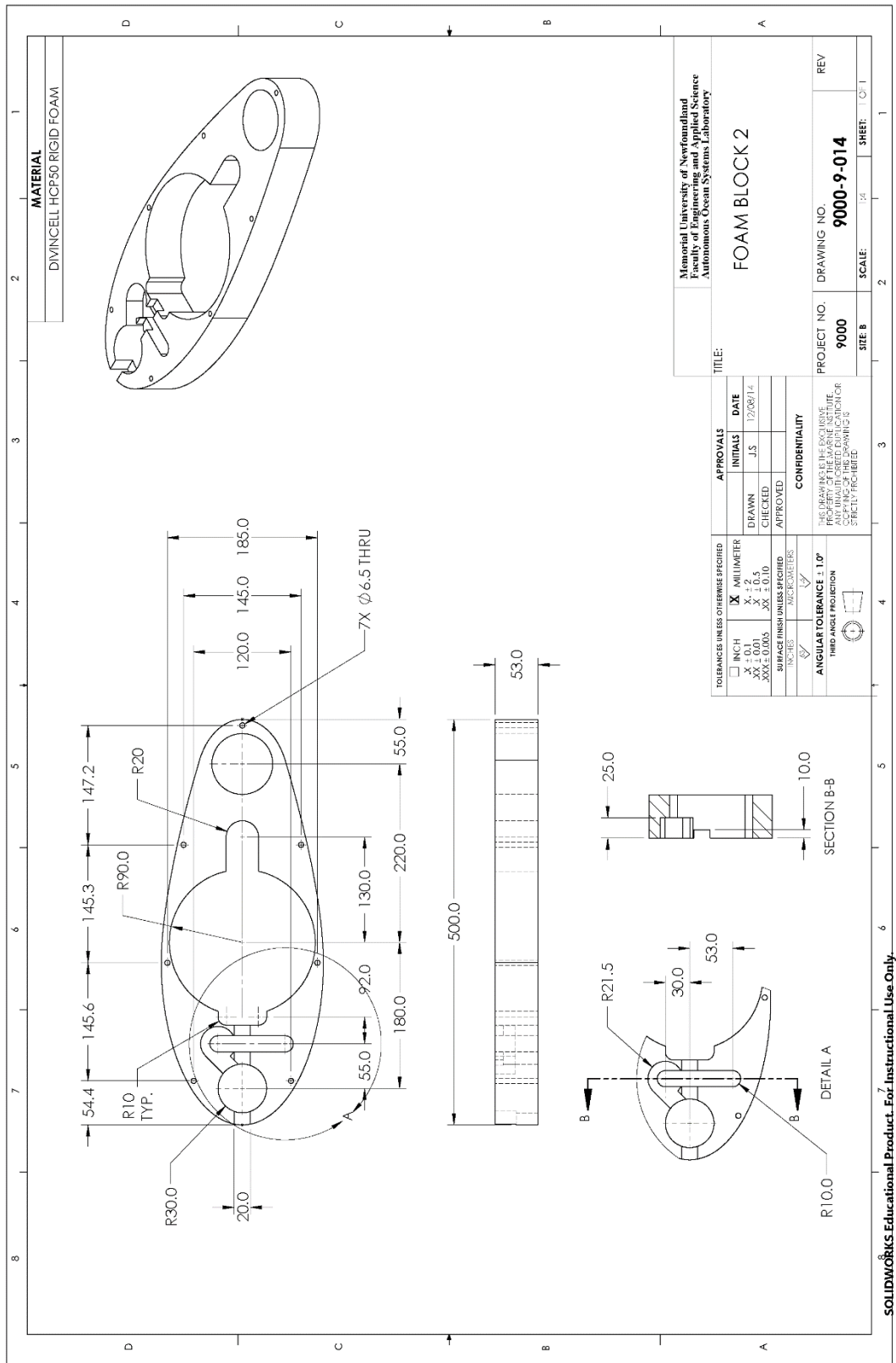


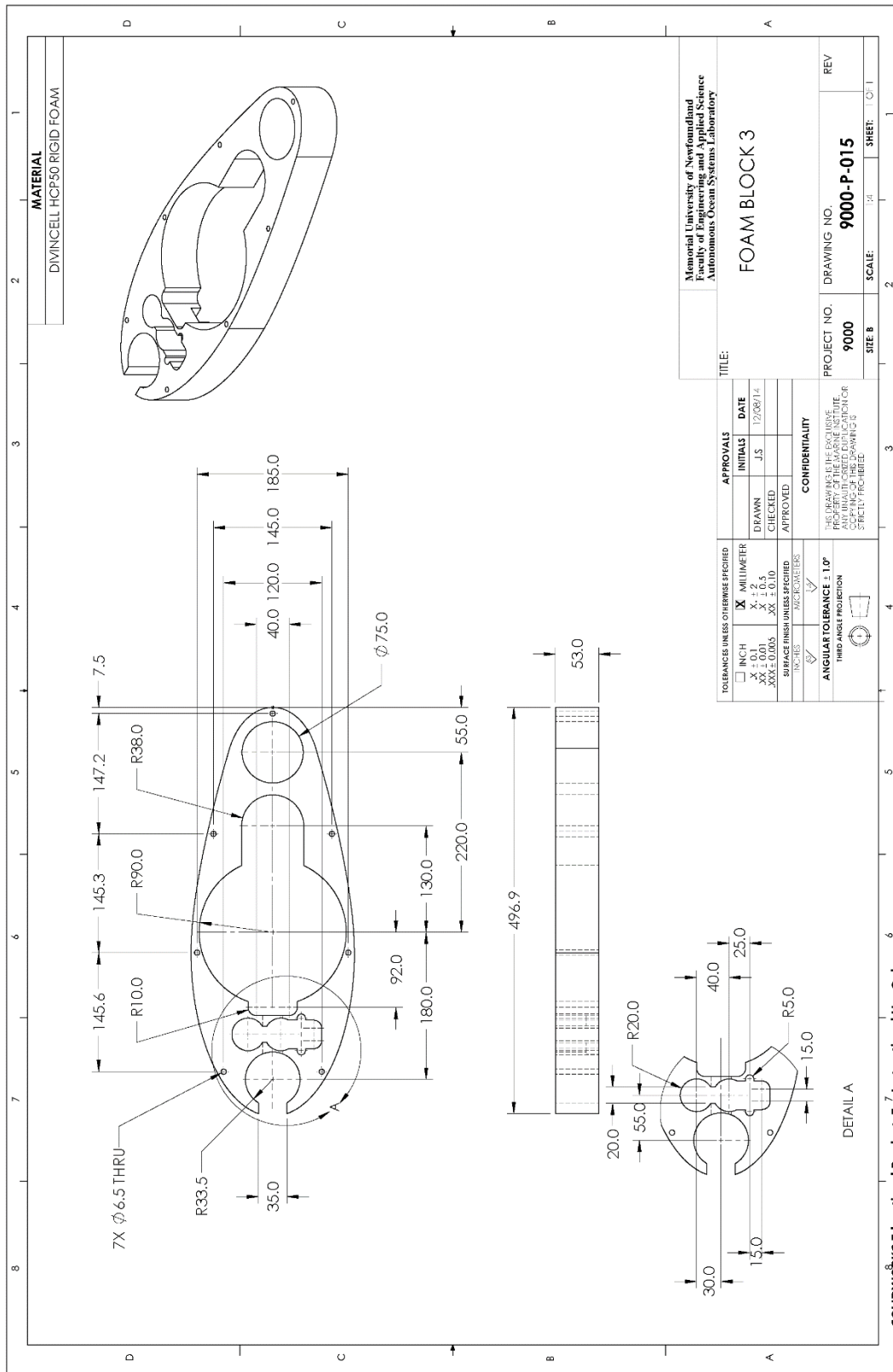


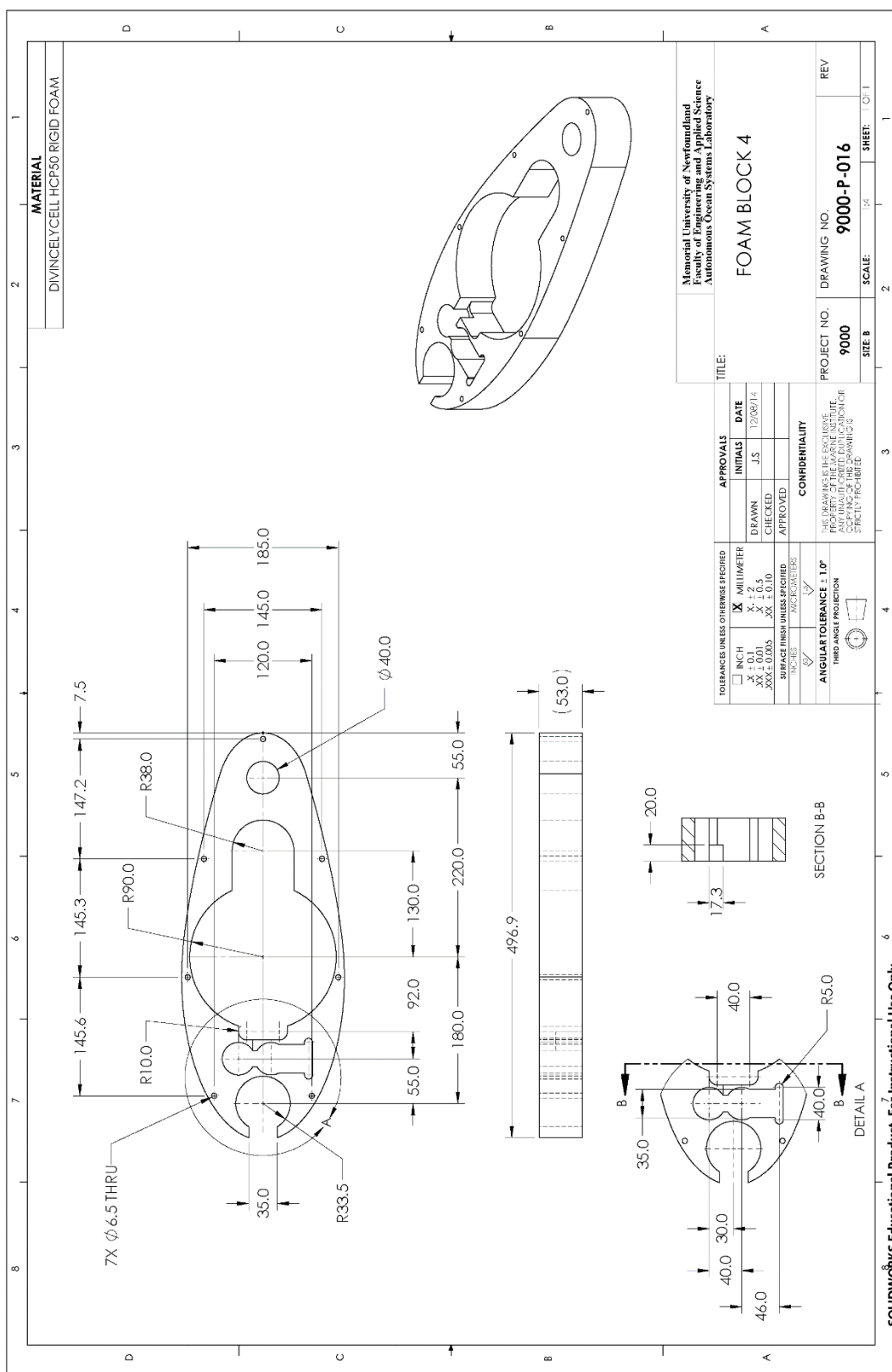
| | | | |
|--|--|--|---|
| <p>MATERIAL</p> <p>6061-T6 ALUMINUM</p> <p>MCMaster P/N: 94669A802</p> |  | | |
| <p>NOTES:</p> <p>1. REMOVE ALL BURRS AND SHARP EDGES</p> | <p>TITLE:</p> <p>TIE ROD ROUND NUT</p> | | |
| <p>APPROVALS</p> <table border="1" style="width: 100%; border-collapse: collapse;"> <tr> <td style="width: 50%;"> <p>INITIALS</p> <p>J.S.</p> </td> <td style="width: 50%;"> <p>DATE</p> <p>12/08/14</p> </td> </tr> </table> | <p>INITIALS</p> <p>J.S.</p> | <p>DATE</p> <p>12/08/14</p> | <p>CONFIDENTIALITY</p> <p>THE DRAWING IS THE EXCLUSIVE PROPERTY OF MEMORIAL UNIVERSITY OF NEWFOUNDLAND. NO PART OF THIS DRAWING IS TO BE REPRODUCED OR TRANSMITTED IN ANY FORM OR BY ANY MEANS, ELECTRONIC OR MECHANICAL, INCLUDING PHOTOCOPYING, RECORDING, OR BY ANY INFORMATION STORAGE AND RETRIEVAL SYSTEM, WITHOUT PERMISSION IN WRITING FROM MEMORIAL UNIVERSITY OF NEWFOUNDLAND.</p> |
| <p>INITIALS</p> <p>J.S.</p> | <p>DATE</p> <p>12/08/14</p> | | |
| <p>TOLERANCES UNLESS OTHERWISE SPECIFIED</p> <table border="1" style="width: 100%; border-collapse: collapse;"> <tr> <td style="width: 50%;"> <p><input type="checkbox"/> INCH</p> <p>.XX ± 0.01</p> <p>.XXX ± 0.005</p> </td> <td style="width: 50%;"> <p><input checked="" type="checkbox"/> MILLIMETER</p> <p>.X ± 0.5</p> <p>.XX ± 0.10</p> <p>.XXX ± 0.10</p> </td> </tr> </table> | <p><input type="checkbox"/> INCH</p> <p>.XX ± 0.01</p> <p>.XXX ± 0.005</p> | <p><input checked="" type="checkbox"/> MILLIMETER</p> <p>.X ± 0.5</p> <p>.XX ± 0.10</p> <p>.XXX ± 0.10</p> | <p>ANGULAR TOLERANCE ± 1.0°</p> <p>THIRD ANGLE PROJECTION</p> |
| <p><input type="checkbox"/> INCH</p> <p>.XX ± 0.01</p> <p>.XXX ± 0.005</p> | <p><input checked="" type="checkbox"/> MILLIMETER</p> <p>.X ± 0.5</p> <p>.XX ± 0.10</p> <p>.XXX ± 0.10</p> | | |
| <p>PROJECT NO.</p> <p>9000</p> | <p>DRAWING NO.</p> <p>9000-P-007</p> | | |
| <p>SCALE:</p> <p>1:1</p> | <p>SHEET:</p> <p>1</p> | | |

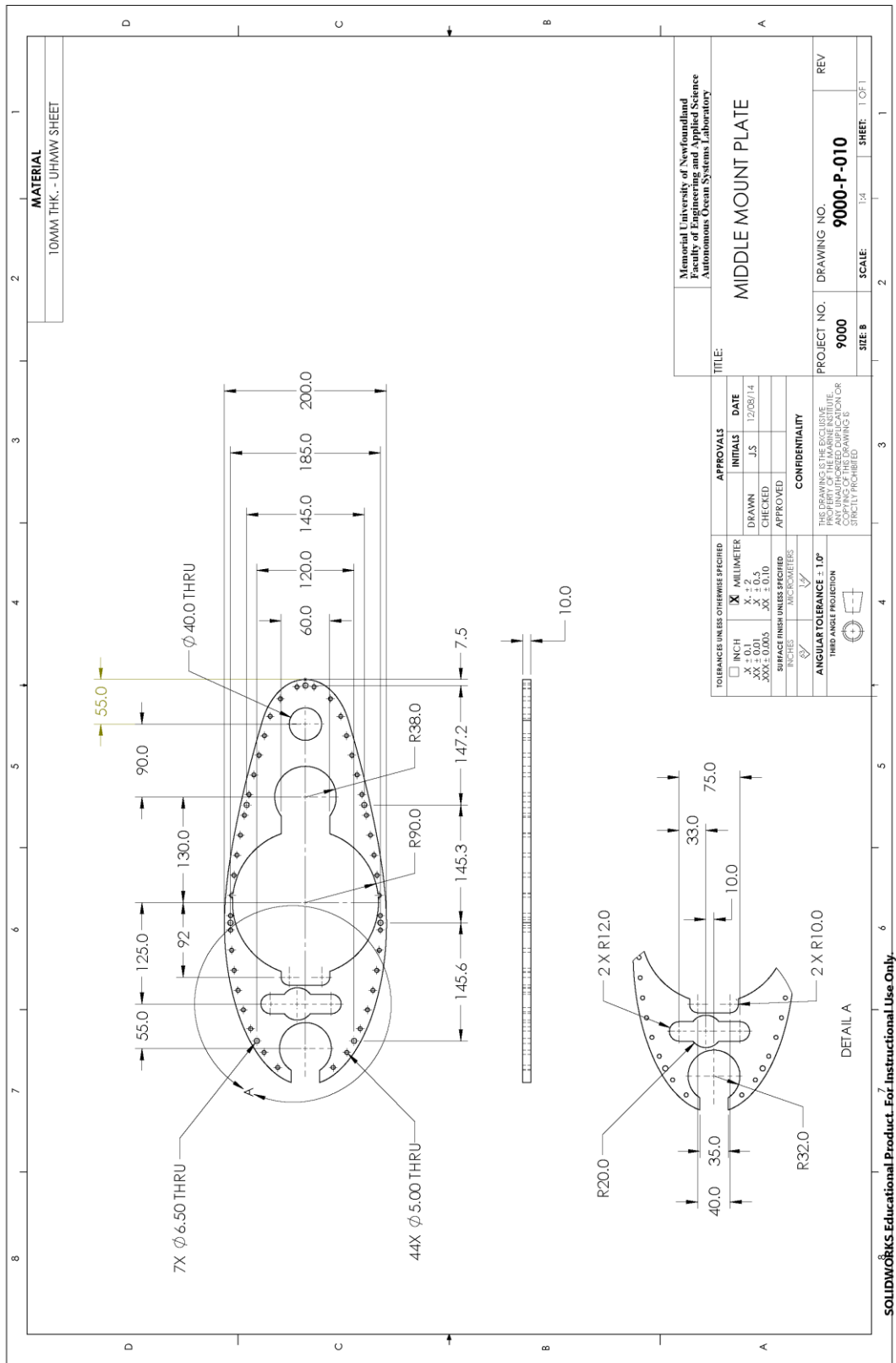


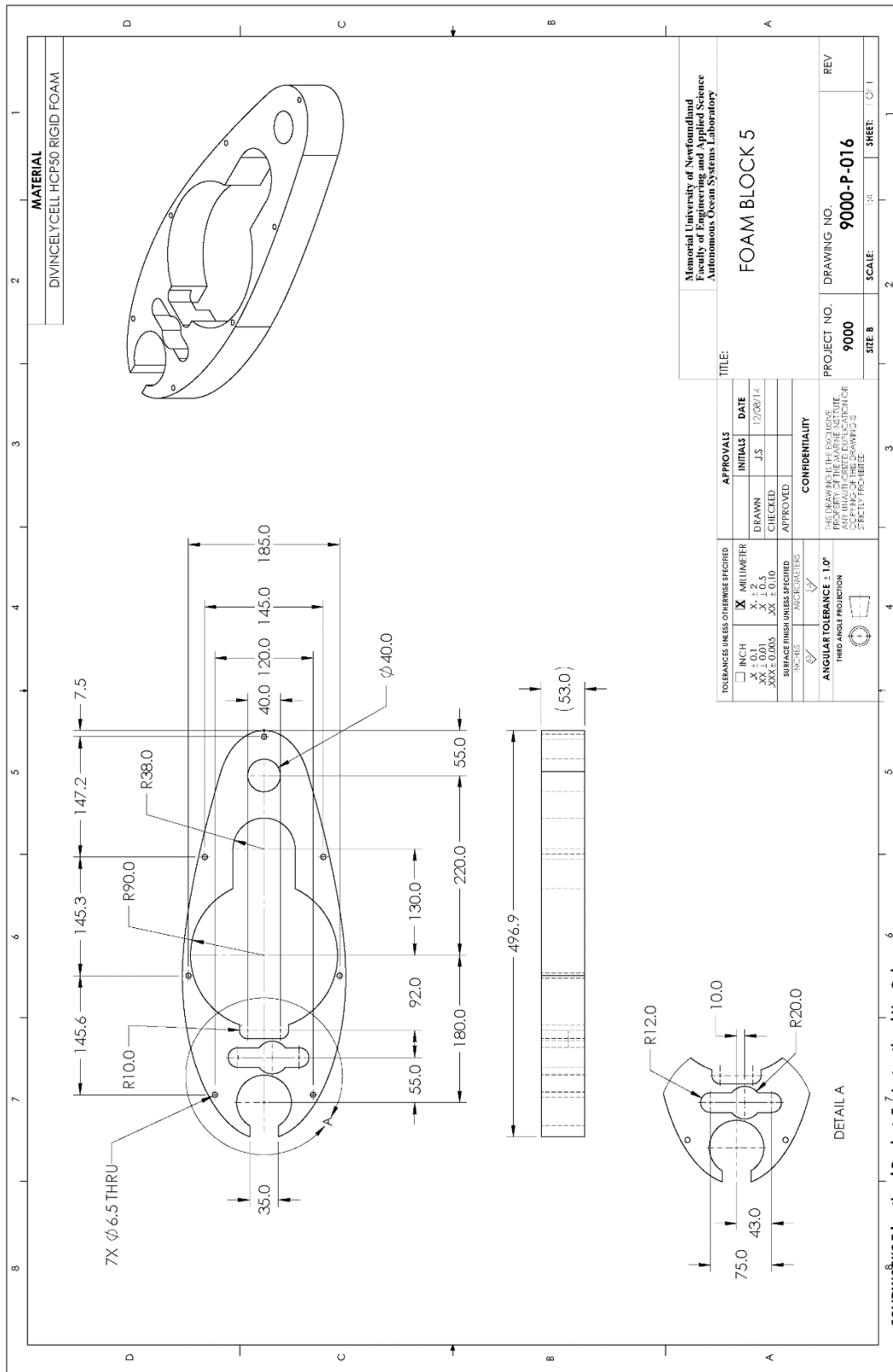


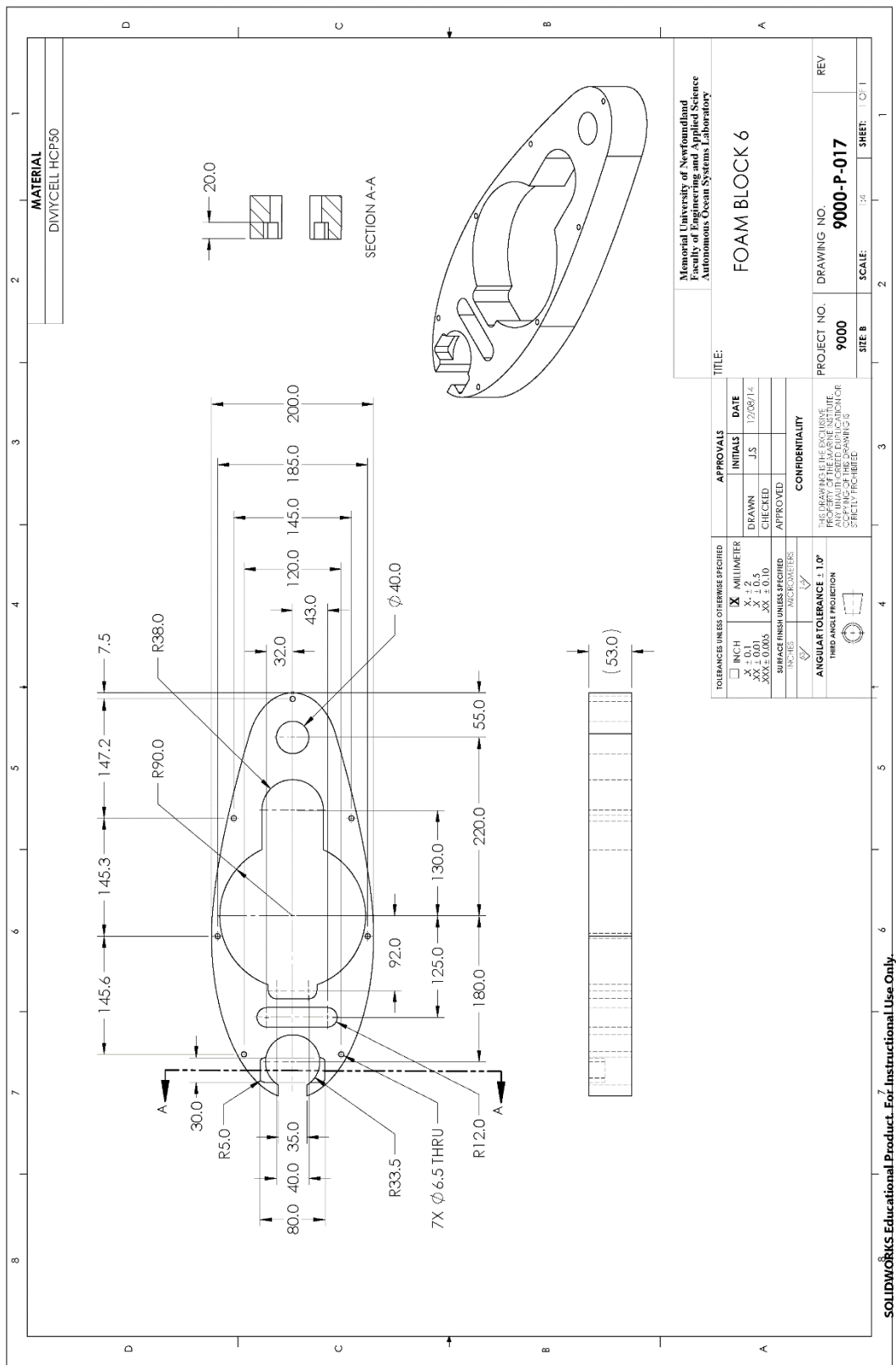


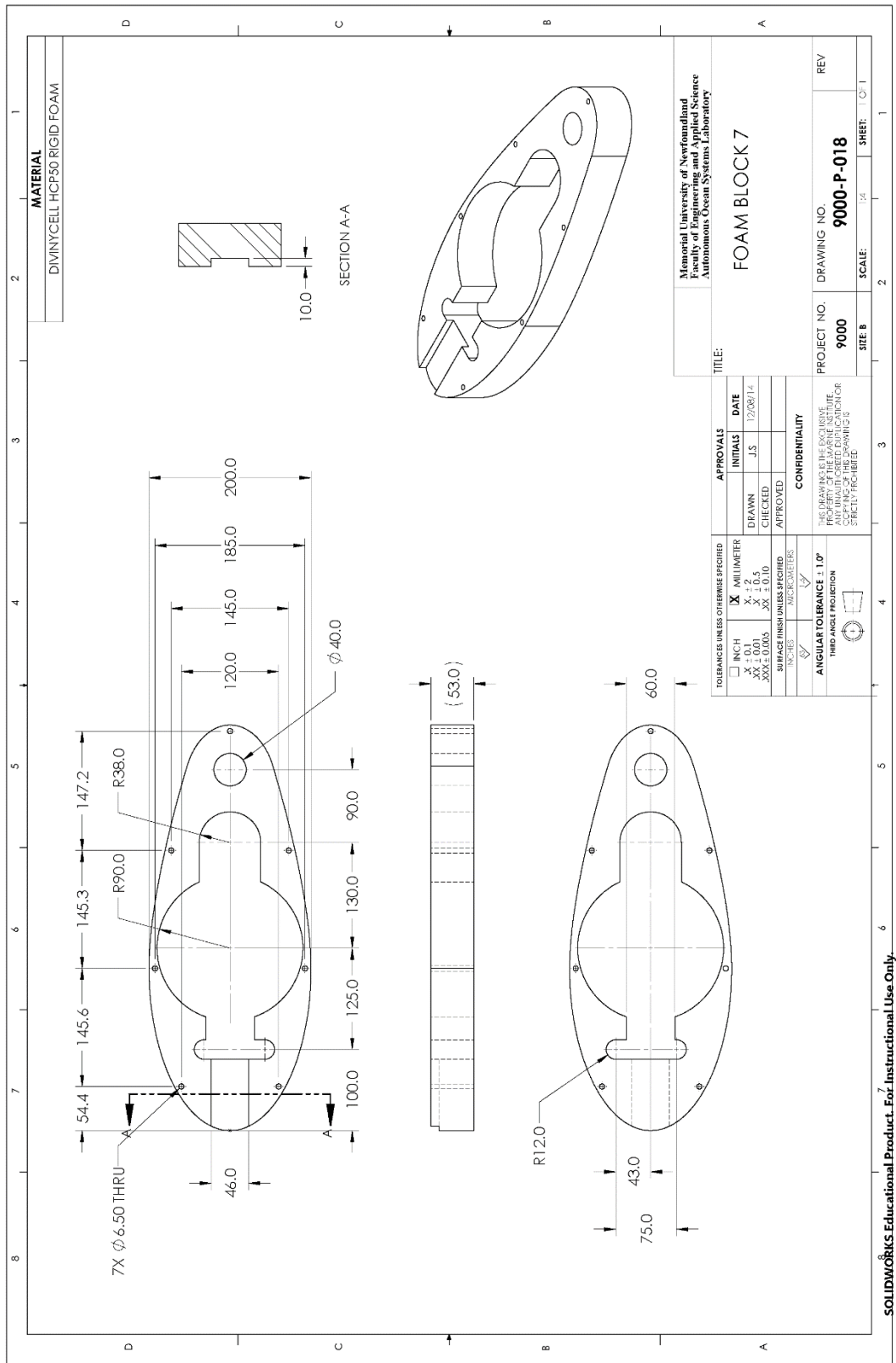


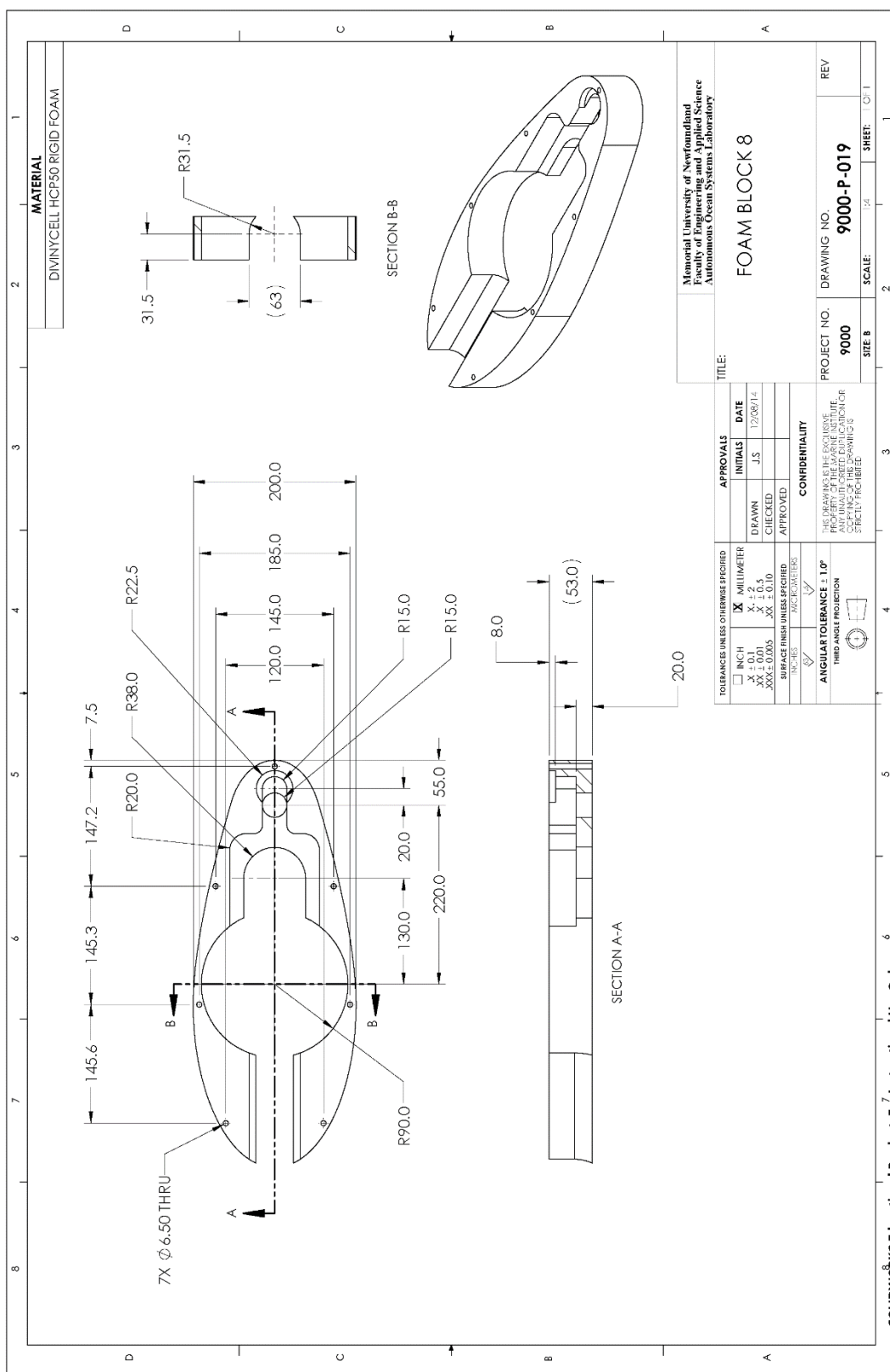


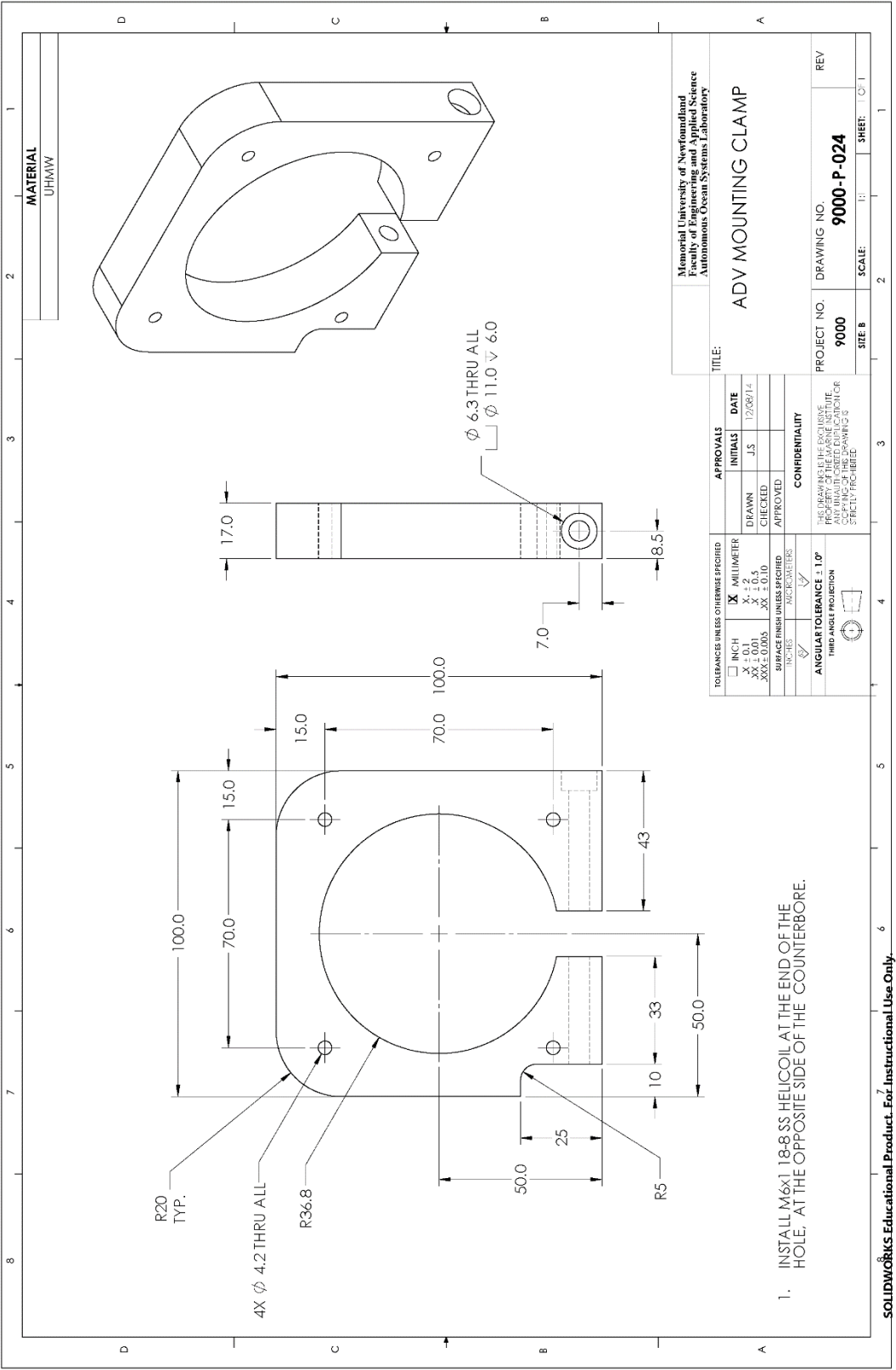


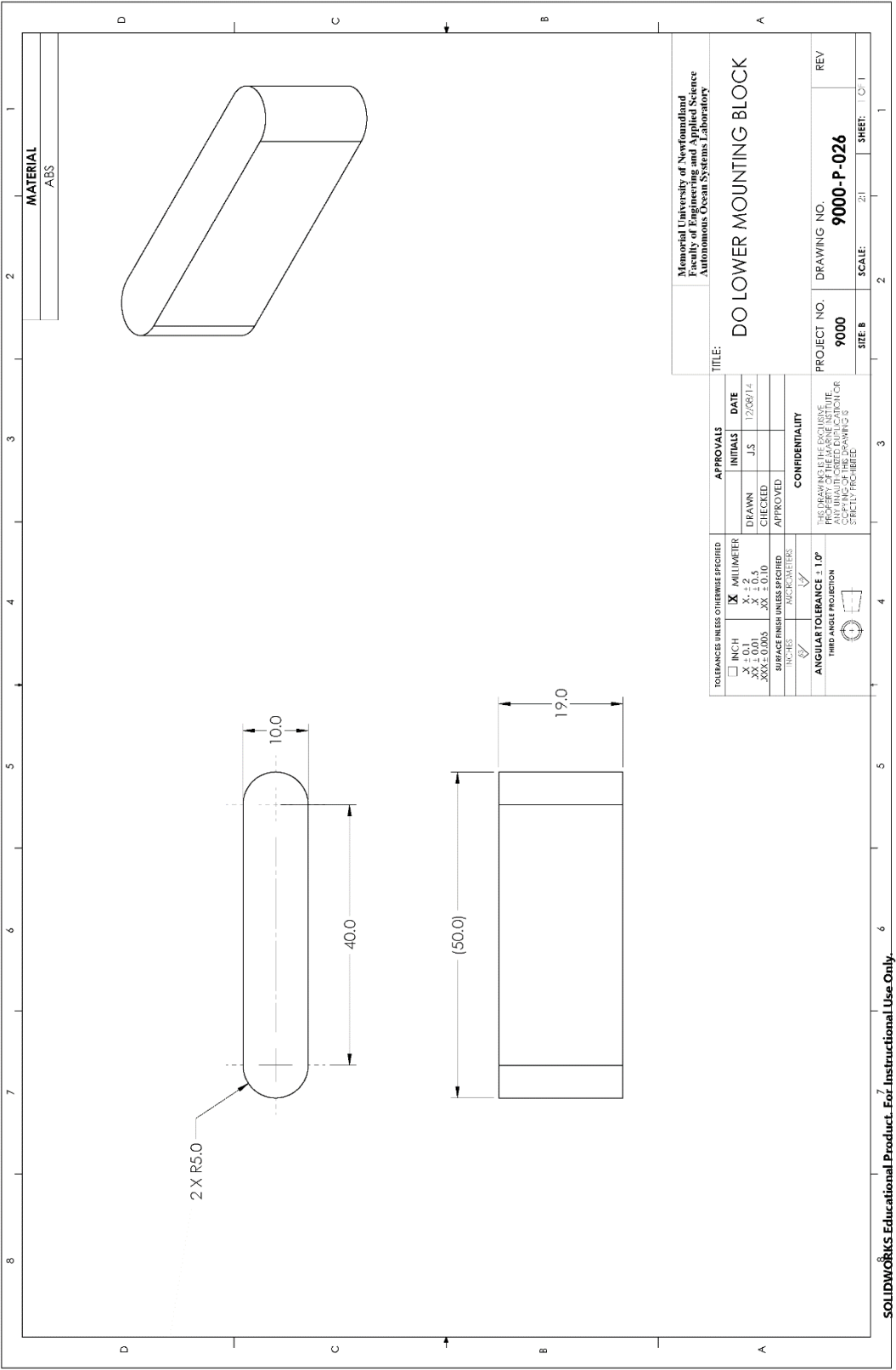


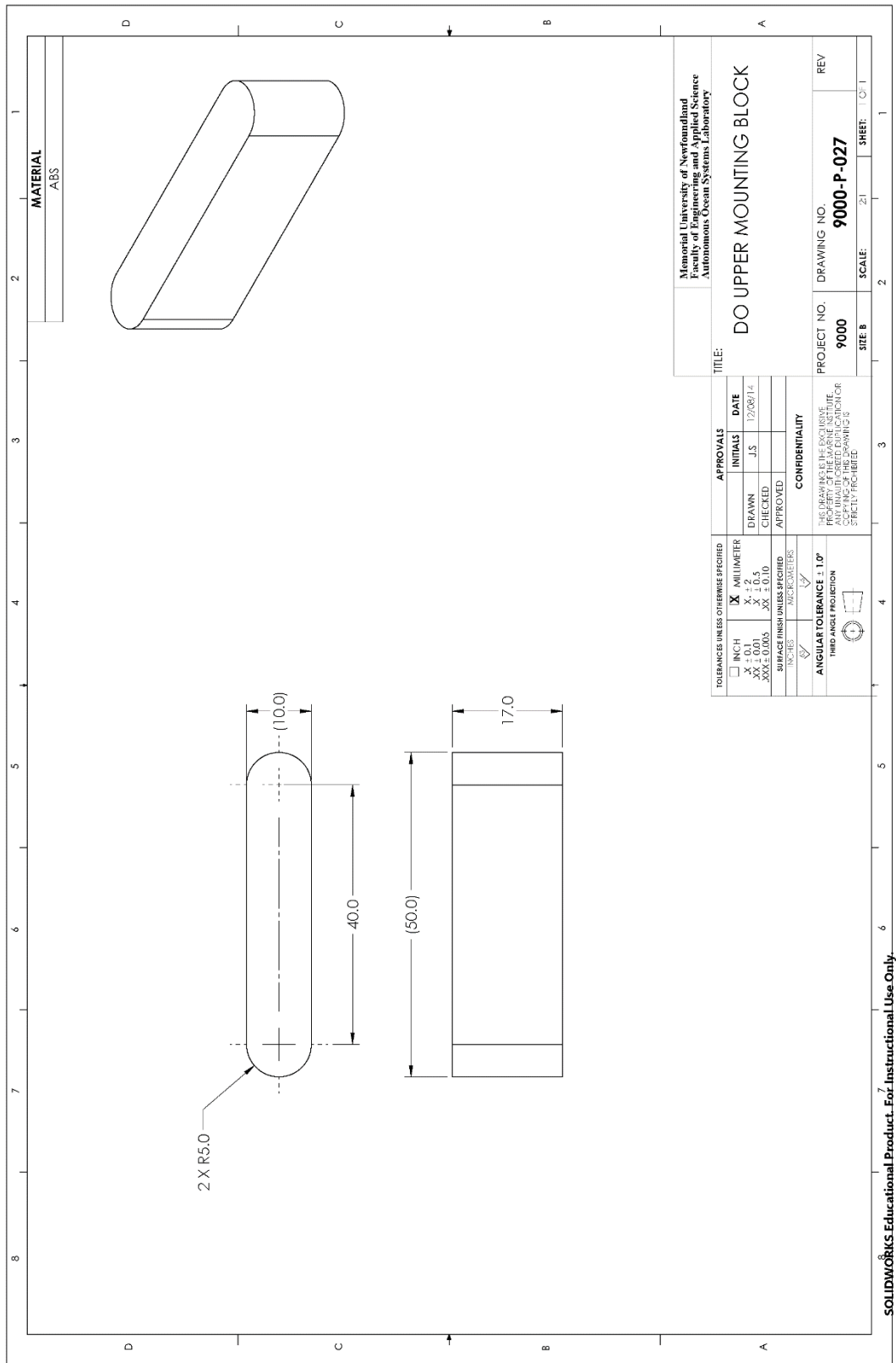


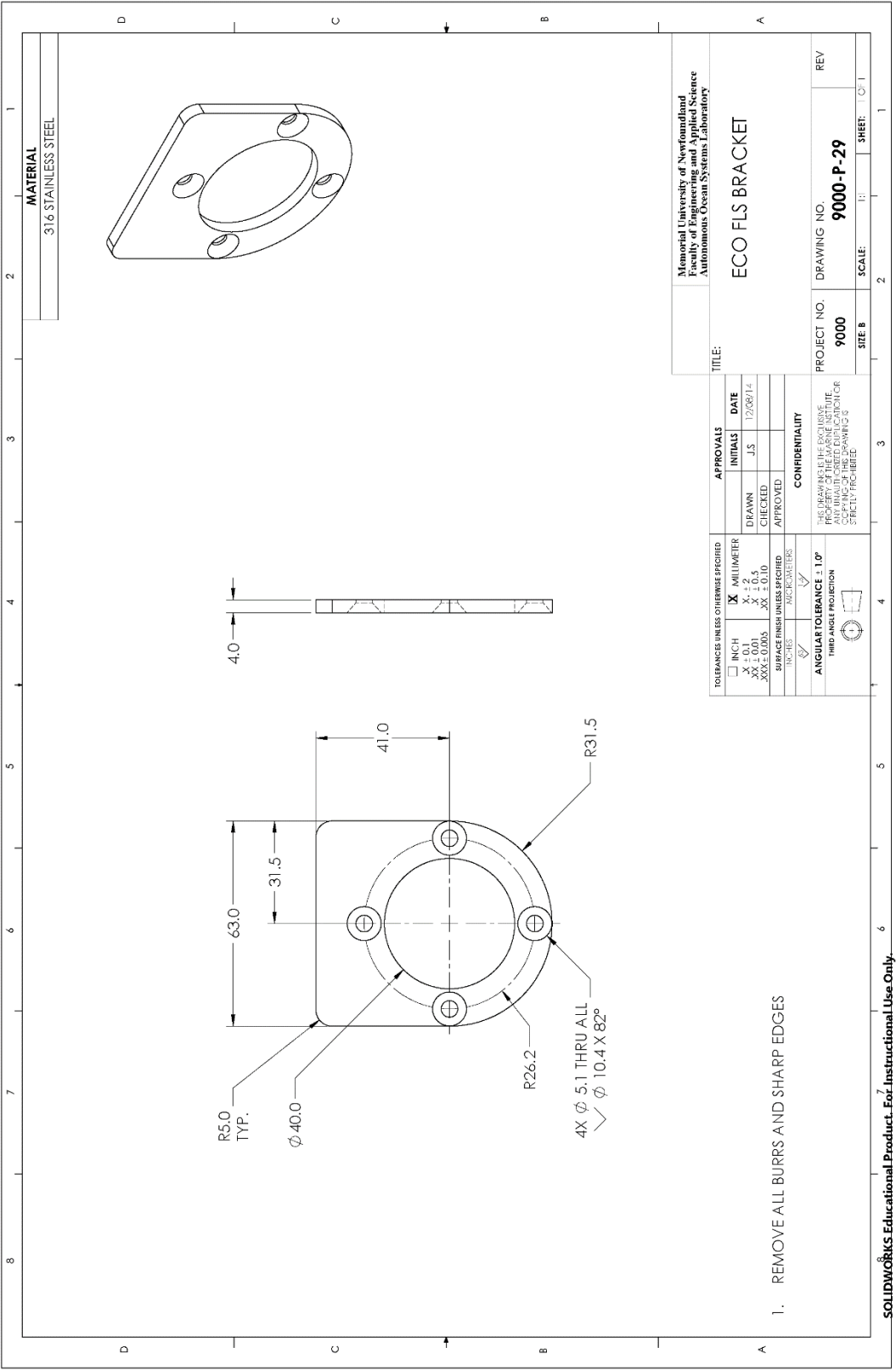


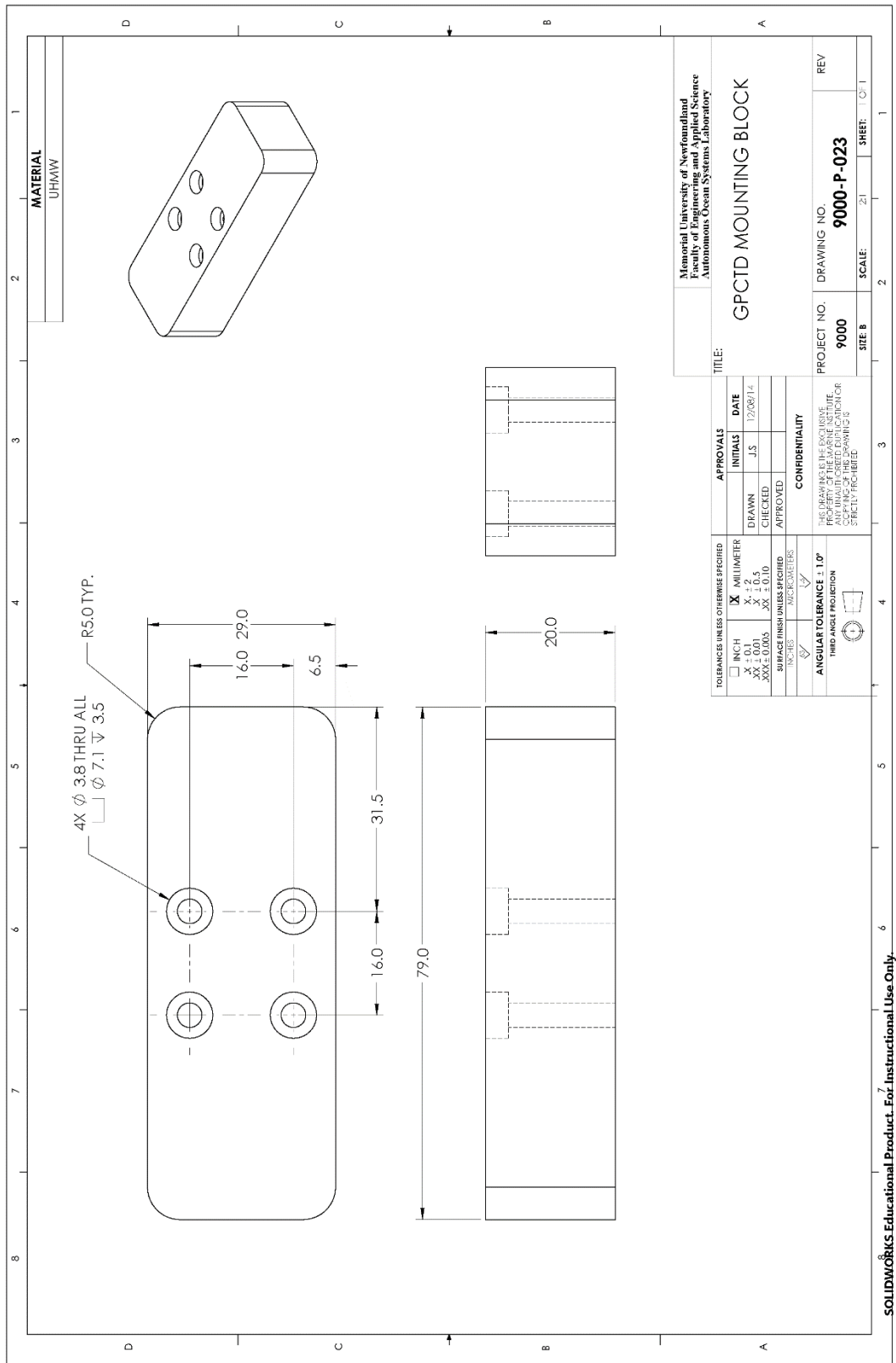


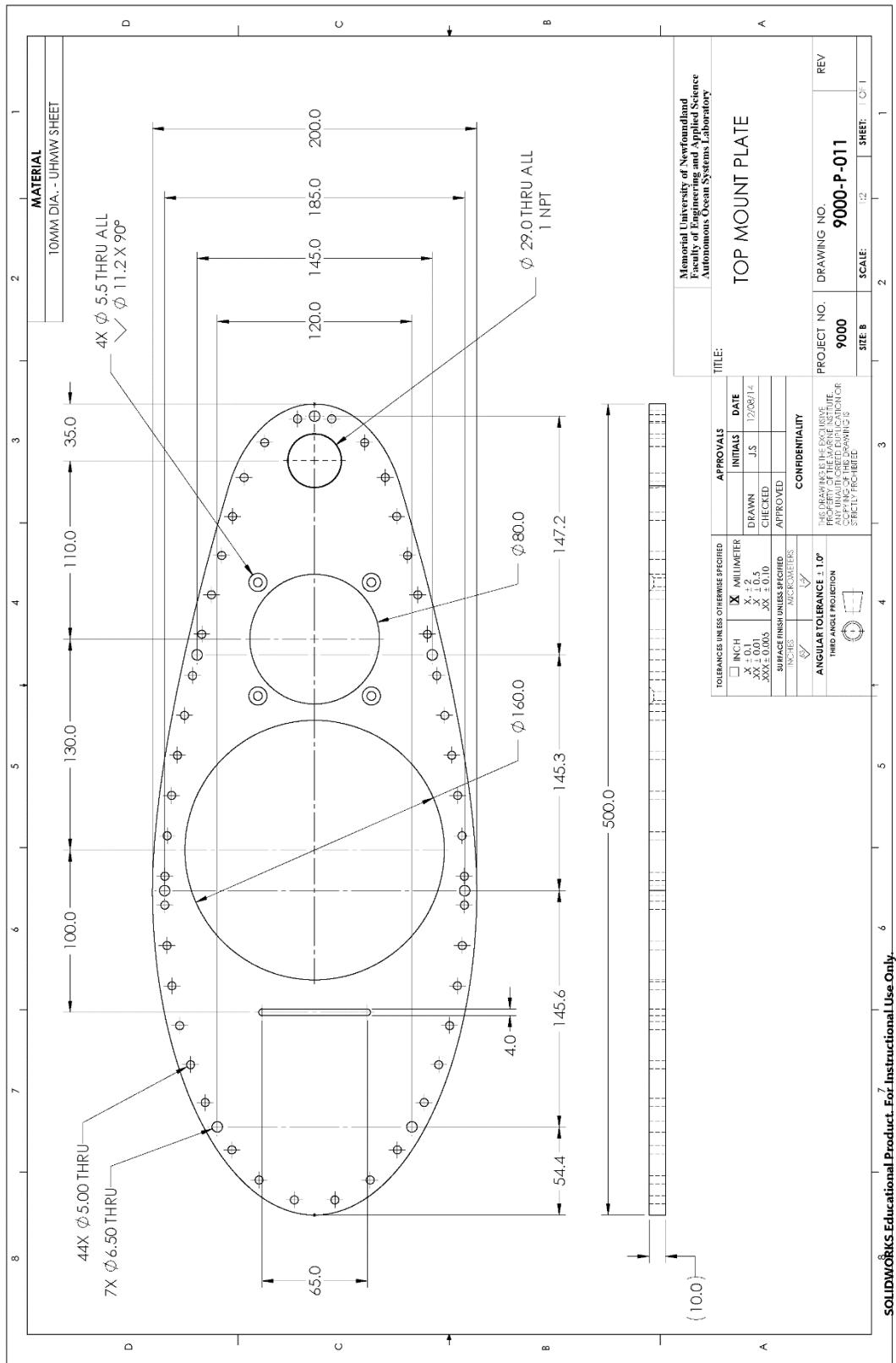


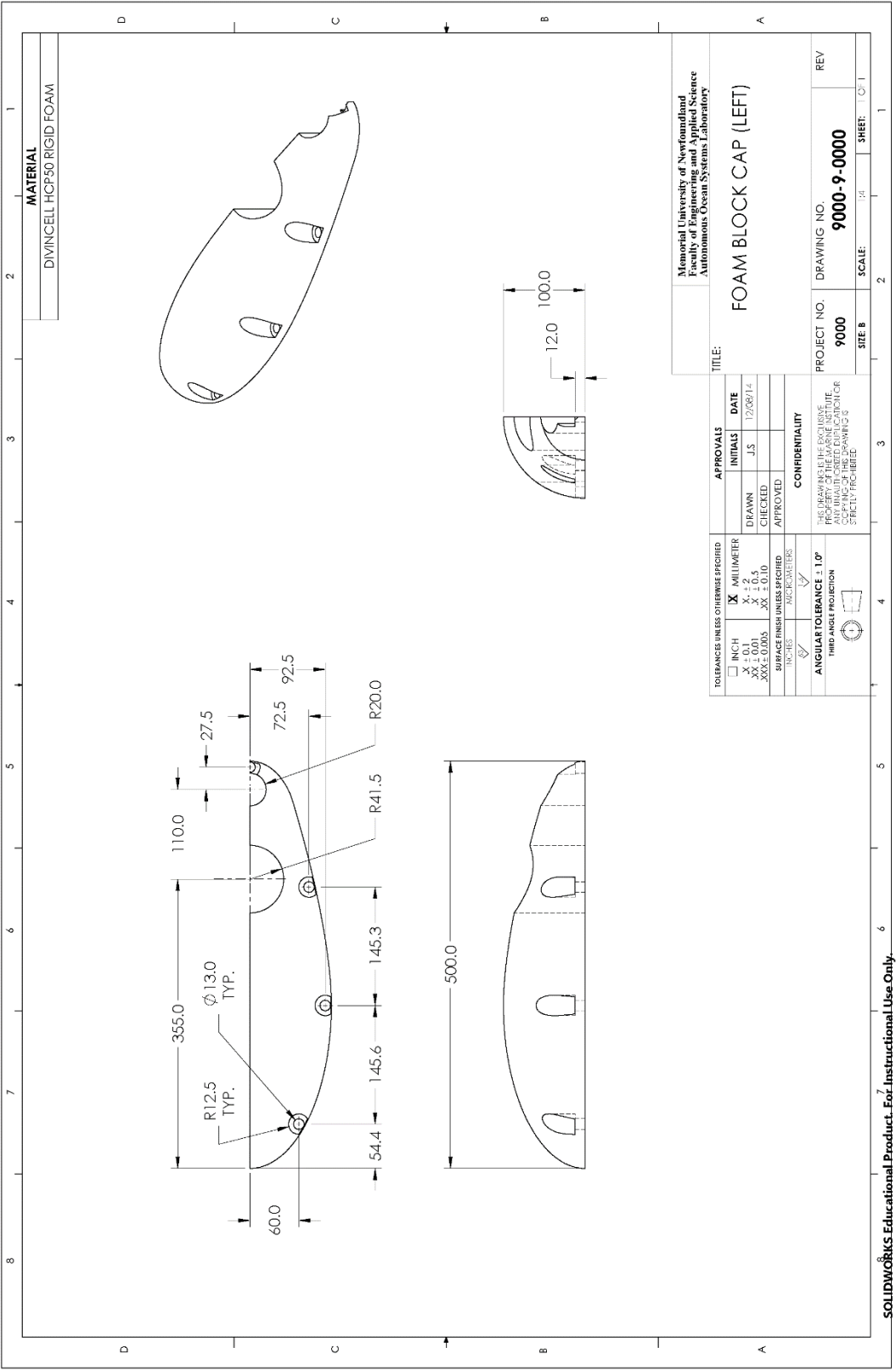


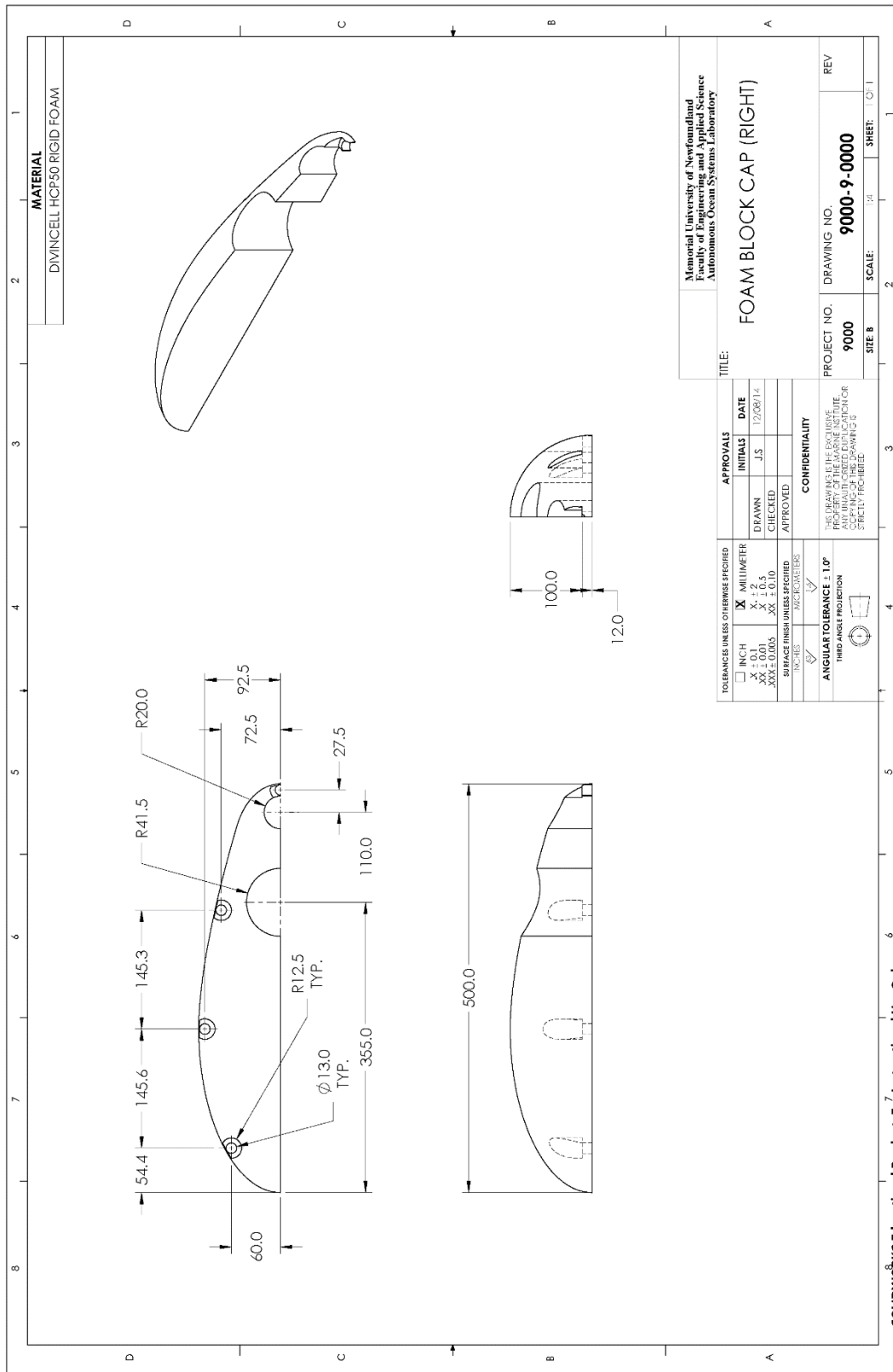


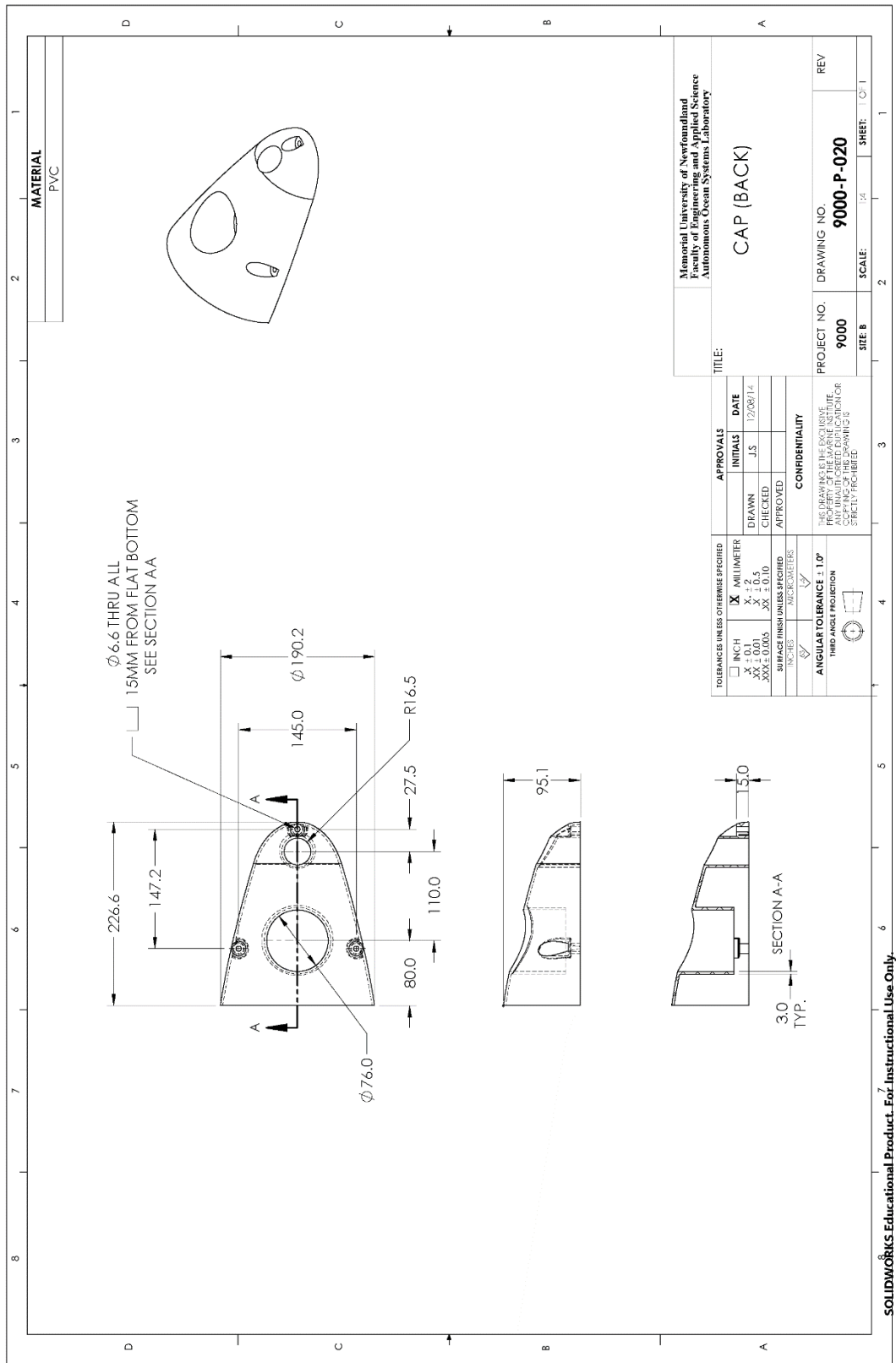


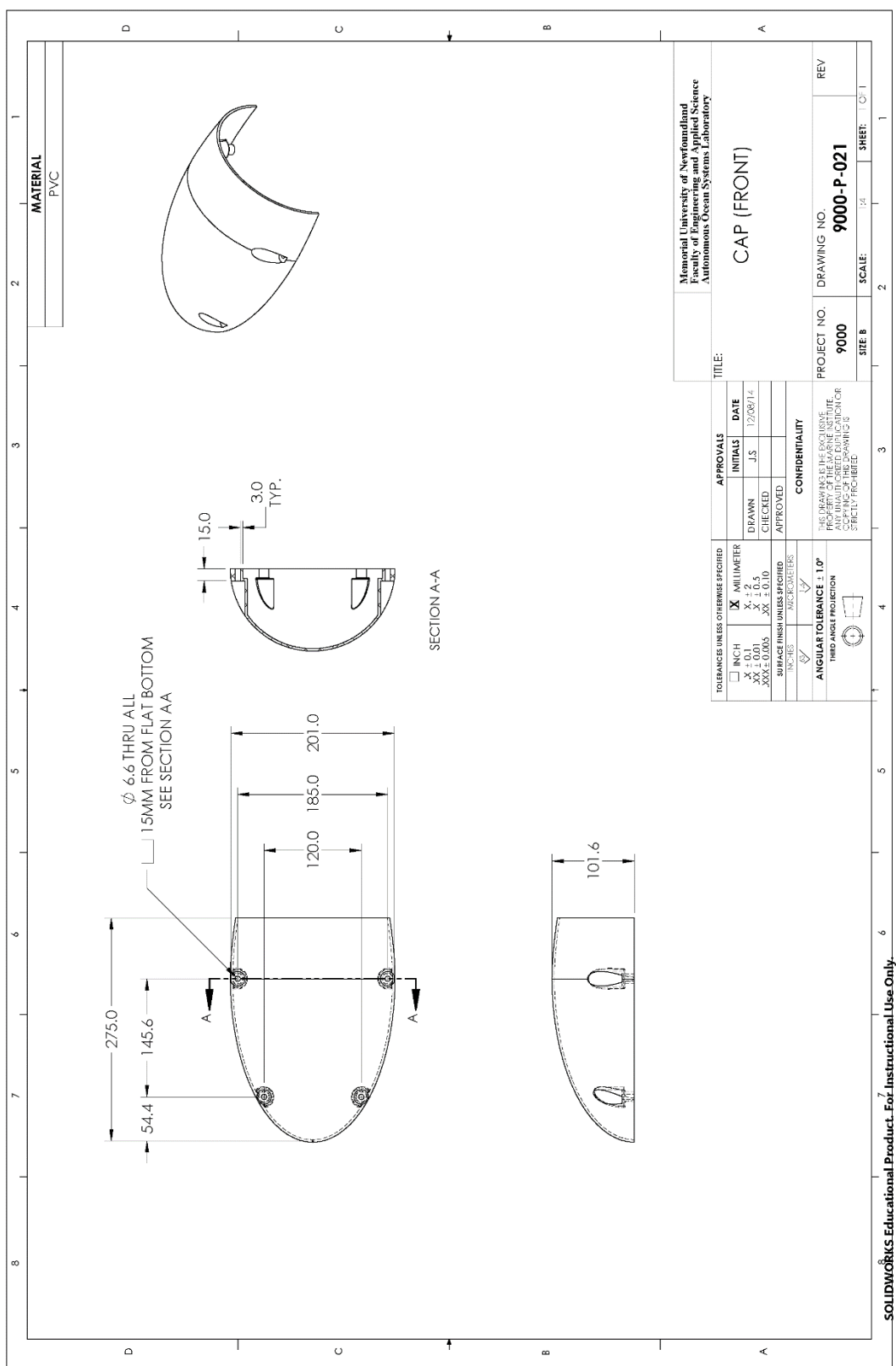


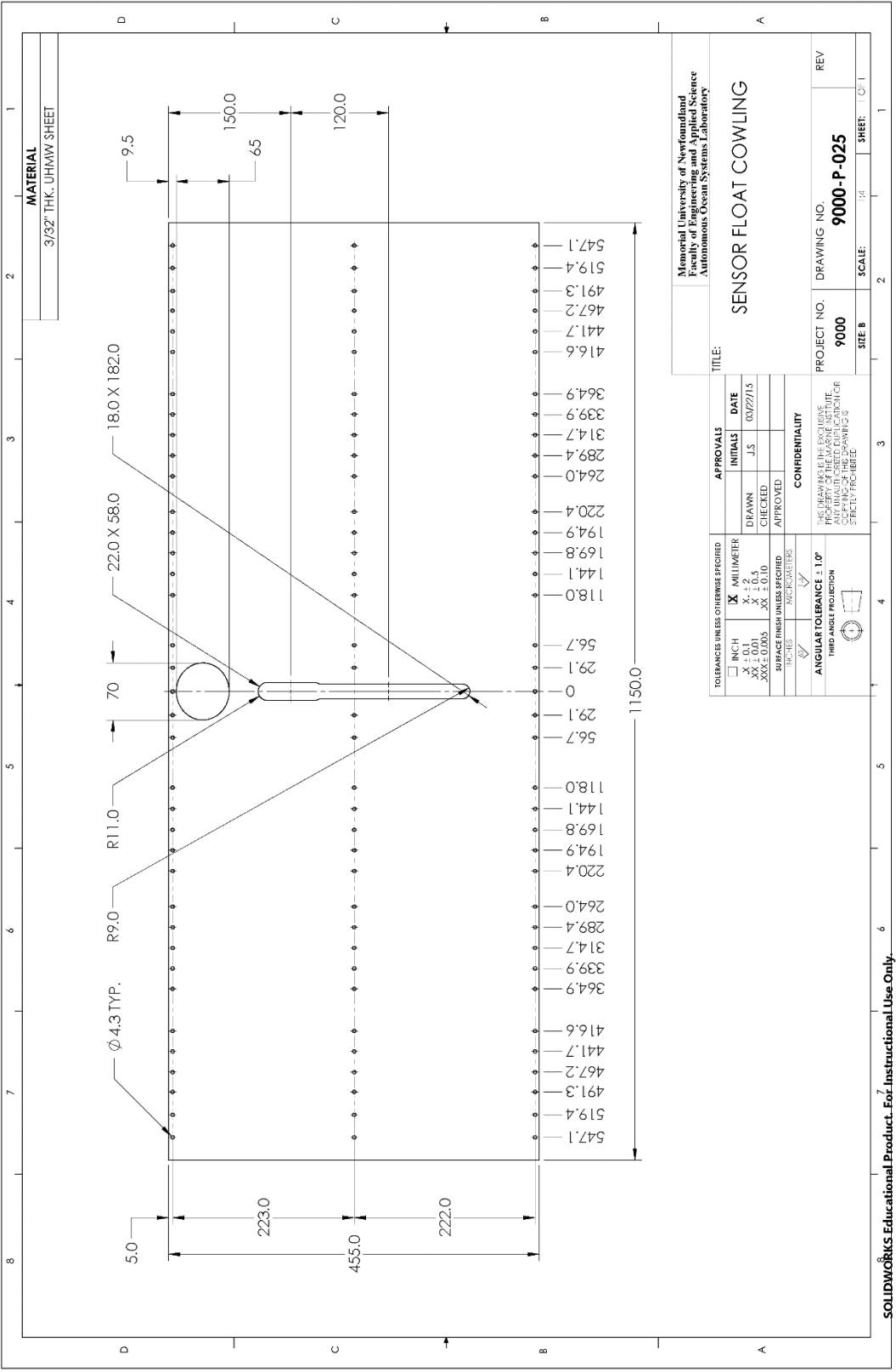


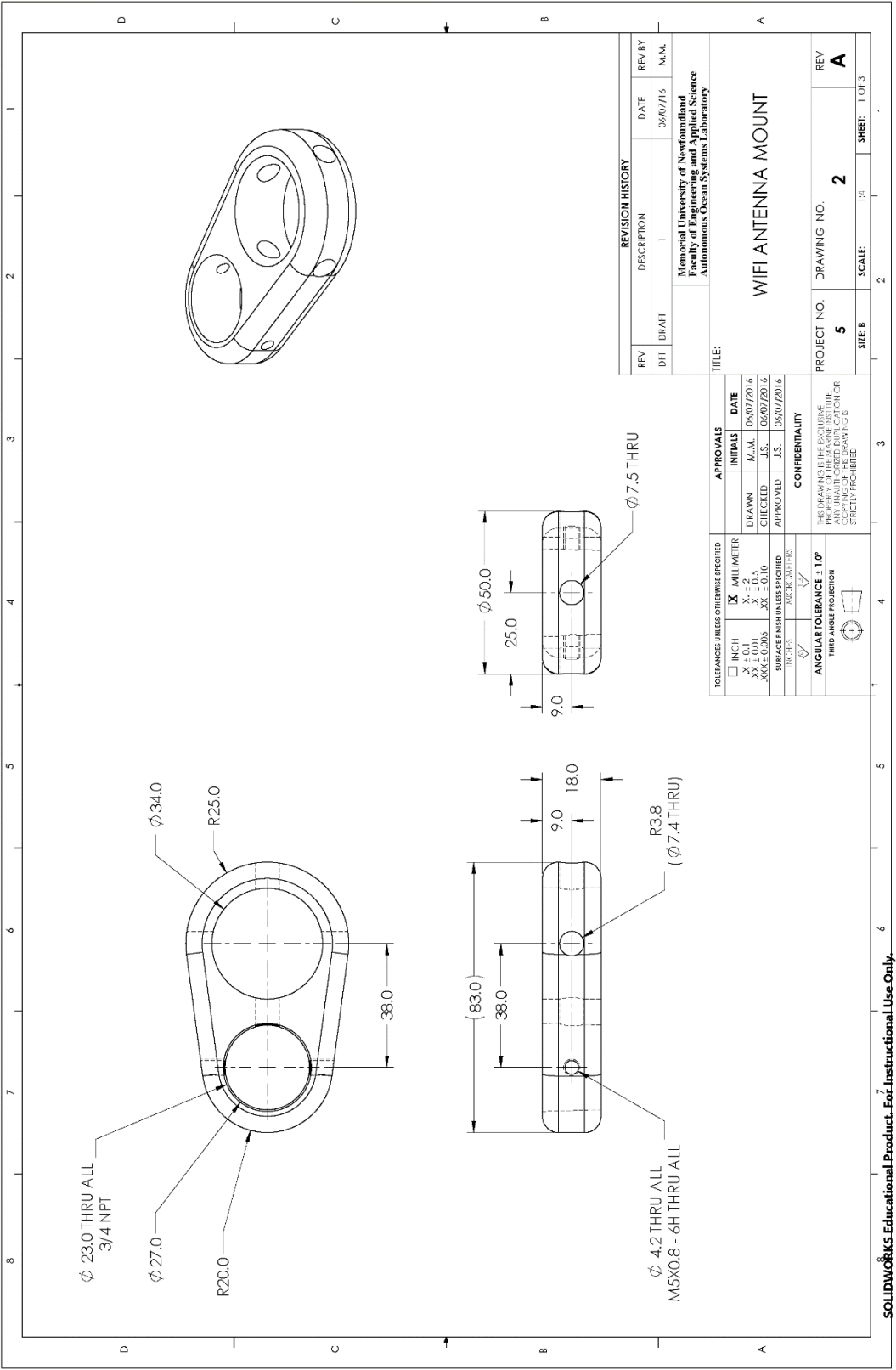


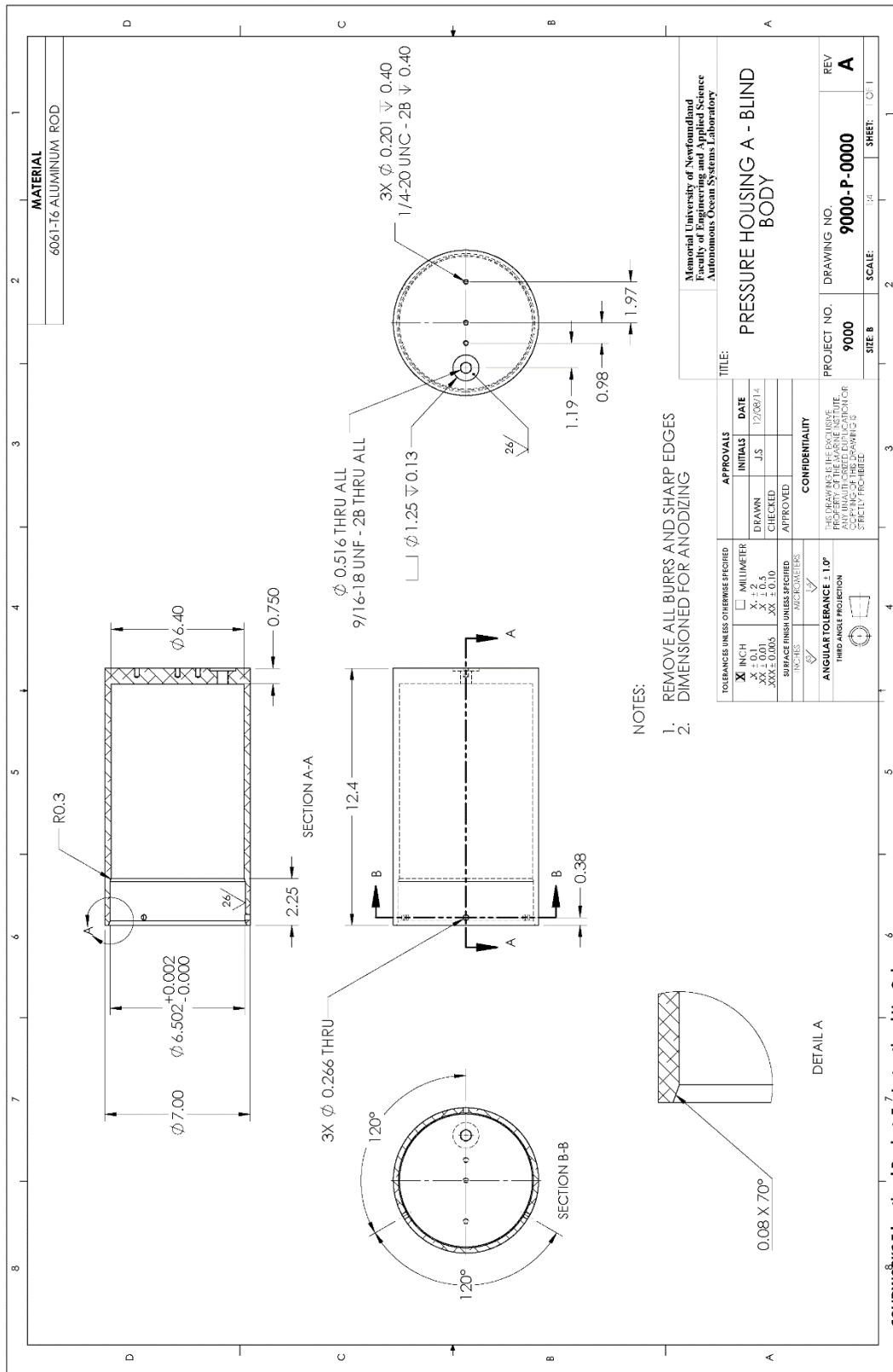


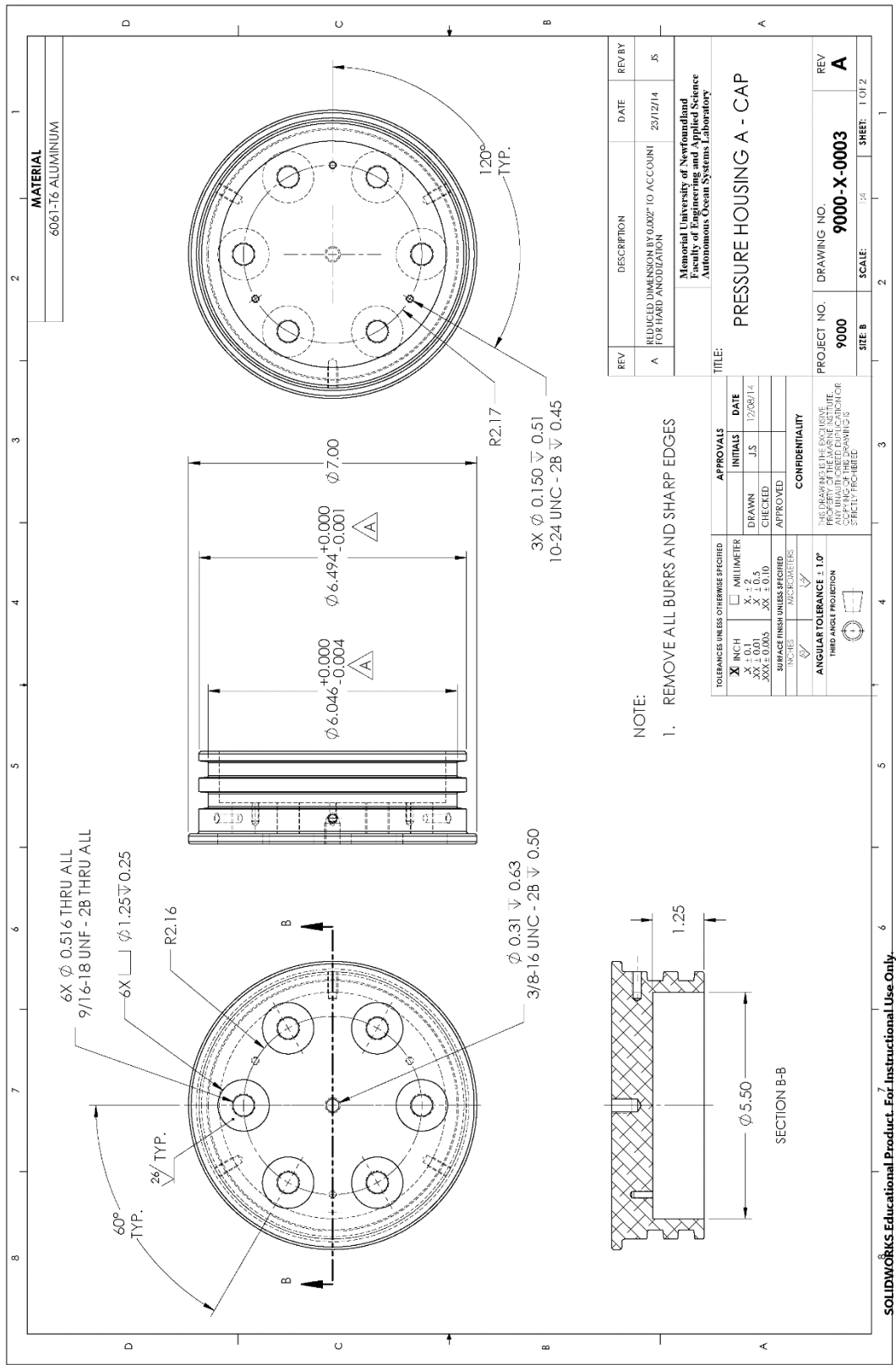


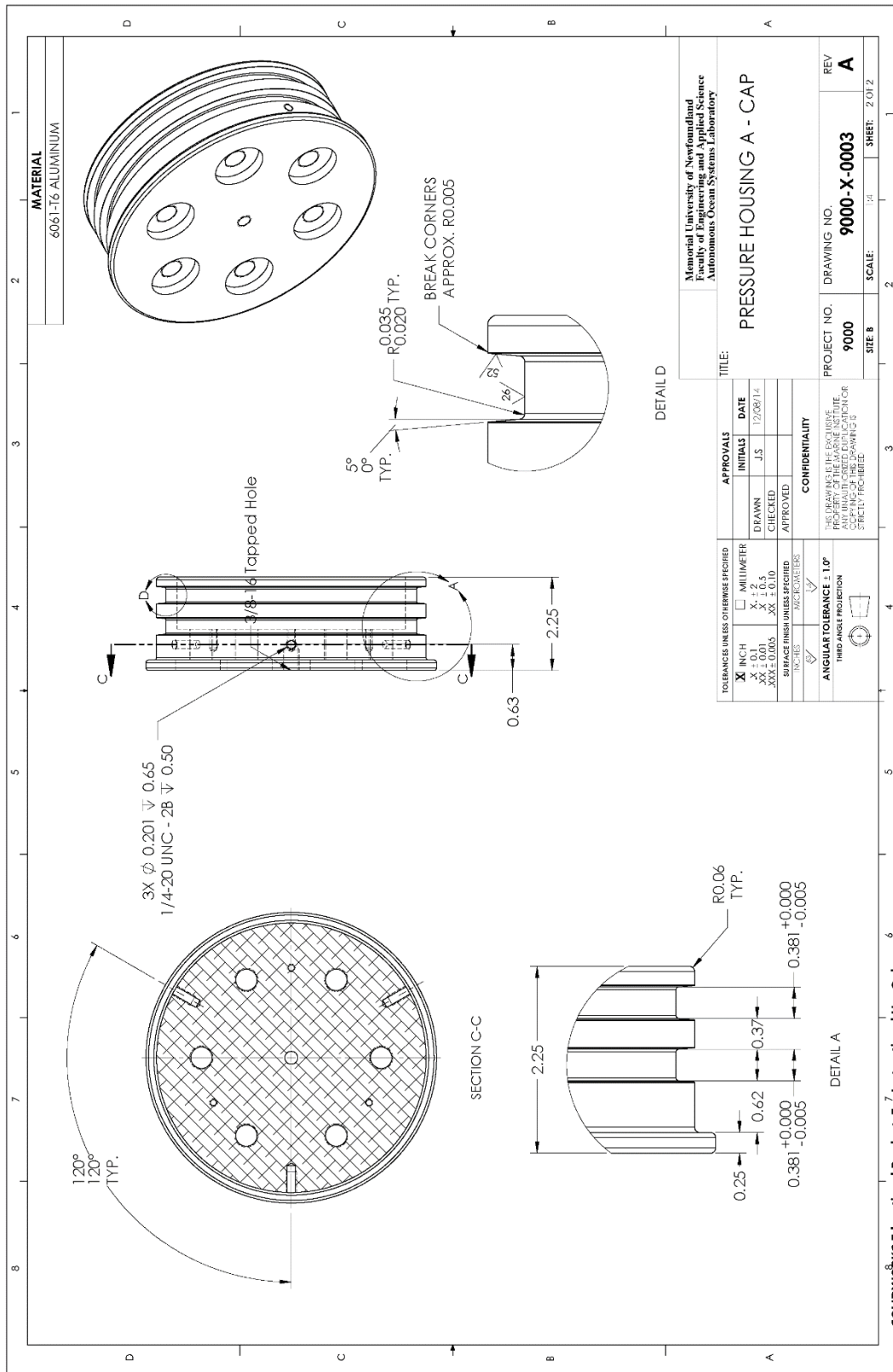




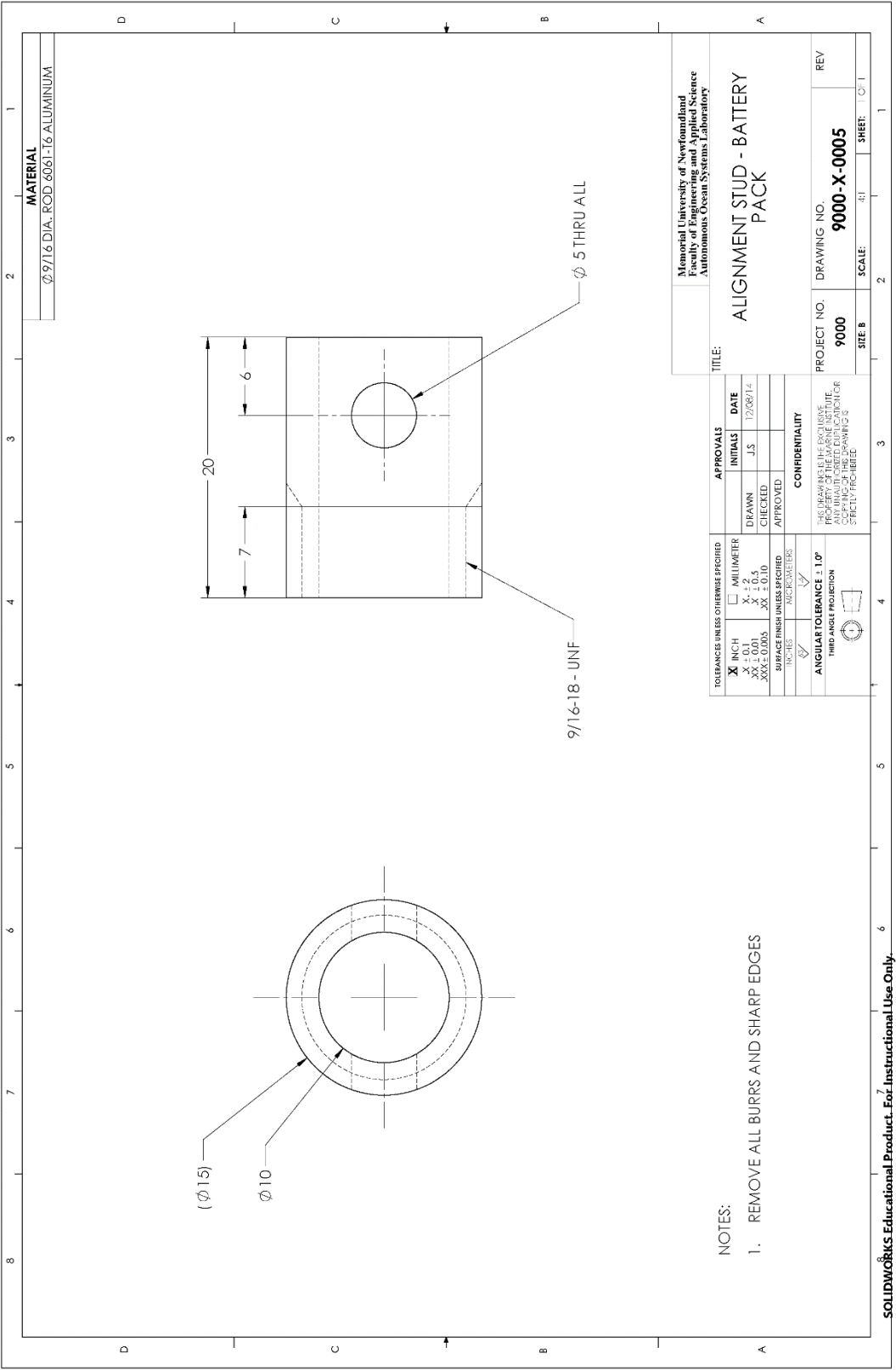


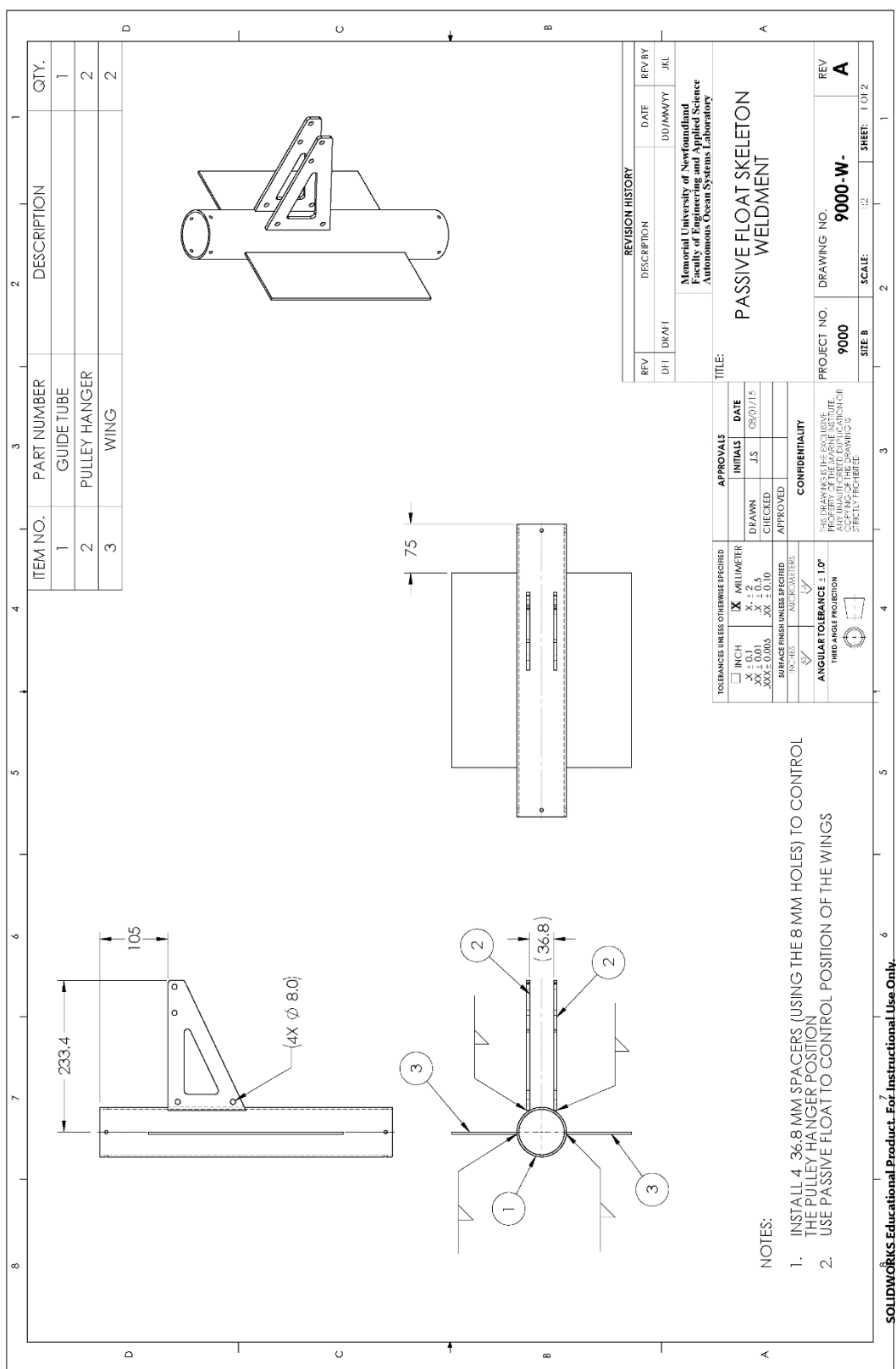


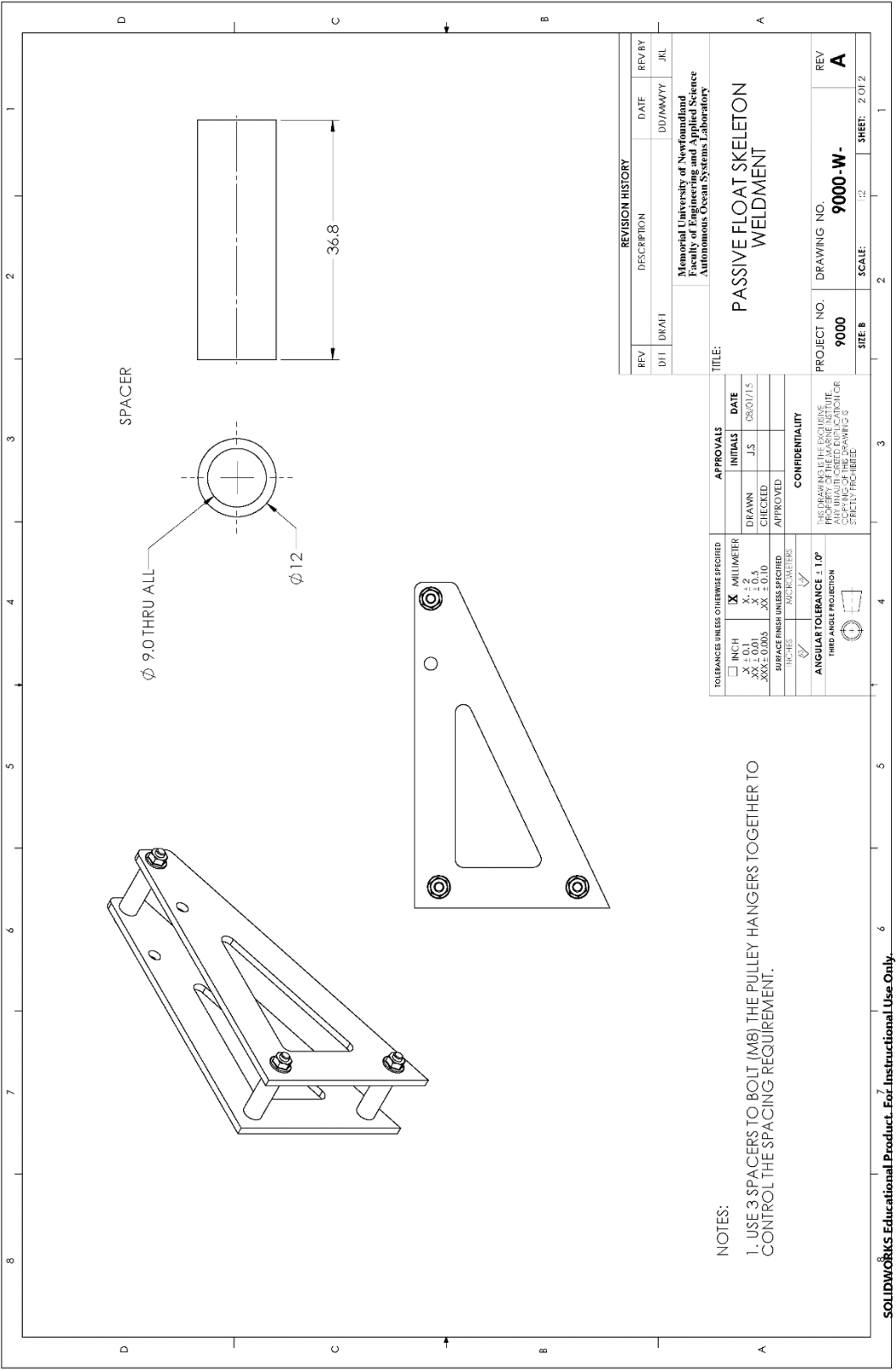


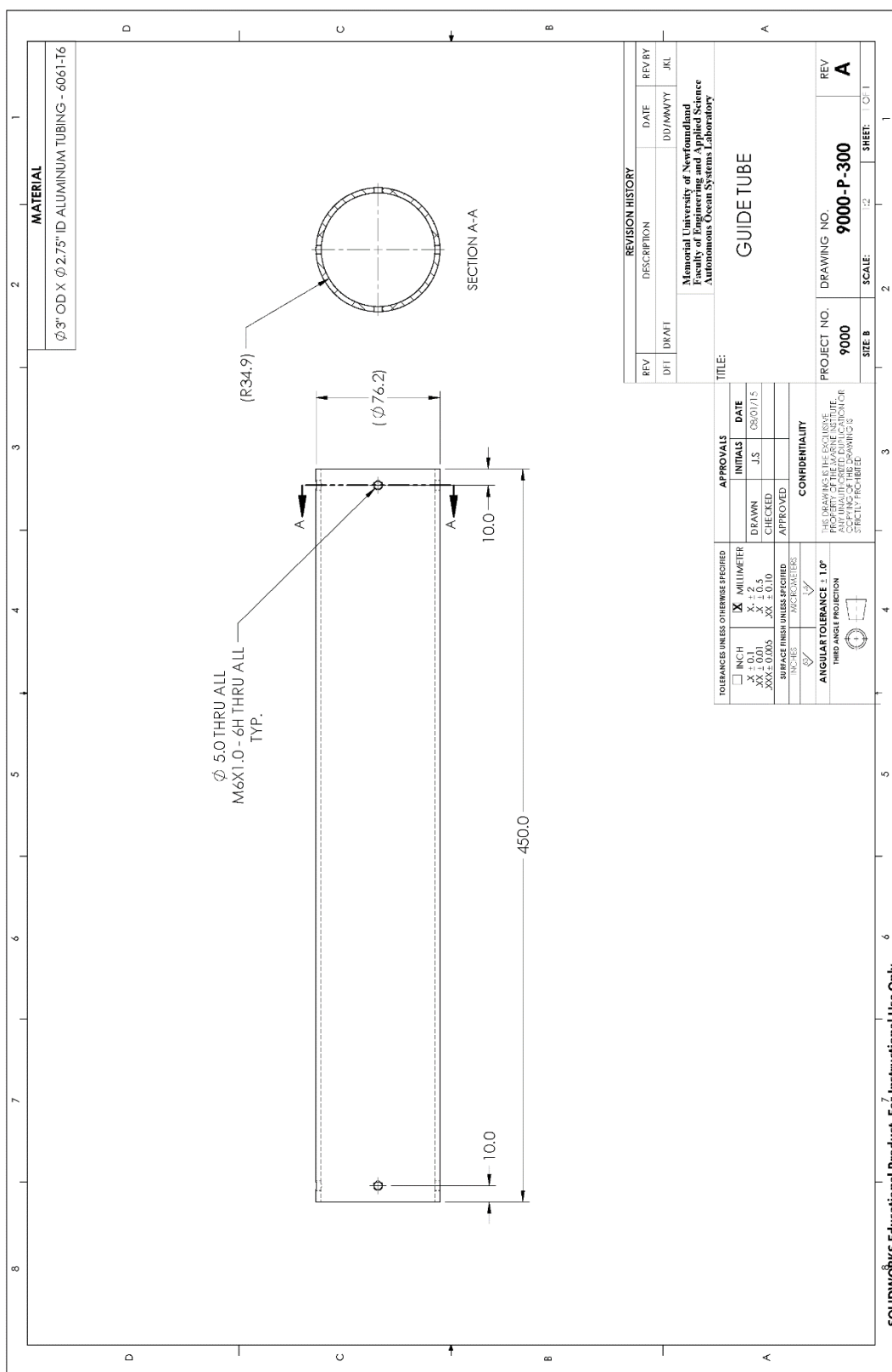


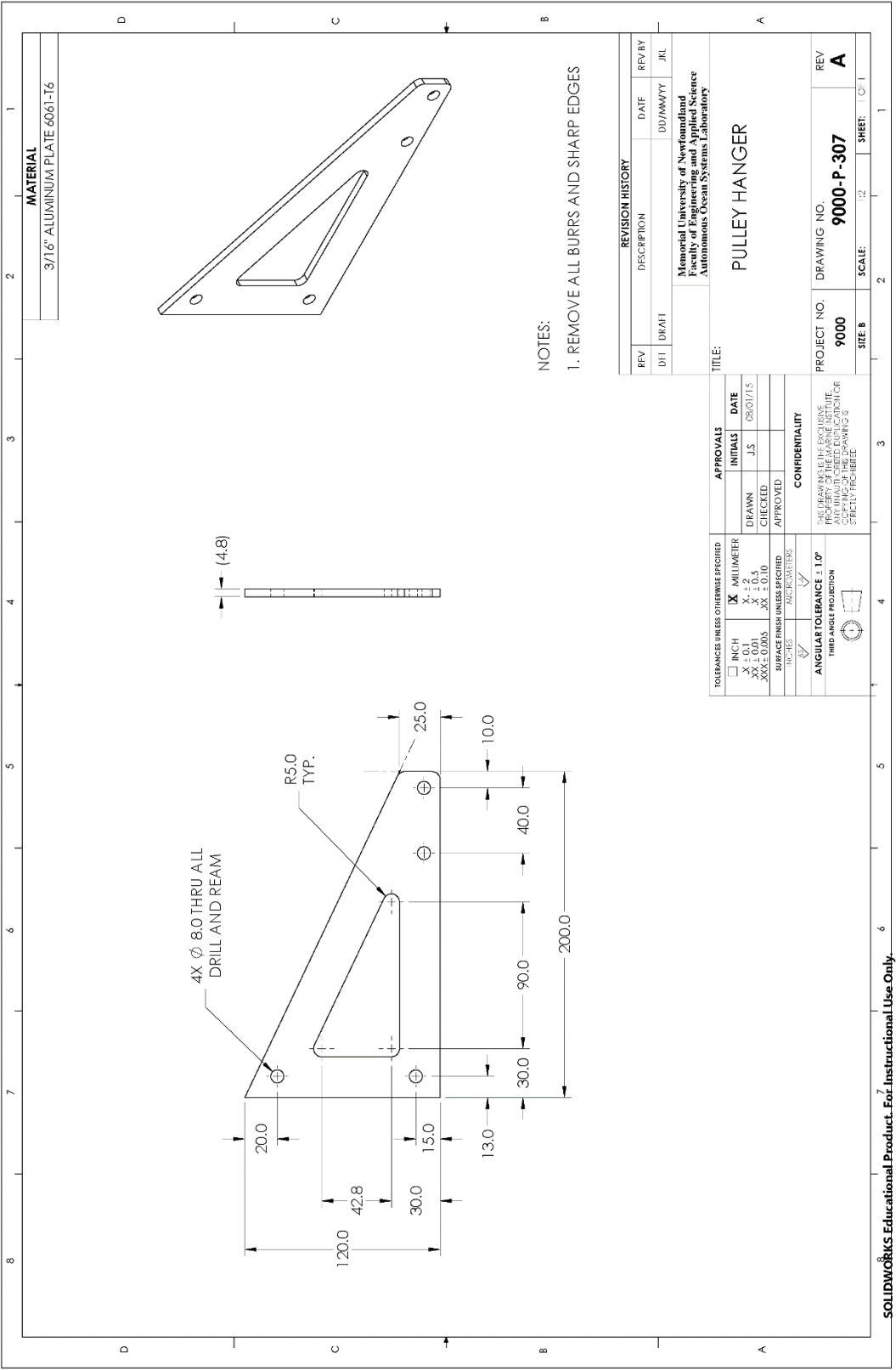
SOLIDWORKS Educational Product. For Instructional Use Only.

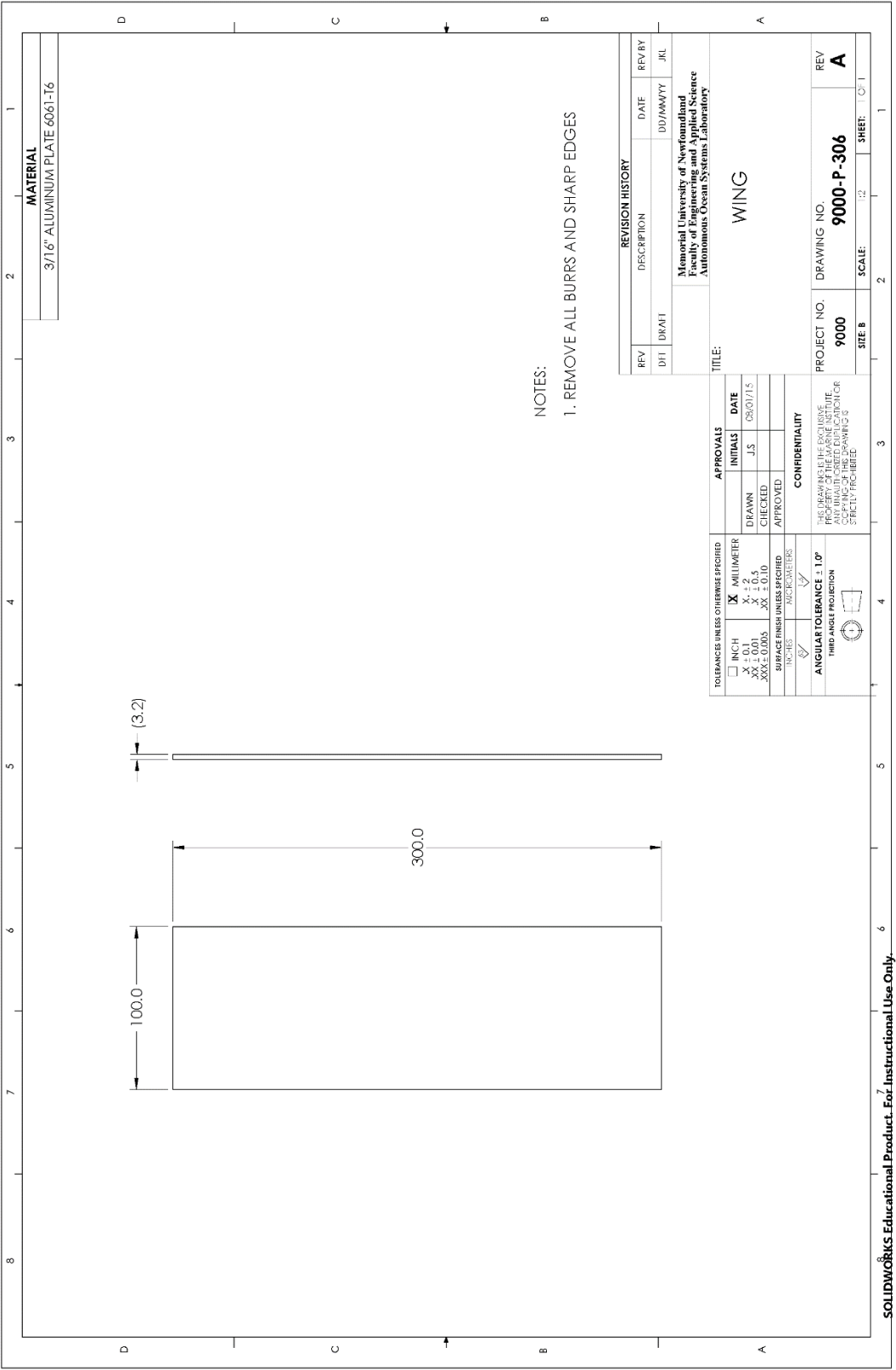


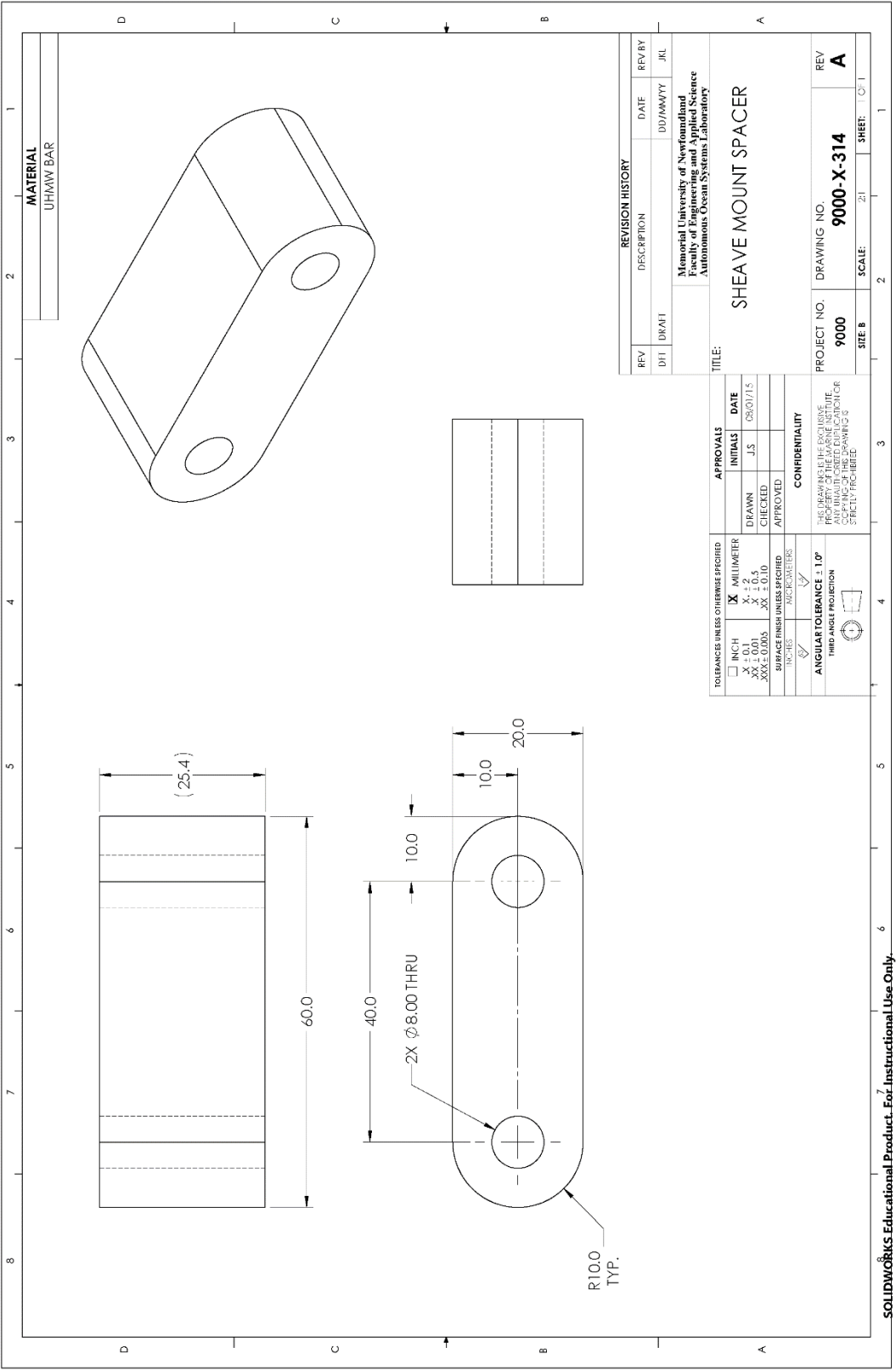


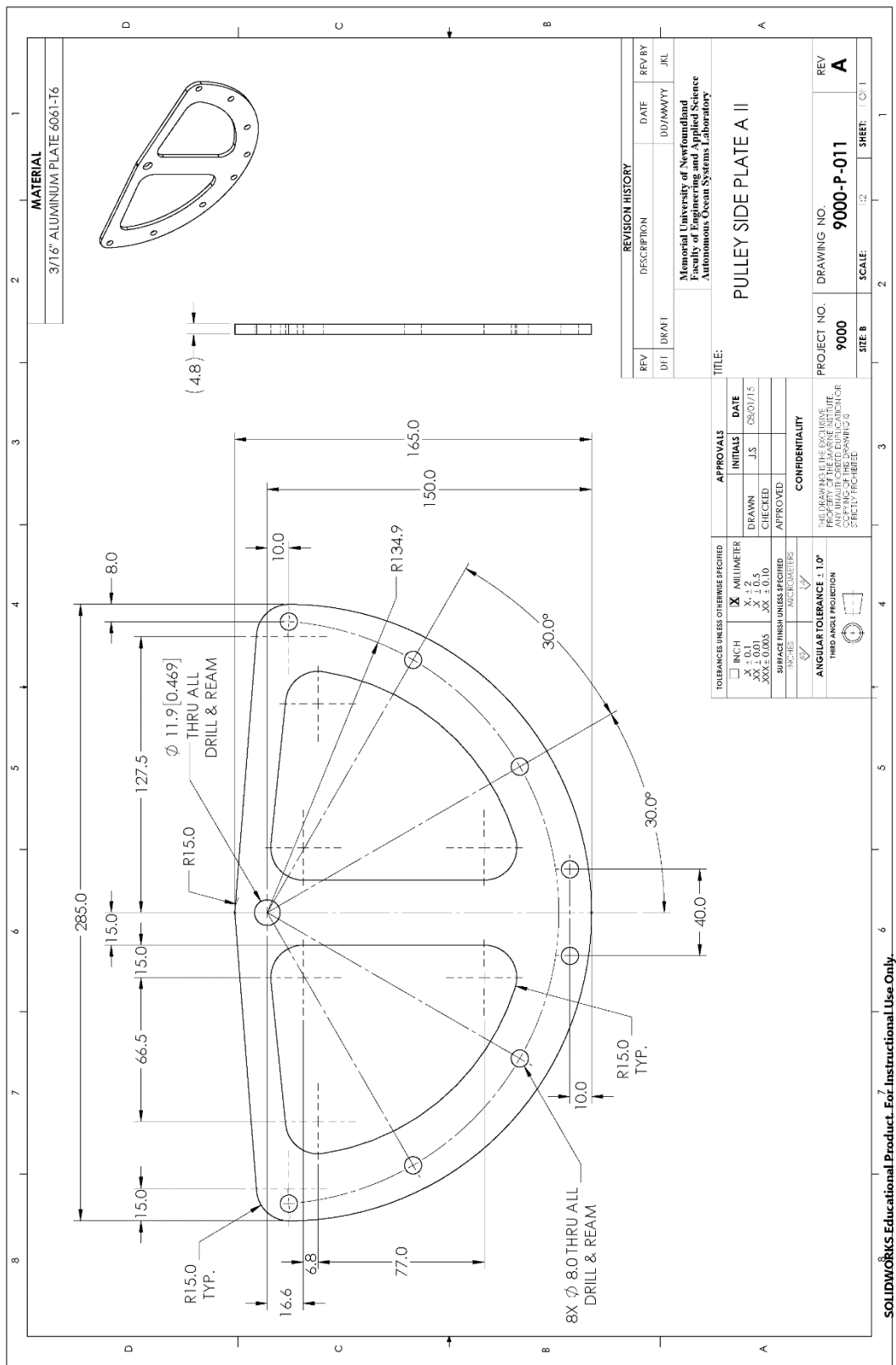


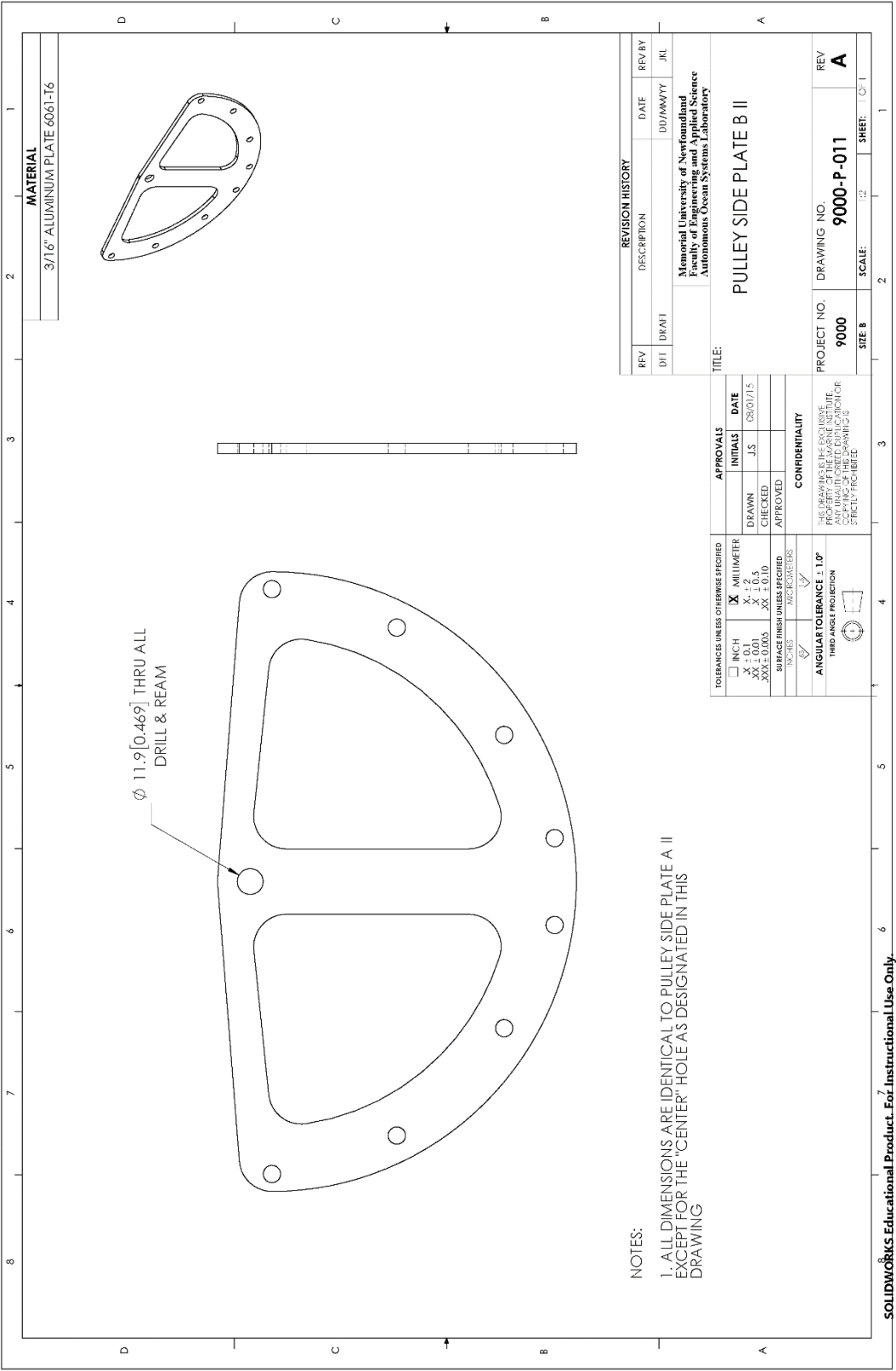


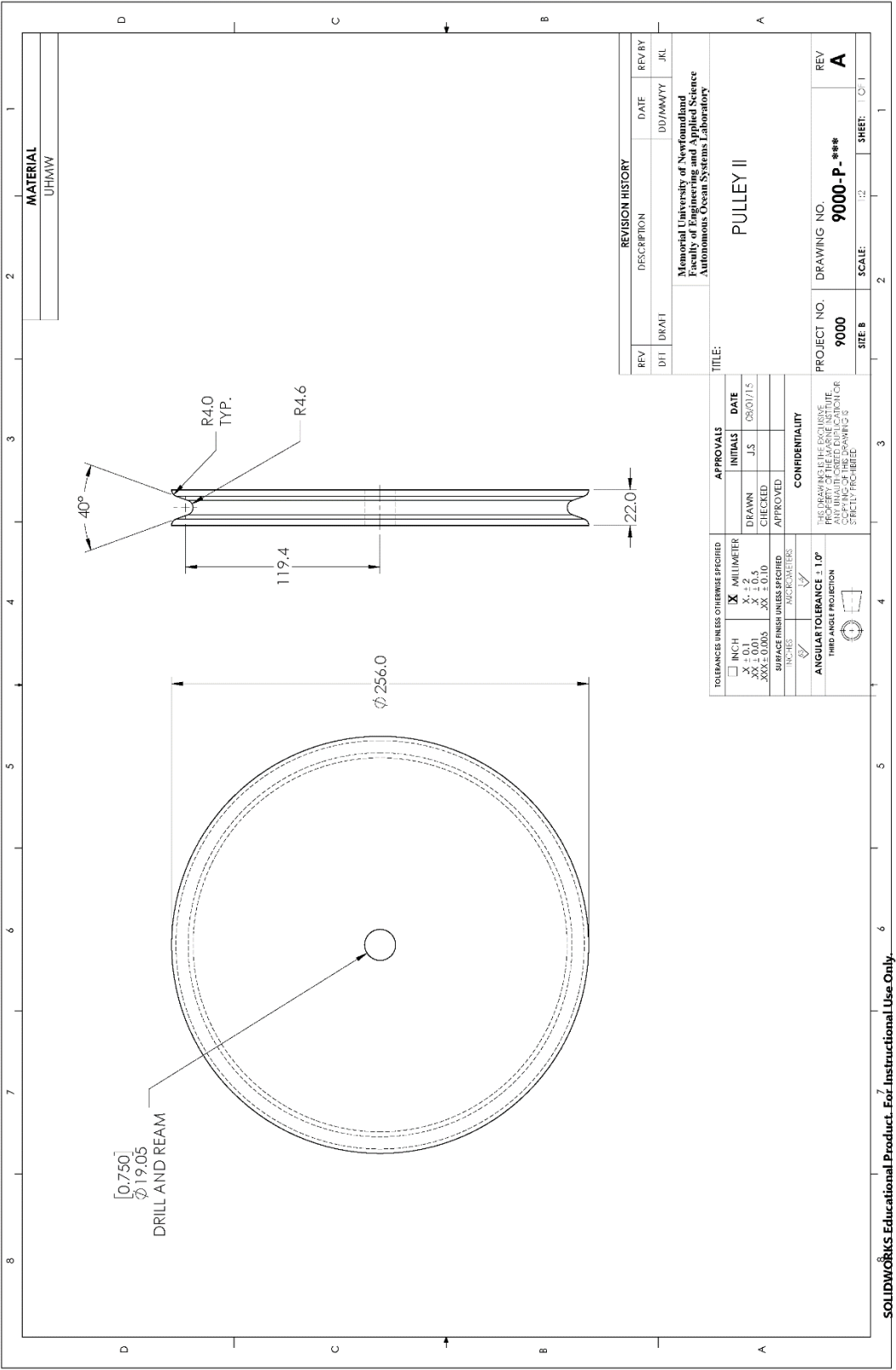


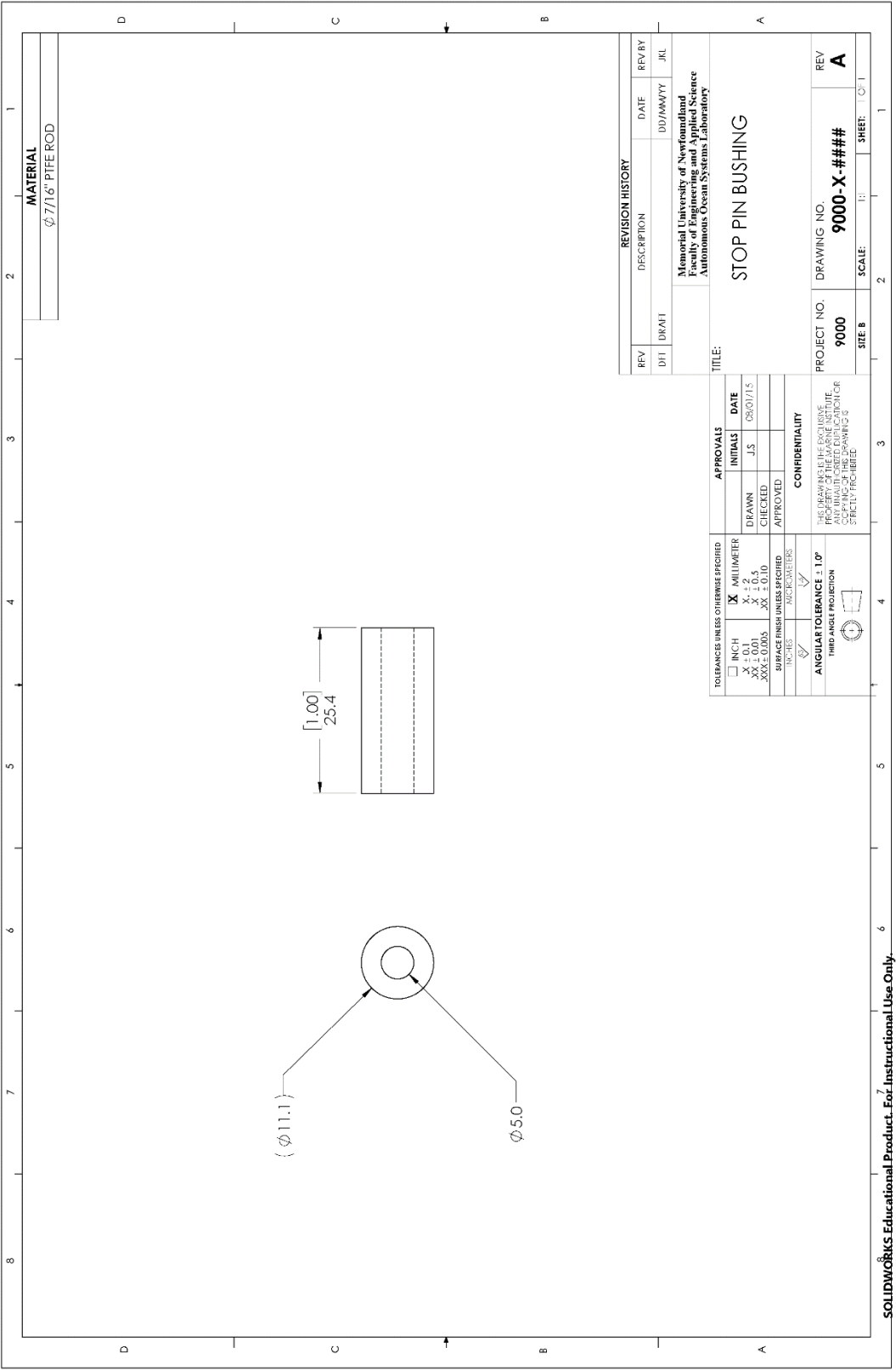


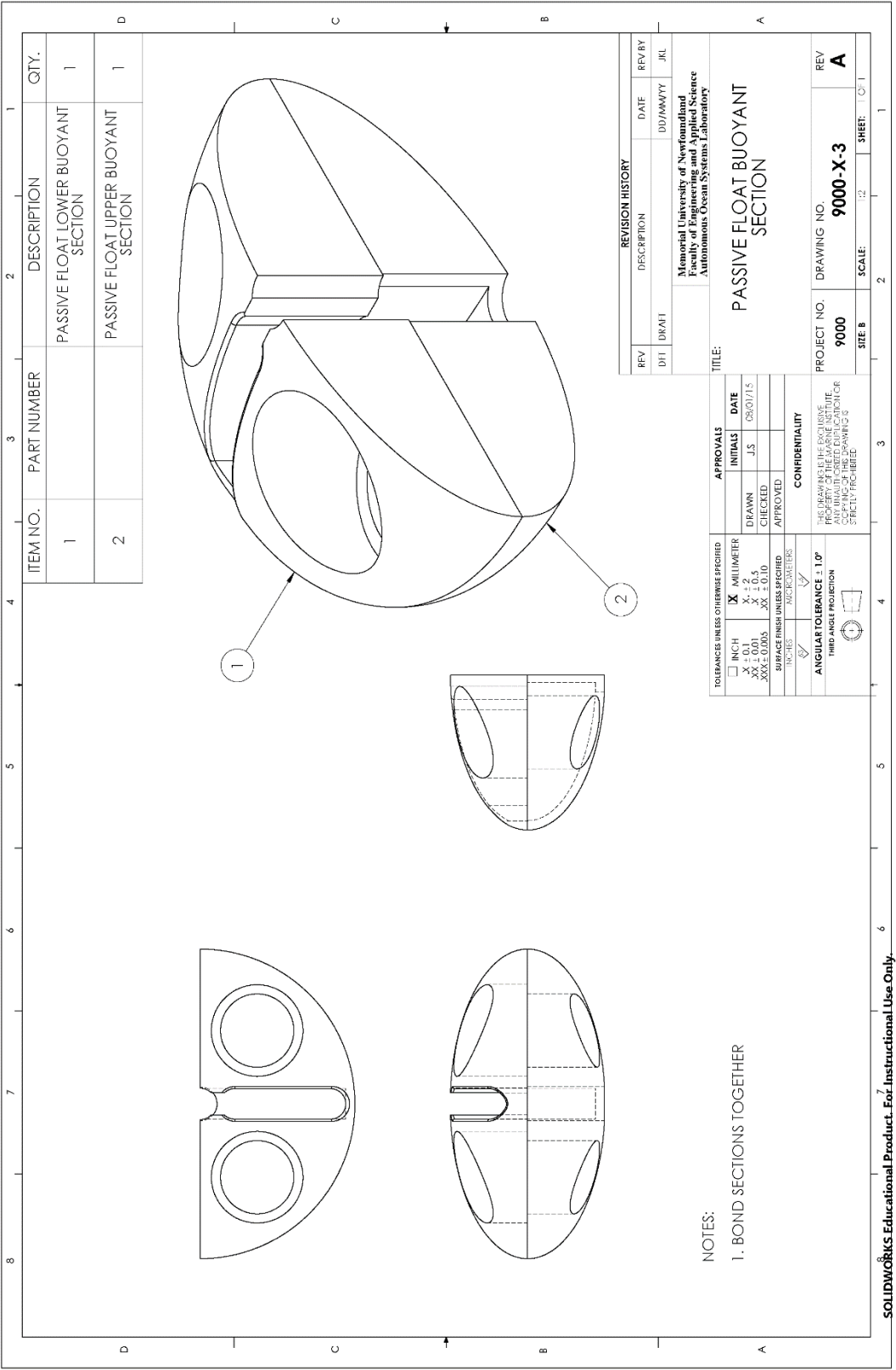


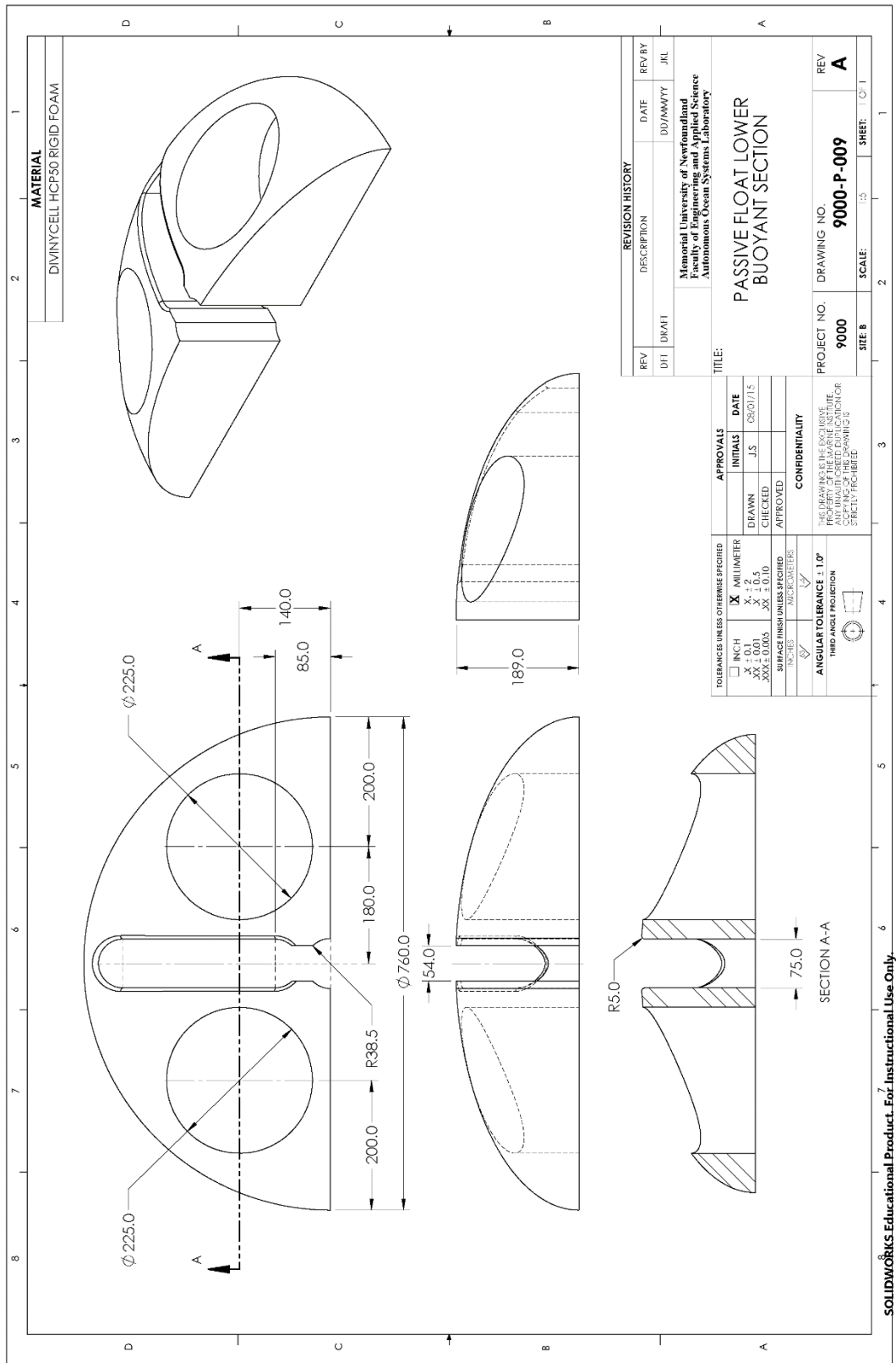


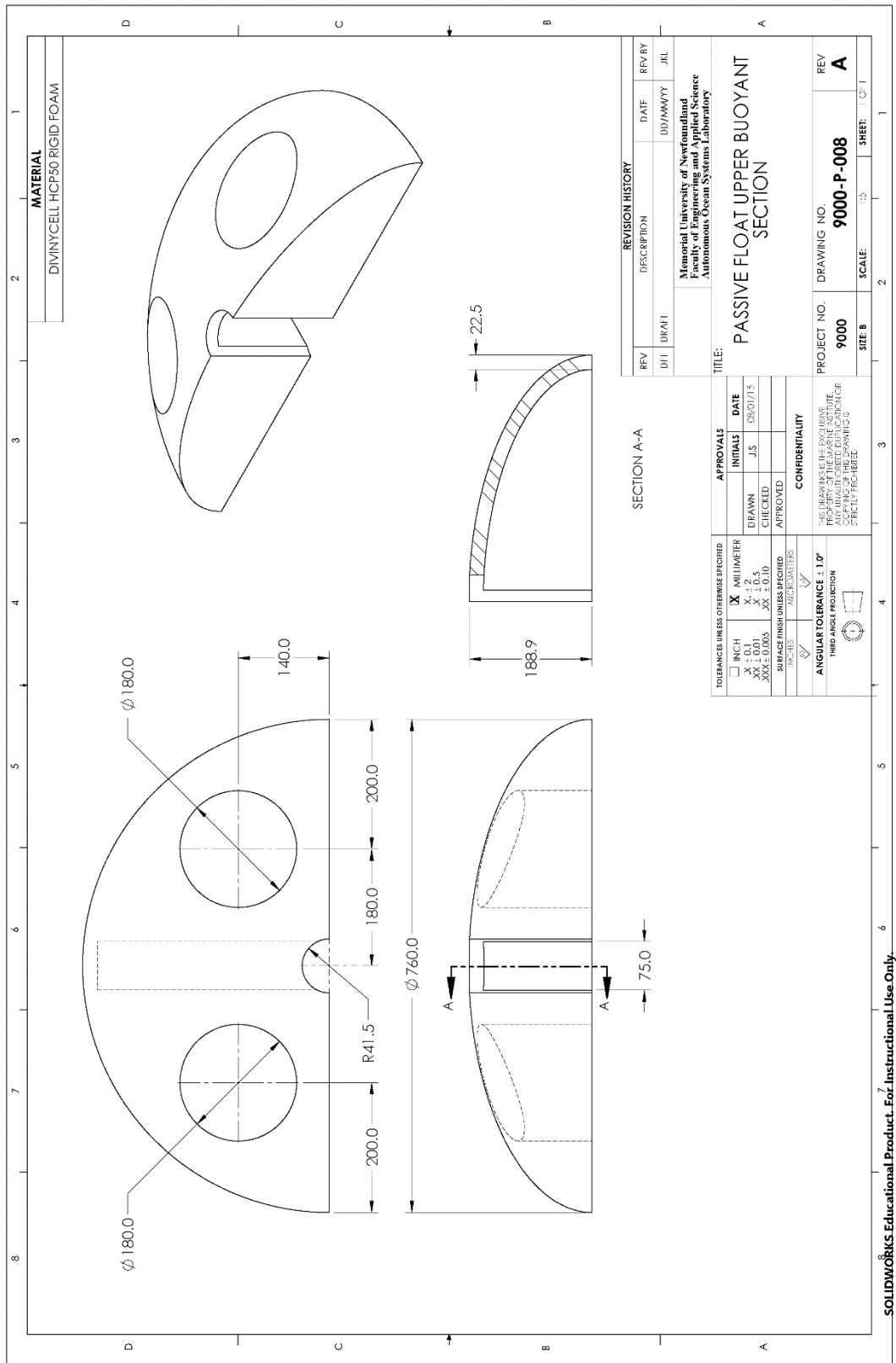


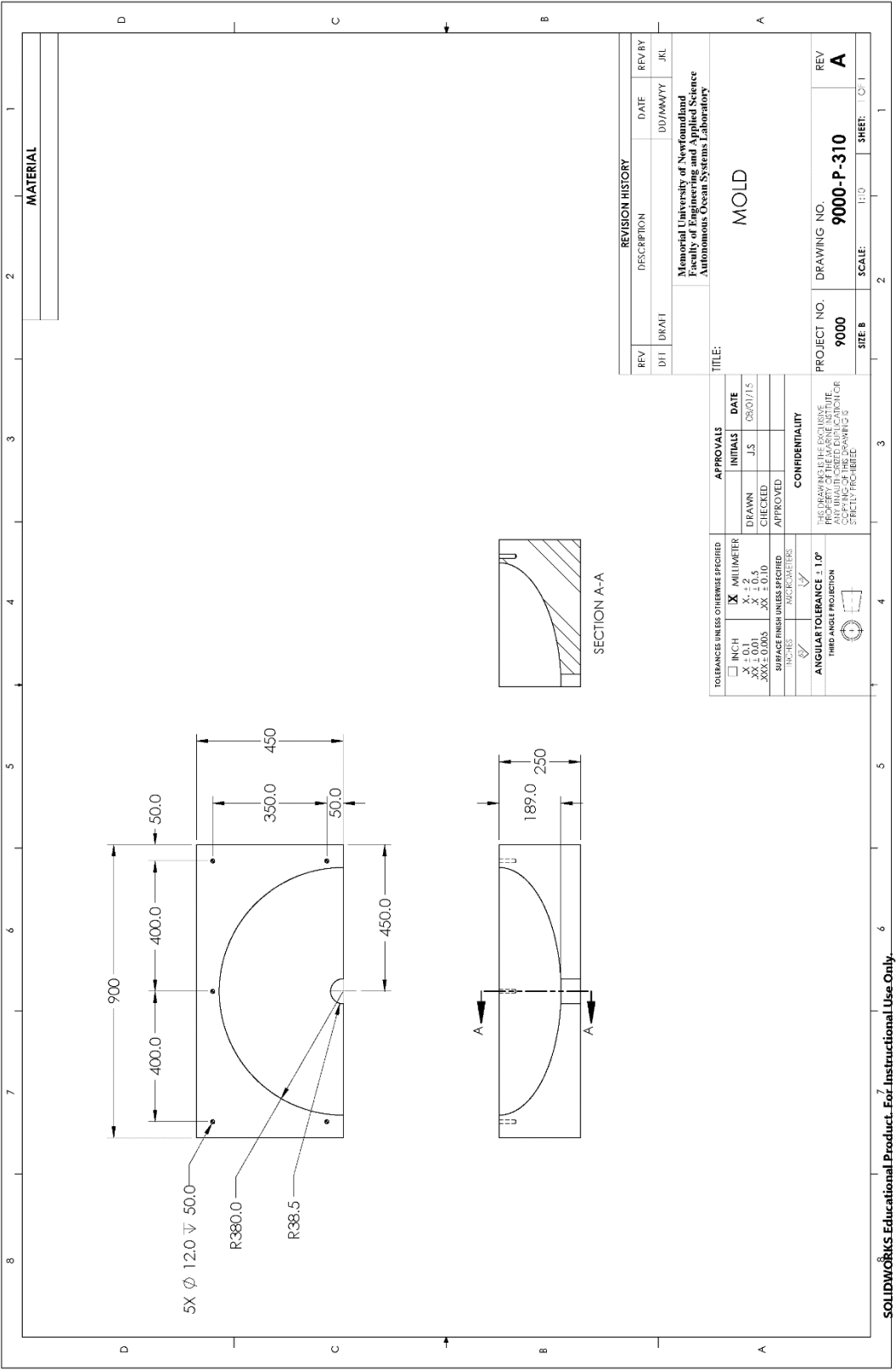


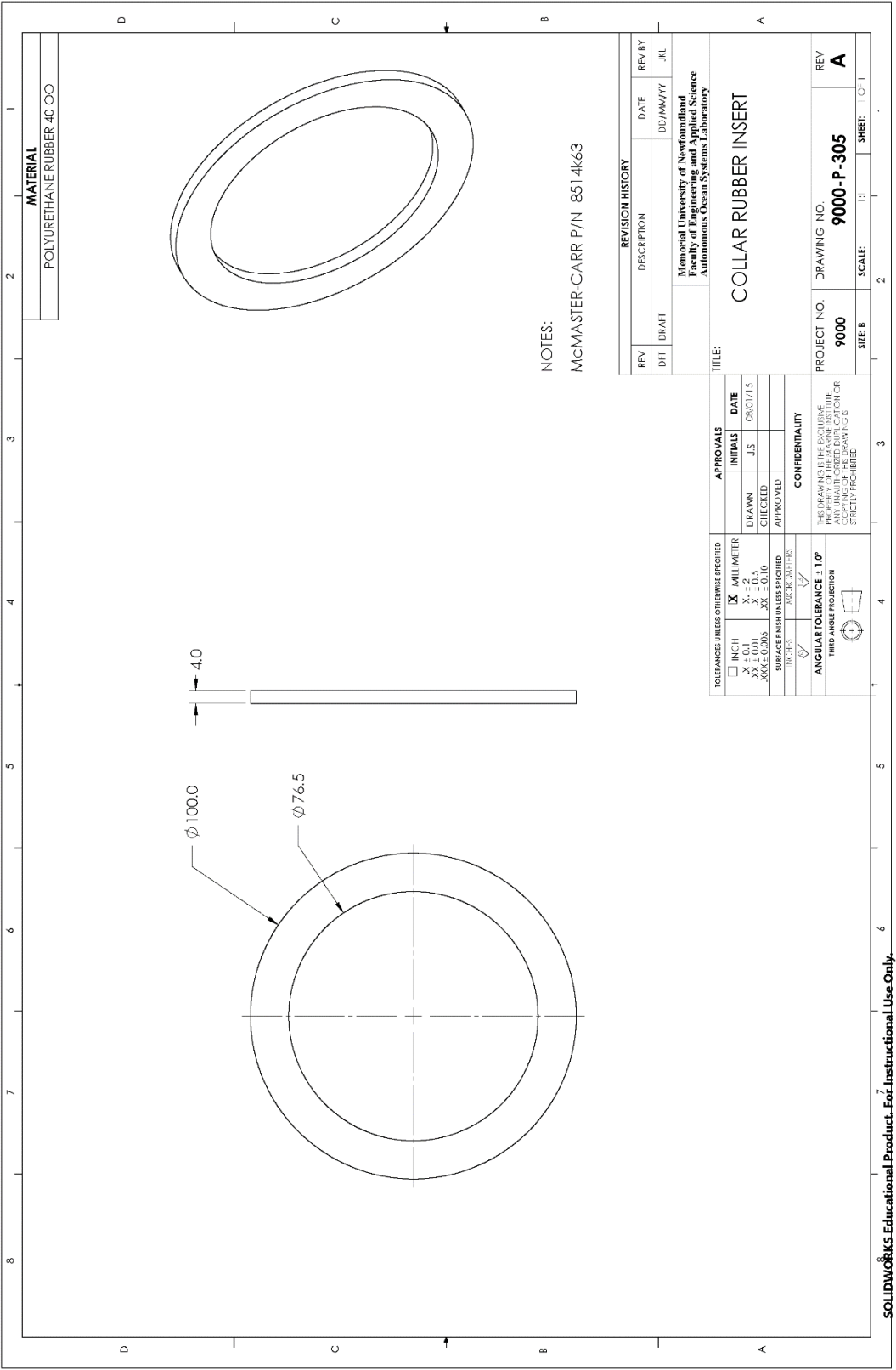


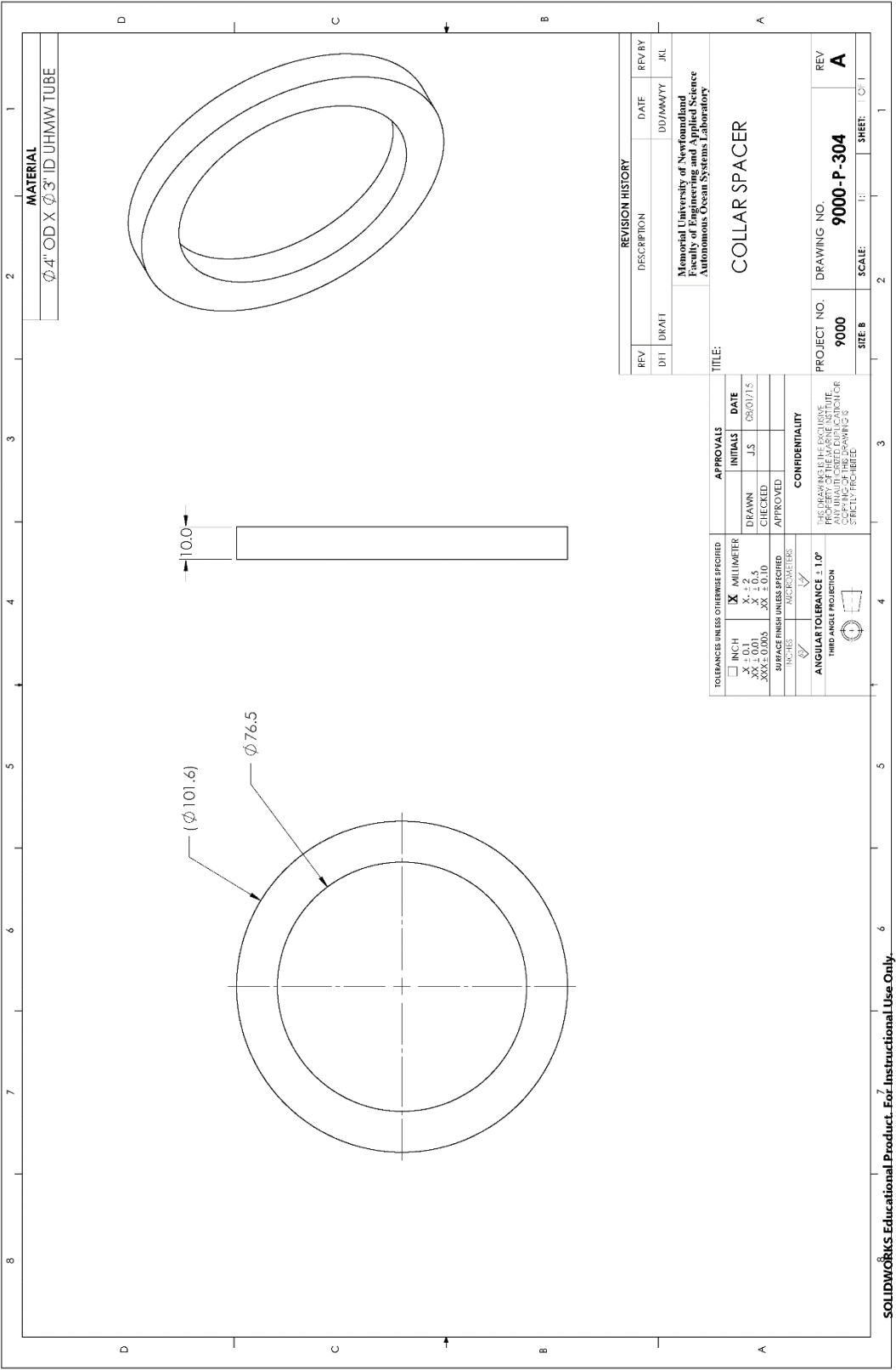


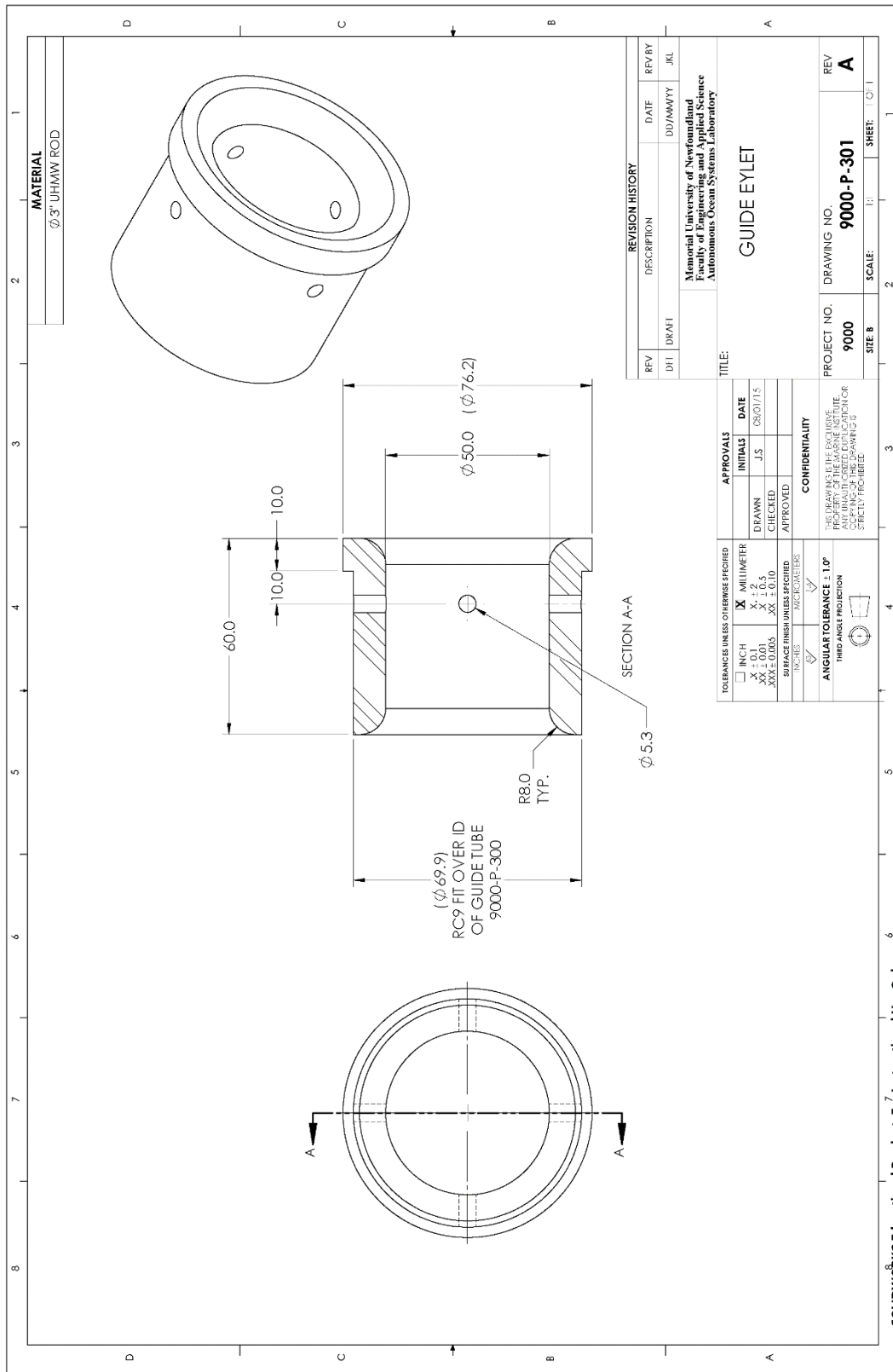


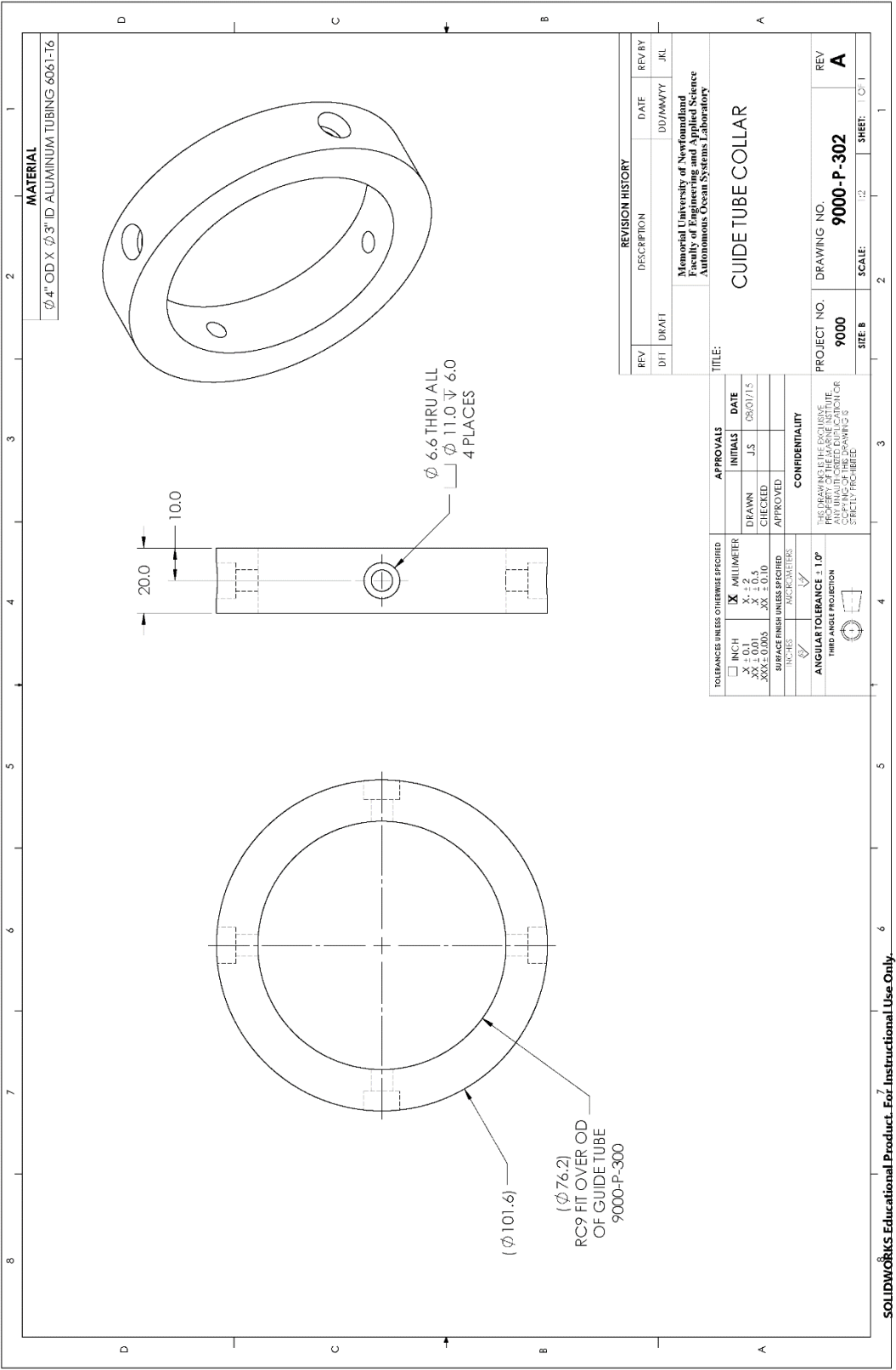


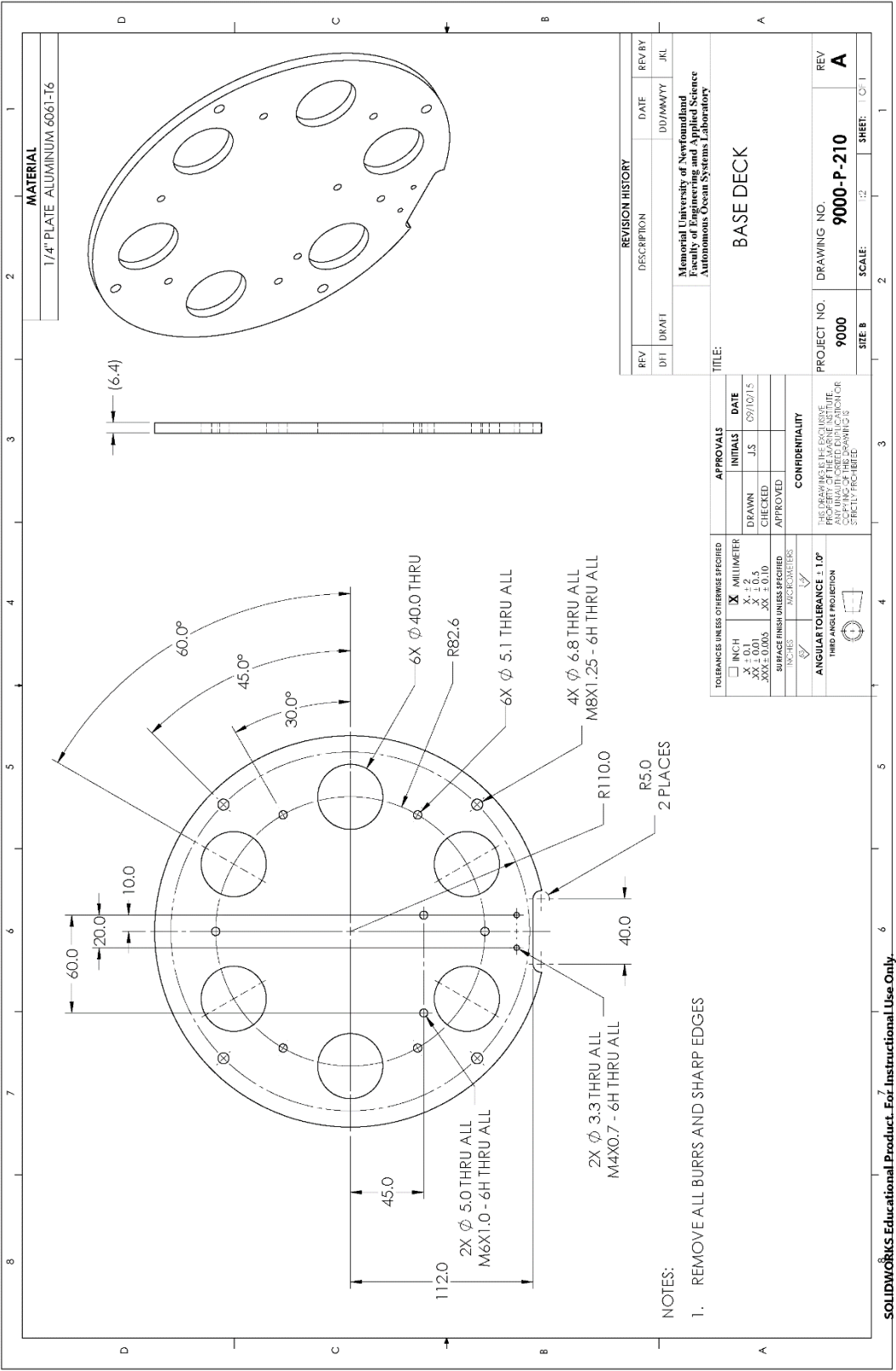


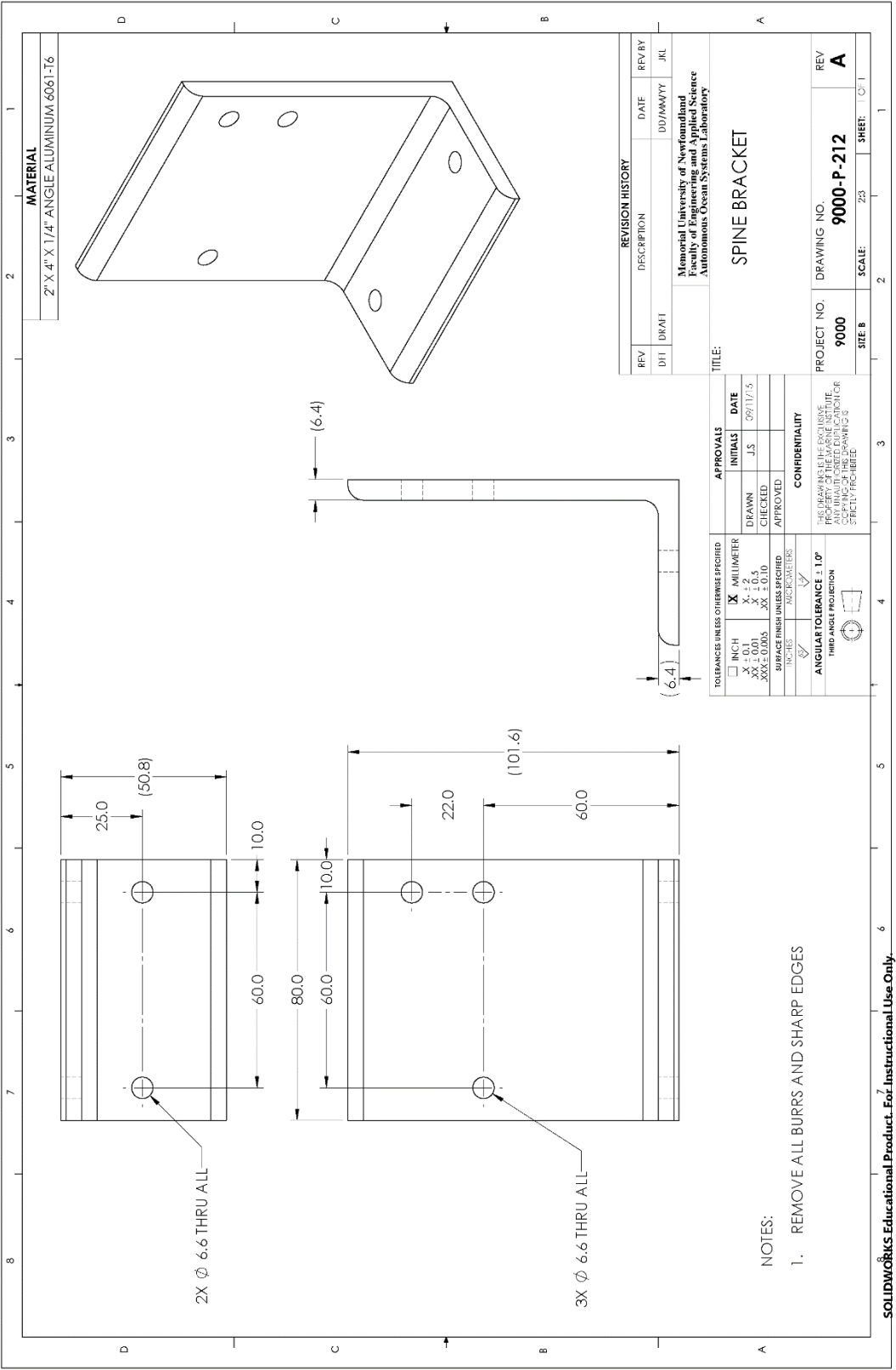


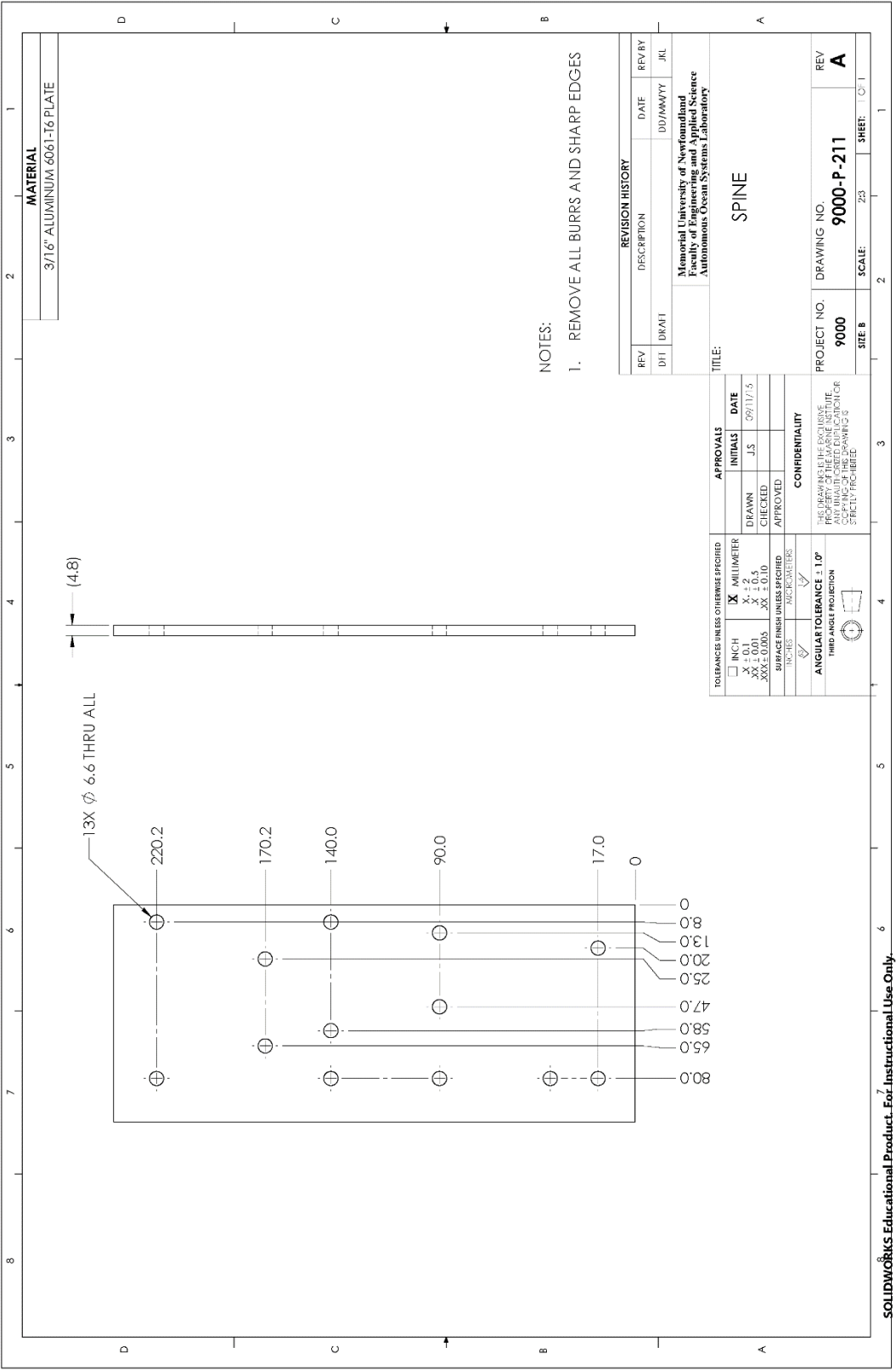








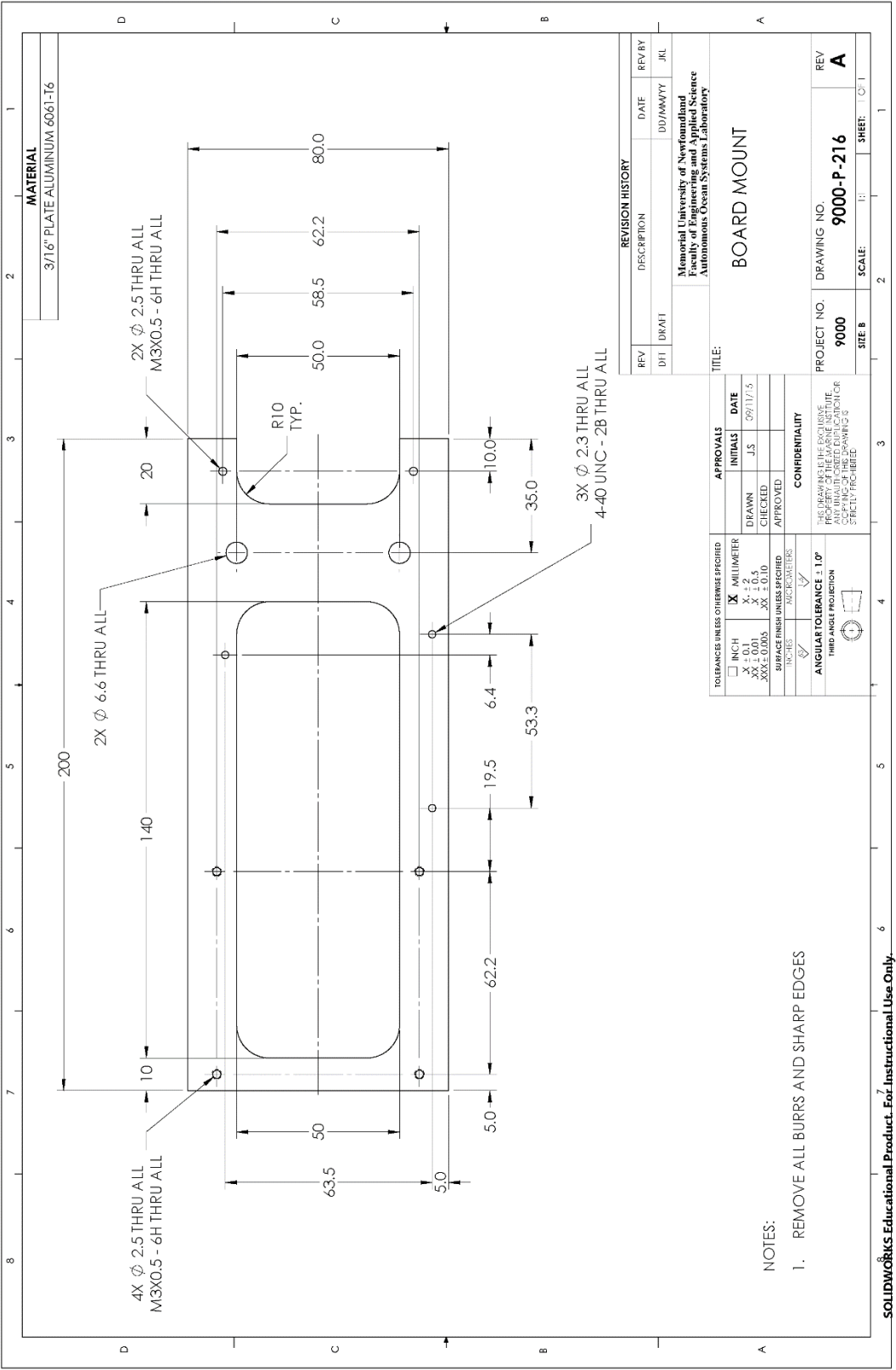


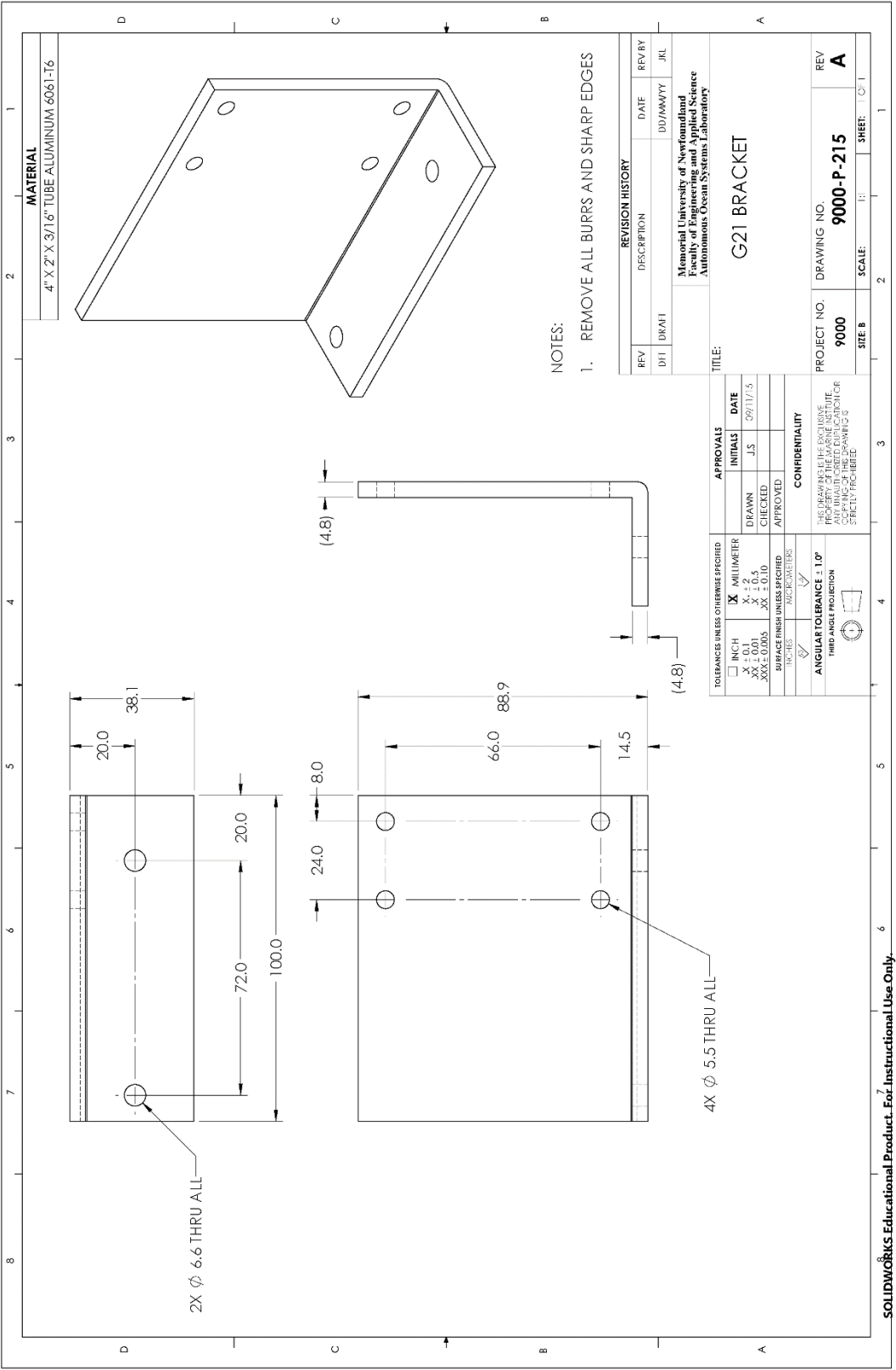


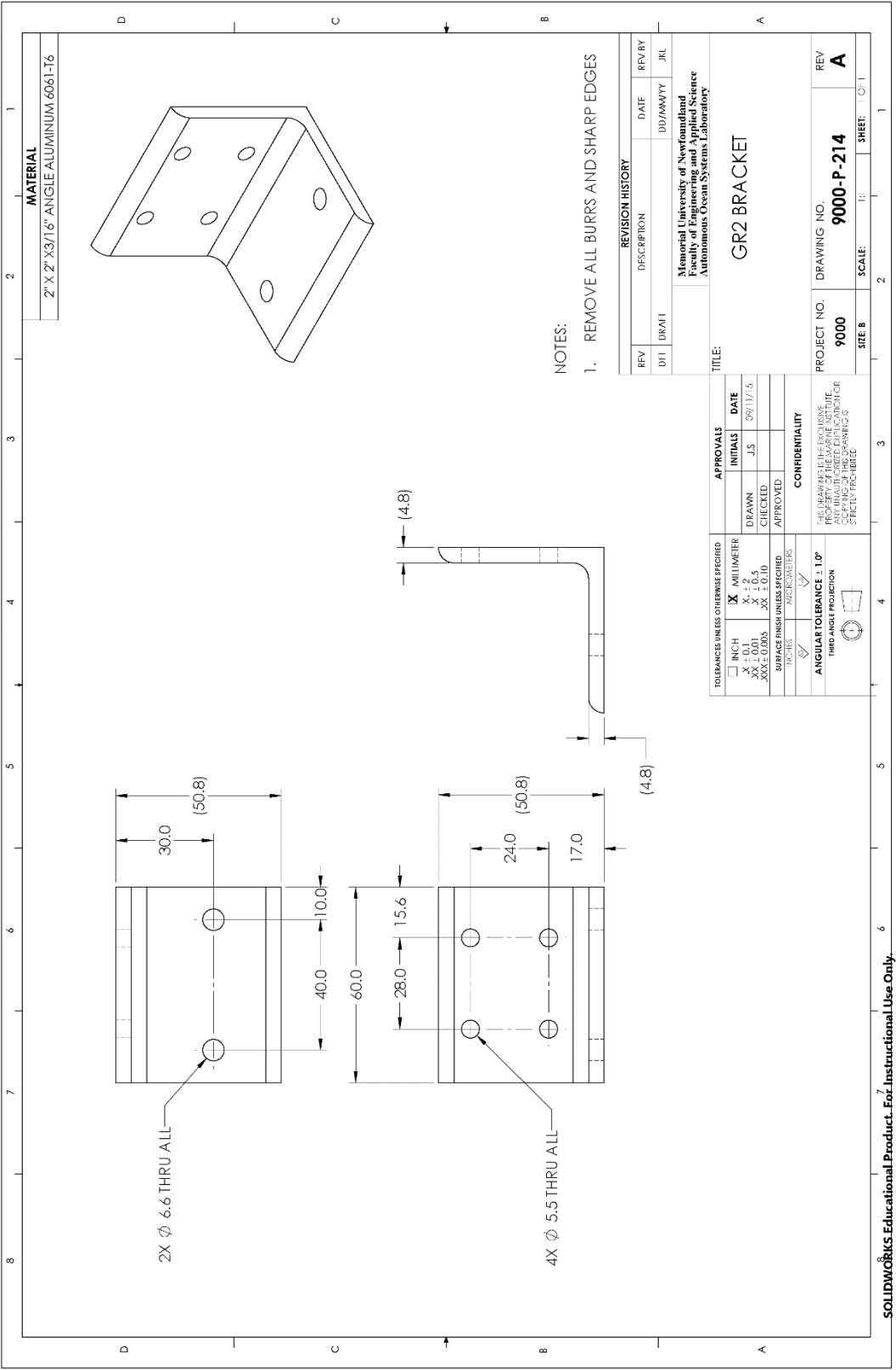
NOTES:
1. REMOVE ALL BURRS AND SHARP EDGES

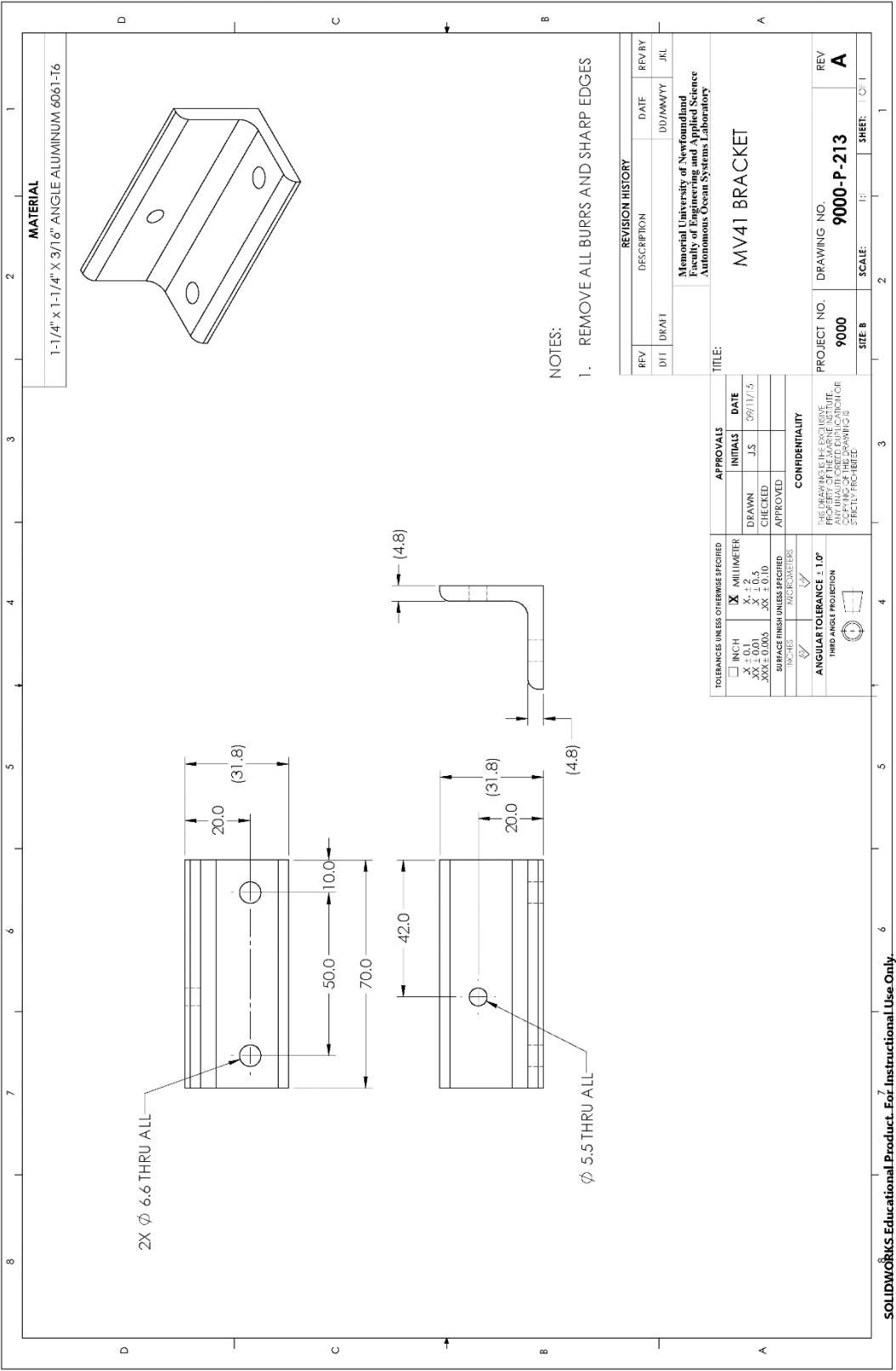
| REVISION HISTORY | | | |
|--|-------------|------------------------|----------|
| REV | DESCRIPTION | DATE | REV BY |
| D11 | DRAFT | DD/MM/YY | JKL |
| Memorial University of Newfoundland Faculty of Engineering and Applied Science Autonomous Ocean Systems Laboratory | | | |
| TITLE: SPINE | | | |
| PROJECT NO. 9000 | | DRAWING NO. 9000-P-211 | REV A |
| SITE 8 | | SCALE: 23 | SHEET: 1 |

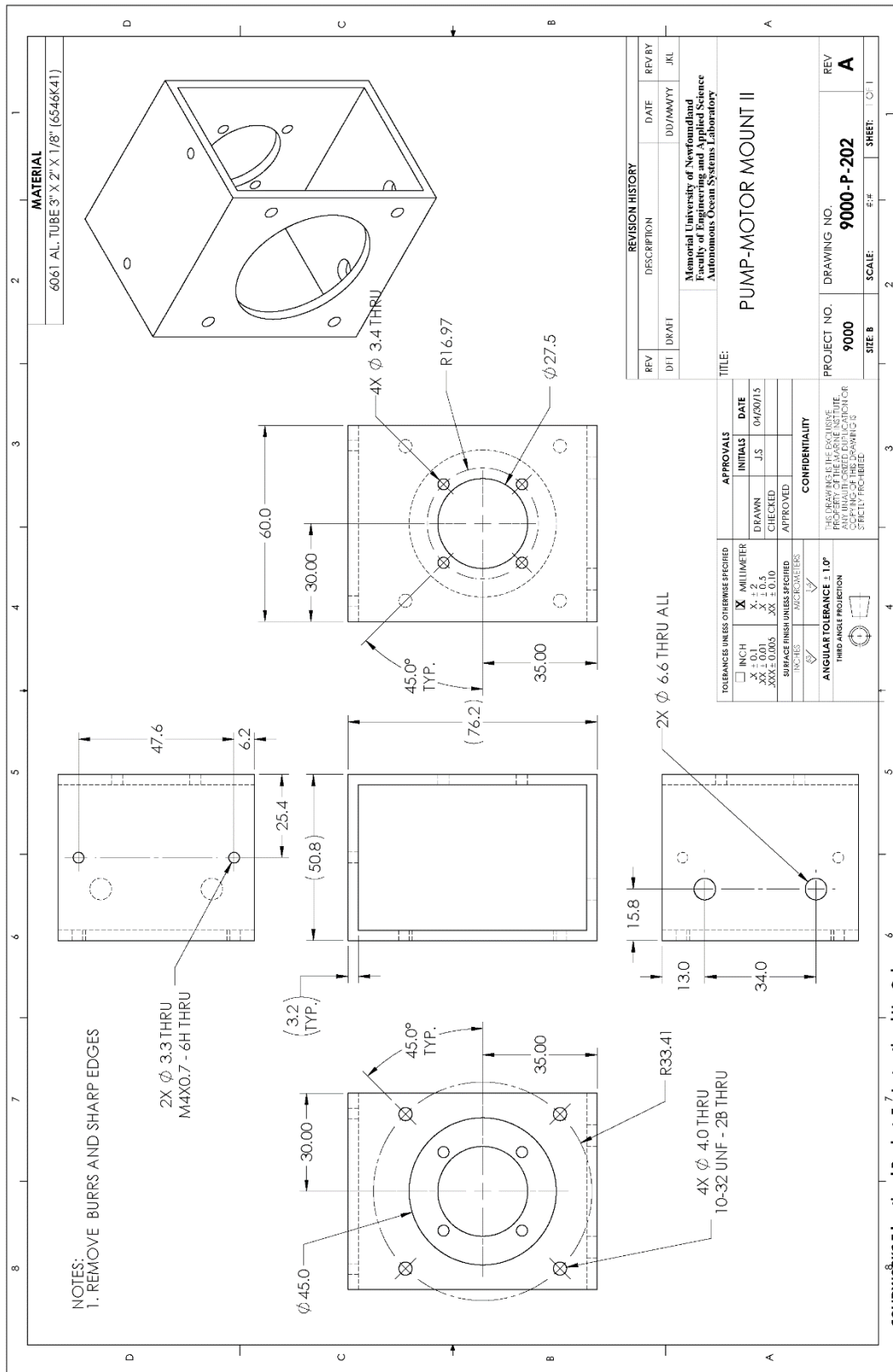
| APPROVALS | | DATE |
|--|------|----------|
| INITIALS | | |
| DRAWN | J.S. | 09/11/15 |
| CHECKED | | |
| APPROVED | | |
| CONFIDENTIALITY | | |
| THIS DRAWING IS THE EXCLUSIVE PROPERTY OF THE MARINE INSTITUTE. ANY UNAUTHORIZED REPRODUCTION OR COPIING OF THIS DRAWING IS STRICTLY PROHIBITED. | | |
| ANGULAR TOLERANCE $\pm 1.0^\circ$ | | |
| THIRD ANGLE PROJECTION | | |

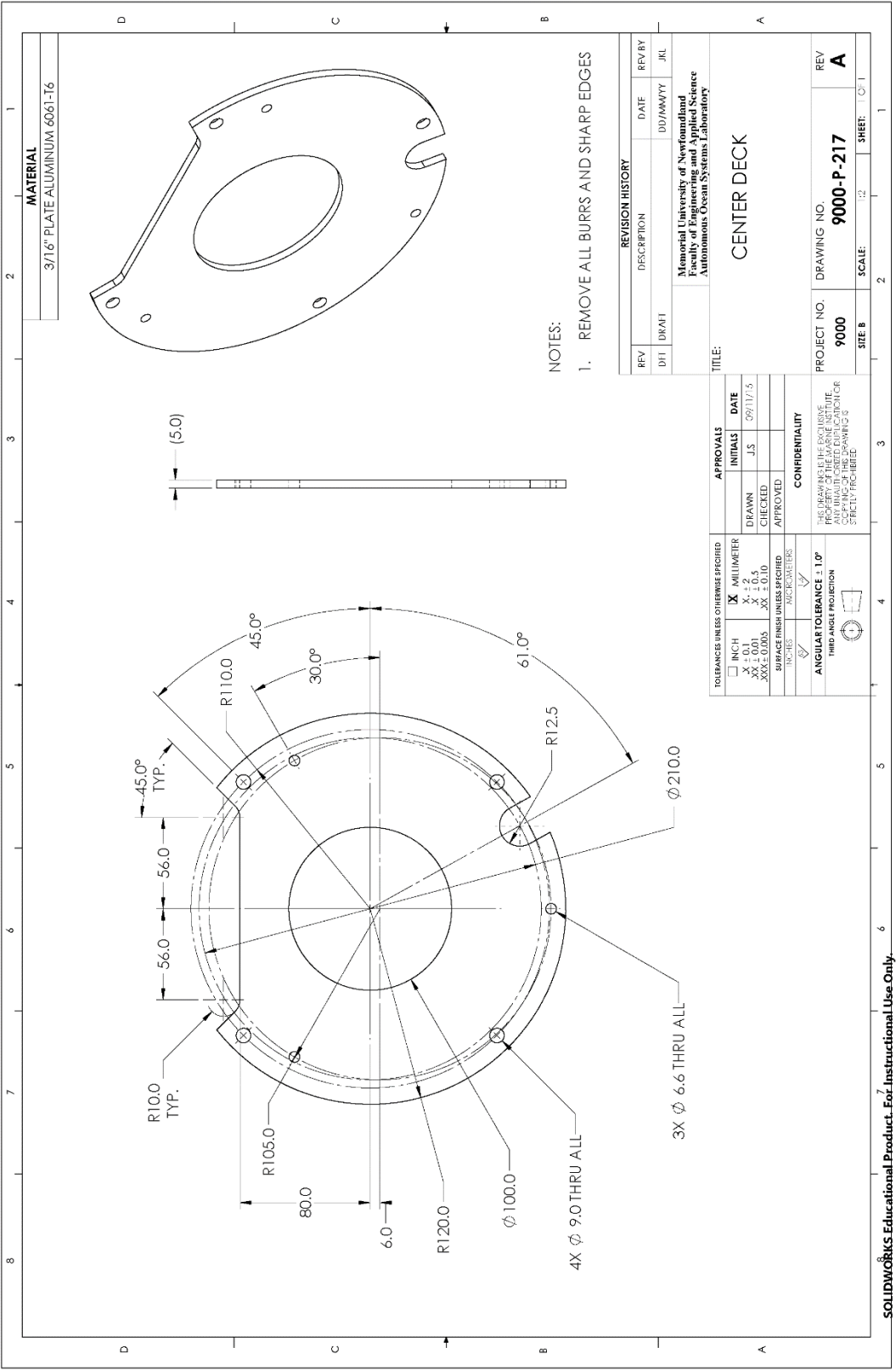


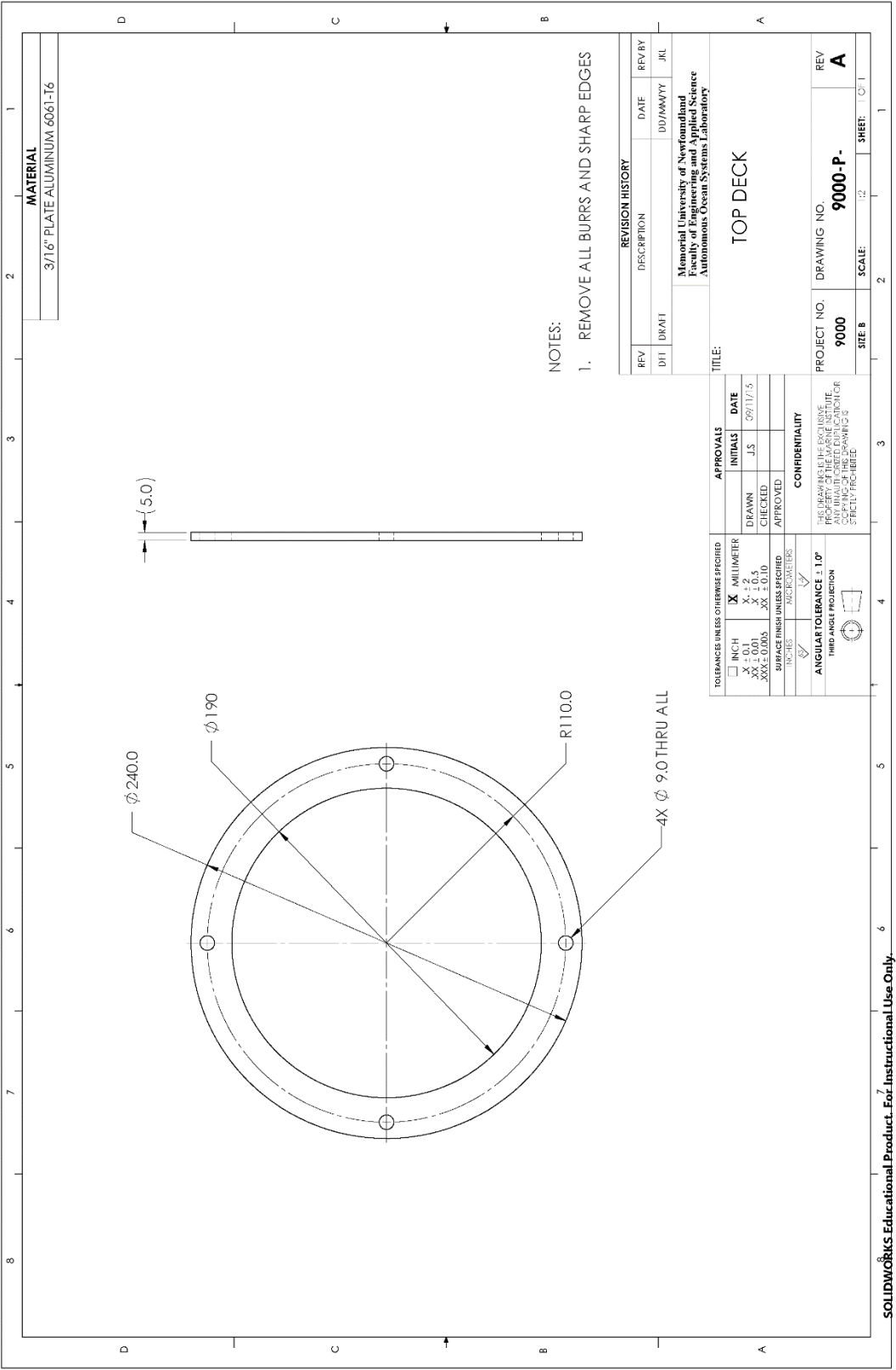








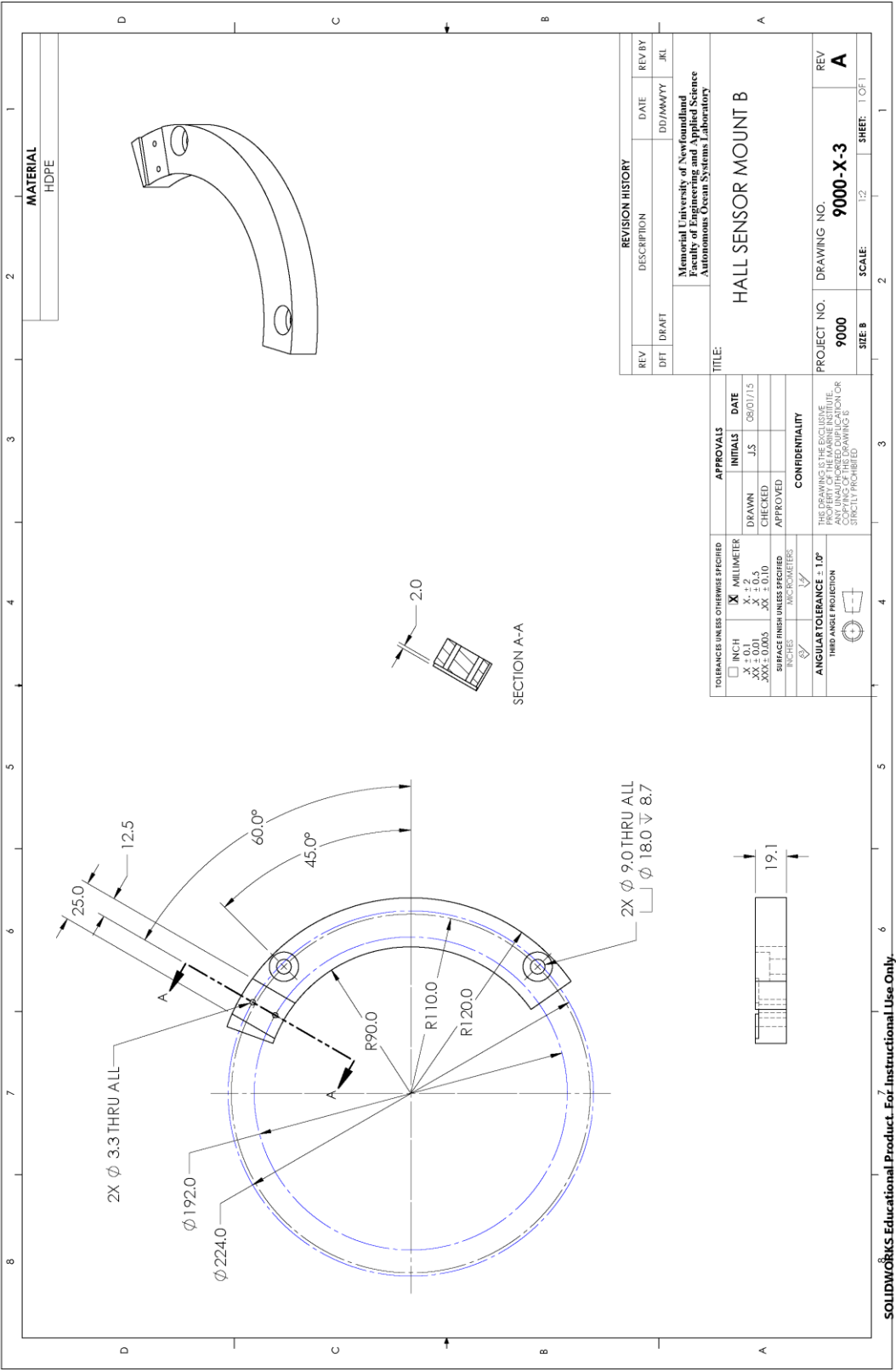


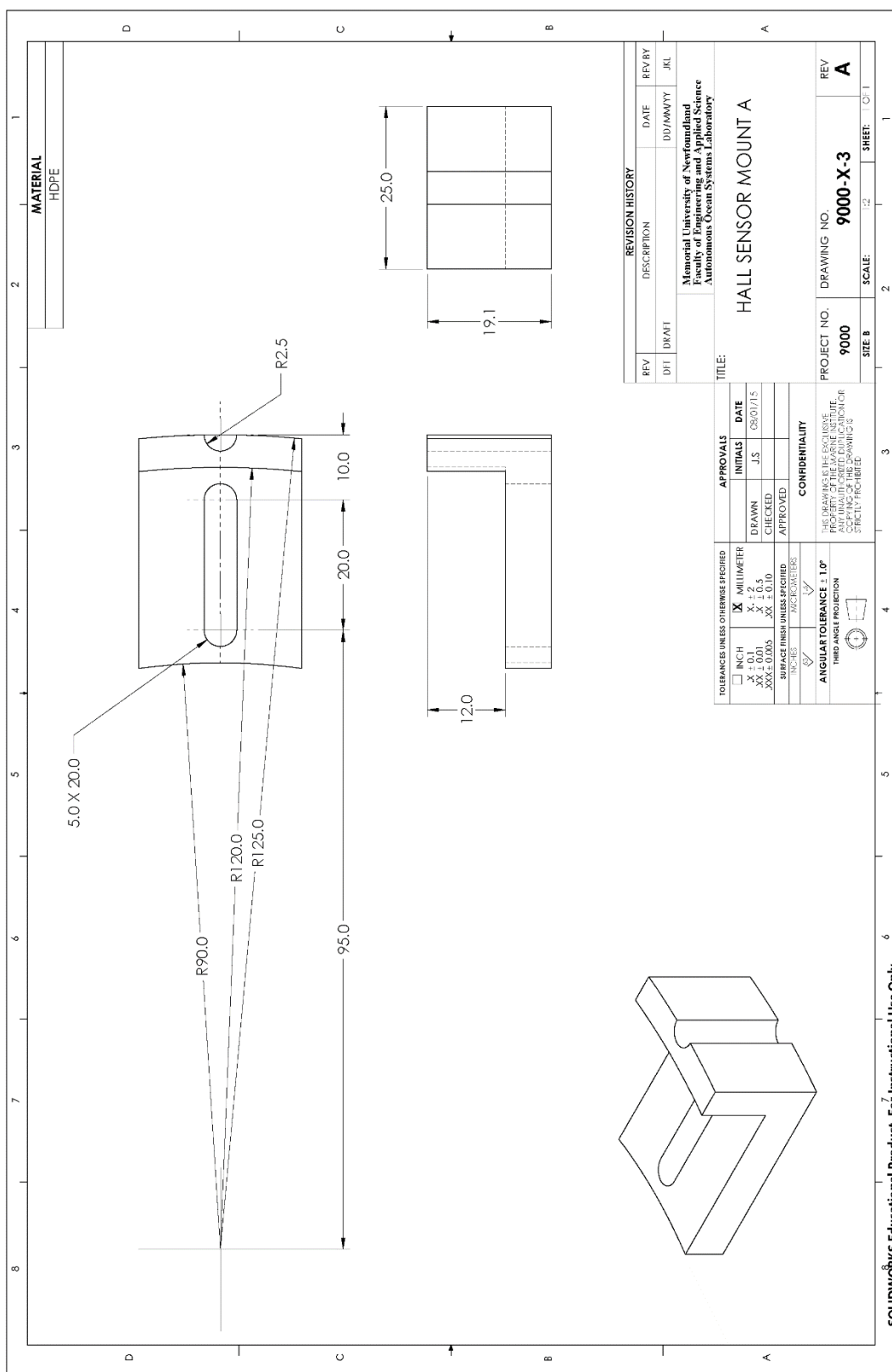


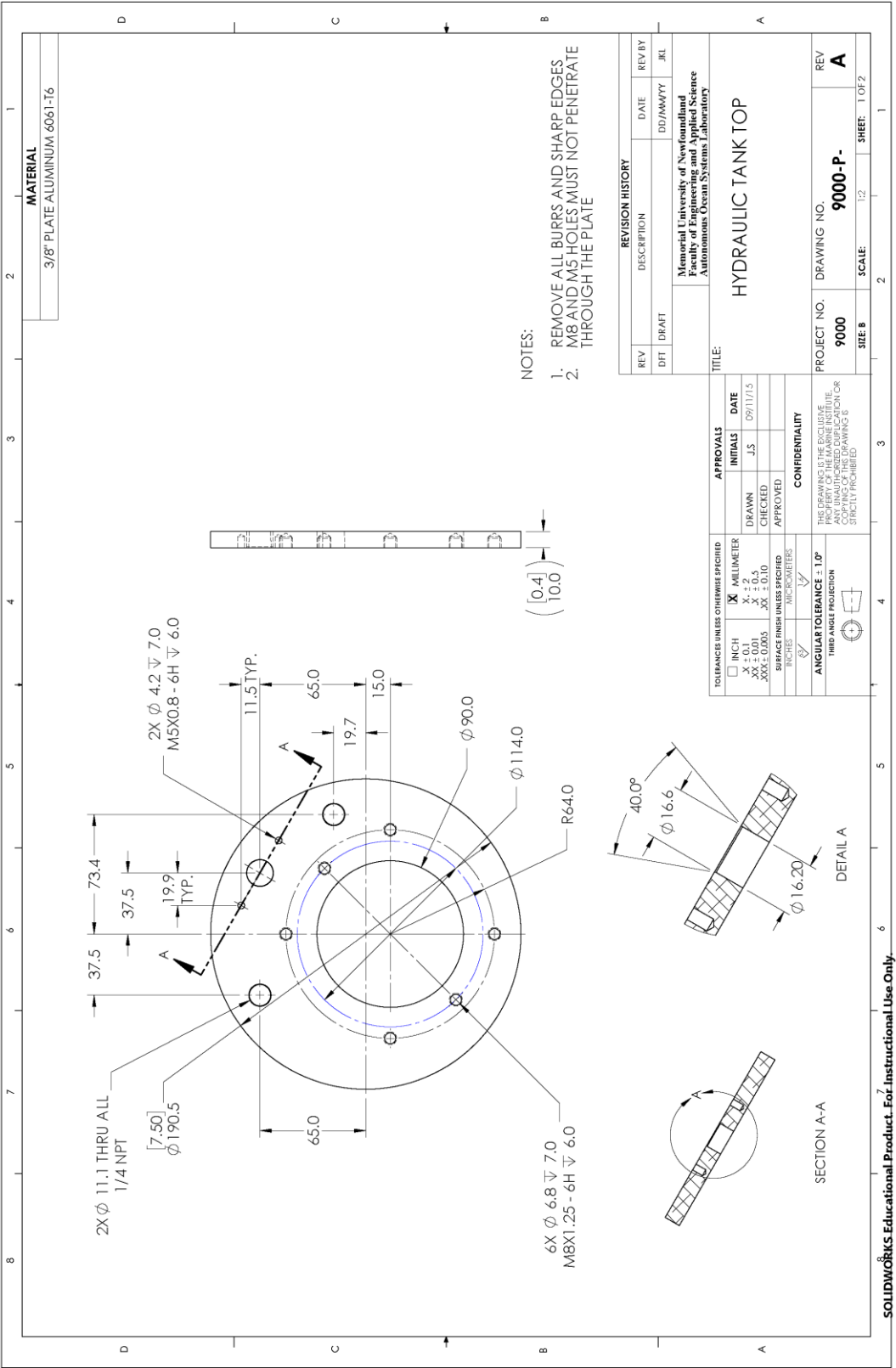
NOTES:
1. REMOVE ALL BURRS AND SHARP EDGES

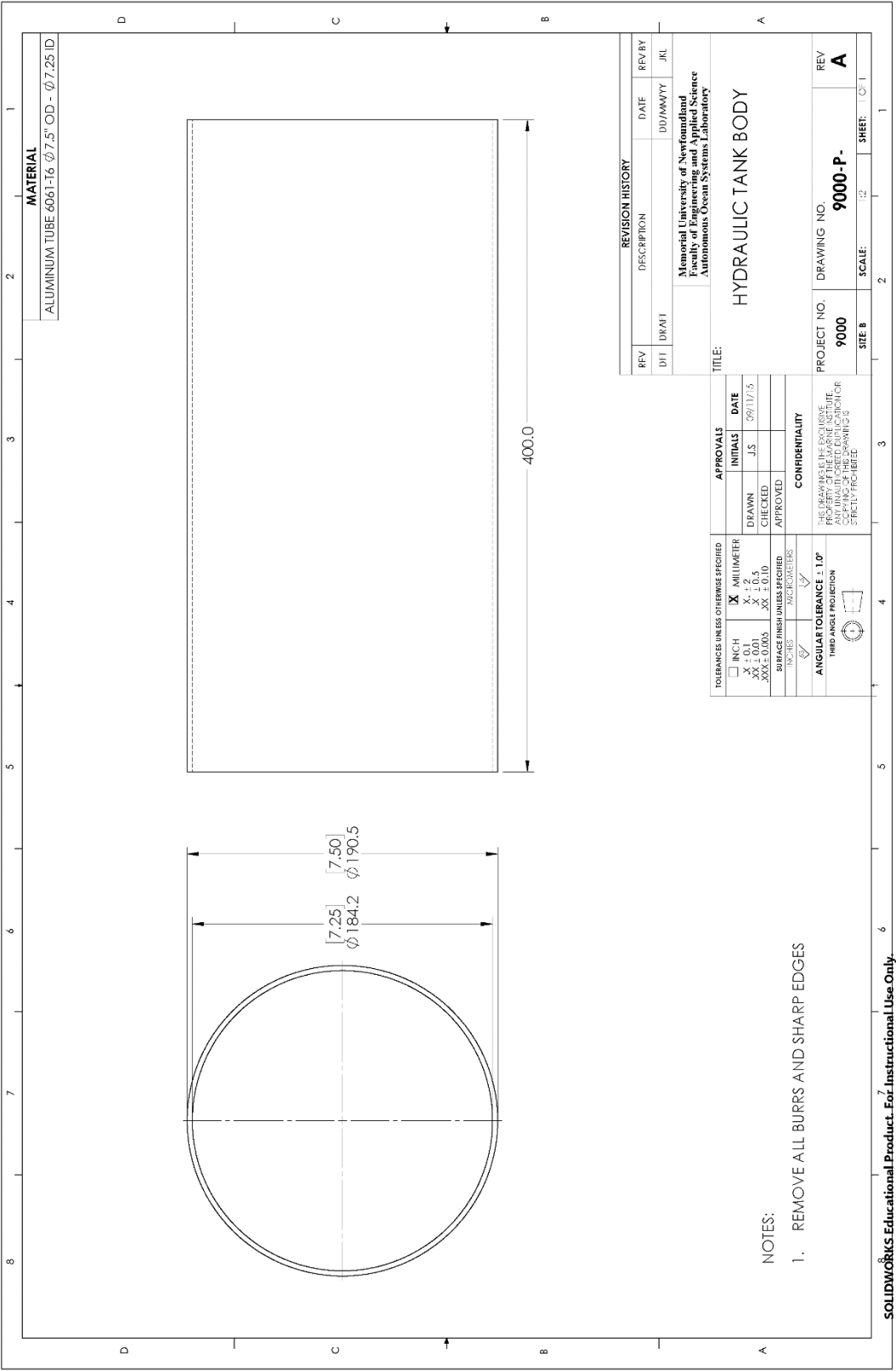
| REVISION HISTORY | | | |
|--|-------------|---------------------|---------------|
| REV | DESCRIPTION | DATE | REV BY |
| D11 | DRAWN | DD/MM/YY | JKL |
| Memorial University of Newfoundland Faculty of Engineering and Applied Science Autonomous Ocean Systems Laboratory | | | |
| TITLE: TOP DECK | | | |
| PROJECT NO. 9000 | | DRAWING NO. 9000-P- | REV A |
| SITE 8 | | SCALE: 1:2 | SHEET: 1 of 1 |

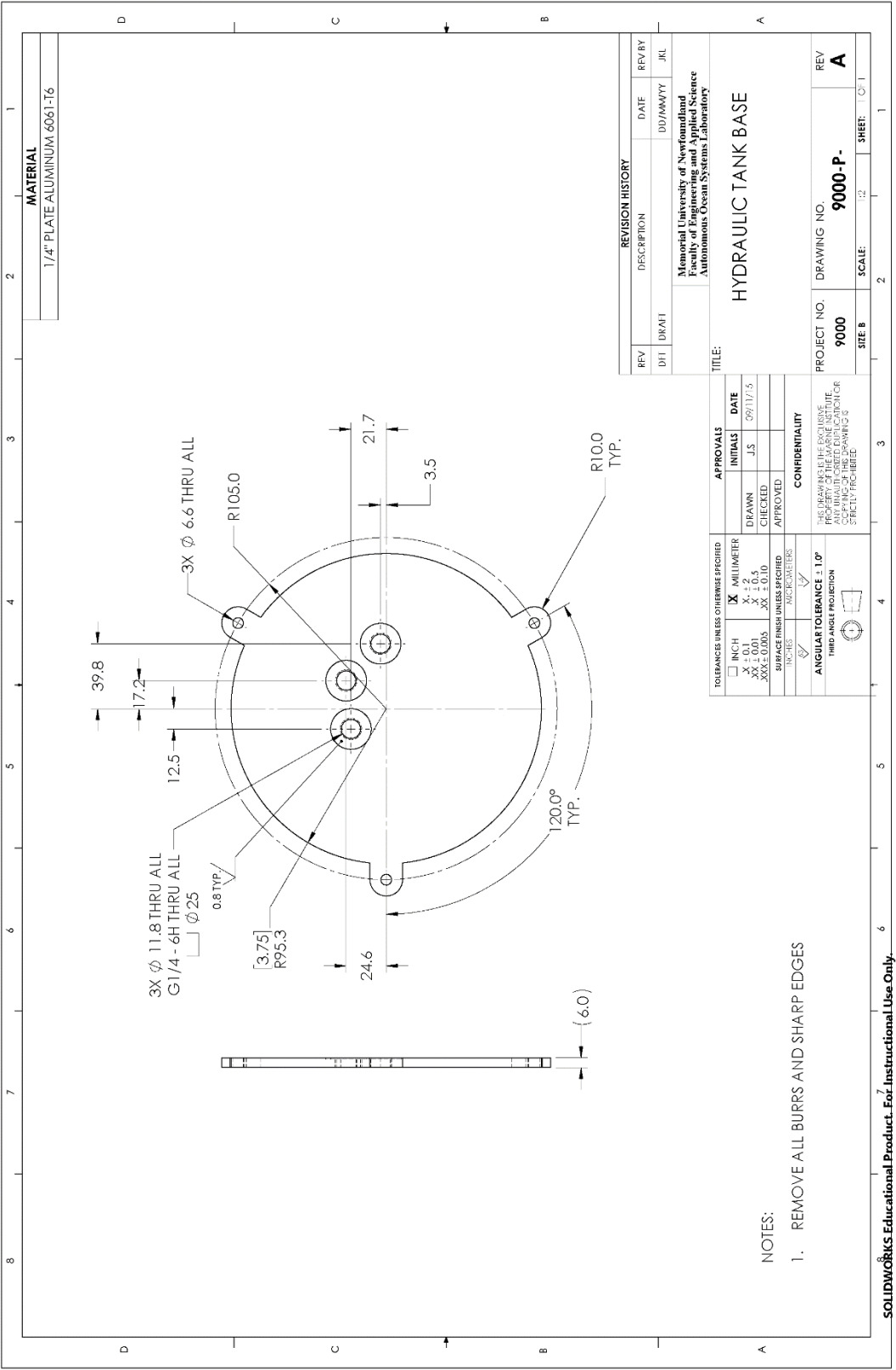
| TOLERANCES UNLESS OTHERWISE SPECIFIED | | APPROVALS | |
|---------------------------------------|--|--|----------|
| <input type="checkbox"/> INCH | <input checked="" type="checkbox"/> MILLIMETER | DRAWN | DATE |
| ± 0.1 | ± 2.5 | CHECKED | 09/11/15 |
| ± 0.005 | ± 0.10 | APPROVED | |
| SURFACE FINISH UNLESS SPECIFIED | | CONFIDENTIALITY | |
| INCHES | | THIS DRAWING IS THE EXCLUSIVE PROPERTY OF THE MARINE INSTITUTE. ANY UNAUTHORIZED REPRODUCTION OR COPIING OF THIS DRAWING IS STRICTLY PROHIBITED. | |
| ANGULAR TOLERANCE $\pm 1.0^\circ$ | | THIRD ANGLE PROJECTION | |

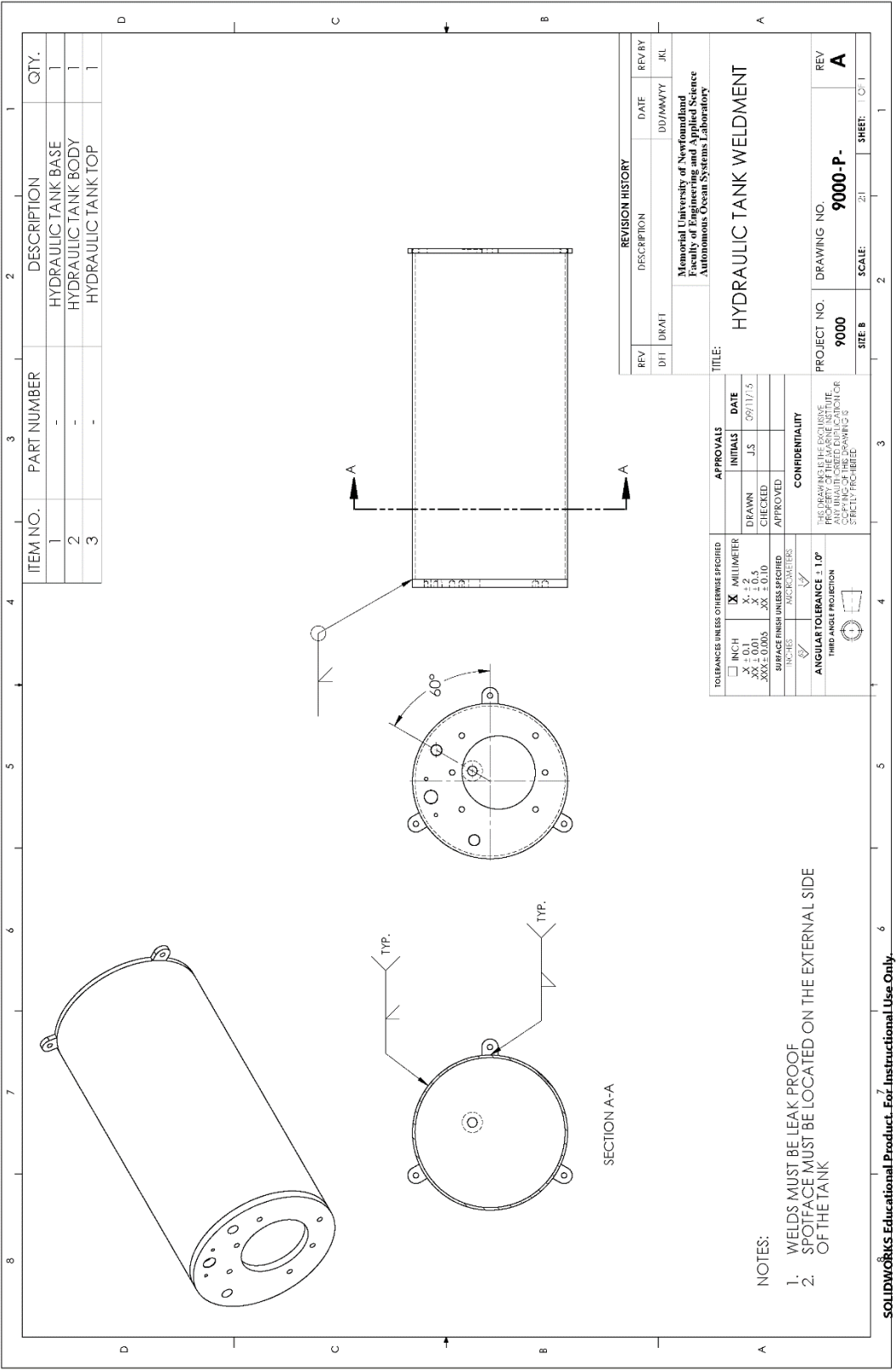


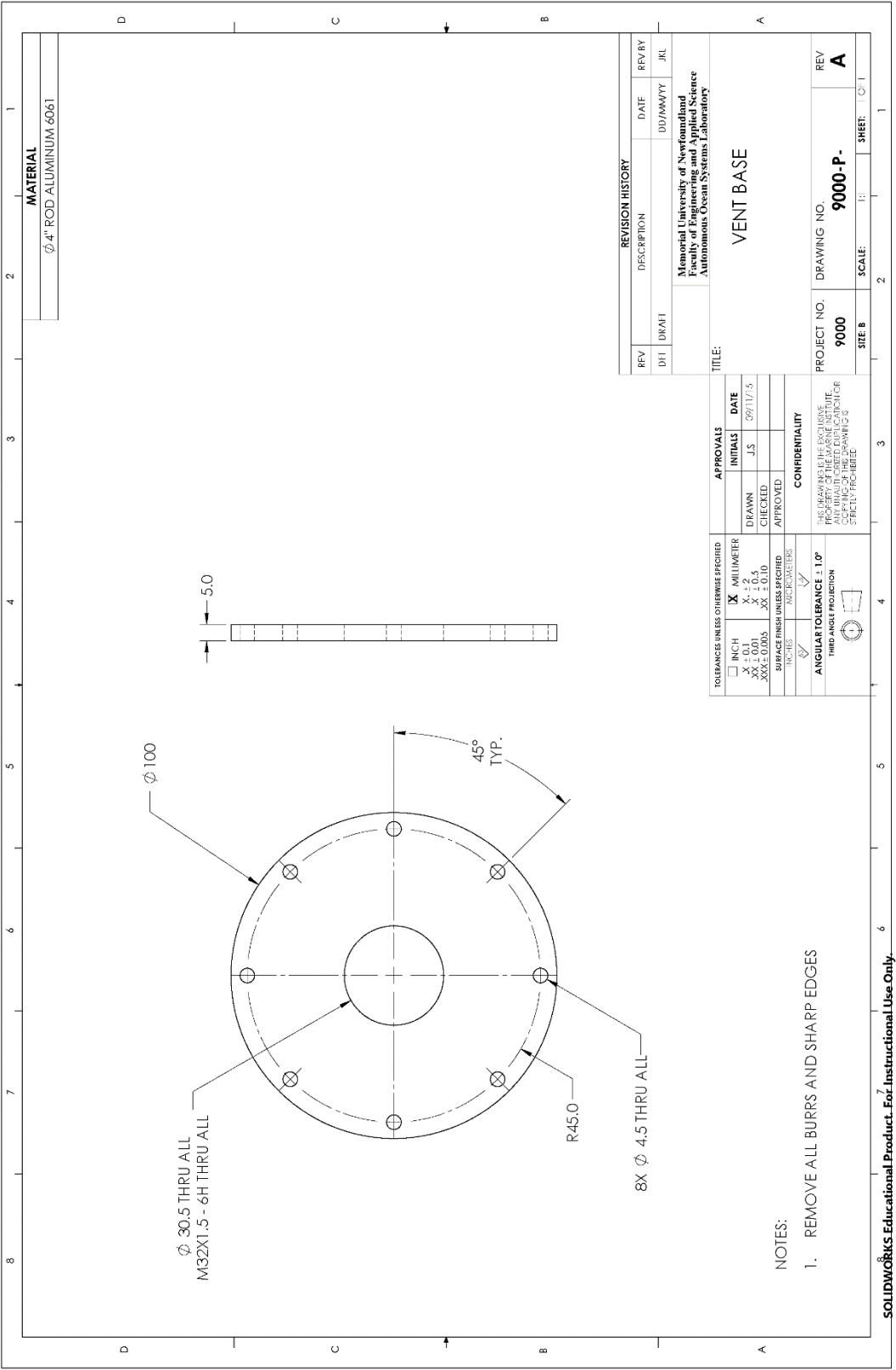


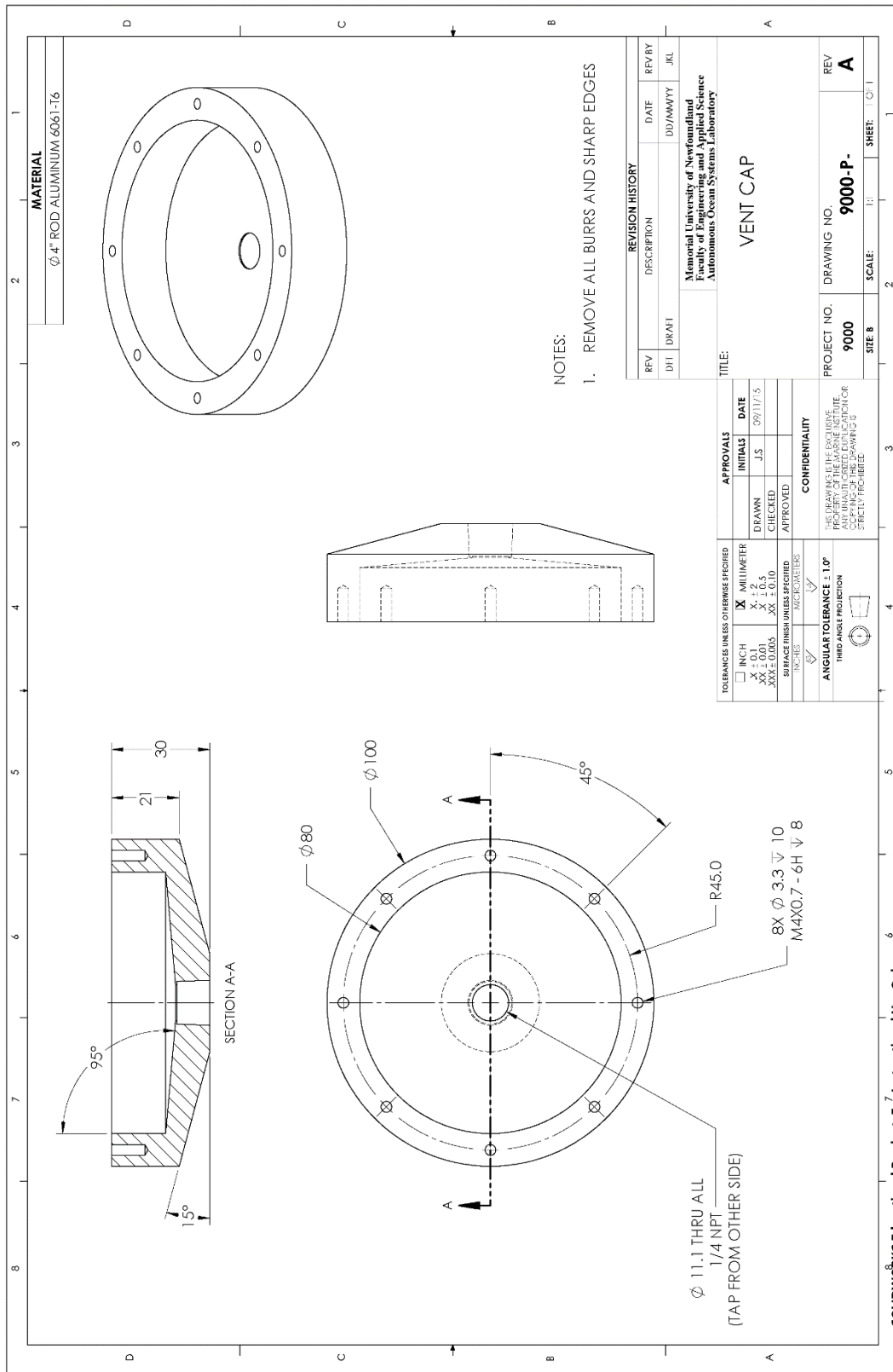


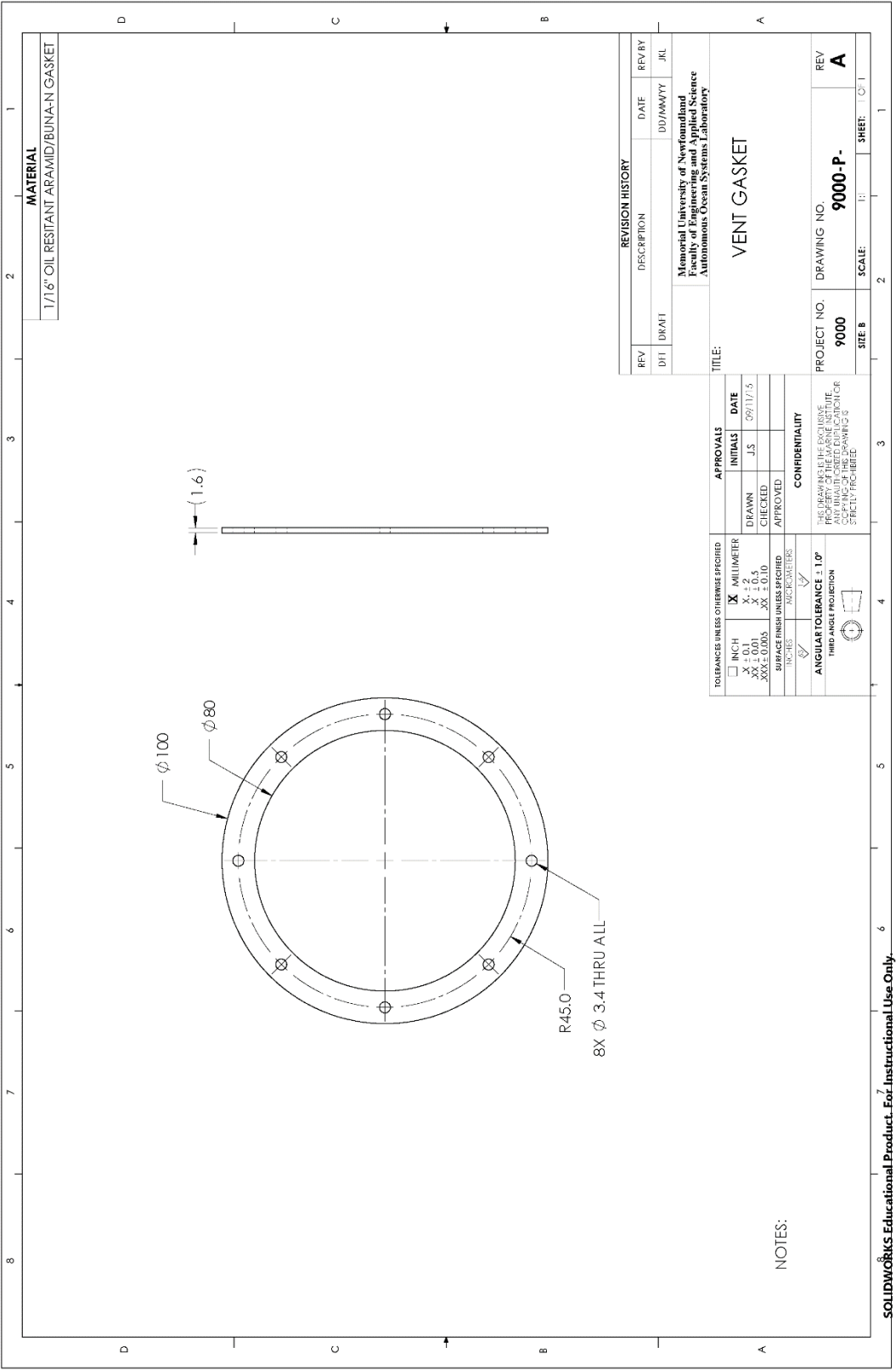


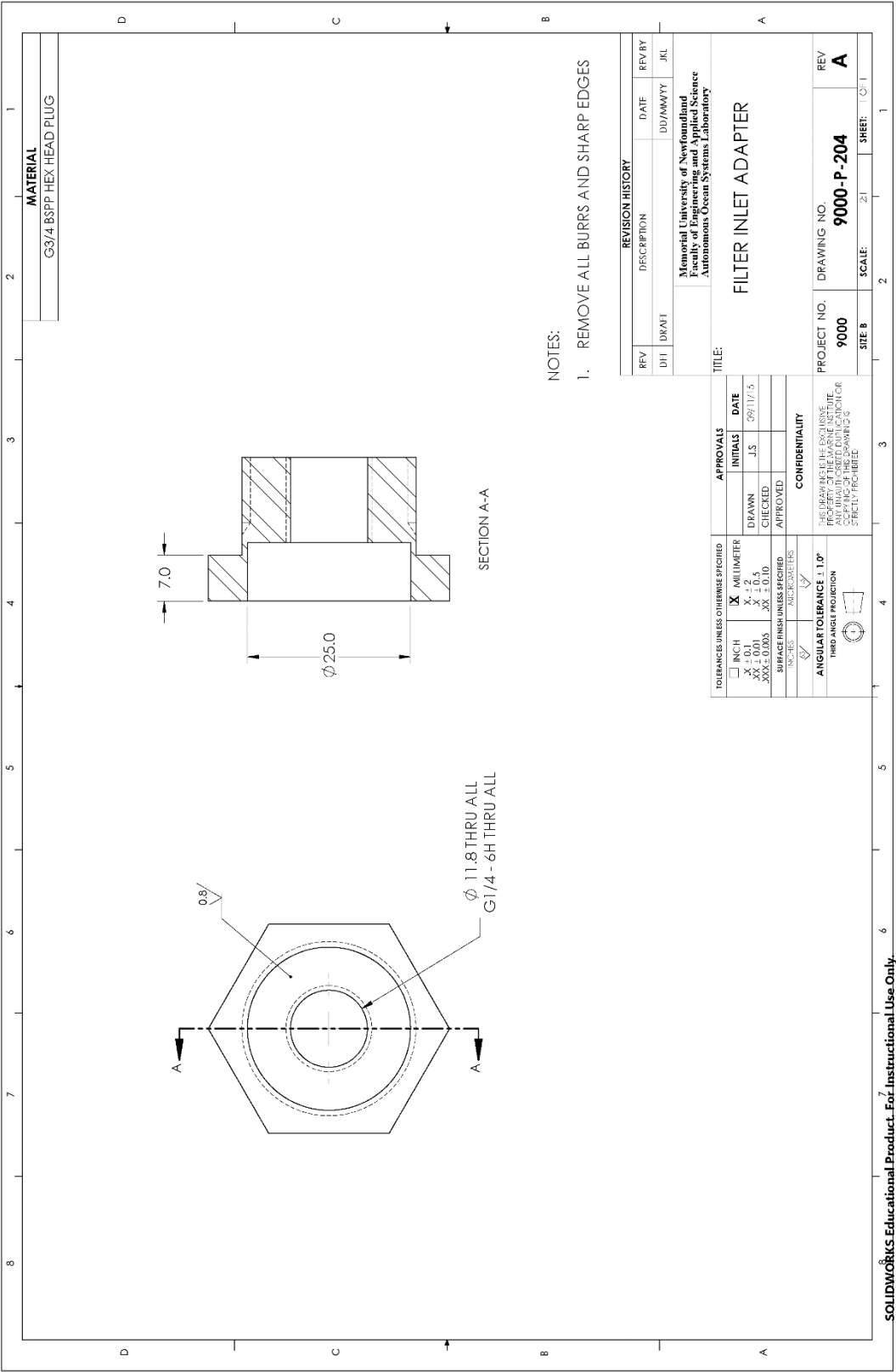


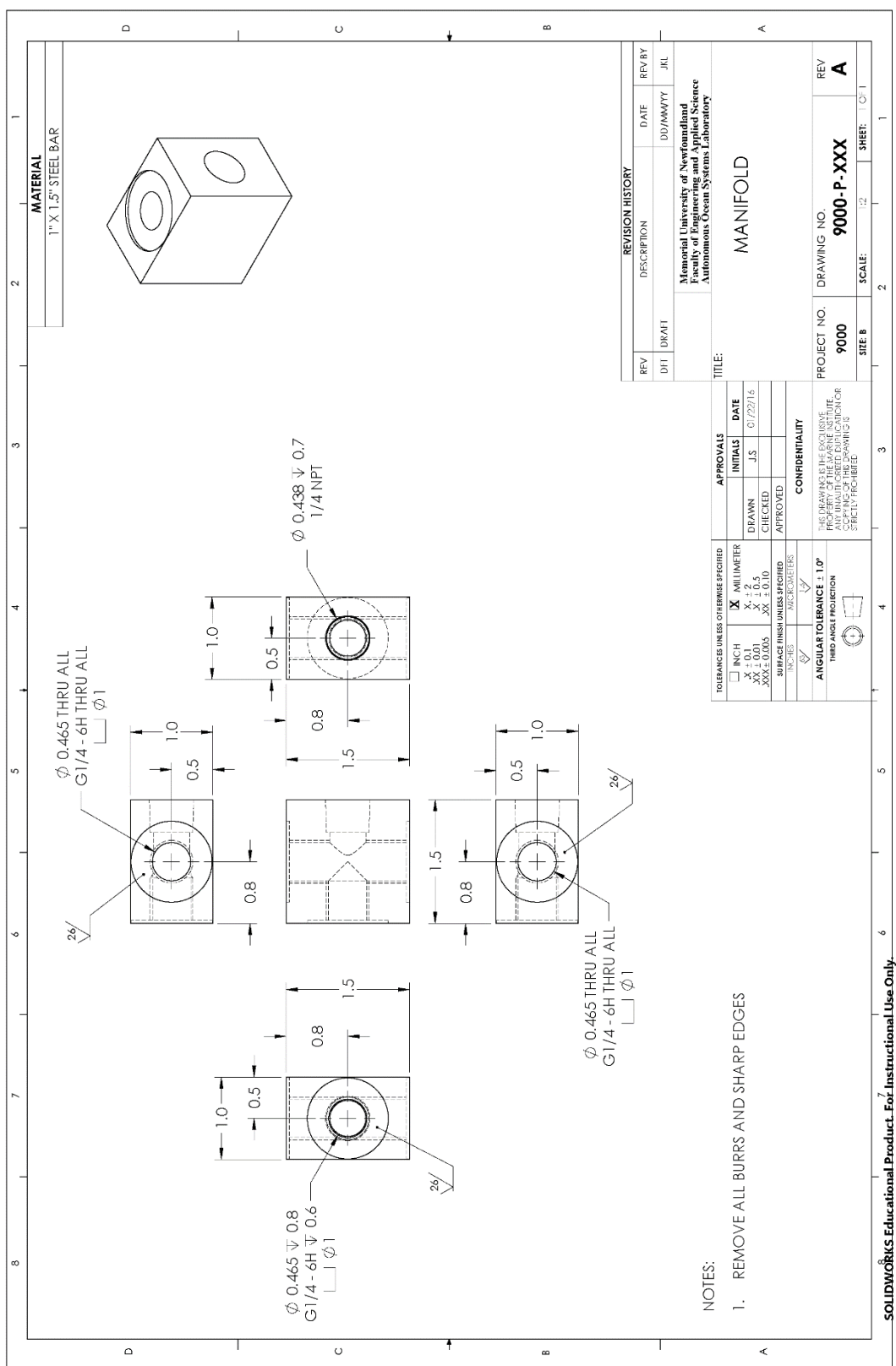


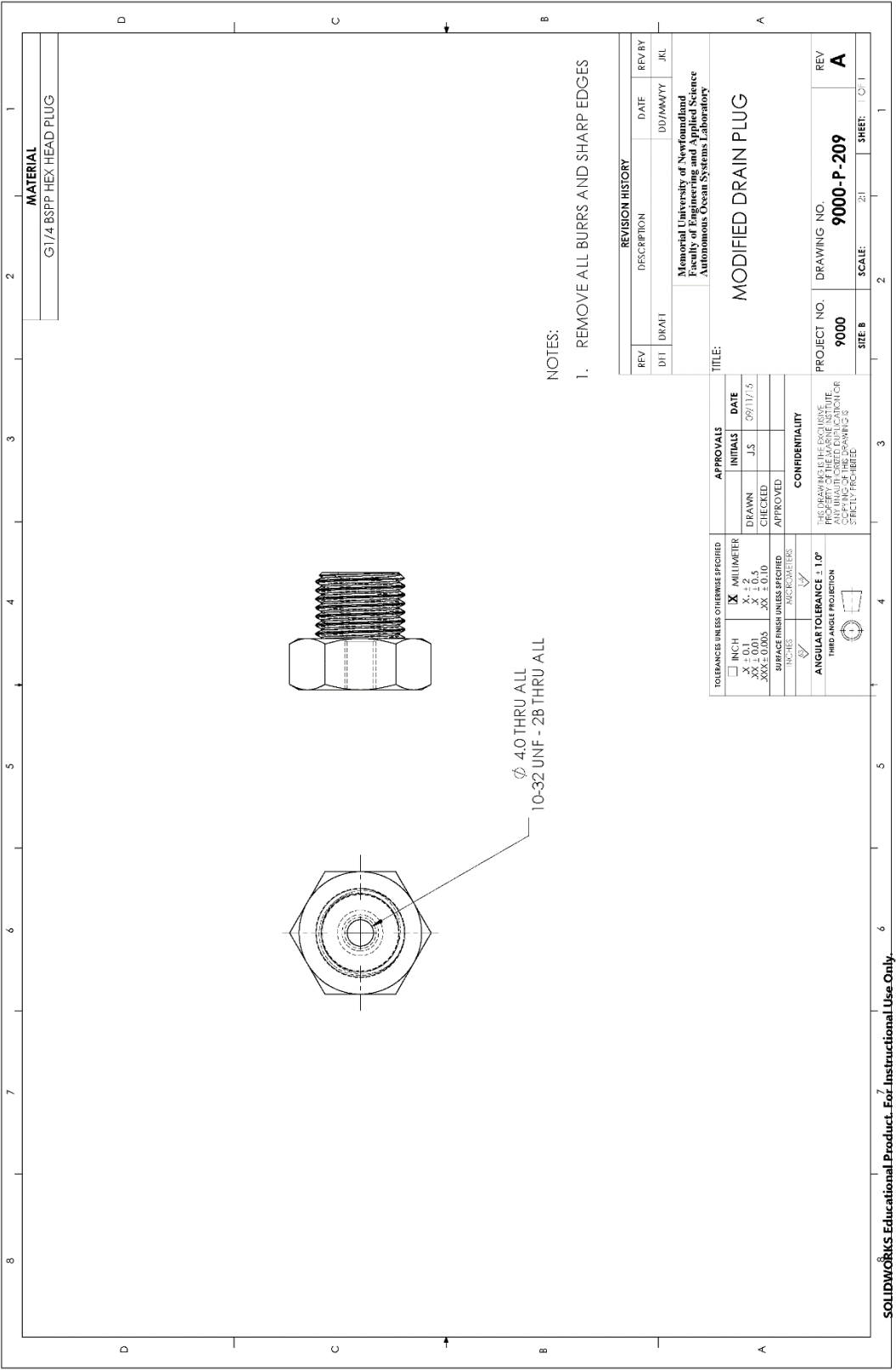


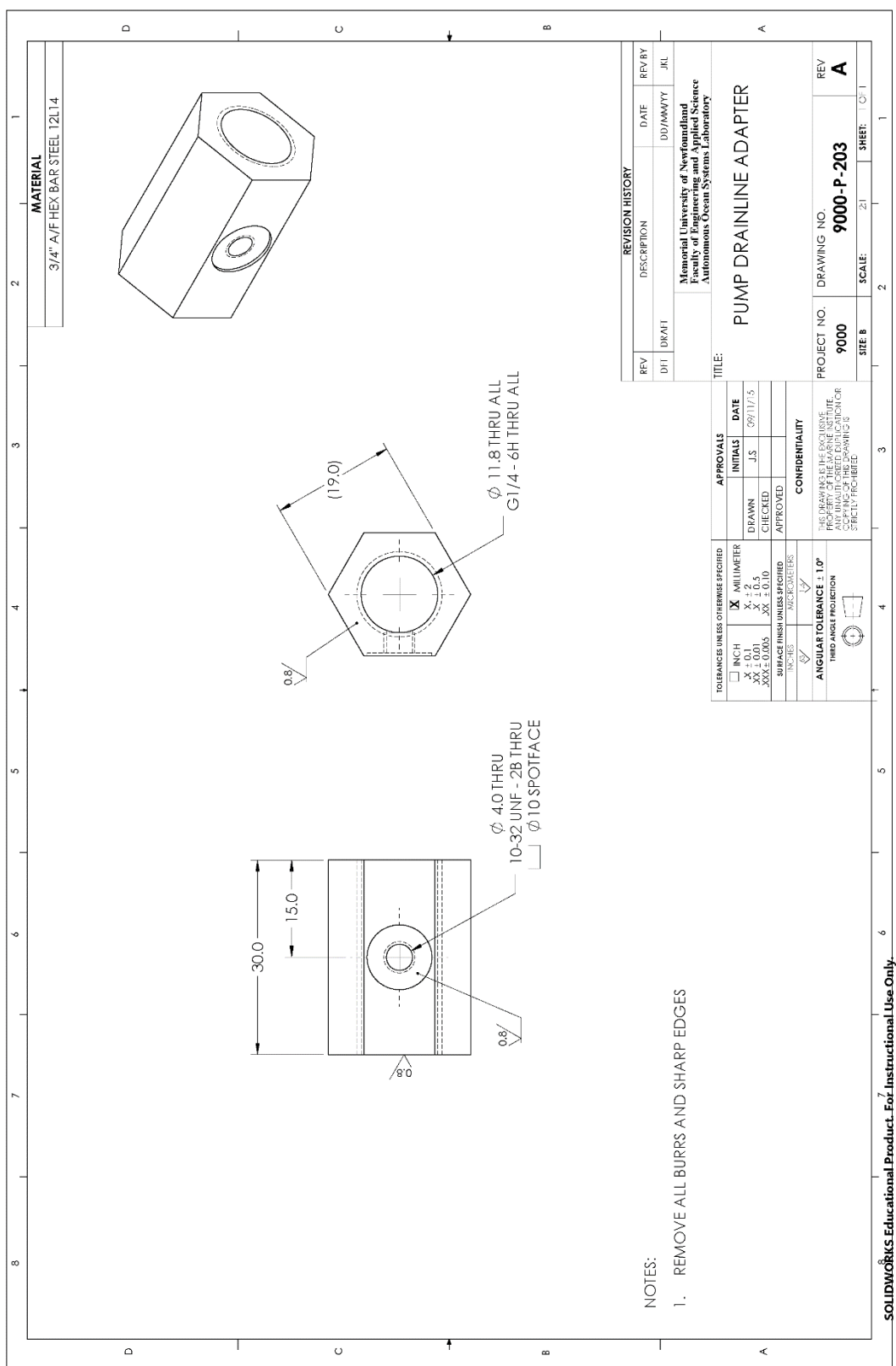


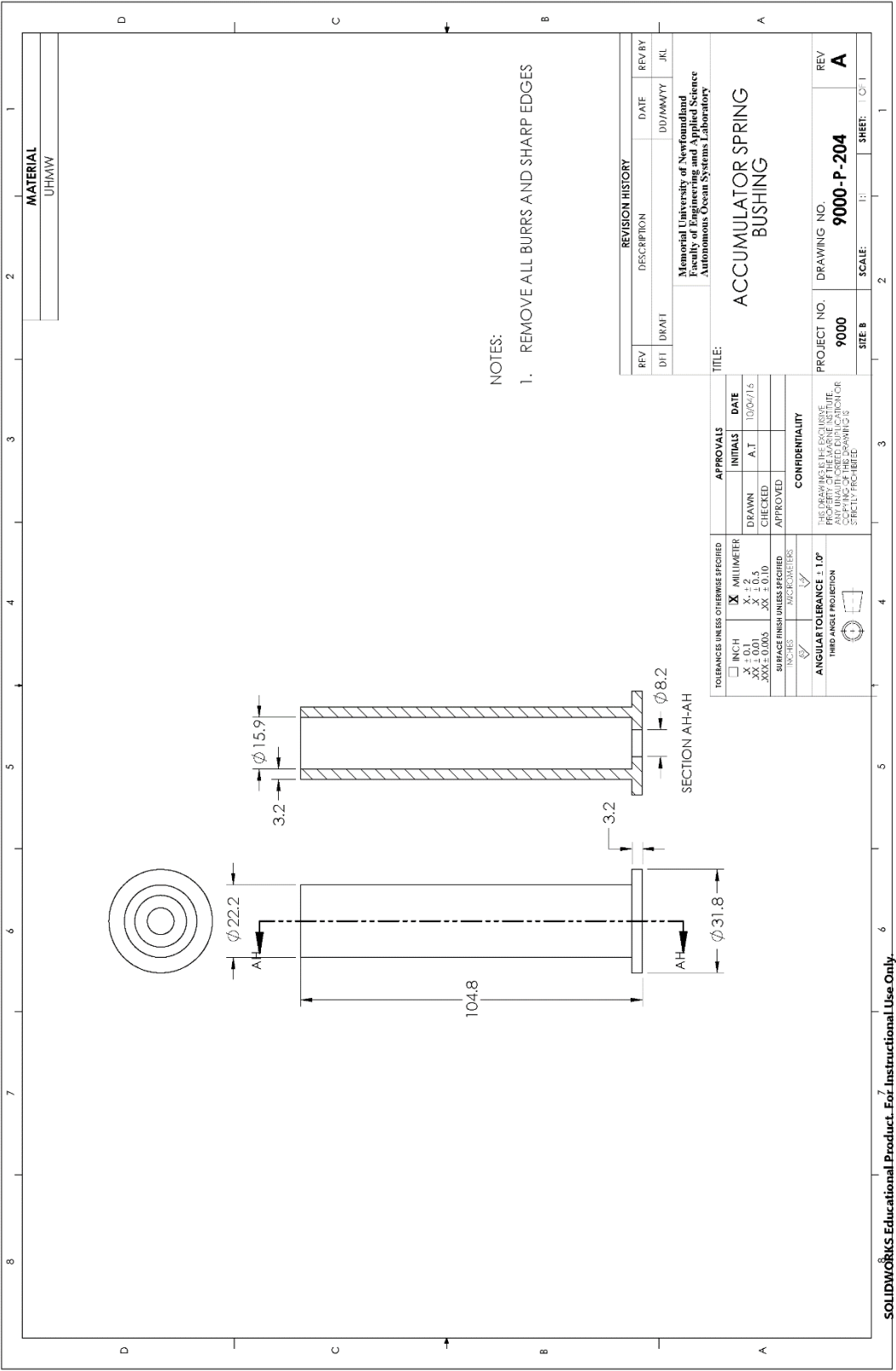


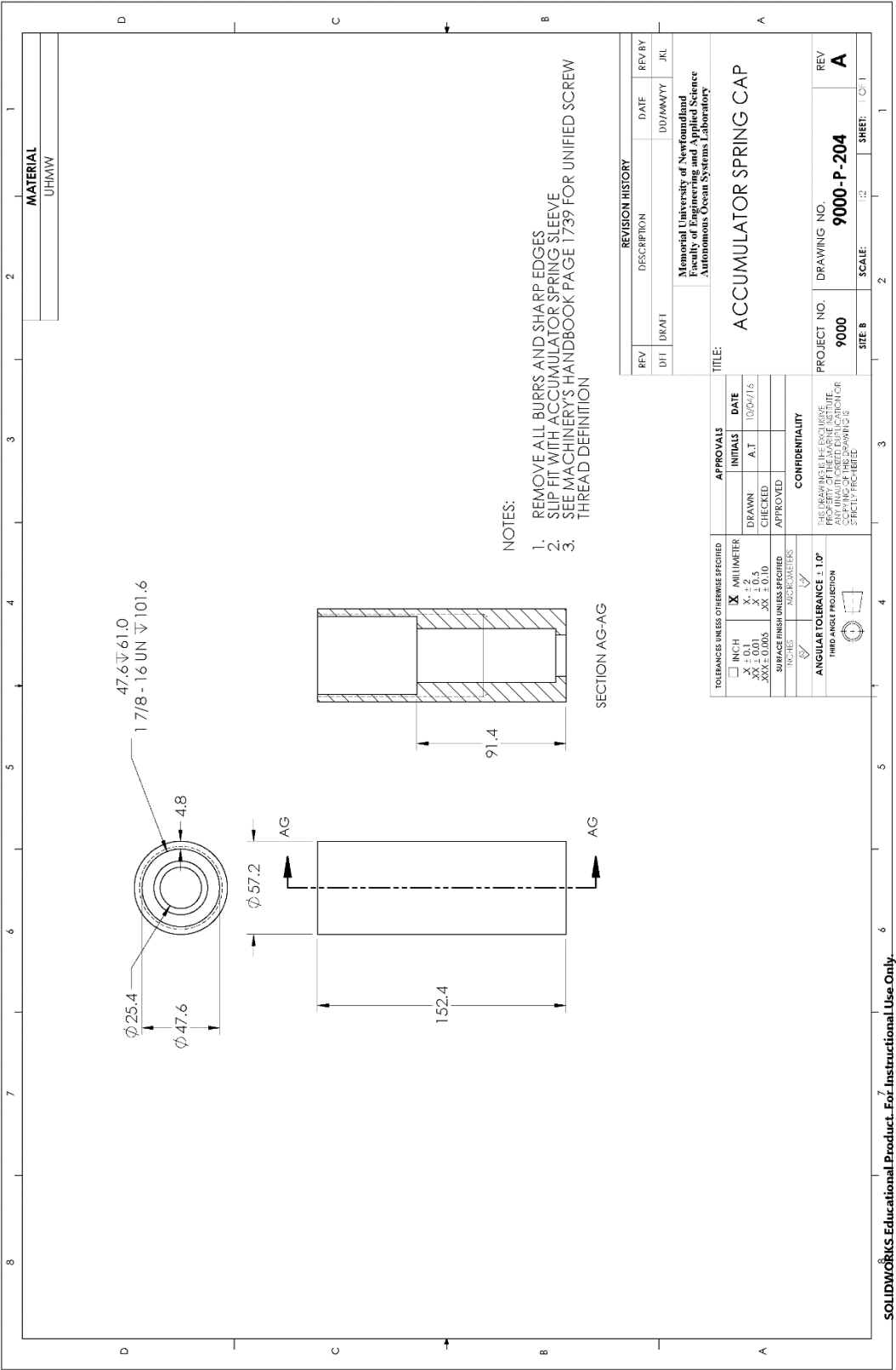


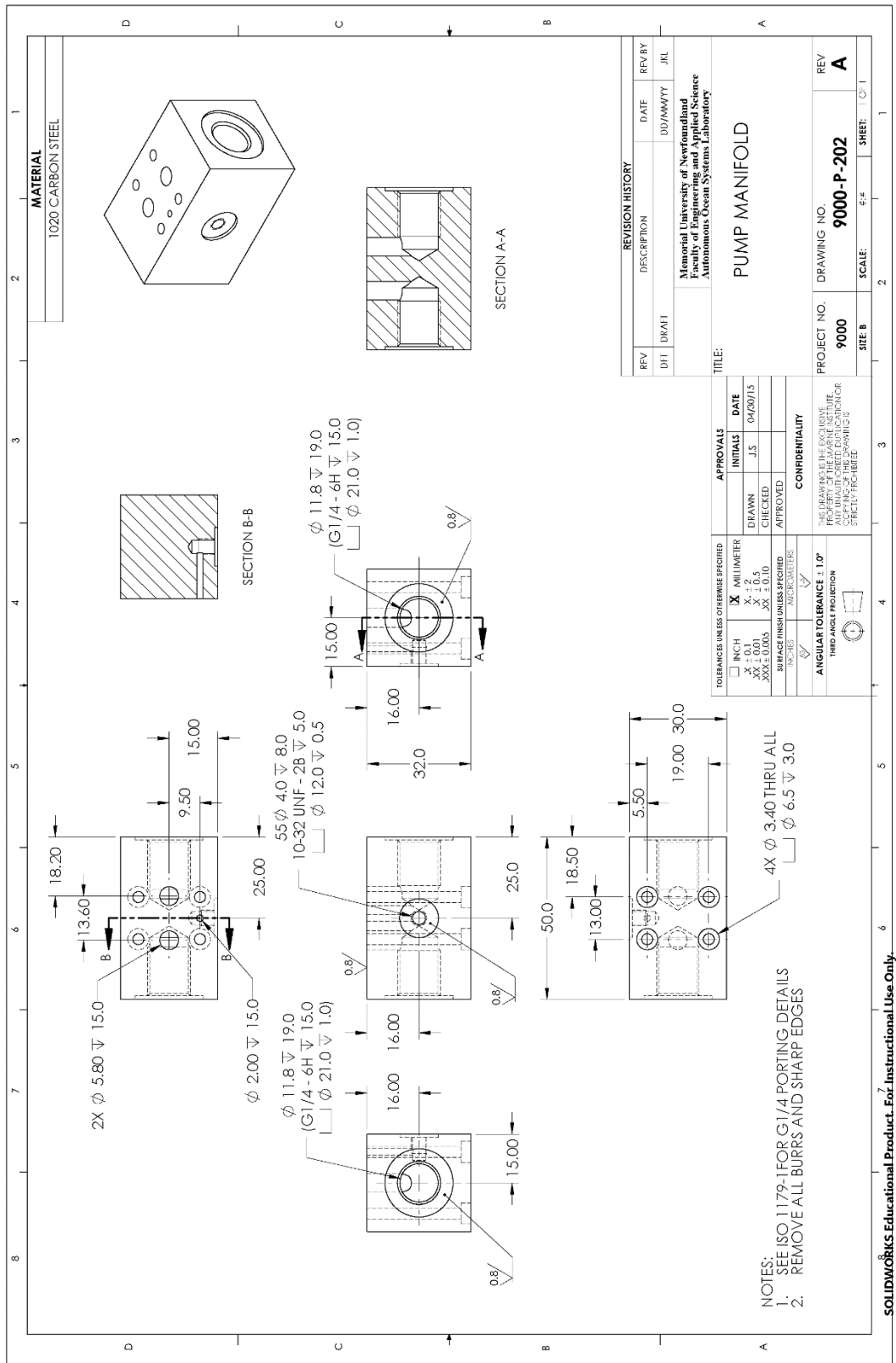


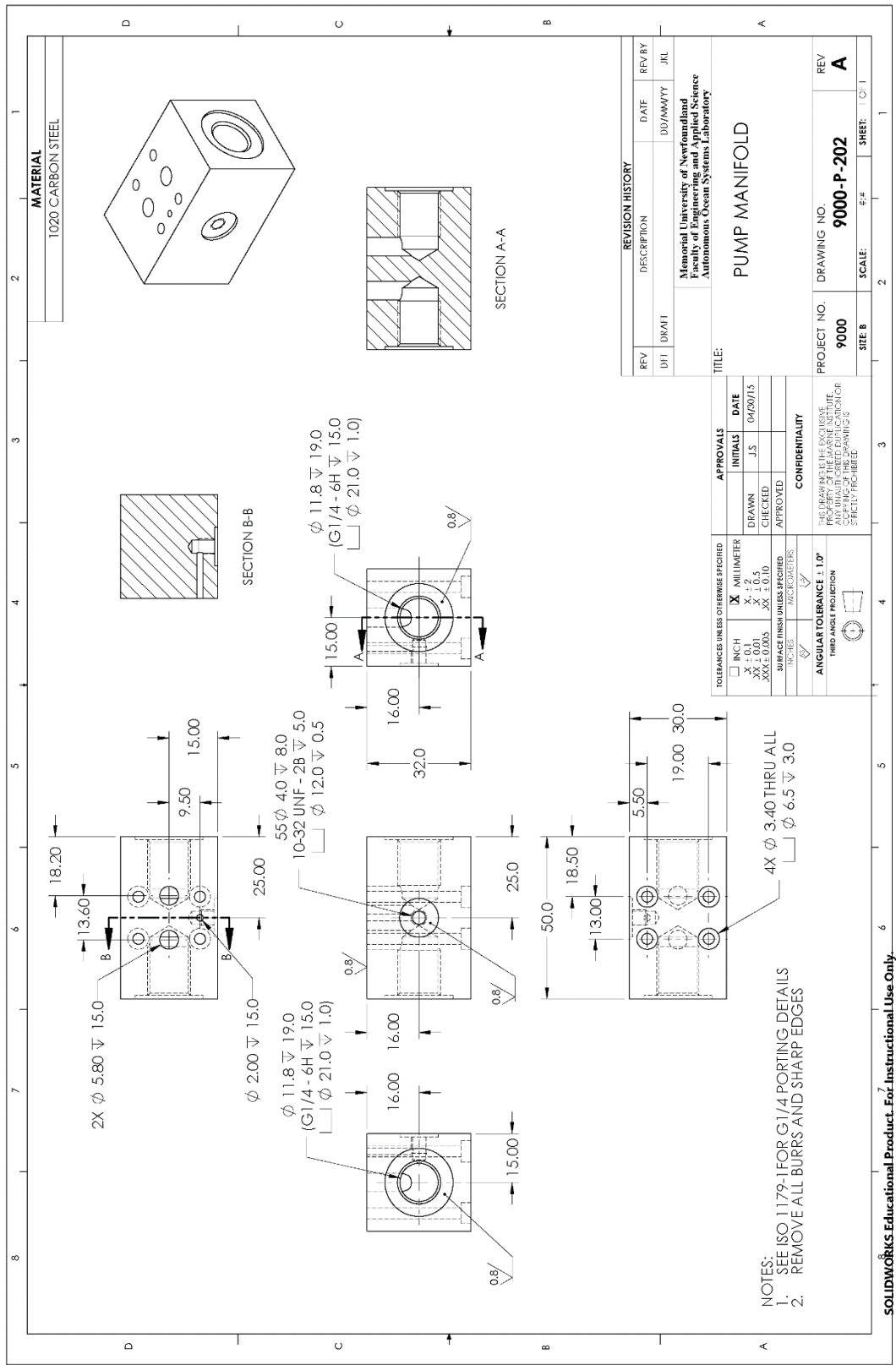


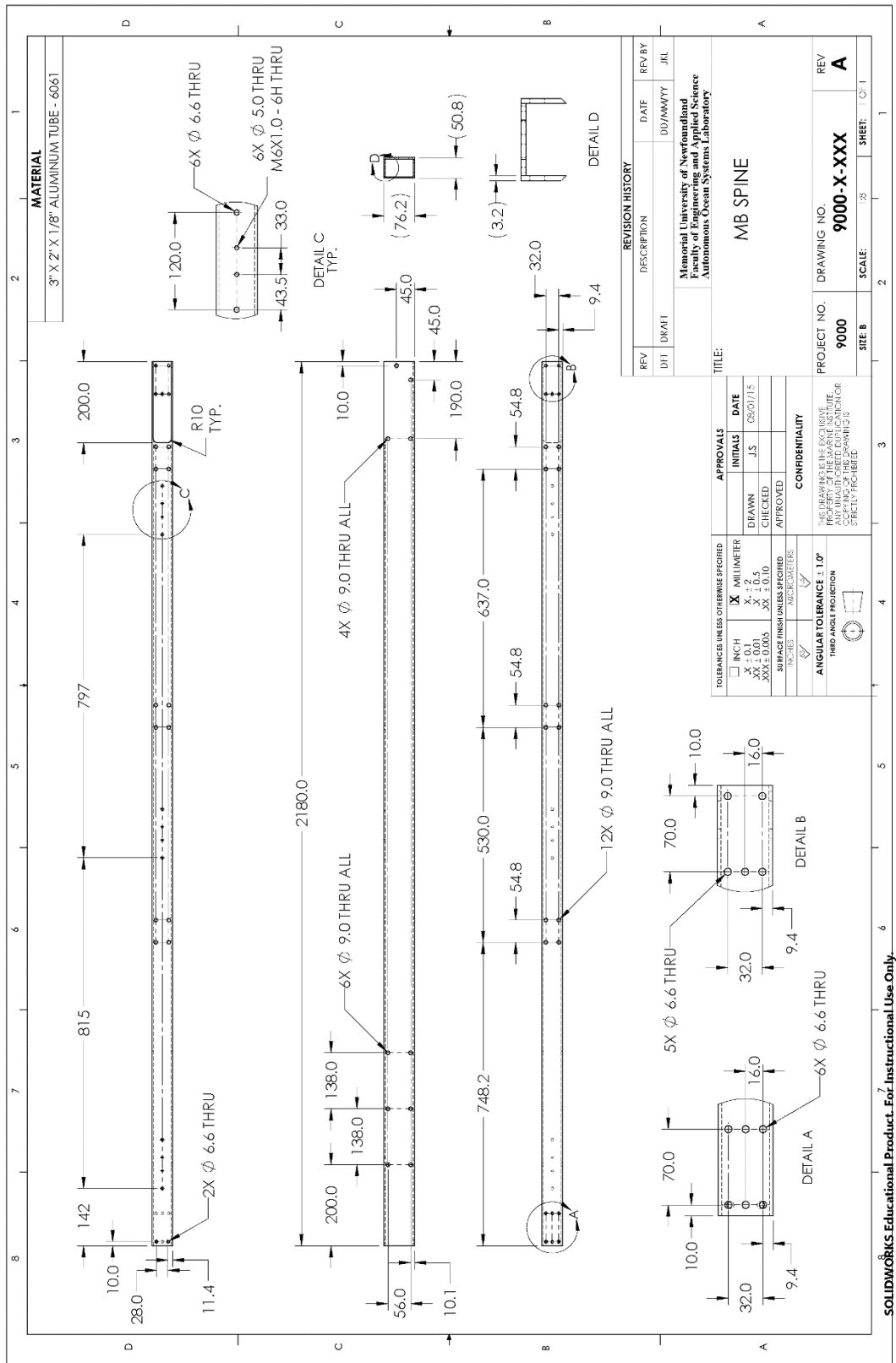


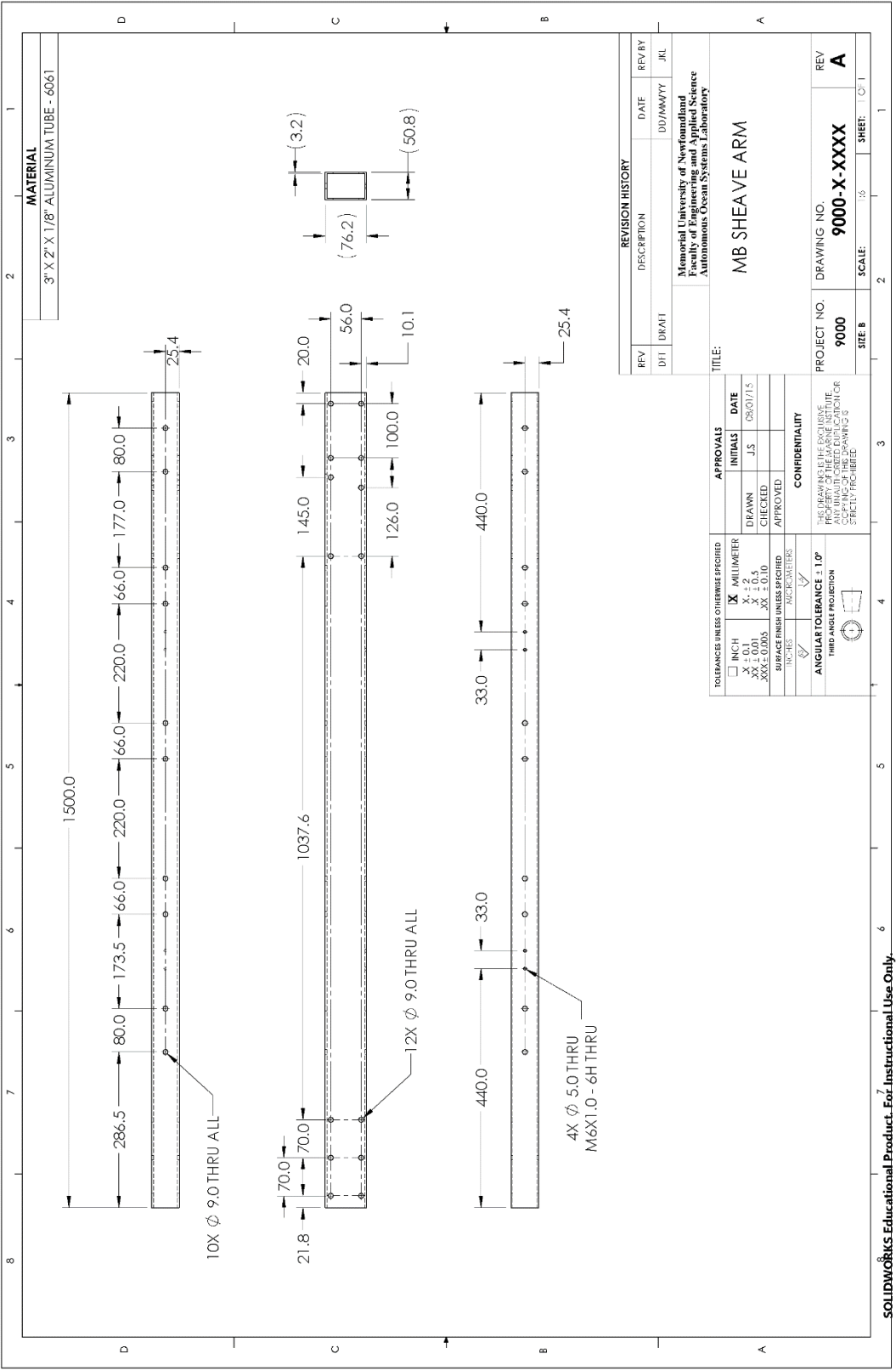


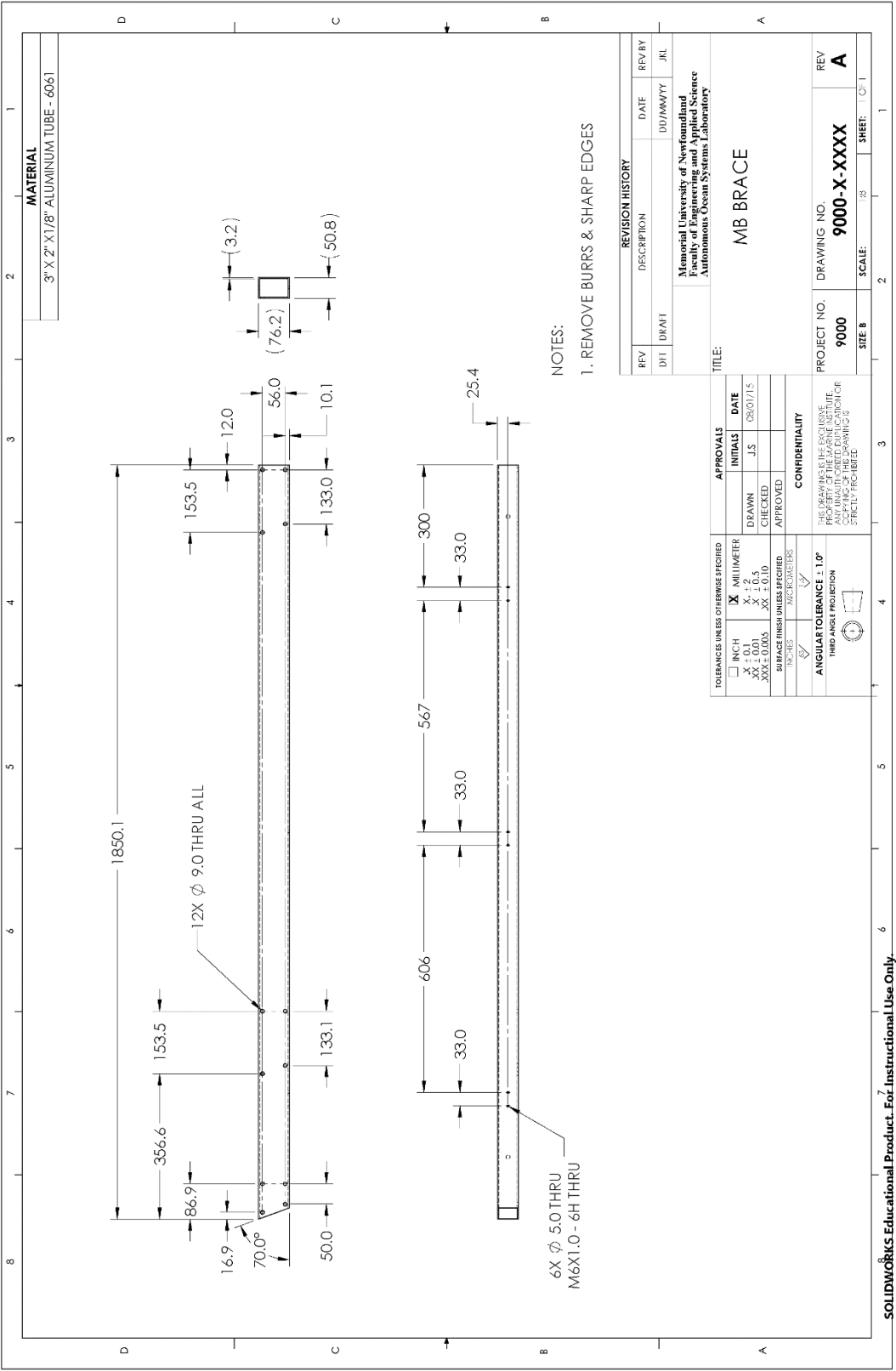


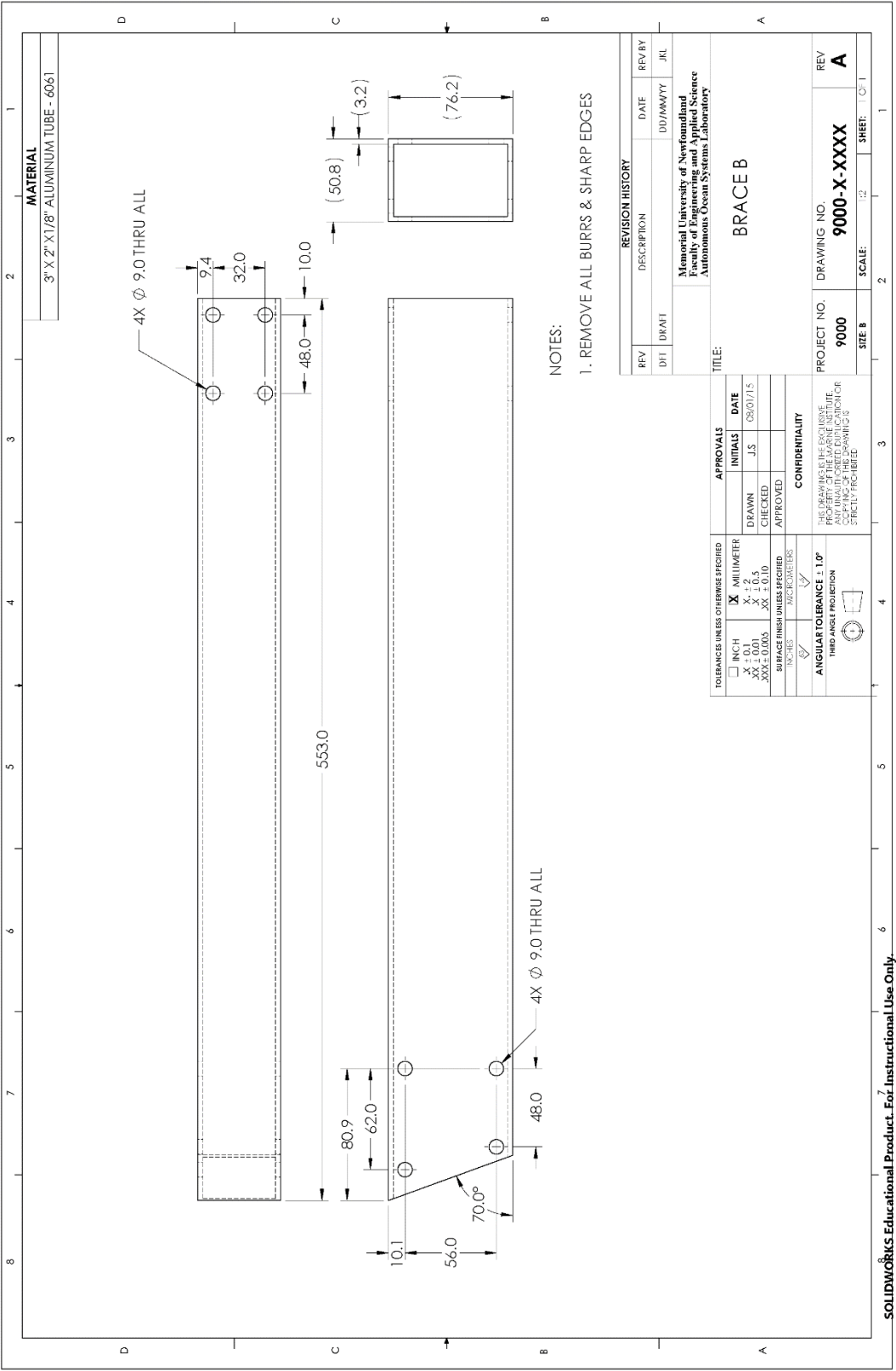


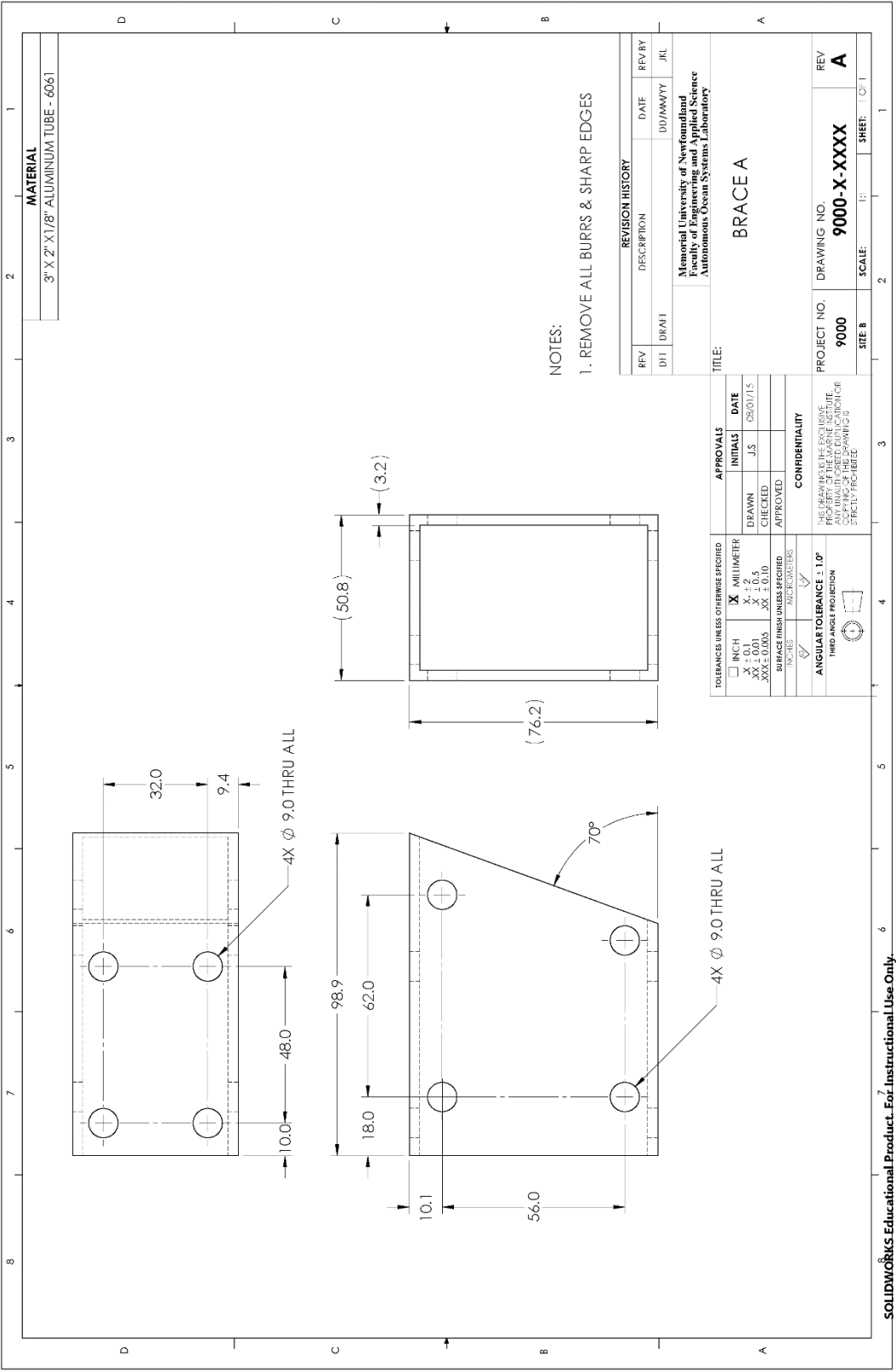


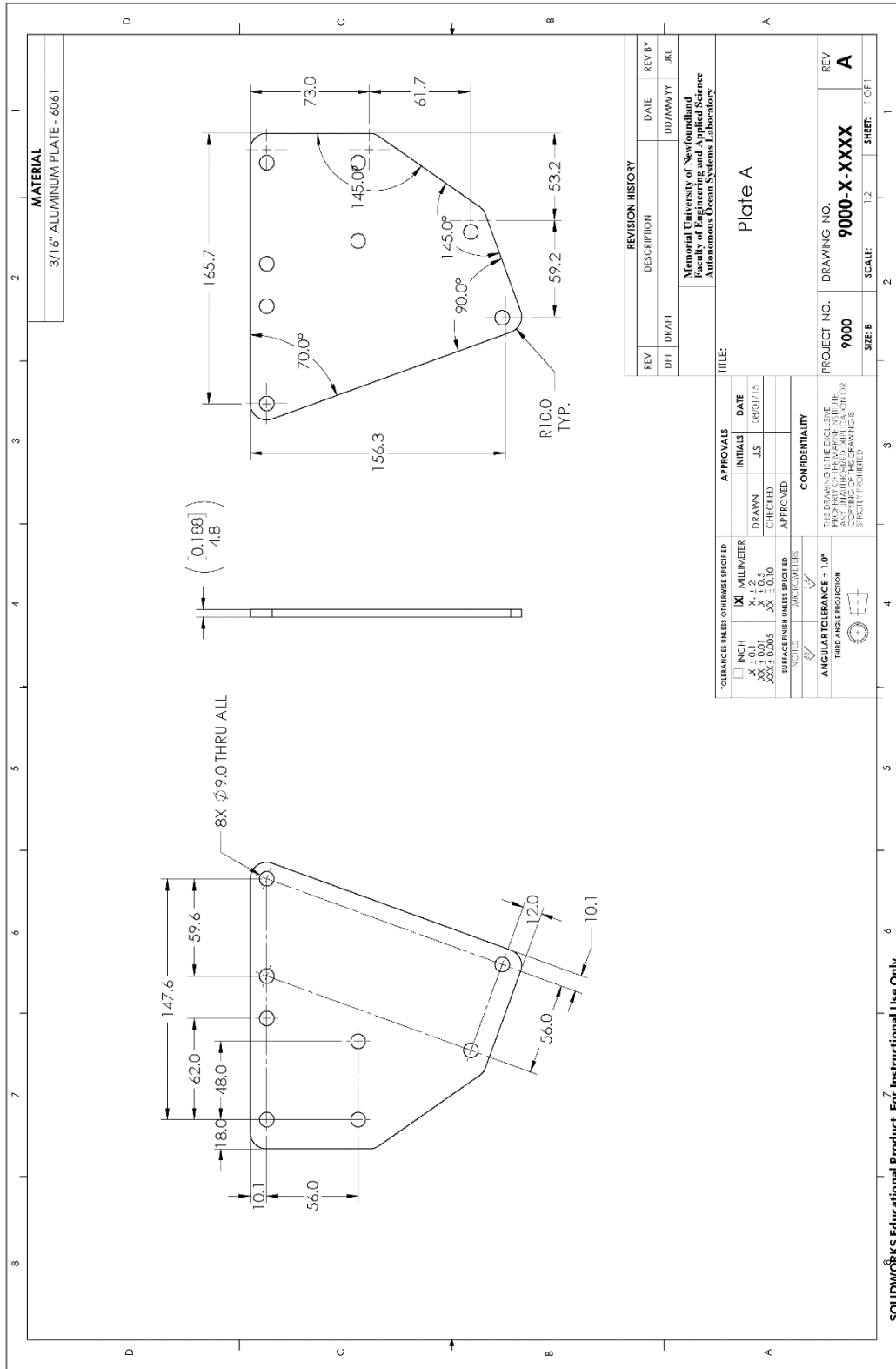


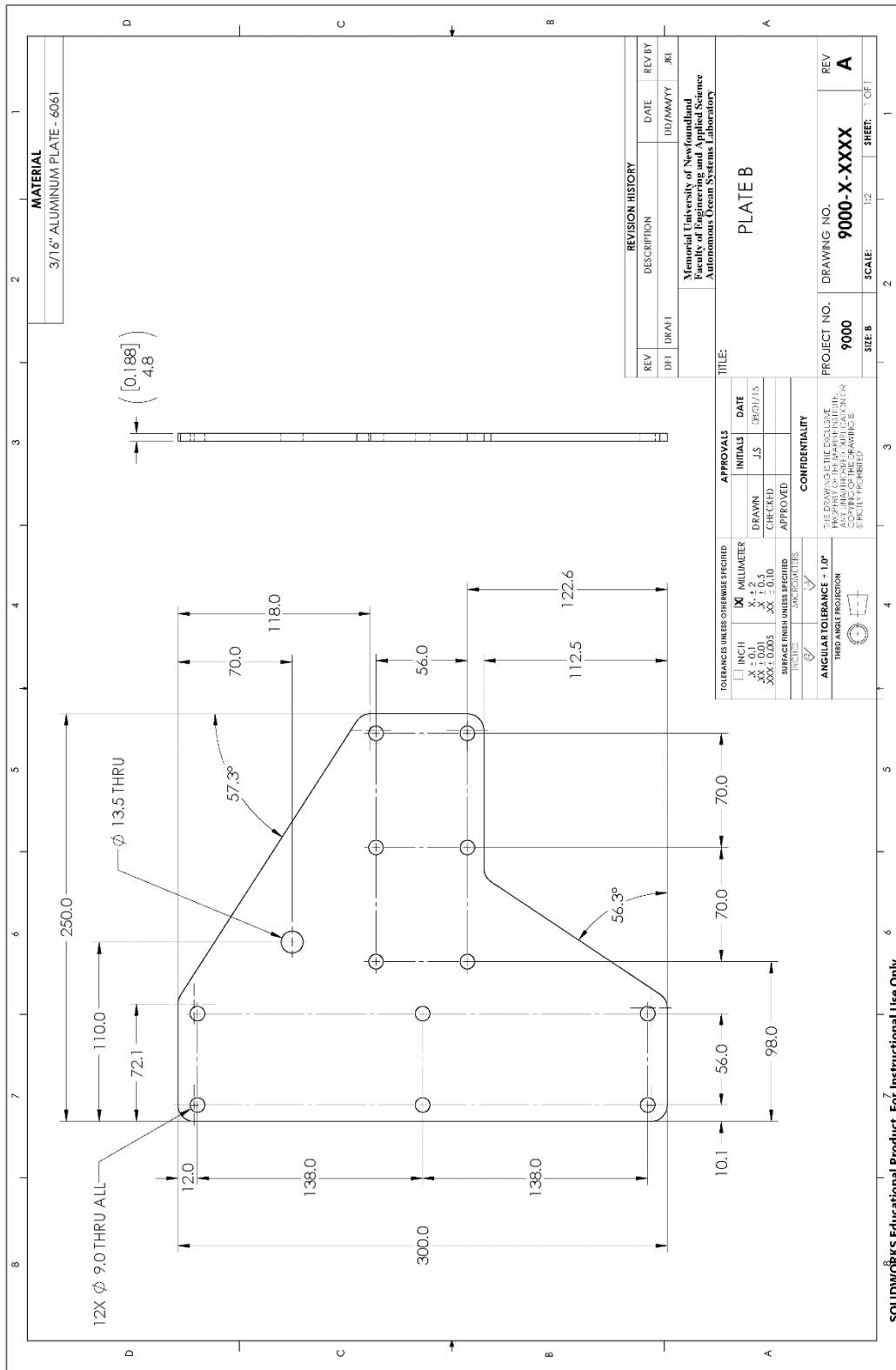


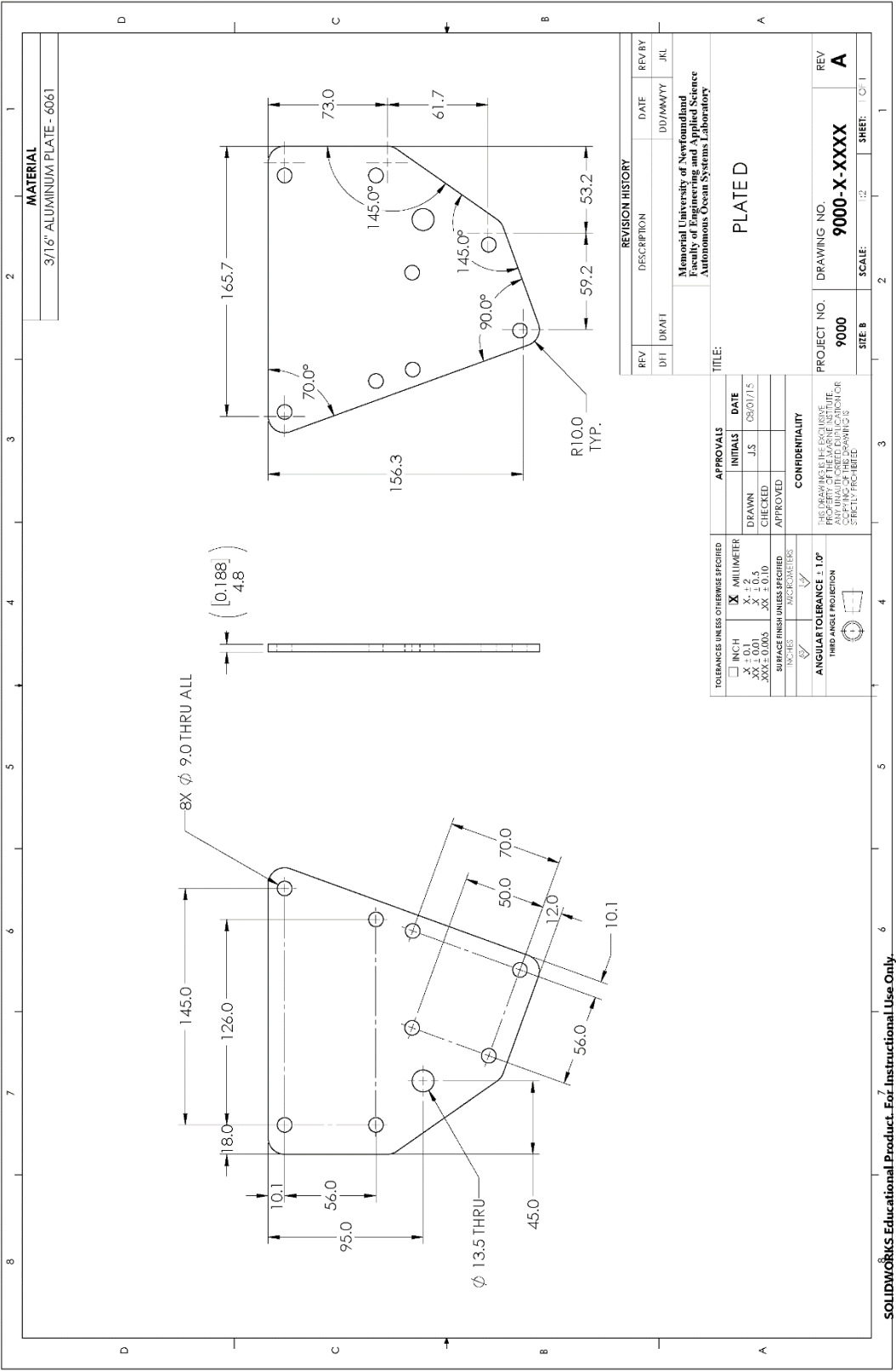


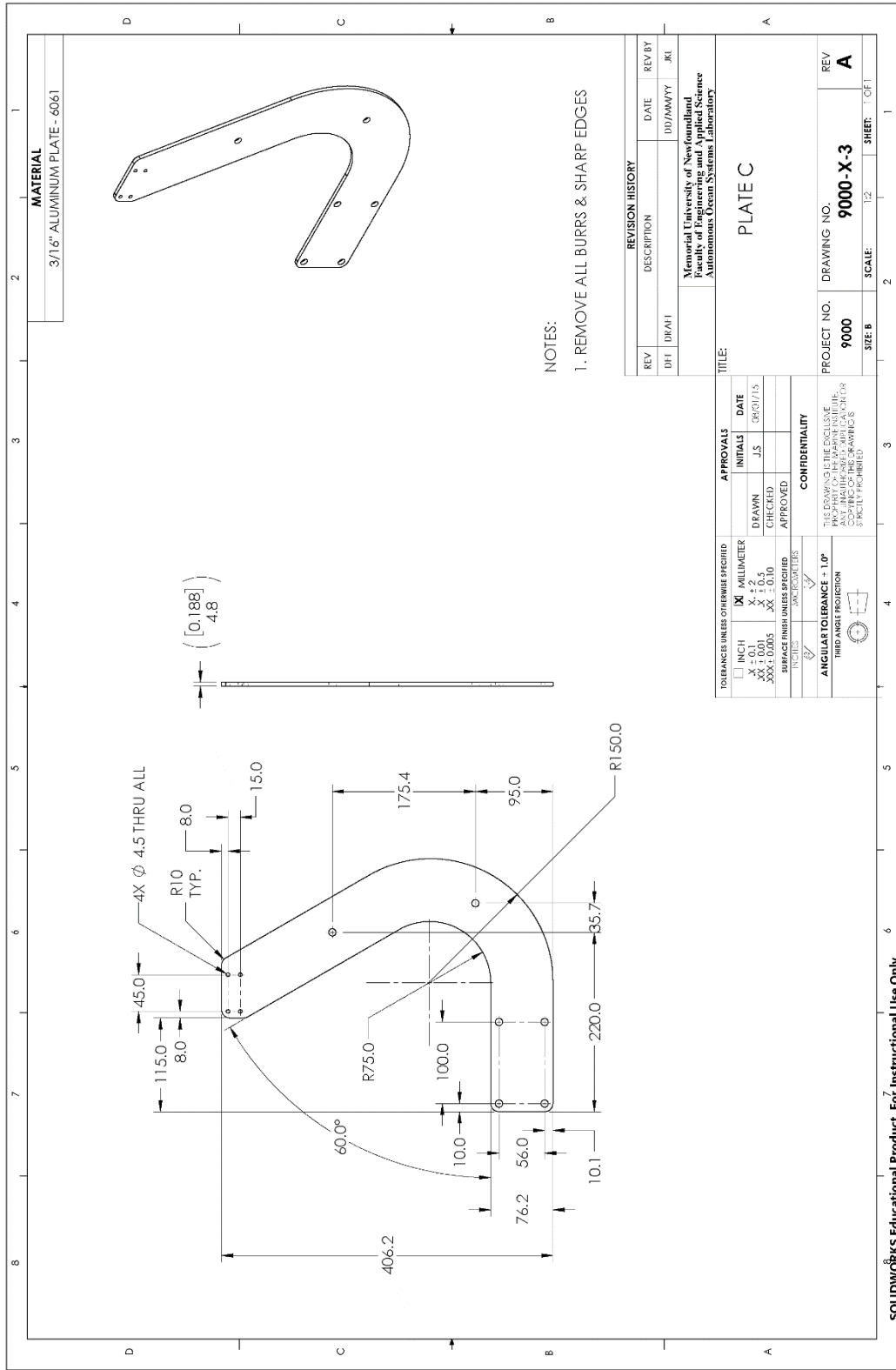


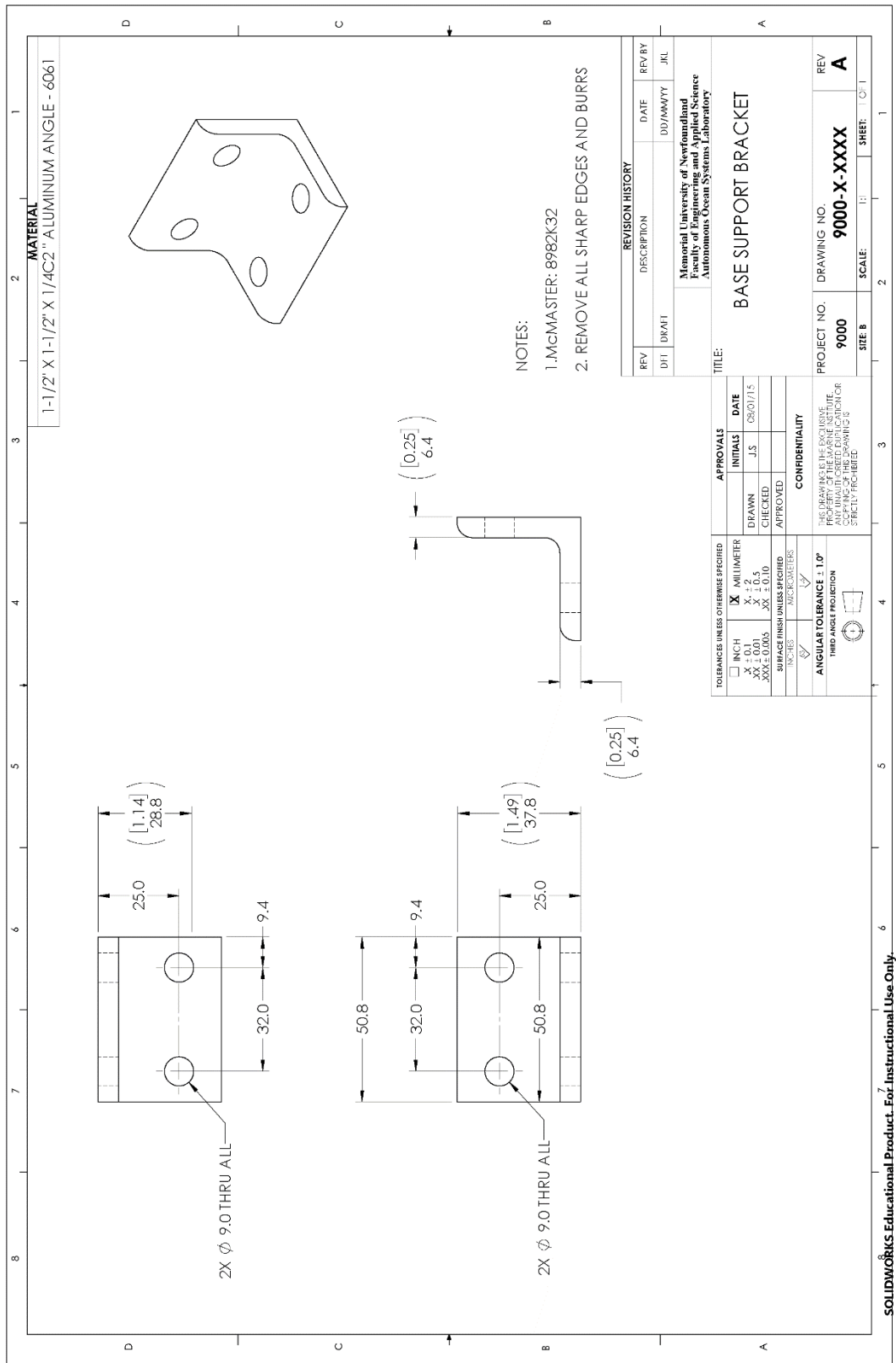


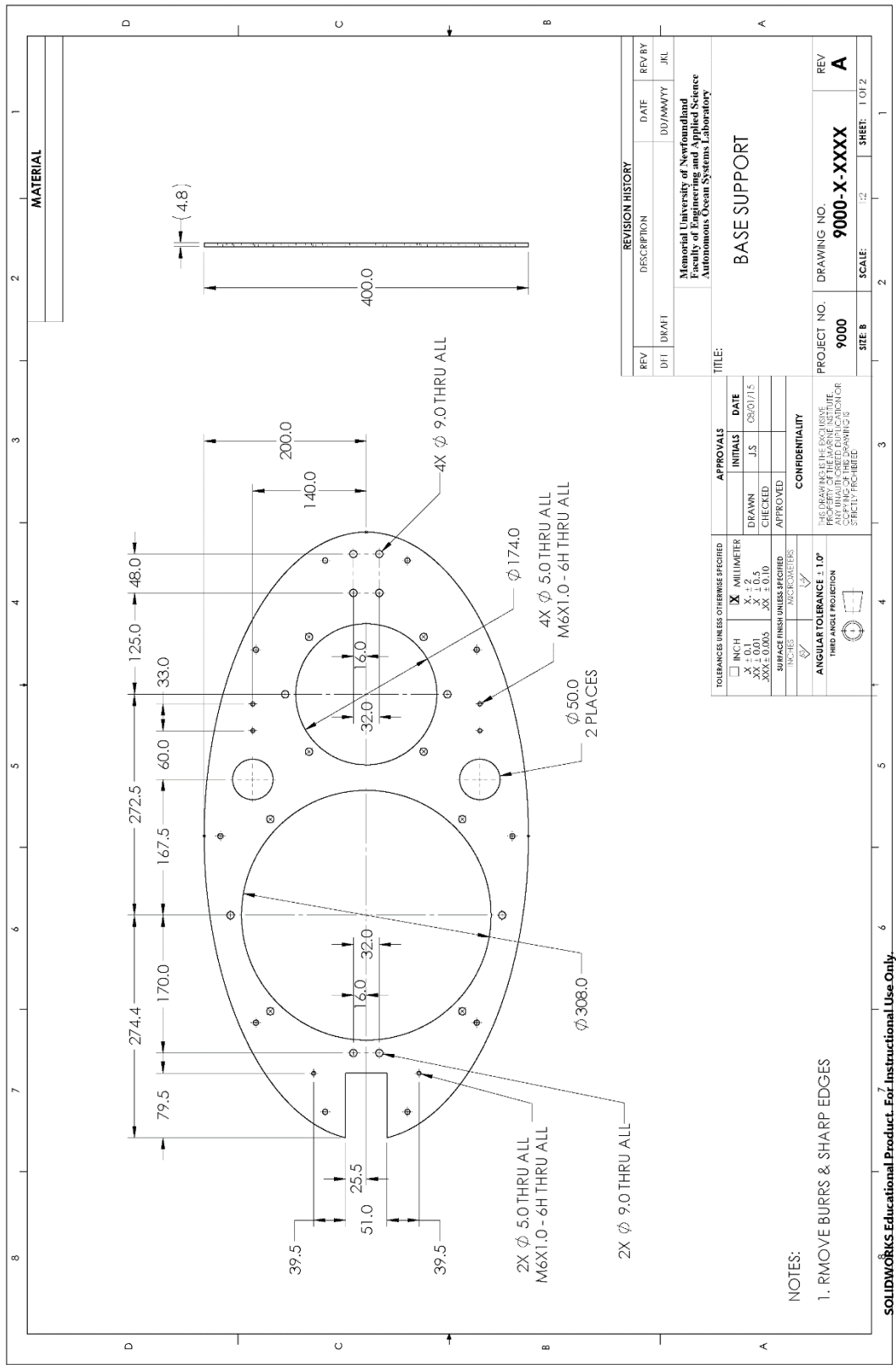


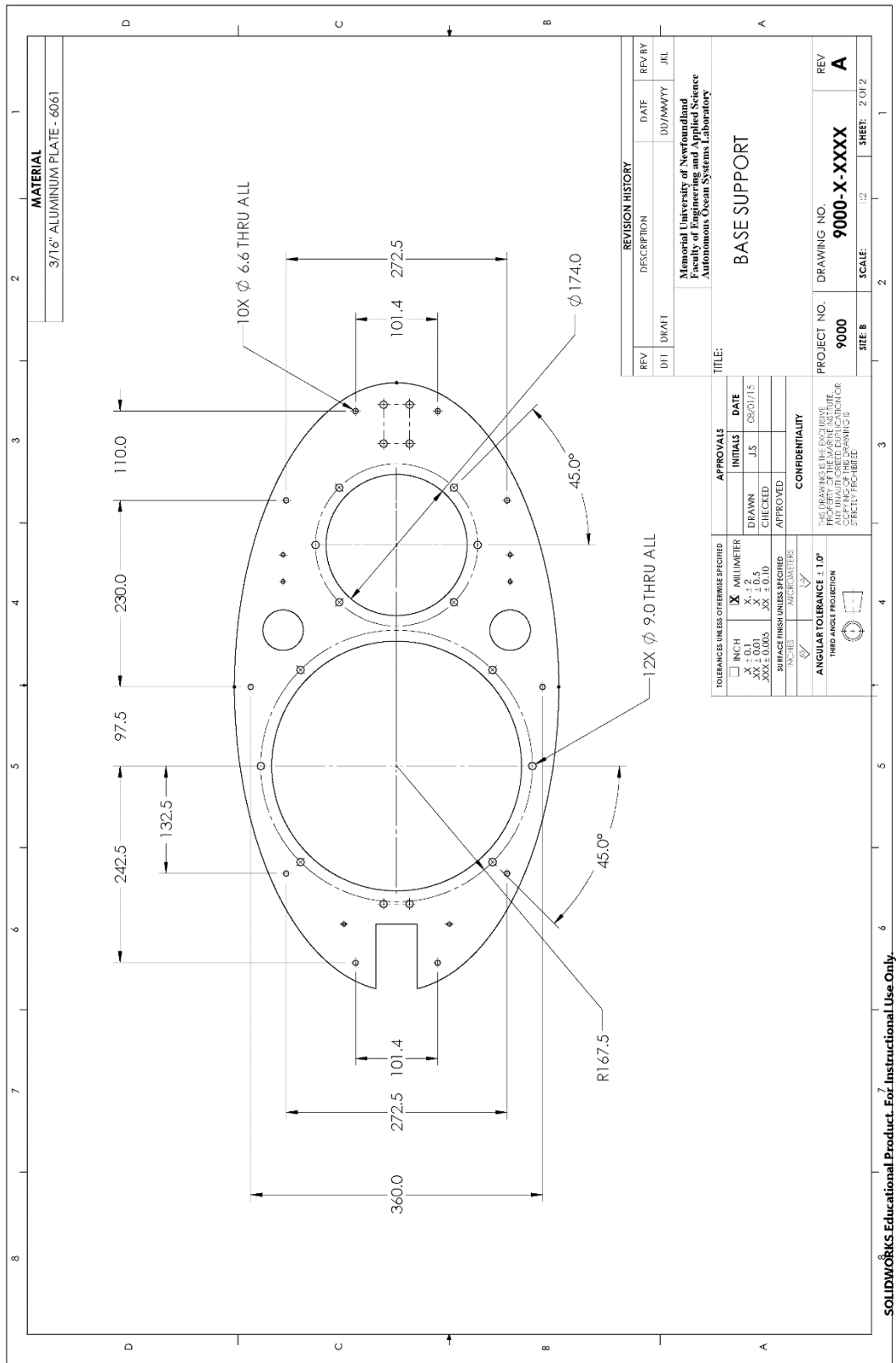


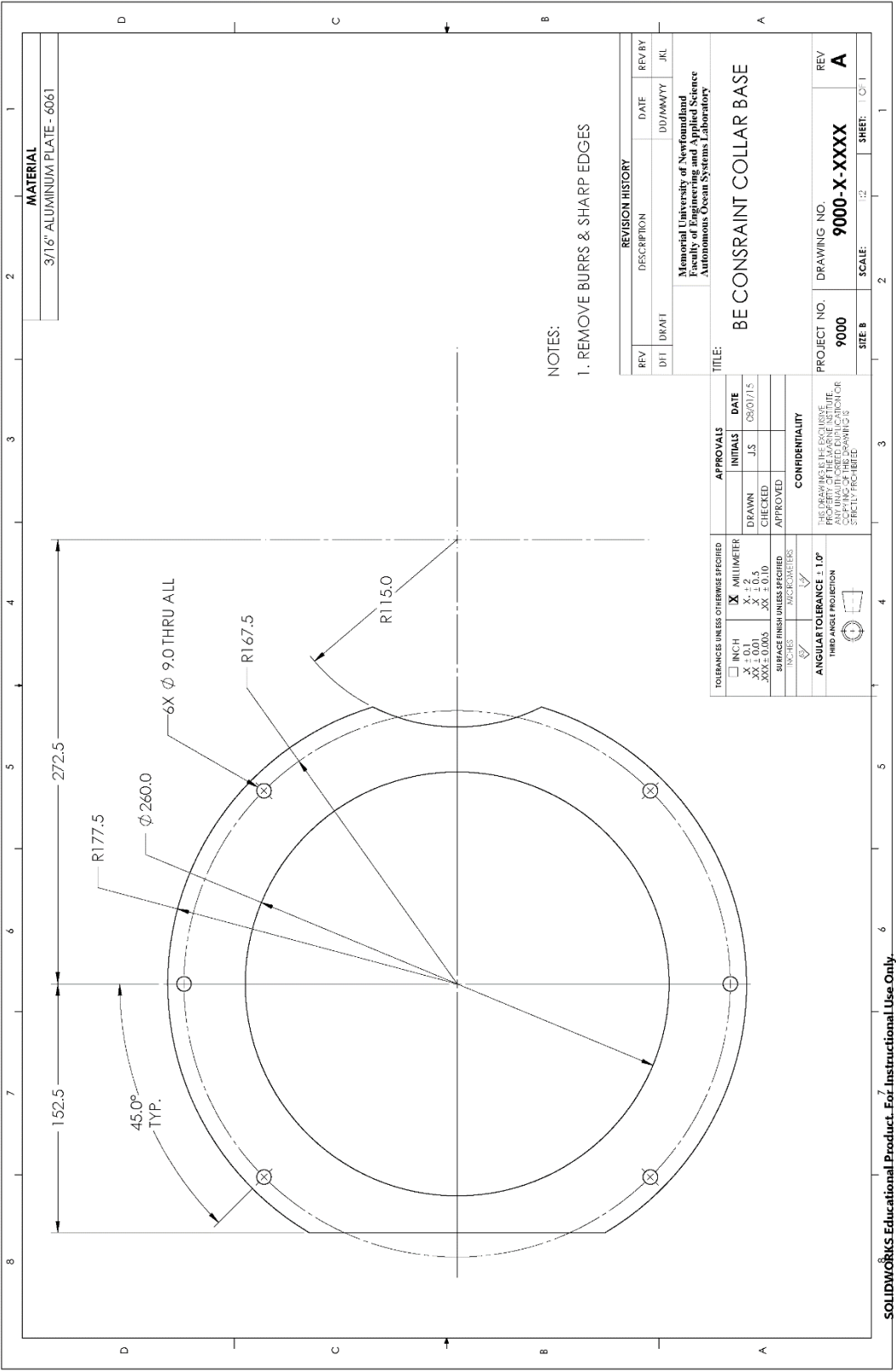








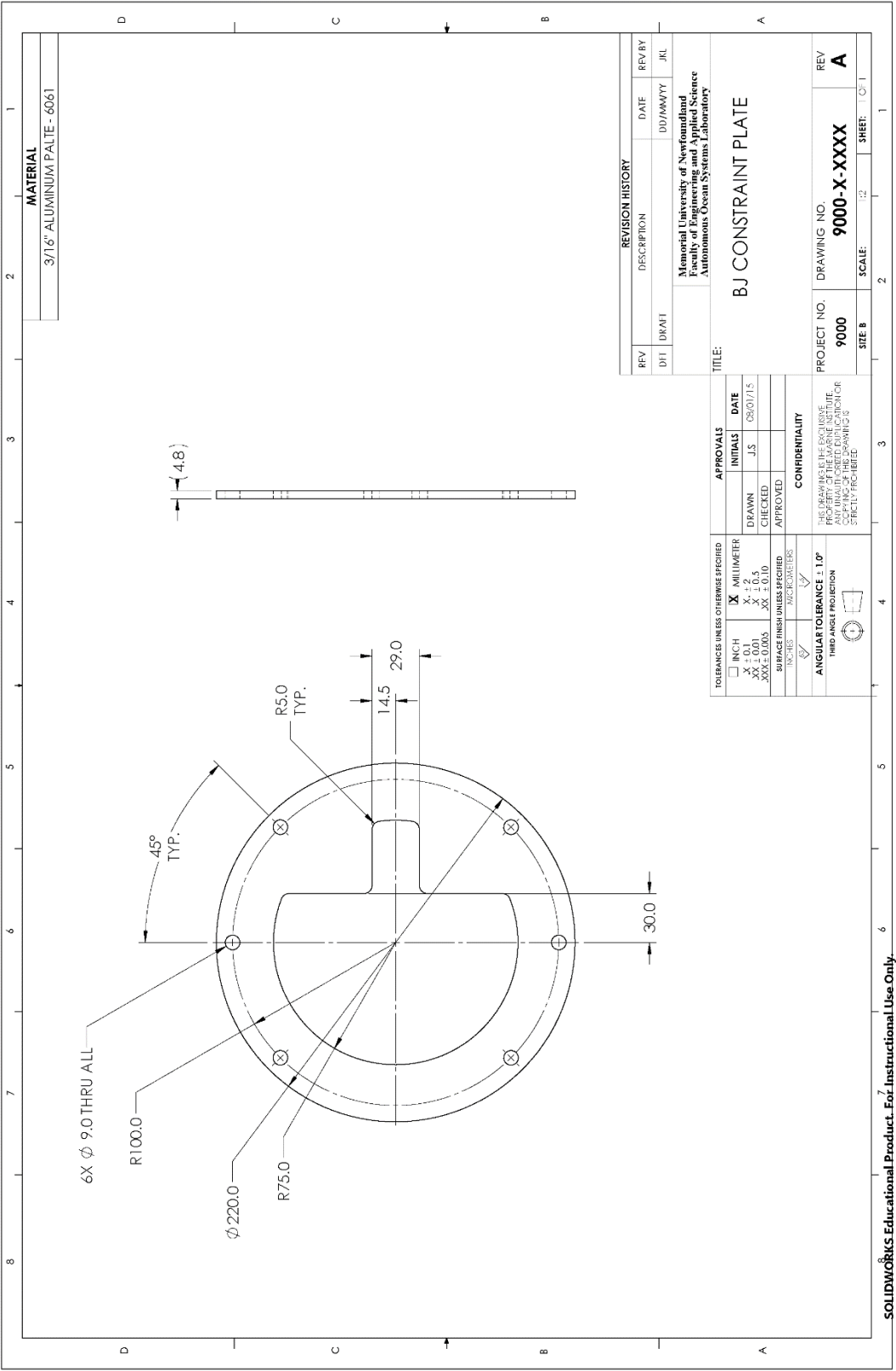


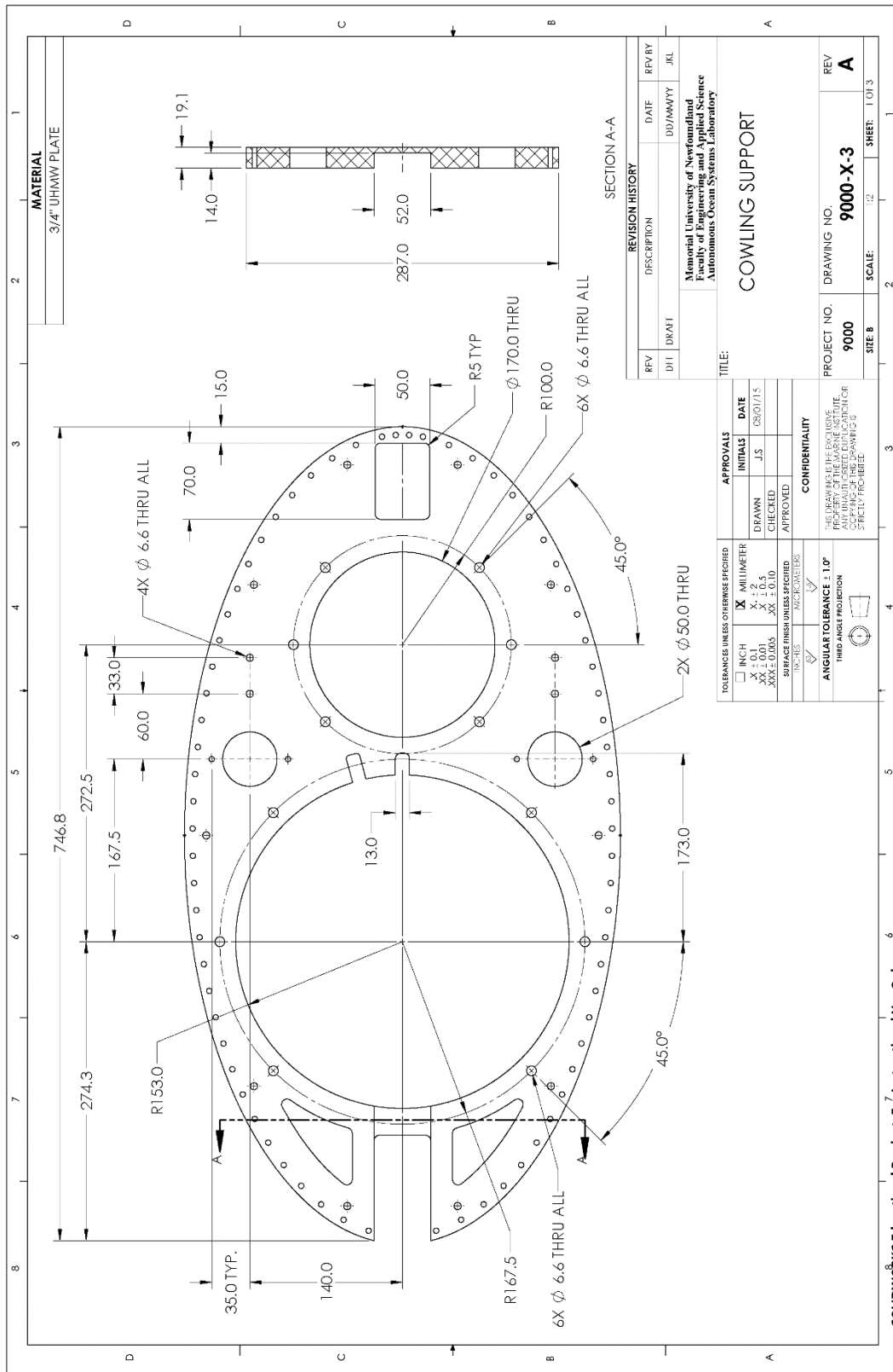


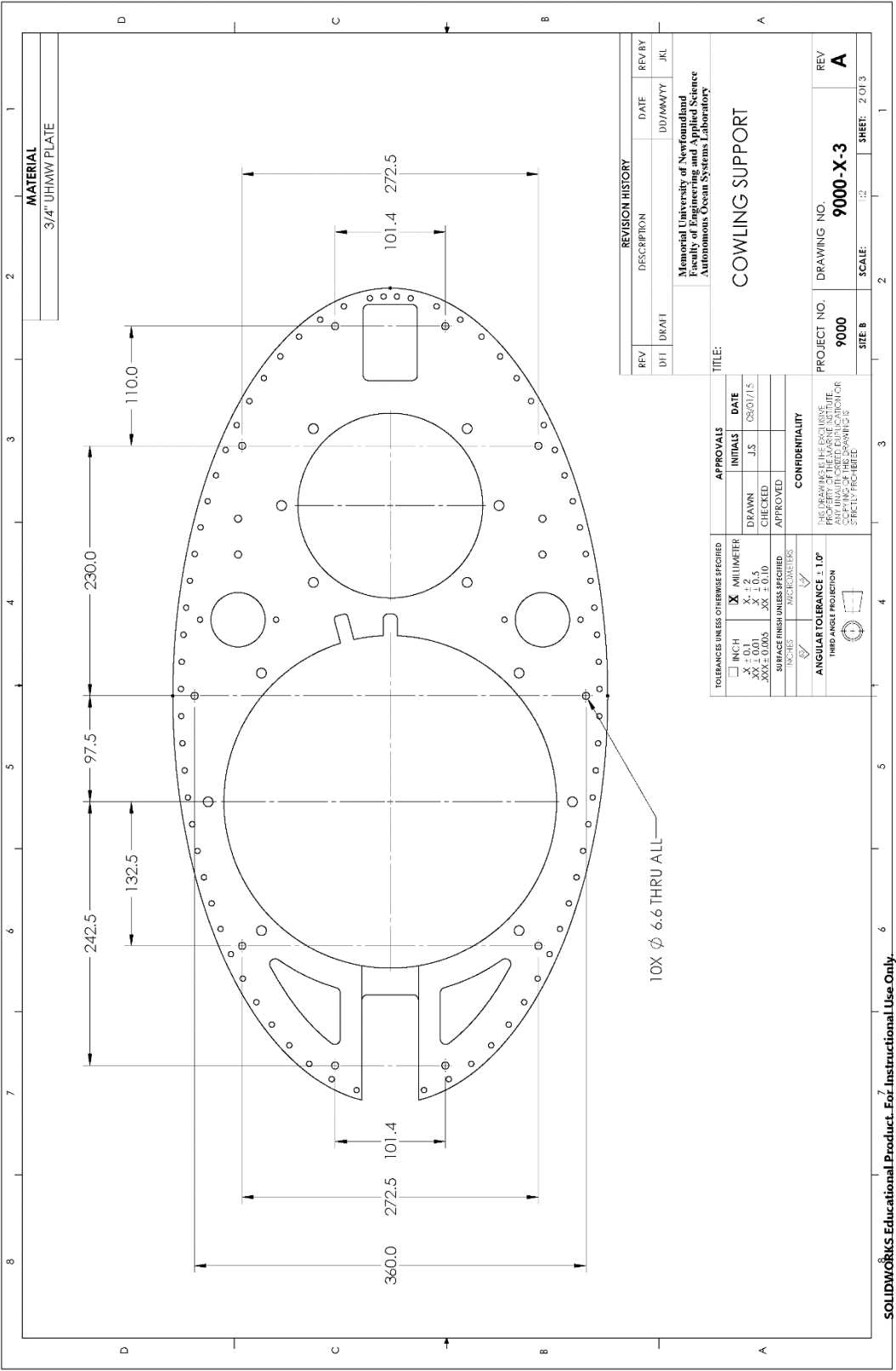
NOTES:
1. REMOVE BURRS & SHARP EDGES

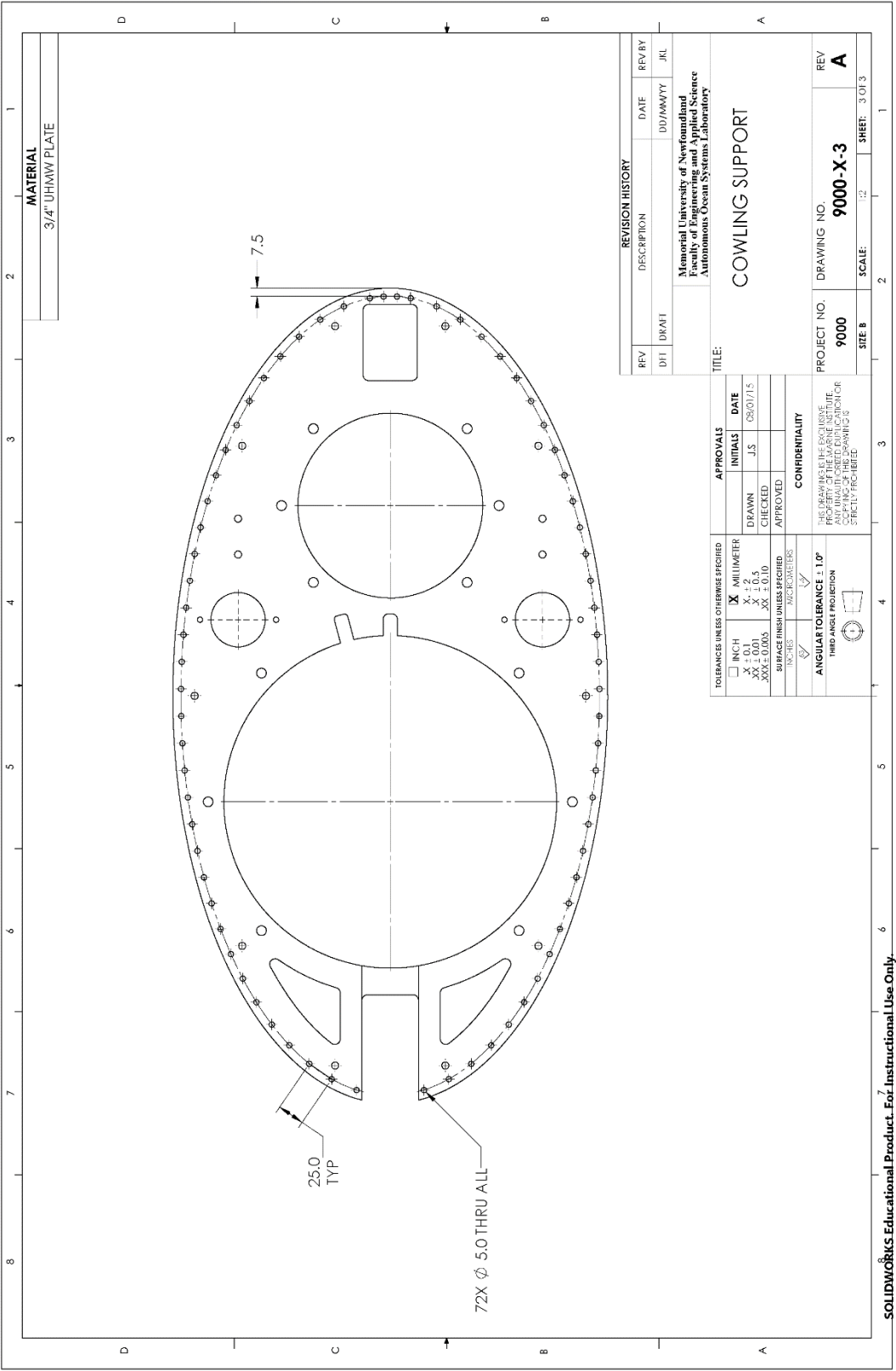
| REVISION HISTORY | | | |
|--|-------------|-------------------------|-----------|
| REV | DESCRIPTION | DATE | REV BY |
| D11 | DRAFT | DD/MM/YY | JKL |
| Memorial University of Newfoundland Faculty of Engineering and Applied Science Autonomous Ocean Systems Laboratory | | | |
| TITLE: BE CONSTRAINT COLLAR BASE | | | |
| PROJECT NO. 9000 | | DRAWING NO. 9000-X-XXXX | REV A |
| SHEET 8 | | SCALE: 1:2 | SHEET 101 |

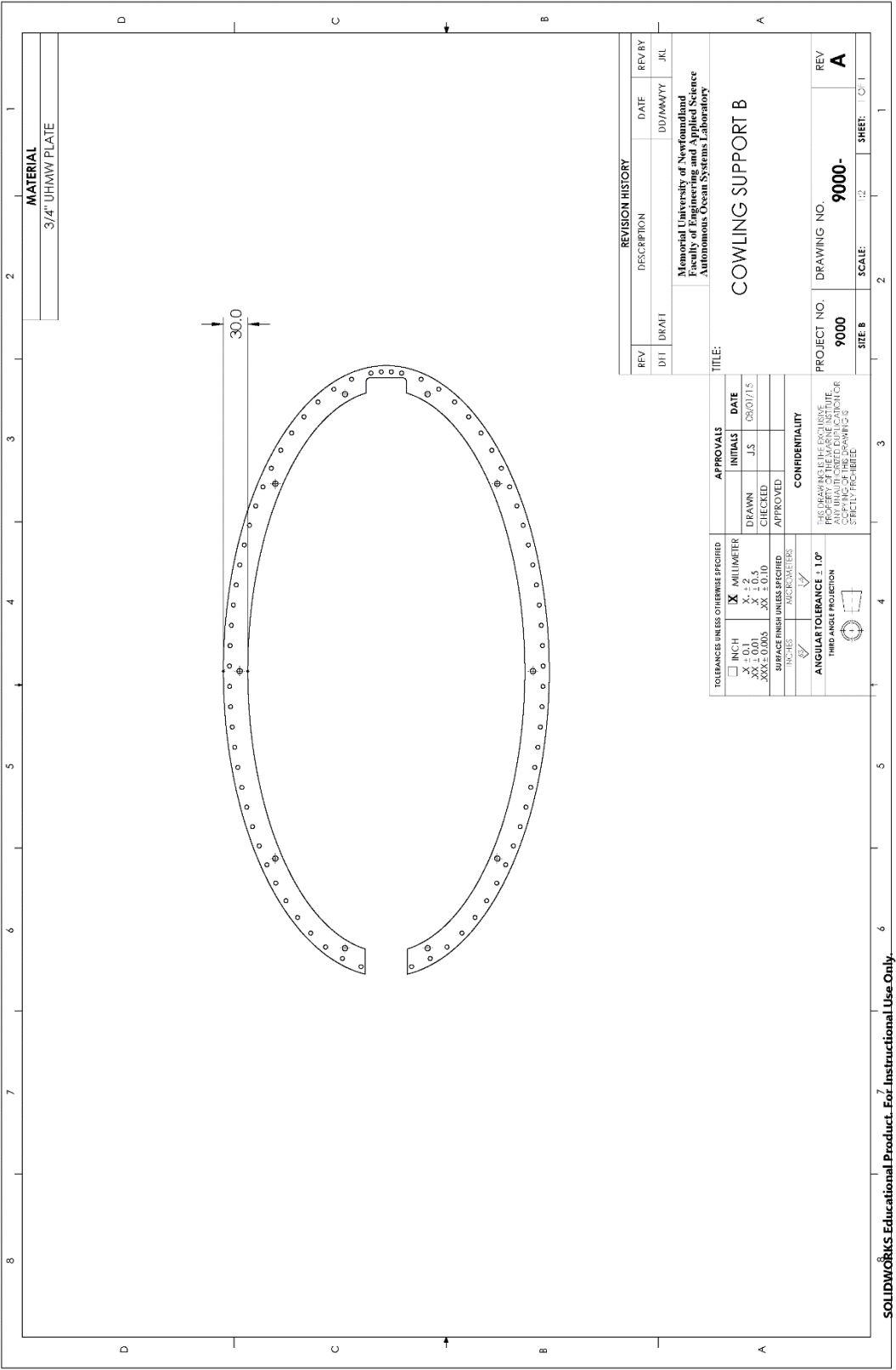
| APPROVALS | | DATE | |
|--|--|--------------------------|--|
| INITIALS | J.S | 05/07/15 | |
| DRAWN | CHECKED | | |
| APPROVED | | | |
| CONFIDENTIALITY | | | |
| THIS DRAWING IS THE EXCLUSIVE PROPERTY OF THE MARINE INSTITUTE. ANY UNAUTHORIZED REPRODUCTION OR COPIING OF THIS DRAWING IS STRICTLY PROHIBITED. | | | |
| TOLERANCES UNLESS OTHERWISE SPECIFIED | | ANGULAR TOLERANCE ± 1.0° | |
| <input type="checkbox"/> INCH | <input checked="" type="checkbox"/> MILLIMETER | THIRD ANGLE PROJECTION | |
| X ± 0.1 | X ± 0.2 | | |
| XX ± 0.05 | XX ± 0.5 | | |
| XXX ± 0.005 | XXX ± 0.10 | | |
| SURFACE FINISH UNLESS SPECIFIED | | | |
| INCHES | | MILLIMETERS | |

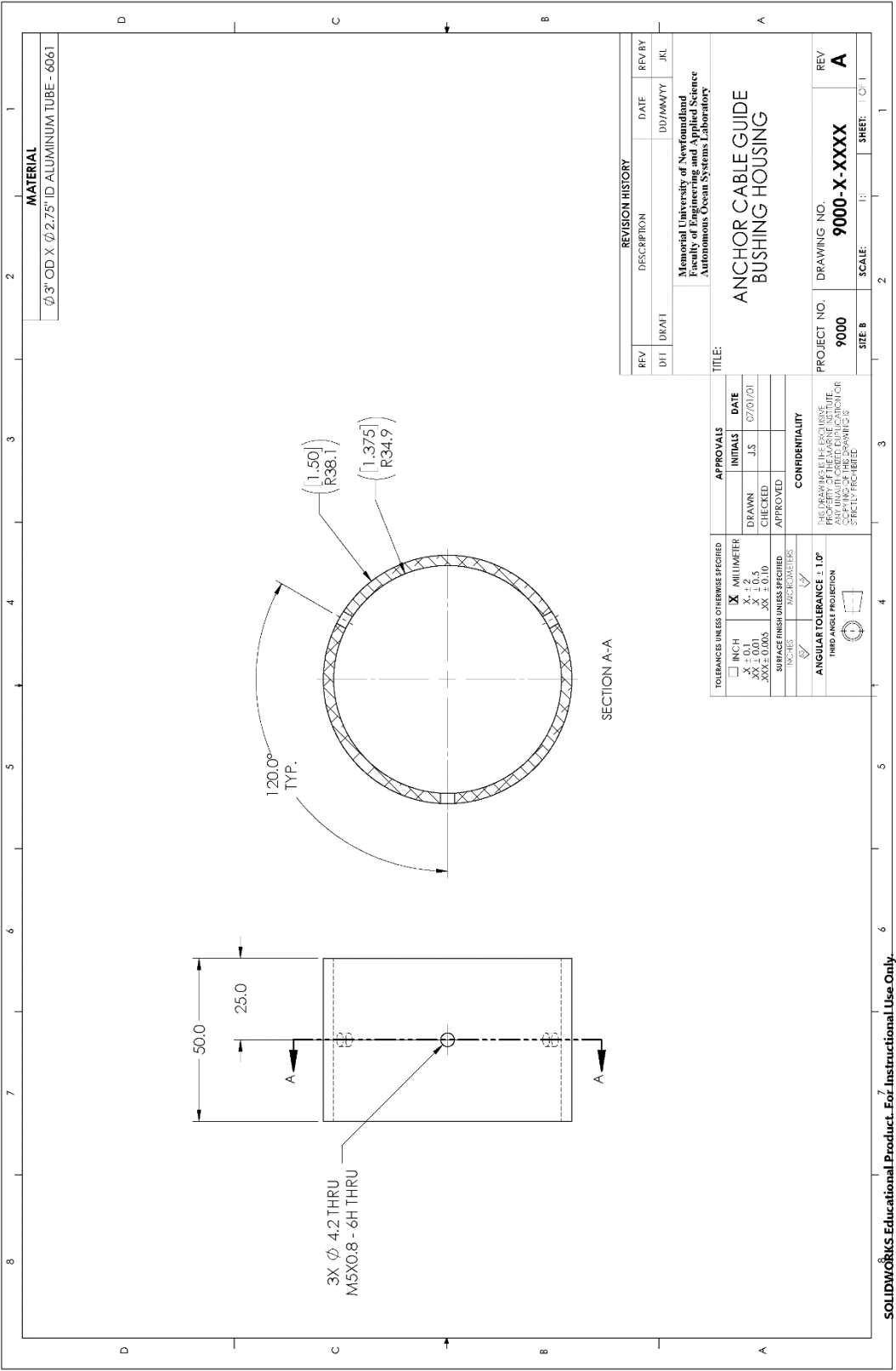


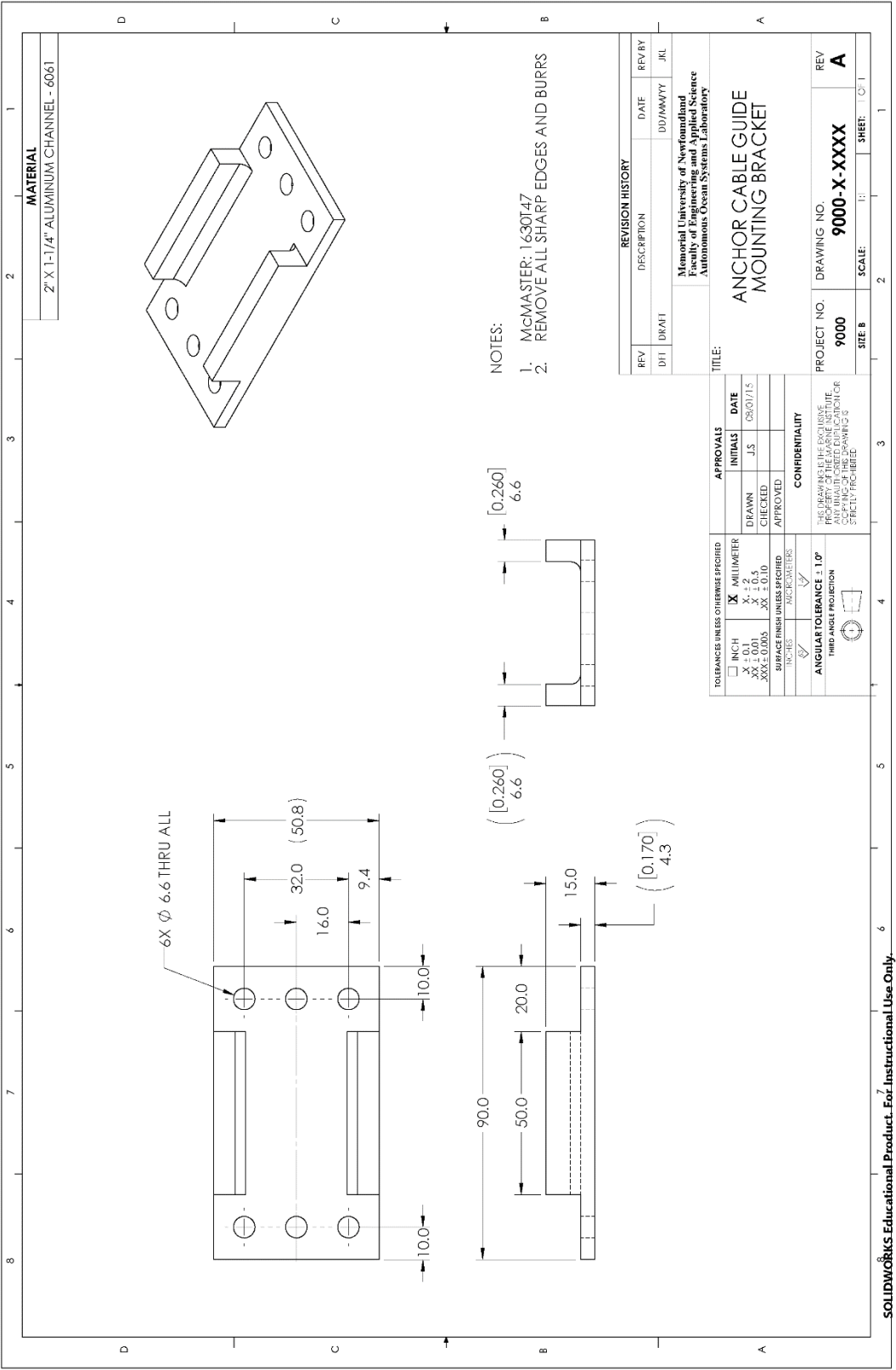


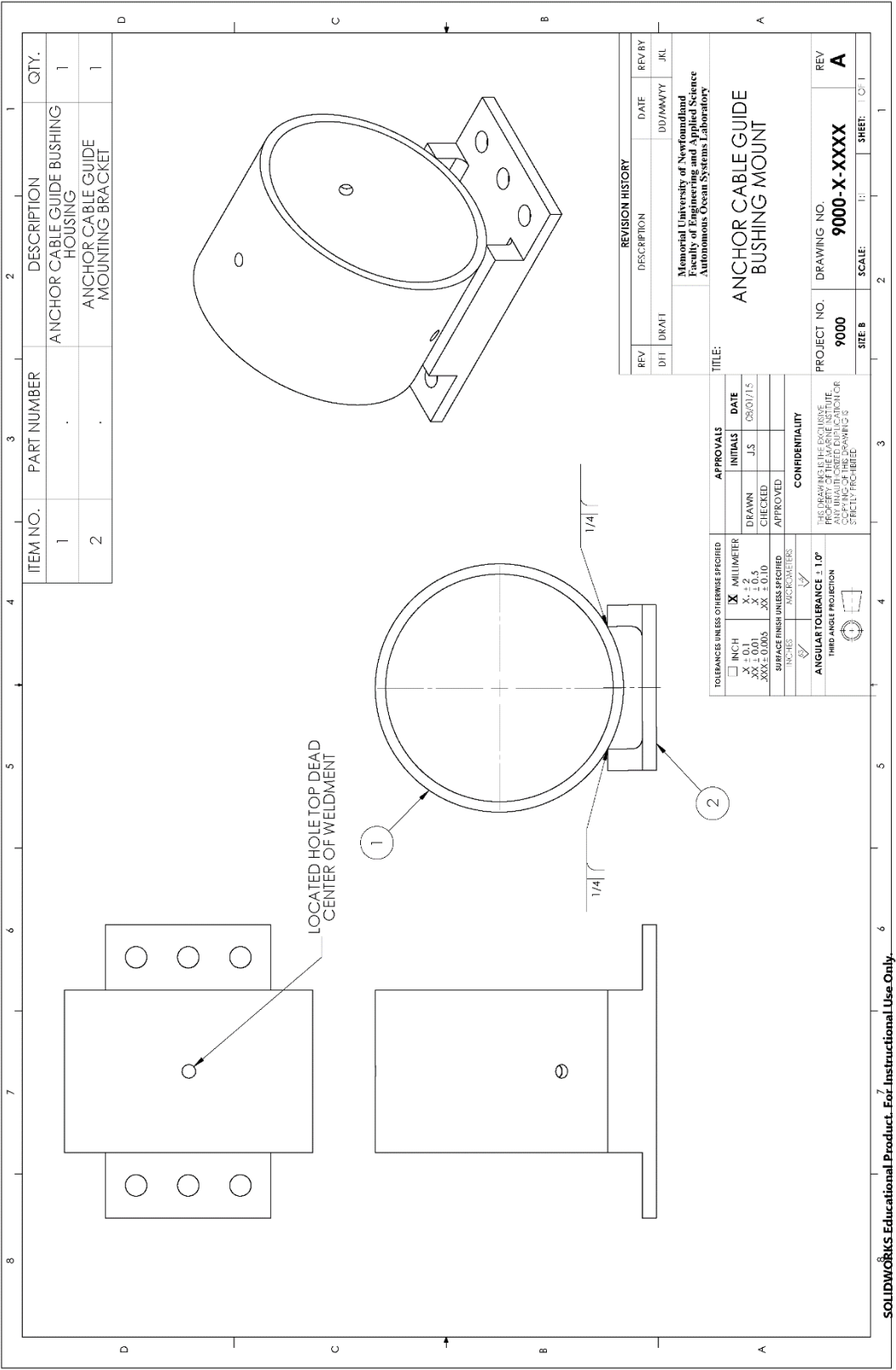


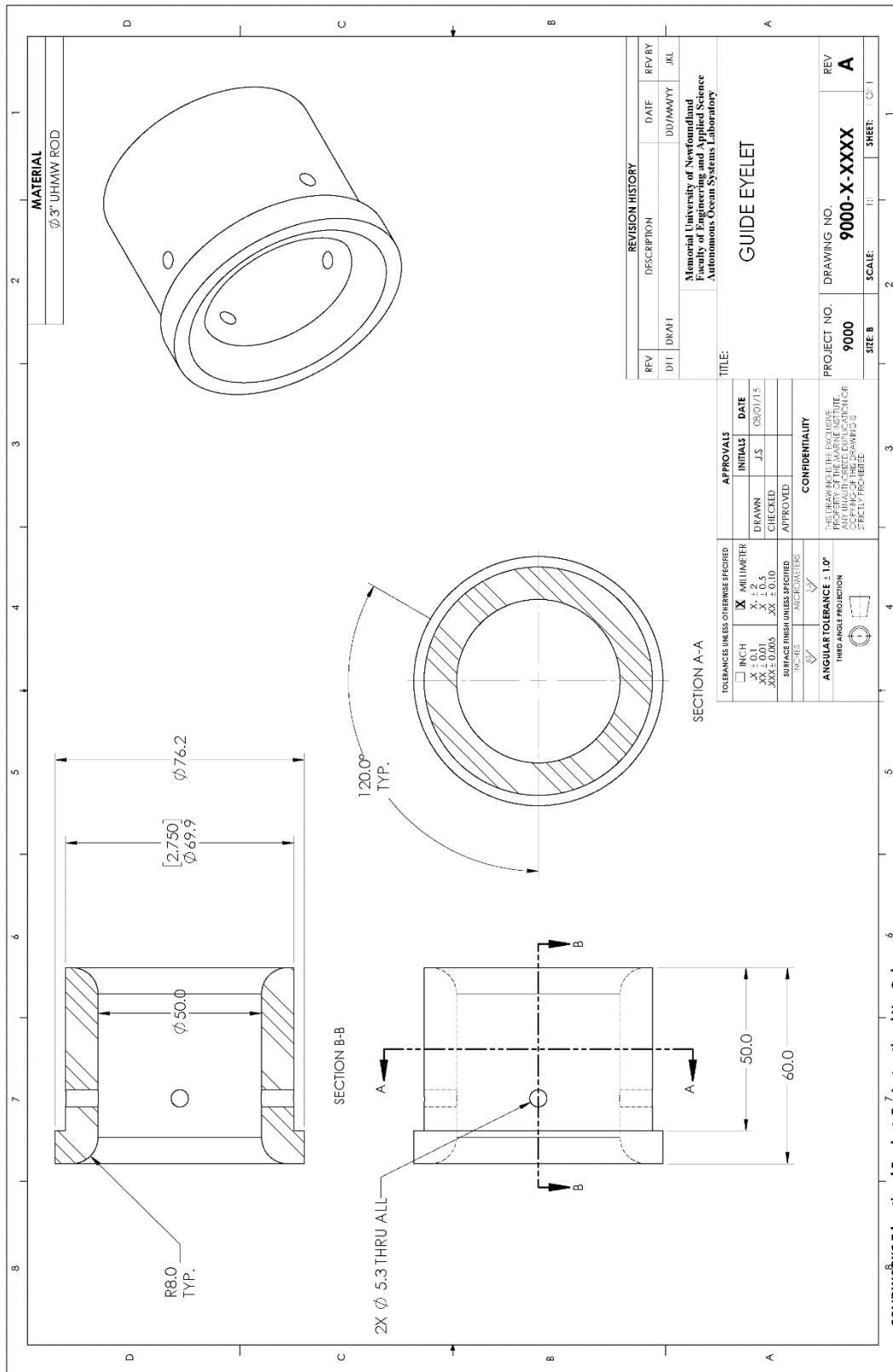


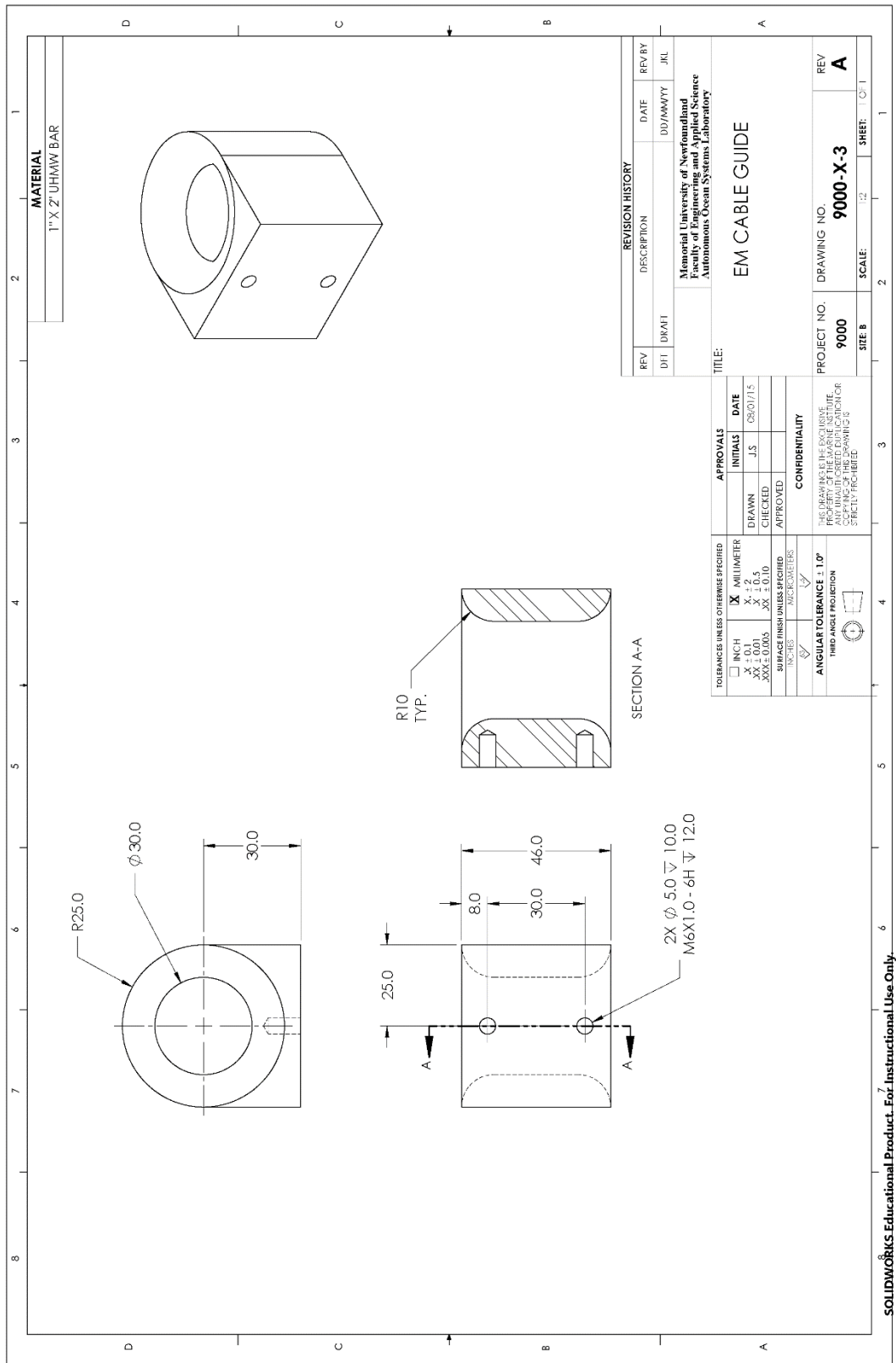


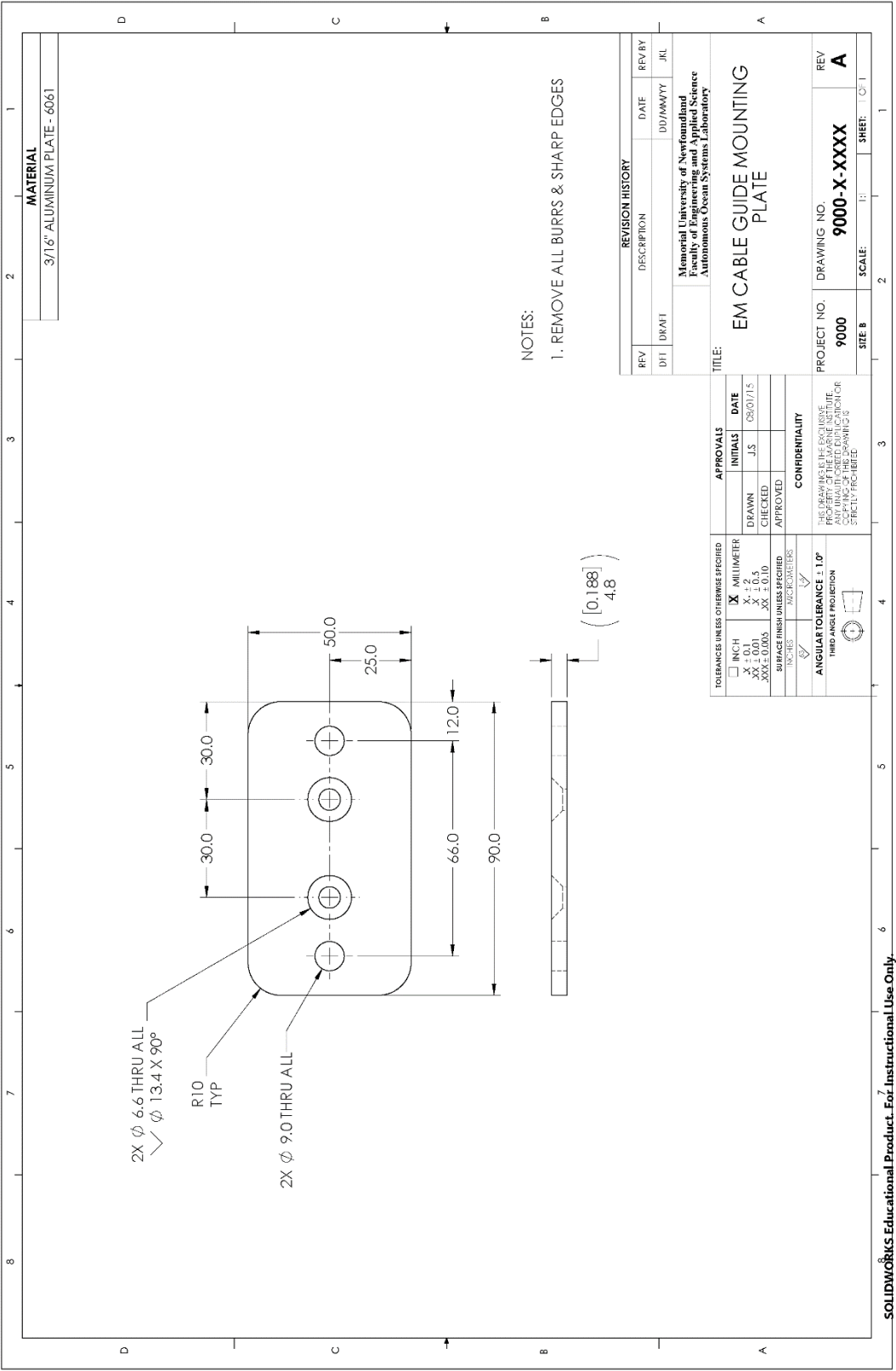


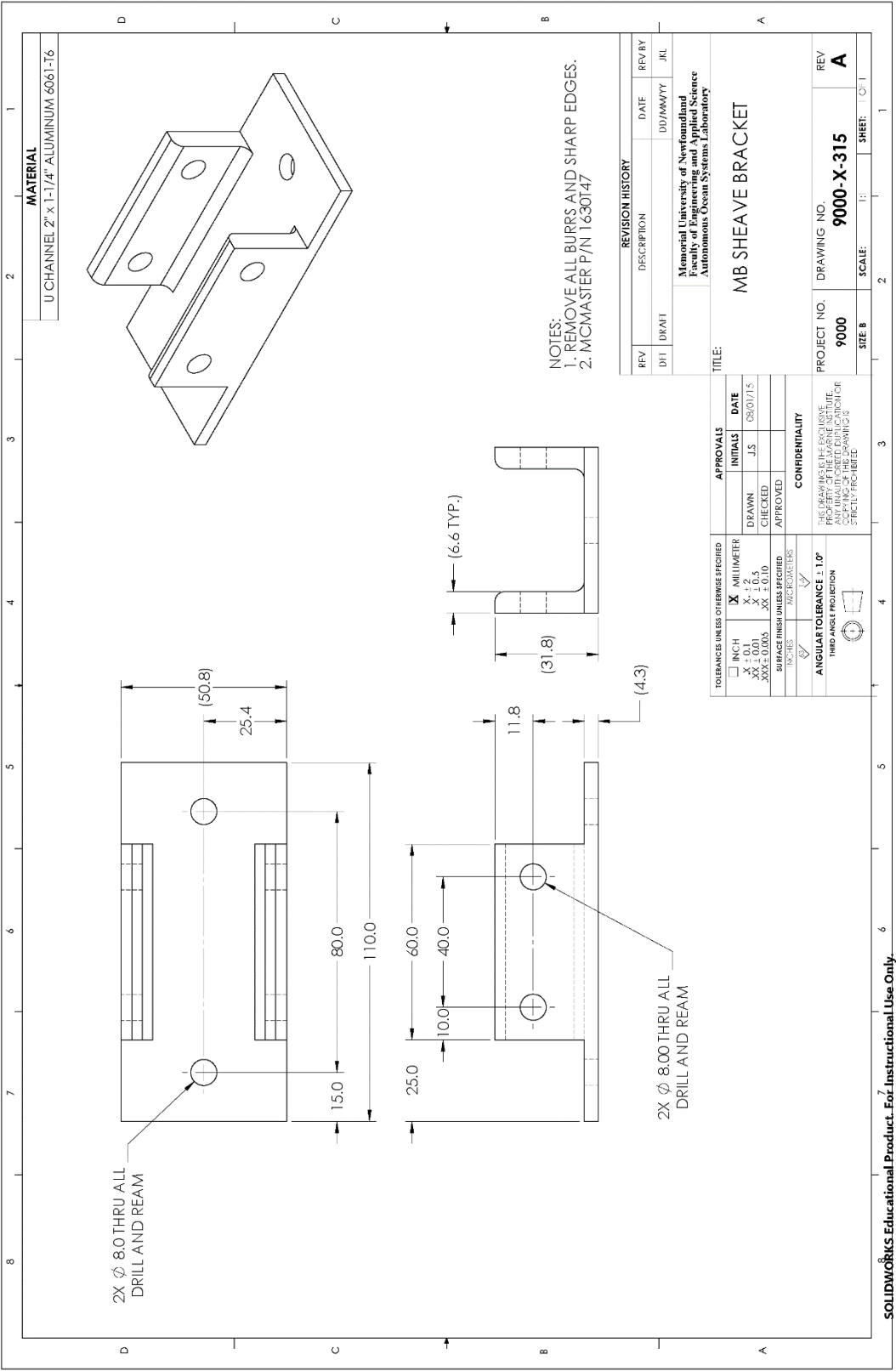


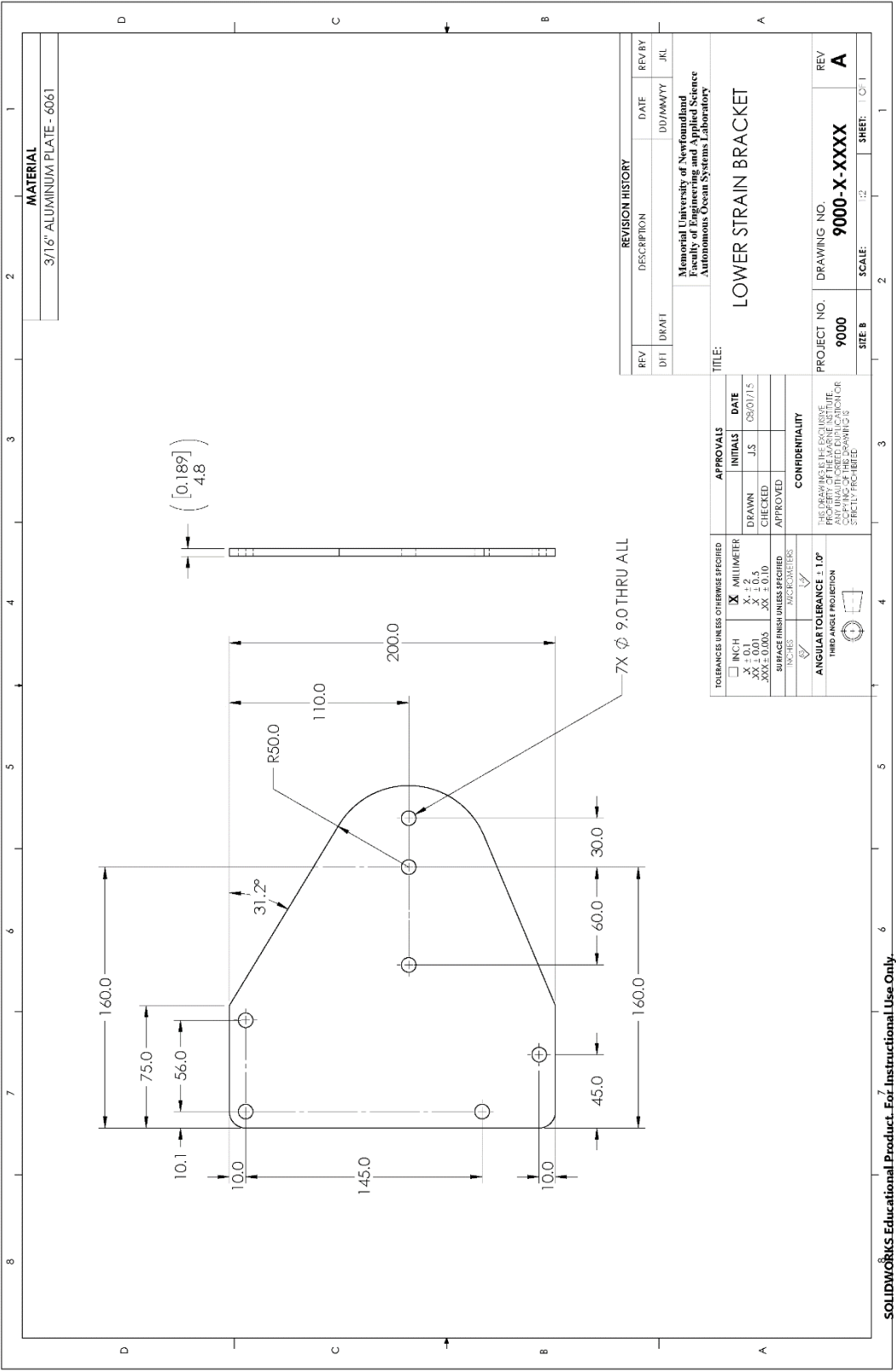


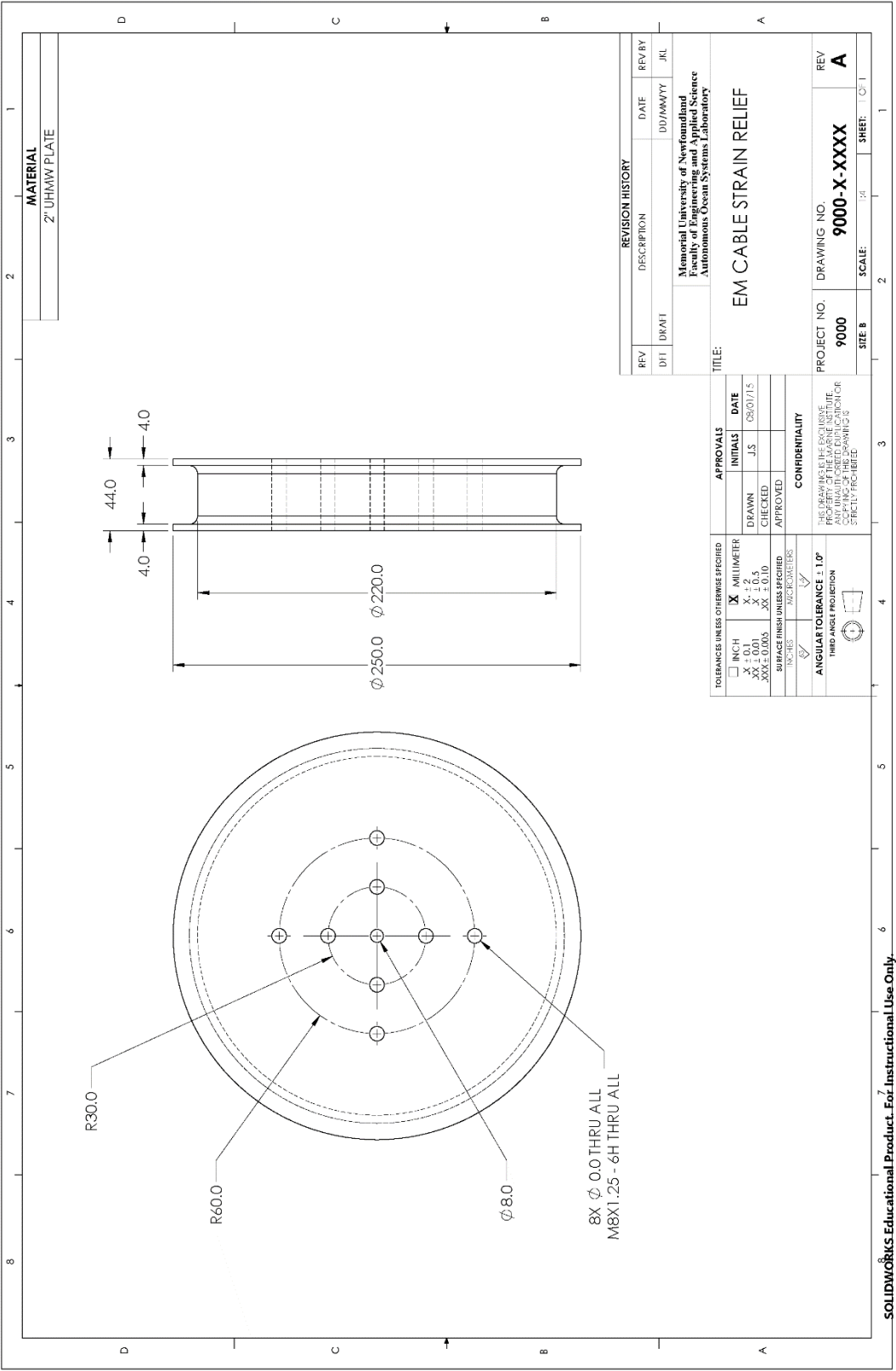


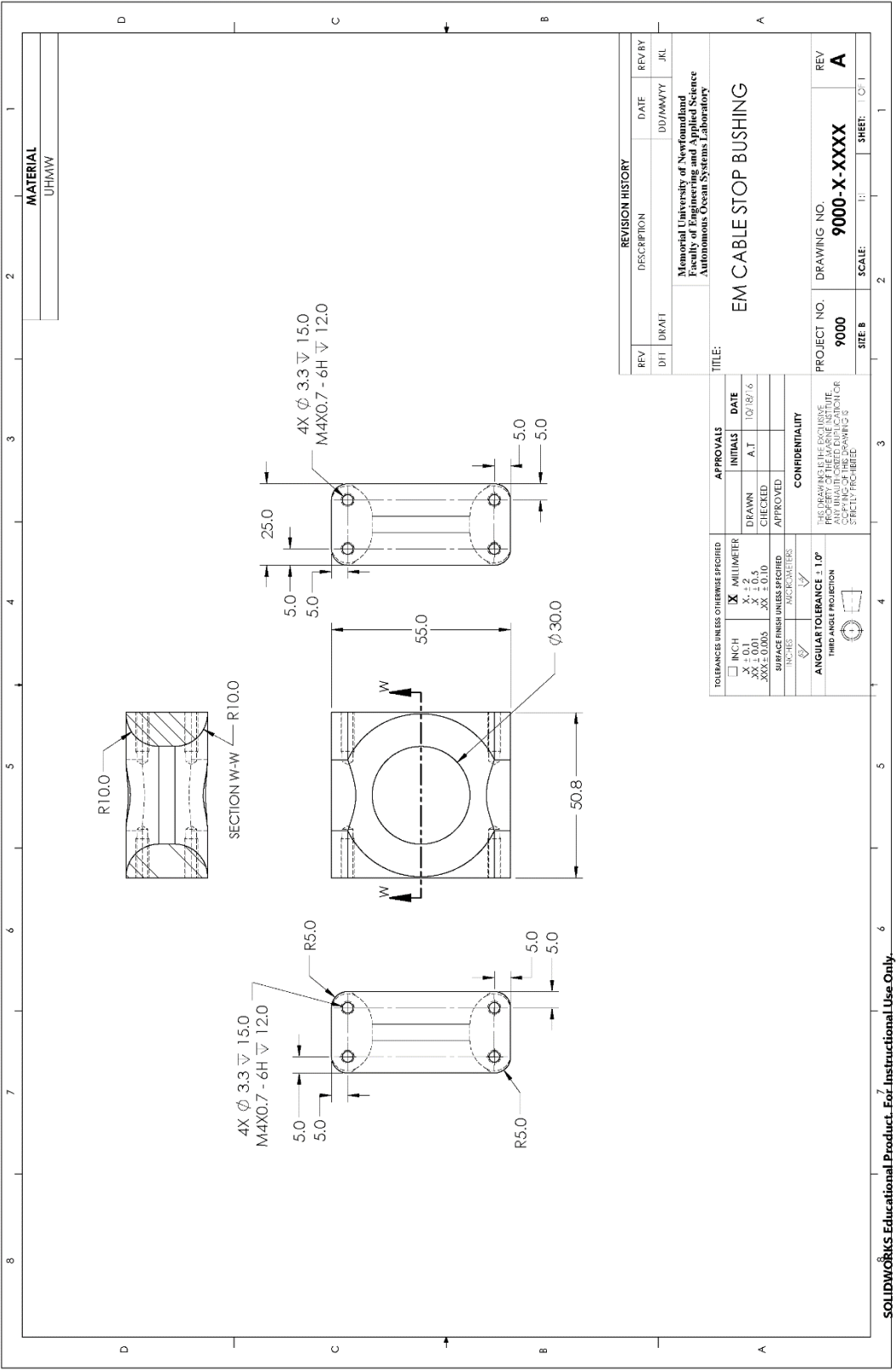


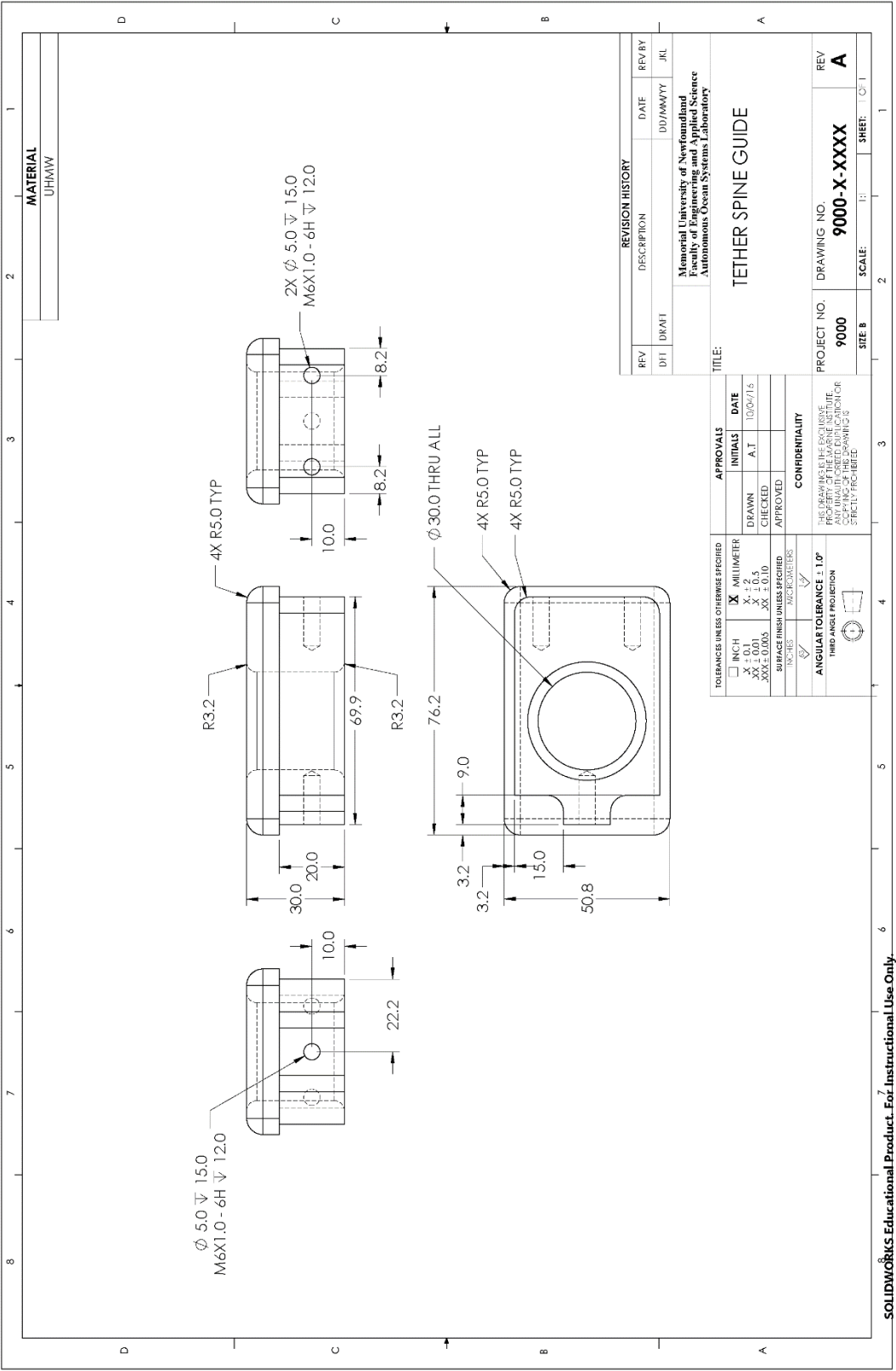


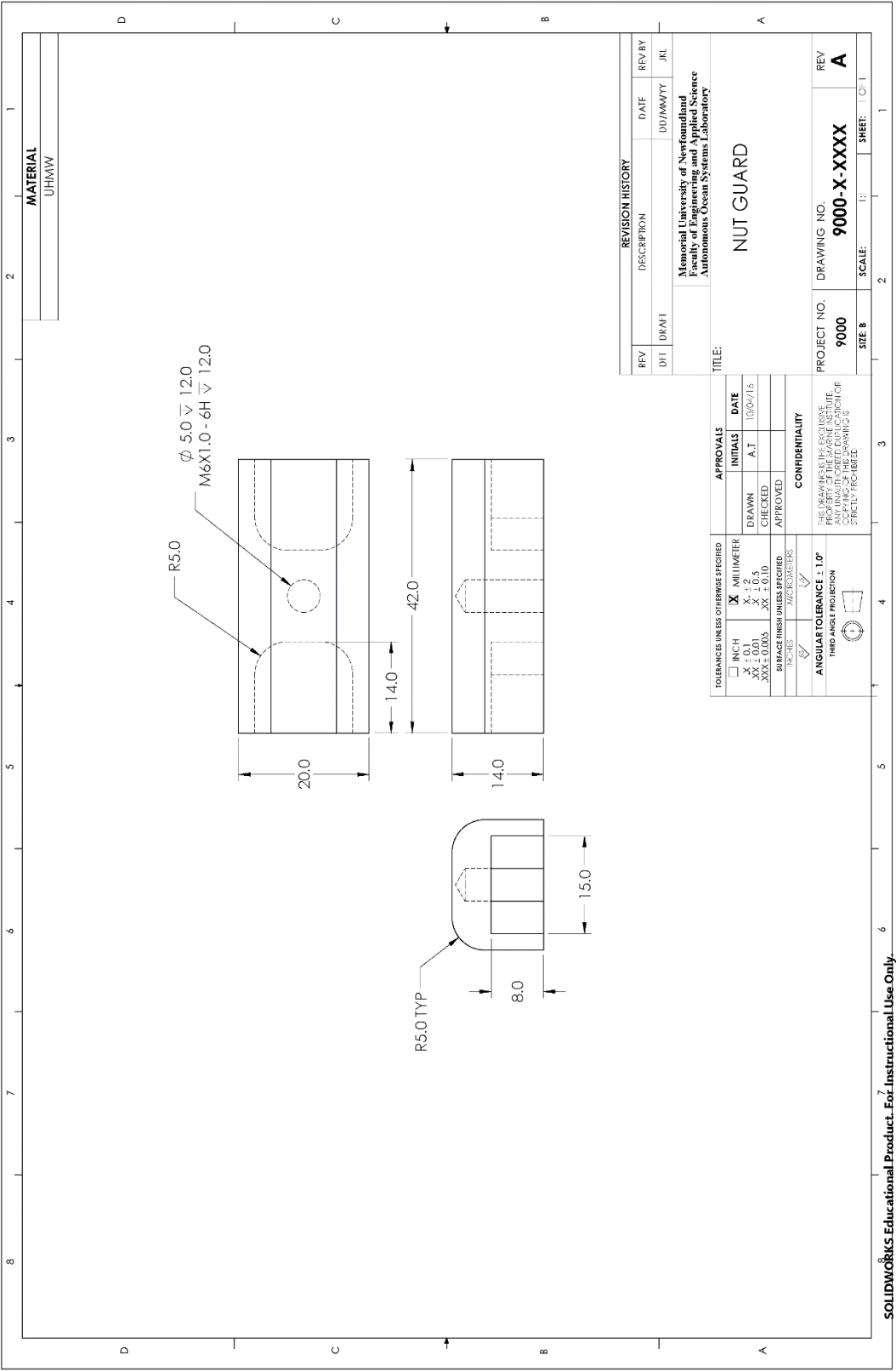


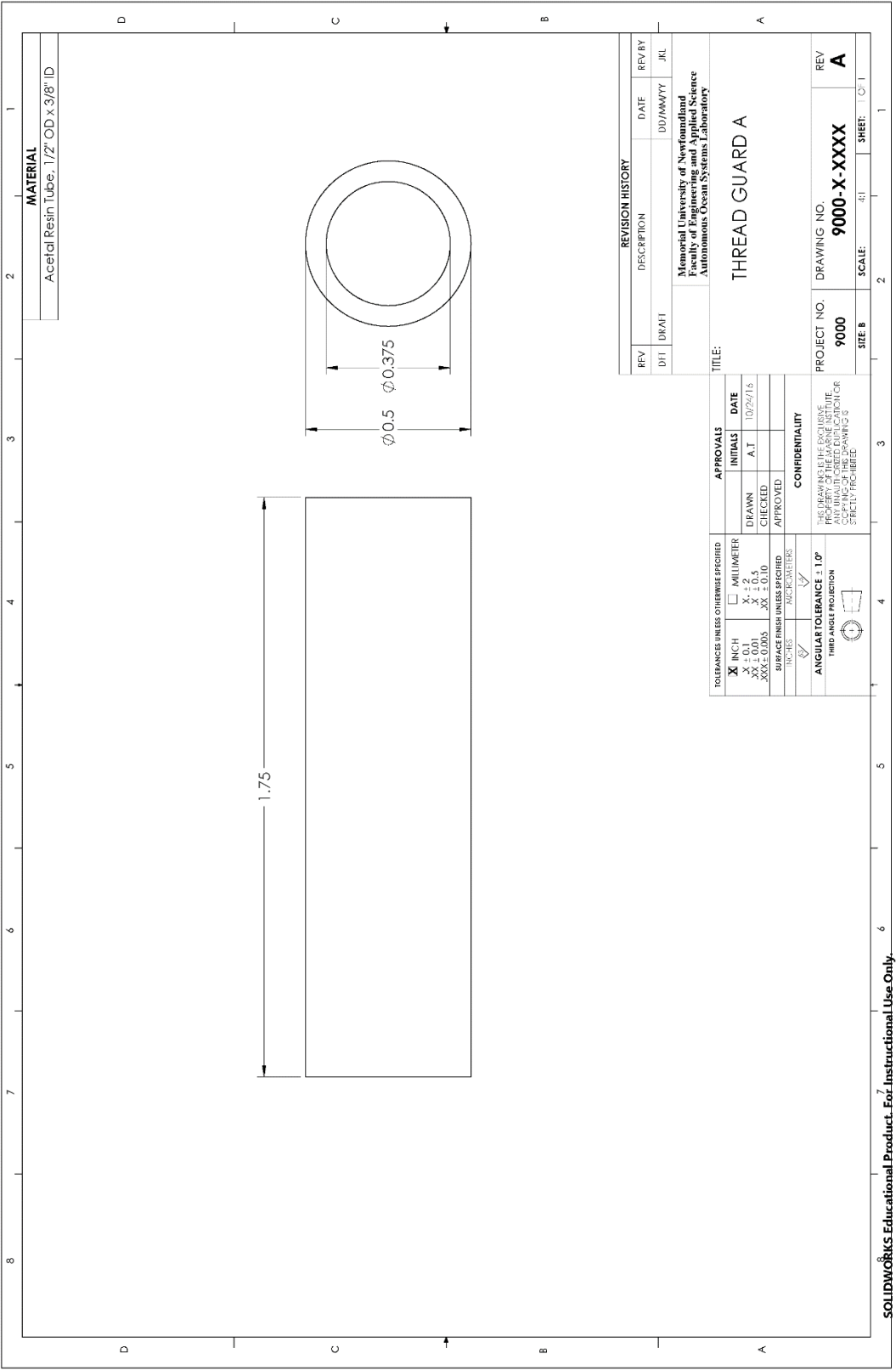


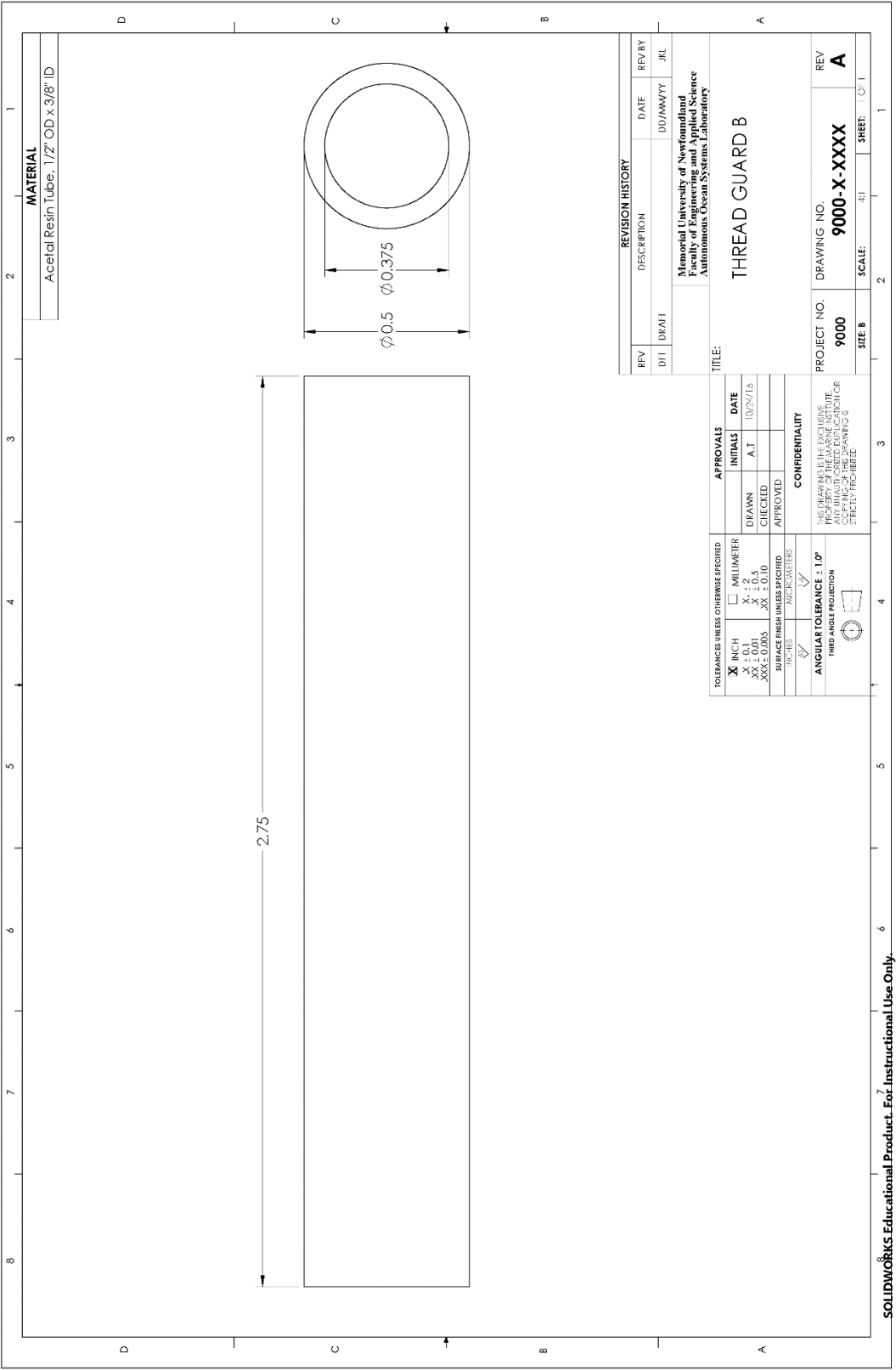


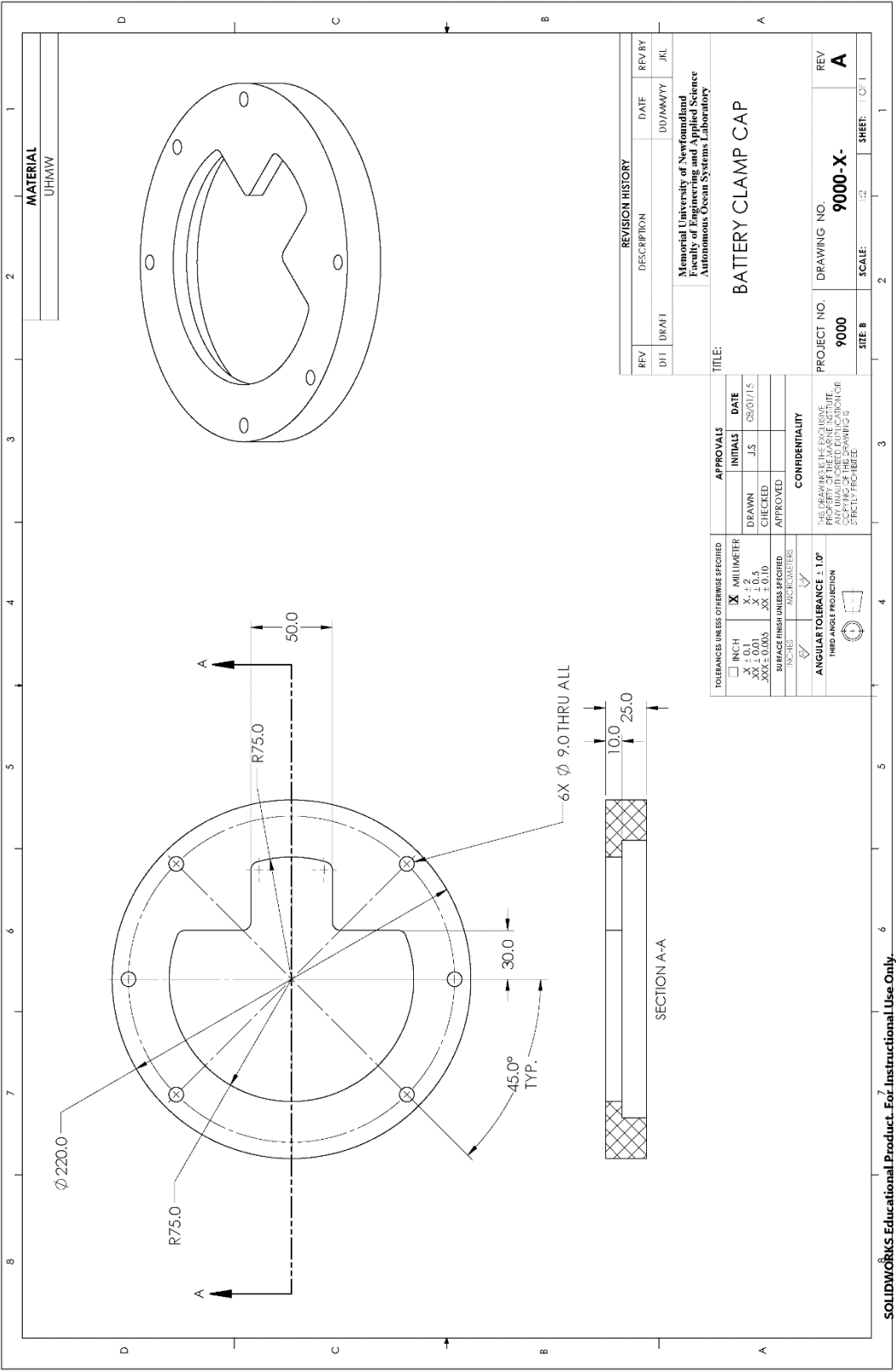


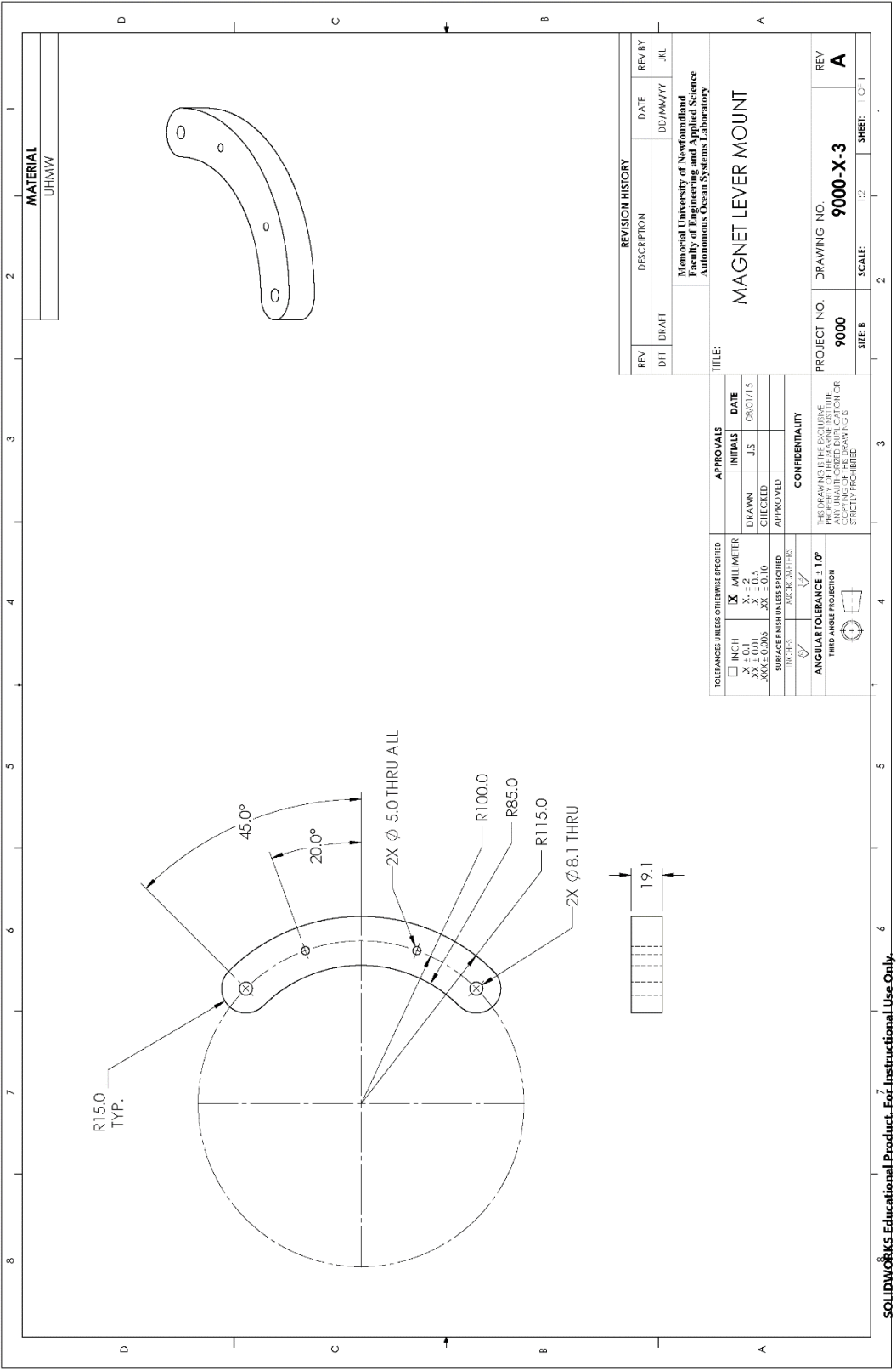


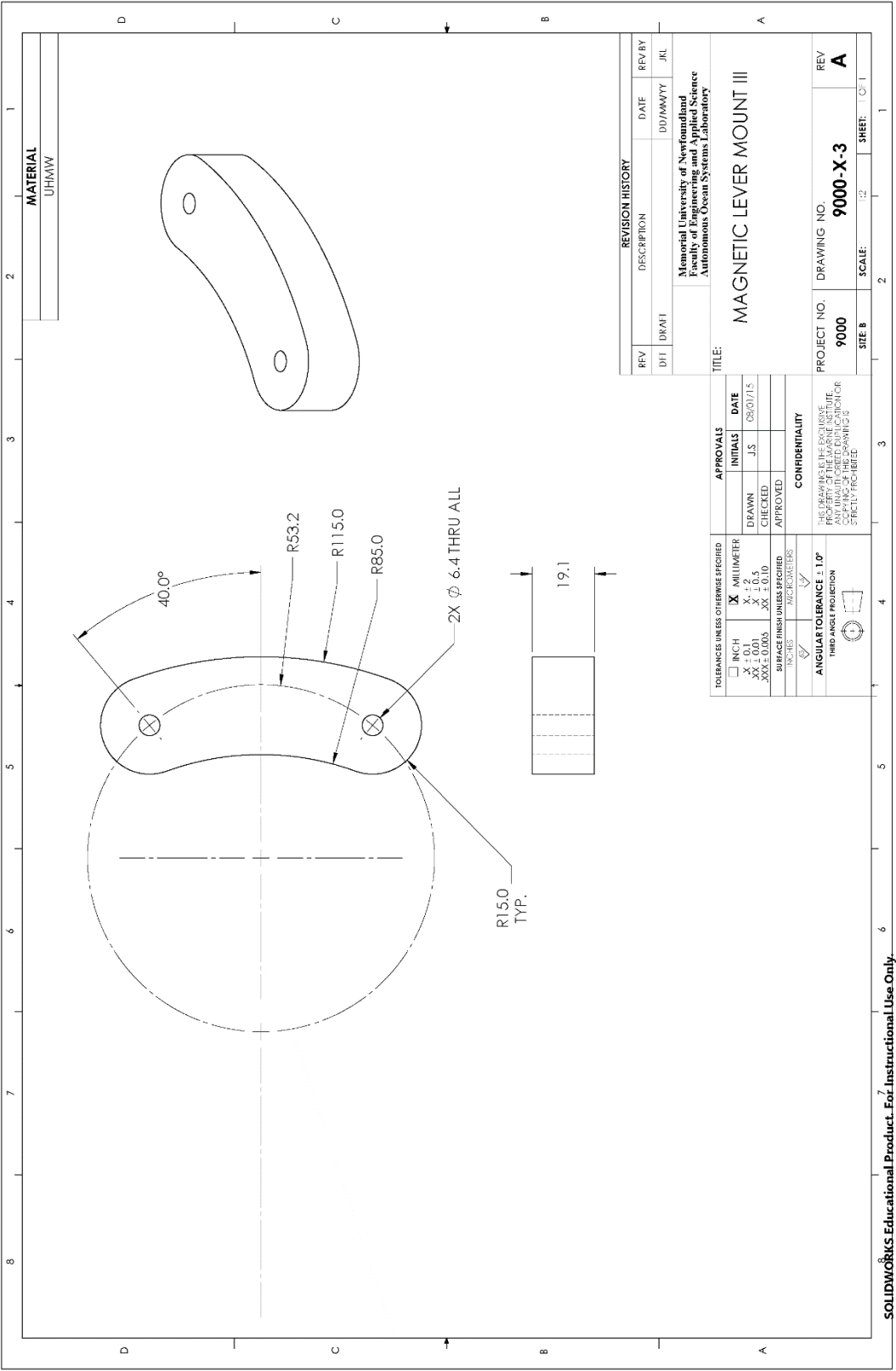


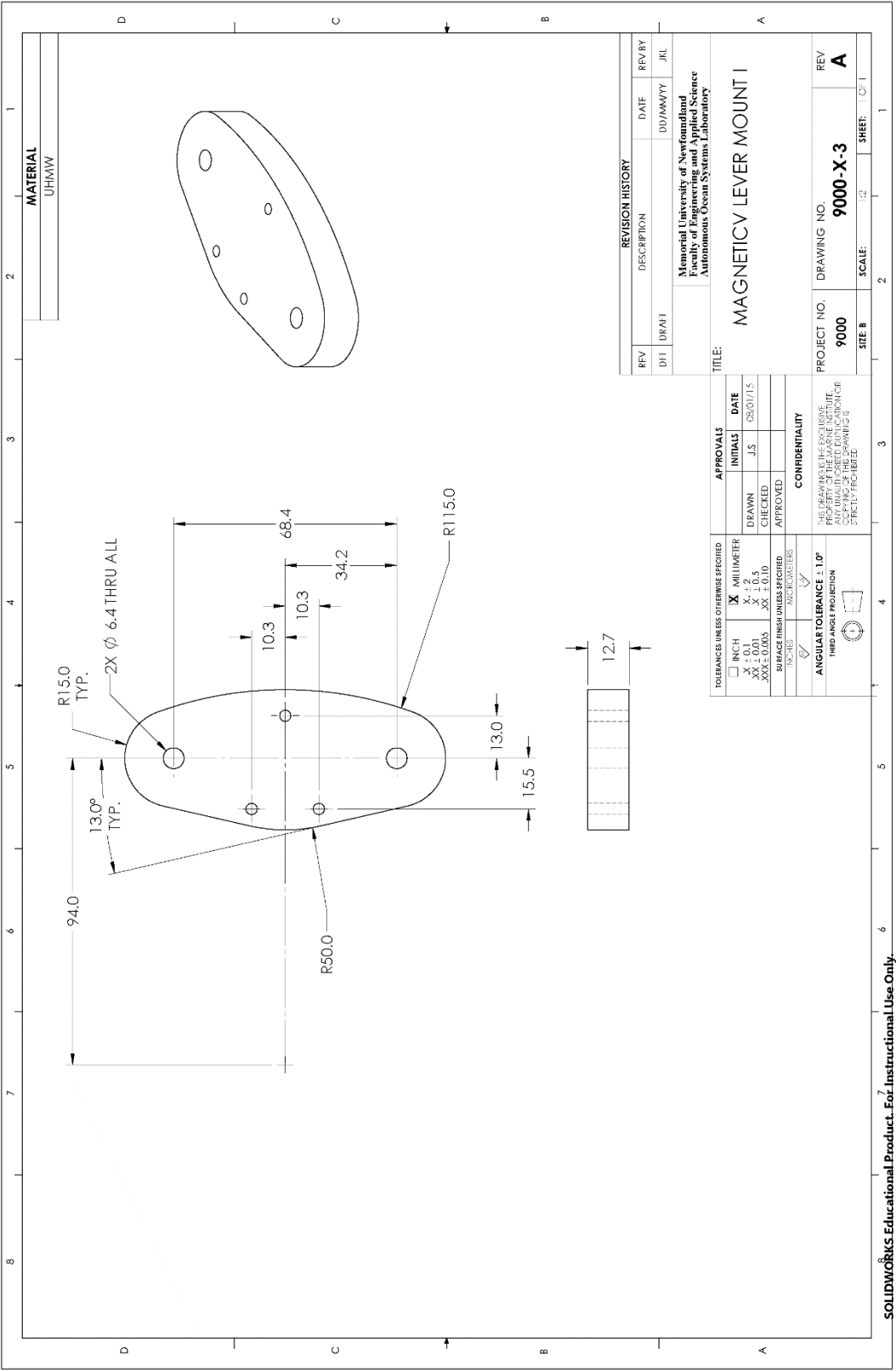


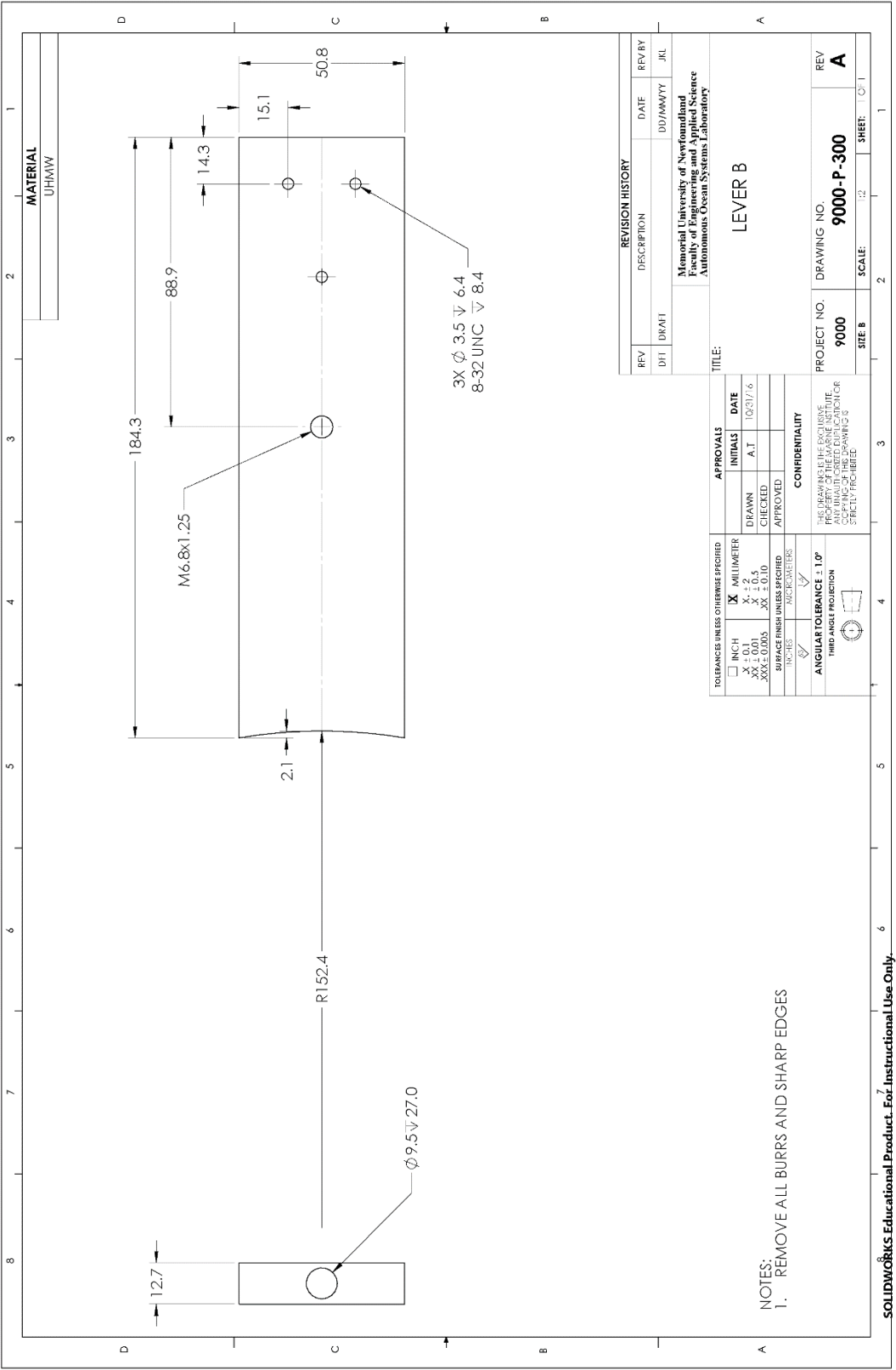


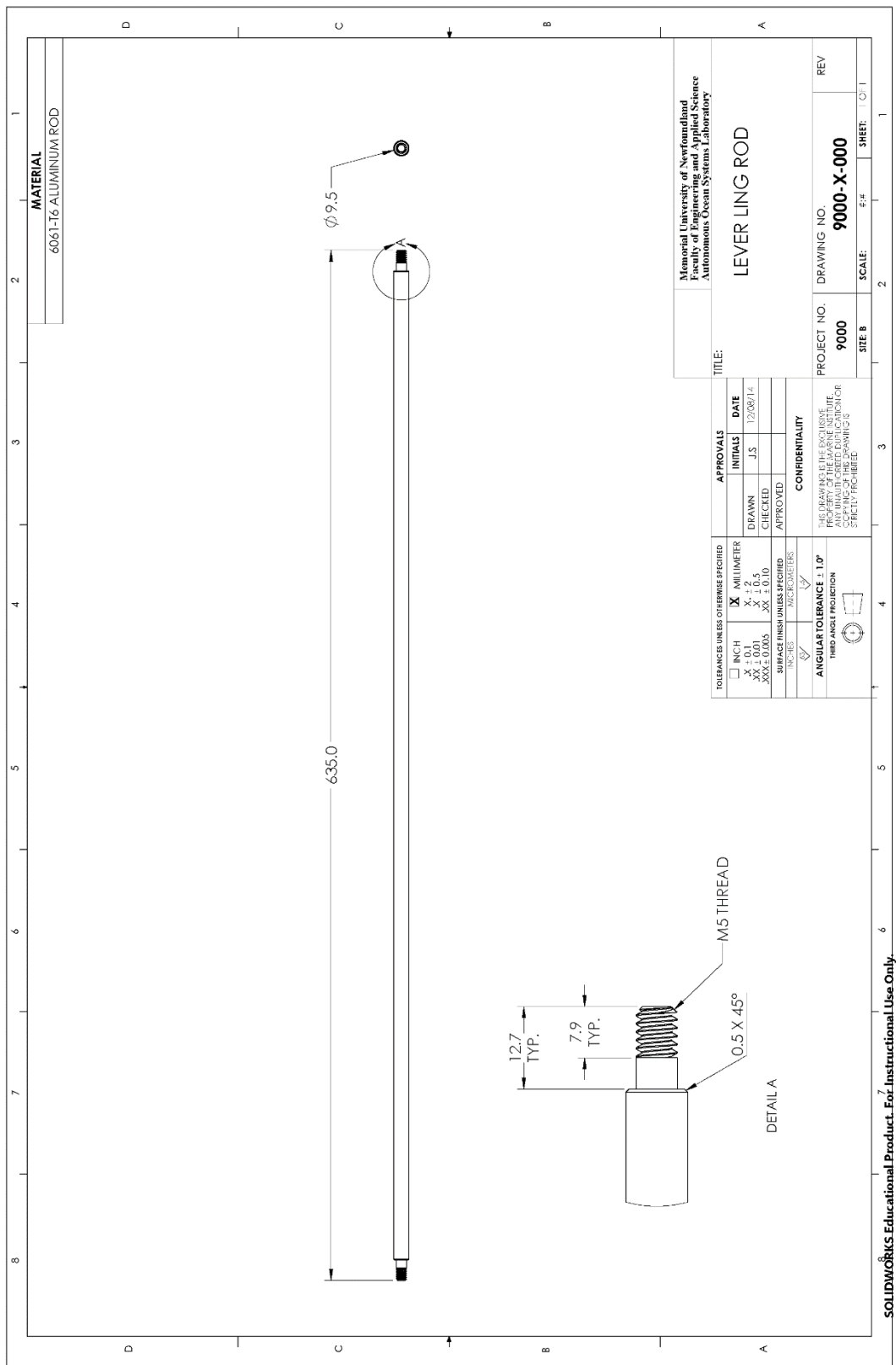


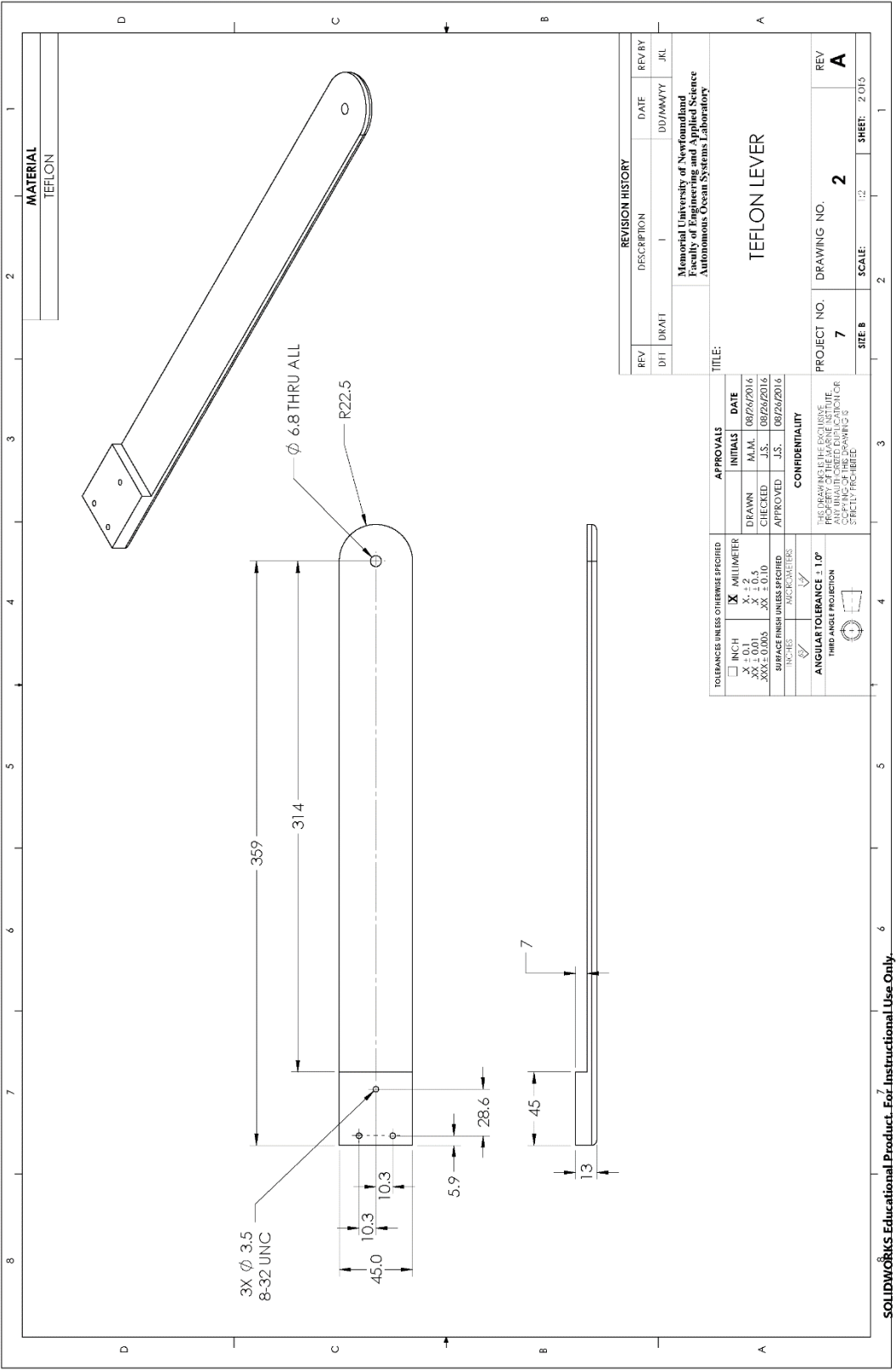


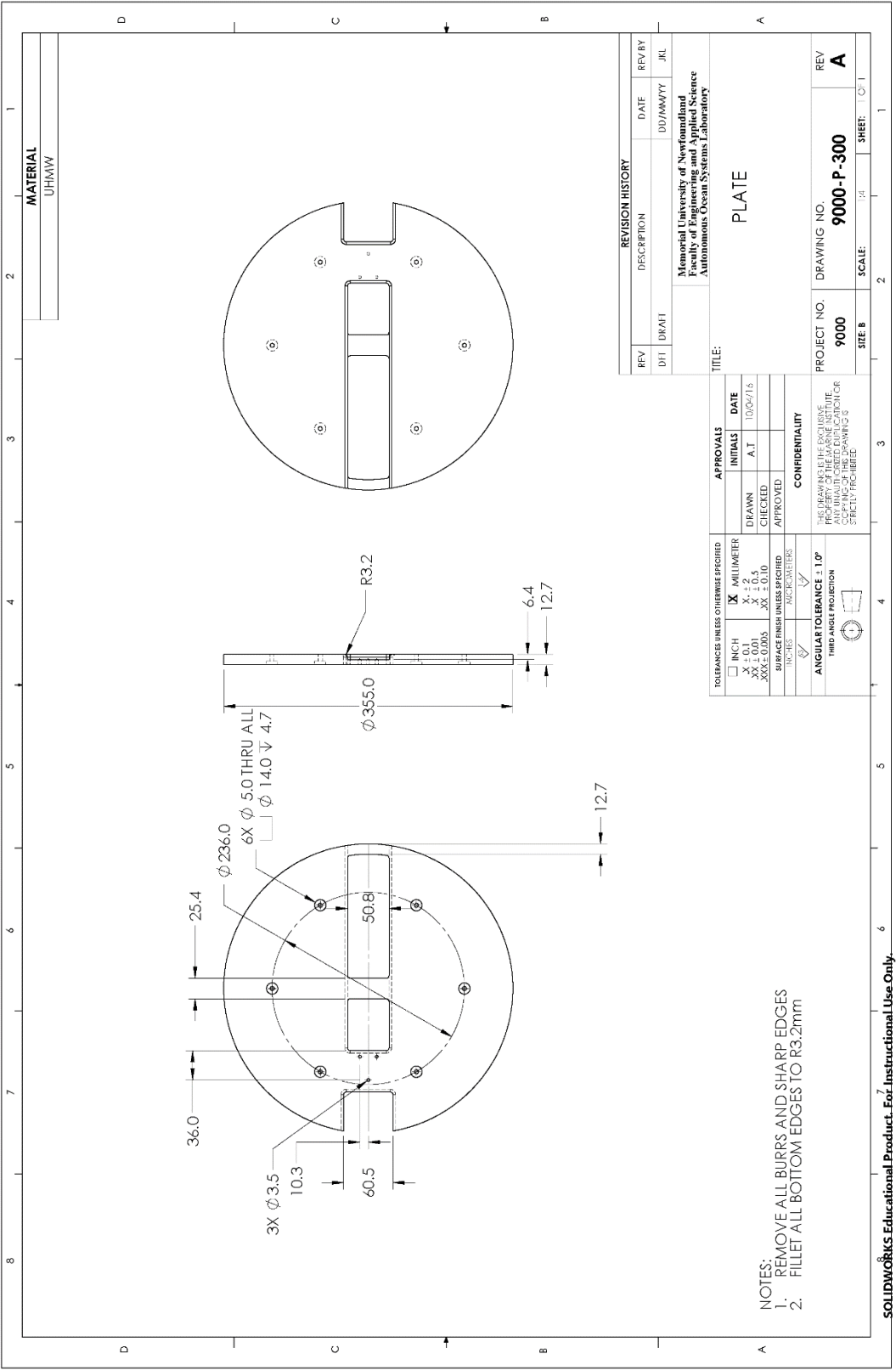


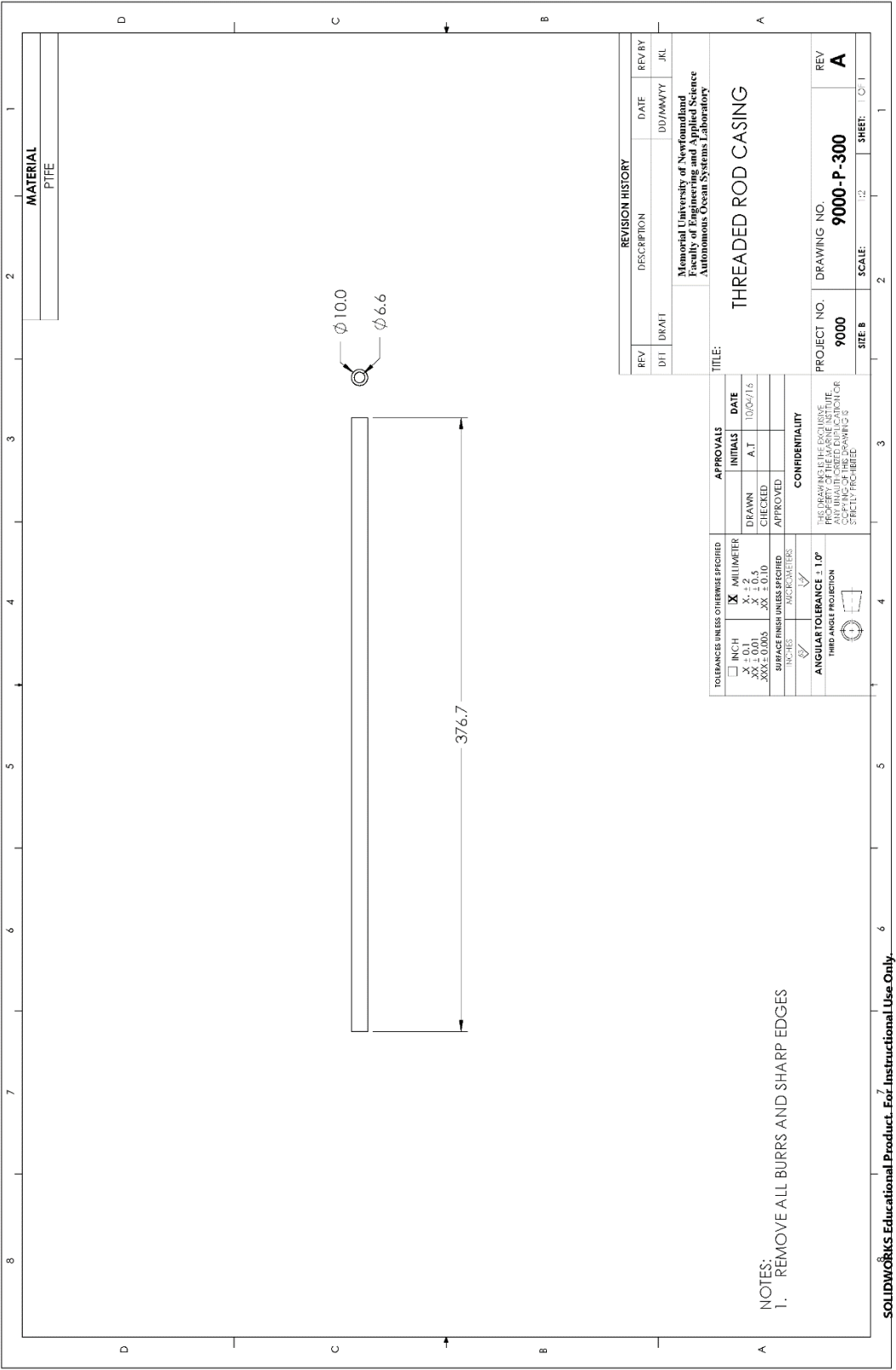


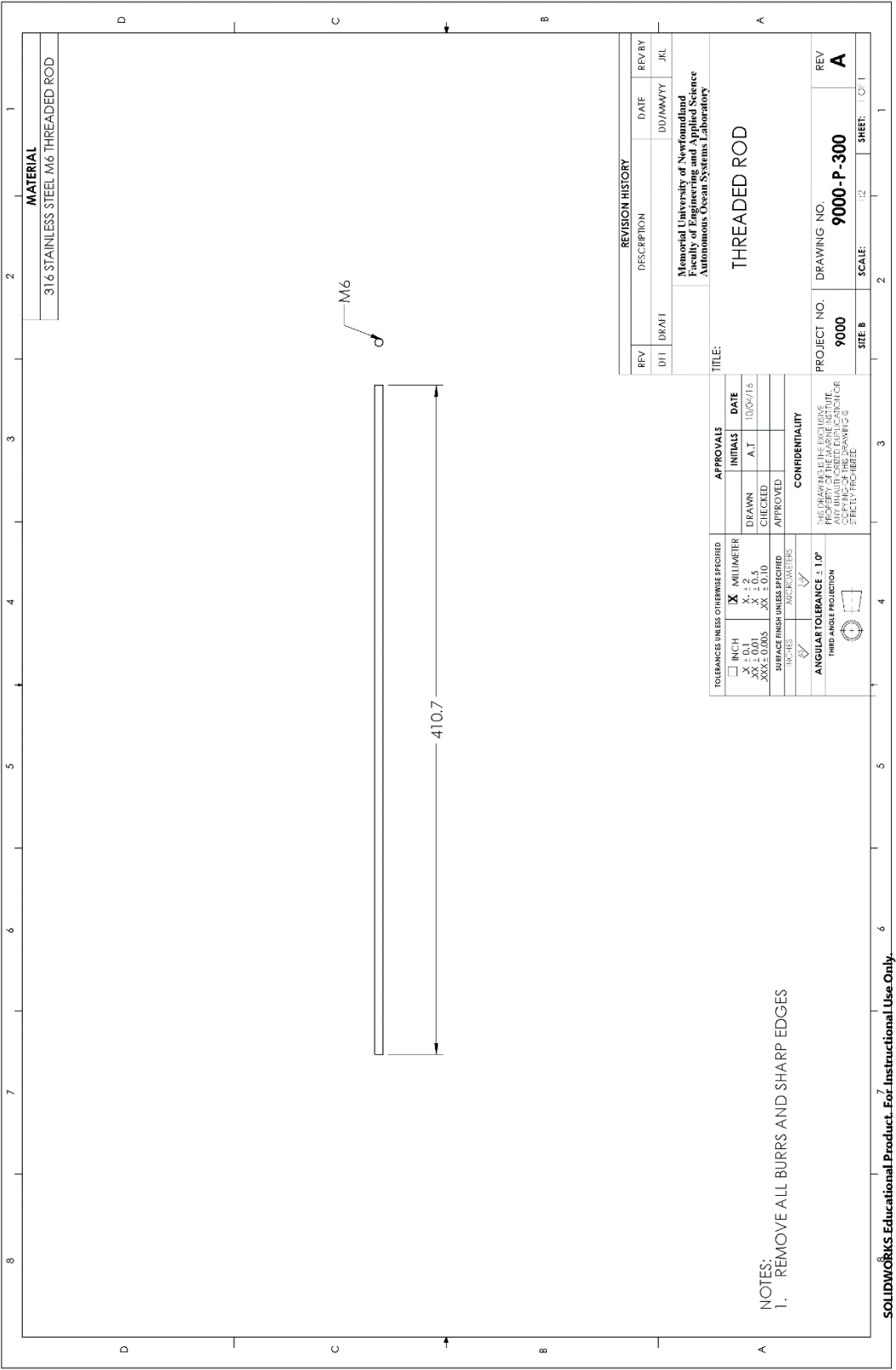


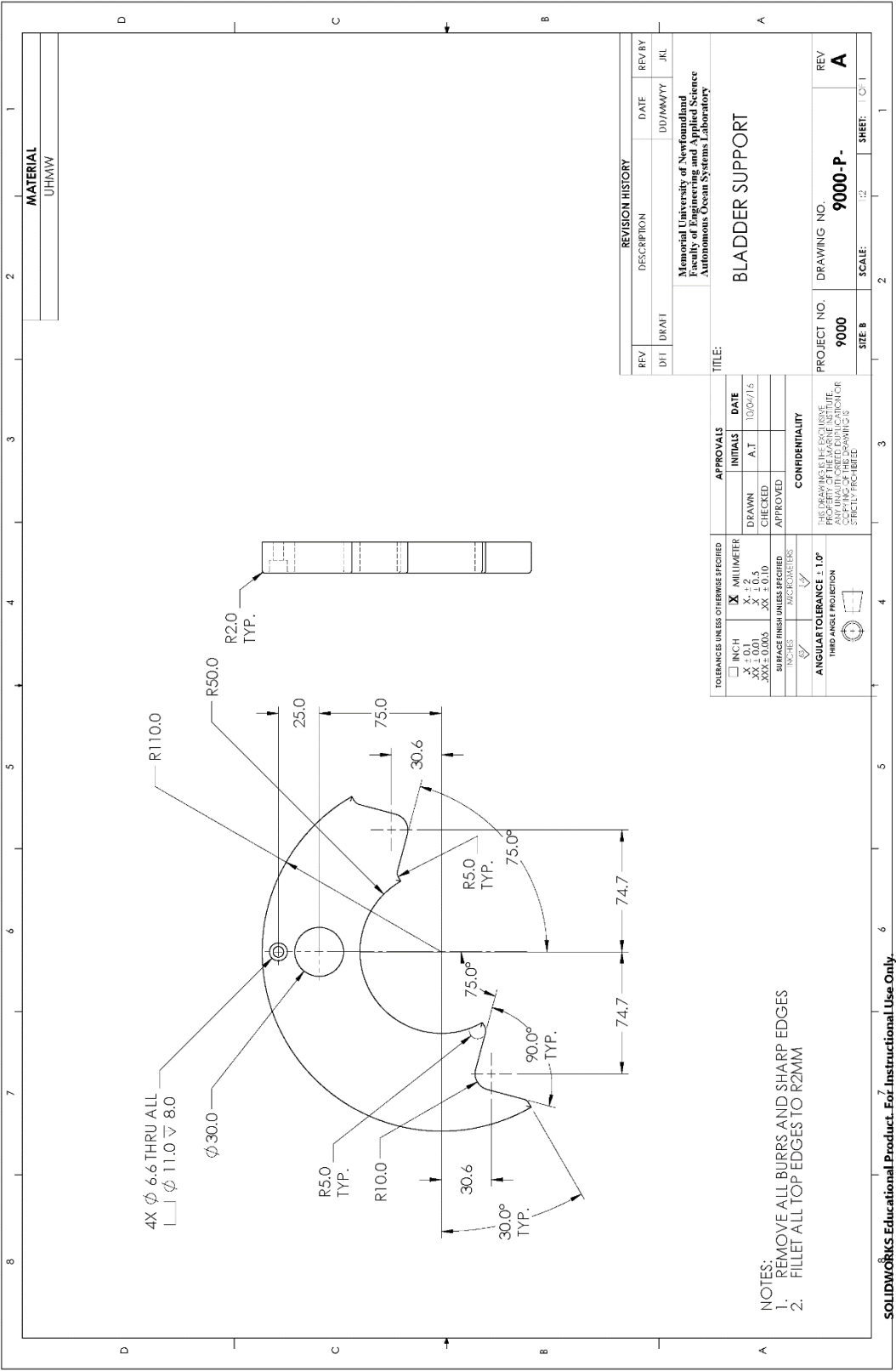


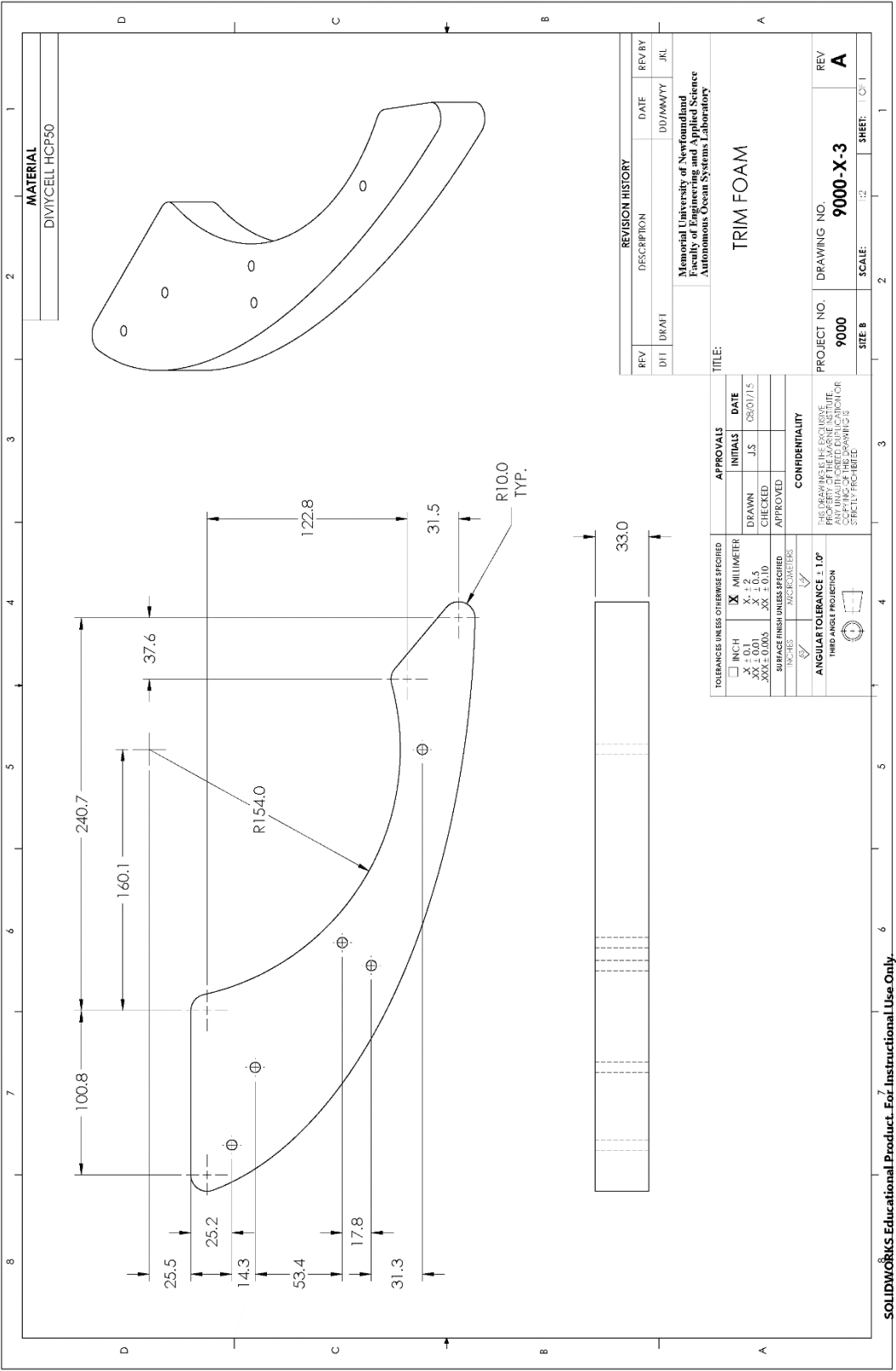


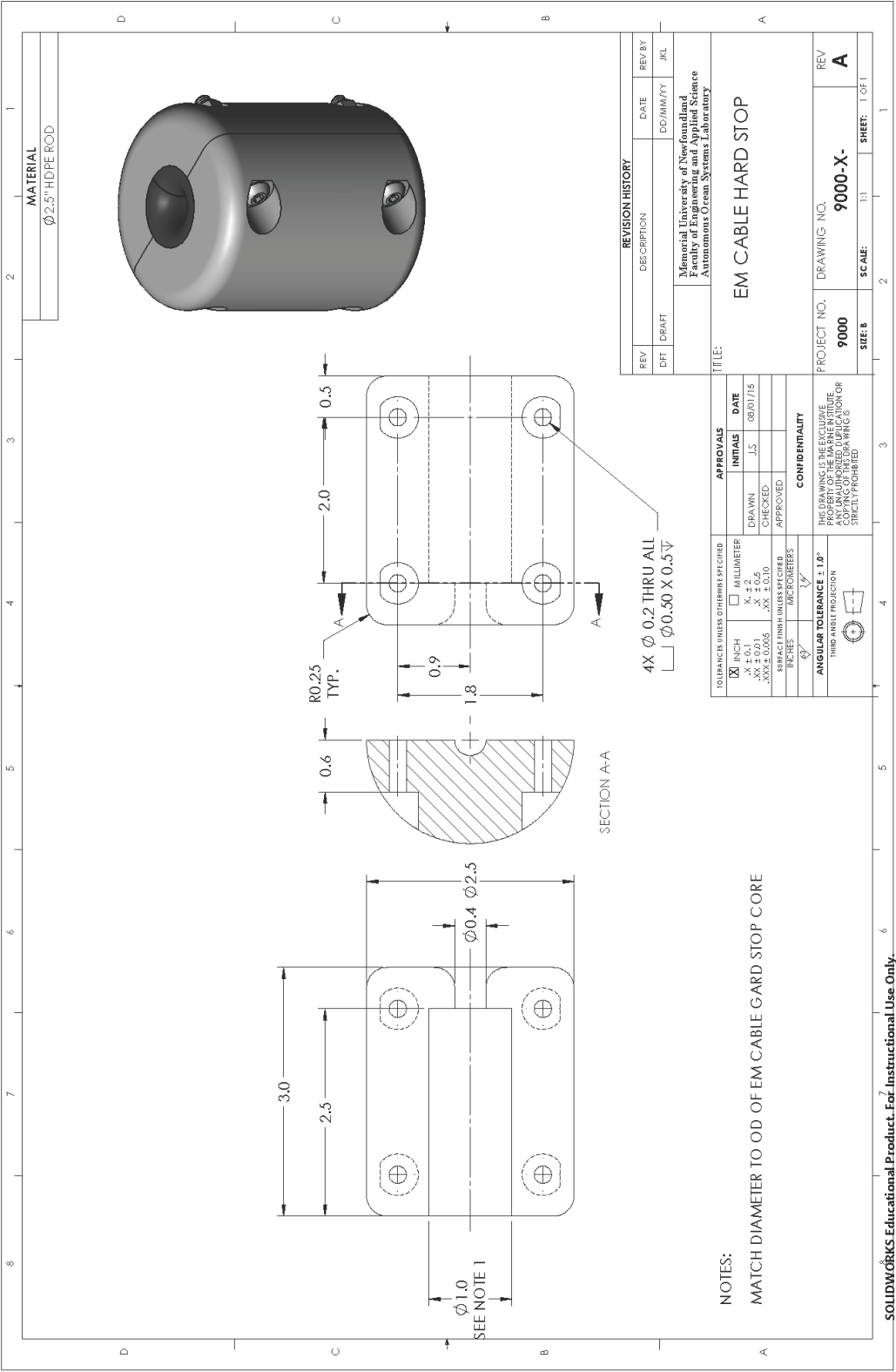


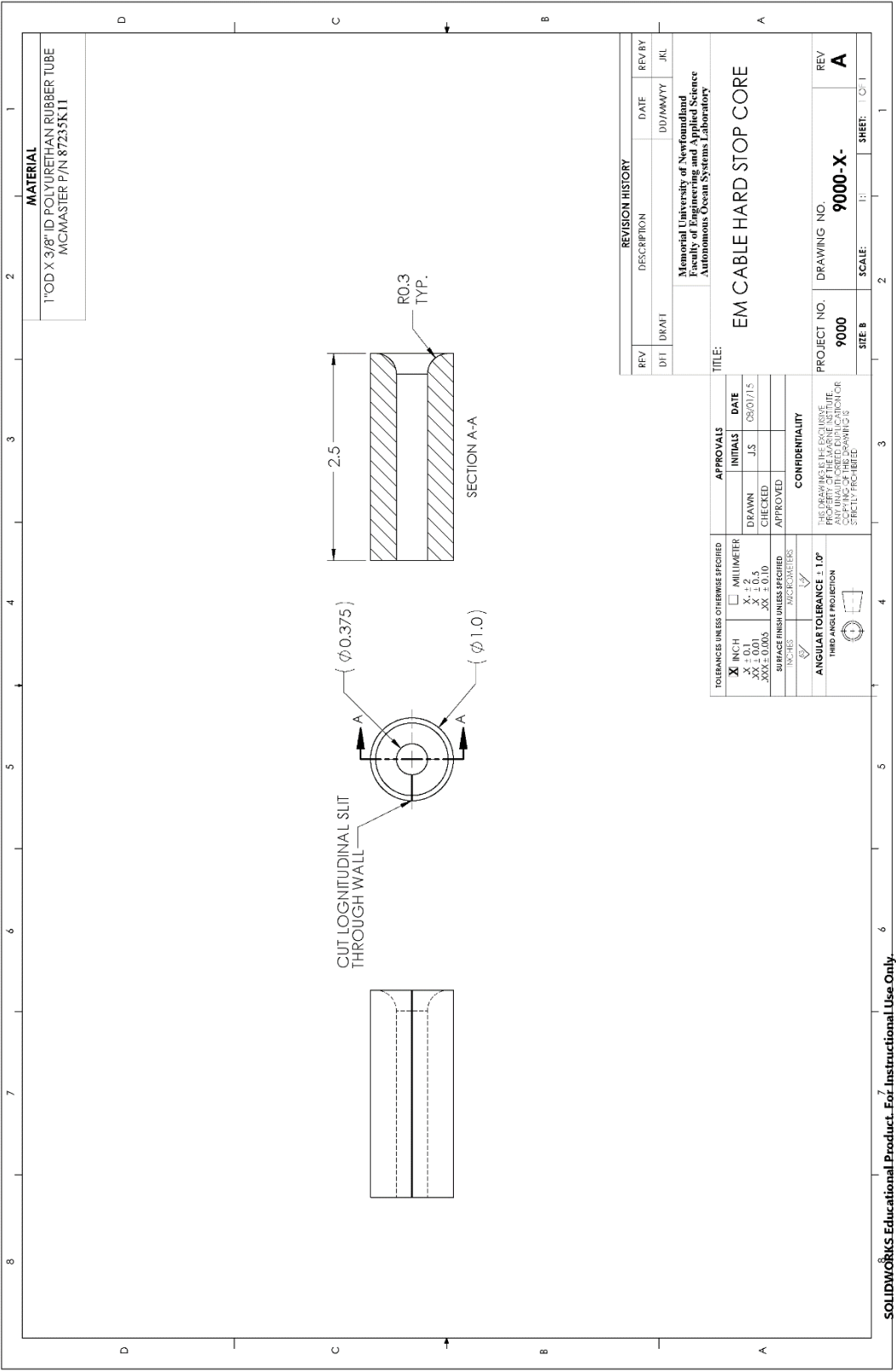


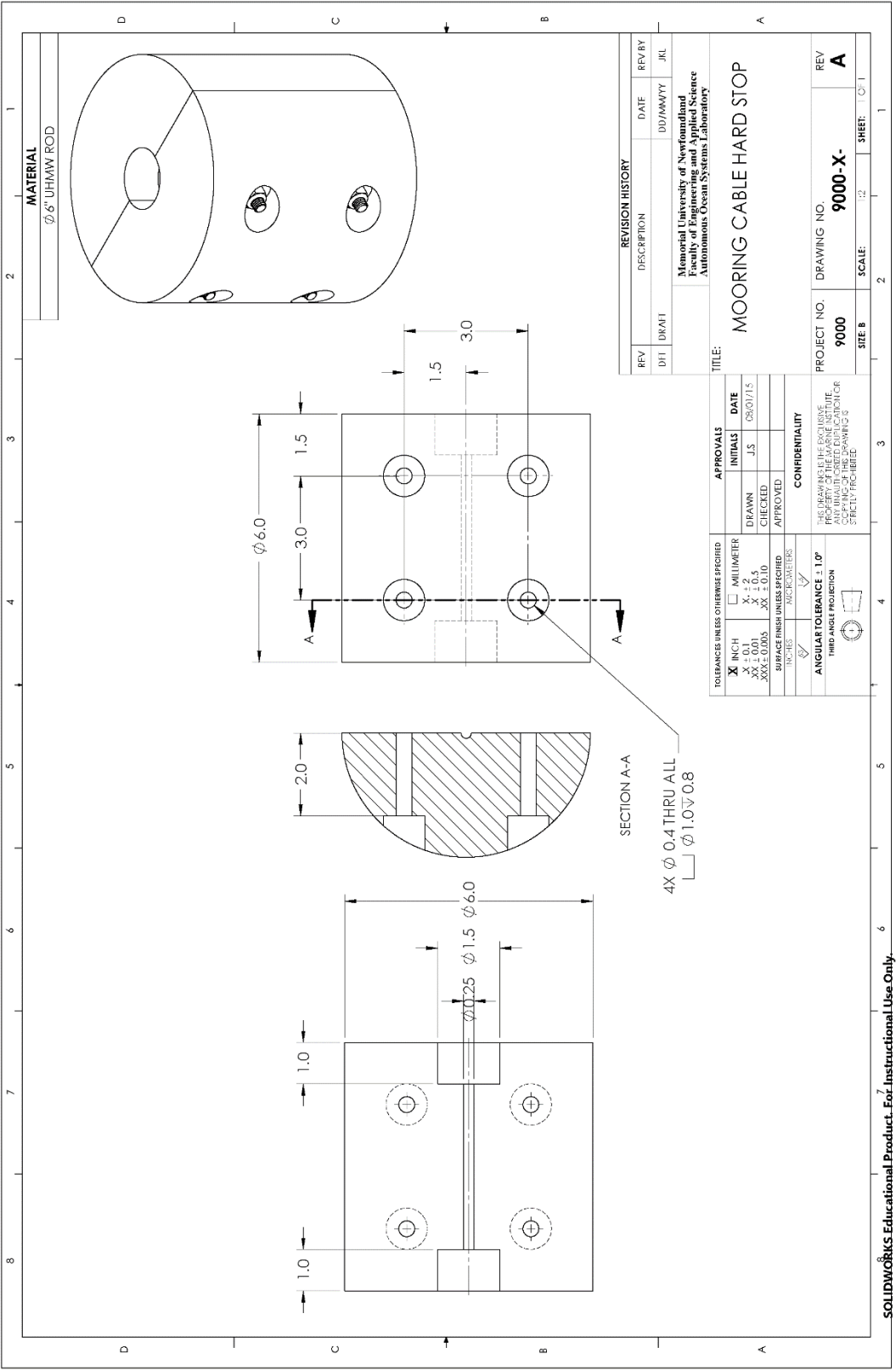


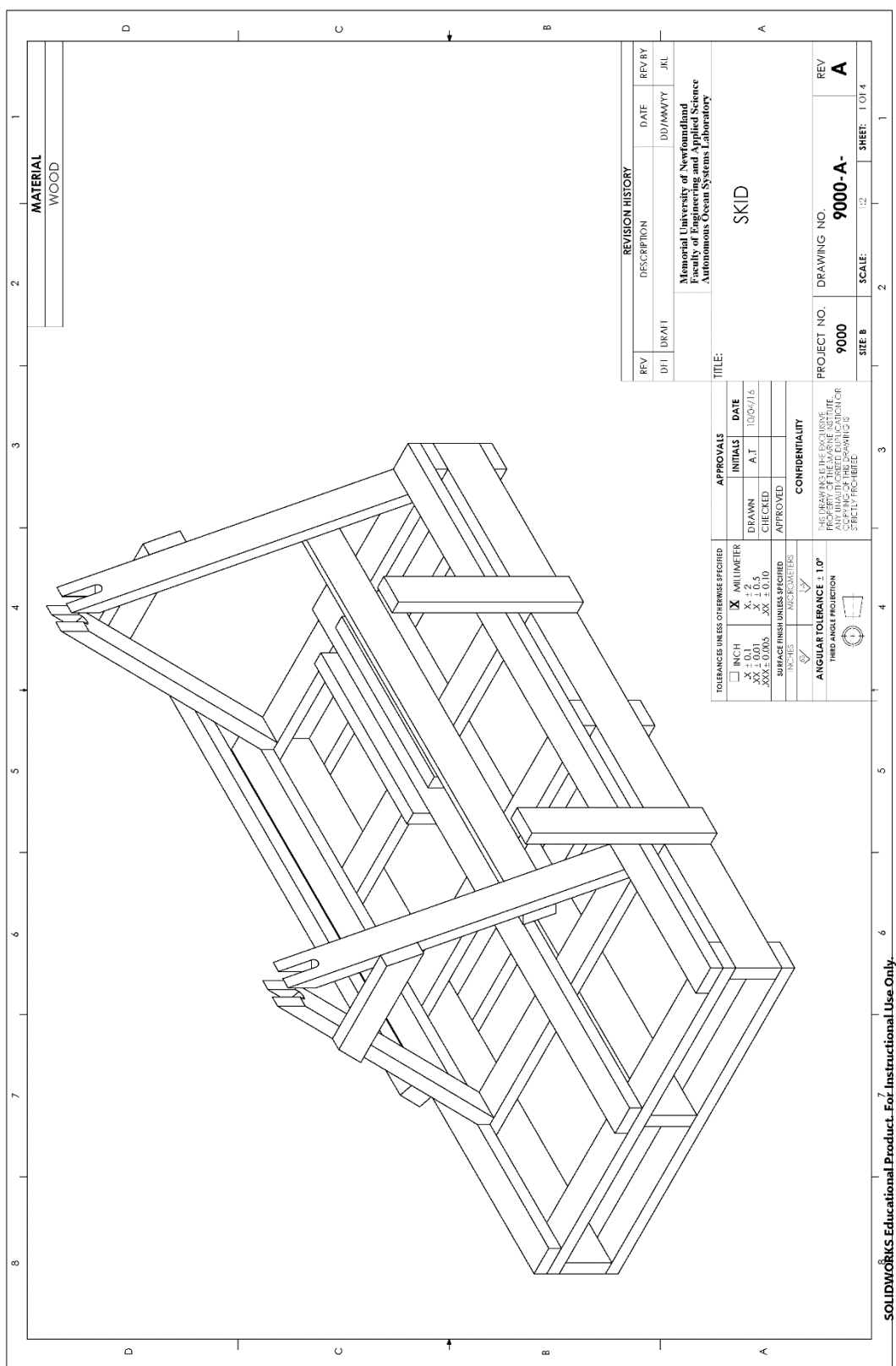


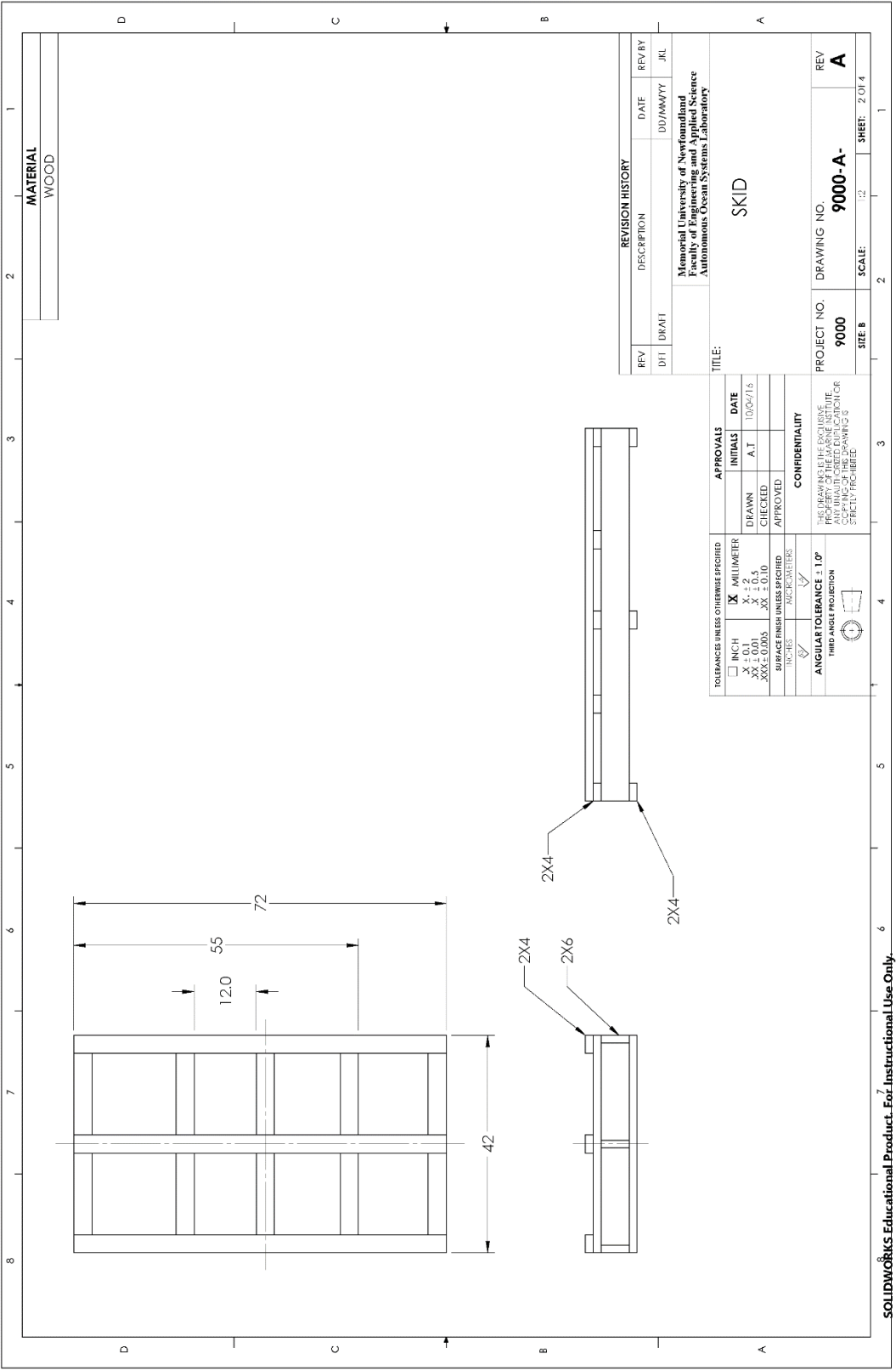


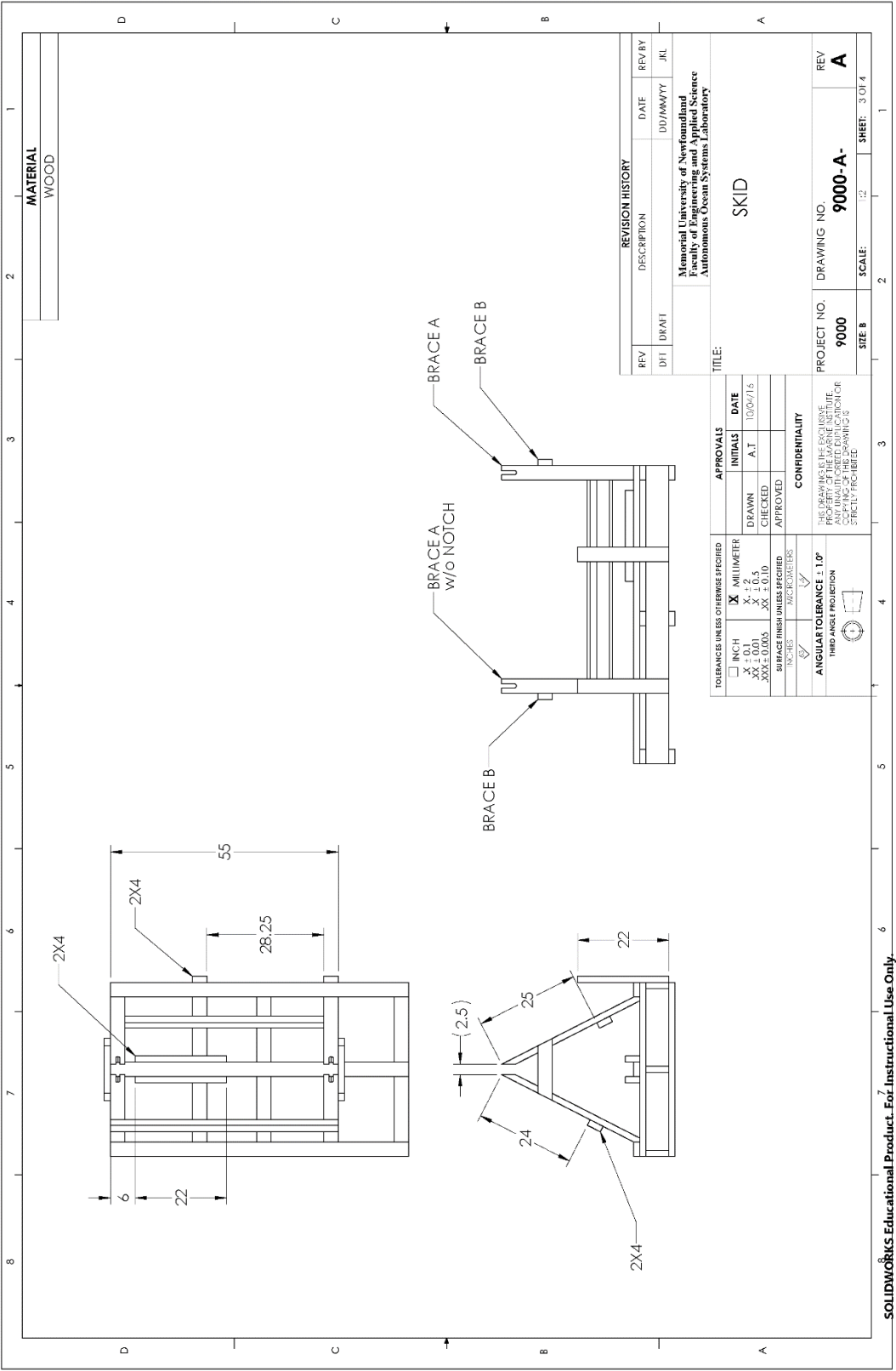












| | | | |
|---|--|--|--|
| TOLERANCE UNLESS OTHERWISE SPECIFIED <input type="checkbox"/> NCH $X \pm 0.1$ $X \pm 0.2$ $X \pm 0.5$ $XX \pm 0.05$ $XX \pm 0.10$ | | APPROVALS INITIALS DATE 10/04/16 | |
| SURFACE FINISH UNLESS SPECIFIED NO FINISH MICRO-FINISH | | CONFIDENTIAL THE DRAWING IS THE PROPERTY OF THE MARINE INSTITUTE. ANY UNAUTHORIZED REPRODUCTION OR DISSEMINATION OF THIS DRAWING IS STRICTLY PROHIBITED. | |
| ANGULAR TOLERANCE $\pm 10^\circ$ THIRD-ANGLE PROJECTION | | CONFIDENTIAL THE DRAWING IS THE PROPERTY OF THE MARINE INSTITUTE. ANY UNAUTHORIZED REPRODUCTION OR DISSEMINATION OF THIS DRAWING IS STRICTLY PROHIBITED. | |
| REVISION HISTORY DESCRIPTION DATE DWT DWT DWT | | TITLE: SKID PROJECT NO. 9000 DRAWING NO. 9000-A- REV A | |
| MEMORIAL UNIVERSITY OF NEWFOUNDLAND FACULTY OF ENGINEERING AND APPLIED SCIENCE AUTONOMOUS OCEAN SYSTEMS LABORATORY | | SITE B SCALE: 1:2 SHEET: 4 OF 4 | |

Appendix C

Custom Accumulator Design Calculations Worksheet

Custom Accumulator Worksheet

From the data available from the specification sheets the Versa BPS-2208 pilot operated check valve can open the valve with a line pressure of 2.8 bar (40 psi) using a pilot pressure of 1.8 bar (20 psi). Since the expected depth of the profiler would be a maximum of 20 meters (2 bar) the 1.8 bar of pilot pressure would be more than enough to operate the check valve.

From the data available from the specification sheets the Vektex 20-0115-04 cylinder has an effective piston area of 1.767 in².

Therefore, the maximum force produced by the cylinder from the when the profiler is at an operational depth of 25 meters (2.5 bar or 36.3 psi) can be calculate using;

$$\text{Maximum Cylinder Force} = \text{Operating Pressure} \times \text{Effective Piston Area}$$

$$\text{Maximum Cylinder Force} = 36.3 \text{ psi} \times 1.767 \text{ in}^2$$

$$\text{Maximum Cylinder Force} = 64.1 \text{ lb}$$

From the data available from the specification sheet for the compression spring selected has a maximum load of 72 lb. Therefore, it is possible to get a 64.1 lb. return force from it. Given the spring rate is 38.4 lb/in the amount of compression can be calculated using;

$$\text{Maximum Spring Compression} = \text{Maximum Cylinder Force} \div \text{Spring Rate}$$

$$\text{Maximum Spring Compression} = 64.1 \text{ lb} \div 38.4 \text{ lb/in}$$

$$\text{Maximum Spring Compression} = 1.70 \text{ in}$$

Since the original spring length is 3" the new spring length is 1.3" after compressing 1.7".

The stroke length required from the cylinder to deliver 1.12 in³ of oil to the pilot operated check valve is calculated using;

$$\text{Stroke} = \text{Volume delivered} \div \text{Effective Piston Area}$$

$$\text{Stroke} = 1.12 \text{ in}^3 \div 1.767 \text{ in}^2$$

$$\text{Stroke} = 0.64 \text{ in}$$

Since the compressed spring length was 1.3" the new spring length after 0.64" stroke is 1.94 in.

The amount of force lost when 1.12 in³ of oil is delivered to the pilot operated check valve is calculated using;

$$\text{Loss of spring force} = \text{Stroke} \times \text{Spring Rate}$$

$$\text{Loss of spring force} = 0.64 \text{ in} \times 38.4 \text{ lb/in}$$

$$\text{Loss of spring force} = 24.6 \text{ lb}$$

The new spring force acting on the cylinder after the 0.64 in stroke is calculated using;

$$\text{New Spring Force} = \text{Maximum Cylinder Force} - \text{Loss of spring force}$$

New Spring Force = 64.1 lb - 24.6 lb

New Spring Force = 39.5 lb.

The pilot oil pressure generated in the cylinder by the new spring force is calculated using;

New Pilot Oil Pressure = New Spring Force ÷ Effective Piston Area

New Pilot Oil Pressure = 39.5 lb. ÷ 1.767 in²

New Pilot Oil Pressure = 22.4 psi

The new pilot oil pressure of 22.4 psi is greater than the required pilot pressure of 20 psi therefore the cylinder and spring combination can form an adequate accumulator for bench testing and field trial in shallow water depths of 25 meters or more.

To achieve a spring force of 64.1 lb the spring must compress 1.7 in. Since the maximum cylinder stroke is 1.5 in the accumulator design must preload the spring by compressing it 0.2 in. Otherwise if the spring only compresses 1.5 in the maximum oil pressure would be 32.6 psi and the reduced spring force after a 0.64 in stroke would be 18.7 psi. This value is lower than the 20 psi pilot pressure required by the pilot operated check valve therefore it will not remain open.

Appendix D

ATL Bladder Design Work Sheet

D.E.W.S.

ATL DESIGN ENGINEER'S WORK SHEET

AERO TEC LABORATORIES INC. RAMSEY, NEW JERSEY, 07446, USA

ATL specializes in the design and fabrication of custom made bladders and other flexible devices. So that our engineers may best assist you, please complete the following interactive DESIGN ENGINEER'S WORK SHEET and a) Save the .pdf and return via e-mail attachment or b) Print, fill out, scan and return via e-mail or fax. If you would like to send a drawing for further clarification, please attach to email. Accepted file types: .PDF, .DXF, .DWG or .IGES.



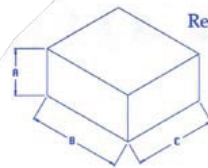
1. Intended application for flexible or collapsible product: Oil Bladder for subsea profiler
2. Operating pressure: 1 bar of differential pressure
3. Operating temperature range: -5 to 30 degrees celcius
4. Chemicals or other substances present in the environment: Sea Water
5. Environmental exposure; (ie. wind, sunlight, radiation, abrasion, bacteria, ozone, impact, ice, etc.): Sea water, periodic sunlight (4 hours a day max)
6. Predetermined specifications for bladder materials; (ie. tensile strength, tear strength, puncture strength, durometer, etc.): _____
7. Specific limitations such as weight, volume, collapsed size, etc.: 8 litre capacity required
8. Is bladder unsupported (free standing), supported (fully restrained), or partially supported? Partially supported
9. Basic size, type and location of fittings required: _____
Bellow style bladder with an SAE-4 ORB bulkhead fitting, center location (see attached schematic)
10. Desired flow rate for filling, discharging or venting if known: _____
11. Quantity desired (no order too small): 1
12. Your name, address, fax, phone, e-mail and best time to call: _____
Joe Singleton, joe.singleton@mi.mun.ca

TOLL FREE: 800-526-5330 TEL: 201-825-1400 FAX: 201-825-1962 E-MAIL: atl@atline.com

WWW.ATLINE.COM

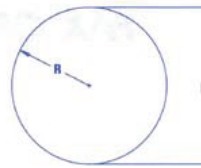
DS-515
3X10

TYPICAL BLADDER SHAPES & VOLUMES



Rectilinear

$$\text{Vol} = A B C$$



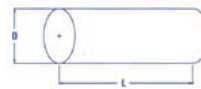
Sphere

$$\text{Vol} = 4.189R^3$$



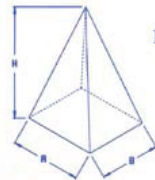
Pillow

$$\text{Vol} = 0.188LW^2 \text{ (APPROX.)}$$



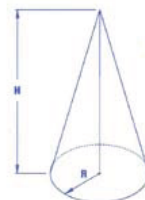
Cylinder

$$\text{Vol} = 0.785LD^2$$



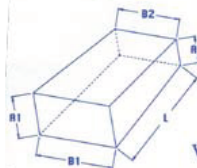
Pyramid

$$\text{Vol} = \frac{H A B}{3}$$



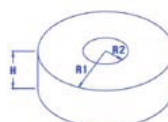
Cone

$$\text{Vol} = 1.047R^2H$$



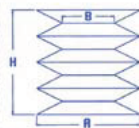
Wedge

$$\text{Vol} = \frac{L (A_1 B_1 + A_2 B_2)}{2}$$



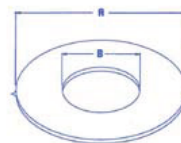
Torroid

$$\text{Vol} = 3.141H(R_1^2 - R_2^2)$$



Bellows

$$\text{Vol} = 0.196H(A^2 + 2AB + B^2)$$



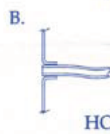
"Pancake Donut"

$$\text{Vol} = \frac{(A+B)(A-B)^2}{7.5} \text{ (APPROX.)}$$

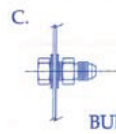
Typical Bladder Fittings



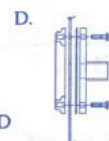
BARB



HOSE



BULKHEAD



FLANGE

CALL, FAX OR E-MAIL OUR SALES ENGINEERS

TOLL FREE: 800-526-5330 TEL: 201-825-1400 FAX: 201-825-1962 E-MAIL: atl@atline.com

WWW.ATLINE.COM

DS-515

PLEASE REVIEW AND PROVIDE SIGNATURE FOR APPROVAL:

SIGN: DATE: April 4, 2016

4 3 2 1

1

| | | | |
|----------|----------|-------------------------|-----------------|
| REVISION | ECN | DETAILS | DRAWN / CHECKED |
| XA | ECN-0443 | INITIAL DRAWING RELEASE | JEC 4/1/2016 |

NOTES:

1. APPLICABLE STANDARDS/SPECIFICATION:
A. ASME Y14.3-10
B. ASME Y14.5
2. APPROXIMATE FINISHED DIMENSIONS OF BLADDER SHOWN
BASED ON CUSTOMER SUPPLIED DRAWING
3. DIMENSIONS ARE IN INCHES (PARENS)
4. TO INCLUDE (1) SAE -40RB S.S. FITTING LOCATED AS SHOWN

| ITEM NO. | PART NUMBER | DESCRIPTION | QTY. |
|----------|-------------|---|------|
| 1 | 10-7400 | Custom ATL Fabricated Bellows Style Bladder | 1 |
| 2 | TF260 | 1.625"-4 Hole Nut-ring Flange Assembly | 1 |
| 3 | TF266 | 1.62x4-Hole Blank Cover Plate | 1 |

| | | | |
|---|---|---|--|
| <p>THIS DRAWING AND CONTENT ARE THE PROPERTY OF AERO TEC LABORATORIES INC. UNAUTHORIZED DISTRIBUTION OR USE WITHOUT WRITTEN PERMISSION FROM AERO TEC LABORATORIES INC IS STRICTLY PROHIBITED.</p> <p>MATERIAL: ATL 648-40</p> | <p>DESCRIPTION: Custom ATL Fabricated Bellows Style Bladder, 1810-7400</p> <p>WEIGHT: lbs</p> | <p>SIZE: A</p> <p>DWG. NO.: 10-7400</p> | <p>REV: XA</p> <p>SCALE: 1:4</p> <p>SHEET 1 OF 1</p> |
|---|---|---|--|

4 3 2 1

Appendix E

Buoyancy Engine Subsea Enclosure Tender Specifications

SPECIFICATIONS FOR A SUBMERSIBLE ENCLOSURE FOR OCEANOGRAPHIC EQUIPMENT

Used to protect oceanographic equipment on an autonomous mobile moored profiler that operates from the surface of the ocean to the seafloor along the continental shelf. The equipment cycles from the sea surface to the floor (200 m depth) five times daily for a twelve month duration.

Please refer to the drawings at the end of the document to complement the written requirements.

Construction Material must be corrosion resistant to a salt water environment; sea water. (Hard anodised aluminum, stainless steel, titanium, composite, etc.). Anodised parts must be machined prior to anodization to ensure all exposed surfaces are protected.

Must not allow the ingress of water. Minimum, the enclosure must be rated and tested to an equivalent depth of 200 meters (20 bar) with a safety factor of 1.5.

Minimum Inside Diameter: 245 mm

Maximum Inside Diameter: 260 mm

Minimum Useable Length: 1000 mm

Maximum Useable Length: 1100 mm

* Useable length is the space between the inside of the endcaps when the enclosure is assembled.

End Caps must have a minimum of 2 seals; at least one must be a bore seal.

End Caps must be mechanically attached to the main body of enclosure.

End Caps must have a means to assist their removal.

End Cap 1 must have an SAE -4 threaded hole (as per SAE J1926 standards) on both sides (port both faces), thru the centre of its face.

End Cap 1 must have 6 equally spaced holes (M6 X 12 mm deep) located on the exterior face of the end cap and located 118 mm from its centre.

End Cap 2 must have 6 equally spaced threaded thru holes located 85 ± 5 mm from its centre.

1 X 9/16"-18 UNF-2A

1 X 5/8"-18 UNF-2A

1 X SAE -4 (as per SAE J1926 standards), ported on the exterior face

3 X SAE -6 (as per SAE J1926 standards), ported on the exterior face

On the external face of End Cap 2, each thru hole must be spot faced to a minimum of 32 mm diameter and with a 0.8 micrometer surface finish.

End Cap 2 must have 6 equally spaced holes (M6 X 12 mm deep) located on the interior face of the end cap and located 100 mm from its centre. They must be spaced between the thru holes.

End Cap 2 must have 1 hole (M6 X 12 mm deep) located at the center exterior face of the end cap.

Fittings:

The SAE -4 hole on the external face of End Cap 1 will be furnished with a 316 Stainless Steel SAE-4 ORB union, coupling, and plug. Parker Part No.; 4 F5OHAO-SS, 4 G5HH5-SS, and 4 P5ON-SS (suggested).

The 3 X SAE – 6 holes on End Cap 2 will be furnished with 316 Stainless Steel Hex Head SAE –6 ORB plugs. Parker Part No. 6 P5ON-SS (suggested).

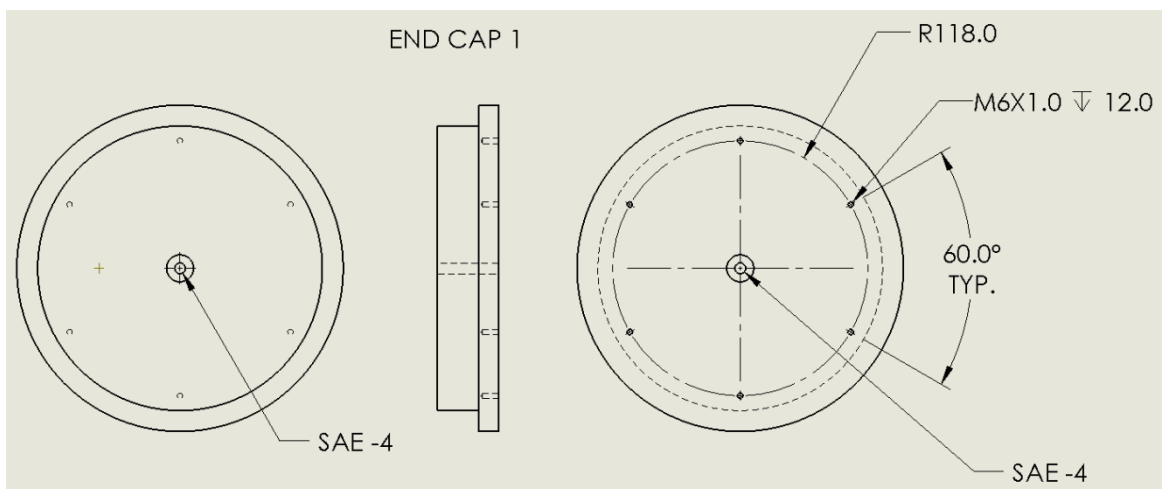
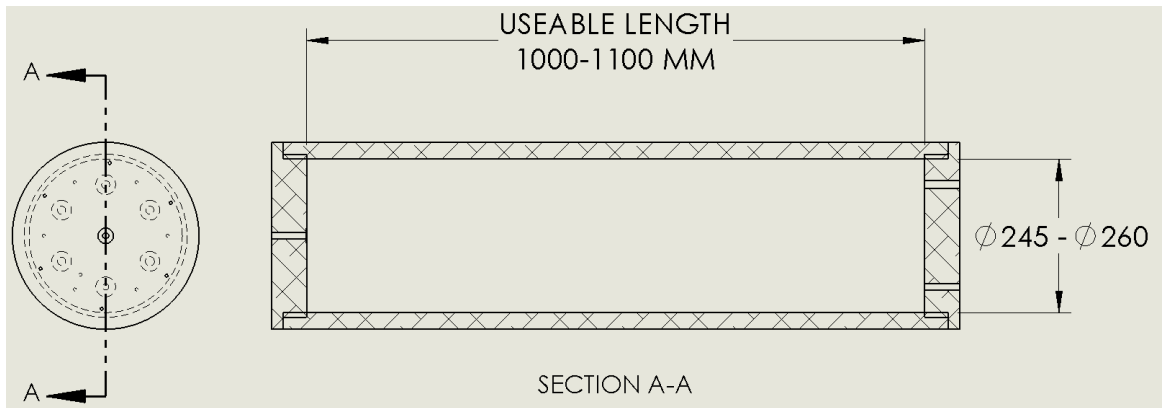
The 1 X SAE -4 hole on End Cap #2 will be furnished with PREVCO Dual Vent Port. Part No. 00669-001 (LBO). <https://prevco.com/products/accessories/vent-plugs>

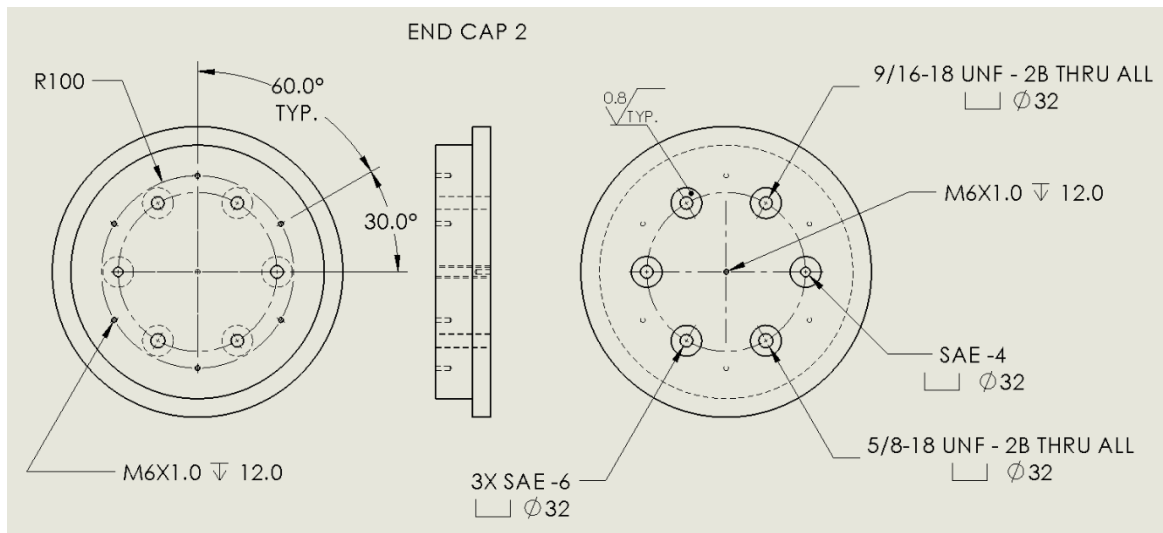
The 1 X 5/8"-18 hole on End Cap 2 will be furnished with a SubConn, BH6M connector, dummy plug DC6F, and sleeves DLSB-F and DLSB-M. The BH6M connector will have 500 mm long lead wires. <http://www.macartney.com/what-we-offer/systems-and-products/connectivity/subconn/subconn-circular-series/subconn-circular-6-8-and-10-contacts/>

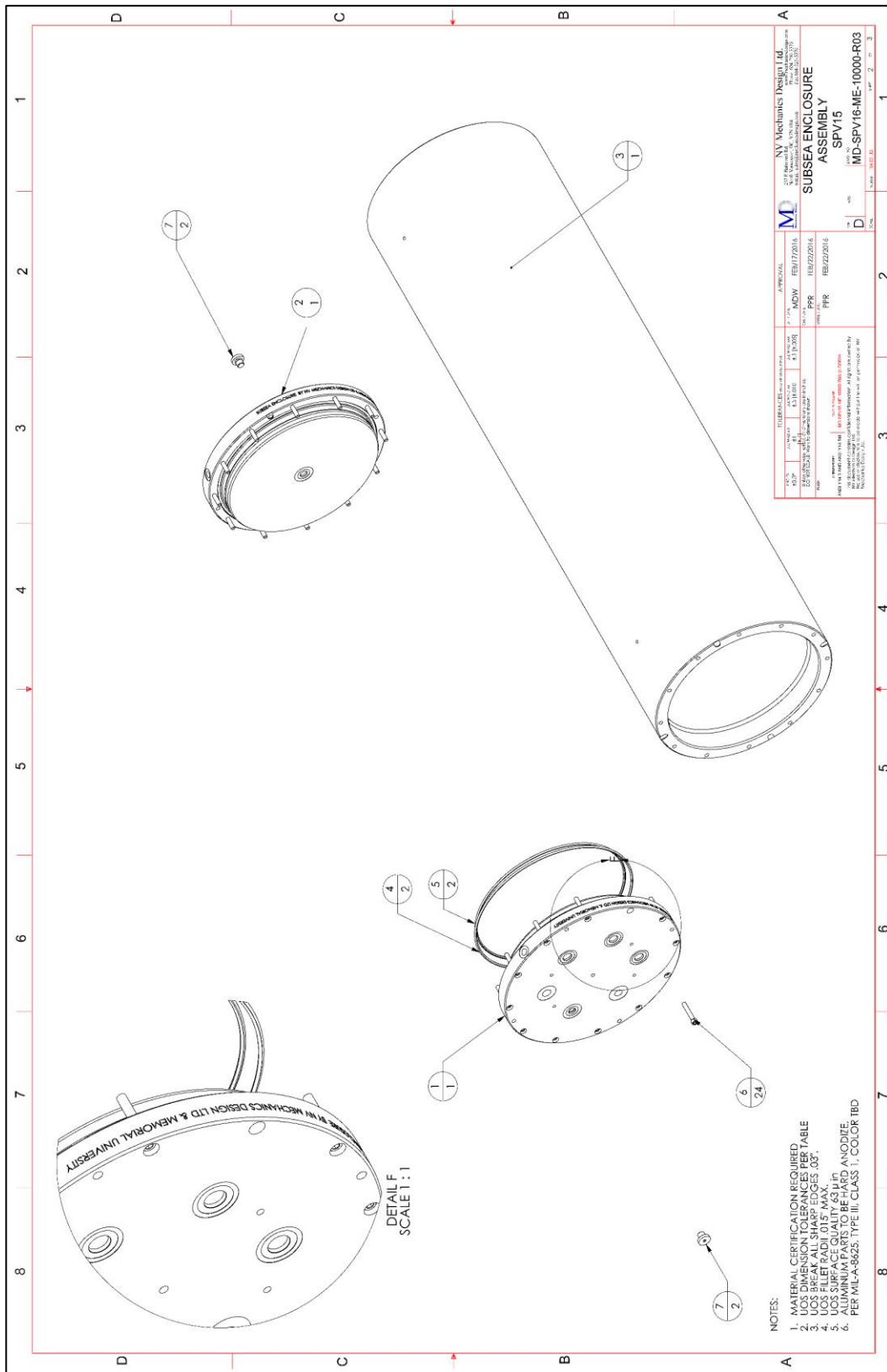
The 1 X 9/16"-18 hole on End Cap 2 will be furnished with a Teledyne MHDG-4-BCR connector, and a dummy plug MHDG-SCP. The MHDG-4-BCR connector will have 500 mm long lead wires.

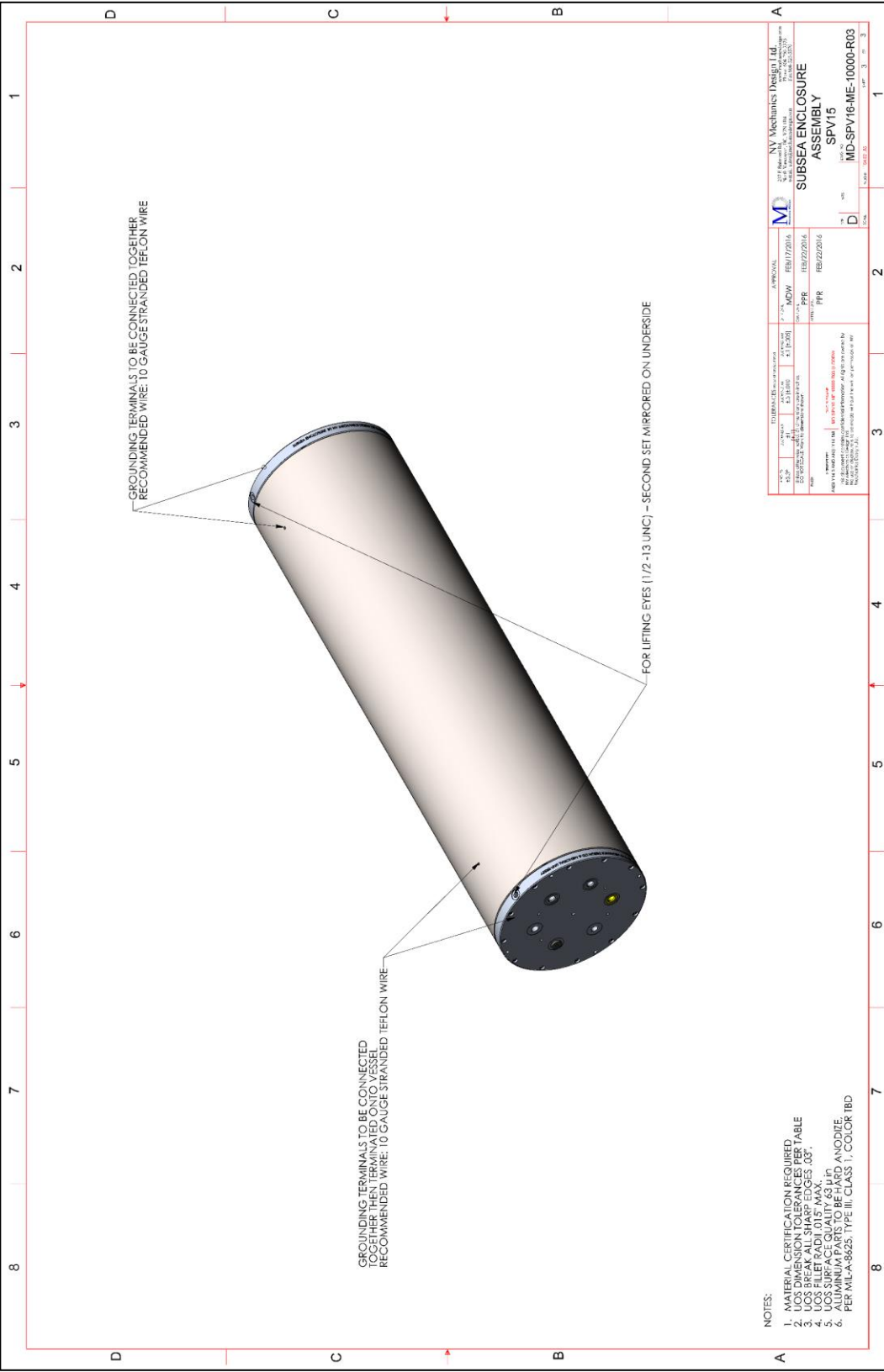
http://www.teledyneoilandgas.com/_document%5CImpulse_MHDG.pdf

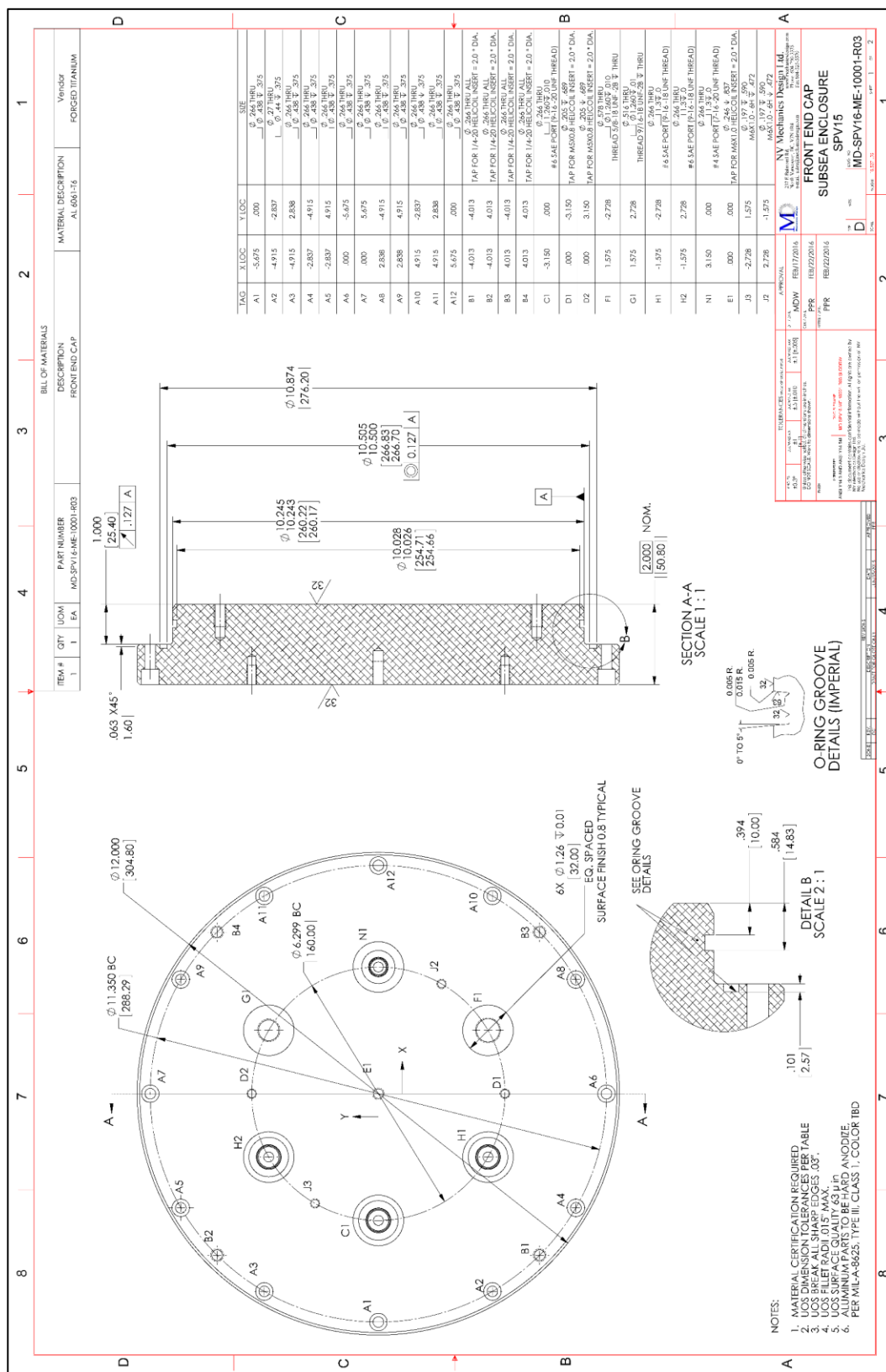
A drawing package must be submitted with the tender to illustrate the basic design (type of seals, method of mechanical attachment of the end caps, etc.).

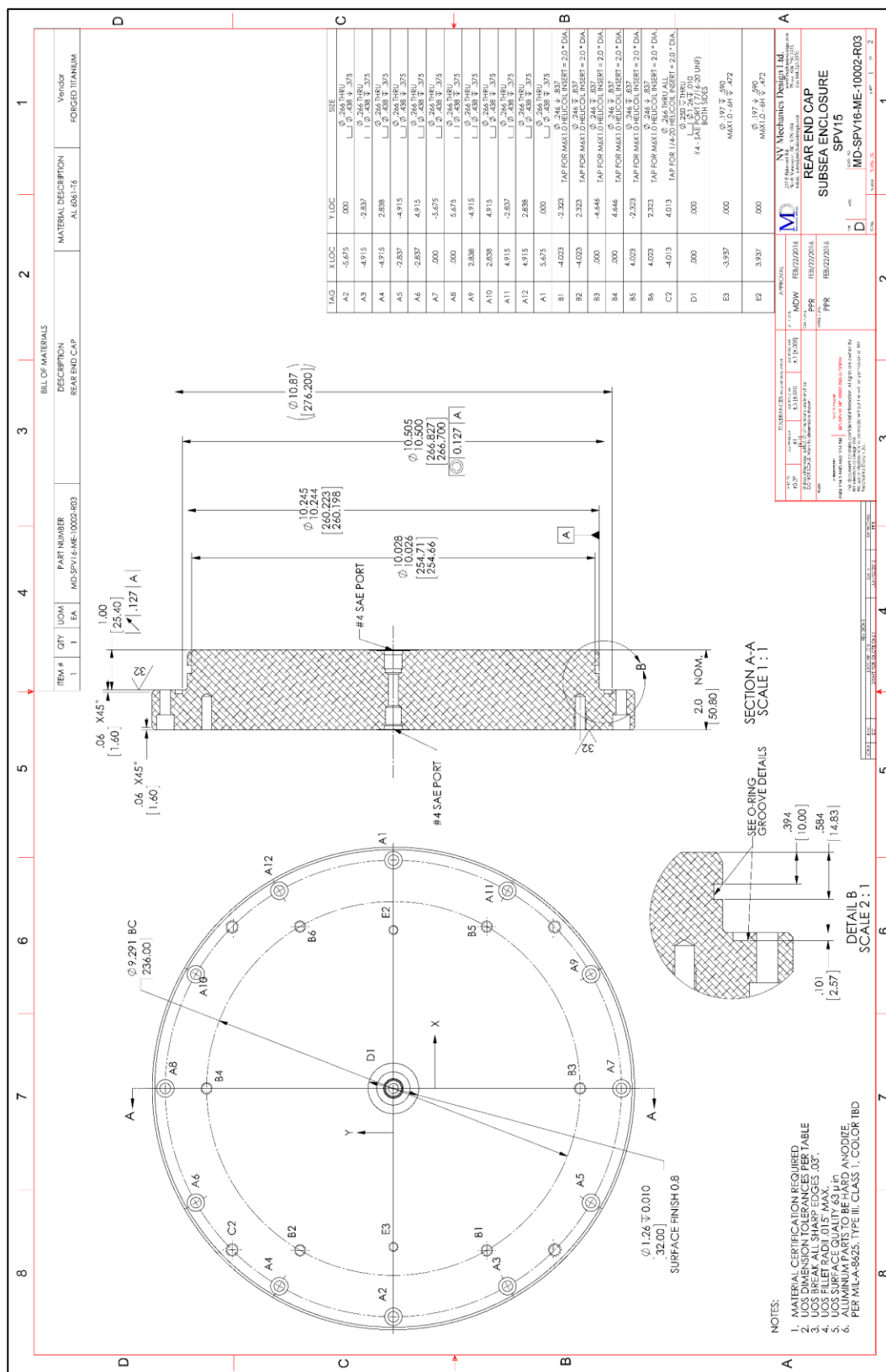


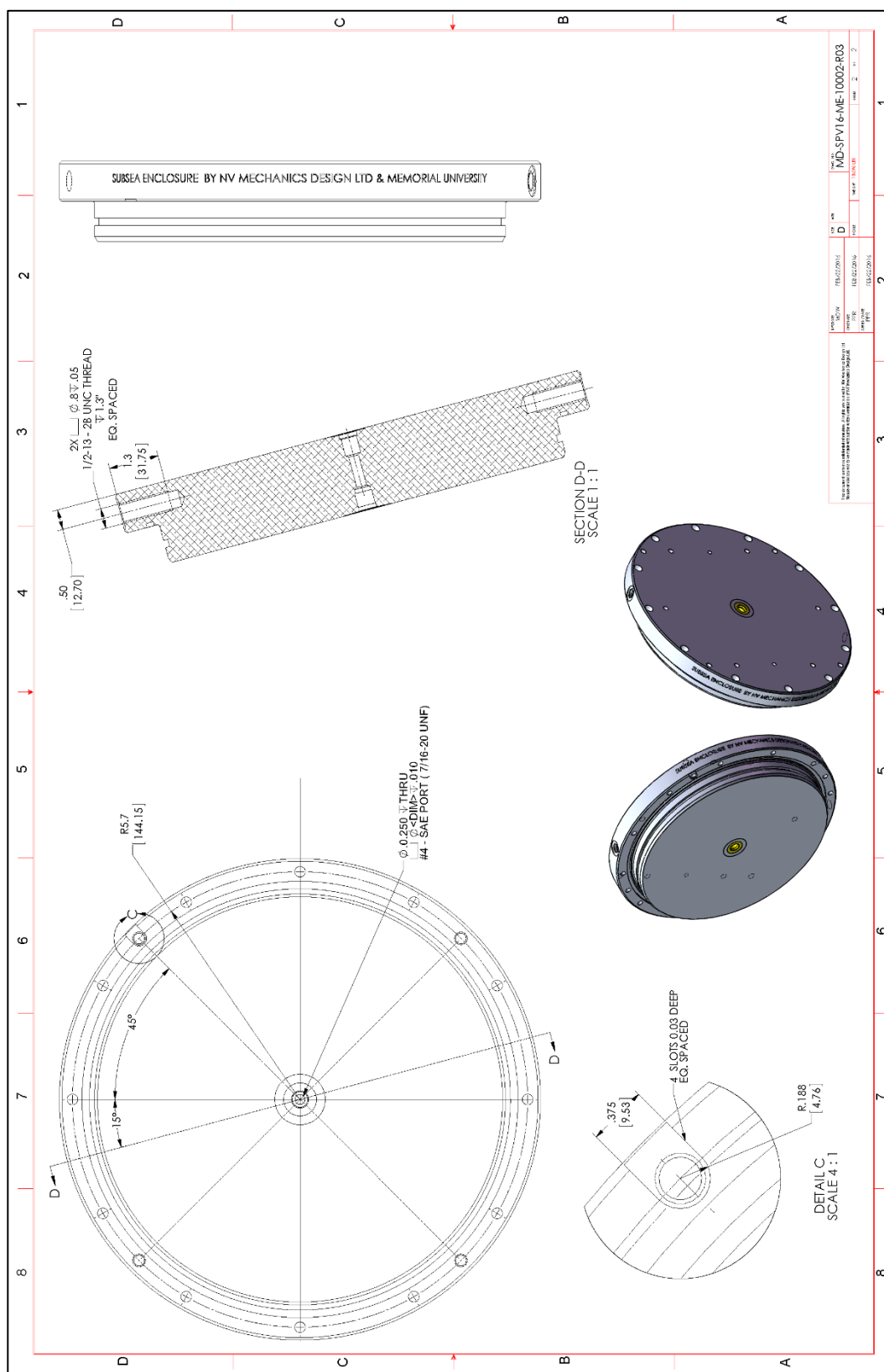


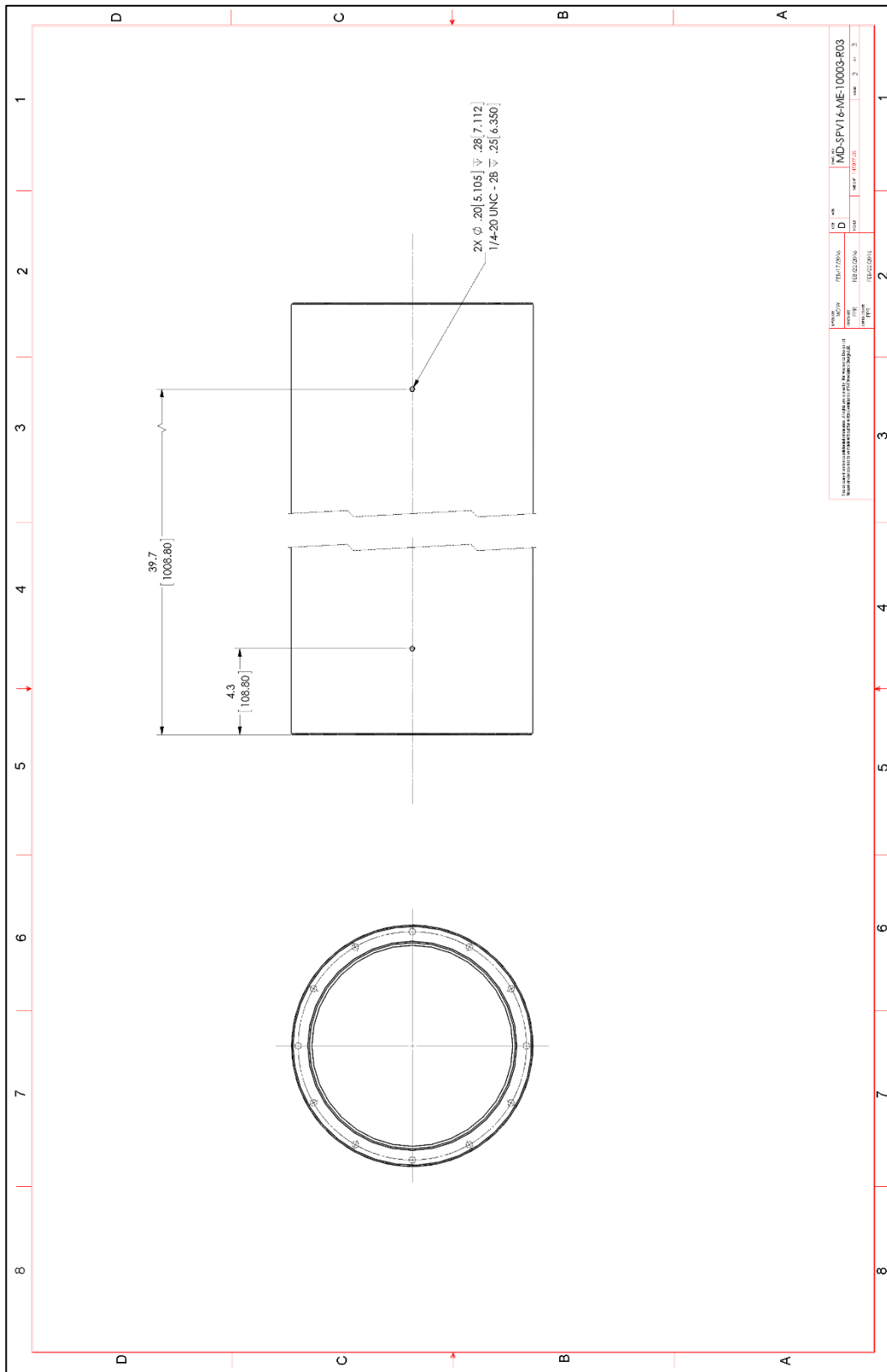












| | | | | |
|----------------------------------|--|--------|--------|--------|
| Part Name: MD-SPV16-ME-10003-R03 | | Rev: 1 | Rev: 2 | Rev: 3 |
| Drawing No: 10003-R03 | | Rev: 1 | Rev: 2 | Rev: 3 |
| Drawing Date: 10/01/16 | | Rev: 1 | Rev: 2 | Rev: 3 |
| Drawing By: [Signature] | | Rev: 1 | Rev: 2 | Rev: 3 |
| Drawing Check: [Signature] | | Rev: 1 | Rev: 2 | Rev: 3 |
| Drawing Appr: [Signature] | | Rev: 1 | Rev: 2 | Rev: 3 |
| Drawing Date: 10/01/16 | | Rev: 1 | Rev: 2 | Rev: 3 |